The impact of dysfunctions in telomere capping

on ageing and cellular senescence

Noshina Shaheen

A thesis submitted in partial fulfilment of the requirements of the Manchester Metropolitan University for the degree of Doctor of Philosophy

School of Healthcare Science
The Manchester Metropolitan University

Manchester, UK

March 2015

Declaration

I declare that this work has not been accepted for any degree before and is not currently being submitted in candidature for any degree other than the degree of Doctor of Philosophy of the Manchester Metropolitan University.

Noshina Shaheen

Acknowledgment

I would like to acknowledge the financial support for this project in the form of a Faculty of Science and Engineering Ph.D studentship. This work would not have been possible otherwise.

It is with immense gratitude that I acknowledge the continuous support and help of my supervisor Dr. Mikhajlo Zubko for his supervision, positive criticism, understanding and personal guidance throughout this project. He was always there to listen positively and provide logical opinion. I am grateful for his valuable comments on the manuscript.

I wish to thank Dr. Muhammad Saeed Ahmad for his constructive criticism, valuable advice and critical comments throughout the progress of this project. Without his support, encouragement and understanding it would have been difficult to complete this project.

I am also very grateful to Professor Claire Stewart for her valuable comments and positive suggestions. I would also like to thank Dr. Nasser-Al-Shanti for his support, guidance and valuable advice related to DNA sequencing work.

I am very much thankful to Dr. Elena Zubko for her help and suggestions during this study.

I cannot find words to express my deepest gratitude to Dr. Ruth Shepherd for proof reading the manuscript. She provided valuable suggestions during the critical review process.

I am indebted to all my colleagues who supported me throughout this work

I would like to extend my gratitude to microbiology technical team for providing excellent support services one can wish for. I express my sincerest thanks to Anne Leahy-Gilmartin, Dr. Paul Benson and especially to Gillian Collier.

I would also like to thank all those who helped me with my work in Cell and Molecular Biology laboratory. Special thanks to my respectable colleague Mr. Mike Head.

I am very much thankful to my loving son Sabeeh Ahmad for his patience, understanding, prayers and encouragement that kept me going.

Finally, I would like to thank my former line manager Mrs. Helen Williams for her support and encouragement to continue my research career.

Table of Contents

Abstract

There is increased evidence of the important roles of telomere capping proteins Cdc13 and Stn1 for cell survival in budding yeast (*Saccharomyces cerevisiae*). Dysfunctional telomeres due to alterations in telomere capping proteins activate DNA damage response and genomic instability causing cellular senescence and eventually cell death. The main aim of this study was to investigate the roles of Cdc13 and Stn1 in ageing and cellular senescence.

Based on the phenomenon of non-essentiality of *CDC13* gene in the absence of *EXO1* gene, *CDC13* full gene deletion and its N-and C-termini disrupted variants were generated using target oriented PCR based approach and verified by automated DNA sequencing. Loss of Cdc13 and/or Stn1 or the presence of defective Cdc13 with truncated N- or C-termini, manifested heterogeneous telomeric DNA profiles with various sizes of unique telomeric bands comparable to type I and type II survivors.

The mutants with telomere capping dysfunctions in the absence of Cdc13 and/or Stn1 disclosed significant differences in survival time under different metabolic conditions. The reduction in viability of the combined deletion mutants (*cdc13Δ* and *stn1Δ*) was much slower in water at 4°C compared to synthetic complete (SC) medium at 30°C, and a similar mortality rate observed at day 6 in (SC) medium was only observed at day 35 in water. The dramatic loss of viability in combined deletion mutant highlighted additive effects of the two capping proteins on chronological survival. The Stn1 deletion mutants (*stn1*::HIS *exo1* LEU2 *rad24*::TRP) showed significantly reduced lifespan as compared to Cdc13 deletion mutants. However, the N- and C-truncated variants of Cdc13 manifested large differences in ageing as compared to WT, indicating different roles of the Cdc13 domains in cell survival.

The strong inhibition of cellular growth of combined deletions mutants of *cdc13* and *stn1* (in the absence of *EXO1* and *RAD24* genes) in responses to genotoxic agents (UV, MMS and HU) suggest the interaction of *cdc13Δ* and *stn1Δ* cooperatively. However, the absence of Stn1 protein made cells highly resistant to H_2O_2-mediated oxidative stress as compared to the combined deletion and *cdc13Δ* mutants. Different extent of growth inhibition was observed for *cdc13Δ* mutants, and its N- and C-terminus truncated variants with the allele dosage effect in N/C-heterozygous diploids.

In conclusion, this study highlighted the significance of Cdc13 and Stn1 in the integrity of telomeres and revealed their important roles in preventing senescence and in cellular responses to oxidative and genotoxic stress. The previously unknown role of Stn1 in chronological lifespan and in cellular responses to oxidative stress observed in this study warrants further investigations about Stn1 in genetic stability, checkpoint control and cellular senescence in the integrated scenario of ageing.

Budding yeast nomenclature

Wild type gene	*CDC13*	uppercase italic for dominant
Mutant allele /		
Recessive mutant	*cdc13-1*	gene symbol, a hyphen and an italic Arabic number
Deletion (null) mutant	*cdc13*Δ	lowercase italic for recessive
Wild type protein	Cdc13p/Cdc13	gene symbol, non-italic, initial letter uppercase and with the suffix ‘p’(optional)
Mutant protein	Cdc13-1p/Cdc13-1	
Dominant allele	uppercase	
Recessive allele	lowercase	

List of proteins

Protein name (name description), protein description

(annotations from the *Saccharomyces* Genome Database (SGD))

- **Bar1p** (**BAR**rier to the alpha factor response) Aspartyl protease secreted into the periplasmic space of mating type a cells, helps cells find mating partners, cleaves and inactivates alpha factor allowing cells to recover from alpha-factor-induced cell cycle arrest.
- **Cdc13p** (**C**ell **D**ivision **C**ycle) Single stranded DNA-binding protein found at TG1-3 telomere G-tails; regulates telomere replication through recruitment of specific sub-complexes, but the essential function is telomere capping.
- **Cdk1p/Cdc28p** (**C**ell **D**ivision **C**ycle) Catalytic subunit of the main cell cycle cyclin-dependent kinase (CDK); alternately associates with G1 cyclins (CLNs) and G2/M cyclins (CLBs) which direct the CDK to specific substrates.
- **Chk1p** (**CH**eckpoint **K**inase) Serine/threonine kinase and DNA damage checkpoint effector, mediates cell cycle arrest via phosphorylation of Pds1p; phosphorylated by checkpoint signal transducer Mec1p; homolog of *S. pombe* and mammalian Chk1 checkpoint kinase.
- **Ddc1p (D**NA **D**amage **C**heckpoint) DNA damage checkpoint protein; part of a PCNA-like complex required for DNA damage response, required for pachytene checkpoint to inhibit cell cycle in response to unrepaired recombination intermediates; potential Cdc28p substrate; forms nuclear foci upon DNA replication stress.
- **Dna2p** (**DNA** synthesis defective) Tripartite DNA replication factor with single-stranded DNA-dependent ATPase, ATP-dependent nuclease, and helicase activities; required for Okazaki fragment processing; involved in DNA repair; cell-cycle dependent localization.
- **Ebs1p** (**E**st1-like **B**cy1 **S**uppressor) Protein involved in inhibition of translation and nonsense-mediated decay; interacts with cap binding protein Cdc33p and with Nam7p; localises to P-bodies upon glucose starvation; mRNA abundance regulated by mRNA decay factors.
- **Est1p** (**E**ver **S**horter **T**elomeres) TLC1 RNA-associated factor involved in telomere length regulation as recruitment subunit of telomerase; has G-quadruplex promoting activity that is required for telomere elongation; possible role in activating telomere-bound Est2p-TLC1-RNA.
- **Est2p** (**E**ver **S**horter **T**elomeres) Reverse transcriptase subunit of the telomerase holoenzyme, essential for telomerase core catalytic activity, involved in other aspects of telomerase assembly and function; mutations in human homolog are associated with aplastic anemia ; Also known as TERT.
- **Exo1p** (**EXO**nuclease) 5'-3' exonuclease and flap-endonuclease involved in recombination, double-strand break repair and DNA mismatch repair; member of the Rad2p nuclease family, with conserved N and I nuclease domains.

- **Kem1p/Sep1p/Ski1p/ Xrn1p** (**K**ar-**E**nhancing **M**utations) Evolutionarily-conserved 5'-3' exonuclease component of cytoplasmic processing (P) bodies involved in mRNA decay; plays a role in microtubule-mediated processes, filamentous growth, ribosomal RNA maturation, and telomere maintenance.
- **Lag1p (L**ongevity **A**ssurance **G**ene) Ceramide synthase component; involved in synthesis of ceramide from C26 (acyl)-coenzyme A and dihydrosphingosine or phytosphingosine, functionally equivalent to Lac1p; forms ER foci upon DNA replication stress; homolog of human CERS2, a tumor metastasis suppressor gene whose silencing enahnces invasion/metastasis of prostate cancer cells; LAG1 has a paralog, LAC1, that arose from the whole genome duplication.
- **Mcd1p/Scc1p** (**M**itotic **C**hromosome **D**eterminant) Essential subunit of the cohesin complex required for sister chromatid cohesion in mitosis and meiosis; apoptosis induces cleavage and translocation of a C-terminal fragment to mitochondria; expression peaks in S-phase.
- **Mec1p** (**M**itosis **E**ntry **C**heckpoint) Genome integrity checkpoint protein and PI kinase superfamily member; signal transducer required for cell cycle arrest and transcriptional responses prompted by damaged or unreplicated DNA; monitors and participates in meiotic recombination.
- **Mec3p** (**M**itosis **E**ntry **C**heckpoint) DNA damage and meiotic pachytene checkpoint protein; subunit of a heterotrimeric complex (Rad17p-Mec3p-Ddc1p) that forms a sliding clamp, loaded onto partial duplex DNA by a clamp loader complex; homolog of human and *S. pombe* Hus1.
- **Mrc1p** (**M**ediator of the **R**eplication **C**heckpoint) S-phase checkpoint protein required for DNA replication; interacts with and stabilizes Pol2p at stalled replication forks during stress, where it forms a pausing complex with Tof1p and is phosphorylated by Mec1p; protects uncapped telomeres.
- **Mre11p (M**eiotic **RE**combination**)** Subunit of a complex with Rad50p and Xrs2p (MRX complex) that functions in repair of DNA double-strand breaks and in telomere stability, exhibits nuclease activity that appears to be required for MRX function; widely conserved.
- **Pdl1p** (**P**rotein **D**isulfide **I**somerase) Protein disulfide isomerase; multifunctional protein of ER lumen, essential for formation of disulfide bonds in secretory and cell-surface proteins, unscrambles non-native disulfide bonds; key regulator of Ero1p; forms complex with Mnl1p that has exomannosidase activity, processing unfolded protein-bound Man8GlcNAc2 oligosaccharides to Man7GlcNAc2, promoting degradation in unfolded protein response; PDI1 has a paralog, EUG1, that arose from the whole genome duplication.
- **Pds1** (**P**recocious **D**issociation of **S**isters) Securin; inhibits anaphase by binding separin Esp1p; blocks cyclin destruction and mitotic exit, essential for meiotic progression and mitotic cell cycle arrest; localization is cell-cycle dependent and regulated by Cdc28p phosphorylation.
- **Rad17p** (**RAD**iation sensitive) Checkpoint protein, involved in the activation of the DNA damage and meiotic pachytene checkpoints; with Mec3p and Ddc1p, forms a clamp that is

loaded onto partial duplex DNA; homolog of human and *S. pombe* Rad1 and *U. maydis* Rec1 proteins.

- **Rad24p** (**RAD**iation sensitive) Checkpoint protein, involved in the activation of the DNA damage and meiotic pachytene checkpoints; subunit of a clamp loader that loads Rad17p-Mec3p-Ddc1p onto DNA; homolog of human and *S. pombe* Rad17 protein; Also known as RS1.
- **Rad50p** (**RAD**iation sensitive) Subunit of MRX complex, with Mre11p and Xrs2p, involved in processing double-strand DNA breaks in vegetative cells, initiation of meiotic DSBs, telomere maintenance, and nonhomologous end joining.
- **Rad53p** (**RAD**iation sensitive) Protein kinase, required for cell-cycle arrest in response to DNA damage; activated by trans autophosphorylation when interacting with hyperphosphorylated Rad9p; also interacts with ARS1 and plays a role in initiation of DNA replication.
- **Rad9p** (**RAD**iation sensitive) DNA damage-dependent checkpoint protein, required for cell-cycle arrest in G1/S, intra-S, and G2/M; transmits checkpoint signal by activating Rad53p and Chk1p; hyperphosphorylated by Mec1p and Tel1p; potential Cdc28p substrate.
- **Rap1p** (**R**epressor **A**ctivator Protein) DNA-binding protein involved in either activation or repression of transcription, depending on binding site context; also binds telomere sequences and plays a role in telomeric position effect (silencing) and telomere structure.
- **Rfa1** (**R**eplication **F**actor **A**) Subunit of heterotrimeric Replication Protein A (RPA), which is a highly conserved single-stranded DNA binding protein involved in DNA replication, repair, and recombination.
- **RFC1** (**R**eplication **F**actor **C**) Subunit of heteropentameric Replication factor C (RF-C); RF-C is a DNA binding protein and ATPase that acts as a clamp loader of the proliferating cell nuclear antigen (PCNA) processivity factor for DNA polymerases delta and epsilon.
- **Rif1p** (**R**AP1-**I**nteracting **F**actor) Protein that binds to the Rap1p C-terminus and acts synergistically with Rif2p to help control telomere length and establish telomeric silencing; deletion results in telomere elongation.
- **Rtg2p (R**e**T**ro**G**rade regulation**)** Sensor of mitochondrial dysfunction; regulates the subcellular location of Rtg1p and Rtg3p, transcriptional activators of the retrograde (RTG) and TOR pathways; Rtg2p is inhibited by the phosphorylated form of Mks1p.
- **San1p** (**S**ir **AN**tagonist) Ubiquitin-protein ligase; involved in the proteasome-dependent degradation of aberrant nuclear proteins; targets substrates with regions of exposed hydrophobicity containing 5 or more contiguous hydrophobic residues; contains intrinsically disordered regions that contribute to substrate recognition.
- **Sae2** (**S**porulation in the **A**bsence of spo **E**leven) Endonuclease required for telomere elongation; also required for telomeric 5' C-rich strand resection; involved in processing hairpin DNA structures with MRX complex; involved in double-strand break repair; sumoylation and phosphorylation both required for function; exists in form of inactive oligomers that are

transiently released into smaller active units by a series of phosphorylations; DNA damage triggers removal of Sae2p, so active Sae2p is present only transiently.

- **Sch9p** (provisional name) AGC family protein kinase; functional ortholog of mammalian S6 kinase; phosphorylated by Tor1p and required for TORC1-mediated regulation of ribosome biogenesis, translation initiation, and entry into G0 phase; involved in transactivation of osmostress-responsive genes; regulates G1 progression, cAPK activity and nitrogen activation of the FGM pathway; integrates nutrient signals and stress signals from sphingolipids to regulate lifespan; Protein serine/threonine kinase involved in regulation of transcription by RNA polymerases I, II, and III; involved in regulation of sphingolipid biosynthesis, cell aging and responses to both oxidative and osmotic stresses; localizes to the nucleus, cytoplasm and vacuole membranes.
- **Sgs1** (**S**low **G**rowth **S**uppressor**)** Nucleolar DNA helicase of the RecQ family involved in genome integrity maintenance; regulates chromosome synapsis and meiotic joint molecule/crossover formation; similar to human BLM and WRN proteins implicated in Bloom and Werner syndromes.
- **Sir2p** (**S**ilent **I**nformation **R**egulator) Conserved NAD+ dependent histone deacetylase of the Sirtuin family involved in regulation of lifespan; plays roles in silencing at HML, HMR, telomeres, and the rDNA locus; negatively regulates initiation of DNA replication.
- **Sir4p** (**S**ilent **I**nformation **R**egulator) SIR4 is one of four silent information regulator genes in budding yeast; SIR protein involved in assembly of silent chromatin domains; silent information regulator (SIR) along with SIR2 and SIR3; involved in assembly of silent chromatin domains at telomeres and the silent mating-type loci; Sir4p participates in silencing the cryptic mating type loci HML and HMR, and helps maintain a repressed chromatin structure near telomeres; unlike repressors that act by binding to promoters, the Sir proteins help repress transcription by creating a silent chromatin structure in a gene- and promoter-independent manner via histones and other DNA binding proteins; Sir4p seems to act in the maintenance rather than the initiation of silencing at HML and HMR; potentially phosphorylated by Cdc28p; some alleles of SIR4 prolong lifespan.
- **Stn1p** (**S**uppressor of Cdc **T**hirtee**N**) Telomere end-binding and capping protein; plays a key role with Pol12p in linking telomerase action with completion of lagging strand synthesis, and in a regulatory step required for telomere capping; similar to human Stn1.
- **Swi4p** (**SWI**tching deficient) DNA binding component of the SBF complex (Swi4p-Swi6p); a transcriptional activator that in concert with MBF (Mbp1-Swi6p) regulates late G1-specific transcription of targets including cyclins and genes required for DNA synthesis and repair; Slt2p-independent regulator of cold growth; acetylation at two sites, K1016 and K1066, regulates interaction with Swi6p.
- **Swi6p** (**SWI**tching deficient) Transcription cofactor; forms complexes with Swi4p and Mbp1p to regulate transcription at the G1/S transition; involved in meiotic gene expression; also binds

Stb1p to regulate transcription at START; cell wall stress induces phosphorylation by Mpk1p, which regulates Swi6p localization; required for the unfolded protein response, independently of its known transcriptional coactivators.

- **Ten1p** (**TE**lomeric pathways with ST**n1**) Protein that regulates telomeric length; protects telomeric ends in a complex with Cdc13p and Stn1p; similar to human Ten1 which is critical for the telomeric function of the CST (Cdc13p-Stn1p-Ten1p) complex.
- **Tel1p** (TELomere maintenance) Protein kinase primarily involved in telomere length regulation; contributes to cell cycle checkpoint control in response to DNA damage; acts with Red1p and Mec1p to promote interhomolog recombination by phosphorylation of Hop1; functionally redundant with Mec1p; regulates P-body formation induced by replication stress; homolog of human ataxia-telangiectasia mutated (ATM) gene.

List of Figures:

List of Tables:

List of abbreviations

µg	Microgram
µl	Microliter
bp	Base pairs
BSA	Bovine serum albumin
CaCl2	Calcium chloride
CFU	Colony forming unit
DLY	David Lydall Yeast
DMSO	Dimethyl sulfoxide
DNA	Deoxyribo nucleic acid
dNTP	Deoxyanucleotide triphosphate
DSBs	Double strand breaks
dsDNA	Double stranded DNA
dTTP	Deoxythymidine triphosphate
EDTA	Ethylene diamine tetra acetic acid
H_2O_2	Hydrogen peroxide
HCl	Hydrochloric acid
his	Histidine
HR	Homologous recombination
HU	Hydroxyurea
K rpm	1000 rpm
LB	Luria-Bertani
leu	Leucine
$MgCl_2$	Magnesium chloride
min	Minutes
MMS	Methyl methanesulfonate
NHEJ	Non-homologous end joining
NaCl	Sodium chloride

NEB	New England Biolabs
ng	Nanogram
nt	Nucleotides
OH	Hydroxyl radical
PKC	Protein Kinase C
RNase	Ribonuclease A
ROS	Reactive oxygen species
rpm	Revolutions per minute
SC	Synthetic complete
SD	Standard deviation
SD/SDC	Synthetic defined
SDS	Sodium dodecyl sulphate
sec	Seconds
ssDNA	Single stranded DNA
TCA	Tricarboxylic acid cycle
trp	Tryptophan
ura	Uracil
UV	Ultraviolet rays
WT	Wild type
YEPD/YPD	Yeast extract peptone dextrose

Chapter 1

General Introduction

1. Introduction

1.1. Ageing and cellular senescence

Ageing is a complex multifactorial process that leads to progressive loss of functionality, increase in the chance of diseases and eventually to death. Ageing therefore results from "a decreasing ability to survive stress," (Weinert and Timiras, 2003). Evolutionary question "Why do we age?" addresses the biological and evolutionary significance and benefits of ageing, while the question "How do we age?" is mainly concerned with the mechanisms and manifestations of ageing process (Davidovic *et al*., 2010).

Ageing is regulated by complex interplay of mechanisms at molecular and cellular levels. Many genetic, epigenetic and environmental factors are involved in the ageing process. Accumulation of genetic mutations due to oxidative stress and radiation, reactive oxygen species-induced damage to mitochondrial functions, accumulation of damaged proteins, alterations of the epigenome and modification of molecular pathways due to changes in nutrition are examples of those. At cellular level methylation of DNA is a part of regulatory mechanisms that drive ageing and could be responsible for ageing-induced changes in gene expression. Patterns of DNA methylation change during ageing and contribute to the ageing process (Jung and Pfeifer, 2015). Tissue culture studies in human have demonstrated that cultured cells lose methylated gene fragments with an increased number of cell divisions (Bork *et al*., 2010).

More than 300 theories exist to explain the nature of the ageing process (Vina *et al*., 2007). The main theories have been categorised as evolutionary, gene regulation, cellular senescence, free radical and immune theories (Weinert and Timiras, 2003). These theories explain various aspects of the ageing process at different levels and attempt to identify particular causes or consequences of ageing process. Ageing itself is described as a sum of all changes that occur at physiological, genetics and molecular level with the passage of time (Rattan, 2008, Weinert and Timiras, 2003).

The main theories of ageing are briefly described below. Three of these, the theory of programmed death, the mutation accumulation theory of ageing, and the antagonistic pleiotropy theory of ageing have been considered as evolutionary theories of ageing as these are closely related to the genetics of ageing (Gavrilov and Gavrilova, 2002).

At present there is no unifying theory of ageing which can explain ageing process completely. These theories have their own strengths and limitations and have been validated on the basis of available experimental data over time. Among these theories, the mutation accumulation theory of ageing is widely employed and considered as the most viable one. The free radical theory of ageing is also universally recognised.

1.1.1. Programmed ageing

This concept suggests that ageing is genetically determined i.e., pre-programmed in DNA or genes that encode the lifespan of an organism. Modern theories of programmed ageing emphasise that ageing is under tight control of biological timetable that regulates maintenance, repair and defence responses by switching on/off certain genes at different stages of development. In a multicellular organism differentiating cells lose some potential to translate genetic information that eventually leads to senescence. Ageing in higher organisms could be a result of evolved balance between functionality and counteracting events (Strehler, 1986). Genetic instability (manifested as chromosome aberrations) is involved in ageing and senescence. DNA damages are different from classical mutations and the changes in DNA could be both endogenous and exogenous. Genome crisis due to accumulation of DNA damages leads to irreversible cell cycle arrest (senescence) or programmed cell death (apoptosis) (Weinert and Timiras, 2003).

The genetic control of ageing by underlying groups of genes (the programmed ageing) has been supported by experimental work on worm, *Caenorhabditis elegans* (Hekimi *et al*., 2001), a fruit fly (*Drosophila melanogaster*) (Ja *et al*., 2007) and mouse (Swindell, 2007, Park *et al*., 2009). The overexpression or silencing of genes, or a specific gene disruption/knockout can also delay or initiate early senescence. A number of mutations have been discovered that extend the lifespan in model organisms (e.g., yeast, fruit flies and mice). Mutations in *RAS2*, *CYR1* and *SCH*9 extend the chronological lifespan in *S. cerevisiae* by activating stress resistance transcription factors and mitochondrial superoxide dismutase (Sod2), however, the overexpression of Sod2 shorten the RLS in yeast (Fabrizio *et al*., 2004, Fabrizio *et al*., 2003). These genes act through evolutionary conserved pathways (IGF, TOR and mitochondrial pathways) that regulate growth (Fabrizio and Longo, 2003).

Intrinsic ageing can be counteracted to extend lifespan of organisms to some extent by genetic factors that determine lifespan of organisms under the influence of environmental factors. Many other factors (like specific dietary restrictions, active life style and regular exercise) also affect ageing positively (Davidovic *et al*., 2010). Two factors, "starvation and "delayed reproduction", extend the lifespan cooperatively with species-specific genetic makeup (Davidovic *et al*., 2010). Caloric restriction and prolonged lifespan are not correlated in all organisms including humans (Shanley and Kirkwood, 2006). Many other factors including improved antioxidant defences, increased responsiveness to insulin, reduced blood sugar levels, reduced body size, and delayed sexual maturation are involved in the longevity mechanisms. For example, the increased level of antioxidants can reduce the level of free radicals or ROS to control the oxidative stress damages and delay ageing.

1.1.2. Mutation accumulation theory

From the evolutionary perspective, ageing is considered as the "decreasing force of natural selection with increasing ageing" (Gavrilov and Gavrilova, 2002). Environmental assaults induce damages at various levels. The mutations with negative effects accumulate passively over successive generations in the population and ultimately lead to pathology, senescence and an increase in mortality rates late in life.

The detrimental late-acting mutations accumulate in the population at a much faster rate as compared to early-acting mutations. The accumulation of DNA damage eventually overtakes the ability of the cells to repair them (cell impairment), leading to cell senescence and death.

1.1.3. Antagonistic pleiotropy theory

The competing model to explain senescence is antagonistic pleiotropy hypothesis. It refers to the expression of a gene with multiple competing effects; some beneficial but others detrimental to the organism (unrelated traits). Expression of genes beneficial at younger age could be deleterious at older ages. Selection will favour actively the retention and accumulation of late-acting deleterious genes in populations if they have any beneficial effects early in life (Weinert and Timiras, 2003, Kirkwood and Melov, 2011).

An antagonistically pleiotropic gene selected for beneficial effects in the prime of life yet has unselected deleterious effects with age, thereby contributing directly to senescence. Antagonism between reproduction and longevity in *Drosophila* and *Caenorhabditis elegans* is an example in which limiting reproduction by destroying germ line cells can extend lifespan in both (Sgro and Partridge, 1999, Arantes-Oliveira *et al*., 2002).

Another example is of p53, a key regulator of cell checkpoint responses. It plays an active role in cell cycle arrest, apoptosis and senescence. Studies show that p53-mediated senescence suppresses tumour formation (Donehower, 2002) by preventing the replicative potential of cells. On the contrary, incidence of cancer and cellular senescence prevalence increase in old age. It suggests that selection of cellular senescence in the early life suppresses cancer whereas unselected effects manifest cancer in the old age. The senescent cells release factors that stimulate neighbouring cells to proliferate and increase in the occurrence of cancer, an age-related pathology (Krtolica and Campisi, 2002, Coppe *et al*., 2010).

1.1.4. Disposable soma theory

T. B. Kirkwood proposed disposable soma theory of the evolution of ageing in 1977 (Kirkwood, 1977, Kirkwood, 2002). This theory explains why different organisms live for a certain period of time and why do they age. It was suggested that organism live with reduced protection of

soma (non-reproductive aspects) to enhance development and specifically reproduction. Reduced accuracy and protection of soma due to accumulation of random errors and damages lead to a deterioration of the organism and eventual death. According to this theory, high level of accuracy is maintained in germ line cells with the elimination of any defective cells (Kirkwood and Holliday, 1979). More resources are allocated to develop and to increase the reproductive capacity of organism rather than protecting soma to live longer. The nurturing of somatic cells is to ensure continued reproductive success while soma becomes disposable after reproduction. According to this theory ageing is not adaptive, and organisms must compromise between energy allocation to growth and reproduction, or somatic maintenance and repair (Kirkwood, 1977, Kirkwood and Rose, 1991, Kirkwood, 2002).

Inherent in this theory is the idea that longevity (somatic maintenance) has a cost: the balance of resources is invested in it adopting an energy saving strategy of reduced accuracy, and reproductive fitness dictates the lifespan. The disposable soma theory, however, does not postulate the specific cause of ageing. This theory is in agreement with antagonistic pleiotropy theory as ageing could be a biological trade-off between beneficial aspect of life (reproduction) and the linked adverse aspect ageing (Kirkwood and Holliday, 1979).

1.1.5. Oxidative stress hypothesis of ageing

It postulates that oxidative damage cause age-related decline in physiological functions (Sohal *et al*., 2002). This hypothesis is supported by the evidence that oxidative damage of macromolecules i.e., proteins, lipids and carbohydrates increases with age (Harman, 2006). An additional evidence for a direct link between oxidative damage and ageing is still required.

Oxidative metabolism produces highly reactive free radicals. It was postulated that toxicity of oxygen is due to its partially reduced form (Gerschman *et al*., 1954). This idea was further developed by D. Harman who proposed the free radical theory of ageing (Harman, 1956, Harman, 1981, Harman, 1992a, Harman, 1992b, Harman, 2006). According to this theory free radicals produced during oxygen metabolism are implicated in ageing process by causing damage to cell and tissues. It was suggested that the ageing could be a cumulative effect of the deleterious free radicals reactions initiated first by UV radiation from the sun in oxygen-free environment of a protocell in the beginning of life, and then by ongoing enzymatic and non-enzymatic reactions within cells during the evolution of life. Within a cell, free radicals are mainly generated in mitochondria during cytochrome P450 metabolism and by, peroxisomes (Inoue *et al*., 2003). The formation of free radicals (reactive chemical species) or oxygen-free radicals (reactive oxygen species, ROS) is ubiquitous in biological systems. Since free radicals are the main by-product of aerobic metabolism, their level increases with increased utilisation of

oxygen in cells (Rahman, 2007). These free radical reactions cause damage of cells and tissues. Due to their high reactivity, free radicals oxidise proteins (Lobo *et al*., 2010), carbohydrates (Gutteridge, 1981, Baynes and Thorpe, 1999) DNA (Valko *et al*., 2004) and polyunsaturated lipids (Gutteridge, 1995) in a random manner, and induce oxidative stress. The damages caused by free radicals increases with the age of the organism (Hekimi *et al*., 2011). It accelerates the ageing process and progressively increase the chances of age-related diseases such as cancer, cardiovascular diseases, strokes, Alzheimer's disease, immune system diseases and ultimately death (Valko *et al*., 2004).

Many free radicals has been identified including superoxide; hydrogen peroxide; hypochlorous acid; hydroxyl (Gutteridge, 1995). The deleterious effects of free radicals are influenced by endogenous antioxidant system, environment and genetics factors to various levels (Rahman, 2007). The enzymatic antioxidants such as peroxidases; catalases, glutathione peroxidase, superoxide dismutase and DNA repair mechanisms counteract the oxidative stress damage (Mates *et al*., 1999, Mittler, 2002, Valko *et al*., 2006). Non-enzymatic antioxidants involve vitamin C, vitamin E, carotenoids (CAR), selenium and others (Valko *et al*., 2004, McCall and Frei, 1999). The dietary manipulation can also lower the rate of production of free radical (decrease oxygen consumption) and their detrimental effects and might decrease the symptoms of ageing and increase the lifespan of an organism. In rodents, calorie restriction reduces the formation of ROS and decreases the accumulation of oxidative damages and prolongs lifespan (McCall and Frei, 1999).

The free radical theory operates with several hypotheses based on the type of damaged molecules and the roles of specific organelles in the ageing process. These hypotheses include: enhanced rate of oxidant production due to mutations in mitochondrial DNA; accumulation of oxidized proteins) and accumulation of genetic mutations in somatic cells. Despite the growing evidences on the involvement of free radicals in degenerative senescence, there is no consensus on the hypothesis that free radicals are the only causes of ageing, as genetic data do not provide a strong support to the free radical theory of ageing. However, they are considered as major contributors in the ageing process.

1.1.6. Cell senescence and telomeres

Cellular senescence theory of ageing was described as limited replicative capacity of normal cells in culture followed by irreversible cell cycle arrest and manifestation of altered physiology (Hayflick, 2000, Campisi, 2003b). Senescence could be replicative senescence (as a result of telomere shortening:) or stress induced senescence (due to other molecular causes) (Weinert and Timiras, 2003).

Replicative senescence is the ultimate result of telomere shortening and altered telomere structure (dysfunctional telomeres) due to loss of telomeric DNA during successive cell divisions. Telomeres are the specialised DNA-protein structures at the end of linear chromosomes (Blackburn, 2000). Stress-induced senescence is caused by other DNA damages including double strand breaks, disrupted heterochromatin and strong signalling from oncogene expression etc. (Weinert and Timiras, 2003).

Normal somatic cells undergo irreversible growth arrest after a finite number of divisions and acquire replicative senescence state. Senescent cells exhibit phenotypic changes with altered physiology that may contribute to ageing and age-related diseases, including cancer (Dimri *et al*., 1995, Krtolica and Campisi, 2002). In contrast, escape from cellular senescence is uncontrolled replication or malignant cancer. In cancer cells, telomere length is maintained either by the expression of telomerase enzyme (Kim *et al*., 1994) or by adopting alternate pathways for telomere elongation (Reddel, 2000). The cellular senescence is controlled by the p53 and RB tumour suppressor proteins through a potent anticancer mechanism (Campisi, 2003a). The p53 transcription factor is a key regulator in controlling cell cycle arrest, apoptosis, and senescence. Cellular senescence is a defence response to prevent aged cells, cells with severe damage or dysfunctional telomere from proliferation by inducing a permanent cell cycle arrest.

Senescent cells resemble quiescent cells in culture and are identified by their inability to undergo DNA synthesis. They are detected by histochemical stain of cells for stress induced biomarkers such as beta-galactosidase (Itahana *et al*., 2007). Cellular senescence can be determined by the reproductive capacity of the cell (Piper, 2006). Chronological ageing reflects the time period an organism can remain viable in a non-dividing state (Bitterman *et al*., 2003). In higher eukaryotes, telomere lengths are associated with ageing (Hayflick, 2000). In mammals germ line cells, early embryonic cells and some stem cells express telomerase, in contrast to most somatic cells which do not express telomerase to regulate their length. The telomeres shorten on each cell division due to the "end replication problem" (Allsopp *et al*., 1995). The process of telomere shortening begins in embryonic development (Kalmbach *et al*., 2013). The critical length of the telomere and telomere uncapping cause genomic instability and the onset of ageing and cellular senescence, due to the accumulation of single-stranded DNA, an established form to explore cellular senescence in yeast due to dysfunctional telomeres (Hayflick and Moorhead, 1961, Hayflick, 2000, Aubert and Lansdorp, 2008).

1.2. Telomeres

Telomeres are the specialised DNA-protein structure at the ends of eukaryotic chromosomes with multiple repeats of TG-rich specific nucleotide sequences (Figure 1.1). Telomeres vary in their length in different eukaryotes (yeast, ciliates, mammals and plants) but share the structural patterns of the conserved sub-telomeric and telomeric repeat DNA and telomerase mediated end replication functions (Chakhparonian and Wellinger, 2003). Conserved structural composition of telomeres also indicates their functional homology in different eukaryotes. In humans, telomeres are composed of several kilobases of repetitive sequences (TTAGGG)n followed by single stranded overhangs of ~100 nt as compared to 12-14 nt in yeast (Chakhparonian and Wellinger, 2003).

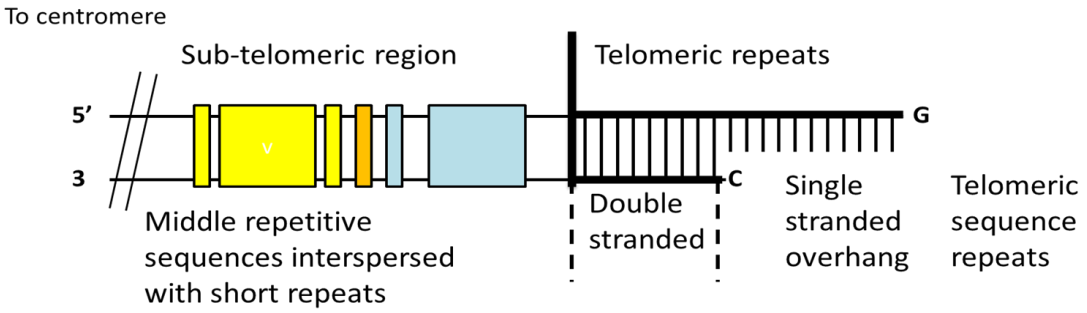

Yeast				
S. cerevisiae	X and Y elements	200-300 bp	12-14 nt; S phase >25 nt	$(TG)_{1\text{-}6}TG_{2\text{-}3}$
Cilliates	Various	14-16 bp	14-16 nt -	-
T. termophila				T_2G_4
O. nova,				T_4G_4
E. crassus				
Mammals	Various		>100 nt	T_2AG_3
H. sapiens		5-15 kb		
M. musculus		up to 100 kb		
Plants	Various	Variable,	Either	T_3AG_3
A. thaliana		>50 kb in some	>20-30 nt or	
Z. mais		cases	<12 nt	
N. tabacum				

Figure 1.1. Organisation of telomeric DNA in different eukaryotes.

Telomeres show variable length in different eukaryotes ranging from a few hundred bp to several kb. They have conserved structural patterns of the sub-telomeric and telomeric repeat DNA. In humans, double stranded telomeres repeat sequences (TTAGGG)n are followed by single stranded overhangs of ~100 nt as compared to 12-14 nt in yeast. The middle sub-telomeric DNA contains conserved repeat sequences of X and Y' elements. (Taken from Chakhparonian and Wellinger, 2003).

In yeast the telomeric repeat DNA contain 200-300 bp of double stranded DNA flanked by middle sub-telomeric DNA of repeat sequences of X and Y' conserved elements. The sub-telomeric X elements are of various sizes (0.3 to 3 kb) and a common feature of yeast chromosomes. The Y' elements of specific sizes (5.2 kb and 6.5/6.7 kb in yeast) together with X-sequences are used to distinguish the telomere length differences in different mutants. The X and Y' repeats contain intergenic located 100-200 bp long autonomously replicating sequence (ARS) elements, which are capable of maintaining extrachromosomal plasmids (Poloumienko *et al*., 2001). Distinct patterns of telomeric DNA are exhibited in mutants with dysfunctional telomere as a result of homologous replication.

Telomeres are characterised by extended single-strand 3' G-overhangs at their end (de Lange, 2002). The G-overhangs in some telomeres fold back and make a loop-like structure with one of the duplex strands to sequester itself within the "large duplex T-loop" generating another small displacement loop (D-loop (Figure 1.2) (de Lange, 2004, Griffith *et al*., 1999). A number of specialised proteins bind with telomeres to single or double strands at specific sequences to form a protective nucleoprotein complex known as a "telosome" (Liu *et al*., 2004) or "shelterin" (de Lange, 2005) (Figure 1.3). Telomere binding proteins also influence the formation of T-loops (Griffith *et al*., 1999). The resulting structural conformation ensures genomic stability by protecting (capping) chromosome ends during the DNA replication process against degradation, rearrangement and end-fusion- by DNA repair machinery.

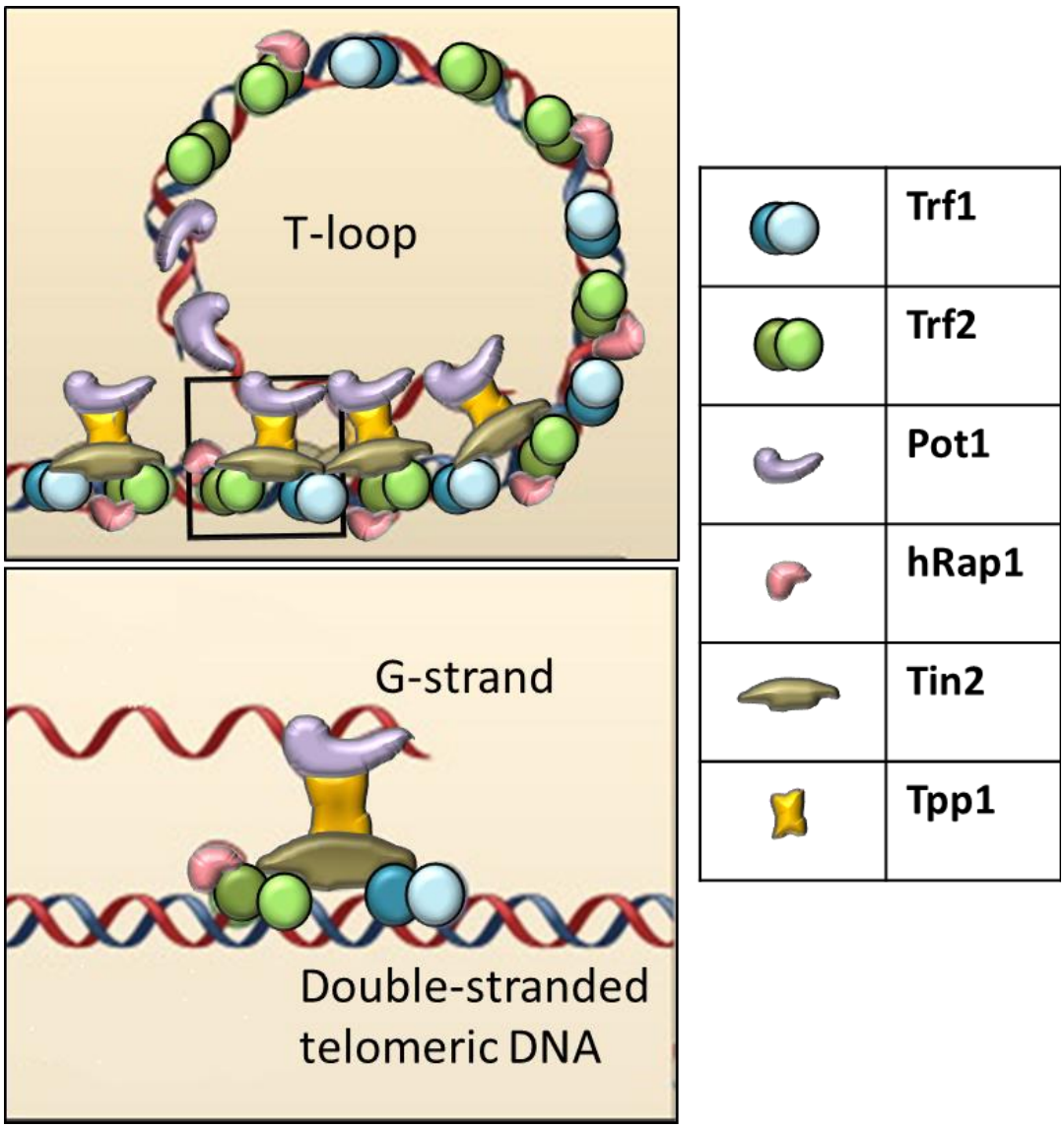

Figure 1.2. Telomeric structure and associated main capping proteins.

Telomeric proteins distinguish chromosome ends from DNA breaks. In mammals, six most important proteins protect chromosome ends and regulate telomere length. Their specific binding and association can bring the single-stranded overhang (G-strand) into close proximity to double-stranded telomeric sequences. Resulting interactions could generate a closed conformation of a telomere in which the single-stranded overhang is fold back and tethered to internal telomeric repeats of homologous sequences through a protein bridge. There could be various possible conformations including linear/open arrangements, T-loops, and other structures which are likely to be interconverted between all of their conformers. **Trf1** (Telomeric repeat binding factor 1): binds to double-stranded TTAGGG repeats, interacts with Pot1 protein indirectly; **Trf2** (Telomere repeat factor-2): binds to double-stranded TG rich repeats; recruits hRap1 and Mre11 complex to telomere; **Pot1** (protection of telomeres): binds to single-stranded TTAGGG repeats; **hRap1** (human repressor activator protein 1): binds indirectly to TRF2 through Tpp1 and Tin2 proteins; **Tin2** (TRF1-interacting nuclear factor 2): binds directly to TRF1 and TRF2 protein to improve localisation of TRF2 and its function to mediate telomere protection; **Tpp1** (Three prime phosphatase: TINT1/PIP1/PTOP1 in mammals): Interacts with Pot1 to make Tpp1/Pot1 heterodimers to recruit telomerase and also binds to Trf2. (Adapted from Baumann, 2006).

Owing to their structural conformation, the ends of telomeres are different from double-stranded DNA breaks (DSBs) (Lydall, 2003) and do not activates DNA damage checkpoint pathways. Telomeres are not recognised as DSBs. In mammals, this is most likely achieved due to protective G-rich T-loop structure conformation that protect chromosome terminus by preventing inappropriate recombination and nucleolytic attacks. Conversely there is no reported evidence of T-loop conformation in yeast, possibly due to short length of telomere i.e., 200-300 bp (Lydall, 2003). However signalling at telomeres and double-strand breaks employs many of the same factors and is supported by increasing evidence that DNA damage response proteins are also involved in telomere maintenance (Slijepcevic, 2006).

Telomereic DNA is considered inert and appears not to induce DNA checkpoint and damage repair responses (Lydall, 2003). Telomere-associated proteins that cap the telomeric ends might function in activating cell cycle checkpoints in response to chromosomal insults. How do cells differentiate between DSBs and telomere ends to prevent chromosome fusion and to ensure genetic stability? With growing knowledge about telomere proteins it is now clear that many DNA damage checkpoint and repair proteins are associated with telomeres. Figure 1.3 shows the various components of DNA-protein complexes of human and yeast telomeres. Telomere capping proteins either bind to the double-stranded DNA (dsDNA) or to the single-stranded telomere DNA (ssDNA). For example, proteins of mammals Trf1, Trf2, Tin2, tankyrase (Tank1 and 2) and hRap1, and proteins of yeast Rap1, Sir2 (silent information regulator 2), Sir3, Sir4 and Yku70/Yku80 bind to duplex region of telomeric DNA. The human Pot1 and yeast Cdc13 proteins, however, bind to telomere at ssDNA. Telomeric proteins play their defined roles in telomere end protection by limiting DNA degradation, preventing ATM (Ataxia telangiectasia mutated) and ATR-activation (signalling) and blocking HR (homologous recombination) and NHEJ (Non-homologous end joining) in human (O'Sullivan and Karlseder, 2010). Other proteins those are involved in DNA replication machinery including Est1 (subunit of telomerase) and Est2 are also associated with telomere DNA.

The number of DNA damage response (DDR) proteins, DNA repair and checkpoint proteins is growing with increasing knowledge of mechanisms involved in cell cycle arrest and in DNA damage pathways. It is still not fully understood how the cell avoids checkpoint/DNA repair activation under normal conditions.

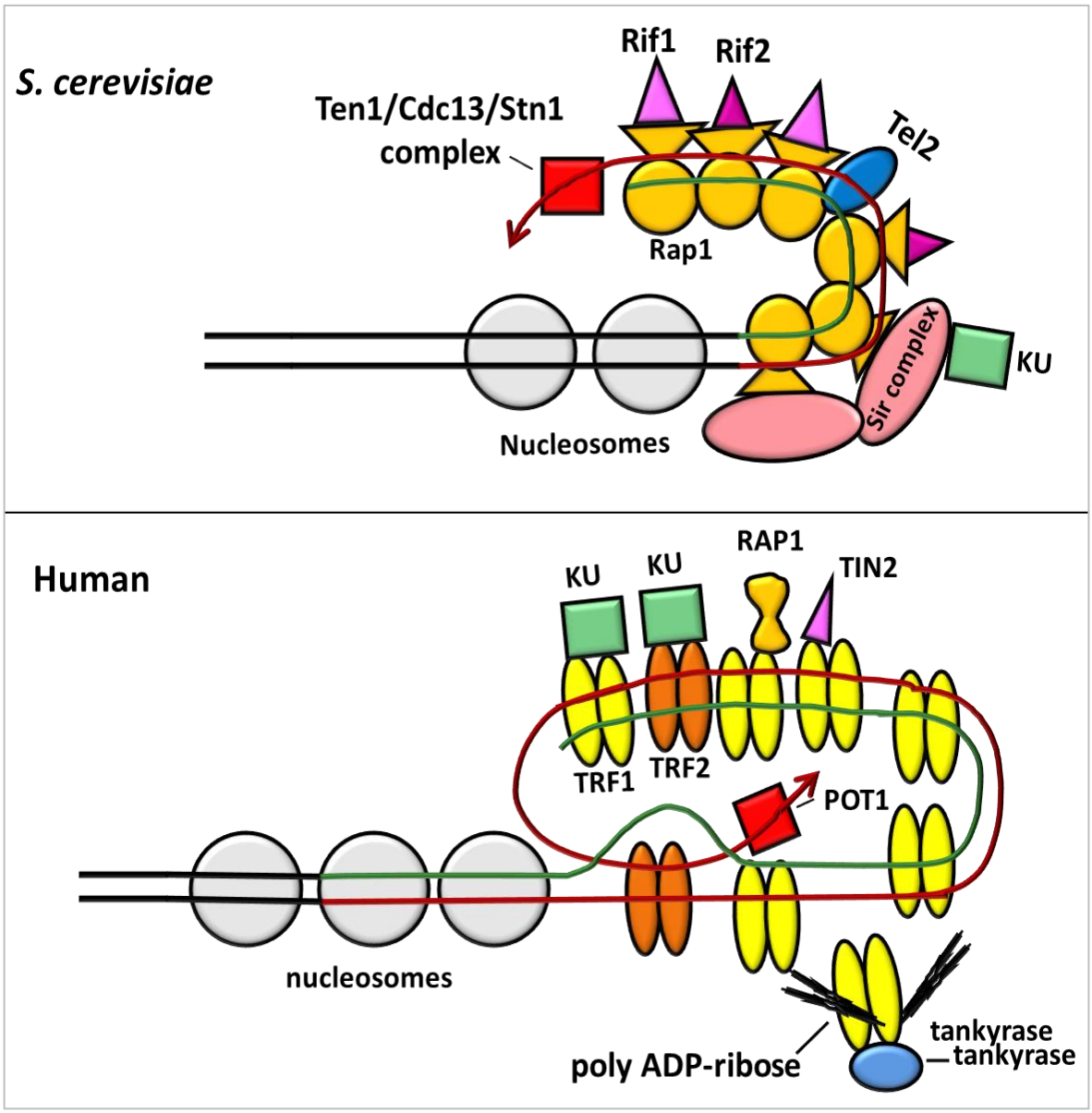

Figure 1.3. The Interactions between different components of the structural DNA-protein complexes associated with telomeres in budding yeast (top) and humans (bottom).

Red line: G-rich telomeric repeat strand (the 3' single-stranded overhang) extended by telomerase; **green line**: complementary C-rich strand; **black lines**: sub-telomeric DNA. The 3' terminal single-stranded telomeric DNA in human telomeres might be in alternative forms: either bound by Pot1 protein or engaged in T-loop formation. (Adapted from Blackburn, 2001).

1.2.1. Telomere maintenance, regulation and genomic instability

The roles of telomeres in chromosome maintenance (Hemann and Greider, 2000, Hemann *et al*., 2001, Price *et al*., 2010) and replication (Blackburn, 1991), in ageing and cellular senescence (Aragona *et al*., 2000, von Zglinicki *et al*., 2005) are well established. Telomere capping proteins stabilise DNA physically by preventing chromosome end fusion and rearrangements and ensure genome integrity. In humans, functional telomere capping with T-loop conformation protects chromosome ends from HR, NHEJ, inhibit recruitment of telomerase and checkpoint proteins, and in association with signalling proteins controls their length (Wu *et al*., 2006, Longhese, 2008). Otherwise, DDR proteins may sense chromosome ends as damaged or double strand DNA breaks and, as a result activate damage response pathways to repair the damage. Studies on budding yeast cells showed that disruption of telomere functions cause strand specific DNA degradation due to dysfunctional capping (Longhese, 2008). It leads to cell cycle arrest and cause genomic instability (Wellinger, 2009). In higher eukaryotes, telomere integrity ensures genetic stability and plays a crucial role to protect organisms from different diseases like cancer and ageing (d'Adda di Fagagna, 2008, Stewart and Weinberg, 2006). Telomere integrity is maintained through complex interaction of mechanisms involving telomere capping proteins (mostly shelterin proteins), telomerase, and DNA damage sensor and repair proteins (Slijepcevic, 2006, Sedivy, 2007, Baumann, 2006).

1.2.1.1. Telomere capping proteins and telomere maintenance

There are a number of proteins that bind telomere to protect chromosome ends and regulate cell proliferation through intracellular signalling (Figure 1.4; Table 1.1). In vertebrates, there are two conserved complexes of telomere binding and capping proteins: the "shelterin complex" that consists of six proteins (Palm and de Lange, 2008, de Lange, 2009) and a recently reported "CST complex" which contains three proteins (Slijepcevic, 2006, Miyake *et al*., 2009, Wellinger, 2009). Within 'shelterin', two proteins TRF1/TRF2 are negative regulators of telomere length, which bind to the double-stranded TTAGGG repeats at telomere T-loops and recruit four more capping proteins (TIN2, RAP1, TPP1 and POT1). The hetero-trimeric complex in mammals, consisting of CTC1, STN1 and TEN1, is an analogue of the *S. cerevisiae* Cdc13-Stn1-Ten1 (CST) complex (Figure 1.4).

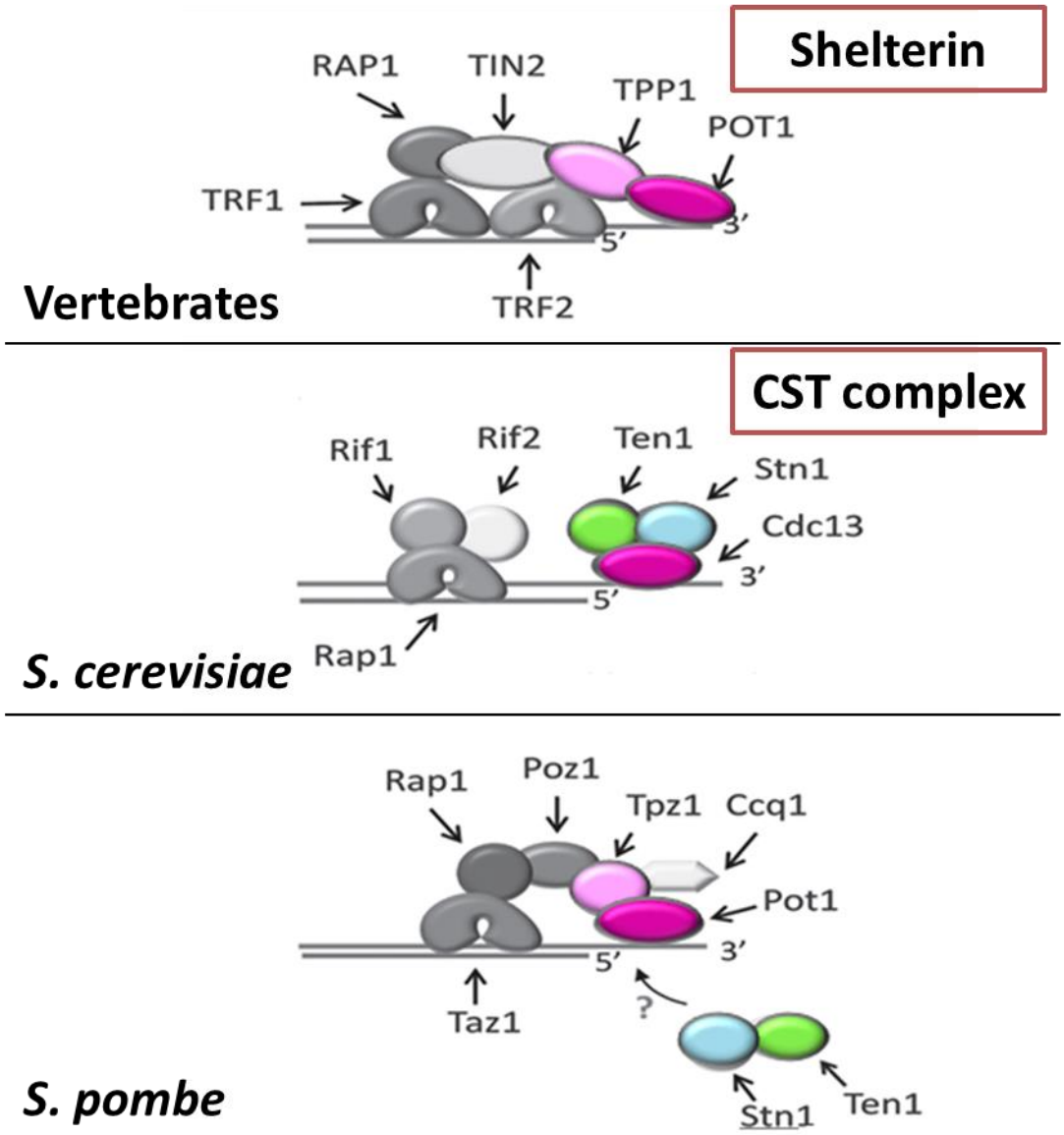

Figure 1.4. Telomere capping complexes in vertebrates and yeast.

The shelterin complex consists of six proteins that bind to single- and double-strand regions of the vertebrate telomeric DNA. In budding yeast the trimeric (CST) complex protect telomere by binding to single- strand G-rich overhangs of telomeres. The dsDNA region of telomere is protected with another complex of proteins containing Rap1, Rif1 and Rif2. In fission yeast, the protecting complex of six proteins resembles shelterin-like complex and contributes to chromosome end protection by interacting with other checkpoint components and DNA damage response proteins. These three complexes show functional and structural homologies that underline conserved regulatory pathways (taken from Price *et al*., 2010).

In lower organisms (e.g., ciliate *Oxytricha nova*), a heterodimeric protein (TEBP-αβ) protects telomeric G-rich overhangs (Horvath *et al*., 1998). In humans, the alpha-homologue of this protein is POT1 (protection of telomeres 1) and the β-homologue of this protein is TPP1 (three prime phosphatase 1) (Wang and Lei, 2011). POT1 binds the telomeric G-rich overhang at single-stranded DNA (ssDNA) and interacts with TRF1 (double-strand binding protein) and

links the double-stranded telomere region to the single- stranded 3' overhang through the TPP1 protein to facilitate communication between (Baumann, 2006, Xin *et al*., 2007). TPP1 interacts with POT1 through the N-terminal and the resulting association increases its affinity for telomeric ssDNA. TRF2 also stabilises the G-strand overhang and prevents telomeric fusion (Figure 1.4). Moreover, it recruits the MRE11 complex (meiotic recombination nuclease subunit of the heterotrimeric MRN complex: Mre11/Rad50/NBS1) that is the key component of the HR and NHEJ pathways involved in DNA double strand break repair (Baumann, 2006). In human the MRN complex plays important roles in the detection and signalling of DSBs, as well as in the repair pathways of HR and NHEJ (Xin *et al*., 2007).

Table 1.1. Telomere binding proteins in mammalian cells.

Name	Name description	Role at telomeres
Telomerase (Tert-Terc)	Telomerase Reverse Transcriptase-Telomerase RNA Component	Elongates telomeres; additional roles in cell survival and proliferation
hPOT1	Human Protection of Telomeres	Binds single-stranded TTAGGG repeats; necessary for telomere length maintenance and telomere protection
TRF1	Telomere Repeat Factor-1, amino terminus with an acidic region	TRF1 present in T-loops; binds double-stranded TTAGGG repeats; a negative regulator of telomere length (telomerase-dependent); interacts with Pot1 and conveys information from double stranded telomeric region to single stranded 3' overhangs
TRF2	Telomere Repeat Factor-2, amino terminus with a basic region	Present in T-loops; binds double-stranded TTAGGG repeats; negative regulator of telomere length (telomerase-independent); recruits hRAP1 and MRE11 complex to telomere; loss of function causes end-to-end fusions and leads to apoptosis and replicative senescence
TANK1 and TANK2	Tankyrase	Telomere-associated poly (ADP-ribose) polymerase 1/2 (PARP); binds to telomere-binding protein TRF1; ribosylates TRF1; overexpression increases telomere length; positive regulator of telomere length
TIN2/TENF2	TERF1 (TRF1)-Interacting Nuclear Factor 2	TRF1-binding protein; negative regulator of telomere length
hRAP1	Human Repressor Activator Protein	TRF2-binding protein; regulates telomere length; (yRAP1 is yeast homologue of hRAP1 that binds to both telomeres and to extra-telomeric sequence sites

Name	Name description	Role at telomeres
		through the (TTAGGG)2 consensus motif; deficiency increase telomere recombination)
TPP1	Three Prime Phosphatase (TINT1/PIP1/PTOP1 in mammals)	Homolog of human polynucleotide kinase/3'-phosphatase; Interacts with POT1 to recruit telomerase
BRCA1	Human breast Cancer 1	Telomere maintenance
hRAD9	Human RADiation sensitive	DDR protein, involved in telomere maintenance
RAD50	Radiation sensitive	DNA repair complex that binds TRF2
RAD51D	Radiation sensitive	DNA repair protein; DNA double strand break repair protein
MRE11	Meiotic Recombination; nuclease subunit of the heterotrimeric MRN complex (Mre11/Rad50/ NBS1)	Negative regulator of telomere length; role in telomere capping; DNA double strand break repair protein; deficiency cause end to end chromosome fusion
NBS1 (Xrs2p is the yeast homologue of NBS1)	Nijmegen Breakage Syndrome 1 protein	Possible role in T-loop formation; DNA double strand break repair protein; mediates elongation by telomerase
Ku (heterodimer, Ku86/Ku70 complex; Regulatory component of DNA-PK)	'Ku' derives from the surname of the prototype Japanese patient (Protein complex composed of a 70 kDa and a 83/86 kDa subunits)	Associates to telomeric repeats and recognizes the ends of linear duplex DNA; recruits and activates the DNA-PK catalytic subunit; role in non-homologous end joining in mammals (Ku86); Prevents telomeric fusions independently of the length of TTAGGG repeats and the G-strand overhang; physically binds to and repairs DNA double-strand breaks (DSB); deficiency leads to telomere shortening in yeast (Ku86); gene inactivation results in cells with growth retardation, premature senescence and increase in chromosomal aberrations in mammals
DNA-PKcs	DNA-dependent Protein Kinase catalytic subunit	Role in telomere capping; putative role in post-replicative processing of telomeres; DNA double strand break repair protein; control non homologous end joining pathways for double DNA break repair

(Adapted from: (Blasco, 2003, Baumann, 2006, Slijepcevic, 2006, Martinez *et al*., 2010)

DNA-dependent protein kinase complex (DNA-PK) consists of three proteins Ku70, Ku86 and the DNA-PK catalytic subunit (DNA-PKcs). These proteins play dual roles, by protecting telomere capping and also by regulating telomere length. Removal of these proteins results in as end-to-end fusion of TTAGGG telomere regions, due to the loss of telomere capping (Dynan and Yoo, 1998). Deficiency in Ku86 or DNA-PKcs also influences telomere length. Ku86 acts as a negative regulator of telomerase e.g., its deficiency causes telomerase-mediated telomere elongation while DNA-PKcs regulates telomere length positively and its deficiency causes telomere shortening (Espejel *et al*., 2002).

In humans, telomere protection is facilitated by the formation of T-loop structure which impedes chromosome end fusions (NHEJ and HR). The ssDNA binding protein, POT1 blocks recruitment of RPA and inhibits ATR mediated signal transduction pathways and repairing (Figure 1.5). The ATM activation is prevented by dsDNA-binding protein TRF2 (Longhese, 2008). POT1 DNA binding domain is homologous to that in yeast Cdc13. It binds to the 3' single strand DNA overhang and blocks the accessibility of MRX (DNA damage response complex, composed of Mre11, Rad50 and Xrs2 proteins), RPA, Mec1 (mitosis entry checkpoint) and telomerase at telomeres. The deletion of *CDC13* is lethal for yeast cells due to its essential role in telomere capping. Cdc13 inactivation by mutation of *cdc13-1* results in telomeric single stranded DNA (ssDNA) formation, recombination and Mec1-dependent cell cycle arrest (Figure 1.5) (Jia *et al*., 2004).

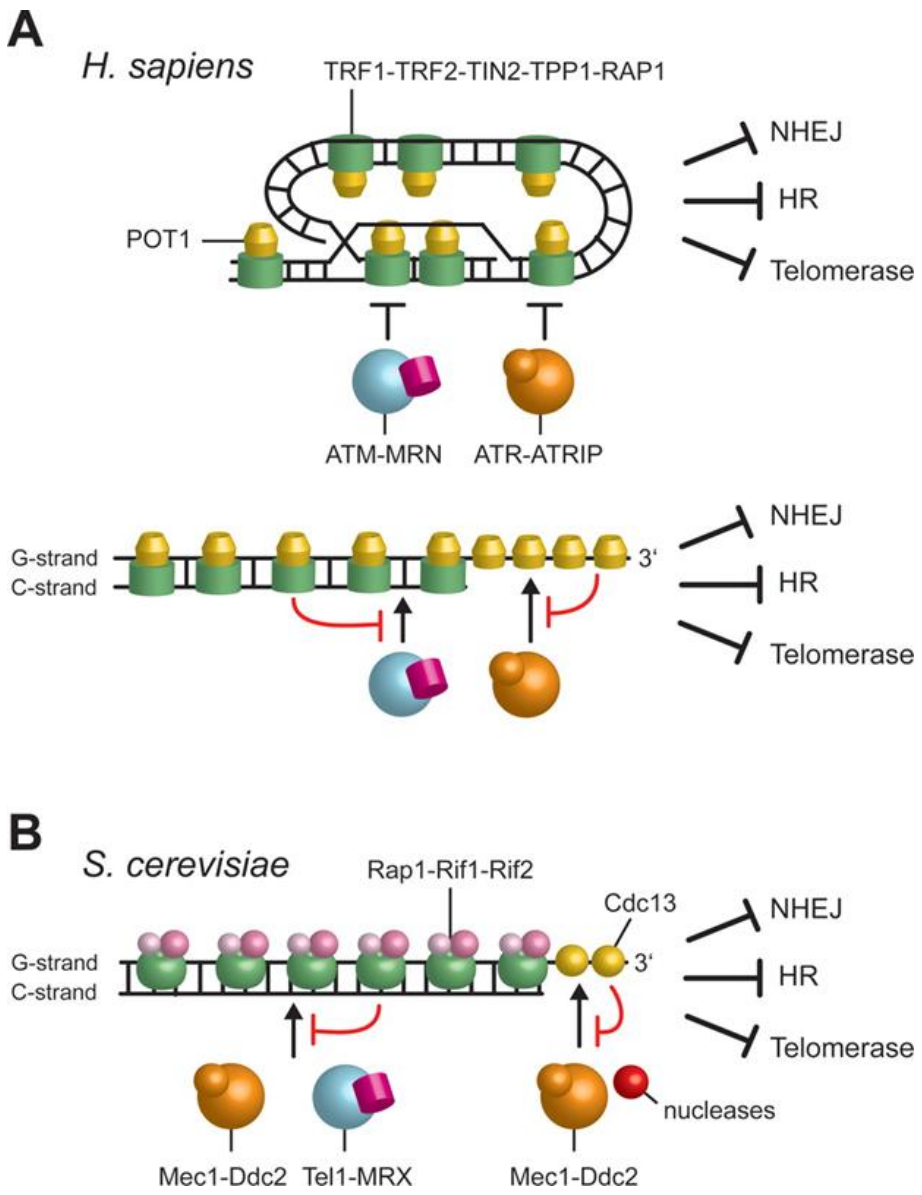

Figure 1.5. Chromosome end protection in humans and budding yeast.

(**A**) In humans T-loop conformation protects the telomere ends.
Formation of T-loop structure at telomere end may protect the chromosome ends from NHEJ and HR and also inhibits the recruitment of telomerase and checkpoint proteins, ATM-MRN and ATR complexes to telomere. In the absence of T-loop, the ssDNA-binding protein POT1 prevents the recruitment of RPA protein and telomerase and inhibits ATR activation.
(**B**) In *S. cerevisiae*, ssDNA-binding protein Cdc13 and dsDNA-binding protein Rap1 protect telomeres. Cdc13 prevents nucleases from binding at single-stranded telomere sequences whereas Rap1 inhibit the recruitment of MRX complex, RPA, Mec1, and telomerase at telomeres, which inhibit RPA recruitment and subsequent Mec1-dependent cell cycle checkpoint activation. (Taken from Longhese, 2008).

Beside their roles in telomere binding and telomere length regulation, capping proteins play essential roles in intracellular signalling (Sedivy, 2007). Critically short telomeres are processed as damaged DNA and senescence signalling is activated. Telomere uncapping and DSB can trigger checkpoint response (Figure 1.6). The ends of the uncapped or dysfunctional telomeres are presumably recognised as DSBs, which activate checkpoint response cascade. This may be the underlying cause of cell cycle arrest/senescence lead by telomere shortening. It is more likely that the capping proteins are unable to bind very short telomeres and to protect telomere.

In yeast, an uncapped telomere (dysfunctional telomere) recruits the phosphatidylinositol 3-kinase-related kinase (PIKK), Mec1 a central player of DNA damage checkpoint signalling (Harrison and Haber, 2006), Tel1 (telomerase maintenance; the ATM orthologue), the checkpoint protein Rad9, and the MRX complex (Lydall, 2003). This type of telomere is a weak inhibitor of cell division based on the fact that the *TEL1*-dependent response to un-resected DSBs is weak and that Tel1p overexpression causes transient arrest (Clerici *et al*., 2001). Tel1 is a key regulator of checkpoint response to BSBs. It promotes lengthening of short telomeres. Tel1 defective strain show chromosomal aberrations and short telomere indicating its role in genomic stability. It is a potent activator of telomerases and contributes to telomere capping (Arneric and Lingner, 2007, Di Domenico *et al*., 2014).

The eukaryotic telomeres are protected from checkpoint activation, end fusions and other events) that might lead to the repair of intra-chromosomal DNA breaks. The involvement of DDR proteins in the regulation of telomere suggest that functional telomere can also be recognised as DNA breaks (Longhese, 2008).

In mammals, during the late S phase after the completion of DNA replication the telomere become susceptible to Clb–Cdk1-dependent (cyclin B-cyclin dependent kinase) nucleolytic processing which can result RPA coated ssDNA. Telomeres exhibit short TG repeats and other features similar to DSBs. The MRX complex binds to telomere and activates transient Mec1- and Tel1-dependent checkpoint activation that elongates telomere and also increases the proteins bound at TG tract. This modification blocks telomerase and Mec1/Tel1 recruitment on telomere. In the successive G1 phase the functional telomere cap could be reassembled when the Cdk1-dependent nucleolytic activity is low.

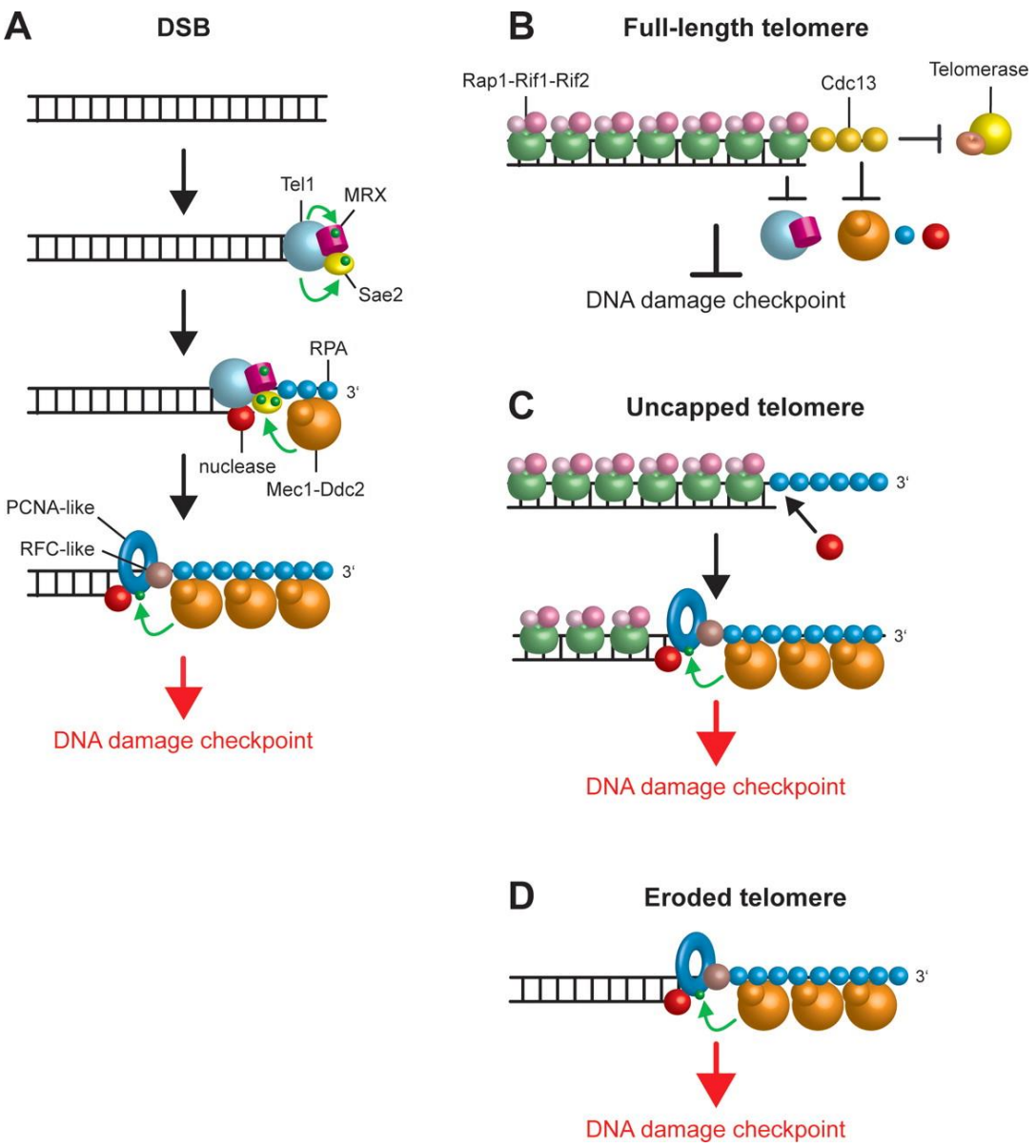

Figure 1.6. A model for different states of budding yeast telomeres: DSB, capped, uncapped and eroded.

(**A**) DSB-like telomere triggers a DNA damage checkpoint response and recruits the core components of DDR machinery including Mec1-Ddc2 (DNA damage checkpoint), Tel1-MRX complex, Rad17-Mec3-Ddc1 proteins to the unprocessed break. Tel1 phosphorylates Sae2 (ssDNA endodeoxyribonuclease) and recruits it independently of MRX to telomeres. Exonucleases resect DSB and generates 3'-ended ssDNA which is the occupied with RPA protein. RPA allow the loading of Mec1-Ddc2 complex and proceed to Mec1-dependent checkpoint activation. Mec1 activation is also supported by independent loading of the PCNA-like Ddc1-Rad17-Mec3 complex by Rad24-RFC.
(**B**) A fully capped telomeres are protected from checkpoint activation. The presence of ssDNA- and dsDNA-binding proteins on full-length chromosomal ends inhibits recruitment of MRX, RPA, nucleases, telomerase, and checkpoint proteins. The protective functions of telomere are lost with the loss of telomeric ssDNA- and dsDNA-binding proteins (uncapped telomere) or telomerase (eroded telomere).
(**C**) An un-capped telomere (dysfunctional telomere): in the absence of the ssDNA-binding protein Cdc13, telomerase recruitment is impaired, and nucleases can resect the chromosome end. This could lead to degradation of C-rich strand and accumulation of RPA-bound ssDNA, which activates a Mec1-dependent DNA damage checkpoint response.
(**D**) Eroded telomere: RPA-bound ssDNA accumulates at telomeres also after telomere erosion, due to telomerase loss. Green arrows indicate phosphorylation events. (Taken from Longhese, 2008).

It has been shown that nucleases are involved in the DNA replication, repair and generation of ssDNA tail at telomere (Longhese, 2008). In yeast, effective checkpoint controls require the generation of ssDNA, a prerequisite for signalling cell cycle arrest (Maringele and Lydall, 2002).

In budding yeast, a number of DDR proteins are involved in the formation of ssDNA and its degradation. Rad24, Rad17 and Mec3, members of clamp loader and sliding clamp, promote the generation of ssDNA while Rad9, Rad53 and Mec1 play opposite roles by inhibiting degradation (Lydall and Weinert, 1995, Jia *et al*., 2004). The checkpoint sliding clamp, (Rad17-Mec3-Ddc2) loaded by Rad24 protein regulates nucleases (Figure 1.7). The activation of Rad53 through Mec1 and Rad9 inhibits nuclease degradation. It further suggests that Rad9 inhibits ssDNA generation by both Mec1/Rad53-dependent and -independent mechanisms. However Exo1 (exonuclease 1) appears to be targeted by the Mec1/Rad53-dependent pathway. Normally Exo1 nuclease does not play important role in telomere maintenance. However on uncapped telomere Exo1 (the 5'-to-3' exonuclease), plays a critical role in generating single-stranded DNA and activating checkpoint pathways (Lydall, 2003). RPA1 (replication protein A) is a ssDNA binding protein and involved in cell cycle signalling. Its phosphorylation is also mediated by Mec1 (Brush and Kelly, 2000). The generation of ssDNA is important for the recruitment of RPA1 on telomere.

Several negative regulators of the nucleases activity at telomere have been identified. These include DNA repair protein Yku70/Yku80, single stranded telomere binding protein, Cdc13, its partner Stn1, Ten1, DNA polymerase α, FLAP endonuclease and telomerase (Lydall, 2003). Many of these proteins contribute to limit ssDNA at telomeres and also have telomere capping roles. The involvement of checkpoint genes in the regulation of nucleases supports the possible role of nucleases at uncapped telomere. For example *RAD9* a checkpoint gene inhibits ssDNA production in strains lacking the telomere-binding protein Cdc13 (Lydall and Weinert, 1995). Rad9 also inhibits ssDNA production at uncapped telomeres by mediating interactions between upstream and downstream checkpoint kinases (Proctor *et al*., 2007). Few positive regulators of the nucleases at telomere have also been reported e.g., *MRX*, *EXO1* and *RAD24* genes encode or regulate nucleases at telomere.

The Exo1 is a 5′-to-3′ exonuclease that appears to function with the MRX complex in resection of DSBs and DNA repair (Raynard *et al*., 2008, Bonetti *et al*., 2010). It is one of the main ssDNA generating nuclease. Exo1 is also involved in meiotic recombination (Tsubouchi and Ogawa, 2000) and mismatch repair (Li, 2008). However, *exo1*Δ mutants show no telomere length defects. Previous studies have shown that Exo1 is essential for ssDNA generation and cell cycle arrest (Zubko *et al*., 2004) under conditions of defective capping. It is involved in

generation of type1 and type11 survivors through recombination mechanism (Maringele and Lydall, 2004). The significance of *exo1* null mutation has also been shown in the generation of immortal yeast cell in telomerase and recombination deficient strain (Grandin and Charbonneau, 2009, Ngo and Lydall, 2010). Exo1 protein is essential in the generation of ssDNA in the sub-telomeric region of X element repeat sequence of *cdc13-1* mutants (Zubko *et al*., 2004). The previous study with mutants, *cdc13-1 rad9* and *cdc13-1 rad9 rad24* suggest that other nucleases beside Exo1 may also act on uncapped telomere though Exo1 generate ssDNA in mutant *cdc13-1*.

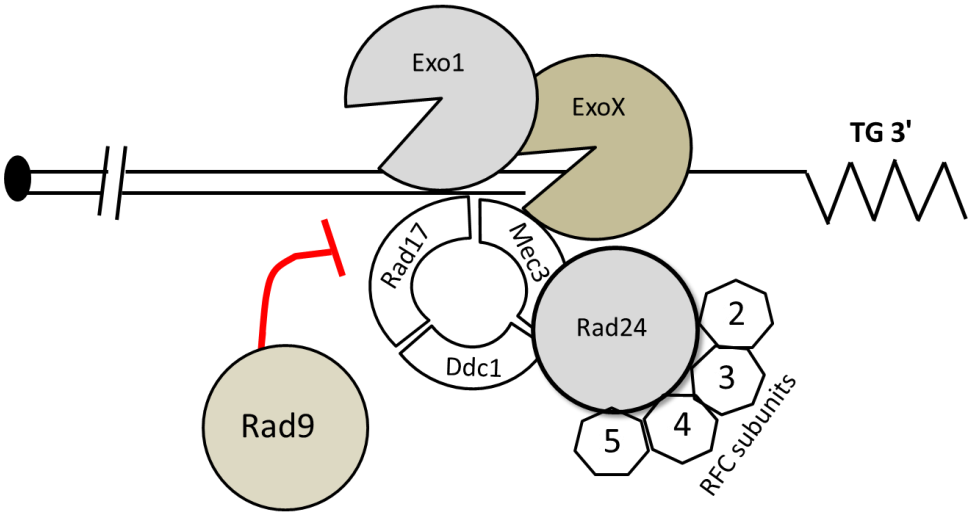

Figure 1.7. A model of checkpoint regulation of Exo1 activity at *cdc13-1* telomeres.
According to this model Rad24 and the small RFC subunits (2, 3, 4, 5) load the checkpoint sliding clamp (Ddc1, Mec3, and Rad17) onto telomeres of *cdc13-1* mutants at 36°C. This sliding clamp tethers Exo1 to DNA. Other unidentified nucleases (ExoX) may also have their roles, while Rad9 inhibits nuclease activity (taken from Zubko *et al*., 2004).

E. M. Holstein's model elaborates (Holstein *et al*., 2014) that diverse groups of proteins including CST complex, nonsense mediated decay (NMD), and DDR proteins, bind to telomere ends in mammals and yeast, and play important roles in telomere capping and replication (Figure 1.8). In the presence of inactive DDR and NMD the Cdc13 essential roles might be bypassed, however, the need for the other two interacting component of the CST complex, the Stn1 and Ten1 cannot be bypassed. This model also emphasises that Stn1 and Ten1 can function in the absence of Cdc13 and bind to telomeres in Cdc13 independent manner, indicating that these two components play more critical roles in CST complex across eukaryotes in telomere maintenance and replication (Holstein *et al*., 2014).

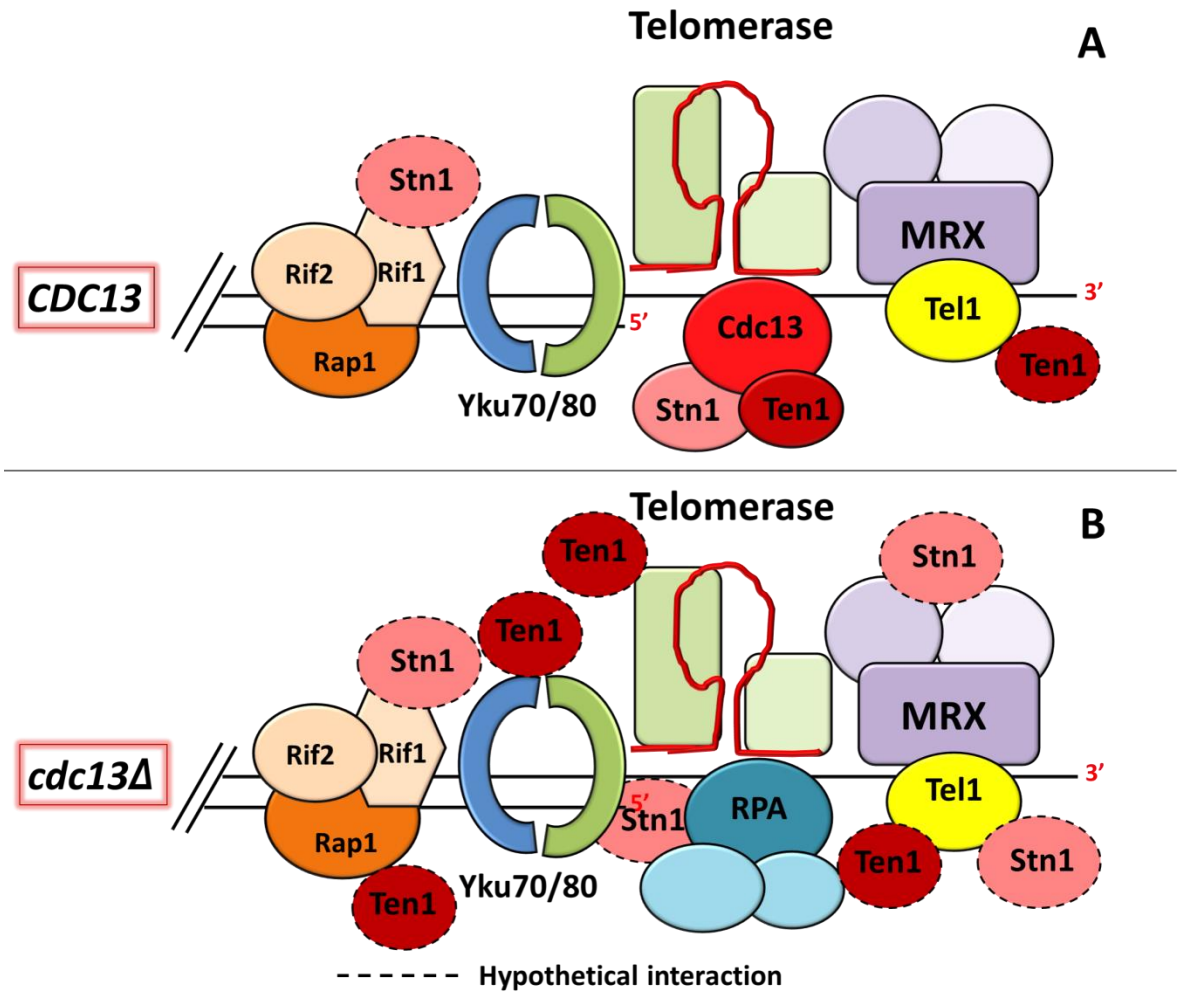

Figure 1.8. Interaction of telomere capping proteins in the presence and absence of *CDC13*. **(A)** In the presence of wild type *CDC13*. **(B)** Without *CDC13* (in *cdc13* deletion mutants). (Taken from Holstein *et al.*, 2014).

The mechanism of telomere chromosome end protection by capping proteins is evolutionarily conserved. DDR mechanisms are activated under the effect of genotoxic stresses. Telomeres interact with the DNA damage repair system as a result of signalling from checkpoint proteins. These checkpoint proteins physiologically maintain uncapped telomeres, a phenomenon that makes telomeres different from 'DNA breaks' (Lydall, 2003).

Telomere defects activate different DNA damage checkpoint proteins to induce cell cycle arrest (senescence) or death (apoptosis) depending upon the damage caused. Many DNA damage response proteins have been implicated in telomere maintenance. They include Brca1 (breast cancer 1) (McPherson *et al.*, 2006), hRad9 (radiation sensitive) (Pandita *et al.*, 2006), PARP1 [TRF2-associated Poly (ADP-Ribose) Polymerase, detect ssDNA breaks and interact with DNA-PKcs, ATM and p53; (Gomez *et al.*, 2006). Cells defective in DNA double strand break repair proteins such as Ku, DNA-PKcs, RAD51D and MRN or having mutated signalling

protein ATM (Metcalfe *et al*., 1996) show loss of telomere functions and involve many DNA damage repair pathways e.g., NHEJ, HR, BER (base excision repair) and nucleotide excision repair (NER) in telomere maintenance. To explain this high level of co-operation between telomere maintenance and DDR, P. Slijepcevic (Slijepcevic, 2006) has proposed an "integrative model" suggesting that telomere maintenance mechanisms are an integral part of the DNA damage response network (Figure 1.9). Telomere maintenance is mediated by the interaction of cell cycle checkpoints with DNA damage response, signalling and repairing complexes of DNA damage response (Slijepcevic, 2006).

According to this model, 'chromosomal repair' is different from DNA repair as it has to preserve its function, not DNA sequence. Such chromosome end should be able to acquire telomeric features at chromosome breakage site or inactivate native telomere and centromere with the initiation of chromosomal rearrangement. Some of these events take place in response to DNA damaging agents causing chromosome rearrangements. An integrative model further suggests that DSB repair and chromosomal healing could be global features with telomere maintenance local function of the single chromosomal repair functional tool (Slijepcevic, 2006). Capping proteins maintain telomeres by interacting closely with DNA damage response networks and telomerase. An example supporting this hypothesis was the observation that TRF2 (double strand binding protein at telomere) is not confined locally but migrated to the site of DNA breakage after exposure of cells to ionizing radiation. Disruption of other DDR proteins exhibited telomere elongation or shortening, end-to-end chromosome fusions, accelerated telomere loss, elevated anaphase bridges, and alternative lengthening of telomere in telomerase independent fashion reflecting their direct link with telomere dysfunctions or interdependence between telomere maintenance and DNA damage response (Slijepcevic, 2006).

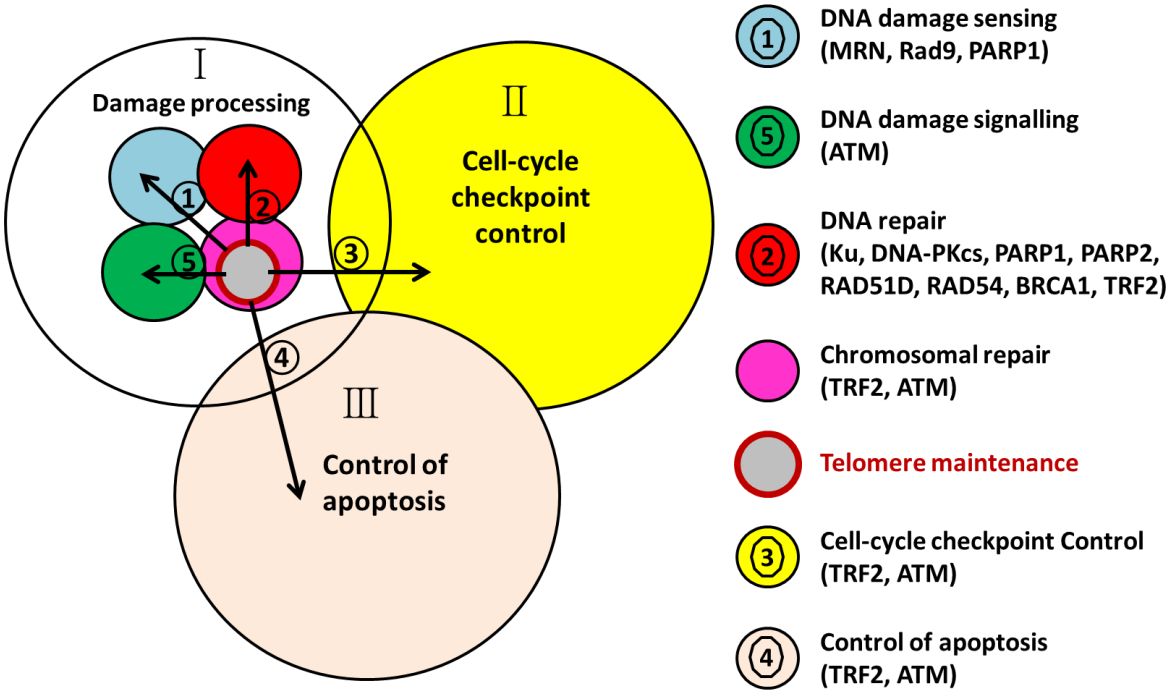

Figure 1.9. An integrative model of telomere DNA damage response mechanisms.

The "integrative" model emphasises the integration of telomere maintenance mechanisms into a complex networks of mechanisms collectively known as the DNA damage response. The major components of DNA damage response include: (**I**) Damage processing, (II) Cell cycle checkpoint control and, (**III**) Control of apoptosis. Arrows indicate the link between telomere maintenance and other components of DNA damage response. Only representative proteins are shown for each link. For example, in the loss of human TRF2 (telomere repeat factor-2, a double strand binding telomere protein) results in apoptosis (link no.4) or cell senescence leading to cell cycle arrest. (Picture is taken from Slijepcevic, 2006).

1.2.1.2. Cell cycle checkpoint and genomic instability

Genomic instability is an increased tendency of alterations in the genome during the life cycle of the cell. Accurate transmission of genetic information from parents to daughter cells is critical for the survival of cells. Cell cycle checkpoint controls ensure accurate duplication of genome and precise division of duplicated genome in daughter cells. The telomere defects such as DNA damages due to external genotoxic agents (Callegari and Kelly, 2007), telomere length shortening (critically short telomere) or other internal replication problems (Sedivy, 2007) are sensed by cell cycle signalling pathways which trigger the cell cycle checkpoints by activating Mec3p, Mec1p, and Ddc2p and lead to cell cycle arrest followed by activation and/or recruitment of telomerase to the short telomeres (Weinert, 1998). The different models of telomere checkpoint propose that the DNA damage pathway signals to Mec3p, Mec1p, and Ddc2p and activate another parallel pathway that involve Tel1p (telomere maintenance) protein (Figure 1.10). Both of these pathways also interact with the Rad9p and Rad53p. Triggering of the DNA damage checkpoint leads to cell cycle arrest and also activate the DNA repair systems, however it does not activate telomerase (Enomoto *et al*., 2002). The cell cycle is delayed by the

signal transduction pathway (G1 checkpoints) and the cell cycle progression is blocked to prevent the defective DNA to enter in replication and undergo segregation and also induce the transcription of several DNA repair genes (Foiani *et al*., 2000).

DNA damage induces the expression of many genes that enhance DNA repair capacities through damage induction subset of pathways. A number of DNA-damage un-inducible (*dun*) mutants have been reported that are sensitive to DNA damages and induce other genes through damage induction pathways (Zhou and Elledge, 1993).

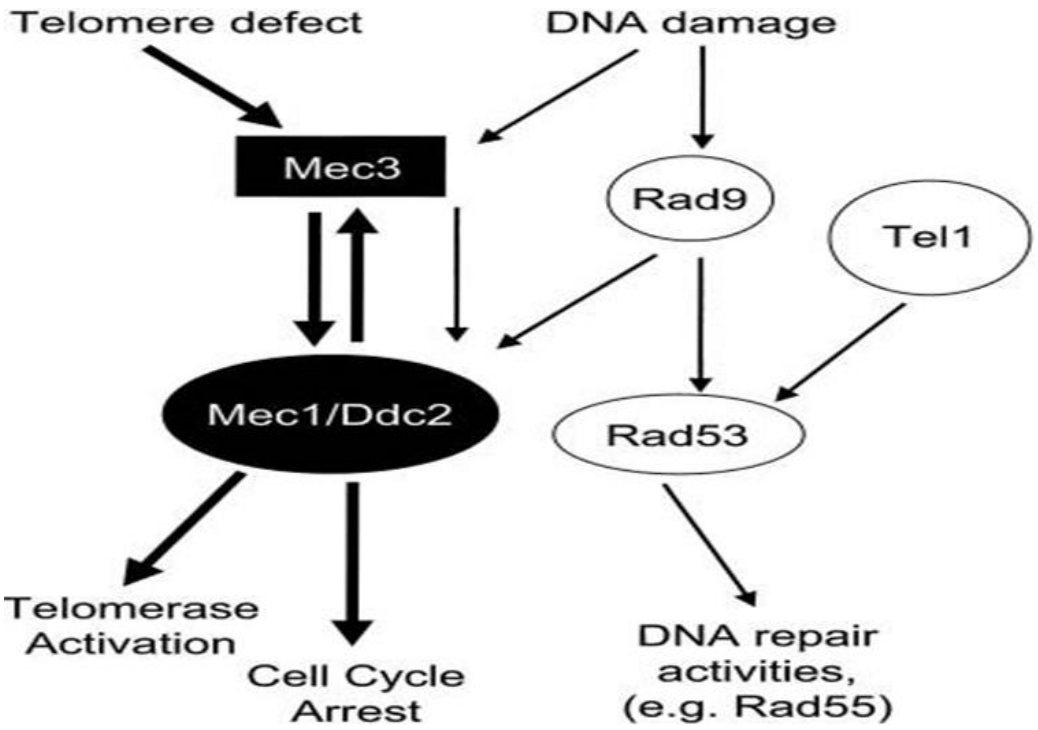

Figure 1.10. The telomere checkpoint model.
(Picture taken from Enomoto *et al.*, 2002)

1.2.1.3. Telomerase and telomere maintenance

Telomerase is a specialised ribonucleoprotein enzyme (RNA-templated polymerase) that is responsible for maintaining the telomere of eukaryotic chromosome ends (Cech, 2004, Sedivy, 2007). It regulates telomere length by adding repeats of TTAGGG onto pre-existing telomeres in mammalian telomeres (Collins and Mitchell, 2002, Cech, 2004). Telomerase complex is composed of two essential components, the catalytic protein subunit or reverse transcriptase subunit known as TERT (telomerase reverse transcriptase: hTERT in human and Est2 in budding yeast) and a small RNA molecule of TERC (telomerase RNA component: hTERC in

human and Tlc1 in yeast) unit which contains the small template for the synthesis of new telomeric repeats and accessory factors (the Est1 protein and dyskerin in humans and Est1, Est3, and Sm proteins in budding yeast (Smogorzewska and de Lange, 2004, Collins, 2000, Autexier and Lue, 2006) for G-rich strand. Telomerase activity is detected only in germ cells, some proliferating stem cells, progenitor cells, cancer cells and transiently in some proliferative cells of renewable tissues (Sedivy, 2007). In human, most normal somatic cells do not have sufficient telomerase. In the absence of telomerase, telomeres are shortened by 50-200 base pairs with each round of replication/cell division because DNA polymerase are unable to fully replicate 3' termini (end-replication problem) (Sedivy, 2007, Lingner *et al*., 1995, Mu and Wei, 2002). DNA replication in the 3'-to-5' direction requires short terminal RNA primers. These RNA primers are lost with each cycle of replication resulting in continuous shortening of the telomere. Telomeres loss in the absence of telomerase activity accumulates and eventually results in various chromosomal aberrations like TTAGGG-exhausted chromosomes, end-to-end chromosome fusion and loss of cell viability (Lee *et al*., 1998, Herrera *et al*., 1999). Telomere shortening destabilises the telomeric loop and increases the possibility of telomere uncapping (Griffith *et al*., 1999). When telomeres become critically short, most cells undergo senescence (Shay and Wright, 2005, Samper *et al*., 2001). Samper *et al*., (2001) has reported in a mouse model that reintroduction of telomerase in cultured cells *in vivo* can overcome the rapid loss of cell viability as a result of senescence triggered by short telomeres, indicating its therapeutic role in cellular senescence.

In yeast, the emergence of post-senescence survivors (cells that escape senescence) with long telomeric DNA repeats have been identified (Kachouri-Lafond *et al*., 2009). Yeast cells can produce recombination-mediated telomere elongation in the absence of telomerase TLC1 moiety (Chen *et al*., 2001). In fission yeast, deletion of single strand telomere binding protein, Pot1 cause rapid loss of telomere DNA and chromosome fusions in most cells (Baumann and Cech, 2001). However survivors with circular chromosomes are generated as a result of intra-chromosomal fusions. These survivors show the ability to replicate and go through mitosis and bypass the need for chromosome end maintenance. Analysis of DNA repair factors have shown that homologs of Rad52 are involved in the generation of telomere dysfunction-induced chromosomal fusions in fission yeast involving NHEJ pathways (Wang and Baumann, 2008).

1.2.1.4. DDR proteins and telomere maintenance

Telomere-induced senescence has been shown to share many components of the DDR triggered by DNA double strand breaks (von Zglinicki *et al*., 2005). There is compelling evidence that a number of DDR proteins including Ku, DNA-PKcs, RAD51D and the MRN (MRE11/RAD51/NBS1) complex and many other are involved in telomere maintenance. Deletion/mutation of these repair proteins causes loss of telomere capping function with

dysfunctional telomeres. Slijepcevic (2006) has reported 18 DDR mammalian proteins that are implicated in telomere maintenance. The DDR is a combination of interacting mechanisms including activities like damage detection, signalling, repairing DNA damage and also activities associated with cell cycle checkpoint control and apoptosis regulation. Alteration of any component of the DDR proteins results in dysfunctional telomeres and genomic instability and is correlated with the number of proteins mutated (due to the combined effect of all mutations). As a result of failure in the telomere's protective function, the ends of chromosomes may fuse to other susceptible chromosomes' ends or double-strand DNA breaks and leads to different chromosomal aberrations besides end-to-end fusion (Goytisolo and Blasco, 2002, Latre *et al*., 2003). The non-homologous end-joining DNA repair machinery detects and signals the presence of dysfunctional telomeres as damaged DNA and repairs them, leading to end-to-end chromosomal fusion and other chromosomal rearrangements.

Telomeric defects could be reflected as telomeric loss (short length), telomeric fusion and accumulation of extra chromosomal telomeric fragments due to disruption of DDR proteins.

1.2.1.5. Telomere length and ageing

In higher eukaryotes telomeres shorten with each cycle of DNA replication due to end replication problem and nucleolytic processing resulting chromosome ends fusion and degradation. Telomerase ribonucleoprotein (RNP) reverse transcriptase counteracts telomere erosion by serving G-overhang as the substrate to replenish telomeric DNA (Shay and Wright, 2001). However the telomerase activity in human cells (stem cells, T cells and monocytes) is either limited at very low level or not observed in most somatic cells after birth to prevent telomere shortening (Wright *et al*., 1996).

In *S. cerevisiae* telomeres are ~350 base pair long with short 3' G-rich strands (Gasparyan *et al*., 2009). It has been established in many studies that telomere length is linked to ageing and cellular senescence (Qin and Lu, 2006). In higher eukaryotes, the length of telomeres plays a decisive role in the onset of ageing and cellular senescence. For example, in human germ line cells (sperm cells), DNA shows long telomeres in comparison to short telomeres in somatic cells which, as a result of sufficient shortening, leads to cellular senescence. Disruption of one of the DDR proteins (*Brca1*) results in significantly shorter telomere (Slijepcevic, 2006) and its deficiency causes end-to-end chromosome fusions. *In vitro* studies of human fibroblasts have shown that shorter telomeres exhibit few doublings of cells (proliferation senescence) as compared to cells with longer telomeres (Bryan *et al*., 1995). It has been revealed through the replicative lifespan (RLS) in cultured human fibroblast cells that telomere length is gradually decreased in ageing culture after a specific number of cell divisions (Cooke and Smith, 1986). Normal fibroblast human cells at the end of RLS show decrease in telomere length and after a specific number of divisions these cells enter in a replicative senescence state (Bodnar *et al*.,

1998). T M Bryan and colleagues have suggested in a study on telomerase that stable and lengthened telomeres are necessary for the immortalisation of cells (Bryan *et al*., 1995). Fibroblasts cells from Hutchinson-Gilford progeria patients show short telomeres consistent with the fact that short telomeres depict reduce replicative potential (few divisions). The cells that express telomerase survive longer than their normal lifespan without shortening of their telomere (Samper *et al*., 2001).

The interaction between the DNA repair protein Ku and the RNA component of telomerase in *S. cerevisiae* has also been shown to be crucial for maintaining telomere length (Sedivy, 2007). Similarly, the hRad9 mutation or its knockdown results in an elevated level of chromatin bridges in anaphase and end-to-end chromosome fusion in metaphase cells. This form of telomere dysfunction results due to its interaction with TRF2 (a capping protein with an additional role of DNA damage-sensing and in cell cycle checkpoint control). On the basis of telomere shortening and its correlation with ageing and cellular senescence, the telomere are regarded "the molecular clock" (Vaziri *et al*., 1994) or "biomarker of ageing" (Mather *et al*., 2011).

1.2.2. Dysfunctional telomeres and genomic instability

In humans, POT1 is one of the essential proteins that binds to single-stranded overhangs and is responsible for telomere capping and maintenance (Wu *et al*., 2006) through chromosome end-protection and telomere length regulation. Pot1-related proteins have also been reported in murine/rodents, mouse (Hockemeyer *et al*., 2006), *Arabidopsis* (Shakirov *et al*., 2005, Surovtseva *et al*., 2007) and ciliate *Euplotes crassus* (Wang *et al*., 1992) and encoded by either single-copy (*POT1* in human and fission yeast) or multiple genes (*POT1* and *POT*2 in *Arabidopsis* and *POT1a* and *POT1b* in rodents/mouse). In budding yeast, *S. cerevisiae*, an ortholog of *POT1* gene is *CDC13* (Baumann and Cech, 2001). Cdc13 is multi-functional protein that plays an important role in telomere end protection, length regulation, telomerase regulation and chromosome maintenance (Lustig, 2001). Cdc13 has been considered an essential telomere capping protein in budding yeast as the yeast cells that lack Cdc13 rapidly accumulate excessive single-stranded DNA at the telomere, arrest of cell division and then die (Garvik *et al*., 1995, Zubko and Lydall, 2006).

In *S. cerevisiae*, Cdc13 binds the G-rich strand of telomeres in close association with two other essential proteins, Stn1 (suppressor of Cdc13) and Ten1 (telomeric pathways with Stn1), and protects the chromosome from degradation and end fusion, and prevents the formation of ssDNA during the S and G2-M phases of the cell cycle (Garvik *et al*., 1995, Grandin *et al*., 1997, Grandin *et al*., 2001, Wellinger, 2009). This heterotrimeric complex physically caps the

telomere end and blocks nuclease activity. Stn1 also promotes telomere C-rich strand extension. The Stn1 protein interacts with Cdc13 and limits ssDNA at the telomere and maintains telomere stability by preventing its degradation. Overexpression of Stn1 N-terminal in the presence of Ten1 protein can protect the telomere even in the absence of *CDC13* (Petreaca *et al*., 2006, Petreaca *et al*., 2007). However, Stn1 requires Pol12 (polymerase alpha-primase regulatory subunit), critical for Cdc13-independent capping (Petreaca *et al*., 2006). Stn1 also interacts with yeast Yku70 to regulate telomerase recruitment. This in turn controls Cdc13 interaction with Est1 (an essential subunit of telomerase) and plays an important role in telomerase regulation (Dubrana *et al*., 2001, Grandin *et al*., 2000). Exo1 is another important protein that is associated with telomere regulation. It is involved in the DNA repair mechanism by coding for 5'-3' exonuclease. In yeast, unprotected telomeres due to non-functional Cdc13p or Stn1p undergo a DNA degradation that is tightly regulated by the cell cycle in the G2/M, but not in the G1 phase of the cell cycle. G1-arrested cells remain viable even with uncapped telomeres while G2-M-arrested cells fail to recover (Wellinger, 2009).

Cdc13 interacts with various other capping proteins through its N-terminal region that is a crucial part for its protective activity (Hsu *et al*., 2004). Mutations in *CDC13* lead to abnormal, uncapped telomeres with long, exposed G-strands, resulting in dysfunctional telomeres that activate the DNA damaged response pathway, cause cell cycle arrest at the G2-M phase (Lin and Zakian, 1996), progress to an ever short telomere (EST) phenotype and eventually lead to cell death. In mouse, conditional deletion of Pot1 activates DNA damage response pathways resulting in replicative senescence with elongated telomere and homologous recombination (Wu *et al*., 2006).

Cdc13 interact with Stn1 and Ten1 proteins of CST complex to form heterotrimeric telomere-capping complex (CST), an activity that is central for telomere end capping and telomerase recruitment for end replication (Figure 1.11). Similarly N- and C-terminus of Stn1 interact independently with Ten1 and Cdc13-Pol12. N-terminus of Stn1 can bind Cdc13 but not to Ten1 and negatively regulate telomerase elongation (Puglisi *et al*., 2008, Sun *et al*., 2011). Structural, biochemical and computational analysis of Stn1 and Ten1 proteins revealed resemblance of these CST proteins to telomere specific replication protein A, RPA32 and RPA14 (Figure 1.12). Multiple sequence alignment of Cdc13 homologs revealed pattern of four conserved regions consisting of 150-200 residues. Cdc13 also exhibited RPA70- (largest subunit of RPA complex) like domain organisation though there was no primary sequence similarity between Cdc13 and RPA70 protein. The crystal structure of Cdc13 N terminal-OB1 folds showed only 8% identity with RPA70 N domain. OB2 fold is involved in homo-dimerization of Cdc13 proteins, a conserved feature of all

Cdc13 proteins and also interact with pol1 (polymerase alpha) for DNA replication. The dimerization of Cdc13 is also involved in telomere length regulation.

An essential function of Stn1 is to cap the telomere end (Zubko and Lydall, 2006). Stn1 interacts with *CDC13* through its C-terminus. Gene over expression studies have shown that the Stn1 C-terminus interferes with the S phase checkpoint response to DNA replication stress. Over-expressed Stn1 distributes on chromosomal DNA outside of the telomere, restores the S phase checkpoint in association with DNA polymerase and maintains genomic stability (Gasparyan *et al*., 2009). Moreover, Stn1 C/N-terminus suppresses *cdc13-1* temperature sensitivity to some extent but cannot bypass the *CDC13* essential function (Petreaca *et al*., 2006). Functional loss of Stn1 leads to excessive ssDNA at the telomere that is a marker of senescence (Petreaca *et al*., 2007, Grandin *et al*., 1997).

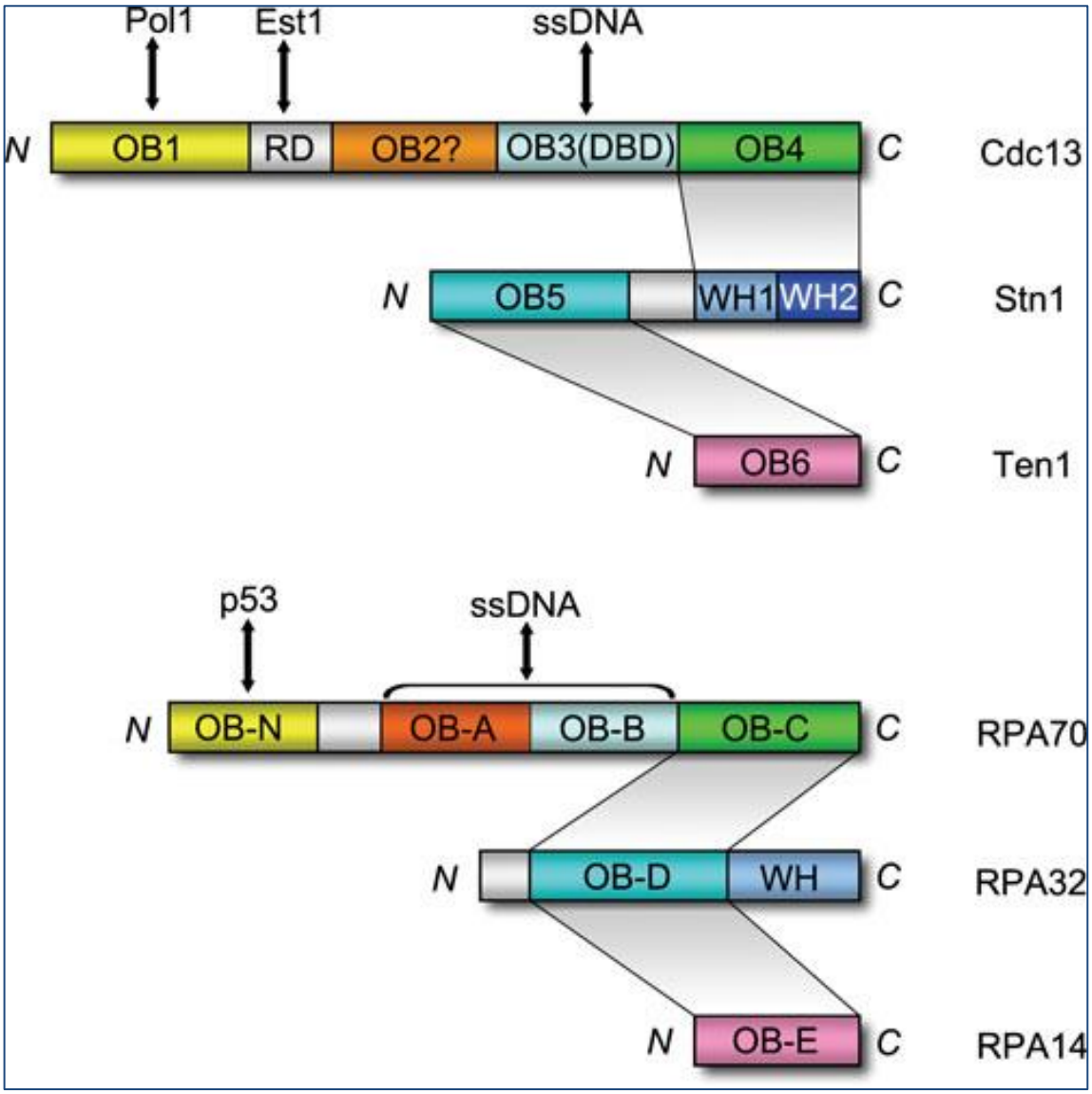

Figure 1.11. The CST and RPA complexes: organisation of conserved domains.

The sequence analysis of Cdc13 shows homology to RPA70 component of RPA-complex. There are four oligosaccharide/oligonucleotide binding (OB) folds in Cdc13 and RPA70 that revealed pattern of conserved regions from N to C-terminus and consisted of 150-200 residues. Cdc13 binds to Pol1 (alpha) through its N-terminal OB-1 fold while it interacts with Stn1 through its C-terminal OB4-fold. (Picture taken from Sun *et al*., 2011).

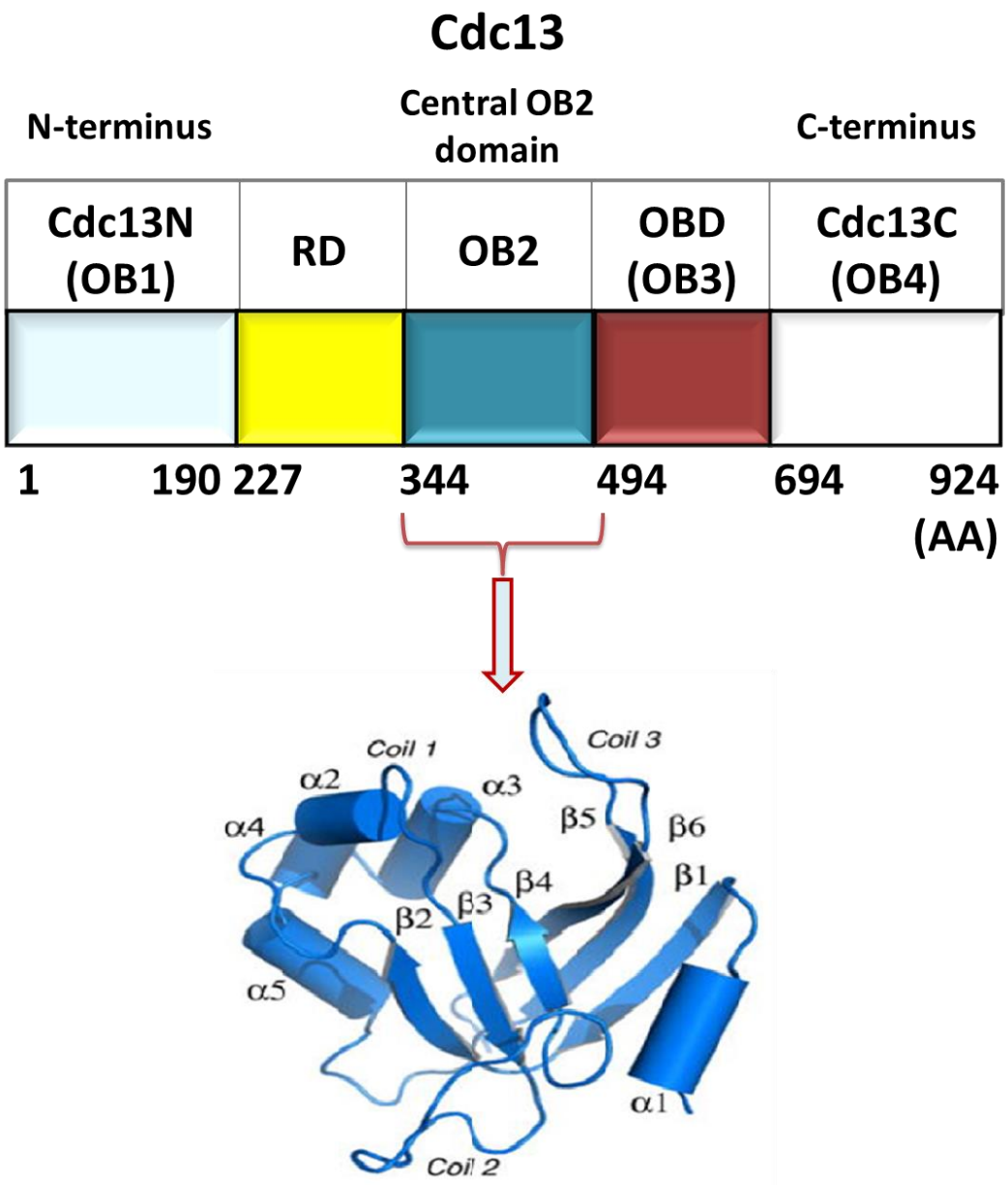

Figure 1.12. A diagram of the Cdc13 protein and its OB2 monomer.

Cdc13 protein exists as a dimer in crystal and in solution form. At least five conserved oligosaccharide binding domains (OBD) exist in Cdc13 protein (**A**). The conserved motifs include Cdc13N-terminus oligosaccharide binding 1 (OB1), recruitment domain (RD), central OB2, DNA binding domain (DBD/OB3), and C-terminus domain (CTD/OB4). The domains between the recruitment domain (RD) and DNA binding domain (DBD) is OB2 that involved in Cdc13 dimerization. In Cdc13-1 the oligomerisation of OB2 is disrupted that affect the Stn1 and Cdc13 binding and telomere maintenance (adapted from Mason *et al*., 2013).

The conditional telomere capping dysfunction leads to sister chromatid rearrangements and genetic instability. The telomere lead genomic instability has been suggested to be regulated due to cellular DNA repair activation (Wellinger, 2009). It has been reported in recent studies in *S. cerevisiae* strains that *cdc13* deletion mutants can survive without Sgs1 (helicase), Exo1 and Rad9, important damage response proteins and maintain linear chromosomes (Ngo and Lydall, 2010). Though continuous sub-culturing of such strains results in progressively shorter telomeres but cells can maintain them by recombination and thus can survive indefinitely.

1.3. Model organisms

Model organisms have been used historically in research to elucidate fundamental and basic principles in evolution, genetics and developmental biology. The animal models have helped to discover many of the conserved pathways underpinning the complex physiology and chemistry of higher mammals. Animal research in medical field has played a vital role in expanding our understanding of different disease (Festing and Wilkinson, 2007). About 60% of the genes involved in different human disease have their counterpart in the fruit fly and worm (Edwards, 1999) and these organisms have been studied universally to characterise the molecular pathways these genes are involved in. The ultimate goal of present day research is to translate scientific finding from model organism into human to improve their health conditions.

At present a range of model systems (Table 1.2) are being utilised to explore the molecular and genetic mechanisms of ageing in relation to mammals. In telomere studies, the significance of ciliates was a powerful tool because of large amount of telomere DNA, budding yeast offered the ease of genetic manipulation; the human cell lines have advantages of their direct applicability to humans (Dehe and Cooper, 2010). There are many aspects to consider when choosing a model organism e.g., it should be simple, economical and easy to manipulate in the laboratory. An important criterion for choosing a model organism is its suitability to address the research question. Due to its high level of conservation with mammalian telomere budding yeast has presents a valuable model for telomere and ageing research.

Table 1.2. Models organisms used in research with their relative advantages and disadvantages.

	Advantages	**Disadvantages**
Human	A higher eukaryote; directly relevant to human biology.	Ethical limitations for conducting many experiments on human; complex organism; long lifespan; complex and slow ageing process; long term development; virtually impossible to study human ageing *in vivo*.
Human cells	Simplified models for human biology; possibility for studying human ageing at cellular level; relatively short life cycle (dividing time of ~18-20 hours for most mammalian cells); availability of immortalised cells; convenient to model genetic, biomedical and biochemical events (e.g., cancerous processes), availability of embryonic stem cells to investigate growth and differentiation; suitable for uncovering mitosis: nuclear envelope breaks down during mitosis; microtubules nucleated by centrosomes.	Subject to tissue act laws; *In vitro* results do not always representative *in vivo* process; not suitable for studying systemic processes.
Bacteria *E. coli*	Simple prokaryotic systems; valuable model with well understood biology; a good tool for fundamental biological research; simple and easy to apply techniques; easy to handle and to manipulate; suitable for cellular and molecular studies of gene expression; a crucial model to study infectious diseases of gut; inexpensive; no ethical issues involved.	Different from human genetic constitution (circular naked DNA) and physiology (not representing human ageing).
Baker's yeast *S. cerevisiae*	The simplest unicellular eukaryotic model with entire genome sequenced; total ~6500 genes on 16 chromosome; short cell cycle (90 min); economical; not a subject of ethical issues; easy to grow and to maintain in laboratory; easily manipulable by genetic methods;	No features of multicellular systems; compartmentalized mitosis: nuclear envelope does not break down during mitosis; microtubules nucleated by spindle pole bodies.

	Advantages	Disadvantages
	asymmetrical division (daughter and mother cells); is ideal model for genetic research of ageing; stable haploid and diploid states; simple molecular tools for gene manipulation; many conserved genes involved in human disease; ideal for fundamental and applied research; observable phenotypes of the mutations in haploids; many genes have human homologs; powerful tool to study checkpoints, telomere maintenance and ageing (replicative cell senescence and chronological lifespan); availability of deletion mutants for functional analysis.	
Fruit fly *Drosophila melanogaster*	Invertebrate model; multicellular; small, easy to grow and to maintain; easy breeding in laboratory; short generation times with large numbers of offspring; short life cycle (~2 weeks); inexpensive to culture; availability of full genome sequenced (14000-16000 genes); independent embryo development; excellent model for genetics and pathology; easy to apply molecular tools to generate gene knockout or to create mutants; mitotic cell cycle; suitable for studying behaviour, learning and memory formation; suitable for high throughput mutation screening; availability of vast biological information.	Restricted to basic biological research; telomere composition is different from human: no evidence of shelterin proteins or t-loop at telomere; Telomere elongation through telomerase independent mechanisms such as chromosome end capping with non-LTR retrotransposons and chromosome end elongation by gene conversion or recombination.
Roundworm Nematode *Caenorhabditis elegans*	Multicellular; simple eukaryotic model; short lifespan of two weeks; easy to manipulate; economical; quick to grow (3-4 days); first multicellular organism with entire genome sequenced; total genome with ~20000 genes with 6 pairs of chromosomes; 40% genes have	Expensive to cultivate *in vitro*.

	Advantages	Disadvantages
	human homologs; a model to study cell division and developmental processes; easy to conduct gene knockout using RNAi; ease of mating, isolating and manipulating gene; less than 1000 somatic cells with fixed position in the body; a hermaphrodite with large numbers of eggs; a useful model for genetics and developmental research; transparent embryo, easy for developmental manipulations; self-fertilisation.	
Rodents (Mice, *Mus musculus;* Rats, *Rattus norvegicus)*	Mammalian models for developmental, molecular and genetic studies; vertebrate model closely related to human; small size, easy to keep; complete generation time of ~10 weeks; ideal model for deeper understanding of physiological mechanisms; similar to human genome, anatomy and physiology; useful to study homologous recombination; models for human diseases: transgenic mice models for Alzheimer's disease, Huntington's disease, sickle cell anaemia and many cancers.	Not an ideal model of ageing as due to subject to animal licensing laws; complex animals with large genomes; internal embryo; limitation to grow and culture embryos; relatively long generation time (3 months); limited mutational screening; long telomeres and telomerase activity in most tissues; telomere shortening not correlated with lifespan (or replicative ageing); expensive to maintain; extremely long (10-80 kb) polymorphic telomeres; not very reliable as preclinical models for human disease.
Amphibians African clawed frog (*Xenopus*)	Long lifespan (~15 years); negligible or very slow senescence; easy to access, manipulation with eggs and embryos; rapid development (~ 4 days); well establish systems; extensive regenerative potential.	A subject to animal licensing laws; complex, genomes are poorly characterised; cannot breed for many generation in laboratory; persistent telomerase activity in somatic cells.
Zebrafish (*Danio rerio*)	Small, economical; large, easily observable eggs and embryos; ease of breeding in the laboratory; small fully sequenced genome; valuable vertebrate model to study development (due to transparent embryo); convenient to	A subject to animal licensing laws; long generation time (2-4 months); high proliferation rates of all somatic cells; telomerase activity in all somatic cells; telomerase activity related to regeneration not to lifespan.

	Advantages	Disadvantages
	study fundamental aspects of blood (iron load or haemochromatosis); molecular tools to manipulate genes; telomere length similar to that in human; a unique model of ageing with different patterns of senescence; long lifespan; excellent model of regeneration , stem cells, DNA repair and cancer; recently being used in cardiac electrophysiology.	
Rhesus monkey	A mammalian model with approximately same number of genes as in humans: most of the genes have human homologs; a valuable model for clinical studies of numerous diseases including cancer and autoimmune disorders.	A subject of animal licensing laws and expensive; complex organism to study; not an ideal model to conduct basic/applied research.

Although debatable animal research has played a vital role in scientific and medical advances with the benefits of better quality of life globally (Festing and Wilkinson, 2007). Model organisms like yeasts, flies, fish and mice have many molecular pathways and genes in common with human (99% of mouse genes have their counterpart in humans) and have been widely used in research to explore evolution, genetics and development, as well as advanced molecular, biological aspects of serious human diseases (like cancer) and ageing.

There is a lack of compelling evidence for *in vivo* telomere-induced senescence. The main reason for that is a fact that laboratory mice are not an ideal model system for ageing studies: these animals have very long telomeres, and many tissues express significant levels of telomerase. A mouse that completely lacks telomerase activity, due to a germ line knockout of the RNA template component, has been apparently normal and healthy. After successive generations, allowing for sufficient telomere shortening, the mice display premature ageing phenotypes (Sedivy, 2007). Similarly, in *Drosophila*, another model system used to study telomere maintenance, there is no evidence for existence of shelterin proteins or t-loops at the telomere (Cenci *et al*., 2005), though it involves many DDR proteins for telomere maintenance. However, telomere maintenance in mammalian and yeast cells is terminal sequence-dependent and maintained by telomerase, indicating similar mechanisms of telomere maintenance. The biological consideration for the suitability of an organism for a type of research question is one of the basic criteria to select a model organism for a study.

1.3.1. Yeast: *Saccharomyces cerevisiae* as a eukaryotic model

Yeasts are one of the simplest, unicellular eukaryotic systems. Commonly known baker's yeast, or budding yeast, *S. cerevisiae* is one of the most studied yeasts in molecular genetics. It has also been studied extensively to explore the fundamental mechanisms of ageing (Steinkraus *et al*., 2008). The biggest advantage of using *S. cerevisiae* in fundamental and applied research is the availability of its entire sequenced genome (Mager and Winderickx, 2005) and methods for genetic manipulations thus facilitating functional genomic analysis. Another advantage includes methods for manual manipulations with individual cells and spores using dissecting microscope.

It was suggested in many studies that genes involved in regulation of ageing have a common evolutionary origin between unicellular *S. cerevisiae* and higher eukaryotes (Longo and Fabrizio, 2012). For this reason *S. cerevisiae* can serve as an alternative, economical model complementing ageing research in higher eukaryotes and mammals. Yeasts have also been very useful for cell cycle and checkpoint research and other fundamental cellular processes. Yeast has additional advantages such as rapid growth, spore formation and simple transformation methods that could be employed in basic research. It is easy to grow and can be manipulated under normal laboratory conditions. *S. cerevisiae* have small genome with ~6,700 genes. It can also exist in stable haploid or diploid state. Yeasts have a short cell cycle i.e., approximately 90 minutes as compared to other simple systems that are currently being utilised to study eukaryotic system like worms, fruit flies and rats. In yeast, comparative analysis of the genomes and the predicted proteins have shown that ~40% of yeast proteins are conserved in eukaryotic evolution (Rubin *et al*., 2000) and 30% of known genes involved in human diseases have yeast homologues (Bassett *et al*., 1997). This aspect presents it as an efficient model system and powerful tool to investigate different diseases and the therapeutic approaches to find solutions in combating human diseases.

1.3.2. Yeast cell cycle and cell cycle checkpoint

A cyclic array of organised events whereby cell grow, divide and bring about accurate DNA replication, duplication and segregation of all essential cell components into daughter cells is known as cell cycle (Elledge, 1996). The cell cycle in yeast has been divided in four easily identifiable stages namely G1, S, G2M and M (Figure 1.13). The G1 phase is characterised by un-budded cells. Cells can be identified as an oval-shaped under the light microscope. Growth and preparation of chromosomes for replication take place in this phase. In the S phase (DNA synthesis phase) cells appear with small buds. DNA and histone proteins (DNA proteins) synthesis, and chromatin assembly take place in this phase. Centromere duplication also occurs in this phase. The G2M phase is a transition phase between the S (DNA synthesis) and M

(division) phases. The newly emerged bud grows and gets to the parental cell size. The M phase (mitosis and nuclear division) is the final stage in the cell cycle in which nuclear division takes place. The cells divided into two, remain still connected to each other but have their separate nuclei.

There is another phase known as G0 or "quiescent" phase (Gray *et al*., 2004) when the cell leaves the cell cycle at the G1 phase either temporarily or permanently and enters in this G0 phase/stationary phase. The stationary phase has been characterised by cell cycle arrest and with a number of physiological, biochemical and morphological changes. The cell wall gets thickened with the accumulation of reserve carbohydrates, and acquires the capability of thermotolerance (Werner-Washburne *et al*., 1993).

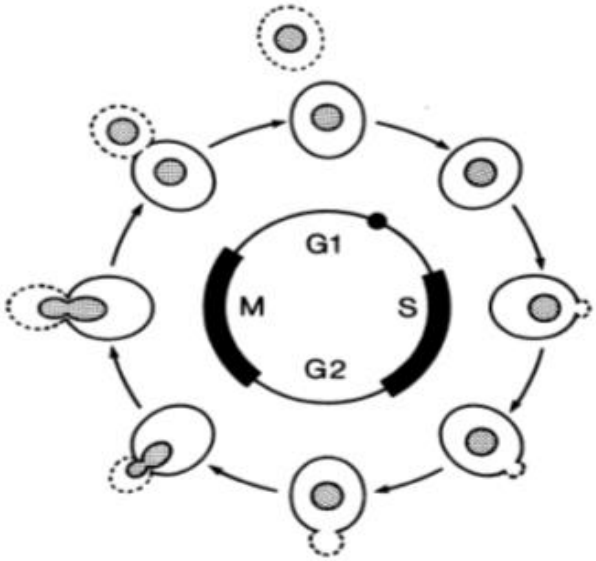

Figure 1.13. The different phases of yeast cell cycle.
Life cycle of yeast shows different phases as they appear under the microscope. Grey areas represent the nucleus, solid lines represent the mother cell and dotted lines show the newly emerging daughter cell (taken from Herskowitz, 1988).

The genetically controlled surveillance and response mechanisms by which cell monitor and control cell cycle events to ensure genomic integrity are known as cell cycle checkpoints (Clerici *et al*., 2001, Mogila *et al*., 2006). They include both intrinsic and extrinsic pathways. Intrinsic pathways regulate successive cell cycle events in an extremely organised sequence (Hartwell and Weinert, 1989). Extrinsic checkpoints prevent cell cycle progression in response to DNA damage. The gene products (checkpoint controls) are involved in monitoring cell cycle events such as chromosome replication, duplication and segregation. The checkpoint controls and DNA damage response pathways and the genes involved to mediate are highly conserved (Gartner *et al*., 2000).

The cell cycle is under tight regulation of different checkpoint mechanisms which constantly monitor the integrity of genome and cell cycle progression e.g., the G1 checkpoint senses DNA damage before the cell enters S phase (transition point G1-S). The G2 checkpoint monitors DNA damage after the S phase (G2-M) and stops progression of the cell cycle into the next phase until the damage is either repaired or, if not, cell self-destruction takes place through apoptosis (Hartwell and Weinert, 1989, Weinert, 1998). The S-M checkpoint detects the error in DNA synthesis (S) such as interruption in DNA replication and delays the onset of mitosis (M) (Boddy and Russell, 2001). The M phase checkpoint similarly senses spindle error. The high order of organisation of cell cycle events is essential to keep the cell viable (Elledge, 1996). Genetic damage is unavoidable if the cell progresses to the next phase of cell cycle without completing the previous phase. An example of an error is a non-disjunction of chromosomes during meiosis when chromosomes segregate in anaphase before the kinetochore of sister chromatid has attached to the microtubule. As a result, daughter cells will either contain one extra or lack one chromosome (trisomy). The normal feature of a eukaryotic cell is to follow one step after another in an accurate and organised way i.e., one round of replication should follow one round of mitosis as a rule to avoid an error to ensure viability.

The cell is under constant threat of endogenous (cellular metabolites) or exogenous DNA damaging factor (Gospodinov and Herceg, 2013, Abbotts *et al*., 2014) which may lead to mutations, genomic instability (cancer) or cellular death (Sancar *et al*., 2004).
DNA damage caused by telomere uncapping is controlled by different checkpoint genes (Table 1.3) that activate an intricate network of protective mechanisms through intracellular signalling to DNA damage response proteins resulting in either arrest or apoptosis of the cell (Longhese *et al*., 1998).

DNA damage checkpoints signalling pathways are activated in response to DNA insult under both intrinsic and extrinsic factors such as ultraviolet radiation (Sinha and Hader, 2002), ionizing radiations, chemotherapeutic drugs, replication error (HU, UV light), alkylating agents (MMS) (Ghosal and Chen, 2013) or reactive oxygen species (Zhang *et al*., 1993). The DNA damage range from DSBs, SSBs (single strand breaks), stalled replication fork, modified bases and intra-strand crosslinking. Eukaryotic cells respond to DNA perturbations by activating checkpoint signalling pathways and recognising damage at different phases of cell cycle e. g., G1-S transition, S phase or G2-M phase either alone or in specialised sub-complexes (cell cycle stage specific) and activate network of systems including DDR. The checkpoint proteins have been described as sensors, transducers and effectors: sensors proteins detect replication blocks or DNA damage; transducers relay this signal; and effectors that act on targets of the checkpoint (Boddy and Russell, 2001). DNA repair response could be HR, NHEJ, BER, NER, and MMR

(mismatch repair). Alteration or mutation of checkpoint genes may result in the failure of checkpoint controls due to defective proteins and may lead cell to senescence or cancer.

Table 1.3. DNA damage checkpoint proteins.

	Budding yeast	**Fission yeast**	**Human**
PIKK	Mec1	Rad3	ATR
PIKK	Tel1	Tel1	ATM
Adaptor	Rad9	Crb2	53BP1, MDC1, BRCA1?
Rfc1 homolog	Rad24	Rad17	Rad17
9-1-1 clamp	Rad17	Rad9	Rad9
	Mec3	Hus1	Hus1
	Ddc1	Rad1	Rad1
MRX complex	Mre11	Mre11	Mre11
	Rad50	Rad50	Rad50
	Xrs2	Nbs1	Nbs1
BRCT domain adaptor?	Dpb11	Rad4/Cut5	TopBP1
Signaling kinase	Rad53	Cds1	Chk2
Signaling kinase	Chk1	Chk1	Chk1
Polo kinase Cdc5	Cdc5	Plo1	Plk1
Securin	Pds1	Cut2	Securin
Separase	Esp1	Cut1	Separase
APC-targeting subunit	Cdc20	Slp1	$p55^{CDC}$

(Taken from Harrison and Haber, 2006).

In *S. cerevisiae*, DNA damages activate signal transduction pathways by protein kinases cascade along with non-kinase mediator proteins (Pfander and Diffley, 2011). Different members of Rad proteins (Rad9, Rad17, Rad24 and Rad53) and Mec1 and Mec3 are required for efficient damage response machinery (Figure 1.14). The mutants defective in or lacking any of these regulatory proteins delay cell cycle at G1-S or G2-M checkpoints. In budding yeast, the sensor kinase, Mec1 (hATR) and the downstream kinase, Rad53 (hChk2) play essential roles in signal transduction pathways (Ohouo and Smolka, 2012). Rad9 as an adaptor or mediator protein recruits Rad53 protein to site of DNA lesion in close proximity of Mec1

(Vialard *et al*., 1998, Blankley and Lydall, 2004). Mec1 (hATR) and Tel1 (hATM), the sensor kinases initiate the activation of the downstream kinase effectors Rad53 and Chk2 in response to DNA damage and delay cell cycle and activate repair proteins (Branzei and Foiani, 2006). Mec1 and Rad53 are crucial for the integrity of genomic DNA as they regulate effector proteins involved in DNA replication, transcription and cell cycle control (Ohouo and Smolka, 2012). Rad53 and Mec3 are involved in S/M checkpoint activation which delays the onset of mitosis when blocked by the presence of replication problem such as stalled replication fork (Enomoto *et al*., 2002).

In *S. cerevisiae*, Mec1-Ddc2 checkpoint protein kinase complex (human ATR-ATRIP) initiates a signal transduction pathway in response to DNA damage and replication stress to mediate cell cycle arrest (Navadgi-Patil and Burgers, 2008). A non-kinase mediator protein Dpb11 activates the Mec1-Ddc2 checkpoint kinase complex (Mordes *et al*., 2008). Yeast Dpb11 (hTop-BP1) binds to and activates checkpoint kinase Mec1 and phosphorylates downstream effector kinase Rad53 (hChk1/2) and RPA (Pfander and Diffley, 2011). Dpb11 interacts directly with the yeast DNA damage checkpoint clamp Ddc1-Mec3-Rad17 (9-1-1: human hRad9-hHus1-hRad1), loaded around effector DNA, Mec1 (Mec1-Ddc2) and recruit Rad9 at sites of DNA damage (Puddu *et al*., 2008). The ternary complex of Dpb11, Mec1 and Rad9 is required for efficient Rad9 phosphorylation/activation by Mec1. The phosphorylation of Rad9 by Cdk generates binding site for Dpb11 protein while inactive Cdk during G1 phase does not induce checkpoint signalling (Pfander and Diffley, 2011).

A number of other DNA repair proteins are activated including serine-threonine kinase, a nuclear protein Dun1 (DNA-damage uninducible) which is involved in post replicative DNA repair and transient arrest of cell cycle at G2-M (Zhou and Elledge, 1993) and proficient in induction of many other repair proteins. Rad53 inhibits the activity of Swi4 and Swi6 (switching deficient) proteins required entering cell in S phase, after damage in G1 phase. Similarly DNA replication factor C (RFC) recognises the damage in S phase and activate Rad53 and deactivate enzyme DNA primase that prevent downstream DNA synthesis.

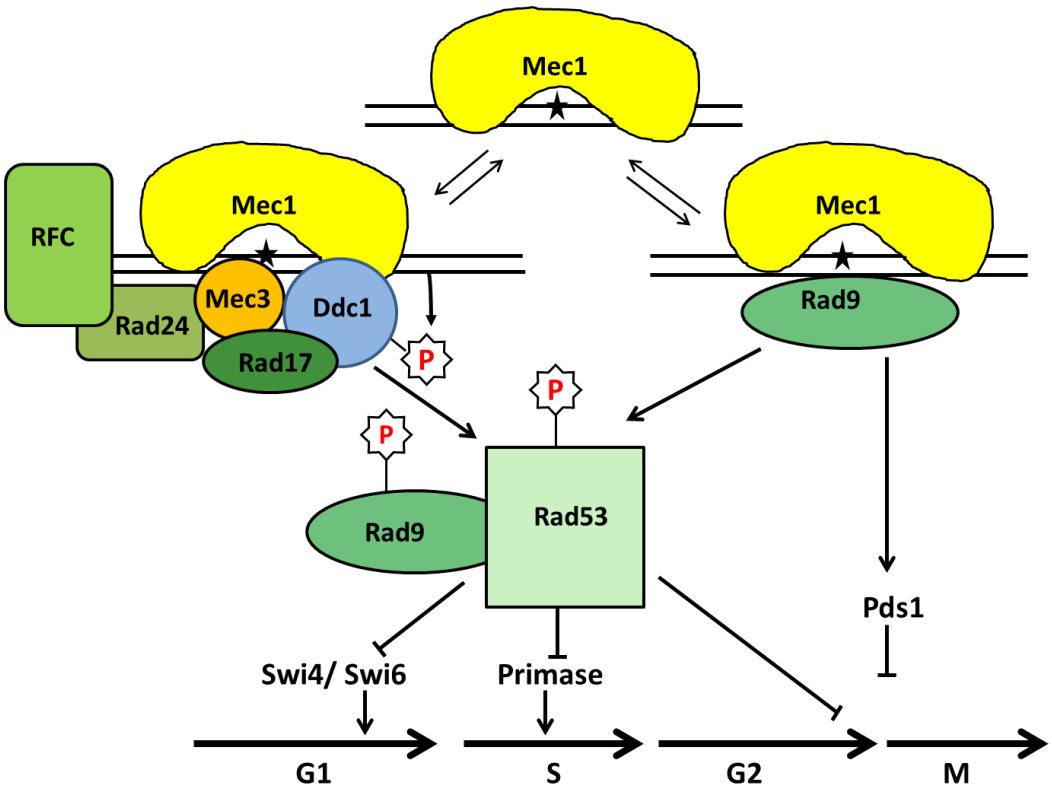

Figure 1.14. A hypothetical model of the DNA damage checkpoint response in yeast *S. cerevisiae*. The first step in DNA damage checkpoint is the recognition of DNA damage. In budding yeast, the products of *RAD9*, *RAD17*, *RAD24*, *MEC3* and *DDC1* genes are essential for an early recognition of damage. The phosphorylation of Ddc1, Rad9 and Rad24 depends on Mec1, initiator of signal transduction. The phosphorylated Rad9 interact with Rad53. The DNA replication protein Pol ε and RFC 5 (subunit of replication factor-C) sense replication block and damage of DNA synthesis. RFC interact with Rad24 and the resulting complex load proliferating cell nuclear antigen (PCNA) like clamp (Mec3-Ddc1-Rad17) on site of DNA damage and recruit DNA polymerase at the site of block. Rad9 and Rad24 belong to different epistasis groups and have different effect in addressing ssDNA accumulation at telomere. The Mec3-Ddc1-Rad17 complex is a homologue of human hRad9-hMec3-hRad17 clamp. Pds1 (precocious dissociation of sisters) is essential for meiotic progression and mitotic cell cycle arrest. (Taken from Longhese *et al*., 1998).

1.3.3. Yeast lifespan

Under favourable environment and in the presence of rich nutrients wild-type cells of yeast in a liquid culture continue to grow. Normally yeast cell completes a round of cell cycle in approximately 90 minutes (Blow, 1993). Growth of yeast cultures is monitored by using a spectrophotometer by measuring optical density of the culture's suspension at 600-660 nm which varies in different species and mutants. In chronological lifespan study samples of ageing culture are measured taking its optical density as a function of time. The data of pooled samples are used to construct the growth curve to measure the differences between wild type and the mutants. Similar to bacteria, yeast cells grow through lag phase (slow

growth of cells to adjust in a new environment), log phase with rapid growth and reach to stationary phase (with a very slow rate of growth as nutrients decreased in medium) (Gray *et al*., 2004). When the nutrients become scarce in a medium or in the environment, the cells shift from fermentation to respiratory metabolism with a slight lag (known as diauxic shift) in growth curve (Figure 1.15) to adjust to new environment and start utilising ethanol produced during fermentation. When all nutrients sugar and ethanol (carbon sources present in the medium) are exhausted, the culture of cells enters in stationary phase with a significant number of cells exiting cell cycle and become quiescent (G0 phase), a dormant or resting state (Gray *et al*., 2004). A number of molecular changes occur in this phase in cell structure; in cell wall and in cytosol along with the storage of sugar trehalose. Functional changes accompany the structural modification. In stationary phase different changes occur at transcription and translation levels (Werner-Washburne *et al*., 1993). A cell remains in this stationary phase until the return of nutrients/carbon source and re-enter the cycle at the availability of the nutrients (medium) and starts dividing again.

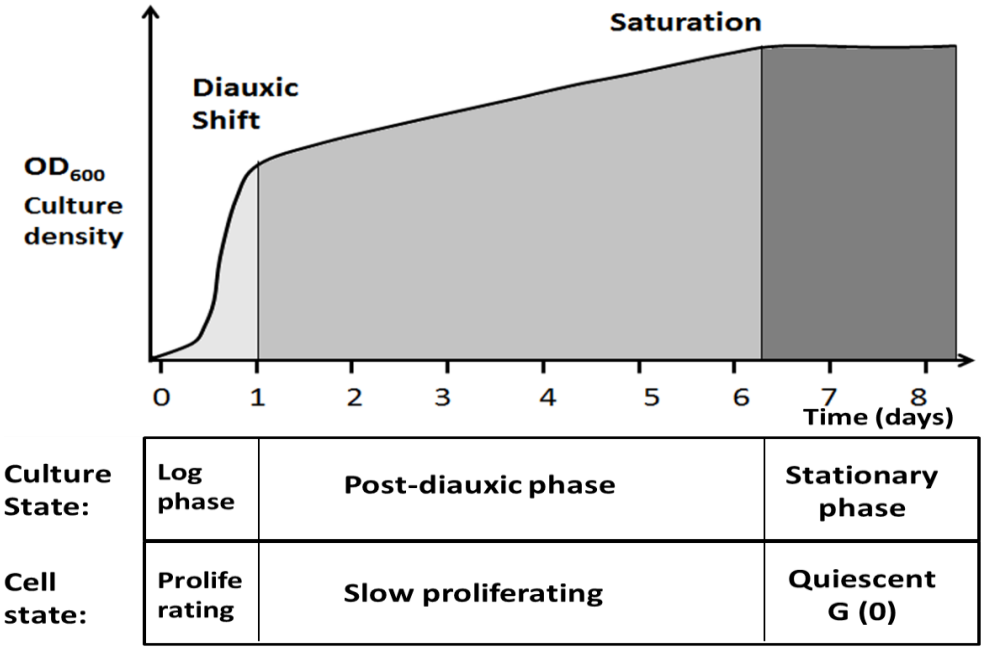

Figure 1.15. A typical growth curve of the yeast culture.

In rich medium (YEPD) containing glucose, yeast cells proliferate exponentially using fermentation. The density of the culture (measured at 600 nm) increases logarithmically with time during log phase. Diauxic shift reaches when all glucose in medium is utilised (after ~ 1 day). The cells shift from fermentation to respiration to use alternative carbon source in the medium with very slow proliferation. When carbon source are exhausted after ~5-7 days the culture reaches saturation state (non-proliferating phase), and cells become quiescent. (Adapted from Gray *et al*., 2004).

Ageing in *S. cerevisiae* has been addressed from two aspects: chronological lifespan (CLS) and replicative lifespan (RLS) (Figure 1.16). CLS is measured by the length of time a stationary phase cell remains viable in a non-dividing state and has been proposed as a model to study

post-mitotic cells in mammals (Fabrizio and Longo, 2003). RLS is expressed as the number of daughter cells produced by the mother cell before senescence (Mortimer and Johnston, 1959, Kennedy *et al*., 1994). These two aspects of ageing have been used in studies on dividing (mitotically active cells) and non-dividing cells (somatic cells) in higher organisms (Piper, 2006). In yeast, RLS studies have been carried out through micromanipulation by dissecting mother cells and separating new daughter cells. It is a time-consuming and laborious technique but the only successful approach for the study of senescence in yeast at present.

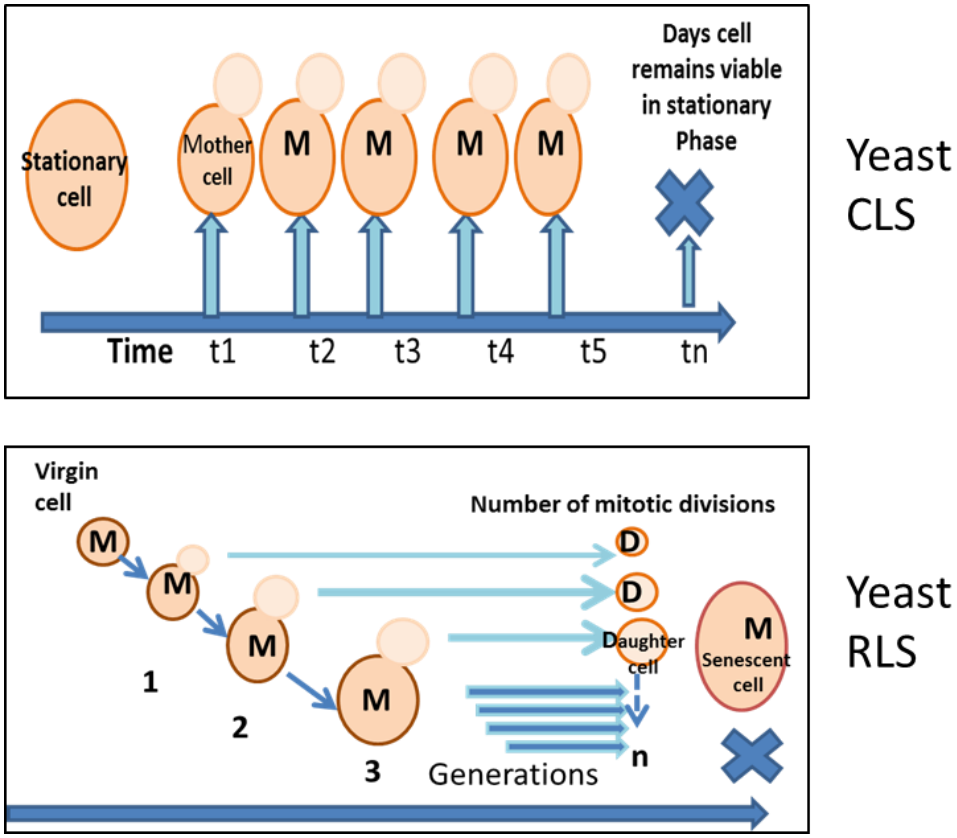

Figure 1.16. Two lifespans of yeast: CLS and RLS
(Adapted from Piper, 2006, Kaeberlein *et al*., 2007).

The CLS of yeast is measured to find out comparative differences in survival time due to different mutations related to ageing. In nature, yeast can survive and age in the stationary (under calorie restriction), or post-diauxic (high metabolic phase) or in a very low metabolic state (spore) (Gray *et al*., 2004, Herman, 2002). Under adverse conditions, yeast cells become arrested in the G1 phase of the cell cycle as unbudded cells, which survive with low metabolism (Herskowitz, 1988). It is not starvation that causes ageing and death as yeast cells can store glycogen and trehalose (reserve sugars) when nutrients are available and utilise these nutrients slowly when they not available (Fabrizio and Longo, 2003). Under favourable environmental conditions with sufficient nutrients, cells resume their growth. For chronological lifespan

measurement yeast cells are grown in a nutrient-rich medium e.g., glucose-containing yeast peptone dextrose (YEPD) or synthetic complete (SD/SC) media and are maintained either in the same media or in water under calorie restriction. Calorie restrictions have been reported to increase the lifespan in many organisms including worms, flies and rodents (Masoro, 2005) and budding yeast (Lin *et al*., 2002). In mammals calorie restriction is known to retard ageing in by causing a metabolic shift toward increased protein turnover and decreased macromolecular damage by reducing oxidative stress (Finkel and Holbrook, 2000). Caloric restriction attenuates the degree of oxidative damage, reduces age-related increase in DNA damage (Hamilton *et al*., 2001), decreases tissue lipid peroxidation (Zainal *et al*., 2000), increases resistance to oxidative stressors (Hall *et al*., 2000) and reduces mitochondrial ROS production (Pamplona and Barja, 2006).

In glucose-containing medium, yeast cells grow rapidly, a post-diauxic phase (high metabolism to growth phase) is followed by a stationary phase (low metabolism phase) until cells stop dividing or die. Post-diauxic and stationary phase cells show resistance to cellular stress and accumulate reserve carbohydrates (Werner-Washburne *et al*., 1993). In YEPD medium, yeast cells grow fast until saturation and stop growing when they pass through the diauxic shift, followed by a very slow growth rate, cell cycle arrest and stationary phase. Cells enter into this stationary phase normally 3-6 days after the diauxic phase (Lillie and Pringle, 1980, Gray *et al*., 2004). Rich medium induces large fluctuations in viability over time due to regrowth of subgroup of the arrested cells which may use nutrients released from the dead cells and re-enter the cell cycle (Zambrano and Kolter, 1996). Synthetic complete medium (SC) is used in high-throughput studies instead of YEPD to overcome the problem of high viability fluctuations due to survivors. Moreover, SC medium promotes a shorter lifespan (5-6 days) with high metabolism in the post-diauxic phase and yeast die rapidly after this phase whereas it may take 3 months before cells start dying in YEPD medium (Fabrizio and Longo, 2003). In CLS experiments with YEPD/SC medium, after the saturation stage, yeast cultures are switched to water that mimics severe caloric restriction. In water, yeast cells enter stationary phase with reduced metabolism and survive much longer. However, in both ways, mutations related to ageing or longevity show potential difference in viability over time (Fabrizio and Longo, 2007, Fabrizio and Longo, 2003).

The principal discoveries associated with yeast ageing might contribute to understand the ageing process in mammals and finding out key pathways and genes involved in the regulation of the ageing process. These pathways have many similarities between yeast and higher eukaryotes due to common evolutionary origins. The knowledge obtained from the simple studies with short lived model organisms can be applied to human genetics and molecular biology, to understand the complicated process of ageing and senescence in higher organisms.

A number of genes/signalling pathways involved in lifespan regulation have been identified e.g., the nutrient/insulin/insulin-like growth factor (IGF)-I-like pathway in mammals, and the Ras/protein kinase A (PKA), TOR (target of rapamycin) kinases, and Sch9 (Serine/threonine-protein kinase) pathways in yeast (Gray *et al*., 2004). Recent investigation in yeast gerontology research have shown that TOR kinases mediate the cellular responses that are involved in cellular longevity with an increasing evidence that the molecular determinants of ageing are conserved in higher eukaryotes including mammals. TOR has also been reported to act as coordinator with other nutrient-responsive kinases PKA and Sch9 and mediate the cellular response with changing nutrient levels with altered glucose and nitrogen levels (Pedruzzi *et al*., 2003). TOR and PKA kinases are activated in the presence of plenty of nutrients and increase ribosome biogenesis to activate protein synthesis machinery and suppress the stress response (Kaeberlein *et al*., 2007, Kaeberlein *et al*., 2005). The activation of TOR and PKA (cyclic AMP-dependent protein kinase) repress features of quiescence. Downregulation of these pathways under depletion of carbon source increases stress resistance, leading cell to G1 progression and extends the CLS (Fabrizio and Longo, 2003). Inactivation of the TOR causes activation of PKC pathway which promotes entry into quiescence cell state. In yeast, SNF1 protein kinase (a member of SNF1/AMPK family; SNF, Sucrose-non fermenting) is inhibited by the presence of fermentable carbon sources such as glucose but activated with the depletion of carbon in the medium and facilitate shift from fermentation to respiratory metabolism, required for entry into quiescence phase (Hedbacker and Carlson, 2008).

Inhibition of TOR and deletion of Sch9 increases both replicative and chronological lifespan (Kaeberlein *et al*., 2005). While deletion of small G proteins Ras1 and Ras2 that activate the PKA pathway have opposite effects on the chronological and replicative lifespans; deletion of *RAS1* increases RLS with slight decrease in CLS, while deletion of *RAS2* decreases RLS with dramatic extension in CLS (Sun *et al*., 1994).

RLS is associated the accumulation of extrachromosomal ribosomal DNA circles (ERCs)which were thought to cause yeast replicative senescence (Sinclair and Guarente, 1997). Several genes e.g., *RTG2 (*retrograde regulation), *LAG1 (*yeast longevity-assurance gene**)**, and *SIR2* involved in the regulation of lifespan have been reported (D'Mello N *et al*., 1994, Borghouts *et al*., 2004). A number of mutations have been identified that play a role in the extension of yeast lifespan by preventing ageing. For example, semi-dominant mutation *sir4-42* of the silencing gene *SIR4* extends lifespan by 30% (Kennedy *et al*., 1995). It prevents Sir3 and Sir4 proteins recruitment to the telomere and increases their concentration at other chromosomal regions like nucleolus (Kennedy *et al*., 1997). Mutation in *SIR4* also enhances rDNA silencing (Smith *et al*., 1998, Smith and Boeke, 1997) possibly by preventing formation of extrachromosomal rDNA circles through homologous recombination.

After systematic sequencing of the *S. cerevisiae* genome, the next challenge is to reveal the function of new genes. In genetics, the function of a gene is analysed by mutation analysis of a gene where mutant phenotypes are known. Most commonly hybrid plasmids are employed to introduce the foreign gene fragment into the yeast host. The limitation of this method is that host yeast sometime tends to lose or alter foreign plasmid or suffer instability. It is challenging to construct and maintain stable recombinant plasmid and its expression in extended cultures. Alternatively, classical methods of gene cloning for the expression of recombinant proteins and gene silencing are employed for new gene's expression both *in vitro* and *in vivo* studies. Another popular approach is PCR-mediated gene iteration in the chromosome DNA.

Since the first report of a targeted gene modification, hundreds of yeast genes have been altered (deleted or modified) for their functional analysis (Scherer and Davis, 1979). The one-step PCR-mediated technique is an easy, simple and rapid approach in the functional analysis of *S. cerevisiae* genes (Rothstein, 1991, Baudin *et al*., 1993, Lorenz *et al*., 1995). Any desired gene can be iterated or deleted with the use of modulating plasmids/'marker swap' plasmids (Cross, 1997) without a time-consuming cloning process (Longtine *et al*., 1998). This process required the desired gene sequence and restriction map of the open reading frame (ORF). A selectable marker (heterologous auxotrophic marker) is used to interrupt the target sequence. The hybrid oligonucleotides that are used for PCR synthesis of the deletion fragment consist of two parts; one that allows the homologous/heterologous recombination at the desired locus (5' end/deleting sequence), the second, which permits the PCR amplification of a selectable marker (3' end). A 5' deleting sequence from the target region of gene could be 35-51 nucleotides (Baudin *et al*., 1993, Lorenz *et al*., 1995) followed by 17-20 nucleotides at the 3' end, homologues to the selectable marker. The PCR amplicon-containing marker gene surrounded by flanking sequences of the target gene is used to transform auxotrophic yeast by a standard method (Gietz *et al*., 1992) with the use of PEG or DMSO (Gietz *et al*., 1995, Soni *et al*., 1993) that increase yeast transformation efficiency. Transformants are selected with complementation of the auxotrophic marker on appropriate dropout medium. Further analysis of the gene for its modification or complete knockout is carried out by its phenotype or Southern blot hybridisation analysis, or with PCR amplification using diagnostic primers.

The auxotrophic markers most commonly used in yeast include deficiencies in 4 syntheses adenine, glutamic acid, histidine, leucine, lysine and uracil (Mulleder *et al*., 2012). Yeast shuttle vectors used for genetic manipulation of *S. cerevisiae* contain antibiotic resistance markers, which can be used in both *S. cerevisiae* and the bacterium *Escherichia coli* (Da Silva and Srikrishnan, 2012), and yeast selectable markers. The latter could be a gene that confers resistance to antibiotic or antifungal toxins (van den Berg and Steensma, 1997) or biosynthetic genes which could complement auxotrophic markers e.g., *HIS3*, *ADE2*, *URA3* and *TRP1*. The

auxotrophic markers that complement the *S. cerevisiae* mutations should have sufficient nucleotide difference to avoid homologous recombination. The use of synthetic markers is a preferred approach in transformation studies instead of using antibiotics that may have their lethal effect on cell survival. Genes can be deleted or overexpressed under regulatable promoters. For PCR-mediated deletion, heterologous marker modules have the advantage over homologous or marker-swap approaches (Wach *et al*., 1997). Plasmids are available that make use of a selectable marker module with the heterologous *his5*$^{+}$ gene (*Schizosaccharomyces pombe*) (Wach *et al*., 1997) or the *S. cerevisiae* TRP1 gene or *Escherichia coli Kan*^{r} gene (Hadfield *et al*., 1990). These marker modules allow full or part of gene deletion/modifications with or without adding a tagging protein under regulatable promotors and are used for efficient analysis of gene functions.

Telomere-binding capping proteins ensure linear chromosome maintenance by end-protection and extension of G-rich strands (Palm and de Lange, 2008). Uncapped telomeres activate DNA damage checkpoint signalling pathways to regulate cellular proliferation. Conditional telomere capping dysfunction leads to sister chromatids' rearrangements and genetic instability (Mathieu *et al*., 2004). However, the direct contribution of telomere uncapping to senescence and ageing is not clear due to the lack of appropriate models. The asymmetrical cell division and availability of different mutants with particular phenotypes makes budding yeast a powerful tool in cellular and genetic studies. The recent mutants lacking Cdc13 and Stn1, in the absence of *EXO1* showed reduced G1 phase with a slow rate of growth due to senescence of large number of cells (Zubko and Lydall, 2006). This slow growth seems to be under genetic control of *RAD24* (an important checkpoint gene). These preliminary observations open the prospect of extensive study of the above mentioned mutants that could link genetic instability, checkpoint control and cellular senescence in the integrated scenario of ageing. Such a study will result in developing a novel approach to better understand the phenomenon of telomere uncapping in ageing by using yeast as a model.

1.4. Aims and Objectives

1.4.1. Aims

This work aims to develop a novel budding yeast model for investigating the impact of dysfunction in telomere capping on ageing and cellular responses.

The main molecular part in addressing this aim was generating *CDC13* deletion mutants in which the whole gene or its C- and N-termini are deleted by gene knock-outs using target oriented PCR mediated technique. The biological part of the work included: 1) studying differences in chronological lifespan in the obtained mutants with telomere capping dysfunction; 2) analyses of telomere length and telomeric DNA patterns of the mutants; 3) studying cellular responses of the obtained mutants to oxidative and genotoxic stress.

1.4.2. Objectives

The following tasks were formulated as main objectives of the study.

A. To carry out *CDC13* disruption (full and partial) by one step PCR mediated technique.

B. To perform genetic crosses to generate new combinations of the obtained mutations.

C. To analyse the telomere length and telomeric DNA patterns in the obtained mutants lacking Stn1 and/or Cdc13 protein and in N- and C-terminus truncated Cdc13 mutants (Southern blot hybridisation).

D. To investigate cellular responses of mutants with telomere capping dysfunctions to genotoxic agents (UV, MMS, HU, H_2O_2).

E. To determine differences in chronological lifespans of mutants without essential telomere capping proteins Stn1 and Cdc13 or mutant strains with N- and C-terminal deletion variants of protein Cdc13-1.

Chapter 2

Materials and Methods

2.1 Materials

- Acetic acid (Fisher Scientific, UK)
- Acrodisc® syringe filters 0.2 µm (Pall Life Sciences, UK)
- Adenine (Amino purine) hemisulphate salt (Sigma-Aldrich, UK)
- Agarose (Melford, UK)
- Albumin from bovine serum (Sigma-Aldrich, UK)
- Amersham gene images AlkPhos direct labelling and detection system with CDP-star (GE Healthcare Limited, UK)
- Amersham Hybond membrane-N (GE Healthcare Limited, UK)
- Ammonium acetate (Sigma-Aldrich, UK)
- Autoradiography film, blue (UltraCruz™) (Santa Cruz Biotechnology, USA)
- Bacteriological agar (Oxoid Limited, UK)
- Bacteriological peptone (Oxoid Limited, UK)
- *Bam*H1-HF (New England Biolabs Limited, UK)
- BD Falcon 125 ml Erlenmeyer Tissue Culture Flask, Flat Base (Scientific Laboratory Supplies, UK)
- Bijoux container sterile, 7 ml (Scientific Laboratory Supplies, UK)
- Blue/Orange Loading Dye, 6x (Promega Limited, UK)
- Calcium chloride (Sigma-Aldrich, UK)
- Chloroform-isoamyl alcohol mixture, 24:1 (Sigma-Aldrich, UK)
- Chromatography paper, Whatman 3MM CHR (Whatman Instruments Limited, England)
- Dextrose (D-glucose anhydrous) (Fisher Scientific, UK)
- Dimethyl sulfoxide (DMSO) (Sigma-Aldrich, UK)
- DNA ladders:
    - 1 kb (Invitrogen™, Life Technologies, USA)
    - 100 bp (Invitrogen™, Life Technologies, USA)
    - 100 bp (New England Biolabs (NEB), UK)
- *Eco*RI-HF® (New England Biolabs Limited, UK)

- Eppendorf tubes (Scientific Laboratory Supplies, UK)
- *Escherichia coli* DH5 alpha cells were kindly donated by Dr Qiuyu Wang (Manchester Metropolitan University)
- *Escherichia coli* K-12 strain NM522 (Manchester Metropolitan University, local stock)
- Ethanol (Fisher Scientific, UK))
- Ethidium bromide (Sigma-Aldrich, UK)
- Ethylene diamine tetra acetic acid (EDTA) (Fisher Scientific, UK)
- Glusulase (PerkinElmer, USA)
- Glycerol (BDH, UK)
- Glycine (Fisher Scientific, UK)
- Go Taq green master mix 2x (Promega Limited, UK)
- *Hin*dIII enzyme (New England Biolabs Limited, UK)
- Hybond-N^+ (GE Healthcare Limited, UK)
- Hydrochloric acid (BDH, UK)
- Hydrogen peroxide (H_2O_2) (Sigma-Aldrich, UK)
- Hydroxyurea (HU) (Sigma-Aldrich, UK)
- Isopropanol (Sigma-Aldrich, UK)
- Lambda *Hin*dIII marker (Invitrogen Life Technologies, USA)
- L-arginine (HCl) (Sigma-Aldrich, UK)
- L-aspartic acid (Sigma-Aldrich, UK)
- L-glutamic acid (monosodium salt) (Sigma-Aldrich, UK)
- L-histidine (Sigma-Aldrich, UK)
- L-Iysine (mono-HCl) (Sigma-Aldrich, UK)
- L-leucine (Sigma-Aldrich, UK)
- L-methionine (Sigma-Aldrich, UK)
- L-phenylalanine (Sigma-Aldrich, UK)
- L-serine (Sigma-Aldrich, UK)
- L-threonine (Sigma-Aldrich, UK)

- L-tryptophan (Sigma-Aldrich, UK)
- L-tyrosine(Sigma-Aldrich, UK)
- L-valine (non-animal source) (Sigma-Aldrich, UK)
- Magnesium chloride (Sigma-Aldrich, UK)
- Mannitol (Sigma-Aldrich, UK)
- 2-β-Mercaptoethanol (Sigma-Aldrich, UK)
- Methyl methanesulfonate (MMS) (Sigma-Aldrich, UK)
- Methylglyoxal (Sigma-Aldrich, UK)
- Methanol (Sigma-Aldrich, UK)
- Microtitre plate flat bottom well sterile (Scientific Laboratory Supplies, UK)
- Nuclease-free water (Sigma-Aldrich, UK)
- Phosphate buffered saline (PBS), 20x (Santa Cruz Biotechnology, USA)
- Phenol:Chloroform:Isoamyl Alcohol (25:24:1) (Sigma-Aldrich, UK)
- Potassium acetate (Sigma-Aldrich, UK)
- Primers (Invitrogen-Life Technologies, USA)
- Q5®high-fidelity DNA polymerase (New England Biolabs, UK)
- QIAprep spin miniprep Kit (50) (cat. no. 27104, Qiagen, USA)
- QIAgen plasmid midi kit (25) (cat. no. 12143, Qiagen, USA)
- QIAquick gel extraction kit(50) (cat. no. 28704, Qiagen, USA)
- RNase A (Qiagen, USA)
- Sodium chloride (Sigma-Aldrich, UK)
- Sodium dodecyl sulphate (Sigma-Aldrich, UK)
- Sodium hydroxide (BDH, UK)
- Sodium phosphate (BDH, UK)
- Spreader sterile (Scientific Laboratory Supplies, UK)
- Sterile needles (BD Plastipak, UK)
- TrackIt™ λ DNA/*Hind* III Fragments (Invitrogen-Life Technologies, USA)
- Tris Base (Fisher Scientific, UK)

- Tris-Borate-EDTA buffer, 10x (Invitrogen-Life Technologies, USA)
- Triton X-100 (Bio-Rad, USA)
- Tryptone (Oxoid Limited, UK)
- Tween-20, 10% (Bio-Rad, USA)
- Universal sterile container, 30 ml (Scientific Laboratory Supplies, UK)
- Uracil (Sigma-Aldrich, UK)
- Urea (Sigma-Aldrich, UK)
- 96-well plates (Scientific Laboratory Supplies, UK)
- Wizard SV gel and PCR clean-up system (Promega Limited, UK)
- *Xho*I (New England Biolabs, UK)
- Yeast extract (Oxoid Limited, UK)
- Yeast Nitrogen Base without amino acids and ammonium sulfate (Sigma-Aldrich, UK)
- Yeast plasmids (pDL 501, pDL 504, pDL 515, pDL 516 etc.) were kindly donated by Professor D. Lydall (Newcastle University)
- Yeast species: *Schizosacharomyces pombe* (fission yeast) and *Saccharomyces cerevisiae* (budding yeast), Manchester Metropolitan University, local stock; DLY strains: 640, 641, 1108, 1195, 1272, 1273, 1296, 1297, 2607, 2608, 2625, 2626, 2684, 2685, 3181, 3182, 3345, 3343, genotypes of which are provided in Table 2.1
- Zymolyase®-20T (AMS Biotechnology Limited, Europe)
- Stock Solutions:
- SDS solution (10 %, w/v): 10 g of SDS in 100 ml of sterile deionized water.
- Sodium chloride (NaCl) 5 M, contained 58.44 g in 200 ml total volume of distilled H_2O.
- Sodium hydroxide (NaOH) 5 M, contained 20 g in total volume 100 ml of distilled H_2O.

2.2 Equipment

- AC power adapter (Transitronix, Taiwan)
- Balance (Sartorius Machatronics Limited, UK)
- Block heater SBH130DC (Bibby Scientific Limited, UK)
- Centrifuge (J2-21) (Beckman Instruments INC., UK)
- Centrifuge 5415 D (Eppendorf, Germany)
- Confocal microscope (Leica DN 2500) (Leica Microsystems CMM, GBH, Germany)
- Digital camera (Coolpix 4500) (Nikon, Tokyo, Japan)
- Electrophoresis tank (Subcell® GT) (Bio-Rad, UK)
- Gene flash bio Imaging (Syngene, UK)
- Glass beads (0.5 mm, soda lime) (BioSpec Product, Inc., supplied by Thistle Scientific, UK)
- Haemocytometer (Weber Scientific International, England)
- Hybridisation Oven (Appligene, UK)
- Ice machine (Scotsman AF 100) (Frimont, UK)
- Incubator (compact)-model C330 (LEEC Limited, UK)
- Incubator (cooled-model 1200) (LMS, UK)
- Incubator (Swallow) (LTE Scientific Limited, UK)
- Incubator IP30 (LTE Scientific Limited, UK)
- Incubator shaker (Excella E25) (New Burnswick Scientific, USA)
- Incubator shaker series-I26 (New Brunswick Scientific, USA)
- Laboratory freezer Bio cold (Scientific Laboratory Supplies, UK)
- Magnetic stirrer hot plate (Stuart Scientific Limited, UK)
- Manipulator system (Singer Instruments Limited, UK)
- Microcentrifuge (Sigma Micro 1-14 with 24 x 1.5 ml tube rotor) (Sigma-Aldrich, UK)
- Microwave oven (Toshiba Corporation, UK)
- Millipore water purification system, RiOs™ and ElixR (Millipore, France)
- Nanodrop 2000/2000c (Thermo Fisher Scientific, UK)

- Orbital shaker R100 rotatest (Luckham Limited, England)
- Paper towels (Scientific Laboratory Supplies, UK)
- Parafilm (Scientific Laboratory Supplies, UK)
- Peltier thermal cycler-200 (MJ Research INC., USA)
- Petri plates 90 mm (Scientific Laboratory Supplies, UK)
- pH/mV/temperature meter model AGB-75 (Scientific Laboratory Supplies, UK)
- Portable autoclave vario 3028 (Dixons Surgical Instruments Limited, UK)
- Power supply (James Electronics, UK)
- Power supply PowerPac™ basic (Bio-Rad, USA)
- Printer digital graphic (Sony Corporation, Japan)
- Quantity one imaging system (Bio-Rad Laboratories INC., Italy)
- Razor blades (Kratos Analytical, UK)
- Refrigerator-Global 48CD (AS Catering Supplies Limited, UK)
- Replica platter (Sigma-Aldrich, UK)
- RunOne electrophoresis cell and multi-caster system, 230V (Embitec, USA)
- Sigma 3-16K centrifuge refrigerated high capacity (Sigma-Aldrich, Germany)
- Spectrophotometer (Jenway 6305) (Bibby Scientific Limited, UK)
- Spectrophotometer (Ultrospec 2000 UV/visible) (Pharmacia Biotech, England)
- Syngene G: Box bio imaging system (Syngene, UK)
- Ultra-low temperature freezer, -80°C (NuAire, Japan)
- Ultraviolet Transilluminator (Ultraviolet Products INC., USA)
- Ultraviolet Translinker, (TL-2000) UVP® (Ultraviolet Products INC., USA)
- Vortex mixer MV17 (Chiltern Scientific Instrumentation Limited, UK)
- Water bath (Bibby Scientific, UK)
- Water bath shaking-GLS 400 (Grant Instruments Limited, UK)

2.3 Methods and Work Programme

This research project involves both molecular techniques and microbiological methods. For simplicity I have divided the methodologies into two parts i.e. yeast methods and molecular biology methods.

2.3.1 Yeast methods

Yeast methodologies used in this work include cultivation of budding yeast, *Saccharomyces cerevisiae* (*S. cerevisiae*) on different media, genotype confirmation by checking genetic markers, spot test assays, testing viability in glycerol, chronological lifespan studies, genetic crosses between different mutants and tetrad analysis of their progenies by using a micromanipulator.

2.3.1.1 Preparation of media

Nutrient-rich media YEPD (yeast extract, peptone and dextrose; Method S2.1), minimal media synthetically defined or synthetic dextrose minimal medium (SD; Method S2.2), synthetic complete (SC; Method S2.3) and dropout media lacking histidine (-H), tryptophan (-T), leucine (-L) and uracil (-U) were prepared as described by (Amberg *et al*., 2005).

2.3.1.2 Growth of budding yeast on agar media

The *S. cerevisiae* strains used in this study had genetic background W303 (two of background BY4741) and are listed in Table 2.1 with their essential genotypes. These strains contain an *ade2-1* mutation; therefore, growth medium YEPD used routinely for their cultivation, was supplemented with adenine sulphate at concentration of 50 mg/L.

All strains were initially streaked out onto YEPD agar plates from -80°C glycerol stock or from old agar plates using sterile tooth picks or culture loops. Media plates were incubated at 23°C for 5-7 days to attain well-separated single colonies. Few colonies (4-5) were selected to grow on dropout solid media lacking histidine, leucine, tryptophan or uracil to confirm genotypic growth markers by testing for their auxotrophies. Two strains were employed for each gene mutation including positive controls. For example strains DLY 640 and 641 were utilised as positive control for *CDC13*. While strains DLY 2607 and 2608 (*cdc13*Δ::HIS *exo1*Δ::LEU2) tryptophan and uracil auxotrophs were used as negative controls of *CDC13.*

Table 2.1. Yeast strains *S. cerevisiae* used in this study and their essential genotype.

	DLY Strain	Strain brief genotype	Genetic background	Strain essential genotype
1.	**640**	WT	W303	MATa ade2-1 trp1-1 can1-100 leu2-3,112 his3-11,15 ura3 GAL+ psi+ ssd1-d2 RAD5
2.	**641**	WT	W303	MATalpha ade2-1 trp1-1 can1-100 leu2-3,112 his3-11, 15 ura3 GAL+ psi+ ssd1-d2 RAD5
3.	**1108**	*cdc13-1*	W303	MATa ade2-1 trp1-1 can1-100 leu2-3,112 his3-11,15 ura3 GAL+ psi+ ssd1-d2 RAD5 cdc13-1-int
4.	**1272**	*exo1*Δ	W303	MATalpha ade2-1 trp1-1 can1-100 leu2-3,112 his3-11,15 ura3 GAL+ psi+ ssd1-d2 RAD5 exo1::LEU2
5.	**1273**	*exo1*Δ	W303	MATalpha ade2-1 trp1-1 can1-100 leu2-3,112 his3-11,15 ura3 GAL+ psi+ ssd1-d2 RAD5 exo1::LEU2
6.	**1296**	*exo1*Δ *cdc13-1*	W303	MATa exo1::LEU2 cdc13-1-int ade2-1 trp1-1 can1-100 leu2-3, 112 his3-11,15 ura3 GAL+ psi+ ssd1-d2 RAD5
7.	**1297**	*exo1*Δ *cdc13-1*	W303	MATalpha exo1::LEU2 cdc13-1-int ade2-1 trp1-1 can1-100 leu2-3,112 his3-11,15 ura3 GAL+ psi+ ssd1-d2 RAD5
8.	**2605**	*exo1*Δ *cdc13-1*	W303	MATalpha exo1::LEU2 cdc13-1-int ade2-1 trp1-1 can1-100 leu2-3, 112 his3-11,15 ura3 GAL+ psi+ ssd1-d2 RAD5, survivor at 36°C
9.	**2606**	*exo1*Δ *cdc13-1*	W303	MATalpha exo1::LEU2 cdc13-1-int rad24::TRP1 ade2-1 trp1-1 can1-100 leu2-3,112 his3-11,15 ura3 GAL+ psi+ ssd1-d2 RAD5 survivor at 36°C
10.	**2607**	*exo1*Δ *cdc13*Δ	W303	MAT not known (initially alpha) cdc13::HIS exo1::LEU2
11.	**2608**	*exo1*Δ *cdc13*Δ	W303	MATnot known (initially alpha) cdc13::HIS exo1::LEU2 ade2-1 trp1-1 can1-100 leu2-3,112 his3-11,15 ura3 GAL+ psi+ ssd1-d2 RAD5
12.	**2625**	*cdc13-1 exo1*Δ *stn1*Δ	W303	MATnot known (initially alpha) cdc13-1-int stn1::HIS exo1::LEU2 ade2-1 trp1-1 can1-100 leu2-3,112 his3-11,15 ura3 GAL+ psi+ ssd1-d2 RAD5
13.	**2626**	*cdc13-1 exo1*Δ *stn1*Δ	W303	MATnot known (initially alpha) stn1::HIS exo1::LEU2 ade2-1 trp1-1 can1-100 leu2-3,112 his3-11,15 ura3 GAL+ psi+ ssd1-d2 RAD5
14.	**2684**	*cdc13*Δ *exo1*Δ *stn1*Δ *rad24*Δ	W303	MATalpha cdc13::HIS stn1::HIS exo1::LEU2 rad24::TRP ade2-1 trp1-1 can1-100 leu2-3,112 his3-11,15 ura3 GAL+ psi+ ssd1-d2 RAD5?
15.	**2685**	*cdc13*Δ *exo1*Δ *stn1*Δ *rad24*Δ	W303	MATalpha cdc13::HIS stn1::HIS exo1::LEU2 rad24::TRP (TR)
16.	**3343**	*yku*70Δ	BY4741	MATa yku70::URA3
17.	**3345**	*yku*70Δ	BY4741	MATalpha yku70::URA3

2.3.1.3 Cultivation of yeast strains in liquid media

Freshly grown, well-separated, same-size colonies (after 3-5 days' incubation on YEPD agar at 23°C), were picked to set starter cultures in YEPD broth in sterile containers (Method S2.1) under aseptic conditions. The inoculated cultures were grown in a shaking incubator at 150 rpm at the desired temperature (23°C or 30°C) to obtain fresh cultures with most of the cells at the exponential phase, required for setting the experiment.

2.3.1.4 Calculation of viability of yeast cells

The viability of cells in stationary/G0 arrested cultures was determined using the traditional colony-forming units (CFUs) method (Fabrizio and Longo, 2007). For this purpose, the stationary cultures were serially diluted to achieve a cell density between $1x10^3$ to $5x10^3$ cells/ml. Fifty microlitres of the final dilution were plated twice onto two halves of a YEPD agar plate and incubated at 30°C for 2-3 days. The resulting colonies were counted manually. All the cultures were presumed to be 100% viable at their maximum value that was either on day 6 or day 9 after inoculum in synthetic defined (SD)/synthetic complete (SC) media (Method S2.2). Subsequent CFU measurements until day 27-30 were normalised to the maximum CFUs value. Averages and standards deviations for at least three to five replicates were calculated for each experiment and the data are presented graphically.

2.3.1.5 Verification of auxotrophic marker by replica plating

In yeast, the use of selectable marker genes is important for efficient detection and selection of transformed cells in gene modification studies. Auxotrophy tests can also be used to counter select against revertants. In genetic studies on yeast, nutritional marker genes offer an alternative to markers of resistance to antibiotics or other toxic compounds. The examples of such genes are *HIS3*, *LEU2*, *TRP1* and *MET15* etc. These are wild type alleles of yeast genes that encode key components of metabolic pathways such as L-histidine, L-leucine, L-tryptophan and L- methionine. Nutrient-requiring auxotrophic yeast strains can be propagated only in media that contain appropriate growth factors. It is an easy and low cost approach to manipulate auxotrophy-complementing genes.

Experimental yeast strains were tested for genetic markers on different dropout media (Method S2.3) by the standard procedure of replica plating with velveteen (Lederberg and Lederberg, 1952) at the beginning and the end of the all chronological lifespan experiments. Auxotrophy complementation approach was also used for marker selection in gene knockout experiments. In genetic crosses of strains, the resulting progenies were selected on dropout media lacking one of the following components: uracil, histidine, leucine or tryptophan.

Yeast cells (4-5 colonies) or cultures were streaked on YEPD agar plates as distinct non overlapping short lines and grown for 2-3 days at 23°C (less growth was encouraged). These agar plates (master plates) carrying the initial cultures were inverted onto a square piece of sterilised velveteen that was firmly placed onto a replica platter (a cylindrical support of ~9 cm in diameter, with a metal flange to hold the fabric firmly). The culture was transferred onto the velveteen with slight digital pressure from the initial (master) plate. Cells imprinted onto the fabric provided the same pattern for replicating replica inocula to subsequent plates with nutrient requirement media. Replica plates were grown at the desired temperature and the

results were documented either by recording data, or by taking a photograph after 3-5 days of growth.

2.3.1.6 Chronological lifespan studies

In yeast, the chronological lifespan (CLS) is a measure of the "length of time a population of yeast strain remains viable under non-dividing conditions in post-diauxic phase (ethanol rich SD medium) or in stationary phase (water) (Fabrizio and Longo, 2003). Viability has been defined by the ability of a single cell to reproduce and form colony (CFUs) within 48 hours (Fabrizio *et al*., 2004). To measure CLS, yeast cells are grown in glucose-containing rich medium (SD) and maintained in this medium in a post-diauxic phase (high metabolism to normal growth with short survival) or in water in a stationary phase (low metabolism growth, with longer survival) until they stop dividing, indicating cell cycle arrest.

For CLS measurement, a modified method of (Murakami *et al*., 2008) was adopted (Protocol S2.1). Yeast cells from experimental strains were streaked out on YEPD and incubated at 23°C for 3-5 days to obtain single colonies. YEPD broth was inoculated in sterile glass tubes with fresh cells from morphologically similar colonies from YEPD plates for six experimental strains each with five replicas, resulting in a total of 30 cultures. Overnight (o/n) cultures were diluted in 20 ml or 50 ml of SD medium in flasks with equal numbers of cells ~1-2 x 10^6/ml based on OD_{660} with 1:5 cultures to flask volume ratio (Protocol S2.1). Cultures were kept at 30°C with agitation (200 rpm) for the entire period of the experiment (~ 30 days) with pooling samples at every third day. The cultures were checked for genetic markers at the beginning and end of ageing studies to ensure the maintenance of the genotype throughout the experiment. Microscopy was carried out at day 3, 6 and 30 to check for stationary phase cell arrest.

For yeast survival, the first reading was taken after 3 days of culture dilution by diluting the ageing culture to approximately 1000 cells/ml in sterile distilled water and plating 50 µl of this dilution in duplicate onto both halves of YEPD plates. Viable cell counts were measured in 50 µl by counting colony forming units (CFU) on YEPD plates for each strain after 2-3 days' incubation at 30°C. Average viable counts/50 µl was taken into account to calculate the total viable cell number in 1 ml by multiplying it by the dilution factor. Plates were incubated for an additional 1-2 days for the last few readings of the survival experiments as older cells re-enter the cell cycle slowly (Fabrizio and Longo, 2003). Percentages of survivals were estimated after every three days until 27-30 days by adjusting the dilution factor according to decreasing viability trends. The maximum number of CFUs at day 6 or 9 was considered to be initial survival point (100% survival) and was used to determine time-dependent % survival. In addition CLS were also measured (Protocols S2.2-S2.4) for 30 days to 90 days under calorie restriction in water for different mutants and wild type strains.

2.3.1.7 Spot tests

Yeast strains were grown at 23°C for 3-5 days for analysis. The loops full of cells from freshly grown single colonies were inoculated into 2-3 ml of sterile water. All samples were vortex mixed to get homogenous suspensions. The cell densities were equalised on the basis of absorbance (~1) at 660 nm wavelength (OD_{660}) using a spectrophotometer. For each strain, 250 µl of this suspension was carefully added into the wells of the first column of a 96-well sterile microtiter plate (one well for each sample). To prepare serial dilutions, 200 µl of sterile water was added to the corresponding rows of each strain (starting from well numbers two to six (2-6). Five-fold serial dilutions were prepared by taking 50 µl of the sample from column 1 and re-suspending it in the adjacent column for each strain using a multichannel pipette. This step was repeated from well 2 to 6. To keep an equal volume in each well from well 1-6, 50 µl of suspension was discarded from well 6. A sterile 48-prong replica plating device (Sigma) was used to spot a drop of 3-5 µl on 2-3 day old YEPD plates to avoid cultures spreading. The plates were allowed to dry and incubated at 23°C or the desired temperature for 3-5 days. This method was used to determine not only the initial viability of different strains on agar media, but also to see the intensity of growth of different strains at defined temperatures, in the presence of different genotoxic agents.

2.3.1.8 Testing viability of cells kept in glycerol

Viability tests were performed to analyse the percentage viability (CFUs) in different mutants under the effects of preservation in 25% glycerol as compared to water at -80°C. Cultures were grown either in YEPD broth (o/n) or on YEPD agar (2-3 days) at 23°C or 30°C. From each plate a loop-full of pure cultures was used to make a suspension in sterile water. Cells were washed three times by centrifugation at 73 x g (1,000 rpm) in a bench top microcentrifuge (Sigma Micro 1-14, Sigma-Aldrich, UK) for five minutes in sterile water. The total cell number was estimated on the basis of OD_{660} in diluted cultures (Amberg *et al*., 2005). Based on OD_{660}, cells were equalised in all suspensions. Total cell concentrations/ml was also measured by haemocytometer (Weber Scientific International, England) by counting cell number randomly in 5, 9 or 13 small squares. On the basis of the cell counts, cultures were serially diluted to get 1000 cells/ml of final dilution. For the final dilution, two sets were prepared: one in water and another in 25% glycerol with 4-5 aliquots of each. Each set was preserved at -80°C for different time periods. The samples (water/glycerol) were plated on YEPD agar in duplicates for zero time periods (0H), one hour (1H), one day (1D), three days (3D) and one week (1W). Viability was calculated by counting colonies from plating of 50 µl of suspension on each half of a YEPD plate. The average number of CFUs was taken to calculate % viability.

2.3.1.9 Mating haploids and sporulation of diploids

Crossing between strains with opposite mating types is a convenient method to generate new combinations of different mutations. Yeast crosses were carried out by mixing approximately equal numbers of cells from two haploid parental strains with opposite mating types, the MATa (a) and MAT alpha (α). A thin smear of one haploid strain was made on YEPD plates followed by a second smear of the opposite strain onto the first strain using a sterile tooth pick. The plates were incubated either at 23°C for 2-3 days or at 28°C overnight (minimum 6-8 hrs) for diploids to form and to grow after mating. Mixed culture was picked up from the surface of the medium and was streaked out on fresh plates of selective medium [dropout media without histidine, leucine, tryptophan and uracil -4 ($HLTU^-$) in this case] to select single colonies of diploid cells. The selective plates were divided in three parts with presumptive diploids cultured in the middle, non-sporulated parental cells at the top on either side as controls, while the bottom part of the plate was used to purify diploids. Haploid parents did not grow due to the lack of essential amino acids in the media, while a single purified colony was picked up to set a culture in 2 ml of YEPD broth and was grown at 28°C until saturation (for approximately 2 days) in a shaking incubator at 150 rpm. The cultures were examined under a microscope at a magnification of 400x to observe cell arrest. From saturated cultures, an aliquot of 500 µl was washed twice with sterile water by spinning at 73 x g (1,000 rpm) for 3 minutes. The washed cell pellets were re-suspended in 2 ml of 1% potassium acetate solution, supplemented with appropriate amino acids (all four in this case) and were grown at 28°C for 2-3 days for sporulation. The culture was examined under a phase contrast microscope to see spores in asci.

A sporulated culture was transferred to a 1.5 ml eppendorf tube and cells were pelleted by spinning at 12,470 x g (13,000 rpm) for 30 seconds in benchtop centrifuge. After discarding the supernatant, the cell pellet was re-suspended in 1 ml of sterile water and washed twice at maximum speed for 30 second to 1 minute. Finally, the pellet was re-suspended in 1 ml of sterile water and was either stored at 4°C for 1 week or used directly for tetrad analysis. From 1 ml of suspension 18 µl was transferred into a fresh tube and mixed with 2 µl of glusulase enzyme (PerkinElmer, USA) commercial product of snail juice. The mixture was vortexed briefly and incubated at 30°C for approximately 5-8 minutes to dissolve the sac surrounding the tetrads. The incubation time is dependent on genetic background of each strain. Sac digestion was monitored by examining a loop-full of the digest under a phase contrast microscope. When most of the asci appeared as discrete spheres, the sample was ready for dissection as tightly packed tetrahedral-shape spores cannot be resolved by micro-dissection. The culture was transferred to ice to terminate digestion and 1 ml of sterile water was added to tube. Cells were treated gently at this stage as extensive treatment can dissociate and disperse the four spores. After gentle rotation the tube, an aliquot of 8-10 µl of the suspension was plated along a line on

one side of the YEPD plate for tetrad dissection, and the plates were allowed to dry before performing tetrad analysis.

2.3.1.10 Tetrad dissection and spore analysis

Sporulated cultures consist of non-sporulated vegetative cells and four-spore asci. Tetrad analysis is a traditional method to study an ascus containing four spores (the product of a single meiotic event).

Micromanipulation was carried out on the surface of plates having digested asci under 100x magnifications. Four-spore clusters were picked individually from agar surface by positioning a microneedle close to the ascus and transferring it to a new area away from the total population. These four spores were separated and arrayed, evenly spaced, on the agar surface and their positions were noted down to keep track of them. In total, more than 100 tetrads were dissected and arranged on different nutrient-rich YEPD plates. Petri dishes containing spores were incubated for 2-3 days at 23°C until the spore colonies produced. The colonies grown from separated ascospores were replica-plated onto nutrient requirement synthetic/dropout media lacking essential amino acids like histidine, leucine, tryptophan and uracil to test the genotype. The growth patterns on selective media revealed the Mendelian segregation of markers, and the genotypes of resulting haploid colonies were assessed on the basis of marker combinations. Further confirmation of the genotypes was carried out by PCR analysis (for *CDC13, cdc13-1* and *STN1* genes)

2.3.1.11 Microscopy

Yeast strains growing in culture or on agar media are prone to contamination. Therefore, phase contrast microscopy was used to confirm the purity of yeast strains or suspected contaminations on the basis of typical cell size or cellular shape. The culture slides were prepared by placing a drop of sterile water onto a slide and resuspending yeast cells in it. A coverslip was placed onto the top of the suspension, and microscopical analysis was carried out. Pictures were taken at a magnification of 400x under a Zeiss KF microscope fitted with Nikon Coolpix 4500 camera (4 Mega pixels 4x optical Zoom) fitted with Zoom Nikkor 7.85-32 mm lens.

2.3.1.12 Spectrophotometry

Measuring OD was used to estimate cell densities in diluted cultures (Hartwell, 1970). Optical densities were measured either against sterile water or media. The spectrophotometer (Jenway 6305, Bibby Scientific Limited, UK) was calibrated for optical density at 660 nm wavelength (OD_{660}). 1 ml of water or medium was used as a blank (setting it as a reference). The samples for OD measurements were prepared by mixing 0.2 ml of culture/suspension and 0.8 ml of sterile water followed by, thorough sample vortexing to obtain a homogenous cell suspension. 1 ml of this suspension was transferred to a cuvette, and the cell density was measured at OD_{660}.

Considering the OD_{660} value, the total cell number/ml was calculated for the diluted suspension. The spectrophotometry technique was used to equalise cells for further inoculum in CLS experiments and also for making suspensions for spot test assays.

DNA concentrations were estimated using scanning spectrophotometry (nanodrop technology). A Nanodrop 2000, a highly sensitive spectrophotometer (Nanodrop 2000/2000c, Thermo Fisher Scientific, UK) was used to measure OD at 260 nm and 280 nm wavelengths.

2.3.1.13 Cell count by using haemocytometer

A haemocytometer (Weber Scientific International, England) counting chamber, was used routinely to determine the number of cells per unit of volume of a suspension. An approximate cell concentration is required for a number of microbiological applications to start culture with specific number of cells, or equalising cell numbers for different cultures in CLS studies.

To estimate total cell counts, homogenous cell suspensions at appropriate dilutions were prepared. A small drop of a suspension was placed at the edge of the coverslip on a haemocytometer. According to the cell density, an appropriate number of small squares within the central square (consisting of 25 small squares, each sub-divided into 16 tiny squares) were taken into account to count the cell number. The total cell number/ml of the suspension was calculated by counting cells in 5, 9 or 13 small squares as below:

Total cell number/ml = (number of cells counted/total volume in cubic mm^3) x 1000 (cm^3 or ml)

Total volume (mm^3) = depth of the chamber (mm) x surface area of squares counted (mm^2)

Where

Depth of chamber = 0.1 mm

Surface area (mm^2) = number of small squares (any number out of 25) x 1/25 (0.04 mm^2)

or

= number of tiny squares (any number out of 16) x 1/25 x 1/16 (0.0025 mm^2)

2.3.1.14 Glycerol preservation

Yeast strains were stored at 4°C on YEPD agar medium for short time periods while for longer periods strains were stored in 15 % (v/v) glycerol at -80°C. To prepare the glycerol stock, cultures were either grown in YEPD broth from purified colonies or from yeast cultured on YEPD plates. From the plates, cells were scraped up with sterile tooth picks and re-suspended in 1 ml of 15% glycerol in 1.5 ml screw cap tubes under sterile conditions. The vials were tightly closed, shaken to make homogenous suspensions and stored at -80°C. The cultures were revived when required by transferring small portions of this frozen stock to YEPD plates and growing at 23°C.

2.3.1.15 Toxicity and genotoxicity assays

In yeast genetics, toxicity tests are carried out to determine the destructive effect of a toxin, a hazardous chemical or radiation on genomic DNA, RNA or expression levels to elucidate the relative role of different genes involved in genome maintenance through cell damage repair pathways.

Yeast cells from fresh colonies were grown overnight at 23°C in 5-10 ml of YEPD broth from test strains. Cells from the log-phase of growth were harvested and washed three times with sterile water. The washed pellets of cells were re-suspended in sterile water. The OD of suspensions was determined by measuring absorbance at 660 nm wavelength to estimate the cell number. The optical density of cultures was subsequently adjusted to ~1-1.5 to keep similar loads of cells. Five-fold serial dilutions of this suspension were prepared in a 96-well plate for each strain as has been described in the spot test section (2.4.1.7) and spotted with a sterile replica plater on media plates prepared with different concentrations of genotoxic agents hydrogen peroxide (H_2O_2), methyl methanesulfonate (MMS) and hydroxyurea (HU) as described below.

To test the sensitivity of mutant strains to ultraviolet (UV) radiation, on the yeast genome, the serial dilutions of cultures were spotted onto YEPD plates. Two plates were used for each irradiation time point. Each group of plates was labelled with their respective UV exposure time (control without UV exposure, 10, 15, 30 seconds and so on) before exposure. Initially, a broad range of UV exposure times (from 10, 15, 20, 30, 40, 50, 60, 70, and 100 seconds) was tested to establish the most effective exposure time. This range was narrowed down to doses obviously effecting the growth of cells. The UV dose was expressed in J/M^2 (1 mJ/cm^2=10 J/m^2). For example if sample was exposed to UV for 10 seconds, the exposure time was multiplied with the unit of system and converted the resulted value to mJ/cm^2 or J/m^2 i.e., 10 second x100 $\mu J/cm^2$ =1000 $\mu J/cm^2$ or 1 mJ/cm^2=10 J/m^2. The plates with sets of cultures were placed inside a UV cross-linker under the UV lamp (TL-2000 UVP®, Ultraviolet Products INC, USA). The lid of the plate was removed and the cells were exposed to UV light (short wave 254 nm) for different exposure times. After UV exposure, the plates were cultivated for 3-5 days at 23° and 30°C.

To test cellular responses to intracellular oxidative stress in the presence of H_2O_2, YEPD medium was prepared according to a standard protocol. Plates were poured with different concentrations of H_2O_2 by mixing stock solution (30% concentration) of H_2O_2 to the melted medium at a temperature of ~55°C. Different deletion mutants, *CDC13* and *STN1* were initially tested on media with 2 to 8 mM H_2O_2. The most effective doses of H_2O_2 were used in the final tests.

Similarly, toxic effects of MMS, a DNA alkylating agent, were studied on YEPD medium containing 0.010%-0.035% of MMS. The sensitivity to HU was monitored on YEPD medium with initial doses of 10, 25 and 30 mM of HU. Based on the responses, concentrations were further increased to 50 mM, 75 mM, and finally to 100 mM of HU. All plates were dried before use.

2.3.1.16 Transformation of yeast cells by lithium acetate method

Competent yeast cells were prepared by inoculating a single colony of freshly grown culture into 10 ml of selective medium/dropout medium with (Gietz *et al*., 1995). The culture was grown o/n in incubator shaker at 150 rpm at 23°C and 30°C for temperature-sensitive and temperature-resistant strains respectively. The starter cultures were diluted with 100 ml of YEPD broth to OD ~ 0.2 at wavelength 660 nm. The inoculated cultures were grown at the required temperature for 4-4.5 hours in an incubator shaker (Excella E25, New Burnswick Scientific, USA) at 200 rpm. The cells were pelleted at 1,377 x g (3,000 rpm) for 5 minutes in a Beckman centrifuge (J2-21, Beckman Instruments INC, UK) and washed in 50 ml of sterile distilled water at the same speed. The resulting pellet of cells was re-suspended in 1.5 ml of lithium acetate/Tris EDTA buffer (Li/TE) (see below for recipe). The cell suspension was transferred to a sterile eppendorf tube. The cells were centrifuged in a benchtop centrifuge for 1 minute at maximum speed and re-suspended in 500 µl Li/TE buffer. In a fresh tube, ~1 µg plasmid DNA was mixed with 160 µg (16 µl of 10 µg/µl stock) of single-stranded carrier DNA to enhance uptake of DNA fragment. Freshly prepared 100 µl of yeast cell suspension, 10 µl of dimethyl sulfoxide (DMSO), and 600 µl of freshly prepared PEG/Li/TE (see below for recipe of PEG/Li/TE buffer) were also added to this vial and mixed gently. The percentage of PEG is crucial in the yeast transformation buffer. The new solution of PEG was used for each transformation to avoid the chances of evaporation. This vial was incubated in a water bath at 42°C for 15-20 minutes for the efficient transformation of yeast cells. To overcome the resistance of cell wall, yeast are generally heat shocked for 15 to 45 minutes. After incubation the mixture was centrifuged for 1 min at maximum speed, and the cell pellet was re-suspended in 1 ml of sterile distilled water. From 1 ml mixture, 100 µl of the cells were plated onto appropriate selective media. For example, tranrsformants with vector pFA6a containing a histidine marker was first selected on the medium without histidine. However, yeast cells used for transformation were with the LEU^+ marker so the medium used for the second round of selection was lacking both histidine and leucine.

Lithium acetate /Tris EDTA buffer (3 ml):

0.3 ml	10x LiAc (Lithium acetate)
0.3 ml	10x TE (Tris EDTA)
2.4 ml	sterile distilled water (SDW)

PEG (Polyethylene glycol 4000)/LiAc/TE solution (3 ml):

0.3 ml 10x LiAc

0.3 ml 10x TE

2.4 ml 50% PEG (sterile solution of PEG 4000 in water by mixing 200 g of PEG in 400 ml of DW)

PEG/Lithium Acetate solution for transformation (10 ml): made fresh just before use.

50% PEG 4000 8 ml

10x TE 1 ml

10x LiAc 1 ml

10x TE (1L, sterile):

1M Tris-HCl pH 7.5 100 ml

500 mM EDTA (pH 7.5) 20 ml

10x Lithium Acetate (LiAc) (400 ml):

Lithium acetate 40.8 g in the final volume of 400 ml. Adjusted to pH 7.5 with diluted acetic acid (autoclaved).

2.3.2 Molecular Biology Methods

2.3.2.1 Preparation of competent *E. coli* cells for transformation

This method was used to concentrate bacterial cells from diluted cultures from the mid exponential phase and to make cells capable of taking up foreign DNA (competent) with a high efficiency of transformation. Foreign DNA, due to its hydrophilic nature, cannot normally pass through the cell membrane. A high concentration of calcium chloride ($CaCl_2$) was used to make small holes in the cell membrane and DNA was forced to enter the cells by heat shock.

Glycerol stock of *E. coli* K-12 strain NM522 was removed from -80°C (15% glycerol), and a loop-full of cells was streaked on nutrient agar medium to get well-separated single colonies. The culture plate was incubated at 37°C overnight (o/n) for optimal growth. A single colony from a freshly grown plate was picked up with a sterile tooth pick and transferred to 10 ml of nutrient broth to set the starter culture in incubator shaker at 37°C with vigorous shaking. Five ml of o/n culture was inoculated into 500 ml of nutrient broth (1:100 dilution) in a 2.5 L flask and grown at 37°C at 200 rpm until the mid-exponential phase; this corresponds to OD 0.4 at 600 nm (approximately 3 ½-4 hours). At this stage, the culture was removed from the shaker incubator and transferred to 250 ml Beckmann tubes under sterile conditions. The cells were harvested by centrifugation at 4°C at 15,302.9 x g (10,000 rpm) for 5 minutes in a Beckmann centrifuge (J2-21, Beckman Instruments INC., UK). The supernatant was discarded, and the

pellet was re-suspended in 100 ml of ice-cold sterile 0.1M $CaCl_2$ solution. The suspension was again spun as before and, after discarding the supernatant, the pellet was re-suspended in 50 ml of ice-cold sterile 0.1M $CaCl_2$, followed by centrifugation and finally re-suspending the pellet in 15% glycerol (8.5 ml 0.1M $CaCl_2$ solution and 1.5 ml glycerol) to adjust the final cell density to OD ~ 0.48 at 550 nm wavelength. Competent cells were mixed gently by pipetting. The suspended cells were aliquoted (200 µl) into 2 ml screw cap tubes and stored at -80°C freezer until further use.

2.3.2.2 Transformation of *E. coli* with plasmid DNA

Competent *E. coli* K-12 cells (strain NM522) were used for various plasmid transformations. Aliquots of competent cells were removed from -80°C and were thawed on ice for 10-15 minutes. Two µl of yeast plasmid (pDL501, pDL504, pDL515, pDL516 etc., Table 2.2) DNA (diluted 5 times from the original concentrated preparation, ~100 ng) were added to the vial containing 200 µl of competent cells and mixed by finger flicking. After incubation on ice during 10 min, vials containing cells were subjected to heat shock at 42°C for 30-45 seconds (Sambrook and Russell, 2001). 800 µl of nutrient broth (rich nutrient medium) was added to the vial, and tubes were placed in an incubator shaker at 37°C for 30-60 min to recover the transformed cells after heat shock. The cell mixture was then plated on nutrient agar media with antibiotic, ampicillin used at the final concentration of 100 µg/ml to select antibiotic resistant *E. coli* cells transformed with different yeast plasmids e.g., pFA6a-His3MX6 plasmid.

Table 2.2. Yeast plasmids used for *CDC13* disruption with modulating marker DNA.

	Vector ID	Alias	Plasmid size (bp)	Size of amplicon (~)	Marker	Construction details
1	pDL501	pFA6a-HIS3MX6	3782 bp	PCR product size 1.403 kb	Amp, His3	HIS3 cassette
2	pDL504	pFA6a-GFP(S65T)-ADH1-HIS3MX6	4698 bp	PCR product size 2.348 kb with GFP tag	Amp, His3	His3 cassette for GFP tagging of yeast fragment (yfg)
3	pDL515	pFA6a-TRP1-PGAL1	3962 bp	PCR product size 1.558 kb	Amp, TRP1	TRP1 cassette for placing yfg under control of the GAL1 promoter
4	pDL516	pFA6a-HIS MX6-PGAL1	4329 bp	PCR product size 1.925 kb	Amp, His3	HIS3 cassette for placing yfg under control of the GAL1 promoter

(Longtine *et al*., 1998)

2.3.2.3 Plasmid DNA extraction

Plasmid DNAs were extracted at small scale (<20 µg) using the QIAgen mini (QIAprep spin miniprep Kit, cat. no. 27104, Qiagen, USA) or at large scale (up to 100 µg) using midi plasmid kits (QIAgen plasmid midi kit, cat. no. 12143, Qiagen, USA) by following the instruction manual provided by the manufacturer.

2.3.2.4 Confirmation of plasmid DNA size by digestion with restriction enzymes

3-5 µl of purified plasmid DNA (~500 ng-1 µg) were digested with single or unique cutter (*Eco*RI, *Bam*HI, *Pst*I or *Hin*dIII restriction enzymes), chosen on the basis of the plasmid restriction map. For example, single cutter *Eco*RI restriction enzyme was used with 20 units per reaction in a 20 µl reaction mixture to linearise vector pFA6a-HIS3MX6, and its double enzyme digestion was performed with two enzymes, *Eco*RI and *Bam*HI for further size confirmation. The digestion mixture was incubated for 2-3 hours at 37°C. Digestion was terminated by adding 1 µl of 0.5 M EDTA and was stored at -20°C until further analysis by agarose gel electrophoresis.

2.3.2.5 Agarose gel electrophoresis

Agarose gel electrophoresis was carried out to confirm the presence of plasmid and genomic DNA after extraction, to quantify purified PCR product/plasmid/genomic DNA in a known volume, to check linearised DNA size after restriction digestion and to confirm the desirable amplicons following PCR. Purified uncut DNA (3-5 µl) and digested DNA (15-20 µl) were resolved on a 0.8% agarose gel with 0.25 µg/ml ethidium bromide (Sigma-Aldrich, UK) in 1x TBE running buffer to estimate the size, yield and purity of DNA. DNA markers 1 kb ladder from Invitrogen™ (Life Technologies, USA) and 100 bp DNA ladder quantitative from NEB/Invitrogen™ (Life Technologies, USA) were included as reference standards on either side of the gel. All DNA gels were photographed with a GeneFlash gel imaging system (Syngene) fitted with a PULNiX TM-300 CCD camera [8-48 mm f1.2 6x manual zoom lens (Computar H6Z0812) under UV illumination].

2.3.2.6 PCR amplification for *CDC13* and *cdc13-1* detection

Polymerase chain reaction (PCR) amplification was carried out to detect *CDC13* or *cdc13-1* in cells of different yeast strains. The primers N1 (forward primer) and N2 (reverse primer) were used to amplify *CDC13* specific N-terminal fragments with an approximate size of 378 bp (from 953 to 1330 bp of the open reading frame (ORF). The isolated colonies were picked from the media plate and denatured at 95°C for 15-20 minutes in 20-25 µl sterile water or 0.02 M NaOH. Samples were centrifuged for 1-3 min to pellet down denatured cell debris. The PCR

reaction was set up using 2 µl of clear supernatant as a template in 25 µl of reaction volume with 2x PCR master mix from Promega (3 mM $MgCl_2$, 400 µM dNTPs, and 50 units/ml Taq polymerase). Each PCR reaction contained 10 µl of nuclease-free water, 0.25 µl each of forward and reverse primers (stock 100 pM/µl), 2 µl template DNA, and 12.5 µl of Promega's green master mix).

PCR conditions were as below:

1.	95° C for 15 min		(Denaturing step)
2.	94° C for 25 sec (seconds)	32 cycles	(Denaturing step)
3.	56° C for 30 sec		(Primer annealing step)
4.	72° C for 30 sec		(Extension step)
5.	32 cycles from steps 2-4		
6.	72° C for 5 min		

Amplified fragments were resolved on 1.5 % agarose gel with 1x TBE buffer to confirm the presence of the fragments of the expected size.

2.3.2.7 Post PCR amplified product restriction enzyme analysis

After confirmation of PCR fragment size on the gel, 10-15 µl of amplified product was digested with 10-20 U of *Eco*R1 restriction enzyme to differentiate between wild type *CDC13* and its mutant form, *cdc13-1*. The *cdc13-1* mutant have an additional *Eco*R1 site (sequence below) that replaced nucleotide 'C' (5'…TGAATCC…3') with 'T' (5'…TGAATT C…3') at sequence position 1111 of *CDC13* ORF.

***Eco*R1 site**

As a result of digestion, *CDC13* showed a single band of ~378 bp corresponding to the sequence from 953 to 1330 bp of the ORF without *Eco*R1 site), and *cdc13-1* generated two bands of sizes ~219 and ~159 bp (due to the *Eco*R1 cut) on 2.5 % agarose gel.

2.3.2.8 *CDC13* modification by PCR and homologous recombination

In gene functional analysis studies, the target gene replacement is a standard technique used to achieve gene replacement in "one step PCR-mediated gene modification, deletion and integration" at the target specific site (Longtine *et al*., 1998). It is a quicker and cheaper alternative to time-consuming gene cloning technique.

The first step in PCR based gene deletion and modification is the choice of yeast plasmids with selectable marker of interest. A number of yeast plasmids are available that serve as template for PCR synthesis of DNA fragment for gene manipulation. The hybrid primers are designed by selecting 5'-ends from the target gene nucleotide sequences and 3'-ends from modular marker sequence for the synthesis of disruption cassettes by PCR using plasmid DNA as template. The amplified DNA fragment with flanking region of gene is transformed into host yeast. Homologous recombinants that carry the deleted gene are identified on the basis of selectable marker and confirmed by diagnostic PCR for the deletion of gene and integration of marker module in yeast genome.

2.3.2.8.1 Yeast plasmid for *cdc13-1* full gene deletion

The plasmid pFA6a-HIS3MX6 (pDL501) with a histidine marker module was chosen as a template for PCR synthesis of the sequence for *CDC13* full gene deletion (Longtine *et al*., 1998, Wach *et al*., 1997) (Figure 2.1).

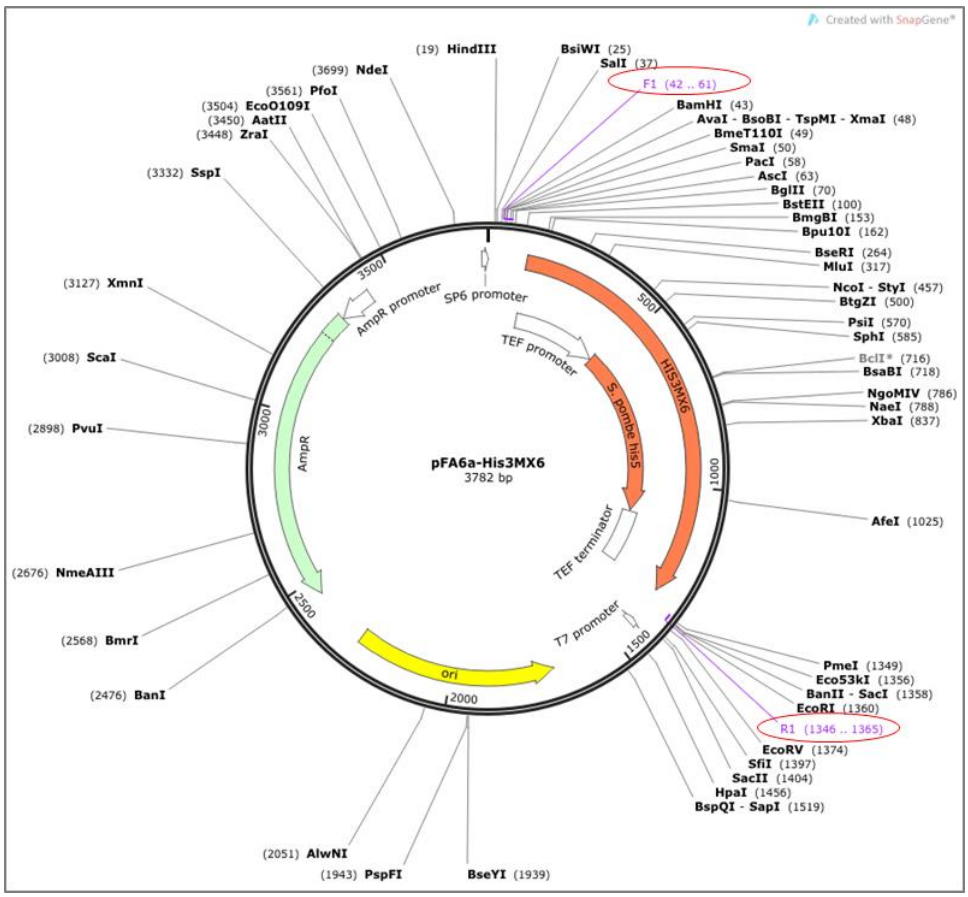

A

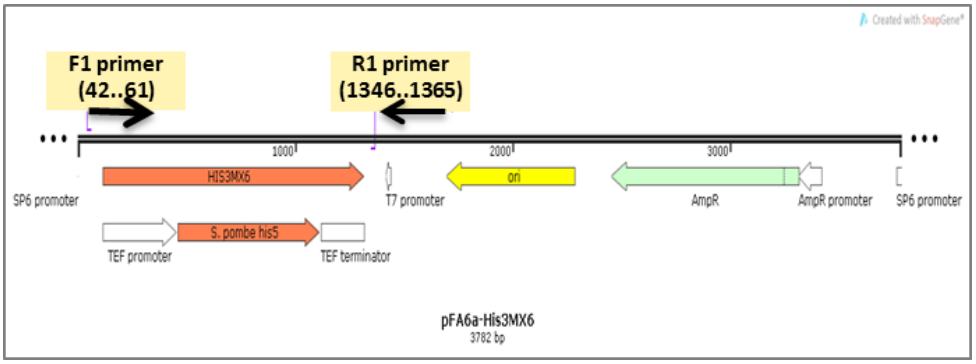

B

Figure 2.1. Map of the yeast plasmid pFA6a-HIS3MX6 (3782 bp).

(**A**) Map of circular plasmid showing unique restriction sites (http://www.snapgene.com/).

(**B**) Map of linear plasmid showing the position of PCR primers (F1 and R1) used as the 3' part of hybrid deletion primers.

The HIS3MX6 DNA module contains a heterologous *his5*$^{+}$ marker gene that complements *S. cerevisiae his3* mutations. The *his5*$^{+}$ gene is basically a hybrid gene from *Saccharomyces kluyveri* and *Schizosacchromyces pombe* adapted for better transformation efficiency. Transformation of yeast *S. cervisiae* with the *HIS3* gene of *S. kluyveri* under its native promoter could result in 5% more false positives as compared to *Sz. pombe* under the strong *TEF* gene

promoter and terminator (Wach *et al*., 1997). The hybrid histidine gene is ~1.4 kb and encodes for imidazole glycerol-phosphate dehydratase required for histidine biosynthesis.

2.3.2.8.2 Hybrid primers for *CDC13* full gene deletion cassettes

The chimeric primers have 100% homology with the target gene sequences as well as with the metabolic marker gene. To delete *cdc13-1*, the 3'ends of forward (N-F1) and reverse (C-R3) hybrid primers were picked from the start and end of the HIS3MX6 marker module sequences corresponding to 20 nucleotides (nt) as shown by sequences F1 and R1 respectively on the circular and linear maps of plasmid pDL501 in Figure 2.1 and 2.2 (Longtine *et al*., 1998). The 5' gene-specific targeting sequences corresponding to 46 and 40 nucleotides were immediately upstream (including start codon ATG and first three nucleotides from the start) and downstream of the *CDC13* open reading frame to be deleted, as shown in Figure 2.3; (Table 2.3).

The 3' marker sequence of primers should hybridize with homologous HIS3 DNA of plasmid pDL501 in the PCR reaction to amplify the ~1409 bp deletion cassette, whereas the flanking 5' guide sequences will recombine with target DNA in their normal chromosomal location during yeast transformation to disrupt *cdc13-1* resulting in *cdc13-1*Δ::HIS3MX6 construct (Figure 2.4).

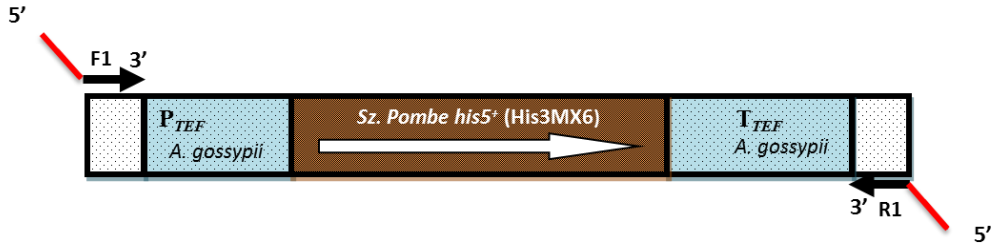

Figure 2.2. Histidine (*HIS3*) marker module: a PCR template to generate fragments for *CDC13* gene deletion and modification**.**

The plasmid pFA6a-HIS3MX6 uses the *HIS3MX6* module that contains the *Sz. pombe his5*$^{+}$ gene, (Wach *et al*., 1997) with *TEF* promoter and terminator sequences from a filamentous fungus *Ashbya gossypii.* The arrow within the box indicates the direction of transcription. Outside arrows indicate forward (F1) and reverse (R1) PCR primers (arrows shown in black represent the 3' part of hybrid primers corresponding to sequences on either side of the *HIS3MX6* module whereas the red parts represent the 5' end of the primers homologous to the yeast target sequences). Gene-specific primer-length dictates the size of PCR product e.g., with 40-nucleotide homologous primers, the size of the amplicon is expected to be 1403 bp (Adapted from (Wach *et al*., 1997).

CDC13 sequence

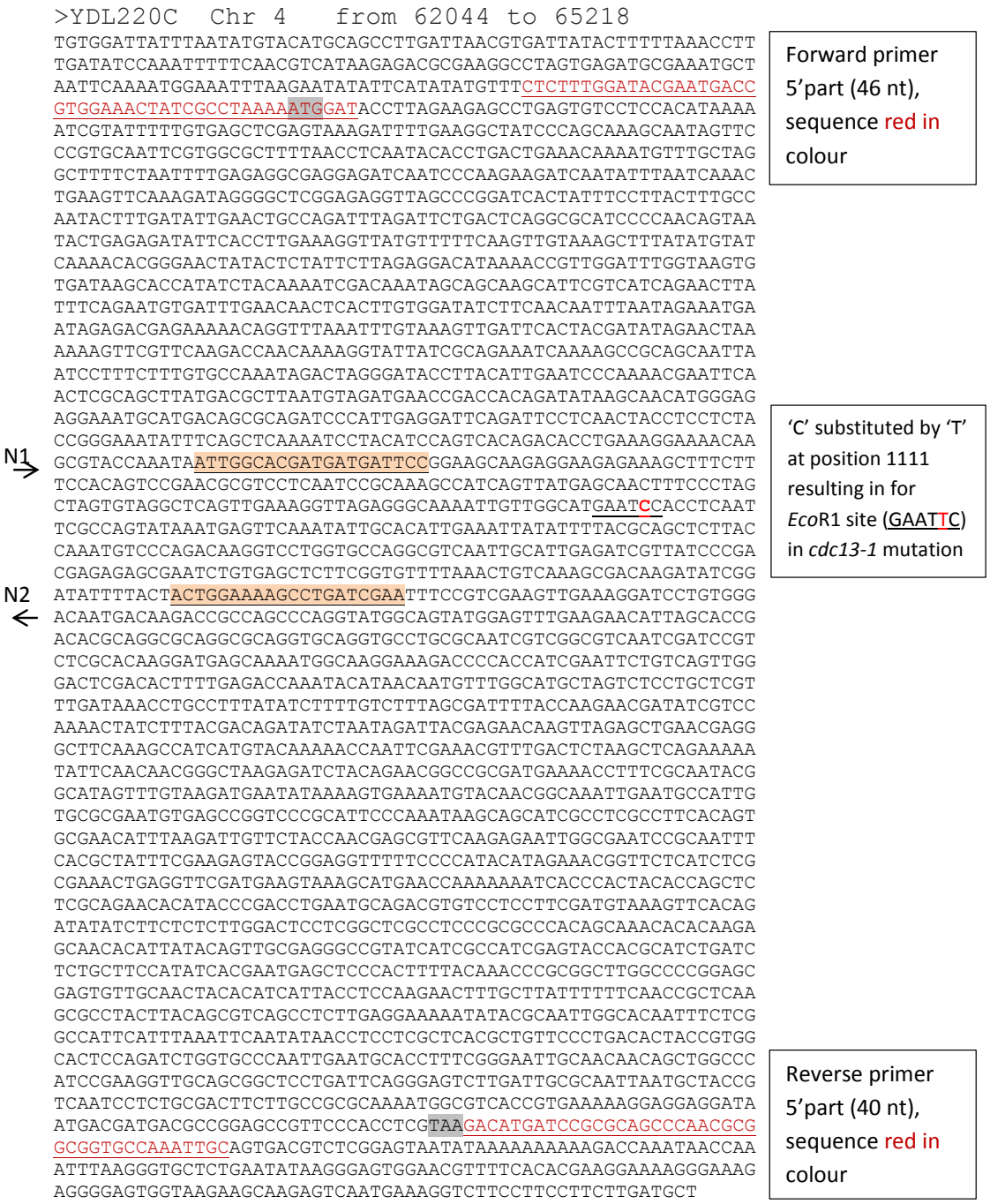

Figure 2.3. Designing of primers for *cdc13-1* full gene deletion: selecting the 5' ends of the hybrid primers.

CDC13 ORF (1-2775) with upstream and downstream sequences with each being 200 nucleotides in length, accessed from Saccharomyces Genome Database (SGD) (http://www.yeastgenome.org/). Nucleotide sequences dark red in colour was selected as 5' end of hybrid primers. Diagnostic primers (N1 and N2) were used to detect the 378 bp fragment for *CDC13* or *cdc13-1*.

Table 2.3. Primer sequences used for the deletion of the *CDC13* full gene or its N- and C-terminus truncation.

Hybrid primers	Primer (3' Part)	objective	Primer sequence
N-F1 (66 nt)	F1 (20 nt)	*cdc13-1* full gene deletion (7-2775)	5'-C TCT TTG GAT ACG AAT GAC CGT GGA AAC TAT CGC CTA AAA **ATG** GAT cg gat ccc cgg gtt aat taa-3'
C-R3 (60 nt)	R1 (20 nt)		5'-GCA ATT TGG CAC CGC CGC GTT GGG CTG CGC GGA TCA TGT C ga att cga gct cgt tta aac-3'
FT-N1 (70 nt)	F4 (20 nt)	TRP1-P_{GAL1} introduction (without tag); *cdc13-1* NTΔ (1-1386 nt)	5'-AT ATA TGT TTC TCT TTG GAT ACG AAT GAC CGT GGA AAC TAT CGC CTA AAA gaa ttc gag ctc gtt taa ac-3'
RT-N1 (68 nt)	R2 (20 nt)		5'-CGC CTG CGC CTG CGT GTC GGT GCT AAT GTT CTT CAA ACT CCA TAC TGC **CAT** ttt gag atc cgg gtt tt-3'
FT-C2 (70 nt)	F3 (20 nt)	ADH1-HIS3MX6 (without tag) Insertion; *cdc13-1* CTΔ (1387-2775 nt)	5'-TC GAA GTT GAA AGG ATC CTG TGG GAC AAT GAC AAG ACC GCC AGC CCA GGT **tga** ggc gcg cca ctt cta aa-3'
RT-C2 (71 nt)	R1 (20 nt)		5'-GAG ACG TCAC TGC AAT TTG GCA CCG CCG CGT TGG GCT GCG CGG ATC ATG TC ga att cga gct cgt tta aac-3'

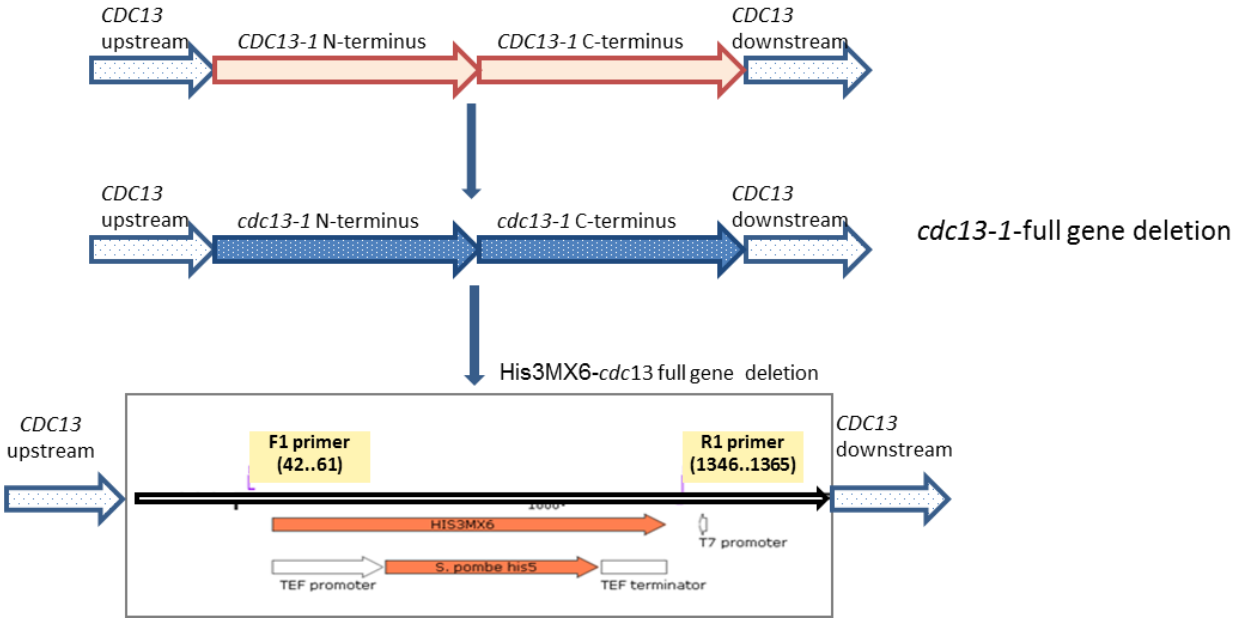

Figure 2.4. A diagrammatic representation of HIS3MX6-*cdc13-1* full gene deletion construct. *cdc13-1* deletion (*cdc13-1*Δ) with modulating plasmid pFA6a-HIS3MX6 (pDL501).

2.3.2.8.3 Plasmid selection for *cdc13-1* N-terminus deletions

The ORF or coding sequence of *CDC13* (1-2775 bp) was theoretically divided into two halves of 1386 and 1389 bp. The first half of *CDC13*, that is N-terminus part of gene (1386 nt plus one ATG codon), was deleted with the yeast plasmid pFA6a-TRP1-PGAL1 (pDL515; 3962 bp) (Figure 2.5) containing the tryptophan marker (*TRP1*) module. The *S. cerevisiae TRP1* marker

gene produces the phosphoribosylanthranilate isomerase enzyme, required for tryptophan biosynthesis and is under the *TRP1* promoter. The integration of this marker in the yeast genome through homologous recombination will result in truncation of the *CDC13* N-terminus, while the remaining C-terminal half of *CDC13* will be expressed under the PGAL1 inducible promoter, regulated by Gal4 substrate. The Gal4-dependent induction in turn is mediated by an upstream activating sequence (UAS) in modular DNA.

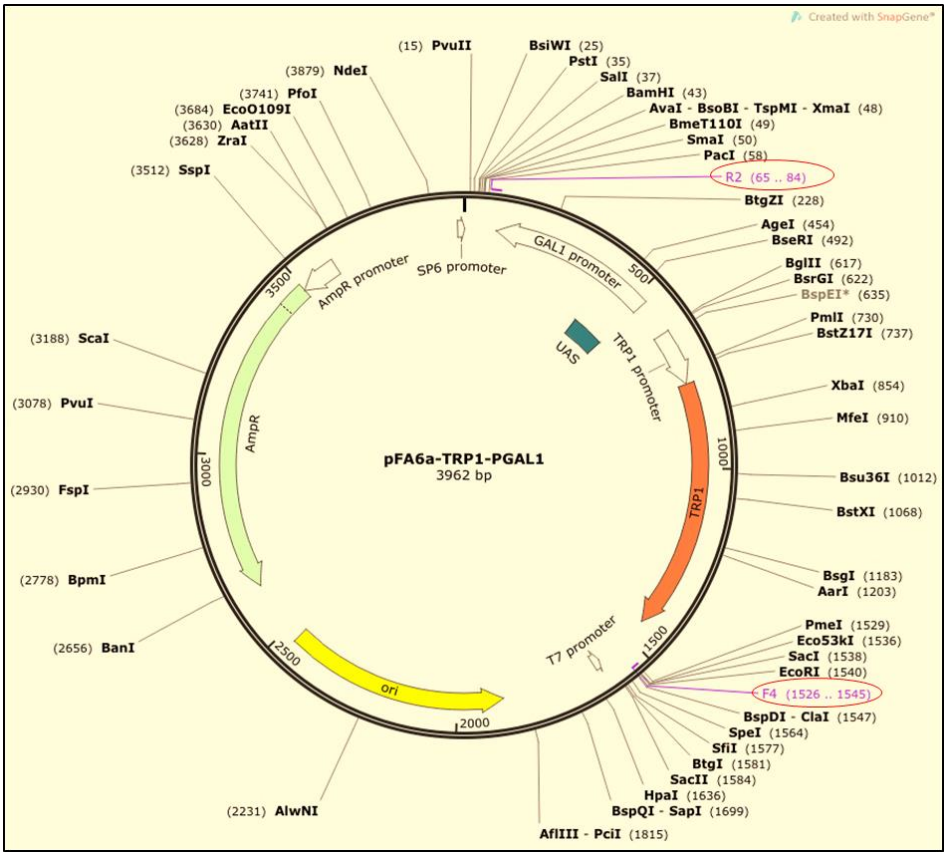

Figure 2.5. The map of yeast plasmid pFA6a-TRP1-PGAL1 (3962 bp) with unique restriction sites.
The map of circular plasmid showing unique restriction sites, primer sites and the TRP1 marker for N-terminus deletion (http://www.snapgene.com).

2.3.2.8.4 Hybrid primers for *cdc13-1* N-terminal deletion cassettes

The hybrid primers for the *cdc13-1* N-terminus deletion (NTΔ) consist of a 50 and 48-mer 5' gene-specific parts (Figure 2.6) and a 20-mer 3' modulating DNA part selected from the yeast plasmids pFA6a-TRP1-pGAL1 (pDL515) (Figure 2.7; Table 2.3) or pFA6a-HIS3MX6-PGAL1 (pDL516); both plasmids utilise common sequences, i.e.,'F4' and 'R2' for forward and reverse primers respectively for 3'ends (Longtine *et al*., 1998)., however, with amplicons of different size. The forward primer (FT-N1) for NTΔ contains 50 nucleotides from just upstream of the *CDC13* start codon whereas the reverse primer (RT-N1) consists of 48 nucleotides from the middle of *CDC13* ORF and with one start codon (CAT) in the complementary strand to start transcription in the middle while preserving the remaining amino acid sequence/protein. The resulting chimeric primers can be used with either plasmid template with a size-specific amplified cassette to delete the N-terminus with tryptophan or histidine marker.

Selection of the gene-specific guide sequence for 5' ends of hybrid primers from the *CDC13* sequence for NTΔ

CDC13 sequence ORF 1-2775: >YDL220C Chr 4 from 62044 to 65218

TGTGGATTATTTAATATGTACATGCAGCCTTGATTAACGTGATTATACTTTTTAAACCTT
TGATATCCAAATTTTTCAACGTCATAAGAGACGCGAAGGCCTAGTGAGATGCGAAATGCT
AATTCAAAATGGAAATTTAAGAATATATTCATATATGTTTCTCTTTGGATACGAATGACC
GTGGAAACTATCGCCTAAAAATGGATACCTTAGAAGAGCCTGAGTGTCCTCCACAT
AAAAATCGTATTTTTGTGAGCTCGAGTAAAGATTTTGAAGGCTATCCCAGCAAAGCAATA
GTTCCCGTGCAATTCGTGGCGCTTTTAACCTCAATACACCTGACTGAAACAAAATGTTTG
CTAGGCTTTTCTAATTTTGAGAGGCGAGGAGATCAATCCCAAGAAGATCAATATTTAATC
AAACTGAAGTTCAAAGATAGGGGCTCGGAGAGGTTAGCCCGGATCACTATTTCCTTACTT
TGCCAATACTTTGATATTGAACTGCCAGATTTAGATTCTGACTCAGGCGCATCCCCAACA
GTAATACTGAGAGATATTCACCTTGAAAGGTTATGTTTTTCAAGTTGTAAAGCTTTATAT
GTATCAAAACACGGGAACTATACTCTATTCTTAGAGGACATAAAACCGTTGGATTTGGTA
AGTGTGATAAGCACCATATCTACAAAATCGACAAATAGCAGCAAGCATTCGTCATCAGAA
CTTATTTCAGAATGTGATTTGAACAACTCACTTGTGGATATCTTCAACAATTTAATAGAA
ATGAATAGAGACGAGAAAAACAGGTTTAAATTTGTAAAGTTGATTCACTACGATATAGAA
CTAAAAAAGTTCGTTCAAGACCAACAAAAGGTATTATCGCAGAAATCAAAAGCCGCAGCA
ATTAATCCTTTCTTTGTGCCAAATAGACTAGGGATACCTTACATTGAATCCCAAAACGAA
TTCAACTCGCAGCTTATGACGCTTAATGTAGATGAACCGACCACAGATATAAGCAACATG
GGAGAGGAAATGCATGACAGCGCAGATCCCATTGAGGATTCAGATTCCTCAACTACCTCC
TCTACCGGGAAATATTTCAGCTCAAAATCCTACATCCAGTCACAGACACCTGAAAGGAAA
ACAAGCGTACCAAATAATTGGCACGATGATGATTCCGGAAGCAAGAGGAAGAGAAAGCTT
TCTTTCCACAGTCCGAACGCGTCCTCAATCCGCAAAGCCATCAGTTATGAGCAACTTTCC
CTAGCTAGTGTAGGCTCAGTTGAAAGGTTAGAGGGCAAAATTGTTGGCATGAATCCACCT
CAATTCGCCAGTATAAATGAGTTCAAATATTGCACATTGAAATTATATTTTACGCAGCTC
TTACCAAATGTCCCAGACAAGGTCCTGGTGCCAGGCGTCAATTGCATTGAGATCGTTATC
CCGACGAGAGAGCGAATCTGTGAGCTCTTCGGTGTTTTAAACTGTCAAAGCGACAAGATA
TCGGATATTTTACTACTGGAAAAGCCTGATCGAATTTCCGTCGAAGTTGAAAGGATCCTG
TGGGACAATGACAAGACCGCCAGCCCAGGTATGGCAGTATGGAGTTTGAAGAACATTAGC
ACCGACACGCAGGCGCAGGCGCAGGTGCAGGTGCCTGCGCAATCGTCGGCGTCAATCGAT
CCGTCTCGCACAAGGATGAGCAAAATGGCAAGGAAAGACCCCACCATCGAATTCTGTCAG
TTGGGACTCGACACTTTTGAGACCAAATACATAACAATGTTTGGCATGCTAGTCTCCTGC
TCGTTTGATAAACCTGCCTTTATATCTTTTGTCTTTAGCGATTTTACCAAGAACGATATC
GTCCAAAACTATCTTTACGACAGATATCTAATAGATTACGAGAACAAGTTAGAGCTGAAC
GAGGGCTTCAAAGCCATCATGTACAAAAACCAATTCGAAACGTTTGACTCTAAGCTCAGA
AAAATATTCAACAACGGGCTAAGAGATCTACAGAACGGCCGCGATGAAAACCTTTCGCAA
TACGGCATAGTTTGTAAGATGAATATAAAAGTGAAAATGTACAACGGCAAATTGAATGCC
ATTGTGCGCGAATGTGAGCCGGTCCCGCATTCCCAAATAAGCAGCATCGCCTCGCCTTCA
CAGTGCGAACATTTAAGATTGTTCTACCAACGAGCGTTCAAGAGAATTGGCGAATCCGCA
ATTTCACGCTATTTCGAAGAGTACCGGAGGTTTTTCCCCATACATAGAAACGGTTCTCAT
CTCGCGAAACTGAGGTTCGATGAAGTAAAGCATGAACCAAAAAAATCACCCACTACACCA
GCTCTCGCAGAACACATACCCGACCTGAATGCAGACGTGTCCTCCTTCGATGTAAAGTTC
ACAGATATATCTTCTCTCTTGGACTCCTCGGCTCGCCTCCCGCGCCCACAGCAAACACAC
AAGAGCAACACATTATACAGTTGCGAGGGCCGTATCATCGCCATCGAGTACCACGCATCT
GATCTCTGCTTCCATATCACGAATGAGCTCCCACTTTTACAAACCCGCGGCTTGGCCCCG
GAGCGAGTGTTGCAACTACACATCATTACCTCCAAGAACTTTGCTTATTTTTTCAACCGC
TCAAGCGCCTACTTACAGCGTCAGCCTCTTGAGGAAAAATATACGCAATTGGCACAATTT
CTCGGCCATTCATTTAAATTCAATATAACCTCCTCGCTCACGCTGTTCCCTGACACTACC
GTGGCACTCCAGATCTGGTGCCCAATTGAATGCACCTTTCGGGAATTGCAACAACAGCTG
GCCCATCCGAAGGTTGCAGCGGCTCCTGATTCAGGGAGTCTTGATTGCGCAATTAATGCT
ACCGTCAATCCTCTGCGACTTCTTGCCGCGCAAAATGGCGTCACCGTGAAAAAGGAGGAG
GATAATGACGATGACGCCGGAGCCGTTCCCACCTCGTAAGACATGATCCGCGCAGCCCAA
CGCGGCGGTGCCAAATTGCAGTGACGTCTCGGAGTAATATAAAAAAAAAAGACCAAATAA
CCAAATTTAAGGGTGCTCTGAATATAAGGGAGTGGAACGTTTTCACACGAAGGAAAAGGG
AAAGAGGGGAGTGGTAAGAAGCAAGAGTCAATGAAAGGTCTTCCTTCCTTCTTGATGCT

Figure 2.6. Primers design for *cdc13-1* N-terminus deletion: selecting the 5' ends of the hybrid primers. *CDC13* ORF (1-2775) with upstream and downstream sequences with each being 200 nucleotides in length, accessed from *Saccharomyces* Genome Database (SGD) (http://www.yeastgenome.org/). Nucleotide sequences shown in red were selected to design 5' targeting sequences for *cdc13-1* N-truncation.

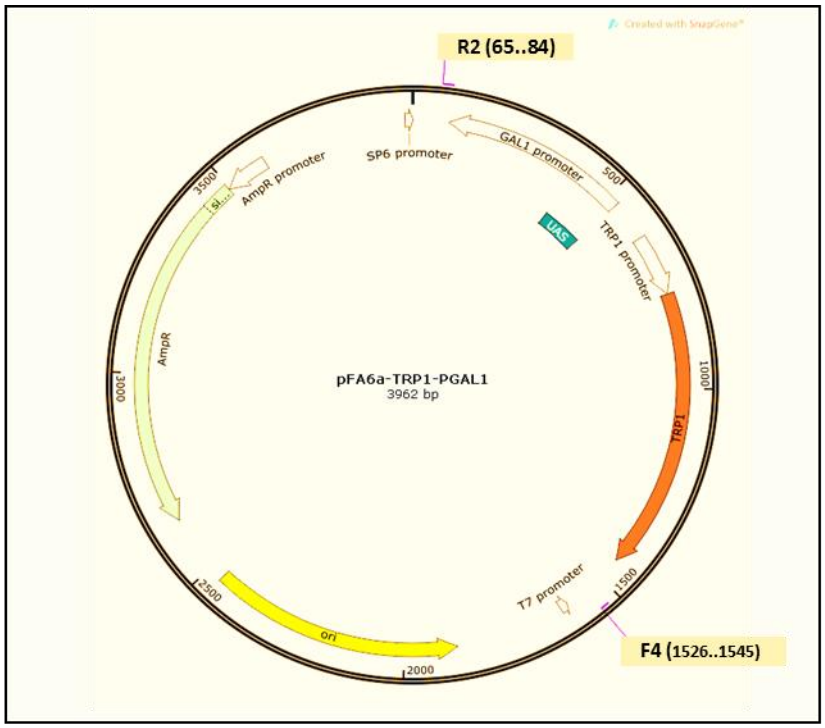

A

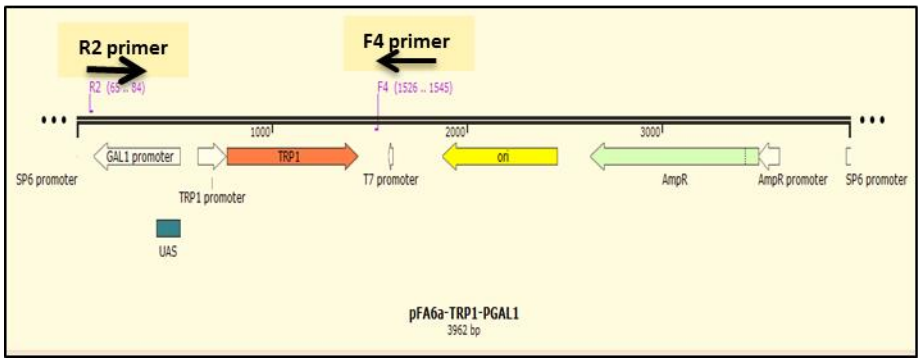

B

Figure 2.7. Map of yeast plasmid pFA6a-TRP1-PGAL1 (3962 bp) showing positions of F4 and R2 primers and inducible promoter.

(**A**) Map of the circular plasmid (http://www.snapgene.com/).

(**B**) Map of the linear plasmid.

Plasmid map shows TRP1 marker under TRP1 promoter and the location of F4 and R2 primers used for truncating N-terminus of *CDC13* without adding any tags (Longtine *et al*., 1998).

The expected PCR product with 40 nucleotide gene-specific hybrid primers has been reported to be 1.558 kb with the TRP1-PGAL1 marker (Longtine *et al*., 1998), however, considering the size of the guide sequence as 50 and 48 nt for forward and reverse primers, the size of the PCR amplicon (deletion cassette) was estimated to be ~1.576 kb for NTΔ.

The marker cassette containing TRP1-PGAL1 or HIS3MX6-PGAL1 will replace the first 1389 nt of Cdc13 ORF sequence resulting in NTΔ::TRP1-PGAL1 (Figure 2.8) or NTΔ::HIS3MX6-PGAL1 depending upon the template plasmid used.

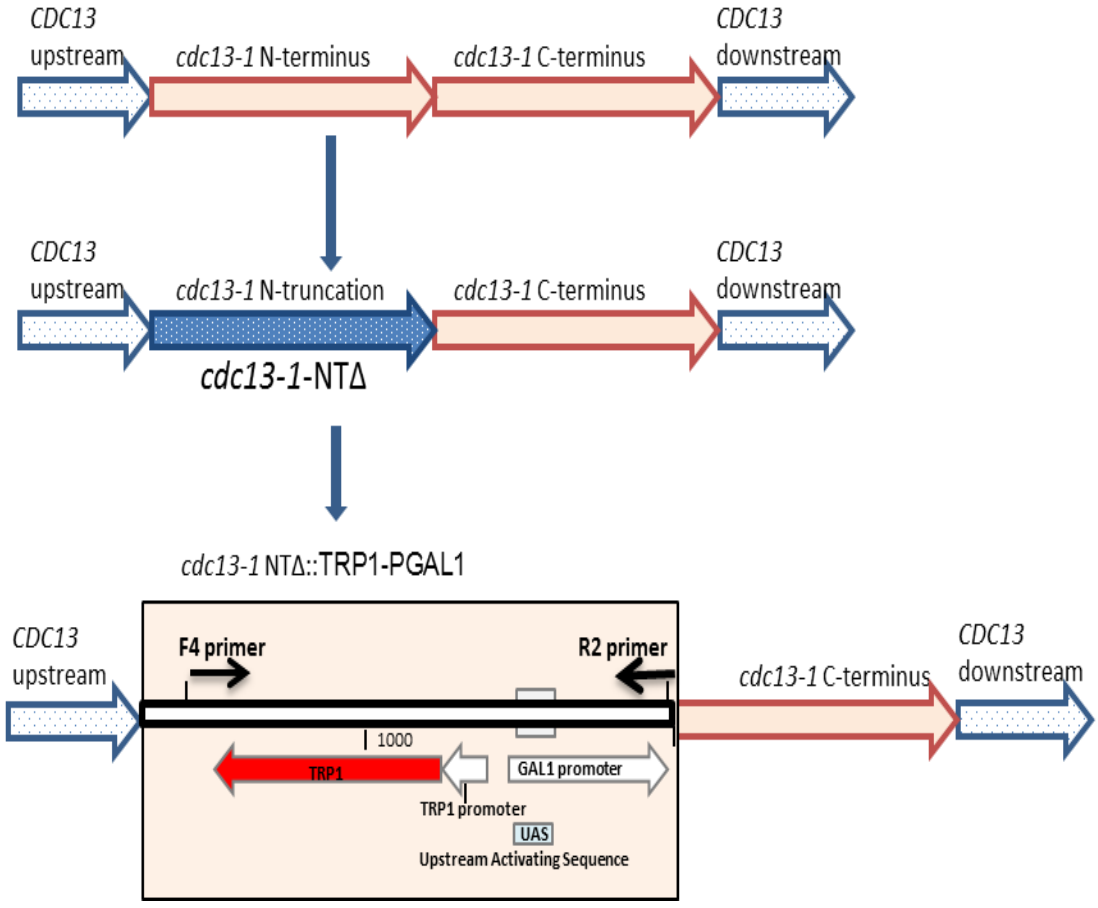

Figure 2.8. Diagrammatic representation of *cdc13-1* N-terminus truncation (NTΔ) using TRP1-PGAL1 deletion cassette.

2.3.2.8.5 Plasmid selection for *cdc13-1* C-terminus deletions

To delete the C-terminus, the second half of the *cdc13-1* yeast plasmid pFA6a-GFP(S65T)-HIS3MX6 (4698 bp) was utilised . The HIS3MX6 DNA module is similar to the marker module of plasmid pFA6a-HIS3MX6 (Figure 2.9) used for the full gene deletion construct with the heterologous *his5*$^{+}$ marker gene of *S. pombe* and *Saccharomyces kluyveri* origin. However, it also contains the ADH1 terminator to stop the replication of truncated transcripts of gene of interest *e g., cdc13-1* C-terminus truncated construct in this case.

The HIS3MX6 produces imidazoleglycerol-phosphate dehydratase, required for histidine biosynthesis. This marker gene is controlled by a strong promoter and terminator from the *TEF* gene of filamentous fungus *A. gossypii*. The marker module is provided with ADH1 terminator to terminate the expression of the N-terminus half of the *CDC13* gene.

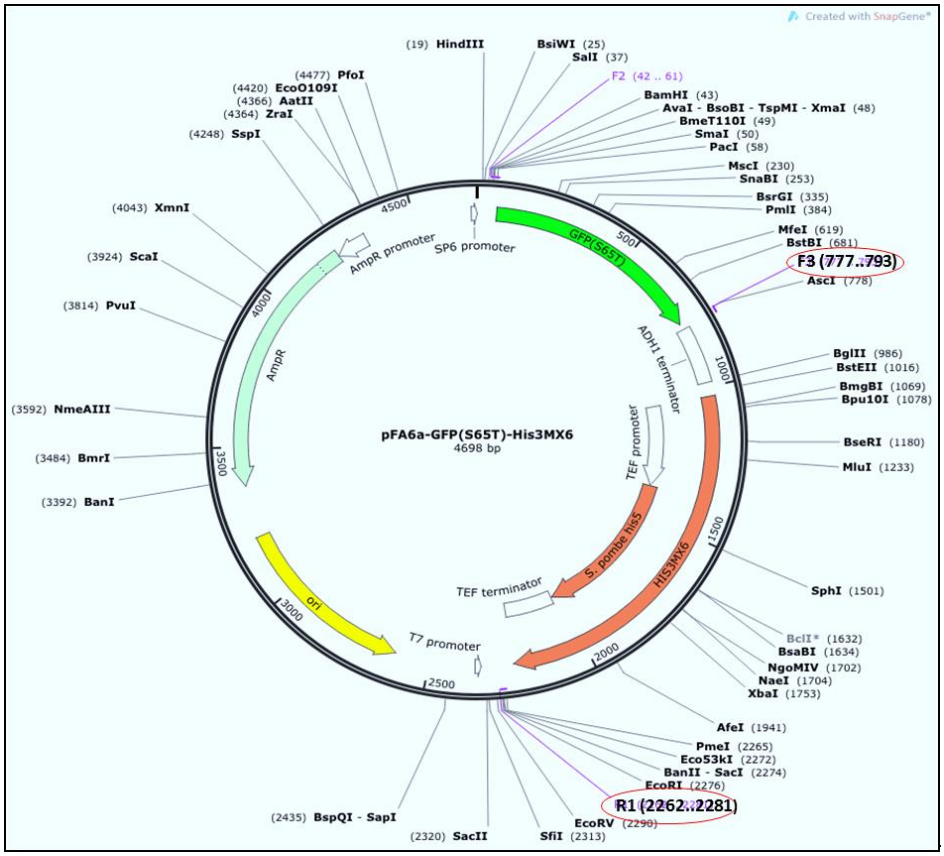

Figure 2.9. The map of yeast plasmid pFA6a-GFP(S65T)-HIS3MX6 (4698 bp) with unique restriction sites. The map of circular plasmid DNA shows primer sites and the HIS marker for C-terminus deletion with or without GFP tag (accessed from www.snapgene.com) under TEF promoter.

2.3.2.8.6 Hybrid primers for *cdc13-1* C-terminal deletion cassettes

The hybrid primers for *cdc13-1* C-terminus deletion (CTΔ) consist of a 50/51-mer 5' gene-specific part and a 20-mer 3' modulating DNA part from plasmid pFA6a-GFP(S65T)-ADH1-HIS3MX6 (pDL504). The forward primer (FT-C2) for CTΔ contains 50 nucleotides from the middle of *cdc13-1* including one stop codon 'TGA' at the end to terminate transcription after the N-terminus half of the Cdc13-1 protein whereas the reverse primer (RT-C2) consists of 51 nucleotides from the end of *CDC13* ORF sequence, just downstream of the stop codon 'TAA' as shown in Figure 2.10.

Selection of the gene-specific guide sequence for 5' ends of hybrid primers from the *CDC13* sequence for CTΔ

CDC13 sequence: >YDL220C Chr 4 from 62044 to 65218

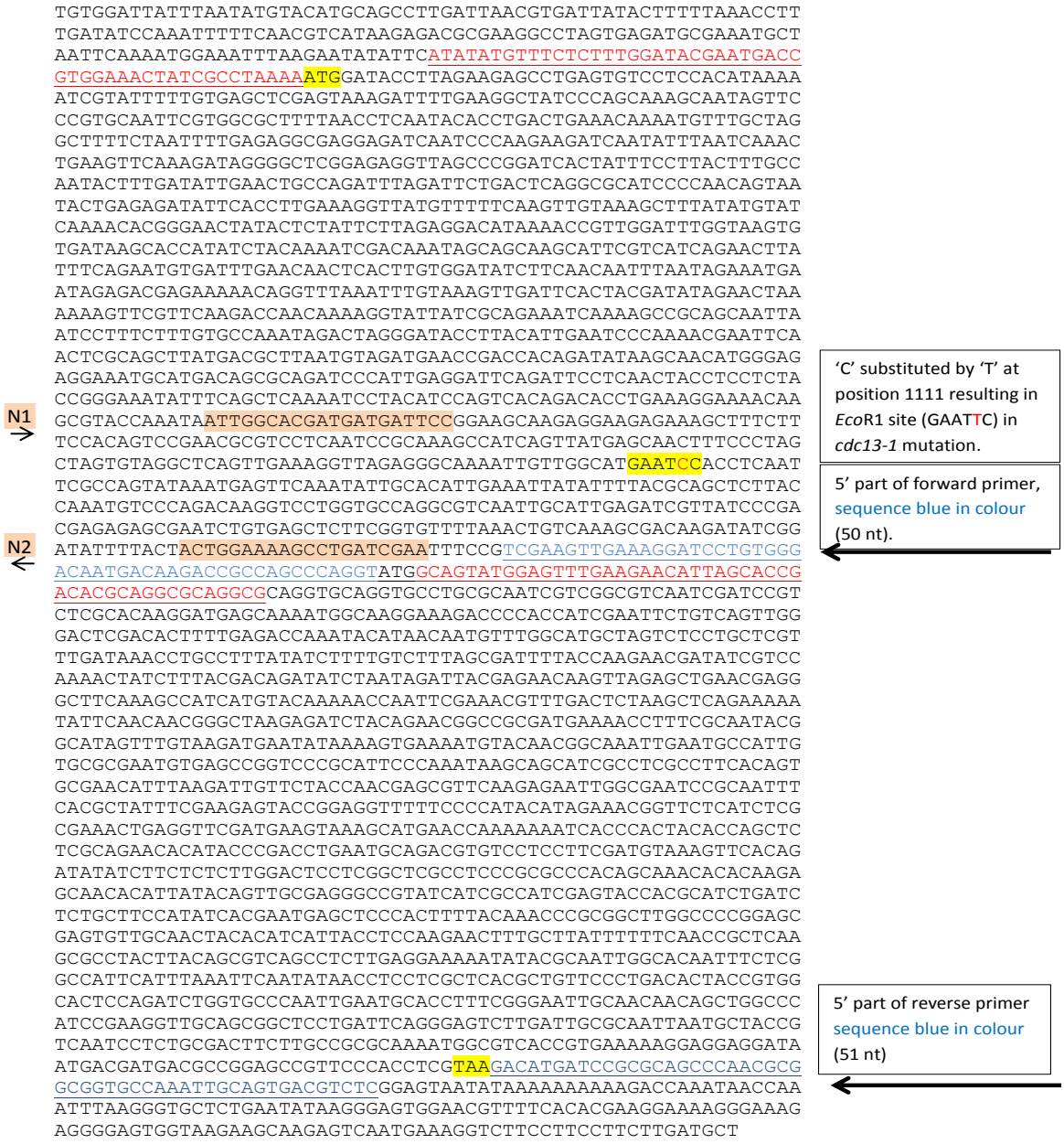

Figure 2.10. Primers design for *cdc13-1* C-terminus deletion: selecting the 5' part of the hybrid primers. *CDC13* ORF (1-2775) with upstream and downstream sequences with each being 200 nucleotides in length, accessed from *Saccharomyces* Genome Database (SGD) (http://www.yeastgenome.org/). Nucleotide sequences shown in blue were selected to design 5' end of hybrid primers for *cdc13-1* C-truncation.

2.3.2.8.6.1 Selection of sequence for 3' part of hybrid primers from the modulating plasmid sequence for CTΔ

The 3' part of hybrid primers 'F3' and 'R1' sequences for forward and reverse primers were picked from the ADH1-HIS3MX6 marker module as shown in Figure 2.11 and Table 2.3 (Longtine *et al*., 1998).

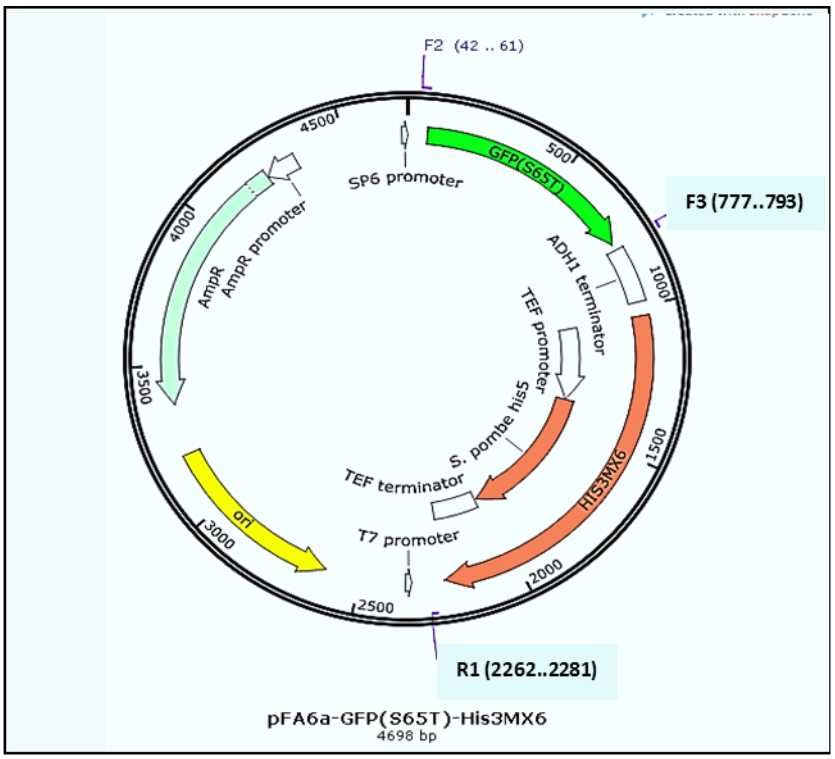

A

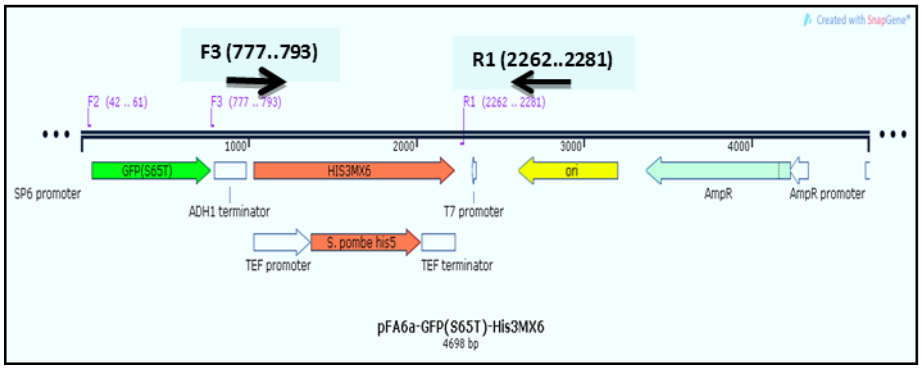

B

Figure 2.11. Map of yeast plasmid pFA6a-GFP(S65T)-HIS3MX6 (4698 bp) showing positions of F3 and R1 sequences and HIS3MX6 marker.

(**A**) Map of the circular plasmid (http://www.snapgene.com/)

(**B**) Map of the linear plasmid.

Plasmid map shows the HIS3MX6 module, a yeast heterologous HIS3 marker (corresponding to *S. cerevisiae HIS3* gene), ADH1 terminator and F3 and R1 sequences used as 3' ends of hybrid primers to amplify the *CDC13*-C-terminus deletion cassette without adding a C-terminal GFP tag.

The expected PCR product with 40 nucleotide gene-specific hybrid primers with the GFP tag has been reported to be 2.348 kb (Longtine *et al*., 1998). However, considering the size of the GFP fragment ~710 bp or 713 bp (Chalfie *et al*., 1994) the size of the PCR amplicon (deletion cassette) for CTΔ was estimated to be ~1.680 kb without the GFP tag.

As shown in Figure 2.12, the PCR-amplified marker cassette HIS3MX6 will replace 1389 nt of the ORF of *cdc13-1* (from 1387 to 2775 nt) in homologous recombinants resulting in *cdc13-1* CTΔ::ADH1-HIS3MX6 construct.

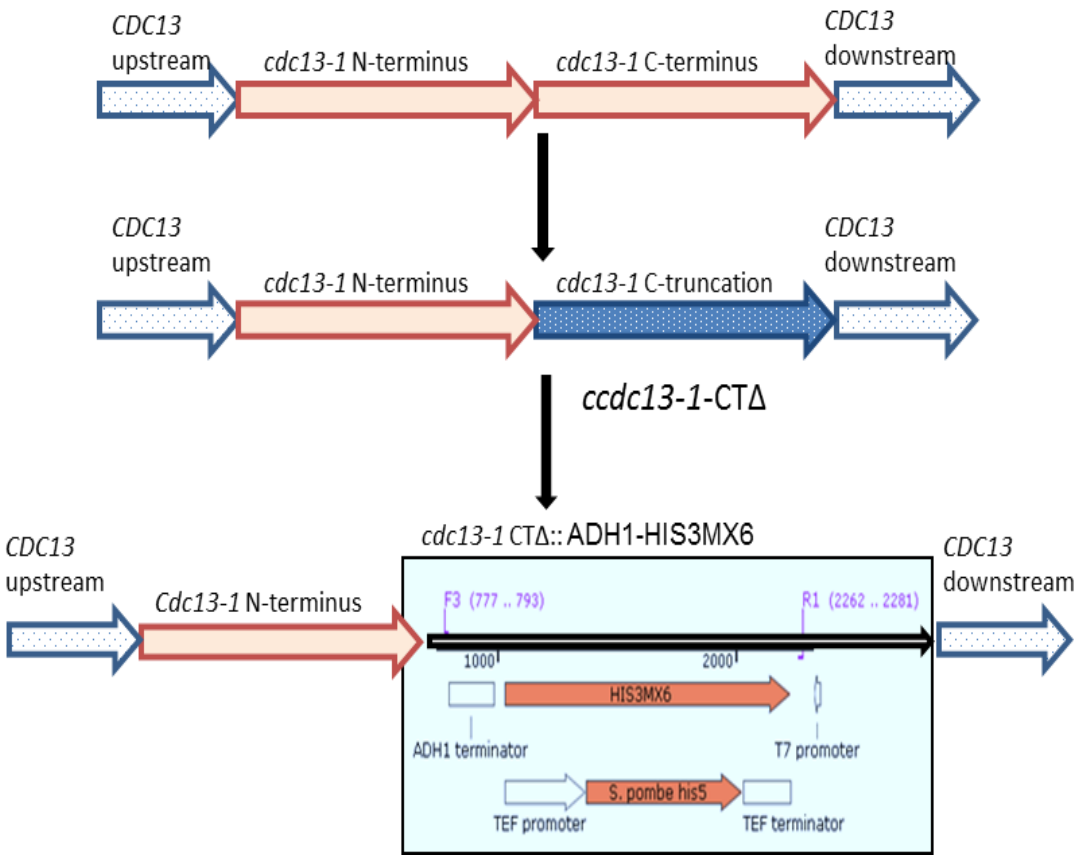

Figure 2.12. Diagrammatic representation of *cdc13-1* C-terminus truncation (CTΔ) using HIS3MX6 deletion cassette of modulating plasmid pFA6a-GFP(S65T)-HIS3MX6).

2.3.2.9 PCR amplification for transforming modules

To amplify the *CDC13* full gene deletion, N-terminus and C-terminus truncation cassettes, yeast plasmids pDL501, pDL515/516 and pDL504 DNA were used as PCR templates with forward and reverse primers (Table 2.3). Plasmid DNA were diluted 10 times to a final concentration of ~0.050 µg/µl in TE buffer or water and used as a template in PCR reaction (~100 ng). The reaction mixture contained 0.5 µl of each forward and reverse hybrid primer from 100 µM stocks, 25 µl 2x PCR master mixes (GoTag Green master mix, Promega #7112) and with ~100 ng of template plasmid in a final volume of 50 µl.

Thermocycler programming carried out as follows:

For full *cdc13-1* deletion cassette with primers N-F1 (C03) and C-R3 (C08):

1.	95°C for 5 min (minutes)		(Denaturing step)
2.	94°C for 1 min	30 cycles	(Denaturing step)
3.	58°C for 1 min		(Primer annealing step)
4.	70°C for 1 min and 20 sec		(Extension step)
5.	30 cycles from step 2 to step 4		
6.	72°C for 10 min		
7.	4°C for ∞		

For *cdc13-1* N-terminus deletion cassette with primers FT-N1 (D09) and RT-N1 (D10):

1.	95°C for 5 min		(Denaturing step)
2.	94°C for 1 min	30 cycles	(Denaturing step)
3.	58°C for 1 min		(Primer annealing step)
4.	70°C for 1 min and 30 sec		(Extension step)
5.	30 cycles from step 2 to step 4		
6.	72°C for 10 min		
7.	4°C for ∞		

For *cdc13-1* C-terminus deletion cassette with primers FT-C2 (D11) and RT-C2 (D12):

1.	95°C for 5min		(Denaturing step)
2.	94°C for 1 min	30 cycles	(Denaturing step)
3.	55°C for 1 min		(Primer annealing step)
4.	68°C for 1min and 40 sec		(Extension step)
5.	30 cycles from step 2 to step 4		
6.	72°C for 10 min		
7.	4°C for ∞		

The amplified fragments (5 µl) were analysed on 0.8% agarose gel to confirm the desired fragment size. PCR amplification generated a *HIS3*-containing deletion amplicon of ~1.4 kb for the full gene deletion with *CDC13*-specific flanking guided sequences. PCR amplicons generated for N-truncation with *HIS3* marker and *TRP1* marker were ~1.9 kb and ~1.5 kb respectively. For C-truncation, the deletion amplicon with the *HIS3* marker was ~1.6 kb. These deletion amplicon DNAs were used to transform yeast to integrate the marker in the yeast genome through a recombination process resulting in full *cdc13-1* gene knockout, N- and C-terminus deletion.

2.3.2.10 Purification of PCR amplicons

For yeast transformation, amplified DNA was purified as follows:

2.3.2.10.1 Sodium acetate and isopropanol precipitation

In the first attempt the PCR product from seven individual reactions was combined (~350 µl) and mixed with 35 µl of 3 M sodium acetate buffer (1/10 volume of combined reactions). An equal volume of isopropanol was added, mixed immediately and centrifuged to precipitate the DNA pellet at 12,470 x g (13,000 rpm) for 25 minutes. Isopropanol was carefully decanted and pellet was washed with 70% ethanol to remove salts at 12,470 x g (13,000 rpm) for 5-10 min in a bench top centrifuge. The pellet was air dried and re-suspended in an appropriate volume of sterile water or 1x TE buffer. Purified DNA was stored at -20°C until further use.

2.3.2.10.2 DNA purification by using gel extraction method

DNA was excised from the gel and purified following the QIAquick (#28704) protocol.

2.3.2.10.3 DNA purification by phenol-chloroform method

The amplified DNA was resolved on agarose gel. The right size DNA band was excised and melted at 37^{o}C in a sterile eppendorf tube. An equal volume of phenol:chloroform:isoamyl alcohol mixture (25:24:1) was added to the DNA, and contents of the tube was mixed thoroughly by vortexing. The turbid mixture was centrifuged at room temperature at 7,378 x g (10,000 rpm) for 5 minutes. The clear upper phase was removed carefully and precipitated with a 1/10 volume of 3 M sodium acetate and 2.5 volume of ethanol, followed by washing in 70% ethanol. The pellet of DNA was re-suspended in the required volume of sterile water or 1x TE buffer and used in transformation experiments.

2.3.2.11 Transformation of yeast competent cells with the deletion modules

A standard technique of lithium acetate transformation (Gietz *et al*., 1995) was used to transform yeast strains DLY 1272, 1296 and 1297 (haploid) with the purified amplified DNA fragments. The strains 1296-TR and 1297-TR include the *cdc13-1* mutant allele while strain 1272 contains *CDC13* gene. However all three strains contain leucine marker (*exo1*::LEU). The transformants were initially selected on medium lacking leucine and histidine for *cdc13-1* full gene deletion or its C-terminus truncated mutants. For the second round of selection, transformants were replica plated on dropout medium supplemented with tryptophan and uracil and without histidine and leucine nutrients for double markers selection. For N-terminal deletion, the transformants were selected on dropout medium lacking leucine and tryptophan to detect recombinants with N-terminus truncated Cdc13-1 mutants. The histidine/tryptophan positive colonies that appeared after 5-7 days of incubation at 30°C, were assumed to be the clones with *cdc13-1* knockout/disruption after successful integration of the marker.

2.3.2.11.1 PCR analysis of transformants

Putative clones were examined for the confirmation of gene disruption and integration of marker within genome. Selected clones were screened using PCR approach for the deletion of N-or C-terminal sequence of *cdc13-1* and for the presence of respective marker module.

2.3.2.11.2 Diagnostic PCR for *CDC13* region and marker modules

Two set of primers were designed based on the ORF of *CDC13* to confirm the N- and C-terminal sequence of gene. Figure 2.13 shows the position of the diagnostic primers and the length of the final PCR product within the coding sequence of *CDC13* (between the 'ATG' start and 'TAA', stop codons).

Diagnostic primers N1 and N2 [D04/D05] and C1 and C2 (D06/D11) were used to amplify *CDC13* N-terminus (~378 bp) and C-terminus specific fragments (~276 bp) respectively to detect full gene knockout or its N- and C-truncation as a result of recombination (Table 2.4) and integration of the *HIS* and *TRP1* markers in the yeast genome. After confirming the *cdc13-1* gene specific sequence PCR was performed to confirm marker genes, *HIS* or *TRP1* in positive transformants. The H1 and H2 primer pair was used to amplify ~1.6 kb ADH1-HIS3MX6 modular DNA, whereas T1 and T2 primers pairs were used to amplify1.9 kb HIS3MX6-PGAL1 and 1.5 kb TRP1-PGAL1 modular DNA in *cdc13-1* CTΔ and NTΔ constructs (Table 2.5).

For PCR screening, single colonies were picked up from the second round of selection and denatured at 95°C for 15-20 minutes. Two µl of clear supernatant was used as a template to set up the PCR reaction in 25 µl of reaction volume using respective forward and reverse primers. Amplified fragments, uncut (N- and C-terminus) and cut (N-terminus amplicon with *Eco*R1 enzyme) were analysed on 2.5% agarose gel for size analysis.

Figure 2.13. Diagnostic primers for the detection of *CDC13* N- and C-terminus.

The primer sequence for N- and C-terminus detection are highlighted in orange and aqua within the ORF sequence (1-2775) of *CDC13* to amplify 378 bp and 276 bp from the N- and C-terminus respectively.

Table 2.4. Diagnostic primers for N- and C-terminus detection of *CDC13* gene.

Objective	Primer name and length	Primers sequence	Origin of nucleotide sequence (*CDC13* ORF)	Length of amplified fragment
cdc13-1/CDC13 N-terminus detection	N1 (D04) 20 nt	5′-ATTGGCACGATGATGATTCC-3′	953-972	378 bp
	N2 (D05) 20 nt	5′-TTCGATCAGGCTTTTCCAGT-3′	1311-1330	
cdc13-1/CDC13 C-terminus detection	C1 (D06) 20 nt	5′-GCAAAATGGCAAGGAAAGAC-3′	1496-1515	276 bp
	C2 (D11) 20 nt	5′-GCTTAGAGTCAAACGTTTCG-3′	1752-1771	

Table 2.5. Diagnostic primers to detect integration of modular DNA in yeast genome.

Objective	Primer name and length	Primers sequence	Origin of nucleotide sequence (yeast plasmids)	Length of amplified fragment
ADH1-HIS3MX6 module detection (in CTΔ construct)	H1 (D07) 20 nt	5′-TGAGGCGCGCCACTTCTAAA-3′	F3 primer (from yeast plasmid pFA6a-GFP(S65T)-ADH1-HIS3MX6 sequence used for CTΔ)	~1.579 kb
	H2 (D08) 20 nt	5′-GAATTCGAGCTCGTTTAAAC-3′	R1 primer (from yeast plasmid pFA6a-ADH1-GFP(S65T)-HIS3MX6 sequence used for CTΔ)	
HIS3MX6-PGAL1 module detection (in NTΔ construct)	T1 (D09) 20 nt	5′-GAATTCGAGCTCGTTTAAAC-3′	F4 primer (from yeast plasmid pFA6a-HIS3MX6-PGAL1 sequence)	~1.845 kb
	T2 (D10) 20 nt	5′-CATTTTGAGATCCGGGTTTT-3′	R2 primer (from yeast plasmid pFA6a-HIS3MX6- PGAL1 sequence	
TRP1-PGAL1 module detection (in NTΔ construct)	T1 (D09) 20 nt	5′-GAATTCGAGCTCGTTTAAAC-3′	F4 primer (From yeast plasmid pFA6a-TRP1-PGAL1 sequence)	~1.481 kb
	T2 (D10) 20 nt	5′-CATTTTGAGATCCGGGTTTT-3′	R2 primer (from yeast plasmid pFA6a-TRP1-PGAL1 sequence)	

2.3.2.12 DNA sequencing

DNA sequencing was used to determine the exact sequence of nucleotides in modified DNA samples (PCR amplified fragments) used in this study and to identify the regions of possible variations and mismatches as a result of PCR amplification and homologous recombination.

To verify the sequence of Cdc13 N- and C-terminus deletion mutants (in 24 genomic clones), mutated DNAs were analysed for their nucleotide sequences at the modified region between 200 nt upstream and 200 nt downstream of *CDC13* in strains 1296-TR and 1297-TR. The DNA sequencing comprised genomic DNA isolation, primer designing for sequencing and PCR amplification of ~3 kb fragment that includes ORF sequence from N- and C-truncated *cdc13-1* clones, purification of the amplified fragment, concentration estimations through gel electrophoresis and spectrophotometry, and sequencing by using GATC-biotech facilities (the ABI Model 3730XL, machine 18127-012 Model 730).

2.3.2.12.1 Designing of primers for sequencing of DNA from N- and C-truncated *cdc13-1* mutants

For single read sequencing four primers, F1, R1, R2 and R3 (Figure 2.14) were designed for N-terminus truncated *cdc13-1* mutants by taking into consideration the primer conditions e.g. melting temperature (TM, between 52°C-58°C), primer length (18-20 bp), and GC content (40-60%) etc. Computer programmes Primer3 (http://bioinfo.ut.ee/primer3-0.4.0/) and NCBI/ Primer-BLAST **(**http://www.ncbi.nlm.nih.gov/tools/primer-blast) were used to design and analyse primers. F1 is the forward primer selected from the upstream sequence of *CDC13*, while R1 is the reverse primer selected from the tryptophan marker module DNA. The R2 primer was selected from the C-terminus half of *CDC13* ORF sequence while the R3 primer was from the downstream region of *CDC13*.

Similarly, primers F1, F2, F3 and R3 (Figure 2.15) were designed to sequence C-terminus truncated *cdc13-1* constructs. The sequencing primers, F1 (forward) and R3 (reverse) were selected from upstream and downstream sequence of *CDC13* ORF. The F2 primer was from the N-terminus half of *CDC13* gene while F3 primer was selected from the histidine marker module DNA.

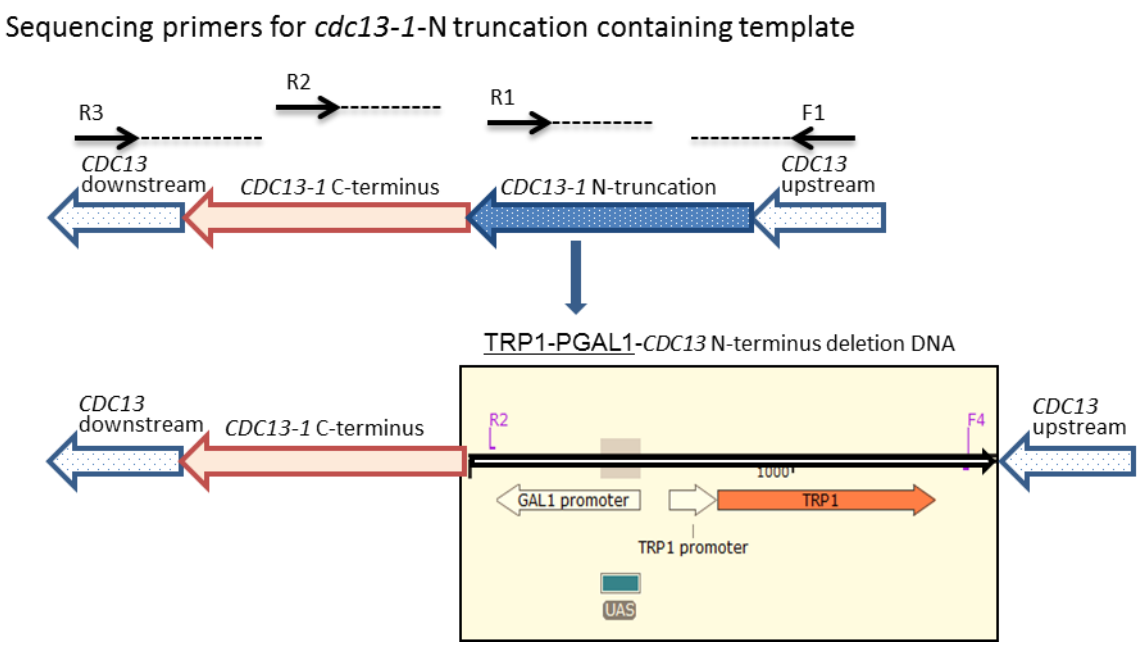

Figure 2.14. Sequencing primers for *cdc13-1*-N truncation.

Sequencing primers F1, R1, R2 and R3 were used to sequence *cdc13-1* NTΔ (TRP1-GAL1) ~3 kb template from N-terminus deletion mutants in strains 1296-TR and 1297-TR.

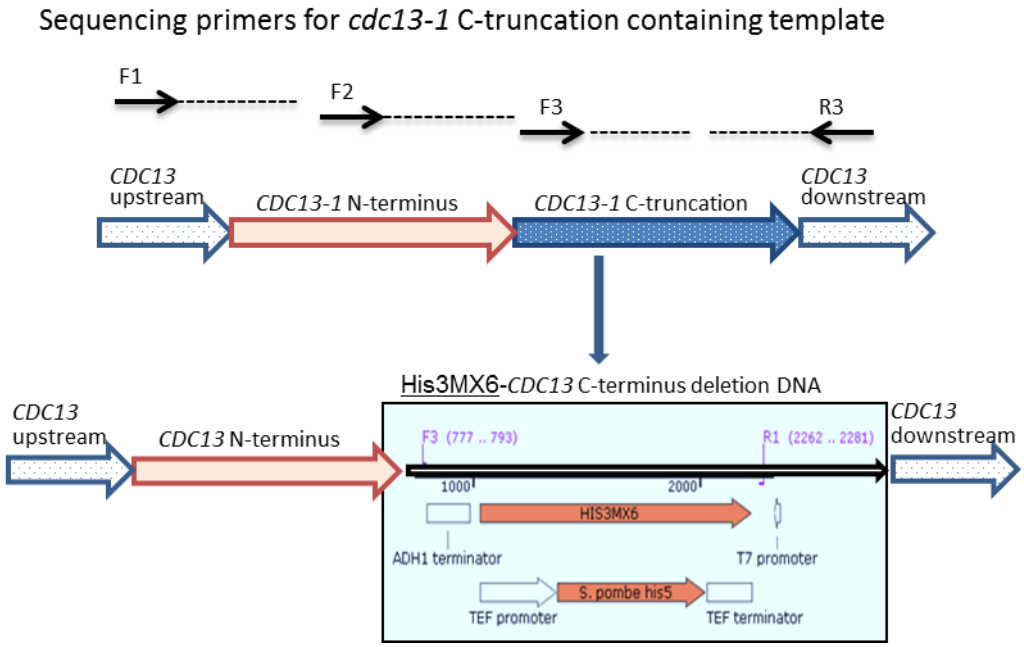

Figure 2.15. Sequencing primers for *cdc13-1*-C truncation.

Sequencing primers F1, F2, F3 and R3 were used to sequence *cdc13-1* CTΔ (His3MX6) ~3 kb template from C-terminus deletion mutants in strains 1296-TR and 1297-TR.

Primers F1, N1, N2 and R3 were used to sequence the open reading frame of *cdc13-1* (Figure 2.16) including upstream and downstream regions from survivor strains 1296-TR and 1297-TR, original strains used for *cdc13-1* N- and C-terminus modification. All these primers used for sequencing were sent in a concentration of 10 pM/µl (10 µM) in 100 µl volume to GATC-Biotech.

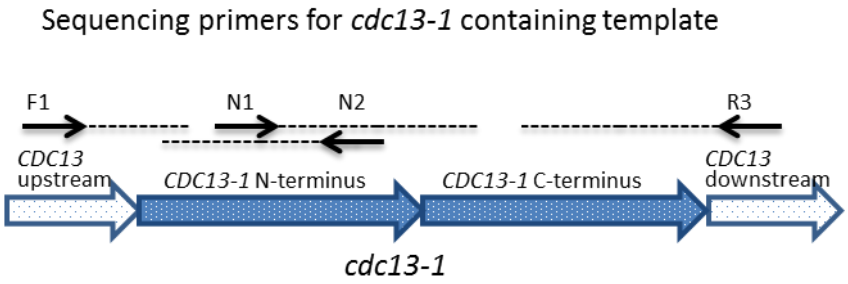

Figure 2.16. Sequencing primers for *cdc13-1*.
Sequencing primers F1, N1, N2 and R3 were used to sequence *cdc13-1* containing template from strains 1296-TR and 1297-TR.

2.3.2.12.2 PCR amplification and purification of sequencing templates

For automated sequencing, the template DNA is required to be free of impurities like proteins, RNA, polysaccharides and genomic DNA that might interfere in nucleotide reading. This was achieved by sequencing the PCR product directly rather than cloning it first. For PCR template yeast genomic DNAs were extracted following the "Yale quick method" for DNA preparation (Adams *et al*., 1998). Un cut DNAs (1-2 µl) were analysed by agarose gels (0.7-0.8 % w/v) electrophoresis in 1x TBE buffer to estimate the quality and quantity of DNA. Genomic DNA was diluted 1:100 for each sample to be used as a template in PCR amplification mixture.

PCR was performed in 50 µl of reaction volume using 1 unit of Q5 enzyme (0.5 µl), Q5 reaction buffer (10 µl of 5x enhancer and reaction buffer), 200 µM of dNTPs (1 µl) and 0.5 µM of forward [F1 (22 nt's) 5'ACATGCAGCCTTGATTAACGTG3'] and reverse [R3 (22 nt's) 5'GGTCTTCCTTCCTTCTTGATGC3'] primers with 2 µl of diluted template DNA. The resulting ~3 kb amplicon (Figure 2.17) consisted of either *cdc13-1* in the case of survivor 1296/1297-TR or N- and C-truncated *cdc13-1* with a gene disrupting modular marker in truncated mutants. The following thermo cycling conditions were used for amplifying the desired PCR product.

PCR conditions:

1.	98° C for 50 sec		(Initial Denaturation)
2.	98° C for 10 sec		(Denaturation)
3.	60° C for 30 sec	32 cycles	(Primer annealing)
4.	72° C for 90 sec		(Extension, 20 sec to 1 min/kb)
5.	32 cycles from steps 2 to step 4		
6.	72° C for 2 min		(Final Extension)

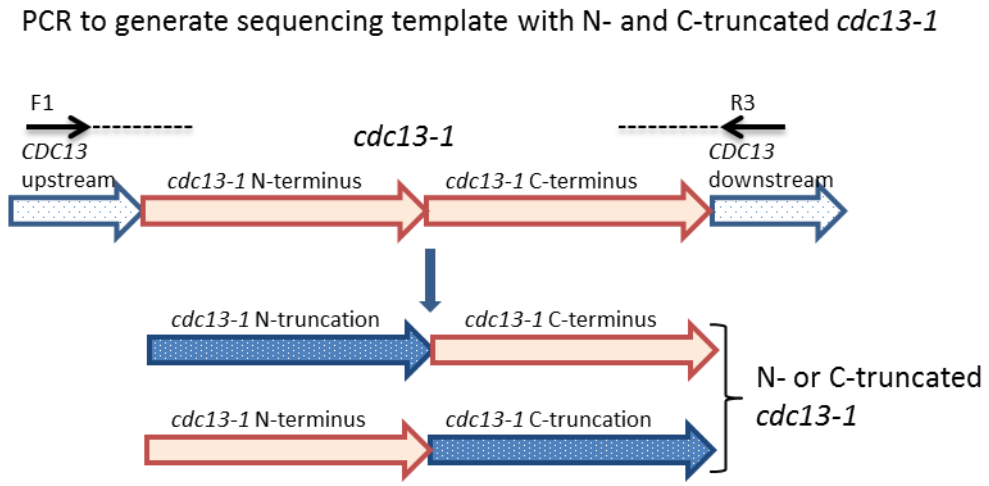

Figure 2.17. PCR to generate template for sequencing *cdc13-1* mutants.

Primers F1 and R3 were used to amplify ~3 kb template containing either fullgene or, N- /C-terminus deleted version of *cdc13-1* from strains 1296-TR and 1297-TR.

Following PCR amplification, agarose gel electrophoresis (0.7% agarose) using 1x TBE buffer was performed to confirm the presence of the desired fragments and also for an estimation of qualitative concentration. More precisely, the concentration of purified amplicons was estimated by spectrophotometer, Nanodrop 2000.

2.3.2.12.3 DNA quantification

DNA samples were prepared as per the "GATC" DNA sequencing facility's recommendation for purity and concentration. Amplicons were purified by the Promega's spin columns method by following the user manual and by phenol-chloroform method. In phenol/chloroform extraction PCR-amplified 3 kb fragments were cleaned up of unwanted PCR products by the phenol/chloroform mixture. An equal volume of amplified products was extracted once with phenol/chloroform/isoamyl alcohol (25:24:1) mixture followed by chloroform/isoamyl alcohol (24:1) extraction. Purified DNA was precipitated with ethanol after addition of 1/10 volume of 3 M potassium acetate buffer followed by washing with 70% ethanol to remove salts. Purified DNA was eluted in sterile water. DNA concentration and purity of the final purified PCR

products was calculated by both gel electrophoresis (see section 2.4.2.5) and spectrophotometric analysis at 260 and 280 nm in 1 µl volume using the Nanodrop 2000). For DNA quantitation by gel electrophoresis the known volume of purified DNA were run along with known masses of quantitative marker. Using ladder bands as a reference the intensity of band of interest was compared to reference standard that was similar to band in question and calculated after correction in for the difference in volume. Typical DNA concentrations were estimated to be between 15 and 42 ng/µl. All 26 samples (50 µl for each mutant) were prepared in similar manner and sequenced in GATC-Biotech (platform Sanger ABI 3730xl).

2.3.2.12.4 Sequencing data analysis from text data and chromatograms

Purified amplicons (10-50 ng) and 10 pM/µl of each primer were sent to the GATC-Biotech sequencing service. The Applied Biosystems 3730xl DNA analyser was used for automated sequencing. DNA sequencing data was evaluated by the Phred20 system using the Basecaller KB 1.4.1.8. Sequencing results (electronic files) were obtained in the form of text files (nucleotide sequences) and chromatograms. Four chromatograms were obtained for each sample DNA in accordance with each of the four primers used for sequencing PCR products. The expected nucleotide sequences for ~3 kb PCR product containing either *cdc13-1* or as a result of marker module integration *cdc13-1* NTΔ-TRP1-GAL1 or *cdc13-1* CTΔ-HIS3MX6 were constructed using free online resources for yeast *CDC13* gene (http://www.yeastgenome.org) and for yeast plasmids (https://www.snapgene.com/resources/plasmid_files/yeast_plasmids/) and were used as a reference sequences for the analysis of N-and C-truncated mutants's sequenced DNA.

Due to design of primers, the automated sequencing of each mutant (N- or C-truncated) resulted in four overlapping chromatograms and text data files (sequence data). Using online software for DNA sequence analysis and alignments such as NCBI's BLAST engine (http://blast.ncbi.nlm.nih.gov/Blast.cgi), each text file was compared and aligned with the reference sequence (theoretical construct) to map fragments and to find any mismatches. Multiple nucleotide sequence alignment was conducted using online tool MUSCLE (MUltiple Sequence Comparison by Log-Expectation; http://www.ebi.ac.uk/Tools/msa/muscle/). All mismatches, especially possible errors near the end and beginning of each run were manually double-checked and further verified against the sequence chromatogram of that text data file. The position of all mismatches or mutations, i.e., insertion, deletion or point mutation were mapped on the related construct sequence and determined for each of 24 mutants and also for *cdc13-1* for the original strains used for N- and C-truncation. Finally, the coding sequence of each construct was analysed for the amino acid sequence through translation by using online resources (http://bio.biomedicine.gu.se/edu/translat.html) and any mutations found in the protein sequence were documented.

2.3.2.13 Total DNA isolation of yeast

"Yale quick method" was adopted for the extraction of total DNA (Adams *et al*., 1998) from *S. cerevisiae* strains. Different strains of *S. cerevisiae* including wild type, *cdc13-1* N- and C-truncated mutants and *CDC13* and *STN1* single and double deletion mutants were grown on YEPD agar media at 23°C, 30°C and 37°C for three days. Two independent mutants of each genotype were used. A loop-full of cells was collected for each sample and transferred in 2 ml eppendorf tubes. Cells were re-suspended in 250 µl of lysis buffer A [containing 0.1 M EDTA (pH 7.5) and 14 mM β-mercaptoethanol and ~1 mg/ml of zymolyase]. The resulting cell suspension was incubated at 37°C with intermittent vortex mixing to facilitate cell wall digestion and rendering the cells to spheroplasts. After incubation of approximately 45-60 minutes, 100 µl of buffer B [containing 0.25 M EDTA (pH 8.5), 0.5 M Tris base and 2.5% (w/v) SDS] was added to each tube. Cells were mixed by inversion and the mixture was incubated further at 65°C for 30 minutes for lysis. Following the lysis, 100 µl of neutralising buffer (5 M potassium acetate) was added to each sample. After quick mixing by inversion, cell lysates were incubated on ice for 30 minutes to precipitate the denatured proteins. Precipitated cell debris was collected by spinning tubes at 16,162 x g (14,800 rpm) for at least 20 minutes. The supernatant was transferred to new tubes containing 720 µl of 100% ethanol and mixed by inversion. The precipitated DNA was spun out by centrifugation at maximum speed for 5 minutes. Supernatant was discarded by decanting tubes thoroughly and un-dried DNA pellets were mixed with 200 µl of TE buffer (containing 100 mM Tris-HCl pH 7.5 and 10 mM EDTA) and 1 mg/ml of RNAase A. DNA was re-suspended slowly by incubating tubes at 37°C for 35 minutes with occasional vortex mixing. Total DNA was re-precipitated with 200 µl of isopropanol through bench top centrifugation for 10 minutes at maximum speed. The supernatant was discarded and DNA pellets were washed with 150 µl of 70 % ethanol to remove salts through centrifugation. Finally, DNA pellets were air-dried and dissolved in an appropriate volume of TE buffer (50-100 µl) by incubating the tube at 37°C followed by 4°C incubation o/n. For each sample, 2 µl of DNA (mixed with 2 µl of 5x DNA dye and 6 µl of 1x TE buffer) was examined on 0.7% agarose gel to roughly estimate the quantity and quality of DNA. The resulting preparation was diluted to a desired concentration, or used directly for downstream applications such as PCR reactions and for *Xho*1 digestion for Southern blot hybridisation analysis.

2.3.2.14 Southern blot hybridisation analysis of telomeric DNA

Southern blot hybridisation was performed to find if there are any differences in telomeric DNA patterns and telomere length in the presence or absence of essential telomere capping proteins Cdc13 and Stn1. Southern blot hybridisation analysis comprised the digestion of genomic DNA, its separation on the gel, transfer onto membrane and finally detection of terminal

restriction fragments of telomeric DNA by an enzyme labelled probe hybridising with Y'+TG telomeric regions. This probe was used to hybridise and detect telomere length patterns.

2.3.2.14.1 Digestion of total DNA and agarose gel resolution

Total DNA extracted from different yeast cells was digested with the *Xho*1 enzyme using 1 µl (20 U) of restriction enzyme, 2.5 µl of 10x reaction buffer and 0.25 µl of 100x BSA in 25 µl of reaction volume at 37°C overnight (16-18 hrs). The digested DNA (8-12 µl with 1x DNA dye) was resolved by electrophoresis on 0.8 % agarose gel at low voltage (40 volts) overnight in 1x TBE buffer containing 0.5 µg/ml ethidium bromide in gel. The gel with well-separated DNA restriction fragments was photographed and further processed for blotting DNA fragments on Hybond-N^+ positively charged nylon membrane.

2.3.2.14.2 Blotting of separated DNA fragments onto membrane

Acid depurination: The agarose gel containing resolved DNA fragments was rinsed briefly in deionised water. The gel was soaked three times for 10 minutes in diluted acid (0.25 M HCl solution) with gentle shaking. The acid treatment depurinates the DNA resulting in the partial dehydrolysis of the DNA. The covalent bond between a purine base and deoxyribose sugar in DNA is more sensitive to HCl than the bond between sugar and pyrimidine base, the treatment of gel with acid will remove purines from DNA to make transfer of large pieces of DNA easy. At the end of acid treatment the fragile gel was rinsed quickly and carefully in deionised water.

Alkali denaturation: The DNA in gel was denatured further by soaking the gel twice for 20 minutes in alkaline solution containing 1.5 M NaCl and 0.5 M NaOH. The alkali treatment rendered DNA single stranded to facilitate its binding with the membrane and eventually with the complementary probe sequence. The gel was rinsed again briefly in deionised water.

Neutralisation: Finally, the gel was soaked twice for 20 minutes in 1 M ammonium acetate ($NH_4CH_3CO_2$) solution to neutralise DNA. The size of the gel was measured. Two pieces of 3 MM Whatman paper and one piece of Hybond N^+ membrane were cut to the size of the gel. The membrane was labelled on one side for orientation and soaked in $NH_4CH_3CO_2$ solution. One piece of the 3 MM paper was also soaked in $NH_4CH_3CO_2$ solution. Figure 2.18 depicts the setup for DNA transfer from agarose gel to the membrane over a weekend (one to two overnights). After DNA transfer, this set up was disassembled, and the side of membrane in contact with DNA was marked. The membrane with blotted DNA was washed briefly with 2x SSC buffer. The wet membrane was exposed to the UV cross-linker (with DNA side towards UV) to bind DNA permanently onto membrane. The membrane was stored at 4°C until hybridisation.

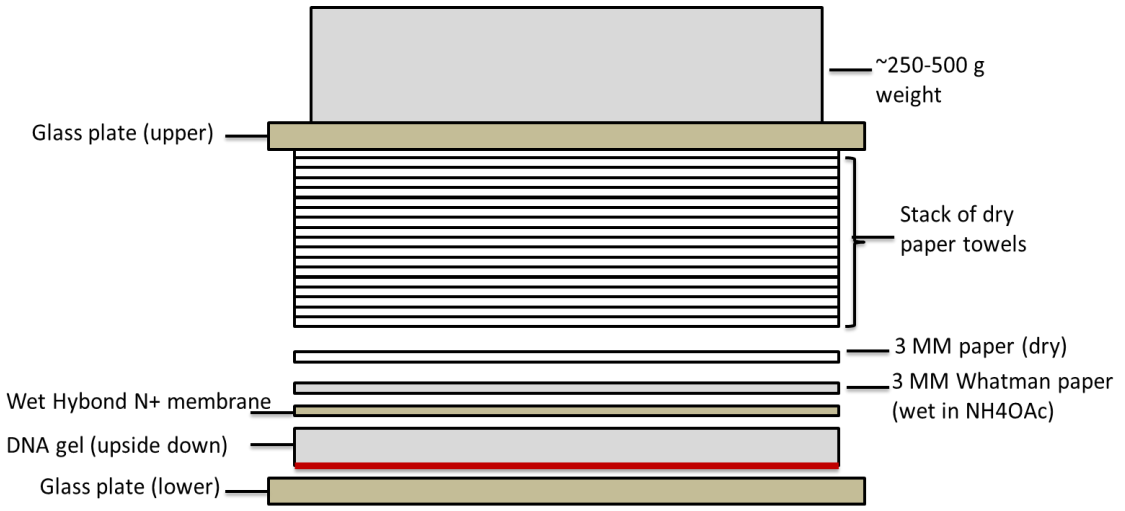

Figure 2.18. Southern blot setup for the transfer of DNA from gel to Hybond N^+ membrane.

2.3.2.14.3 Preparation of the labelled probe

The plasmid 987 that contains Y'+TG fragment of ~1 kb was kindly donated by Professor David Lydall from the University of Newcastle. Plasmid DNA (2 µl) was used for transformation of *E. coli* (K-12 strain NM522) competent cells. Ampicillin-resistant colonies were selected on nutrient agar medium with 100 µg/ml of ampicillin. The plasmid DNA was extracted from ~16 hours grown culture of *E. coli* with a QIAgen kit following the manufacturer's instructions and was re-suspended in 200 µl of sterile 1x TE buffer (10 mm Tris-Cl, pH 8.0; 1 mM EDTA). The purified DNA was digested at 37°C overnight with restriction enzymes *Bam*HI and *Xho*I to release the 1 kb Y'+TG fragment. The digestion was performed in 165 µl of total reaction volume with 140 µl plasmid DNA, 3 µl (60 units) each of *Xho*I and *Bam*HI enzymes with 16.5 µl of 10x buffer and 1.5 µl of 100x BSA. The digested DNA was resolved on 0.8% agarose gel. The fragment of ~1 kb was excised from the gel and the DNA was extracted using QIAgen kit (#28704) by following the user manual.

The approximate concentration of purified fragment was estimated to be ~10-15 ng/µl. The amount of the probe DNA required for hybridisation was estimated according to the size of the filter (equivalent to 0.125 ml/cm^2 to 0.25 ml/cm^2). The DNA was labelled with the Amersham Gene Images AlkPhos direct labelling and detection system with CDP-star (RPN 3690, GE Healthcare) with the thermostable alkaline phosphatase enzyme. The DNA was denatured for 10 minutes in a boiling water bath. Denatured probe DNA was cooled immediately on ice for 10-15 minutes and centrifuged briefly to collect the contents at the bottom of the tube. 20 µl of reaction buffer, 4 µl of labelling reagent and 20 µl of the diluted cross linker were added to 20 µl of denatured DNA (~200 ng). The contents of the tube were mixed thoroughly and spun to bring the contents to the bottom. The reaction was incubated at 37°C for 30 minutes. The freshly labelled probe was kept on ice and used within half an hour.

2.3.2.14.4 Hybridisation and detection of probed DNA

The hybridisation buffer (Amersham's AlkPhos direct labelling and detection system) was prepared with the addition of salt, NaCl and blocking reagent as recommended in the manual. The required volume of pre-hybridisation/hybridisation buffer was preheated to 56°C. The membrane with DNA was placed inside the hybridisation tube with pre-warmed buffer and pre-hybridised for 15-30 minutes in the hybridisation oven. The labelled Y'+TG telomeric probe was added in the tube at a concentration of ~5-10 ng/ml of buffer and left overnight at 56°C in the hybridisation oven. Next morning, the membrane was washed with the primary wash buffer [2 M urea, 0.1% (w/v) SDS, 50 mM sodium phosphate buffer pH 7, 150 mM NaCl, 1 mM MgCl2 and 0.2% (w/v) blocking reagent] twice at 55°C for 10 minutes, with excess of buffer and gentle shaking followed by a secondary wash with 1x wash buffer (0.05 M Tris base and 0.1 M NaCl, pH 10) twice for 5 minutes at room temperature to remove excess non-specific bound probe.

Chemiluminescent detection was carried out with CDP-star solution. Excess of the wash buffer was drained without drying the membrane. Detection reagent (~50 µl/ml) was pipetted onto the blot and left for 5 minutes. Excess of detection reagent was drained off by touching the blot onto a non-absorbent surface. The blot with DNA side up (wrapped in saran wrap) was placed in the film cassettes, exposed and developed on a sheet of autoradiograph film following the user manual for an appropriate length of time (15 minutes, 3 hrs, one night and 3 days).

2.3.2.15 Statistical analysis

Colony count data were statistically analysed using Microsoft office Excel 2010, version, 14.0.7151 5001 (32 bit), part of Microsoft office professional plus 2010 (Microsoft Corporation, USA) to calculate mean, standard deviation (SD), standard error of the mean (SEM) and viability % etc. One way ANOVA was applied to test the significance of difference between control and test groups. The resulting values were considered significant if the *p*-values were below 0.05. Data were presented as mean ±SEM from three independent experiments unless stated otherwise.

Chapter 3

Cdc13 disruption in yeast *Saccharomyces cerevisiae*

3.1. Introduction

In yeast, the availability of full deletion collections (comprising thousands of individual gene deletions) and complete genome sequencing (Winzeler *et al*., 1999, Kastenmayer *et al*., 2006) has made it possible to detect the unknown functions of genes in cellular processes. Out of numerous approaches available nowadays, gene disruption analysis using modular plasmids, PCR techniques and yeast transformation are economical, time saving and easy studies to conduct as compared to the traditional *in vitro* creation of constructs through multiple cloning steps (Wach *et al*., 1997, Longtine *et al*., 1998). The elaborate one step PCR technique followed by guided homologous recombination directly modifies targeted DNA within the genome with the added advantage of a genetically linked auxotrophic marker for an easy selection of transformants. This approach is utilised not only to identify the role of a particular gene, but also to investigate the significance of truncated and mutated genes in cellular processes.

Cdc13 is a multifunctional protein that plays key roles in cellular processes, mainly telomere replication, length-maintenance, end-protection and telomerase regulation (Qi and Zakian, 2000, Sun *et al*., 2011). Cdc13 binds the single-stranded telomere DNA at $TG_{1\text{-}3}$ repeats (~300-350 repeats in *S. cerevisiae*) of telomere G-tails (Nugent *et al*., 1996). Cdc13 plays an important role to prevent the chromosome ends from nuclease degradation and to elongate the DNA after its replication by recruiting telomerase enzyme to telomere. For its capping function, Cdc13 physically binds to long single-stranded telomere ends during late S to G2 phases of the cell cycle. There are several lines of evidence that Cdc13 interacts with its regulatory partners Stn1 and Ten1 and collectively forms a CST protective cap (Wellinger, 2009). This assembly provides a loading platform for other proteins and telomerase to regulate telomere length and genomic stability.

For its protective activity, Cdc13p interacts with various other capping proteins through its N- and C-terminal regions, conferring their crucial roles in telomere protection and length regulation (Hsu *et al*., 2004). The Cdc13 N-terminus is composed of the telomerase activation domain, required for telomerase recruitment. Furthermore, Cdc13 protein dimerisation, required to bind the telomere, is also facilitated through its N-terminus. Conversely, the C-terminus supports the Stn1-Ten1 interaction and consists of a DNA binding domain that is utilised to bind single-stranded telomeres with high affinity and specificity to cap the chromosome throughout the cell cycle (Mason and Skordalakes, 2010). Lack of Cdc13 causes single-stranded DNA accumulation at the telomere that leads to cell cycle arrest and cell death (Nugent *et al*., 1996).

In the first part of the Cdc13 disruption studies, a one-step PCR-mediated technique was employed to construct a *cdc13-1* full gene deletion module through genetic transformation and recombination to enable its functional analysis. In the second part, partial *cdc13-1* deletion mutants were generated with *cdc13-1* N- and C-terminus truncations to provide molecular dissection of their function.

3.2. Aims and objectives

The main aim of this part of the study was to construct *cdc13-1* full ORF deletion and partial deletion mutants (Cdc13 with N-and C-terminus truncations) in temperature-resistant survivors of *cdc13-1 exo1Δ* mutants. This aim included the following objectives:

- To identify appropriate yeast plasmids and design hybrid primers for *CDC13* full gene deletion, *CDC13* N- or C-half deletion cassettes.
- To integrate the deletion cassettes into genome of *cdc13-1 exo1Δ* mutants by genetic transformation.
- To confirm *cdc13-1* knock-out by performing diagnostic PCR.
- To perform genetic crosses to obtain new combinations of deletion.

3.3. Results

The first part of the results is devoted to *CDC13* full gene deletion. In the next sections, N- and C-terminus truncations are described in detail.

3.3.1. *CDC13* full gene deletion

CDC13 is located at chromosome IV. The open reading frame of *CDC13* gene consists of 1-2775 nucleotides (nt) that encodes a protein of 924 amino acids with a molecular weight of ~104895.2 Da (Wu and Zakian, 2011). A single nucleotide change in the coding sequence results in mutant *cdc13-1* that is sensitive to enhanced temperature and shows phenotypic growth retardation. The full deletion of *CDC13* results in immediate cell cycle arrest and cell death (Weinert and Hartwell, 1993). The mutant *cdc13-1* cannot grow at higher temperatures. Nevertheless *cdc13-1* conditional mutants in the absence of *EXO1* gene form rare survivors able to grow at high temperatures (up to 36°C). It was decided to delete the full coding sequence of *cdc13-1* in *exo1*Δ mutants (Figure 3.1).

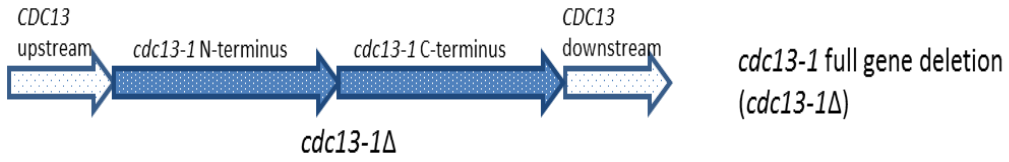

Figure 3.1. Deletion of *cdc13-1* full ORF (1-2775 bp).

A simple scheme describing the *cdc13-1* disruption module is shown in Figure 3.2 and Figure 3.3. The process of disruption includes the choice of a yeast plasmid, chimeric primer design based on the selected plasmid and target gene sequences (Figure 3.2A), PCR amplification of the marker module with a flanking sequence of the target gene (deleting sequence for homologous recombination, Figure 3.2B), transformation of the host yeast strain and confirmation of transformants on the basis of marker integration and diagnostic PCR for the gene sequence (Figure 3.2C).

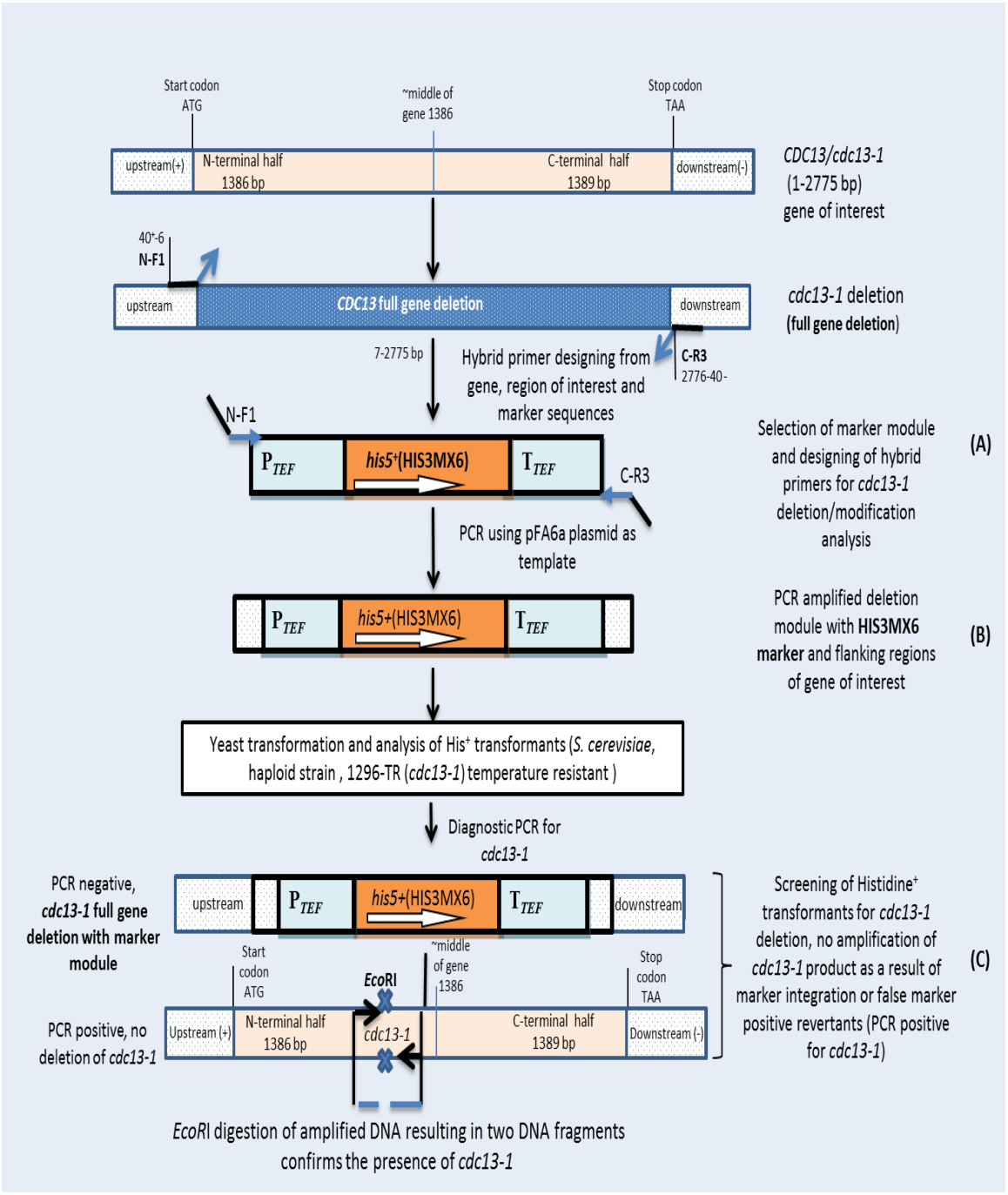

Figure 3.2. Diagrammatic scheme for transformation of *S. cerevisia*e strain with the PCR product carrying *HIS3* disruption module with guided sequences to delete *cdc13-1* (adapted from (Wach *et al*., 1997).

(**A**) Selection of hybrid primers for deletion of *cdc13-1* ORF specific sequence.

(**B**) Synthesis of disruption cassettes by PCR using HIS3MX6 marker DNA (Longtine *et al*., 1998) as a template.

(**C**) The identification of replaced ORF of *cdc13-1* with diagnostic primers from the middle of the *cdc13-1* gene spanning between 953 and 1330 nucleotides whereas nucleotide 'C' at position 1111 has been replaced with 'T' that creates an *Eco*RI site in the *cdc13-1* mutant strain.

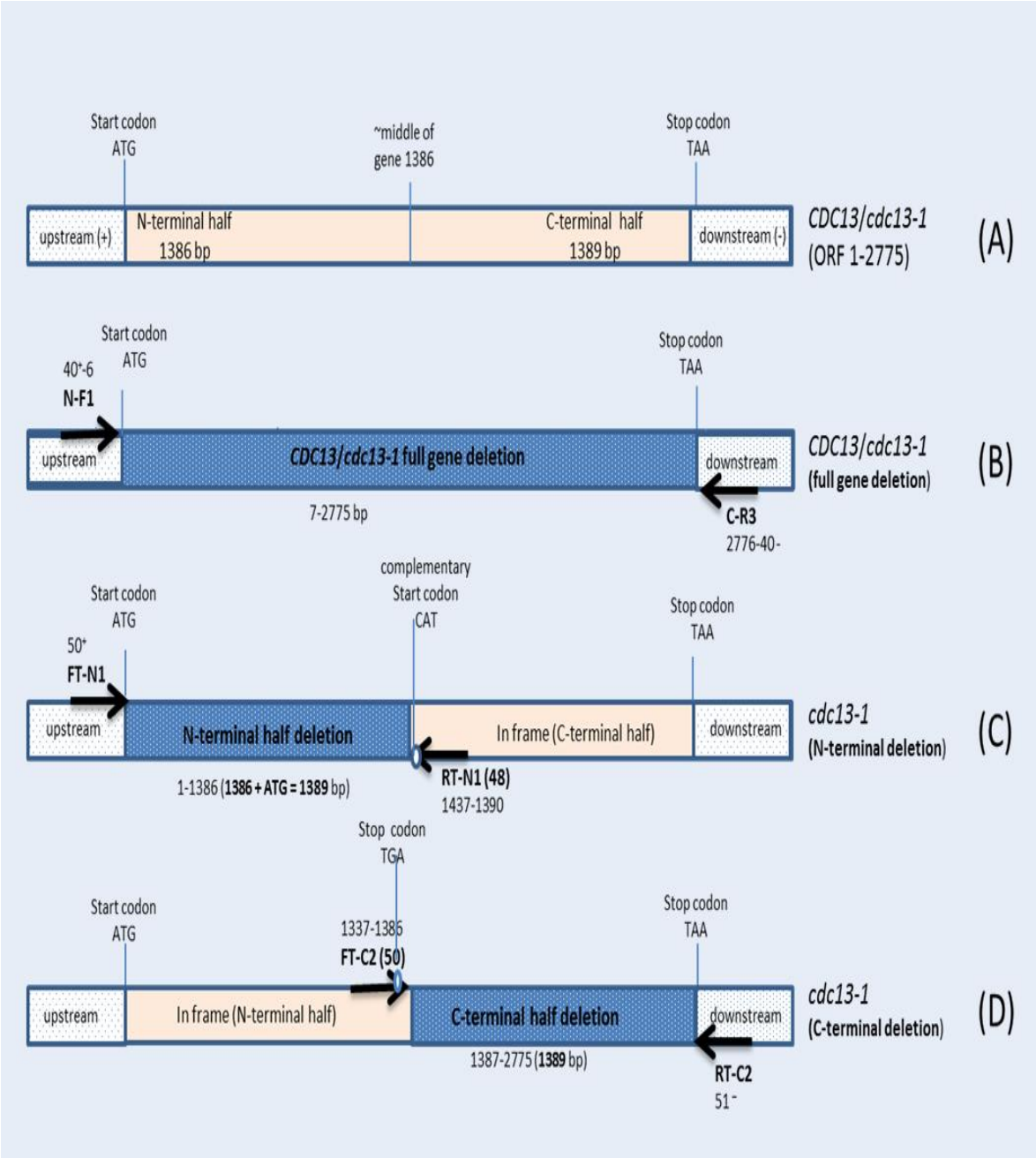

Figure 3.3. *In silico* manipulation of *CDC13* ORF sequence at specific nucleotide positions. Arrow showing the position of flanking sequences homologous to target sequences.

(**A**) *CDC13* ORF with 1-2775 bp sequence, divided in two halves (N- and C-terminus).

(**B**) *CDC13*, full gene deletion (7-2775 bp).

(**C**) *CDC13*, N-terminus deletion (1-1389 bp).

(**D**) *CDC13*, C-terminus deletion (1387-2775 bp).

3.3.1.1. Plasmid DNA extraction and DNA size evaluation via digestion with restriction enzymes

For *CDC13* full gene deletion, plasmid pFA6a (with the histidine marker gene) was used (Longtine *et al*., 1998). The plasmid DNA was transformed in *E. coli* using a standard protocol and resulting transformants were selected on nutrient agar plates with 100 µg/ml of ampicillin as it has been described for *E. coli* transformation. Plasmid DNA was extracted using a QIAgen kit by following the manufacturer‘s instruction manual.

It was decided to conduct *CDC13* full gene (ORF 2775 bp) deletion in the yeast strain DLY 1296 (Table 2.1) in temperature resistant/survivors (TR) and to compare the transformation efficiency of 1296-ts (temperature sensitive) cells with its TR survivors. The method for “TR and ts cell preparation and genotype selection for auxotrophies requirement” has already been mentioned in the Yeast Methods section.

Agarose (0.8%) gel analysis of plasmid (pFA6a-HIS3MX6; pDL501) DNA extracted from transformed *E. coli* NM522 from four independent preparations presents purified uncut DNA, linearised plasmid and double-digested plasmid (Figure 3.4). Purified DNA exhibits multimeric forms of plasmid with supercoiled DNA at the front (owing to its smallest size) being ~3 and 4 kb in size (Figure 3.4, lanes 1-4). The single digestion with restriction enzyme *EcoR*I (unique cut at position 1360 on plasmid map) resulted in a linearised DNA fragment with a size of approximately ~4 kb (3.782 kb; Figures 3.8 and 3.9A, lanes 5, 6, 7, 8). Conversely, double enzyme digestion with *EcoR*I and *BamH*1 resulted in two fragments, approximately 2.465 kb and 1.317 kb in size, corresponding to their sites on the DNA map at positions 1360 and 43 respectively (Figures 3.8 and 3.9A, lanes 9-12). *In silico* analysis of plasmid pFA6a-HIS3MX6 DNA with *EcoR*I and *BamH*1 also confirms the sizes of the linear DNA and fragments generated through double digestion of plasmid on a simulative gel (Figure 3.5B). However, the concentration of plasmid DNA varied in all four preparations that is consistent with uncut and digested DNA samples. The purified plasmid DNA was diluted in a ratio of 1:5 and 1:10 and used as a DNA template to produce PCR amplified modules for *CDC13* gene disruption in transformation experiments.

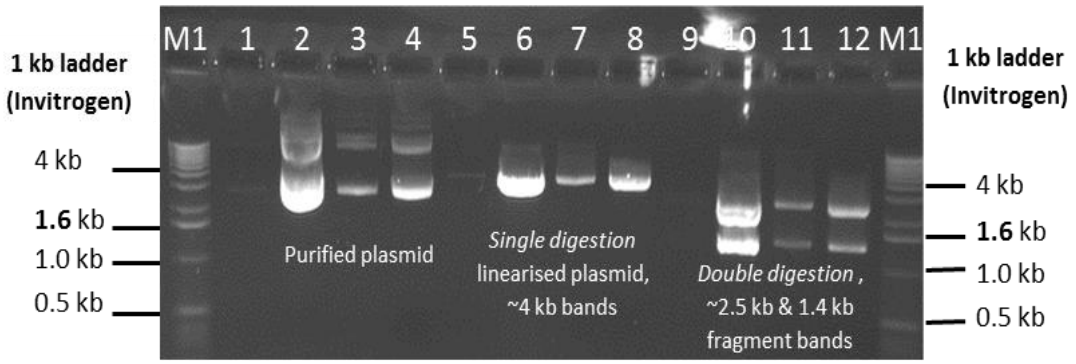

Figure 3.4. Plasmid (pFA6a-HIS3MX6) DNA isolation and size estimation through restriction enzyme analysis. Agarose gel electrophoresis of digested plasmid DNA was carried in 1 x TBE buffer. Uncut (3 µl) and digested DNA (5 µl) were analysed on 0.8% (w/v) agarose gel with ethidium bromide dye at a concentration of 0.25 µg /ml.

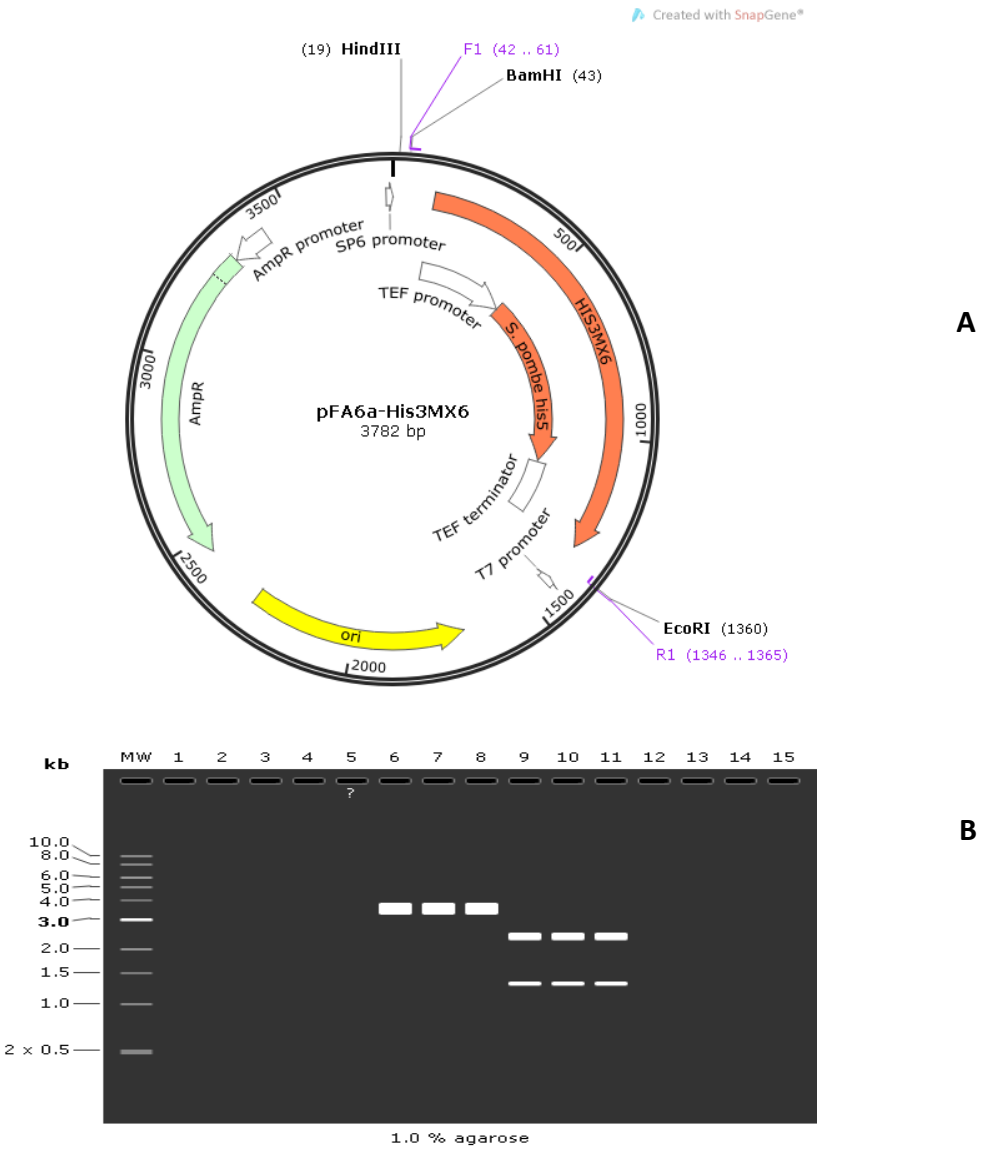

Figure 3.5. *In silico* size analysis of yeast plasmids pFA6a-HIS3MX6 (pDL501).

(**A**) Circular map of plasmid DNA showing *Eco*R1 and *Bam*H1 sites utilised for digestion with restriction enzymes.

(**B**) Simulative gel showing fragments after single(lanes 6-8) and double digestion (lanes 9-11) with the above enzymes (www.snapgene.com/resources)

3.3.1.2. PCR amplification for *CDC13* full gene (ORF) deletion cassettes

The plasmid pFA6a-HIS3MX6 contains a histidine marker module that was used as a PCR template to generate amplified transforming fragments of 1403 bp for *CDC13* gene manipulation. This selectable marker module contains the *Shizosaccharomyces pombe his5+* gene (Wach *et al*., 1997), which complements *S. cerevisiae his3* mutations, with *TEF* strong promoter and terminator sequences from a filamentous fungus *Ashbya gossypii* (*A. gossypii*).

After evaluating the yield, purity and size of yeast plasmid (pFA6a-HIS3MX6), purified DNA was diluted (1:10) and used as a template to produce a PCR-amplified linear module for *CDC13/cdc13-1* deletion using hybrid primers N-F1 (forward) and C-R3 (reverse) in a 50 µl reaction volume. The 0.9% agarose gel analysis revealed the presence of the desired amplified fragments in all seven individual reactions analysed through electrophoresis (Figure 3.6, lanes 3-9). The size of the amplified fragments was estimated to be ~ 1.403 kb as expected. The amplified products were pooled from individual reactions (50 µl/reaction) and purified using either a QIAquick PCR purification kit or the phenol chloroform extraction method or absolute ethanol precipitation with 3 M potassium acetate buffer followed by washing with 70% ethanol.

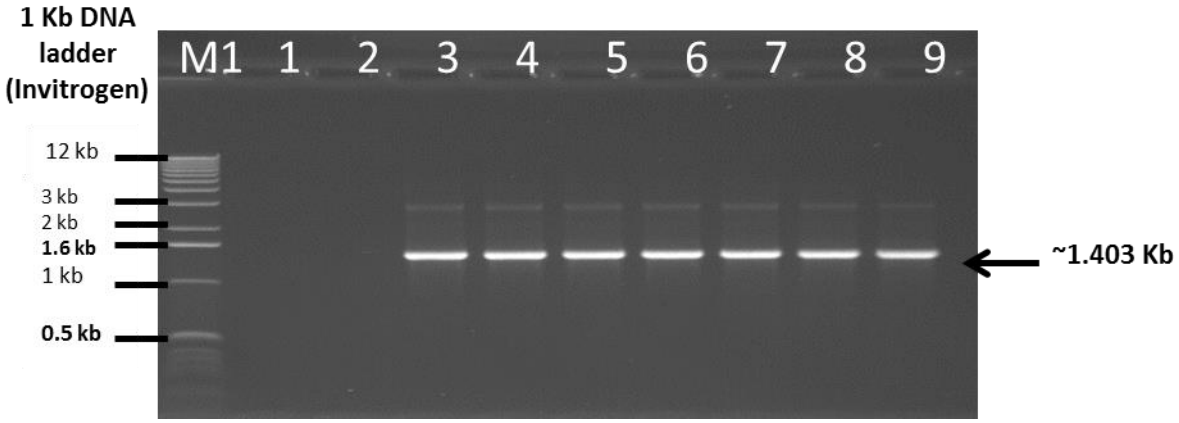

Figure 3.6. PCR amplification for *CDC13* full gene deletion amplicon using the pFA6a-HIS3MX6 marker module. PCR was performed in a 50 µl reaction volume with forward primer (N-F1; 5'C TCT TTG GAT ACG AAT GAC CGT GGA AAC TAT CGC CTA AAA ATG GAT cggatccccgggttaattaa 3' and reverse primers (C-R3; 5'GCA ATT TGG CAC CGC CGC GTT GGG CTG CGC GGA TCA TGT C gaattcgagctcgtttaaac 3') resulting in a ~1.403 kb gene disruption module fragment. Lanes 1 and 2 represent non-template negative controls without DNA. Lanes 3-9 present PCR amplicons from independent reactions. All samples were checked in a 5 µl volume. Lane 'M1' represents 1 kb DNA marker (Invitrogen), loaded as 500 ng per 10 µl volume.

3.3.1.2.1. Estimation of concentration of purified amplicon

The purified DNA was estimated to be ~100 ng per 3 µl as compared to the quantitative marker on 0.8% agarose gel (Figure 3.7, lanes 1-3). This precipitated, amplified DNA was used to transform temperature-resistant survivo rs of yeast strains DLY 1296 and DLY 2605 possessing *cdc13-1* mutation.

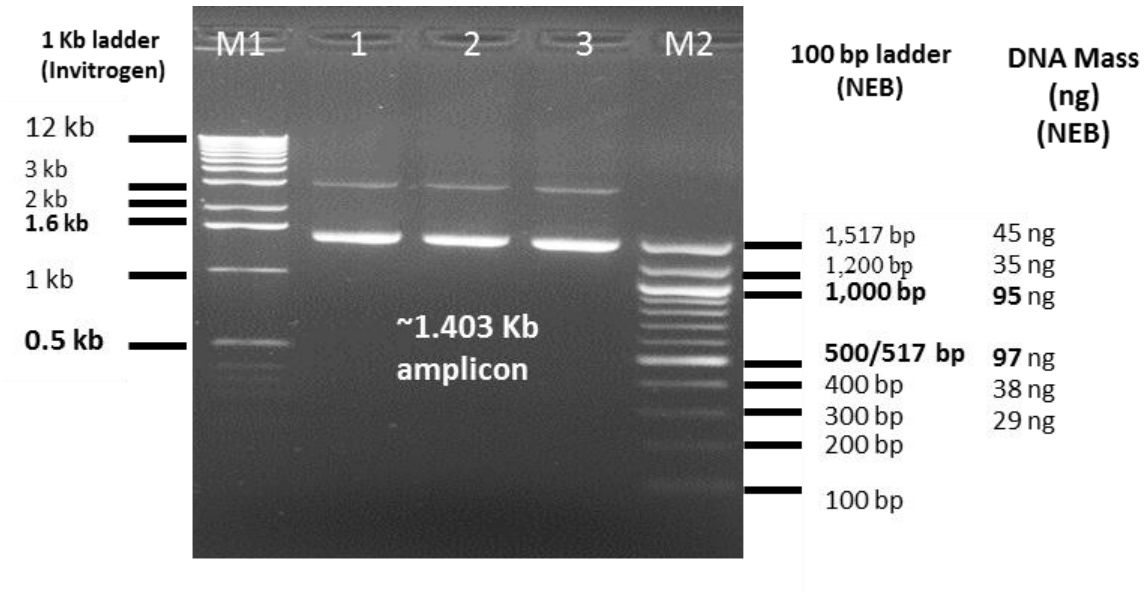

Figure 3.7. Estimation of concentration of purified DNA.

Amplified DNA was precipitated with 1/10 volume of 3 M potassium acetate buffer and ethanol, and washed in 70% ethanol. M1 and M2 represent DNA ladders; 1kb DNA marker (Invitrogen) and 100 bp DNA markers (NEB), were loaded 10 and 5 µl each per lane respectively. 3 µl of purified DNA was analysed by gel electrophoresis.

3.3.1.3. Generation and analysis of temperature-resistant (TR) survivors

Temperature-resistant survivors were selected as rare colonies produced at high temperature (36°C) by three temperature-sensitive (ts) *cdc13-1* mutant strains DLY 2605, DLY 1296 and DLY 1108 after 5-7 days of growth on YEPD medium followed by 2-3 passages at 30°C. To test the possibility of the emergence of spontaneous revertants due to gene conversion or recombination, ts mutants of *cdc13-1*; DLY 2605, DLY 1296 and DLY 1108 and their TR survivors were initially examined for nutritional markers by replica plating, and finally genotyped for the presence of mutation *cdc13-1* by using PCR. Amplified products were further investigated for the presence of *cdc13-1* or *CDC13* by restriction enzyme analysis.

3.3.1.3.1. Confirmation of genetic markers in survivors by replica plating

Genetic marker analysis by replica plating at 23°C and 30°C (with four colonies A-D for each strain) on four dropout media each lacking one of the essential components (-H, -L, -T, -U) confirmed the presence of leucine markers in survivor cells from strains 2605-TR and 1296-TR (Figure 3.8). Strains 1296-ts (3) and TR (6 and 7), 2605-TR (8 and 9) showed growth only on YEPD (replicas 1 and 2) and dropout media lacking amino acid leucine (replicas 4) at 23°C indicating the presence of the *LEU2* marker gene for *de novo* synthesis of l-leucine. Conversely, control strains 1108-ts (4) and 1108-TR (5) grew only on rich nutrient medium

YEPD (replica 1 and 2 at 23°C). Lack of growth of ts or TR cells of strain 1180 (control) at 23°C and 36°C respectively on any of the dropout media corroborated the absence of the above four auxotrophic markers in this strain.

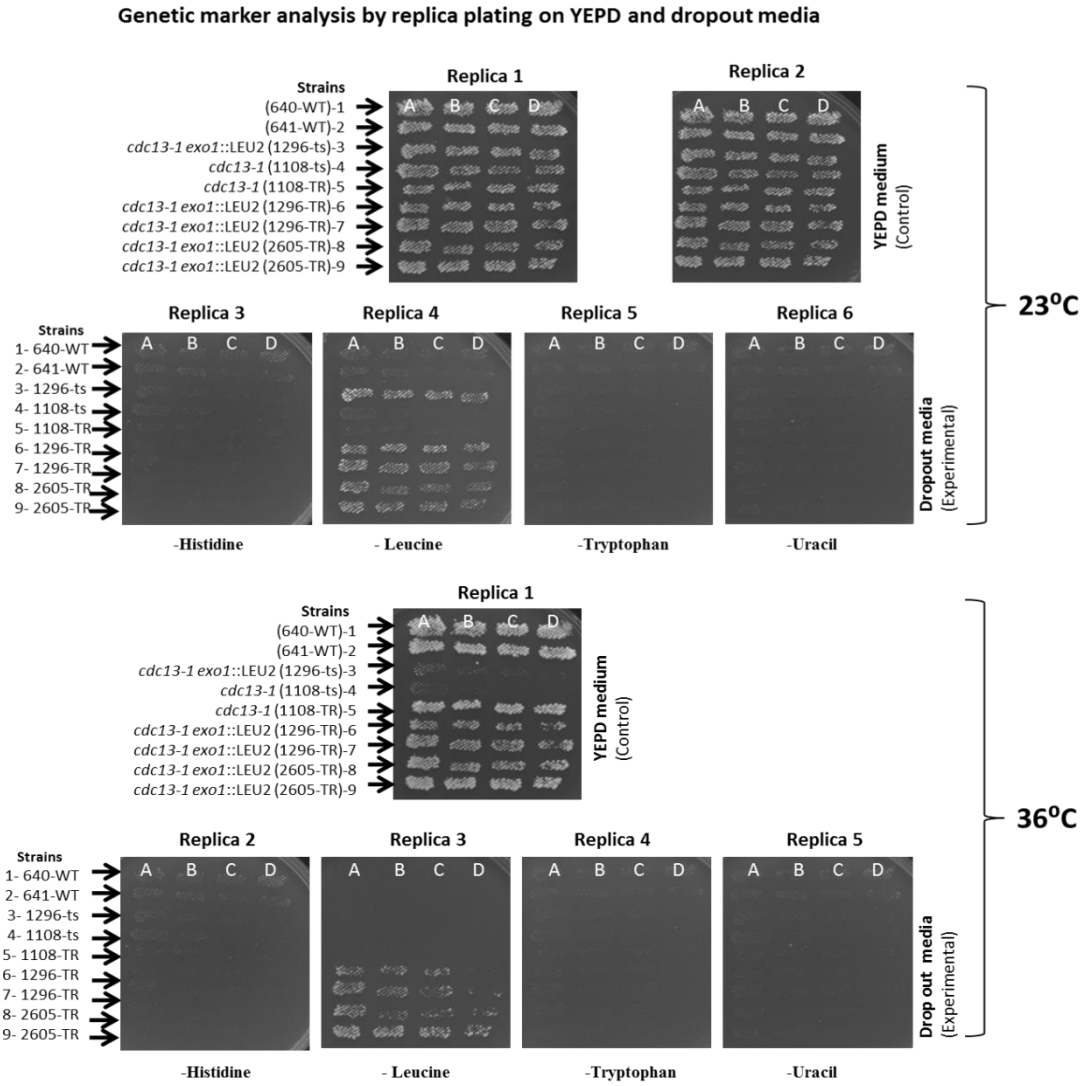

Figure 3.8. Auxotrophic marker analysis through replica plating on YEPD and dropout media at (23°C) and (36°C).

Experimental strains from ts mutants of *cdc13-1*; DLY 1296-ts (3), DLY 1108-ts (4) and DLY 2605-ts and their TR survivors 1296-TR (6 and 7) and 2605-TR (8 and 9) were grown on YEPD. For each strain, four random colonies A-D with approximately same sizes were streaked on a master plate (YEPD) as distinct short lines and were cultivated at 23°C for ~24-36 hours to attain less growth of cultures. These initial cultures were replica plated on two sets of nutrient requiring dropout media (replica 3-6 at 23°C and 2-5 at 36°C) each lacking one essential metabolic component (-H, -L, -T or -U and on YEPD medium (replica 1 and 2 at 23°C and replica 1 at 36°C control). Wild type strains 640 (1), 641 (2) (WT), and *cdc13-1* mutant strain 1108-ts (4) and TR (5) lacking four genetic markers were used as experimental controls. Replica plates were grown at 23°C and 36°C for 3 days before photography. Photographs were taken using a gel documentation system.

Strains 1296-ts (3) and 1108-ts (4) did not grow at 36°C on YEPD medium (replica 1) as expected exhibiting sensitivity to high temperature due to *cdc13-1* mutation. At 36°C strains 1296-TR (6 and 7) and 2605-TR (8 and 9) showed growth only on (YEPD, replica 1) and dropout medium in the absence of amino acid leucine (replica 3) indicating the presence of the *LEU2* marker gene. Strains 640 (1) and 641 (2) (wild type) were used as controls and their growth on YEPD medium only indicates the absence of four genetic markers.

3.3.1.3.2. Confirmation of *cdc13-1* mutation in survivors by PCR

The *cdc13-1* mutation has an additional *Eco*RI restriction site "GAATTC" where 'C' is replaced with 'T' at position 1111 of the *CDC13* ORF (Figure 3.9). This *Eco*RI site was used to differentiate between *CDC13* and *cdc13-1* mutants by analysing cells from ts strains, 2605, 1296 and 1108 and their TR survivors by PCR amplification using N1 and N2 primers and restriction enzyme analysis of amplified product.

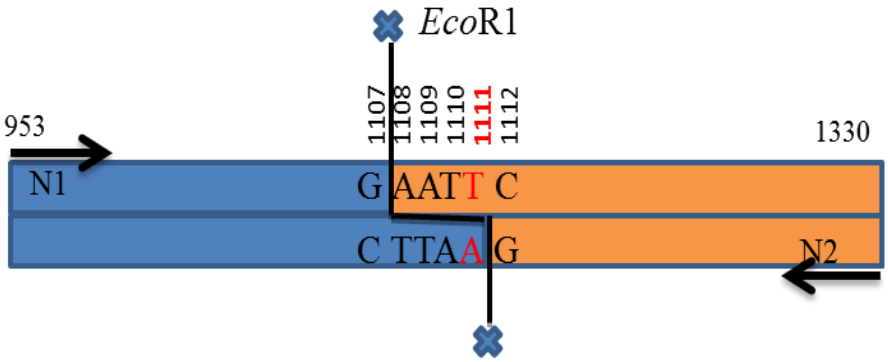

Figure 3.9. PCR amplicon contains *Eco*RI restriction site within the ORF sequence (953-1330 nucleotides) of *cdc13-1.*

The amplified fragment between nucleotides 953 and 1330, with diagnostic primers N1 and N2 was subjected to *Eco*R1 restriction digestion that released two fragments, ~219 bp and ~159 bp with *cdc13-1*, and a single, intact fragment of 378 bp in the case of wild type *CDC13*.

Restriction analysis of PCR products verified the presence of the *cdc13-1* mutation in cells from survivors. Agarose gel analysis of undigested PCR amplicons revealed a single fragment of approximately 378 bp (Figure 3.10A) in mutant cells analysed corresponding to *CDC13* ORF sequence from 953-1330 nucleotides. However, as shown in Figure 3.10B, *Eco*RI restriction digestion generated two fragments of ~159 bp (ORF from nucleotides 953-1111) and ~219 bp (ORF from nucleotides 1112-1330) confirming the presence of *cdc13-1* in the mutant strain 2605-TR (lanes 3 and 4), strain 1296-TR and -ts (lanes 5, 6 and 8) and strain 1108-TR and -ts

(lanes 7 and 9). The single intact fragment of ~378 bp corroborates *CDC13* in wild type strains 640 and 641 used as controls (Figure 3.10B (lanes 10 and 11).

After confirmation of *cdc13-1* mutation, the survivors from strains 1296 and 2605 were utilised in transformation experiments for *CDC13* knockout.

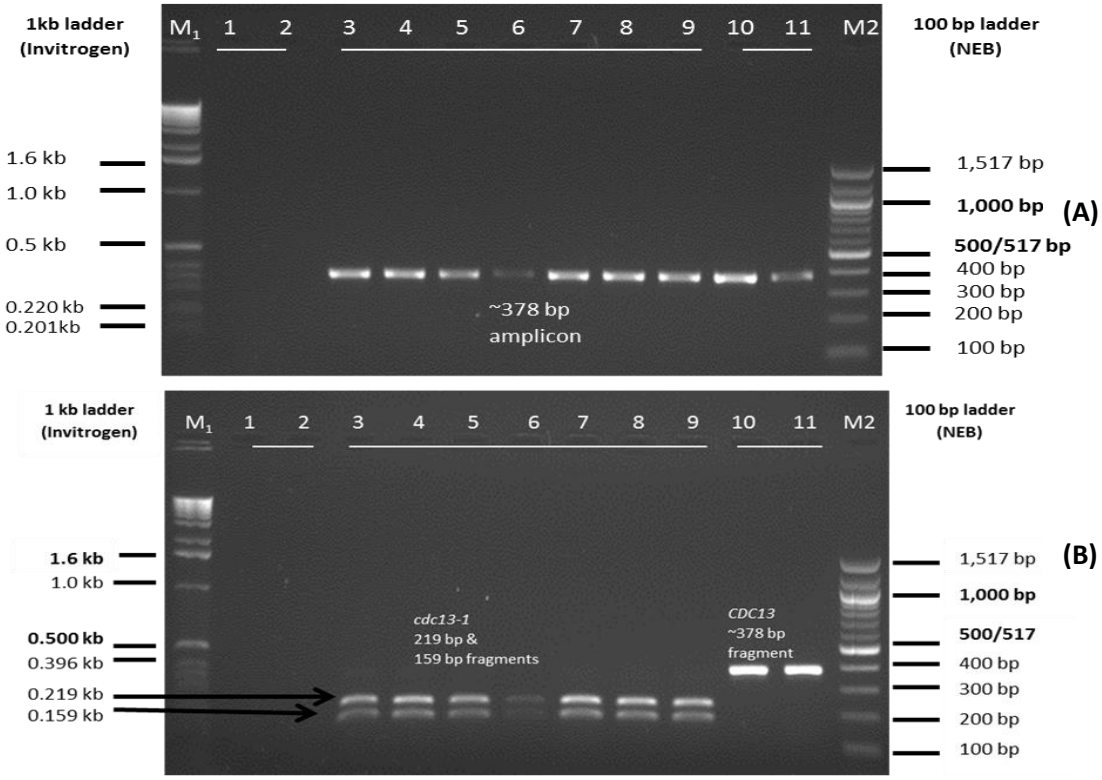

Figure 3.10. Confirmation of survivors: verification of genotypical mutation *cdc13-1* by PCR amplification and *Eco*RI restriction analysis of amplified fragment in ts strains and their TR survivors.

Lanes M1: 1kb ladder, 500 ng (Invitrogen); 1-2:-ve control [Non template control (NTC) without cells or DNA]; 3-4: Strain 2605-TR (*cdc13-1* mutant cultivated at 36°C); 5-6: Strain 1296-TR (*cdc13-1* mutant cultivated at 36°C); 7: Strain 1108-TR (*cdc13-1* mutant cultivated at 36°C); 8: Strain 1296-ts (*cdc13-1* mutant cultivated at 23°C); 9: Strain 1108-ts (*cdc13-1* mutant cultivated at 23°C); 10: Strain 640 WT (control, cultivated at 23°C); 11: Strain 641 WT (control, cultivated at 23°C); M2: 100 bp ladder, 500 ng (NEB).

Temperature-sensitive (ts) strains and their survivors (TR) were cultivated at 23°C and 36°C respectively for 2-3 days. The cells from freshly grown cultures were denatured at 95°C for 10 minutes. PCR was carried out in a 25 µl reaction volume with primers N1 and N2.

(**A**) Agarose gel analysis of uncut PCR amplicons (5µl) from individual reactions.

Gel electrophoresis presents a distinct fragment of ~378 bp (*CDC13*/*cdc13-1*) from ts and TR cells of strains 1108, 1296 and 2605 which were digested and analysed on 2% agarose gel for the verification of *cdc13-1* mutation.

(**B**) Electrophoretic analysis of *Eco*RI digested PCR products to verify the genotypic mutation *cdc13-1* in ts and TR survivors. Gel electrophoresis of *Eco*RI digested PCR product showed a single fragment of ~378 bp in strains 640 and 641 (WT) (lanes 10 and 11) with respect to nucleotides sequenced from 953-1330 of the ORF while two fragments of ~159 bp (from nucleotides 953-1111) and ~219 bp (from nucleotides 1112-1330) were released with strains 1108-TR and -ts (lanes 7 and 9), 1296-TR and -ts (lanes 5, 6 and 8) and strain 2605-TR (lanes 3 and 4) after *Eco*RI digestion. Digestion was performed in 30 µl of total reaction with 15 µl of amplified product at 37°C for 2 hours. Digested products in 15 µl was analysed on 2% agarose gel.

3.3.1.4. Transformation of *cdc13-1* survivors with *CDC13* disruption module

In order to transform *cdc13-1* survivors (strains 1296 and 2605) ~1.3 µg of potassium acetate precipitated amplified module DNA was used. Transformation of survivors was carried out with freshly prepared 100 µl competent cells with a viable count of ~7.6 x 10^7 cells/ml. As it has been demonstrated in Figure 3.11, the transformants were initially selected on dropout medium lacking histidine for strains 1296-TR (plates no. 3 and 4) and 2605-TR cells (plates no. 7 and 8). For positive controls, the competent cells were plated on dropout medium without leucine (plates no. 2 and 6), and for negative controls, cells were plated on media lacking histidine (plates no. 1 and 5). Three his^+ transformants were obtained with strain 1296-TR as compared to two clones with strain 2605-TR after 5-7 days of incubation at 30°C. Transformation efficiency (homologous recombination) was estimated to be one cell out of $2.53x10^6$ cells for 1296-survivors and one transformant out of $3.8x10^6$ cells for 2605-survivors with 15 minutes incubation at 42°C (heat shock). The colony shape in strain 1296-transformants was rough with wavy margins as compared to circular colonies with smooth margins observed in strain 2605-transformants. In the following experiment, transformation efficiency through homologous recombination was increased to one transformant out of $2.14x10^5$ cells (28 his^+ transformants) with 1.6 µg of modular DNA after 35 minutes of incubation at 42°C (data not shown), that was almost 12 times higher as compared to the initial efficiency.

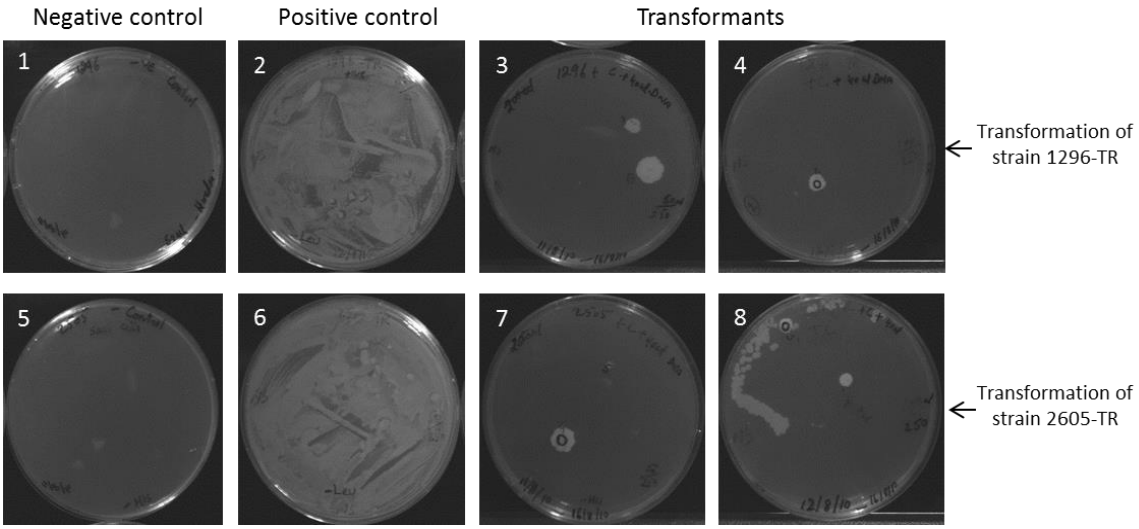

Figure 3.11. Transformation of cells from strains 1296-TR and 2605-TR with *CDC13* PCR deletion module (HIS3MX6). Plates 1 and 5 with medium lacking histidine were used as negative controls for cells of strain 1296-TR and 2605-TR. Plates 2 and 6 with medium lacking leucine were positive controls for cells of strain 1296-TR and 2605-TR. Plates 3, 4 and 7, 8 show transformants in cells from strain 1296-TR and 2605-TR respectively on medium lacking histidine.

3.3.1.4.1. Confirmation of *CDC13* knockout in his$^+$ transformants by diagnostic PCR

The six histidine-positive transformants were analysed by PCR for *cdc13-1* deletion in strain 1296 and 2605 survivors after a second round of selection on medium lacking histidine. Gel analysis manifested a fragment of ~378 bp in positive controls only (Figure 3.12**,** lanes 9-12). However, no amplification was observed in transformants analysed (lanes 3-8) indicating deletion of the *cdc13-1* gene by target-guided homologous recombination. Strains 2607 and 2608 with *cdc13* deletion were used as negative controls (lanes 1 and 2).

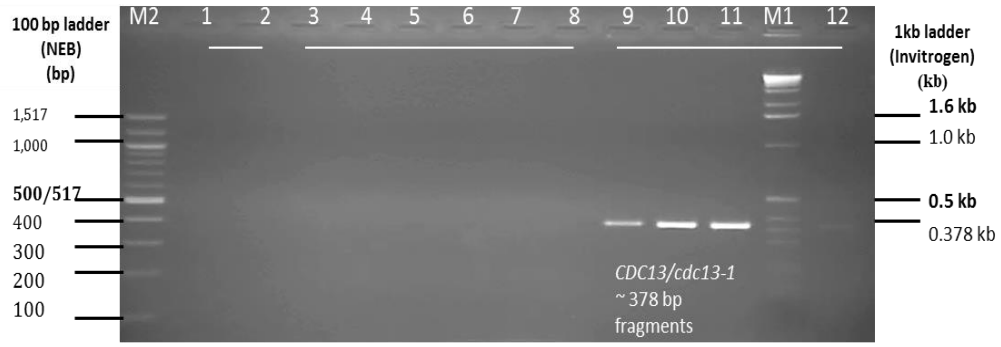

Figure 3.12. PCR screening for confirmation of *cdc13-1* deletion in his3^{+} transformants of strains 1296 and 2605.

Lane M2: 100 bp ladder 500 ng (NEB); 1: Strain 2607 cells (*CDC13Δ*), negative control;
2: Strain 2608 cells (*CDC13Δ*), negative control; 3-8: 1296-TR, transformant #1-#6 cells;
9: 1296-TR cells (*cdc13-1* mutant) positive control; 10: 2605-TR cells (*cdc13-1* mutant) positive control; 11: Strain 640 (wild type) cells, positive control; M1: 1kb ladder 500 ng (Invitrogen); 12: Strain 641 (wild type cells, positive control.
PCR was performed in a 25 µl reaction volume with GoTaq green master mix from Promega. Uncut PCR product (5µl) was analysed electrophoretically on a 1.6% agarose gel.

3.3.1.5. Comparative analysis of *cdc13-1* disruption efficiency in temperature-sensitive strain and its temperature-resistant survivors

In this experiment, the temperature-sensitive *cdc13-1* strain 1296-ts (23°C) and its temperature-resistant survivor 1296-TR (36°C) were used for *CDC13* deletion. The competent cells were prepared following the standard protocol as described in the methods section. Transformation was carried out using a purified PCR DNA module (~1 µg) with flanking guided oligonucleotide from upstream and downstream of *CDC13* and freshly prepared cells (100 µl) with a viable count of $9.66x10^{8}$ cells/ml for temperature-sensitive strain 1296-ts and $8.35x10^{8}$ cells/ml for its survivor 1296-TR. Transformants (his^{+}) were selected initially on dropout medium lacking histidine (Figure 3.13, plates no.1-2 and 5-6) followed by a second round of selection on dropout medium lacking both histidine and leucine (Figure 3.13, plates no. 3 and 4). Transformation efficiency of 1296-TR cells was estimated to be one cell out of $2.4x10^{6}$ cells with 30 minutes' incubation at 42°C (heat shock). Conversely, 1296-ts cells showed transformation efficiency (homologous recombination) of one cell out of $9.66x10^{6}$ cells (~four times less as compared to 1296-TR cells) under the same experimental conditions.

Transformation of 1296-TR and 1296-ts cells using the *CDC13* disruption module

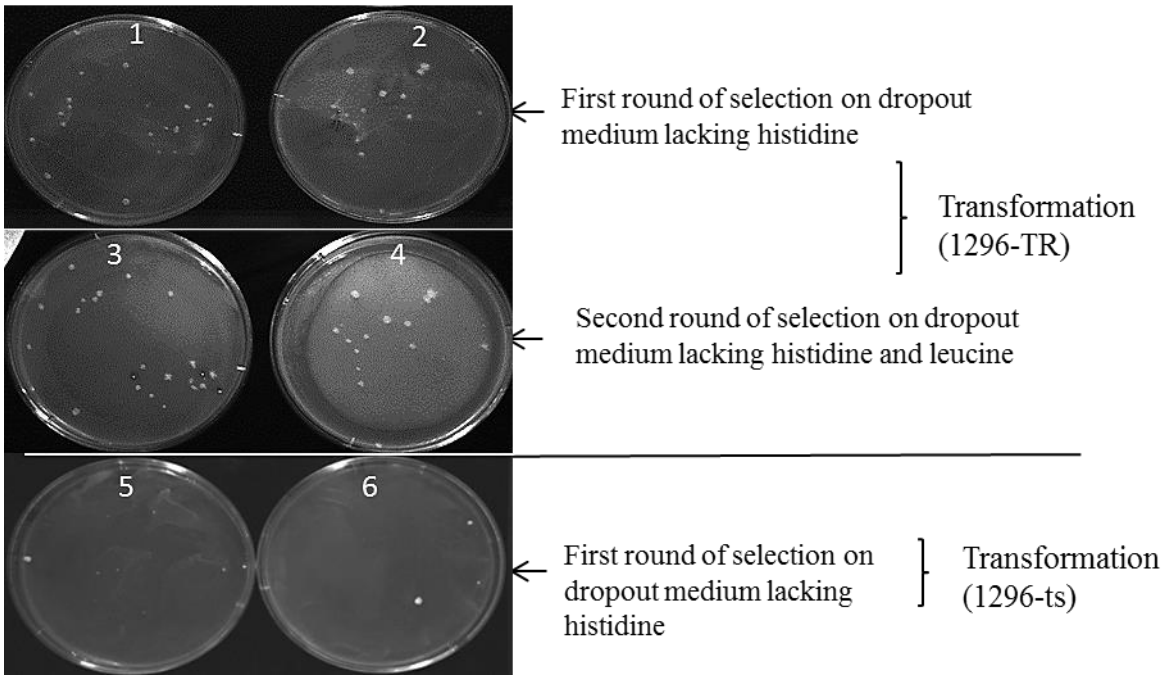

Figure 3.13. Transformation of *cdc13-1* temperature-sensitive strain 1296-ts and its temperature-resistant survivor with PCR-based *CDC13* disruption module. Modular DNA with guided sequences was purified from gel using a Qiaquick PCR purification kit. Approximately 1 µg of DNA was used to transform suspension (100 µl) of competent cells. In strain 1296-ts, 10 his^+ transformants were obtained as compared to 35 transformants for the survivor (1296-TR).

3.3.1.5.1. Confirmation of the histidine marker in transformants by replica plating

The HIS^+ putative clones obtained after transformation of cells of strain 1296-TR and -ts were further analysed through marker analysis and diagnostic PCR for the confirmation of *cdc13-1* deletion and the integration of the histidine marker. Ten transformants (#1-#10) each for both 1296-ts and its TR survivors were systematically tested for the genotypic markers by replica plating to confirm prototrophy for histidine and leucine markers (Figure 3.14).

Figure 3.14A-B (streak 1) demonstrates that the parental strains 1296-ts and 1296-TR respectively did not grow on dropout media lacking histidine, tryptophan or uracil (replica 2, 4 and 5) but exhibited growth on nutrient-rich medium YEPD (replica 1) and medium without leucine (replica 3) confirming its prototrophy (the presence of LEU2 marker gene for the *de novo* synthesis of l-leucine). All 1296-ts and TR transformants examined contained histidine marker (replica 2) owing to their growth on medium without histidine. However, further analysis of transformants for *CDC13* gene deletion by PCR is required for the final confirmation of its knockout.

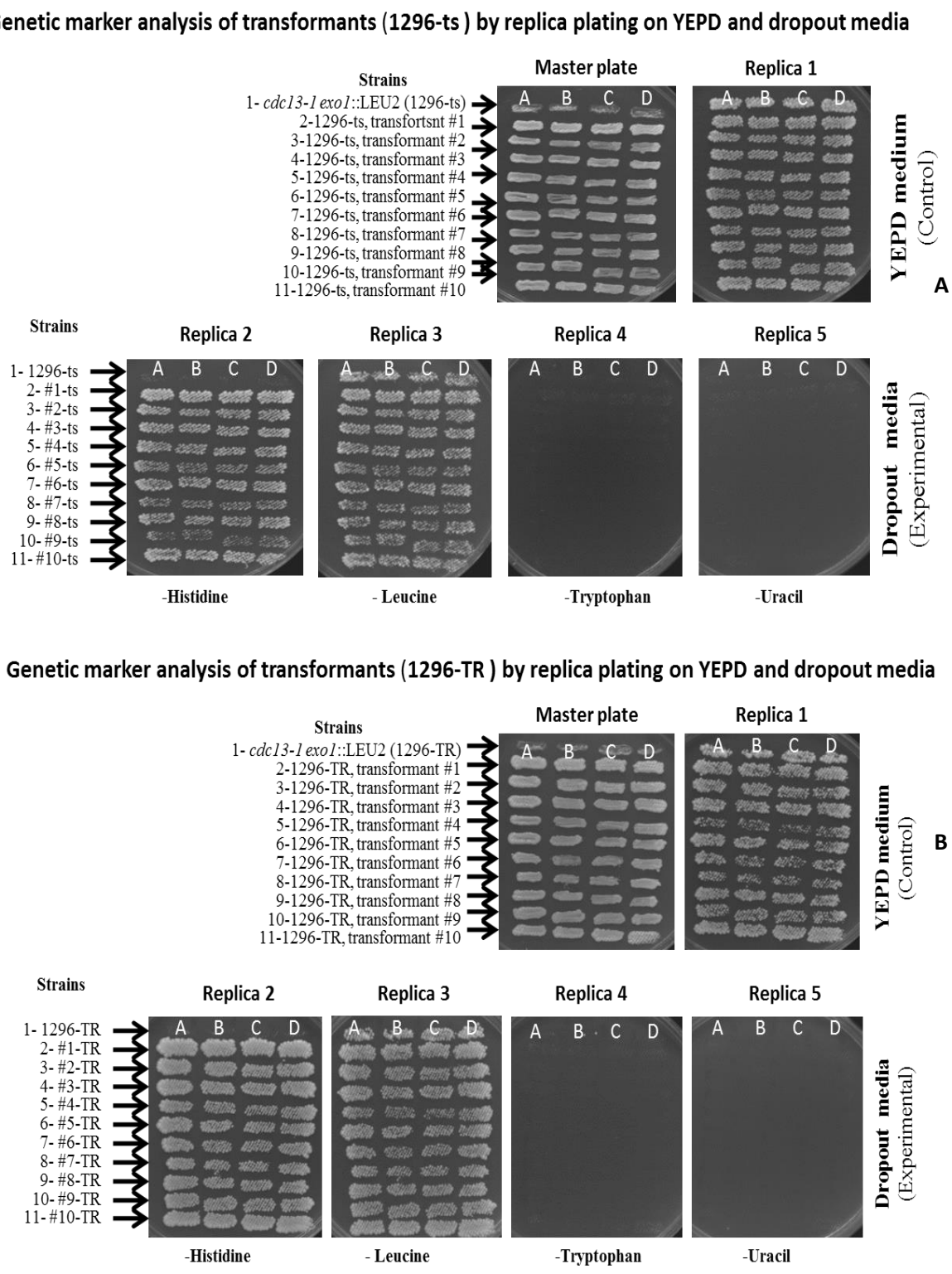

Figure 3.14. Analysis of metabolic markers in ts and TR transformants by replica plating.

Ten transformants from ts (1296-ts) and TR survivors (1296-TR) of strain 1296 were randomly picked for marker analysis. The strains 1296-ts and 1296-TR (1) did not grow on dropout media lacking histidine, tryptophan or uracil (replica 2, 4 and 5, lane 1) indicating its auxotrophies for these markers but grew only on dropout medium lacking leucine (A and B respectively, replica 3). All 1296-ts and -TR transformants (#1-#10) exhibited prototrophy to histidine and leucine markers owing to their growth on

the plate lacking these markers (A and B, replica 2 and 3). Replica plates were grown at 23°C and 30°C for 3 days before photography. Pictures were taken using a gel documentation system (Syngene).

3.3.1.5.2. Confirmation of *cdc13-1* deletion in his$^+$ transformants by diagnostic PCR

3.3.1.5.2.1. Agarose gel analysis of PCR products in uncut and *Eco*R1 digested amplicons

Further analyses of clones for *CDC13* gene knockout were carried out by diagnostic PCR. Ten his$^+$ transformants (#1-#10) were screened by PCR for *cdc13-1* deletion in strain 1296-ts and its survivor (1296-TR). The PCR amplification results are shown in Figure 3.15 (A, undigested PCR fragments) and (B, *Eco*R1 digested PCR fragments) confirming *cdc13-1* knockout in 1296-TR-transformants #1-#10. Gel analyses revealed a fragment of ~378 bp (Figure 3.15A, lanes 20-29) and two smaller fragments of 219 bp and 159 bp (Figure 3.15B, lanes 20-29) in all temperature-sensitive transformants examined (1296-ts) with varying intensity. However, none of the fragments were observed in 1296-TR transformants (Figure 3.15A, lanes 10-19). Wild type strains 640 and 641 (*CDC13*) were used as controls (lanes 5-6 respectively) along with the strains 1296-TR and -ts and 2605-TR cells (lanes 7-9 respectively), originally used for transformation.

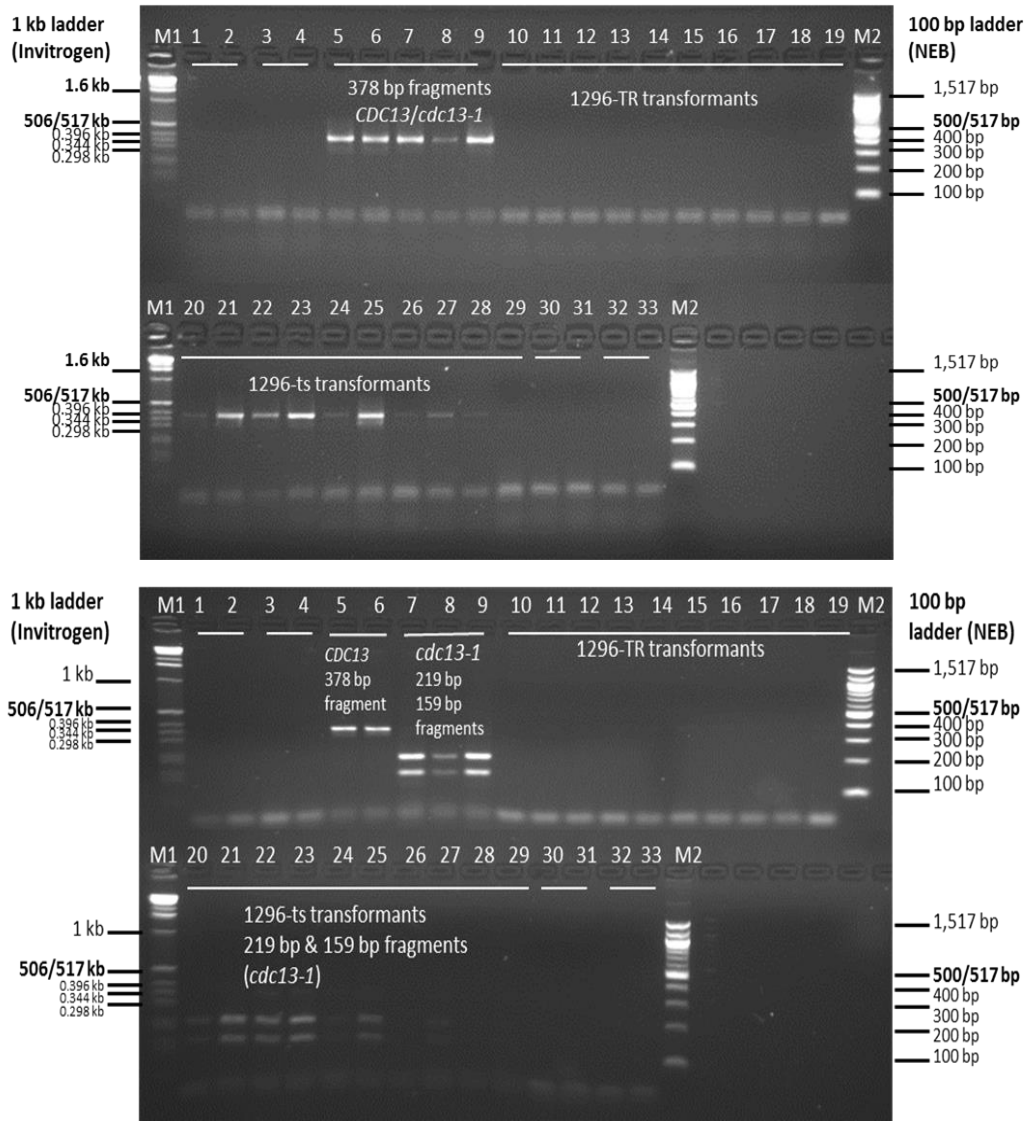

Figure 3.15. Confirmation of *cdc13-1* deletion through PCR screening: analysis of uncut and *Eco*R1digested amplicons.

Lanes M1: 1kb ladder, 500 ng (Invitrogen); 1-2: NTC-1, -ve controls; 3-4: Strain 2607 and 2608 (*cdc13*Δ), -ve controls; 5-6: Strain 640 and 641 (wild type, *CDC13*), +ve control; 7-9: Strain 1296-TR, 1296-ts and2605-TR respectively (*cdc13-1* mutant), +ve controls; 10-19: 1296-TR transformant #1-# 10; 20-29: 1296-ts transformant #1-# 10; 30-31: *cdc13-1* deletion clone (1296-TR) #1-#2, (control); 32: *cdc13-1* deletion clone (2605-TR) #1, (control); 33: *cdc13-1* deletion clone (1296-TR) #1, (control); M2: 100 bp ladder (NEB).

(**A**) Agarose gel electrophoresis of uncut amplicons.

(**B**) Agarose gel electrophoresis of *Eco*R1 digested amplicons.

Gel analysis revealed a fragment of 378 bp in all HIS^+ ts-transformants (putative) analysed (A, lanes 20-29). However, TR survivors-transformants did not show any fragment (A, lanes 10-19). PCR was performed in a 25 µl reaction volume with GoTaq Green master mix from Promega. PCR amplified uncut product (5 µl) and digest (10 µl) was analysed on 2% agarose gel.

Table 3.1 shows the comparative analysis of HIS^+ transformants with 1296 temperature sensitive strain and its temperature-resistant survivors.

Table 3.1. Comparison of *cdc13-1* gene knockout, by PCR mediated homologous recombination in temperature-sensitive *cdc13-1* strain and its temperature-resistant survivor.

Strain (DLY)	**1296-TR**	**1296-ts**
Growth temperature	30°C	23°C
Marker module DNA	100 µl (1µg)	100 µl (1µg)
Incubation temperature and time period for yeast transformation	42°C for 30 minutes	42°C for 30 minutes
Transformants obtained	35	10
Transformation efficiency	1 out of $2.4x10^6$ 4 times > than ts cells	1 out of $9.66x10^6$
Clones tested for genetic makers	Transformants #1-#10 histidine and leucine positive	Transformants #1-#10 histidine and leucine positive
Diagnostic PCR for *cdc13-1* disruption	Transformants #1-#10; No amplification, *cdc13-1* knockout in all clones tested	Transformants #1-#10; amplification with varying intensity, *cdc13-1* present in genome in all clones tested

On the basis of these results it could be concluded that appropriate mutants were successfully generated using the above mentioned protocols. Yeast cells can survive without *CDC13* in survivor strain 1296-TR in the absence of *EXO1*. Growth of these temperature-resistant survivors without Cdc13 indicates that *CDC13* might be dispensable in temperature-resistant survivors. However it was not possible to disrupt *cdc13*-1 in temperature-sensitive cells, presumingly owing to the essential function of the Cdc13 protein at low temperature. It can be hypothesised that at higher temperatures Cdc13 capping is not necessary for telomere function and that an alternative mechanism exists to maintain telomeres and ensure genomic stability. These results are in agreement with a recent report (Ngo and Lydall, 2010) illustrating that the absence of Cdc13 can allow cell division with the inactivation of three DNA damage proteins (Sgs1, Exo1 and Rad9). It would be interesting, in future studies, to investigate the mechanism that exists in temperature-resistant cells that maintain telomeres in the absence of Cdc13 and makes cell survival possible.

3.4. *cdc13-1* N- and C-terminus deletion

3.4.1. *cdc13-1* N-terminal deletion (NTΔ)

The sequence for open reading frame of *CDC13* or *cdc13-1* (1-2775) was divided into two halves, termed N- and C-terminus (see part 1 of this chapter; Figure 3.3). The first half, or N-terminus, consists of 1386 nt with respect to the N-terminus of Cdc13, and the second half from the C-terminus half of the protein composed of 1389 nt (Figure 3.3, A, C and D). *CDC13* modification for N- and C-terminus deletion was carried out in *cdc13-1 EXO1* deletion (strains 1296-TR and 1297-TR) and *CDC13 EXO1* deletion (1272) mutants.

The PCR-based homologous recombination strategy that was used for full gene deletion (Figures 3.2 and 3.3), was also adopted to generate C- and N-terminus deletions of *CDC13*. However, the yeast plasmids and gene-specific target sequence for the hybrid primers were different.

3.4.1.1. Modulating DNA template preparation for N-terminal truncation

The plasmid pFA6a-TRP1-PGAL1 (pDL515) (Chapter 2, Figure 2.5) with a tryptophan marker module was used as a template for PCR synthesis of the fragment for *CDC13* N-terminal deletion (Wach *et al*., 1997, Longtine *et al*., 1998).

The TRP1-PGAL1 DNA module is provided with an inducible promoter PGAL1 (~569 bp, *S. cerevisiae* origin), regulated by Gal4 for the transcription of the C-terminus half of protein after the deletion of its N-terminus with target-specific primers. In the marker module another upstream activating sequence (UAS) (~118 nt) mediates Gal4-dependent induction. The yeast TRP1 marker encodes a protein of 24 kDa required for the biosynthesis of the tryptophan marker.

3.4.1.1.1. Plasmid DNA extraction and size evaluation

3.4.1.1.1.1. Transformation of bacterial cells with yeast plasmid DNA

Three yeast plasmids pDL504 (pFA6a-GFP(S65T)-His3MX6) for CTΔ, pDL515 (pFA6a-TRP1-PGAL1) and pDL516 (pFA6a-His3MX6-PGAL1) for NTΔ were transformed to *E. coli* K-12 (NM522) (Figure 3.16). A single, well-isolated colony was used to set culture in nutrient broth (NB) for plasmid DNA extraction. DNA of three plasmids was extracted from host *E. coli* NM522 and dissolved in 200 µl sterile distilled water. The purified DNA (5 µl) was digested in total volume 20 µl with 20 units of a restriction enzyme.

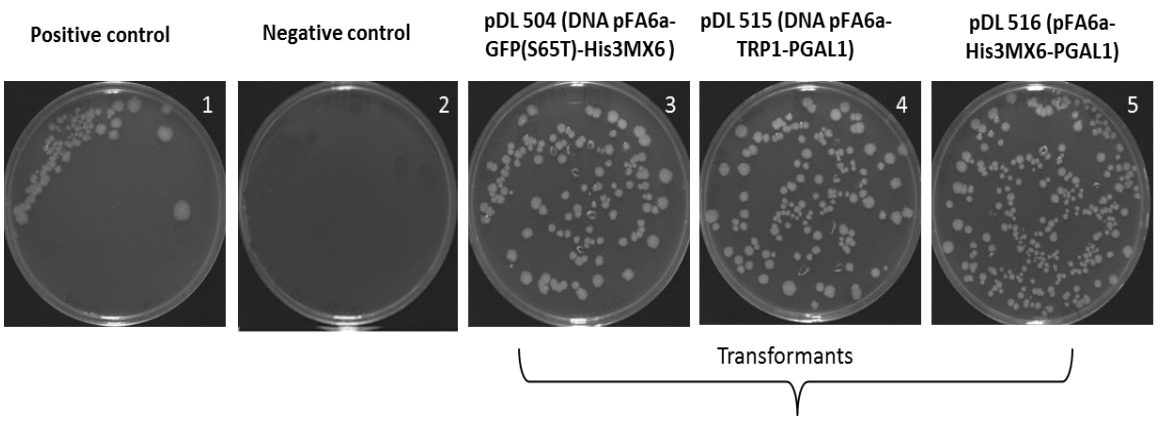

Figure 3.16. Transformation of host bacterial cells with yeast plasmids DNA.
Transformation was carried out with *E. coli* K-12 (strain NM522), chemically competent cells (200 µl) with ~200 ng of plasmid DNA (pDL 504, 515 and 516). Transformants were selected on nutrient agar (NA) medium containing 100 µg/ml of ampicillin (**3-5**). For positive control, untransformed NM 522 cells were grown on NA medium without ampicillin (**1**), while for the negative control, untransformed *E. coli* cells were grown on NA plates containing ampicillin (**2**). Transformation was carried with 45 second heat shock at 42°C. The transformed mixtures, 100 µl of each, were plated and incubated at 37°C overnight.

3.4.1.1.1.2. Plasmid DNA extraction and size estimation

Figure 3.17 represents agarose gel (0.8%) electrophoresis of extracted plasmids DNA pDL504 (4.698 kb), pDL515 (3.962 kb) and pDL516 (4.298 kb), respectively (lanes 1-3) with their approximate sizes. Purified DNA band patterns exhibited multimeric forms of plasmids with supercoiled DNA running at the front because of its smallest size. Relative size analysis shows that the plasmid in lane 1 (pDL504, 4.698 kb), is comparatively larger in size as compared to DNA in lane 2 and 3 (pDL515, 3.962 kb and pDL516, 4.298 kb respectively). However, it was difficult to estimate the exact size of the plasmids from undigested samples.

Plasmid DNA size estimation was carried out by digesting DNA with a single cut restriction enzyme, *Eco*RI, that resulted in linearised DNA fragments (lanes 4, 5 and 6), between 4 and 5 kb in size. Restriction enzyme digestion of the plasmids with *Eco*RI and/or *Pst*1 resulted in two to three fragments. Digestion of the plasmid pDL504 with *Pst*1 (lane 7) resulted in three fragments 3.086 kb, 1.165 kb and 447 bp in size corresponding to three restriction sites at 35, 1200 and 1647 on the map (Figure 3.18A). The double digestion of plasmid pDL515 with *Eco*R1 and *Pst*1 (lane 8) resulted in 2.457 kb and 1.505 kb fragments corresponding to sites 1540 for *EcoR1* and 35 for *Pst1* (Figures 3.17, 3.18A). The plasmid pDL516 produced three fragments of 3.086 kb, 796 bp and 447 bp that correspond to three sites of *Pst*1 at 35, 831 and 1278. The 447 bp fragments from plasmids pDL504 and pDL516 are not visible on the gel.
The simulative gel (Figure 3.18B) with single- and double-digested plasmids also confirms the same restriction fragment pattern.

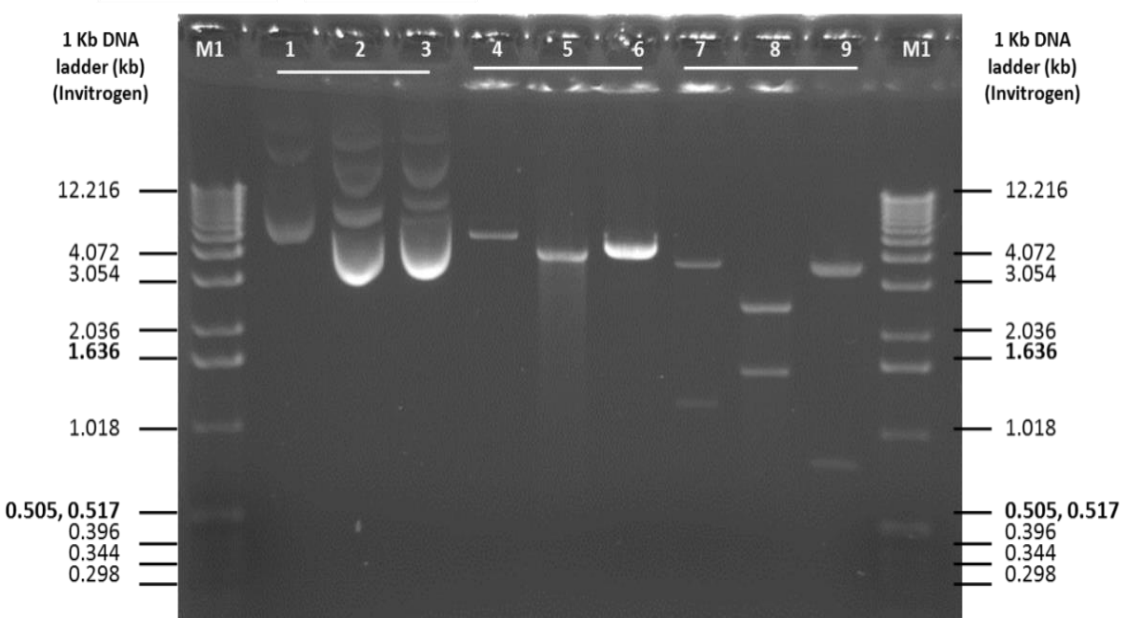

Figure 3.17. Isolation of yeast plasmid DNA and analysis of its size after digestion with restriction enzymes.

Lanes M1: 1 kb DNA marker, 500 ng (Invitrogen); **1-3**: undigested plasmid DNA (pDL504, pDL515, pDL516 respectively); **4-6**: *Eco*RI digested (linearised) DNA, pDL504 (4.698 kb), pDL515 (3.962 kb) and pDL516 (4.329 kb) respectively; **7**: *Pst*1 digested plasmid pDL504 DNA, with two fragments of approximately 3.086 kb and 1.165 kb and one fragment of 447 bp (not visible); **8**: *Pst*1 and *EcoR*I double digested plasmid DNA pDL515, with two fragments of approximately 2.457 kb and 1.505 kb; **9**: *Pst*1 digested plasmid pDL516 with two fragments of approximately 3.086 kb, 796 bp and 447 bp (not visible); **M1**: 1 kb DNA marker, 500 ng (Invitrogen).

Agarose gel electrophoresis presents uncut DNA (lanes 1-3), linearised DNA (lanes 4, 5 and 6) and double digested DNA (lanes 7, 8 and 9) for plasmid DNA pDL504 (pFA6a-His3MX6, 4.698 kb), pDL515 (pFA6a-TRP1-GAL1, 3.962 kb) and pDL516 (pFA6a-His3MX6-GAL1, 4.329 kb) respectively. Estimation of approximate size was carried out by comparing DNA with reference markers. Uncut DNA (2 µl) and digested DNA (3 µl) from each sample was analysed on 0.8% agarose gel.

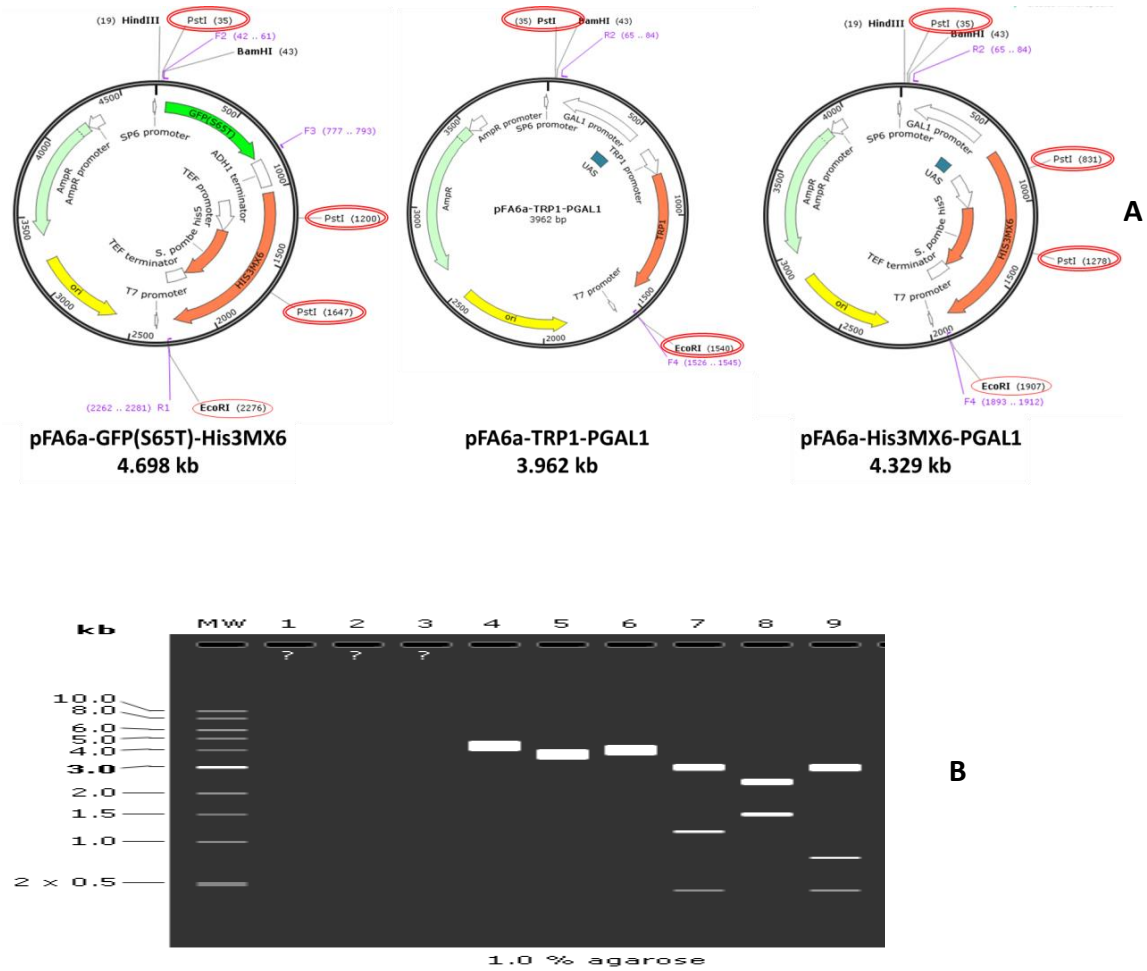

Figure 3.18. *In silico* size analysis of yeast plasmids used for N- and C-truncation.

(**A**) Maps of yeast circular plasmid DNAs showing *Eco*R1 and *Pst*1 sites utilised for digestion with restriction enzyme.

(**B**) Simulative gel showing fragments after single and double digestions.

After confirming sizes of plasmids, the diluted DNAs were diluted use as a DNA template to produce the PCR amplified module for *CDC13* gene disruption (N- and C-terminus deletion).

3.4.1.1.2. PCR synthesis of HIS3MX6-PGAL1 and TRP1-PGAL1 modulating DNA for *cdc13-1*-NTΔ

After electrophoresis analysis of extracted DNA, the purified plasmid DNAs were diluted in a ratio of 1:10 and used as DNA templates in PCR reactions. PCR was performed to produce DNA module possessing HIS3MX6-GAL1 and TRP1-GAL1 deletion cassettes for NTΔ (Figure 3.19). The sizes of the amplified fragments were examined on an analytic gel and were estimated to be ~1.9 kb for HIS3MX6-PGAL1 module (lanes 2-7) and ~1.5 kb for TRP1-PGAL1 deletion amplicons (lanes 9-14) as expected.

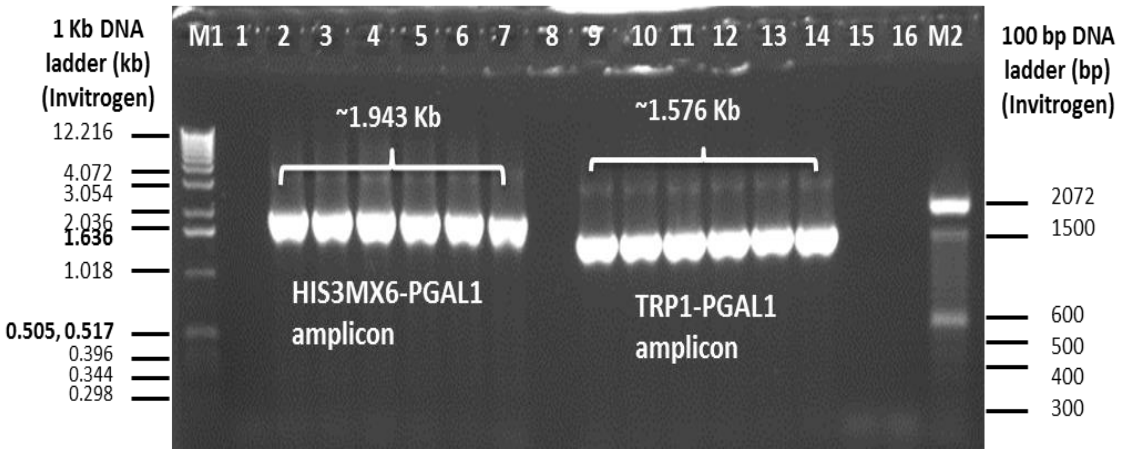

Figure 3.19. PCR amplification of HIS3MX6-PGAL1 and TRP1-PGAL1 DNA modules for *cdc13-1* NTΔ.
The N-terminal deletion modules were amplified using yeast vector pFA6a-HIS3MX6-PGAL1 (pDL516) and pFA6a-TRP1-PGAL1 (pDL515) as a template in a 50 µl reaction volume with FT-N1 and RT-N1 hybrid primers. For each sample 5 µl of PCR reaction mixture was examined on 0.8% agarose gel to confirm the presence of expected fragments.
Lanes M1: 1 kb DNA marker, 500 ng (Invitrogen); **2-7**: Amplified fragments with the plasmid template pDL516 (pFA6a-HIS3MX6-PGAL1); **9-14**: Amplified fragments with the plasmid template pDL515 (pFA6a-TRP1-PGAL1); **15-16**: Negative controls (NTC without cell or DNA); **M2**: 100 bp DNA marker, 500 ng (Invitrogen).

Amplified fragments were extracted by the phenol-chloroform method. Gel electrophoresis (Figure 3.20) shows PCR products unpurified fragments (lanes 1 and 5) and the phenol-chloroform extracted, ethanol precipitated purified fragments, each for HIS3MX6-PGAL1 (lanes 2 and 3) and TRP1-PGAL1 (lanes 6 and 7) modulating DNA respectively. The approximate concentrations of purified PCR products for both fragments were estimated to be ~40-50 ng/µl with approximately 90-95% recovery (Figure 3.20, lanes 2-3 and 6-7 respectively), based on intensities of marker bands on the analytic gel. The purified PCR products ~1-3 µg of DNA was used to transform yeast cells (*cdc13-1* mutant strains) for NTΔ.

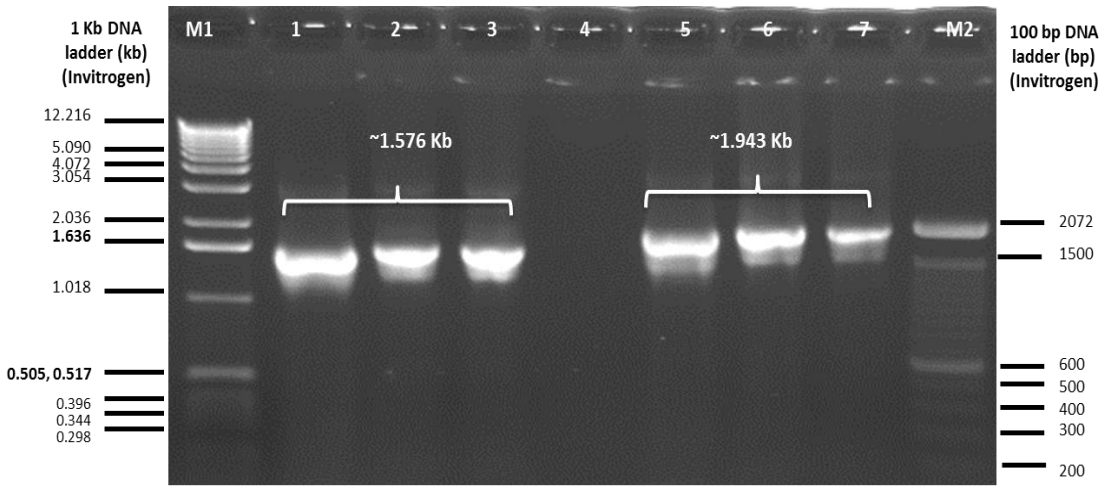

Figure 3.20. Purification and estimation of concentration of PCR amplicons for *cdc13-1* N-terminus deletion cassettes.

Lanes M1: 1 kb DNA marker, 500 ng (Invitrogen); **1**: PCR product with TRP1-PGAL1 containing plasmid DNA (not purified); **2-3**: PCR product for NTΔ (purified); **4**: Blank; **5**: PCR products for HISMX6-PGAL1 for NTΔ (not purified); **6-7**: PCR products for HIS3MX6-PGAL1 marker for NTΔ (purified); **M2**: 100 bp DNA marker, 500 ng (Invitrogen). 2 µl each for HIS3MX6-PGAL1 and TRP1-PGAL1 (lanes 6 and 7) modulating DNA respectively were analysed on the analytical gel. The PCR products 2 µl were examined on 0.8% agarose gel.

The purified linear DNA with target-specific oligonucleotides (5' ends of hybrid primers) were used to transform yeast strains 1296-TR (*cdc13-1*), 1297-TR (*cdc13-1*) temperature resistant survivors and 1272 (*CDC13*) to disrupt *CDC13* N-terminus in its normal chromosomal location.

3.4.1.1.3. Generation and analysis of temperature resistant survivors

Temperature-resistant survivors were generated at high temperature (36°C) from two temperature-sensitive *cdc13-1* mutant strains DLY 1296 and DLY 1297. Strain DLY 1272 with wild type *CDC13* was also grown at 36°C (Figure 3.21A). The survivors from 1296-TR and 1297-TR produced heterogeneously sized (minute and large irregularly shaped colonies with rough edges (Figure 3.21A, 1 and 2), that could be genetically unstable cells. In contrast, strain 1272 generated homogenous, uniform size colonies with smooth edges, (Figure 3.21A, 3).

At 23°C, strains 1296 (*cdc13-1*), 1297 (*cdc13-1*) and 1272 (*CDC13*) exhibited growth in all three suspensions including one concentrated and two diluted suspensions tested [(Figure 3.21B, plate (p) 1, 2 and 3, non-diluted culture (a), 10^{-2} dilution (b) and 10^{-4} dilution (c)], while at 36°C strains 1296 and 1297 showed growth in only non-diluted concentrated suspension (p 4 and 5, dilution a) that is remarkably low as compared to growth at 23°C. However, strain 1272 containing intact *CDC13* gene, presented more or less similar growth patterns at both 23°C (29 cells per 50 µl) and 36°C (16 cells per 50 µl) (p 3 and 6).

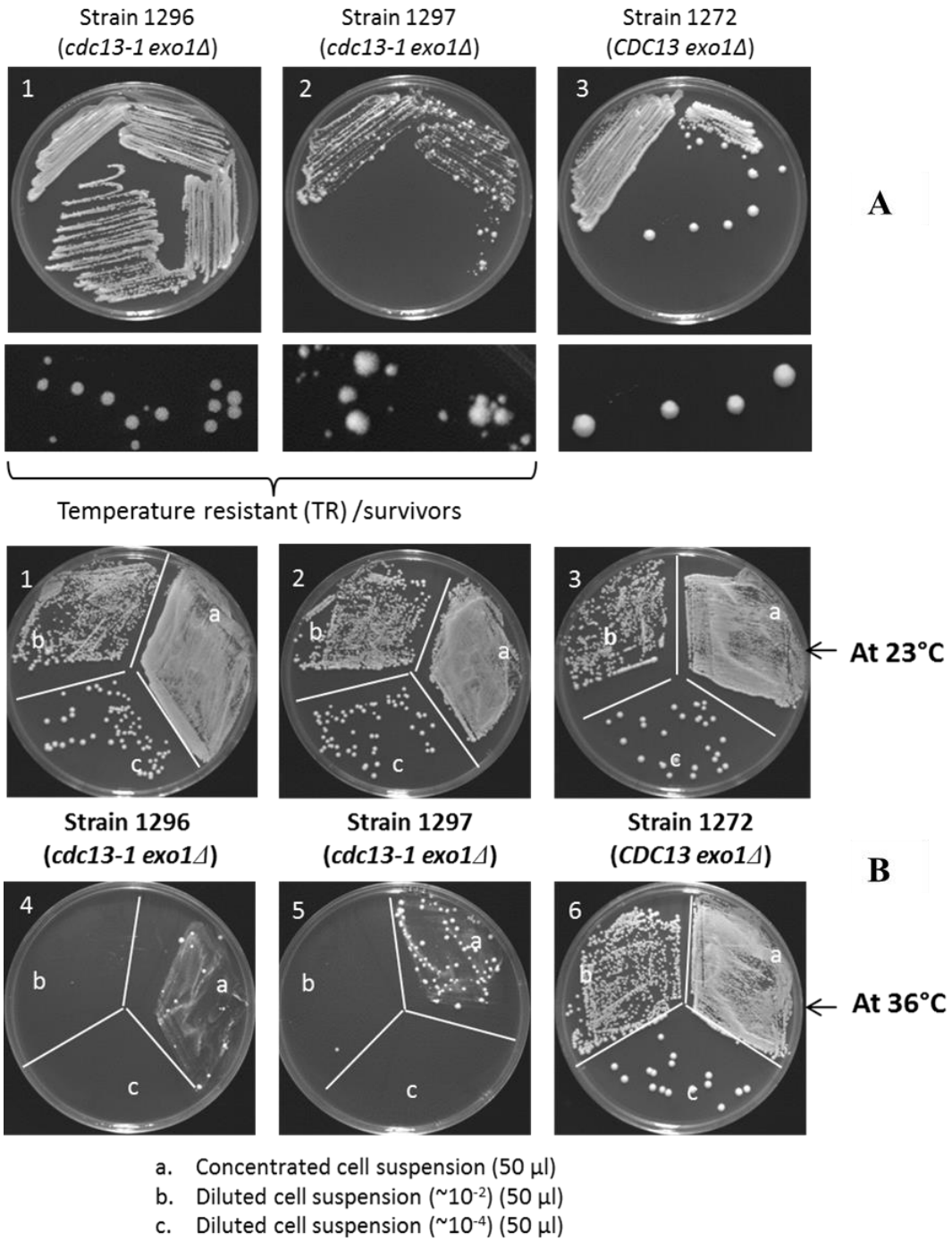

Figure 3.21. Generation of survivors at high temperature (36°C).

(A) Yeast strains 1296 and 1297 (*cdc13-1 exo1Δ*) produced TR colonies (plates 1-2 respectively). Strain 1272 (*CDC13 exo1Δ*) grows at high temperature but does not show survivors (plate 3). Strains 1296 and 1297 (*cdc13-1 exo1Δ*, 1 and 2) showed rough edges and non-uniform sizes of colonies while strain 1272 (*CDC13 exo1Δ*, 3) at high (36°C) temperature shows colonies with smooth edges and uniform size with no growth retardation.

(B) The freshly grown cells from strains, 1296-TR, 1297-TR and 1272 were serially diluted. The cells from concentrated suspension (a) and two different dilutions, 10^{-2} (b) and 10^{-4} (c), were plated on YEPD medium. Plates were cultivated for five days at 23°C and 36°C. Each section (a, b, or c) of the plate showed the comparable growth of cells from 50 µl of the suspension at 23°C or 36°C.

3.4.1.1.4. Selection of temperature-resistant survivors to prepare competent cells

TR cells from strains 1296 and 1297 (*cdc13-1 exo1Δ*), and 1272 (*CDC13 exo1Δ*) were further analysed for the incidence of spontaneous revertants and for the presence of metabolic markers by replica plating. Ten colonies each from strains 1296-TR and 1297-TR cells (previously selected at 36°C) were randomly picked and were replica plated at two different temperatures, 30°C and 37°C (Figure 3.22 and 3.28 respectively). Strains 1296-TR and 1297-TR (colonies 1-10) showed growth only on YEPD and leucine-deficient media (replica 1 and 3) confirming their auxotrophy for histidine, tryptophan and uracil. However, a few colonies from both strains grew on tryptophan- and uracil-deficient media. Strain 1296-TR displayed tryptophan revertants, not very obvious at 30°C (Figure 3.22, replica 4) but prominent at 37°C represented by replica 4 (streak 1B, 3C, 4A, 4D and 8D) and uracil revertants, by replica 5, (colony number 7 in streaks C) at 37°C as shown in Figure 3.22. Strain 1297-TR also produced tryptophan revertants observed at 30°C (Figure 3.23, replica 4, colony number 3B and 7D), and at 37°C (replica 4, colony number 1D, 4A, 4B, and 7B-7D), and uracil revertants observed at 37°C (replica 5, colony number 10, in B-D streaks).

On the basis of revertant analysis, the colony numbers '3A' and '2A' were selected for strain 1296 and strain 1297 respectively to set overnight cultures to prepare competent cells avoiding revertants.

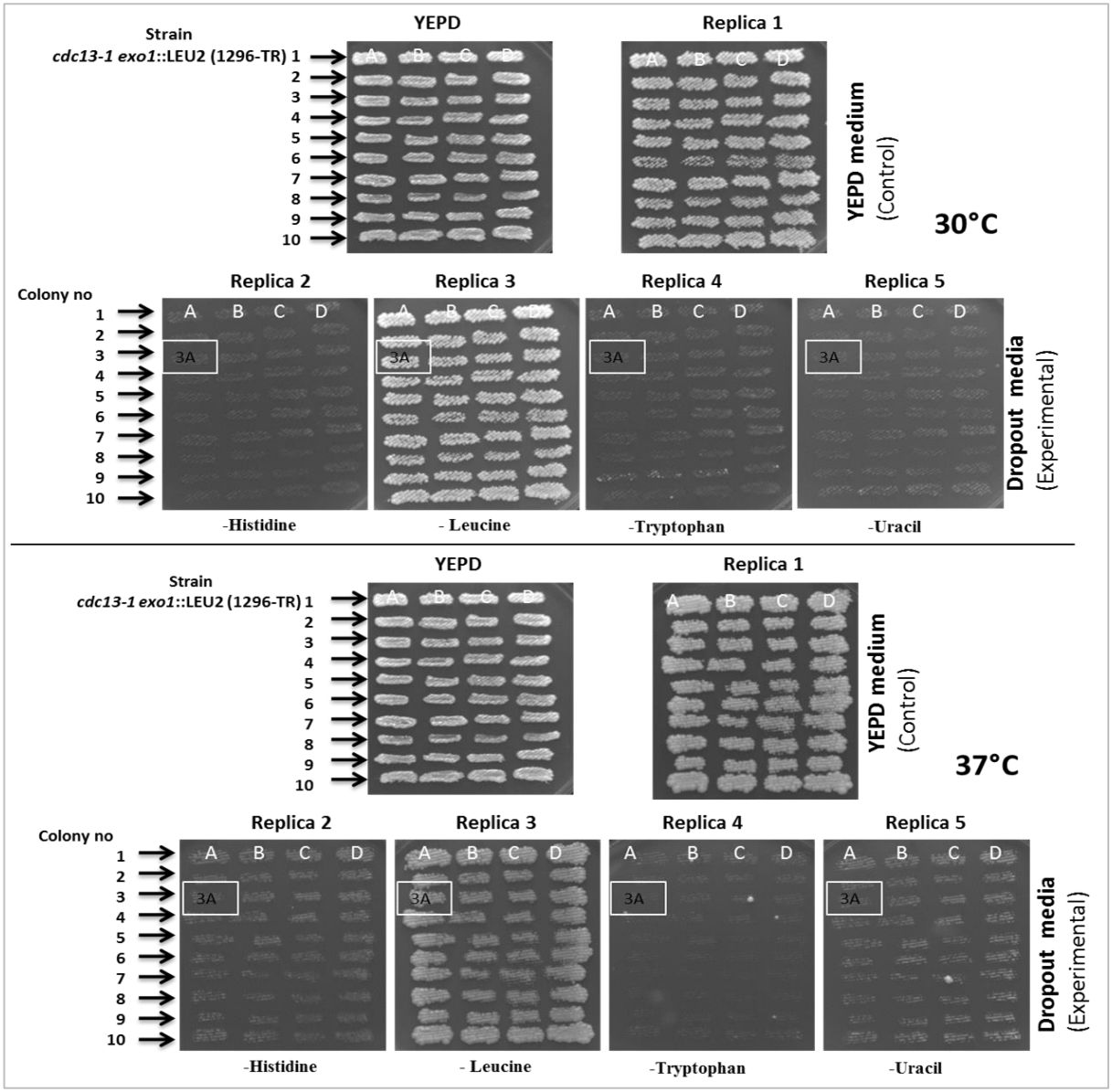

Figure 3.22. Confirmation of genetic markers in survivors strain 1296-TR cells by replica plating on YEPD and dropout media by exposing cells at 30°C and 37°C.

For strain 1296-TR, 10 colonies, each with four streaks (A-D) were analysed by replica plating (1-5) for metabolic markers and revertants. All tested colonies (1-10) showed growth at YEPD (replica 1) and medium lacking leucine (replica 3). However, a few colonies (revertants) grew on tryptophan deficient (replica 4) and uracil lacking (replica 5) media.

The cells from streak '3A' (replica 3) were used to set overnight culture for preparation of competent cells.

Replica plates were incubated at 30°C and 37°C for 5 days before photography. Pictures were taken using a Syngene gel documentation system.

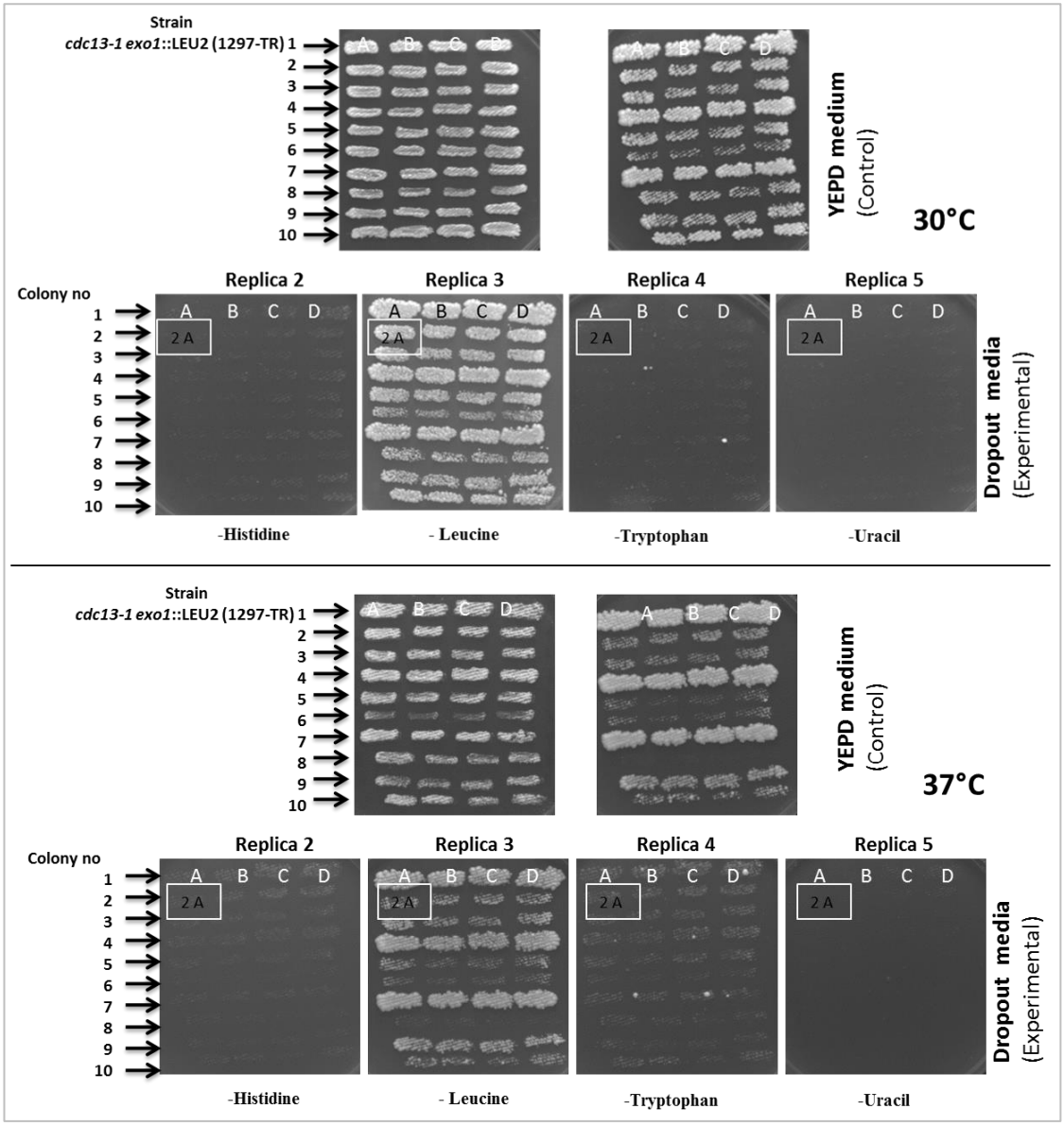

Figure 3.23. Confirmation of genetic markers in survivors strain 1297-TR cells by replica plating on YEPD and dropout media by exposing cells at 30°C and 37°C.

For strain 1297-TR, 10 colonies, each with four streaks (A-D) were analysed by replica plating (1-5) to examine metabolic markers and revertants. All tested colonies (1-10) showed growth at YEPD (replica 1) and medium lacking leucine (replica 3). Few colonies (revertants) also emerged on medium lacking tryptophan (replica 4) at both 30°C and 37°C. Few cells from streak '2A' (replica 3) were used to set overnight culture for preparation of competent cells.

Replica plates were incubated at 30°C and 37°C for 5 days before photography. Pictures were taken using gel documentation system (Syngene).

3.4.1.1.5. Checking genetic markers in competent cells

To verify further that no revertants grew in the cells selected to set cultures for the preparation of competent cells, the overnight starter cultures grown for competent cells were initially analysed for the incidence of revertants in 5 µl of the suspension. As presented in Figure 3.24, all three strains showed growth on YEPD (1) and leucine-deficient media (3) indicating the presence of LEU2 marker. However, scarce revertants were emerged on T^{-} medium (4). The total number of tryptophan revertants was counted in 5 µl of suspension (x8 streaks in total) with 10 colonies in strain 1272, 5 colonies in 1296-TR and 6 in strain 1297-TR. However, only one histidine revertant (Plate 2, 3A) was observed in strain 1296-TR.

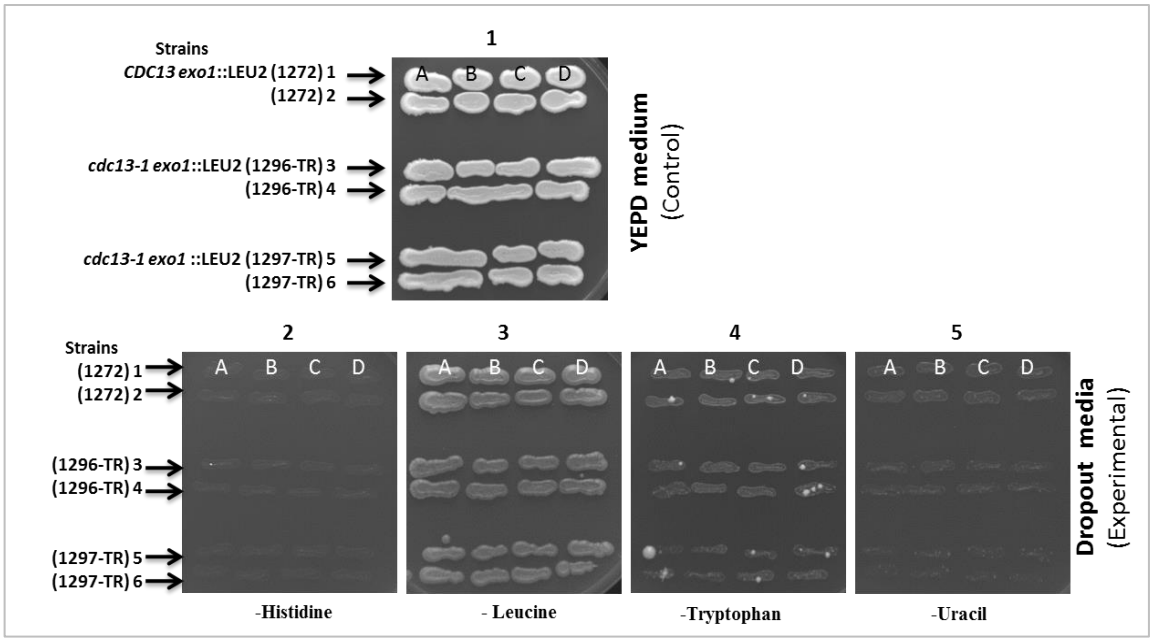

Figure 3.24. Analysis of recovery of revertants from strains 1272, 1296-TR and 1297-TR cells on dropout media.

Cells from the overnight cultures of strains 1272, 1296-TR and 1297-TR were streaked (5 µl per streak) on YEPD (**1**) and dropout media (**2-5**). The plates were incubated at 30°C for 5 days before photography. Pictures were taken using a gel documentation system (Syngene).

The frequency of revertants was further estimated in 50 µl volume of the competent cell suspension (Figure 3.25) by comparing it with the total viable count and is presented in Table 3.2. All three strains exhibited revertants for the tryptophan markers. However, no obvious revertants were observed for the histidine marker for strain 1297-TR.

It appears from the above observations that the tryptophan marker could generate an unavoidable background of spontaneous revertants (as a result of gene conversion or other recombinations) that might result in false positives in gene disruption by homologous

recombination. The 100 µl of freshly prepared competent cell suspension for each sample were used to transform with yeast modulating DNA for *CDC13* disruption.

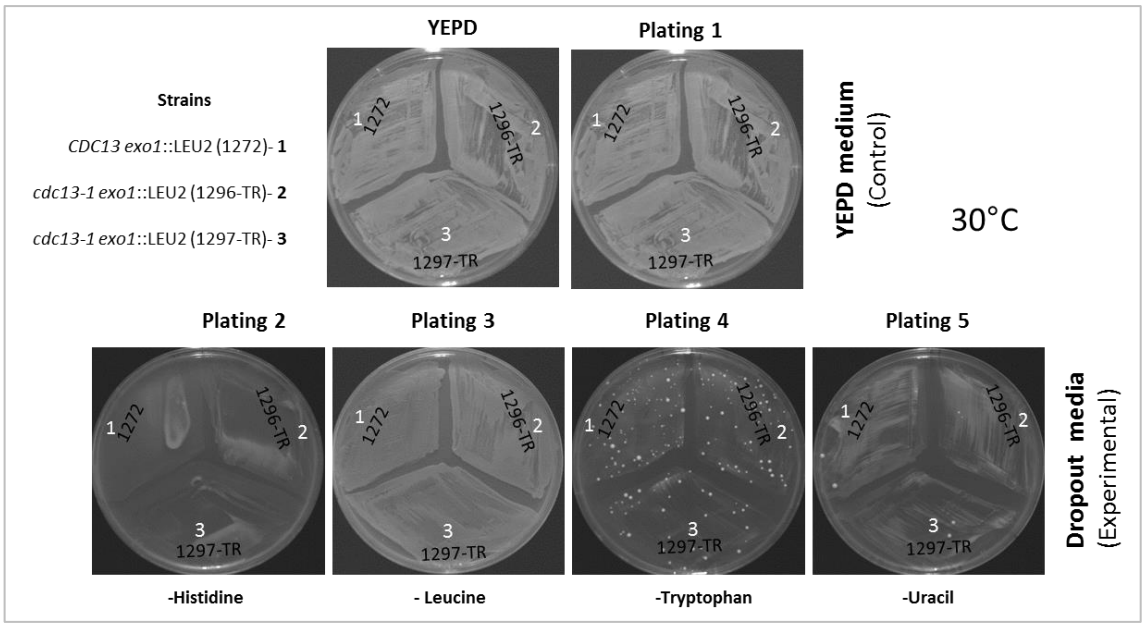

Figure 3.25. Analysis of competent cells for spontaneous revertants in population of 1272, 1296-TR and 1297-TR by testing cells for the incidence of prototrophies on dropout media.

Competent cells from strains 1272, 1296- and 1297-TR showed abundant growth on YEPD and medium lacking leucine (–L) confirming their genetic markers (plating 3). However, a few colonies appeared on tryptophan- and uracil-deficient media (plating 4 and 5 respectively). The total numbers of revertants in 50 µl of cell suspension were 92, 75 and 39 colonies for tryptophan and 2 colonies each for uracil in strains 1272, 1296-TR and 1297-TR respectively.

Plates with suspension were incubated at 30°C for 5 days before photography. Pictures were taken using gel documentation system (Syngene).

Table 3.2. Frequency of revertants in strains 1296-TR, 1297-TR and 1272 grown at 30°C.

	Strains (DLY)	No of Revertants/50 µl (on medium lacking T*)	No of Revertants/50 µl (on medium lacking H)	Total viable count/50 µl	Frequency of revertant in TR cells (revertants/viable count)
1	1272 (36°C) (L^+)	92	0 colony	$110.5x10^6$	$0.83x10^{-6}$
2	1296-TR (L^+)	75	1	$26x10^6$	$2.88x10^{-6}$
3	1297-TR (L^+)	39	0	$84x10^6$	$0.46x10^{-6}$

*Multiple number of tryptophan revertants appeared on medium deficient in T in all three strains tested, in contrast to other media (L^- and U^-), where no revertants were observed.

3.4.1.1.6. Analysis of survivors for genotypic *CDC13* status

Finally, survivors were analysed for the presence of *cdc13-1* and *CDC13* through PCR in order to exclude clones with *CDC13* alleles resulted from possible reversions of *cdc13-1* to *CDC13*. Figure 3.26 confirmed the presence of 378 bp fragments in cells of ts strains and TR survivors.

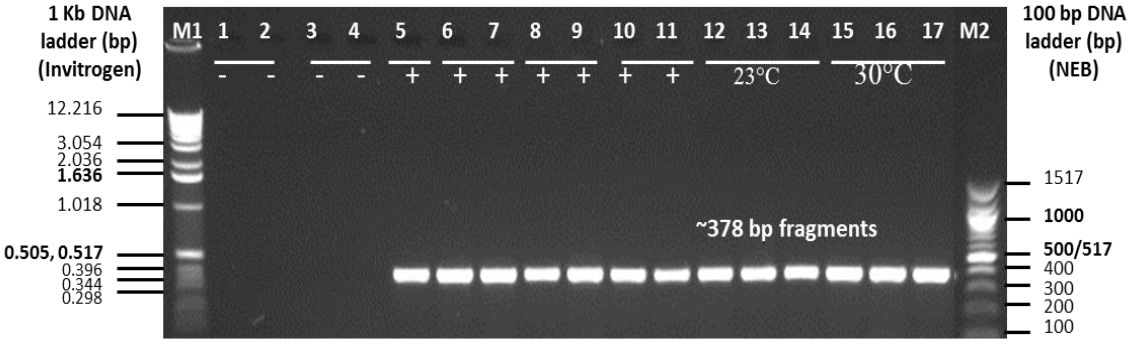

Figure 3.26. PCR analysis of cells grown at 30°C for the presence of *cdc13-1* and *CDC13.*

Lanes M1: 1 kb ladder, 500 ng (Invitrogen); **1-2**: NTC, -ve control; **3-4**: strains 2607, 2608 (*cdc13*Δ),-ve controls; **5**: strain 640 (WT), +ve control; **6-7**: strains 2625 and 2626 (*cdc13-1* mutant) +ve controls; **8-9**: strains 2605-ts and 1108-ts (*cdc13-1* mutant) +ve controls; **10-11**: strains 2605-TR and 1108-TR (*cdc13-1* mutant) +ve controls; **12-14**: strains 1272 *(CDC13)*, 1296 and 1297 (*cdc13-1*) 23°C; **15-17**: strains 1272 *(CDC13)*, 1296 and 1297 (*cdc13-1*) 30°C; **M2**: 100 bp ladder, 500 ng (NEB).

The strains used for transformation were analysed by PCR from colonies treated by heat (95°C). For PCR, temperature-sensitive strains 1296 and 1297 and their temperature-resistant survivors, and strain1272 were cultivated on YEPD medium at 23°C and 30°C for three days. A loopful of cells from a pure culture were denatured at 95°C for 15 minutes prior to PCR. PCR products from these strains exhibited a single fragment of ~378 bp size (lanes 12-17) with diagnostic primers (N1 and N2) for the N-terminus.

Wild type strain 640 (*CDC13*) as well as mutant strains 2625, 2626, 2605 and 1108 (ts and TR) with *cdc13-1* were used as positive controls (lanes 5-11). Uncut PCR products (5µl) were analysed on a 1.5% agarose gel.

3.4.1.2. Transformation of yeast cells with amplified *CDC13* N-terminus disruption modules

Tranformations of cells from three strains 1296-TR, 1297-TR and 1272 were carried out according to the standard protocol (Materials and Methods). Freshly prepared competent cells (100 µl each) were transformed with ~1.5 µg of purified PCR product for N-terminus truncation with TRP1-PGAL1 and HIS3MX6-PGAL1 deletion modules.

3.4.1.2.1. Transformation with TRP1-PGAL1 marker module for *CDC13* N-terminus deletion

The transformants with TRP1-PGAL1 deletion cassettes were selected on T^-L^- dropout medium (Figures 3.27, 3.28 and 3.29; 1a-5a) for strains 1296-TR, 1297-TR and 1272 respectively with appropriate negative (non-transformed cells on T^-L^- medium) and positive controls (non-transformed cells on L^- dropout medium). There was moderate growth of revertants in the negative controls for all three strains as compared to abundant growth for positive controls.

To purify transformants from background growth, colonies were replica-plated for a second round of selection (Figures 3.31, 3.32 and 3.33; 1b-5b). From the second selection, 24 T^+L^+ colonies each from strains 1296 and 1297 and 16 transformants from strain 1272 were screened for N-terminal deletion using a diagnostic PCR assay. The rapid screening assay involved PCR amplification for the N- and C-terminus specific DNA sequences directly from colonies and detection of amplicons on the basis of their molecular sizes by agarose gel electrophoresis.

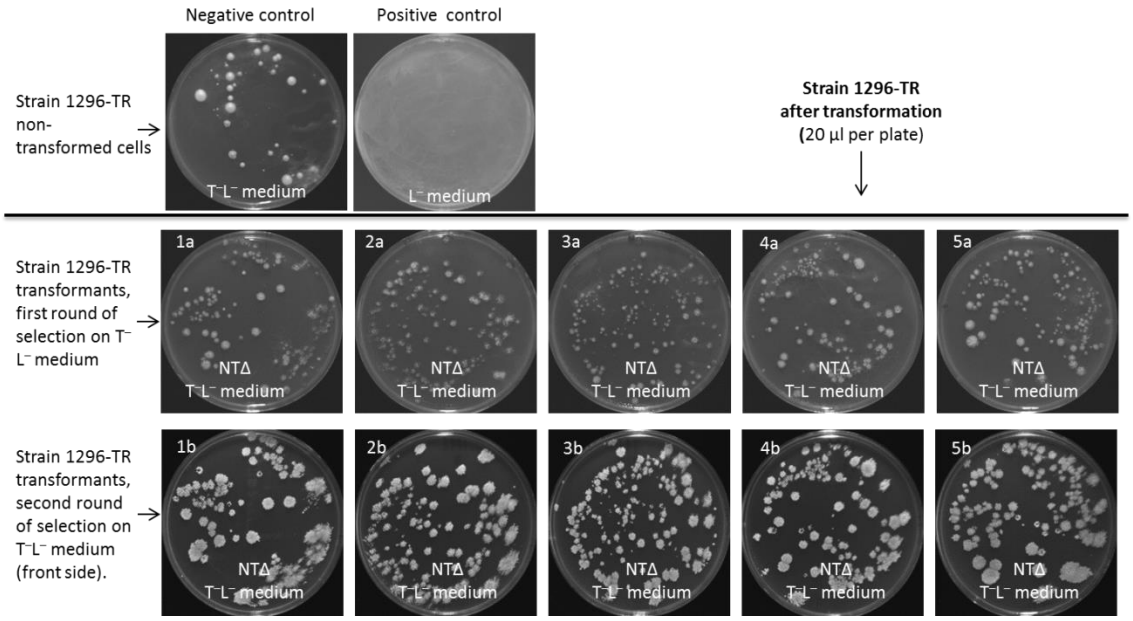

Figure 3.27. Transformation of 1296-TR cells for NTΔ and selection of trp^+ transformants (1-5) through the first (1a-5a) and second (1b-5b) round of selection on T^-L^- medium. Approximately 685 T^+L^+ colonies per 100 µl of competent cells grew after five to seven days of incubation at 30°C. These were replica-plated at 30°C for a repeated selection. Negative control shows approximately 39 colonies grown after plating 20 µl of competent cells. They could be spontaneous revertants.

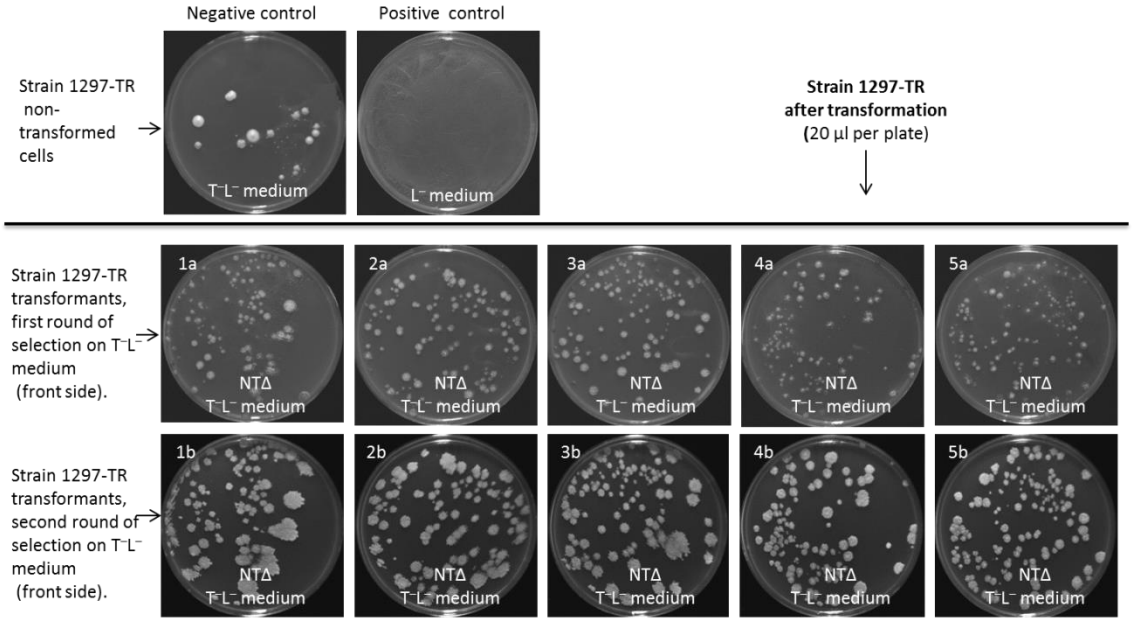

Figure 3.28. Transformation of 1297-TR cells for NTΔ and selection of trp^+ transformants (1-5) through first (1a-5a) and second (1b-5b) rounds of selection on T^-L^- medium. Approximately 550 T^+L^+ colonies per 100 µl competent cells grew after five to seven days of incubation at 30°C. These were replica plated at 30°C for a repeated selection. Negative control shows approximately 25 colonies per 20 µl of competent cell suspension. They could be spontaneous revertants.

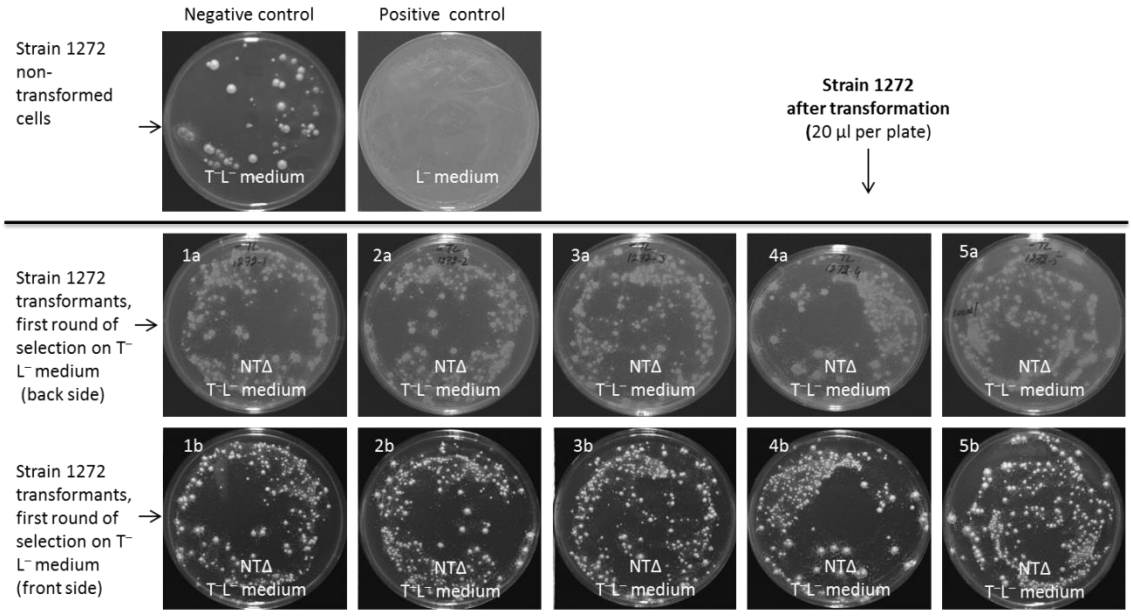

Figure 3.29. Transformation of 1272 cells for NTΔ and selection of trp^+ transformants (1-5) through first (1a-5a) round of selection on T^-L^- dropout medium.

Numerous T^+L^+ colonies (from plating 100 µl of competent cells) grew after five to seven days of incubation at 30°C. They were replica-plated at 30°C for the second of selection. Negative control also shows approximately 25 colonies (spontaneous revertants) resulted from plating 20 µl of competent cells. Sixteen well separated colonies were picked randomly for PCR screening for NTΔ and were analysed through PCR.

3.4.1.2.2. Transformation with HIS3MX6-PGAL1 marker module for *CDC13* N-terminus deletion

Tranformation of three strains (1296-TR, 1297-TR and 1272) were carried out with deletion cassettes containing the HIS3MX6-PGAL1 module marker according to the protocol adopted for NTΔ. The transformants were selected on dropout medium lacking histidine and leucine. There was no growth on H^-L^- dropout plates used as negative controls. However, positive controls (the plates with L^- medium) showed abundant growth for all of these three strains.

3.4.1.3. Screening for *CDC13* disruption and marker module integration through analytical PCR

All three initial strains 1296-TR, 1297-TR and 1272 were auxotrophs for tryptophan and histidine markers. The selection of transformants for NTΔ on tryptophan-deficient medium (in case of the TRP1-PGAL1 deletion module) and histidine-deficient medium (HIS3MX6-PGAL1 deletion module) indicates the presence of the respective markers. However, to confirm whether these markers had replaced the N-terminus of *CDC13*, further analysis of these transformants was required to confirm the integration of these markers and deletion of the desired sequence from *CDC13*. Analytical PCR for the detection of N-terminus (using N1 and

N2 primer pair) and C-terminus (C1 and C2 primer pair) of *CDC13* were performed. Analysis of the transformants was carried out with diagnostic PCR to detect TRP1-PGAL1 and HIS3MX6-PGAL1 (using T1 and T2 primer pair), and HIS3MX6 (using H1 and H2 primers) to verify the integration of the tryptophan or histidine marker module into the genome. Amplicon were determined for their molecular size by electrophoretic separation of PCR reaction products on agarose gel.

3.4.1.3.1. Diagnostic PCR for the confirmation of *CDC13* region

To check the primers' specificities, diagnostic PCR was performed with cells from strains 1296-TR, 1297-TR (*cdc13-1* mutants) and wild type strain 640. Electrophoresis analysis (Figure 3.30) manifested a single fragment of 378 bp for the N-terminus of *cdc13-1* or *CDC13* (lanes 1-4) and 276 bp for the C-terminus (lanes 5-8) in all four samples examined with almost the same intensity, confirming the presence of both halves of *CDC13* in chromosomal DNA of the tested cells.

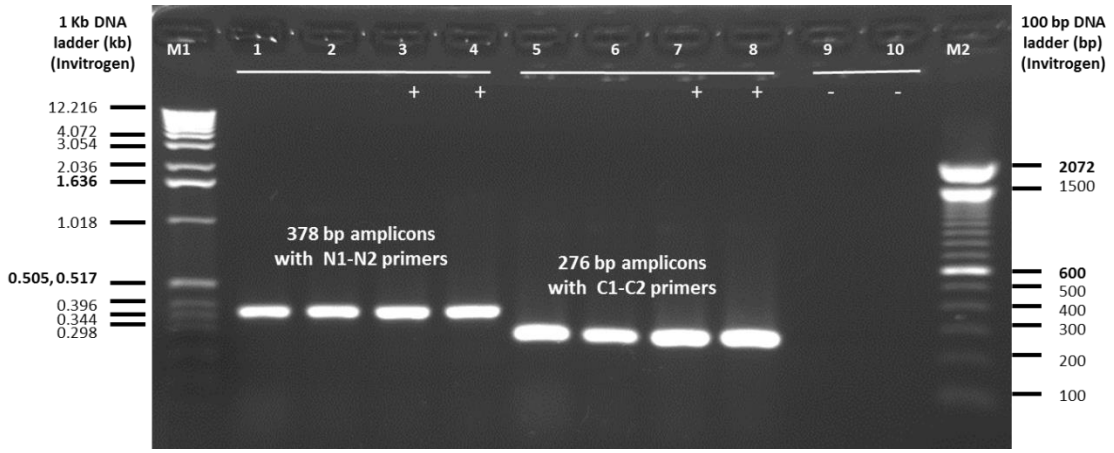

Figure 3.30. Diagnostic PCR to detect *CDC13* (N- and C-terminus): analysis of PCR products on agarose gel.

Lanes M1: 1 kb ladder, 500 ng (Invitrogen; **1-2**: PCR products with cells from strains 1296-TR and 1297-TR (*cdc13-1* mutants); **3-4**: PCR product with cells from strain 640 x2 (WT, *CDC13*), +ve control; **5-6**: PCR products with cells from strain 1296-TR and 1297-TR (*cdc13-1* mutants); **7-8**: PCR products with cells from strain 640 x2 (WT, *CDC13*), +ve control; **9-10**: NTC, -ve control; M2: 100 bp ladder, 500 ng (Invitrogen).

Two set of PCR were carried out with freshly grown yeast cells (phenotypically pure culture). Cells from the subculture of single colony were re-suspended in sterile water (20 µl), denatured in a heat block for 15 minutes. The supernatant was separated by centrifugation and used as a template source for PCR. The PCR was carried out in 25 µl volume with 2 µl supernatant of heated cells (genomic DNA) with 1x master mix (Promega's GoTaq Green master mix) and 2 µM of primers. PCR amplified products (7 µl) were examined on 1.5% agarose gels. Agarose gel analysis of PCR products for *CDC13* N- (N1 and N2 primer pair) and C-terminus (C1 and C2 primer pair) shows discrete bands of DNA fragments from different strains.

3.4.1.3.2. Diagnostic PCR for the detection of marker-specific fragment to confirm marker integration

Diagnostic primers for the confirmation of marker modules were selected from the reported sequence (Longtine *et al*., 1998). DNA of plasmids pDL504, pDL516 and pDL515, were analysed using primer pairs H1-H2 and T1-T2 to check for their specificity. H1 and H2 primers allowed amplifying a fragment of ~1.6 kb (1.579 kb) specifically from plasmid DNA pDL504 possessing the HIS3MX6 marker module only (Figure 3.31, lane 2). Conversely, T1 and T2 primers allowed amplification of ~1.8 kb (1.845 kb) and ~1.5 kb (1.481 kb) fragments of the HIS3MX6-PGAL1 (lane 6) and TRP1-PGAL1 (lane 7) marker module from plasmids pDL516 and pDL515 (DNA) respectively. However, H1 and H2 primers produced a faint band of ~1.6 kb in plasmid pDL516 (lane 3) and using T1 and T2 primers resulted in a faint band of ~1.8 kb in plasmid pDL504 with HIS3MX6 (lane 5). There was no amplification for the TRP1-PGAL1 module (with template DNA of plasmid pDL515, lane 4) using the H1 and H2 primer pair, confirming their specificity for the pDL504 template only. As the screenings of mutants by diagnostic PCR were performed with heated cells rather than DNA this further reduced the intensity of non-specific faint bands. Considering primer specificity, the H1 and H2 primers could only be utilised to screen C-terminus truncated mutants with the histidine marker whereas primers T1 and T2 could be used to screen N-terminus truncated mutants with either HIS3MX6-PGAL1 or TRP1-PGAL1 module with resulting in size-specific PCR products.

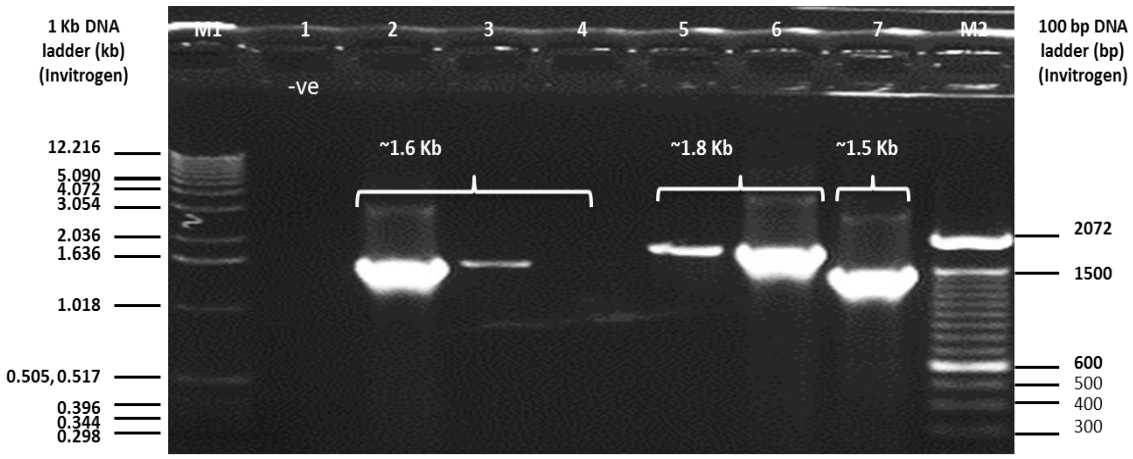

Figure 3.31. Diagnostic PCR to detect integrated modulating DNA sequences (HIS3MX6 and TRP-PGAL1): analysis of PCR products on agarose gel.

Agarose gel analysis of PCR products of HIS3MX6 (H1-H2 primer pairs) and TRP1-GAL1 (T1-T2 primer pairs) DNA shows primers' specificities for template DNA.

Lanes M1: 1 kb DNA marker, 500 ng (Invitrogen); **1**: negative control (NTC); **2**: H1-H2-PCR products with template DNA pDL504 (pFA6a-GFP(S65T)-HIS3MX6); **3**: H1-H2-PCR reaction product with template DNA pDL516 (pFA6a-HIS3MX6-PGAL1; **4**: H1-H2-PCR reaction product with template DNA pDL515 (pFA6a-TRP1-PGAL1); **5**: T1-T2-PCR amplified fragment with template pDL504 (pFA6a-GFP(S65T)-HIS3MX6); **6**: T1-T2-PCR amplified fragment with template pDL516 (pFA6a-HIS3MX6-PGAL1; **7**: T1-T2-PCR amplified fragment with template pDL515 (pFA6a-TRP1-PGAL1); **M2**: 100 bp DNA marker, 500 ng (Invitrogen).

DNA of plasmids pDL504, pDL516 and pDL515, were analysed using primer pairs H1-H2 and T1-T2 to check for their specificity.

PCR was performed in 25 µl reaction volume using 1x master mix (Promega's GoTaq Green master mix) and 2 µM of forward and reverse primers with ~100 ng of plasmid DNA template. Amplified products (7µl) were analysed on a 0.8% agarose gel.

3.4.1.3.3. Genotypic analysis of transformed cells

To verify disruption of *cdc13-1* or *CDC13* with marker cassettes TRP1-PGAL1 and HIS3MX6-PGAL1 for NTΔ, the $T^+L^+$and H^+L^+ transformants were screened by diagnostic PCR for N-terminus with appropriate controls.

3.4.1.3.4. Diagnostic PCR for the confirmation of *cdc13-1* NTΔ in $TRP1^+$ transformants

After the second round of selection, T^+L^+ transformants from strains 1296-TR, 1297-TR and 1272 were analysed by diagnostic PCR to verify N-terminus disruption and integration of the marker. In total, 24 transformants (each from strains 1296-TR and 1297-TR and 16 transformants from strain 1272) were analysed systematically for the detection of the N-

terminus (PCR with N1-N2 primers), TRP1-PGAL1 marker module (PCR with T1-T2 primers) and finally for the C-terminus (PCR with C1-C2 primer pair, data not shown).

3.4.1.3.5. Screening of *cdc13-1* NTΔ::(TRP1-PGAL1) in mutants of strain 1296-TR

3.4.1.3.5.1. Analytical PCR for the N-terminus

The 24 tryptophan-positive transformants were analysed by diagnostic PCR for *cdc13-1* NTΔ in survivor strains 1296. Gel analysis revealed a fragment of ~378 bp in 18 transformants #N1, N3 and N8-N14 (Figure 3.32, lanes 9, 11 and 16-22 respectively) and transformants #N15-N20 and #N22-N24 (Figure 3.34, lanes 9-14 and 16-18 respectively) in consonance with controls *cdc13-1* (Figures 3.32 and 3.34, lanes 5-6) and *CDC13* (Figures 3.32 and 3.34, lanes 7-8) indicating the presence of *cdc13-1* or *CDC13*, however no amplification was observed in other transformants analysed (Figure 3.32, lanes 10 and 12-15; Figure 3.34, lane 15) confirming successful deletion of *cdc13-1* gene by target guided homologous recombination. As the N-terminus fragment of *cdc13-1* should be replaced by a marker cassette of TRP1-PGAL1 resulting in *cdc13-1*-NTΔ::TRP1-PGAL1, the correct integration of TRP1-PGAL1 was confirmed by second analytical PCR with the marker specific primers T1 and T2.

3.4.1.3.5.2. Analytical PCR for the TRP1-PGAL1 modular marker

In parallel to diagnostic PCR, the same supernatant from heated cells was examined for the tryptophan marker module with the T1 and T2 primer pair. The presence of the tryptophan marker module was confirmed in six mutants out of a total of 24 examined for NTΔ (Figure 3.33, lanes 8 and 10-13; Figure 3.35, lane 13). The all six T^+L^+ transformants (#N2, N4-N7 corresponding to lanes 8 and 10-13 in Figure 3.33, and #N21 in Figure 3.35, lane 13) respectively, displayed discrete marker-specific bands of the TRP1-PGAL1 module with varying intensity and did not amplify the gene-specific N-terminus fragment, confirming the replacement of the N-terminus with the TRP1 marker module. Conversely, all other $TRP1^+$ transformants that did not amplify the marker but showed *cdc13-1*-N-terminus fragment, could be spontaneous revertants, (rather than recombinants) emerging as a result of gene conversion.

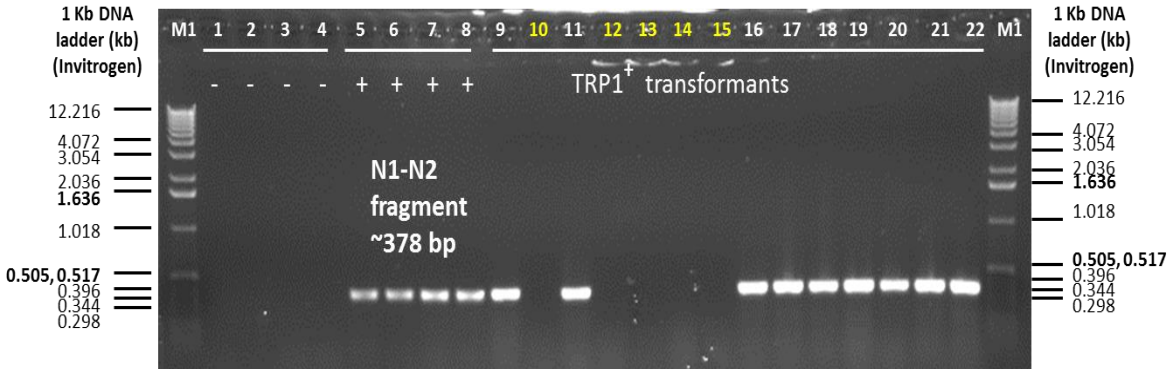

Figure 3.32. PCR screening (1-14) for *cdc13-1* N-terminus deletion (NTΔ::TRP1) in the strain 1296-TR: agarose gel electrophoresis of PCR products (N1-N2 primer pair).

The putative, *cdc13-1* NTΔ transformants (#N1-N14) were screened by PCR for *cdc13-1* N-terminus. The PCR was carried out with N1-N2 diagnostic primers in 25 µl reaction volume with 2 µl of denatured genomic DNA from cells. The PCR products (10 µl) were examined on a 1.5% agarose gel.

Lanes M1: 1 kb ladder, 500 ng (Invitrogen); **1-2**: NTC, -ve control; **3-4**: PCR products from cells of strain 2607 and 2608 respectively (*cdc13*Δ); **5-6**: PCR products from cells of strains 1296-TR, 1297-TR respectively (*cdc13-1*); **7-8**: PCR products from cells of strain 640 X2 (WT, *CDC13*) cells; **9-22**: PCR products from cells of transformants #N1-N14 in strain 1296-TR (anticipated *cdc13-1*-NTΔ mutants).

Gel analysis showed fragments of sizes ~378 bp in nine transformants #N1, N3 and N8-N14 (lanes 9, 11 and 16-22), all other NTΔ mutants examined, #N2, N4-N7 (lanes 10, 12-15) exhibited no fragment indicating the absence of the N-terminus.

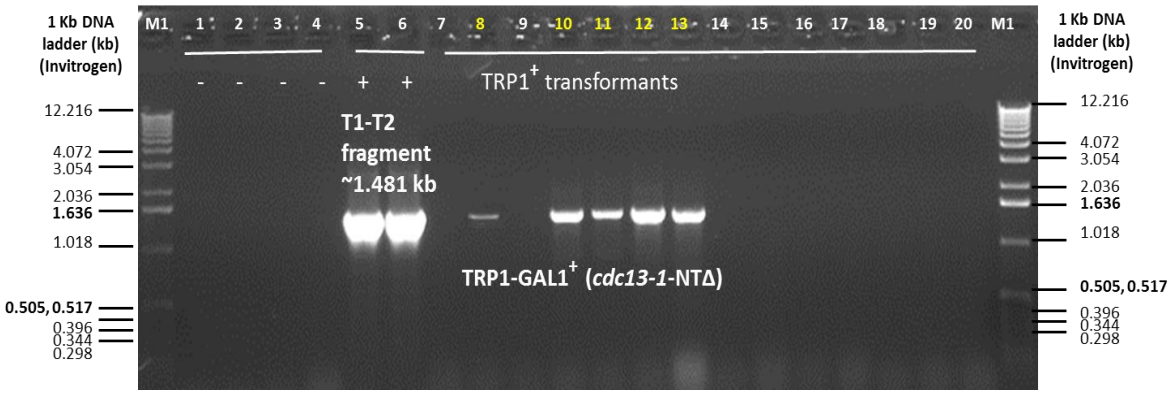

Figure 3.33. PCR confirmation for TRP1-GAL1 marker module in *cdc13-1*-NTΔ mutants (1-14) in strain 1296-TR: electrophoretic analysis of PCR products (T1-T2 primer pair).

The putative *cdc13-1* NTΔ transformants (#N1-14) were screened by diagnostic PCR for the TRP1-PGAL1 marker module. The PCR was carried out with T1-T2 diagnostic primers in 25 µl reaction volume with 2 µl of denatured genomic DNA from cells. The PCR products (10 µl) were examined on a 0.8% agarose gel.

Lanes M1: 1 kb ladder, 500 ng (Invitrogen); **1-2**: NTC, -ve control; **3-4**: PCR products from cells of strains 1296-TR, 1297-TR (*cdc13-1* mutants), control; **5-6**: PCR products with plasmid DNA (pDL515 containing TRP1-PGAL1) +ve control; **7-20**: PCR products from cells of transformants #N1-N14 in strain 1296-TR (anticipated *cdc13-1*-NTΔ mutants).

Gel analysis showed the fragments of ~1.481 kb in five NTΔ transformants out of a total 14 examined (N2, N4-N7, lanes 8, 10-13 respectively), indicating the replacement of the N-terminus by the tryptophan marker integrated by homologous recombination.

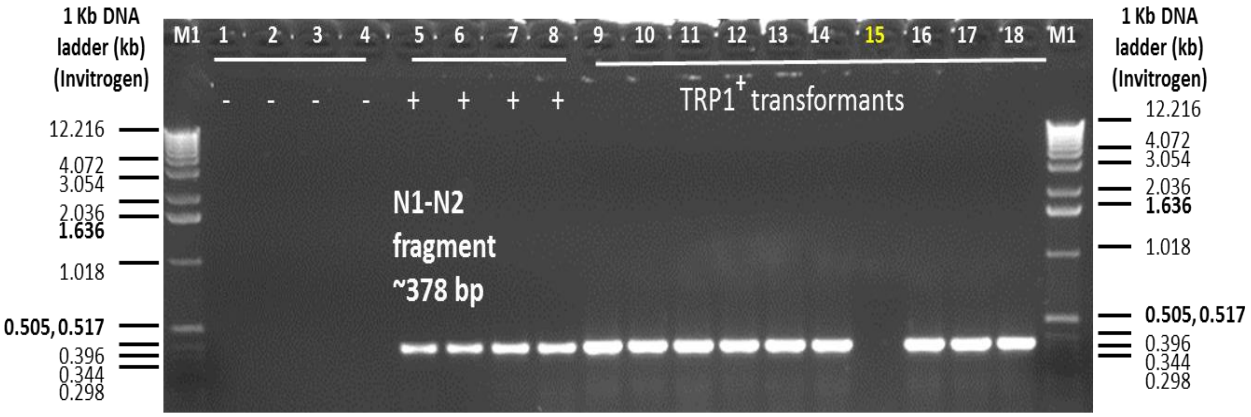

Figure 3.34. PCR screening (15-24) for *cdc13-1* N-terminus deletion (NTΔ) in the strain 1296-TR: agarose gel electrophoresis of PCR products (N1-N2 primer pair).

The putative, *cdc13-1* NTΔ transformants (#N15-#N24) were screened by PCR for *cdc13-1* N-terminus. The PCR was carried out with the N1-N2 diagnostic primers in 25 µl reaction volume with 2 µl of denatured genomic DNA from cells. The PCR products (10 µl) were examined on a 1.5% agarose gel.
Lanes M1: 1 kb ladder, 500 ng (Invitrogen); **1-2**: NTC, -ve control; **3-4**: PCR products from cells of strains 2607 and 2608 (*cdc13Δ*) respectively; **5-6**: PCR products from cells of strains 1296-TR, 1297-TR (*cdc13-1*) respectively; **7-8**: PCR products from cells of strain 640 X2 (WT, *CDC13*); **9-18**: PCR products from cells of transformants #N15-N24 in strain 1296-TR (anticipated *cdc13-1*-NTΔ mutants).
Gel analysis showed discrete DNA band of ~378 bp in nine transformants #N15-N20 and N22-N24 (lanes 9-14, and 16-18), whereas one NTΔ mutant (N21, lane 15) exhibited no N-terminus-specific fragment.

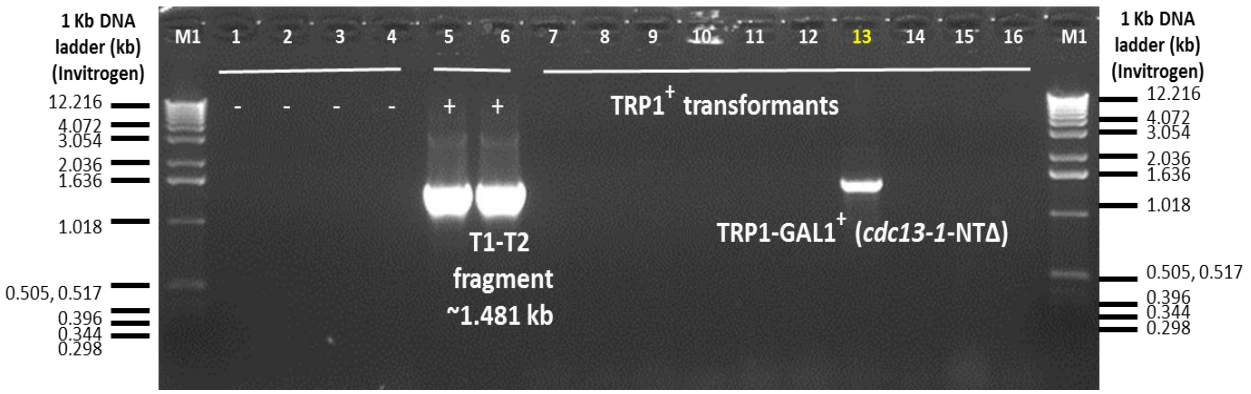

Figure 3.35. PCR confirmation for TRP1-PGAL1 marker module in *cdc13-1*-NTΔ mutants (15-24) in strain 1296-TR: the electrophoretic analysis of the PCR products (T1-T2 primers).

The putative, *cdc13-1* NTΔ transformants (#N15-24) were screened by diagnostic PCR for the TRP1-PGAL1 marker module. The PCR was carried out with the T1-T2 diagnostic primer pair in a 25 µl reaction volume with 2 µl of denatured genomic DNA from cells. The PCR amplified products (10 µl) were examined on a 0.8% agarose gel.
Lanes M1: 1 kb ladder, 500 ng (Invitrogen); **1-2**: NTC, -ve control; **3-4**: PCR products from cells of strains 1296-T, 1297-TR (*cdc13-1* mutants), control; **5-6**: PCR products with plasmid DNA (pDL515 possessing TRP1-PGAL1) +ve control; **7-16**: PCR products from cells of transformants #N15-N24 in strain 1296-TR (anticipated *cdc13-1*-NTΔ mutants).
Gel analysis presented a fragment of ~1.481 kb in one NTΔ transformant (N21, lanes 13), indicating replacement of the N-terminus by the tryptophan marker.

3.4.1.3.6. Screening of *cdc13-1* NTΔ::(TRP1-PGAl1) in mutants of strain 1297-TR

3.4.1.3.6.1. Analytical PCR for N-terminus

The tryptophan-positive transformants (24) were analysed by diagnostic PCR for *cdc13-1* NTΔ in strain 1297 survivors. Gel analysis revealed a fragment of ~378 bp in 15 transformants #N2-3, N6, N9-10, and N12-13 (Figure 3.36, lanes 10-11, 14, 17-18, 20 and 21 respectively) and transformants #N15, N17-N21 and N23-N24 (Figure 3.38, lanes 9, 11-15, 17-18 respectively), in consonance with *cdc13-1* (Figures 3.36 and 3.38, lanes 5-6) and *CDC13*-specific bands (Figures 3.36 and 3.38, lanes 7-8) indicating the presence of *cdc13-1* or *CDC13*. However, no amplification was observed in other transformants analysed (Figure 3.36, lanes 9, 12-13, 15-16, 19, 22 and Figure 3.38, lanes 10 and 16) confirming successful deletion of the *cdc13-1* gene by target guided homologous recombination. As the N-terminus fragment of *cdc13-1* should be replaced by a marker cassette of TRP1-PGAL1 resulting in *cdc13-1*-NTΔ::TRP1-PGAL1, the correct integration of TRP1-PGAL1 was confirmed by a second analytic PCR with marker-specific primers T1 and T2.

3.4.1.3.6.2. Analytical PCR for TRP1-PGAL1 modular marker

In parallel diagnostic PCR, the same denatured supernatants were examined for the tryptophan marker module using the T1 and T2 primer pair. The presence of the tryptophan marker module was confirmed in nine mutants out of a total of 24 examined for NTΔ (Figure 3.37, lanes 9, 12-13, 15-16, 19 and 22; Figure 3.39, lanes 10 and 16). All nine T^+L^+ transformants showing discrete marker-specific bands with varying intensity for the NTΔ::TRP1-PGAL1 construct, did not amplify the gene specific N-terminus fragment, confirming the replacement of the N-terminus with the TRP1 marker module. Conversely, all other $TRP1^+$ transformants that did not amplify the marker and showed the N-terminus fragment could be spontaneous revertants.

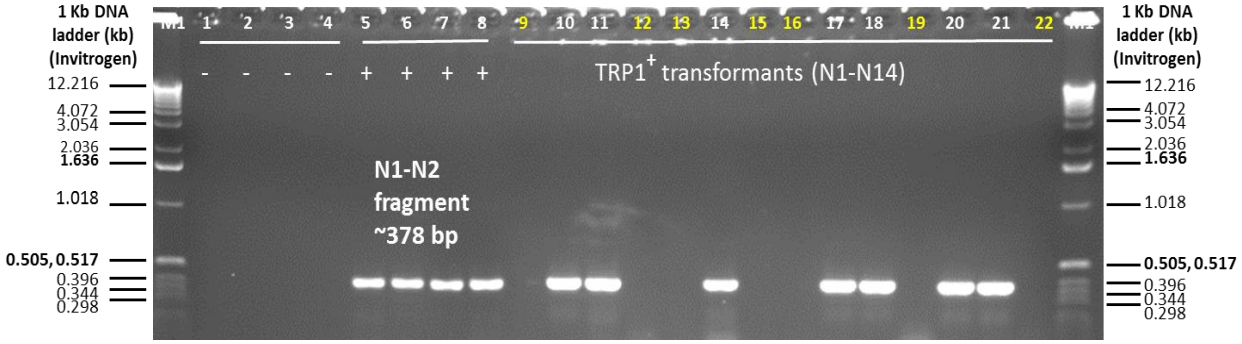

Figure 3.36. PCR screening (1-14) for *cdc13-1* N-terminus deletion (NTΔ) in strain 1297-TR: agarose gel electrophoresis of the PCR products (N1-N2 primers).

The putative, *cdc13-1* NTΔ transformants (#N1-N14) were screened by PCR for *cdc13-1* N-terminus. The PCR was carried out with the N1-N2 diagnostic primers in a 25 µl reaction volume with, 2 µl of denatured genomic DNA from cells. The PCR amplified products (10 µl) were examined on a 1.5% agarose gel.

Lanes M1: 1 kb ladder, 500 ng (Invitrogen); **1-2**: NTC, -ve control; **3-4**: PCR products from cells of strains 2607 and 2608 (*cdc13*Δ); **5-6**: PCR products from cells of strains 1296-TR, 1297-TR (*cdc13-1*); **7-8**: PCR products from cells of strain 640 X2 (WT, *CDC13*); **9-22**: PCR products from cells of transformants #N1-N14 in strain 1297-TR (anticipated *cdc13-1*-NTΔ mutants).

Gel analysis showed the N-terminus specific fragments ~378 bp in seven transformants #N2, N3, N6, N9, N10, N12 and N13 (lanes 10-11, 14, 17-18 and 20-21). All other NTΔ mutants #N1, N4, N5, N7, N8, N11 and N14 (lanes 9, 12-13, 15, 16, 19 and 22) exhibited no fragment indicating the absence of the *cdc13-1*-N-terminus.

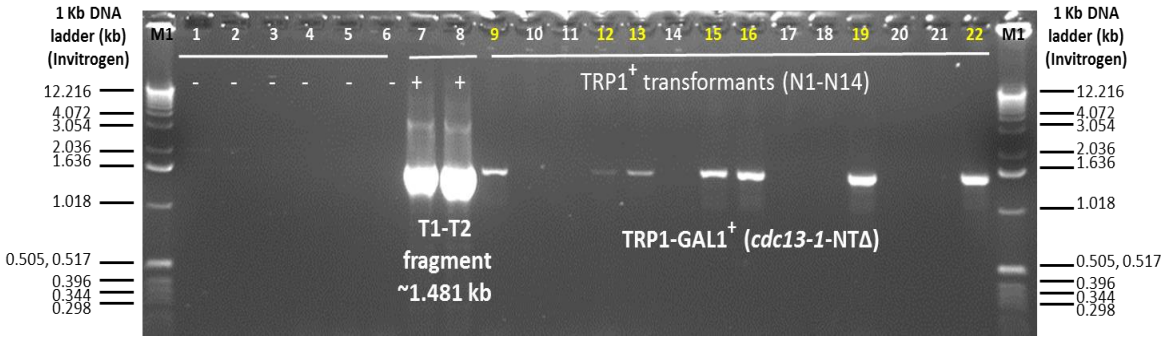

Figure 3.37. PCR confirmation (1-14) for the TRP1-GAL1 marker module in *cdc13-1*-NTΔ mutants in strain 1297-TR: the electrophoretic analysis of amplified products (T1-T2 primers pair).

The putative, *cdc13-1* NTΔ transformants (#N1-N14) were screened by diagnostic PCR for the TRP1-GAL1 marker module. The PCR was carried out using the T1-T2 diagnostic primers in a 25 µl reaction volume with 2 µl of denatured genomic DNA from cells. The PCR amplified products (10 µl) were examined on a 0.8% agarose gel.

Lanes M1: 1 kb ladder, 500 ng (Invitrogen); **1-2**: NTC, -ve control; **3-5**: PCR products from cells of strains 1296-TR, 1297-TR X2 (*cdc13-1* mutant), control; **6**: PCR products from cells of strain 1272 cells (*CDC13*) control; **7-8**: PCR products with plasmid DNA (pDL515 with TRP1-GAL1), +ve control; **9-22**: PCR products from cells of transformants #N1-N14 in strain 1297-TR (anticipated *cdc13-1*-NTΔ mutants).

Gel analysis showed a fragment of ~1.481 kb in seven NTΔ transformants (N1, N4, N5, N7, N8, N11 and N14, lanes 9, 12-13, 15-16, 19 and 22) out of the fourteen examined, indicating replacement of the N-terminus by the tryptophan marker.

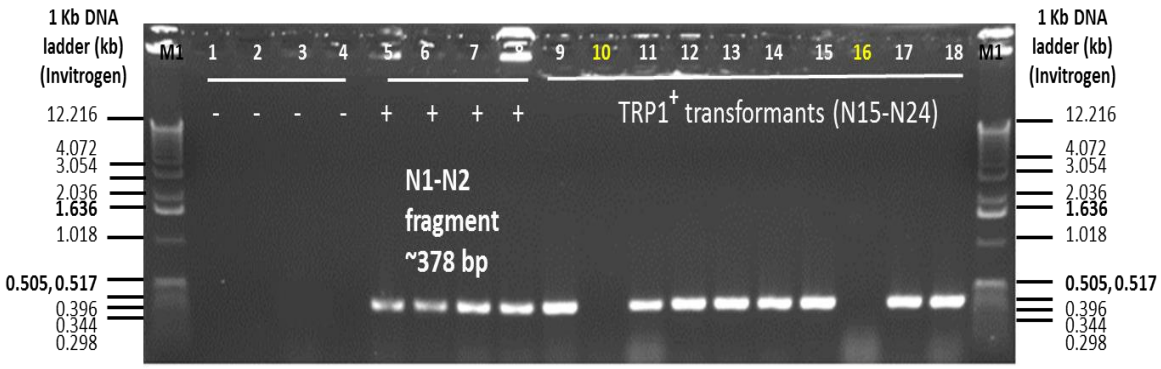

Figure 3.38. PCR screening (15-24) for *cdc13-1* N-terminus deletion (NTΔ) in strain 1297-TR: agarose gel electrophoresis of amplified products with the N1 and N2 primer pair.

The putative, *cdc13-1* NTΔ transformants (#N15-N24) were screened by PCR for *cdc13-1* N-terminus. The PCR was carried out using the N1-N2 diagnostic primers in a 25 µl reaction volume with 2 µl denatured genomic DNA from cells. The PCR amplified products (10 µl) were examined on a 1.5% agarose gel.

Lanes M1: 1 kb ladder, 500 ng (Invitrogen); **1-2**: NTC, -ve control; **3-4**: PCR products from cells of strains 2607 and 2608 cells (*cdc13*Δ); **5-6**: PCR products from cells of strains 1296-TR, 1297-TR (*cdc13-1*); **7-8**: PCR products from cells of strains 640 X 2 (WT, *CDC13*); **9-18**: PCR products from cells of transformants #N15-N24 in strain 1297-TR (anticipated *cdc13-1*-NTΔ mutants).

Gel analysis showed fragments of ~378 bp in eight transformants (lanes 9, 11-15 and 17-18). The other two mutants examined exhibited no fragment (lanes 10 and 16) indicating the absence of the N-terminus (NTΔ).

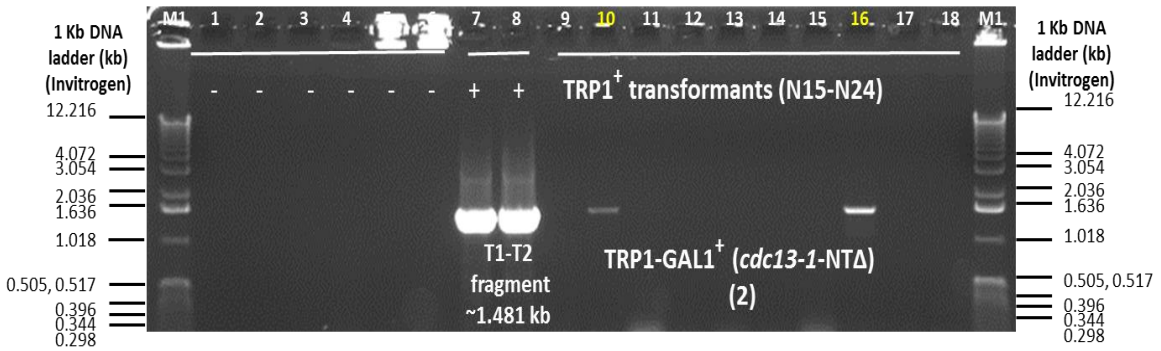

Figure 3.39. PCR confirmation for the TRP1-PGAL1 marker module in *cdc13-1*-NTΔ mutants (15-24) in the strain 1297-TR: electrophoretic analysis of PCR products (using T1 and T2 primer pair).

The putative, *cdc13-1* NTΔ transformants (#N15-24) were screened by diagnostic PCR for the TRP1-PGAL1 marker module. The PCR was carried out with the T1-T2 diagnostic primers in a 25 µl reaction volume with 2 µl denatured genomic DNA. The PCR amplified products (10 µl) were examined on a 0.8% agarose gel.

Lanes M1: 1 kb ladder, 500 ng (Invitrogen); **1-2**: NTC, -ve control; **3-5**: PCR products from cells of strains 1296-TR, 1297-TR X2 (*cdc13-1* mutant), controls; **6**: PCR products from cells of strain 1272 (*CDC13*); **7-8**: PCR products with plasmid DNA (pDL515 with TRP1-GAL1) +ve control; **9-18**: PCR products from cells of transformants #N15-N24 in strain 1297-TR (anticipated *cdc13-1*-NTΔ mutants).

Gel analysis showed the fragments of ~1.481 kb in only NTΔ transformants which were negative for the *cdc13-1*-N-terminus (N16 and N22, lanes 10 and 16), indicating replacement of the N-terminus by the tryptophan marker by homologous genomic integration. The PCR amplified products (10 µl) were examined on a 0.8% agarose gel.

3.4.1.3.7. Screening of *CDC13* NTΔ::(TRP1-PGAL1) in mutants of strain 1272

3.4.1.3.7.1. Analytic PCR for the N-terminus

The 16 tryptophan-positive putative transformants (N1-N16) were analysed by diagnostic PCR for *CDC13*-NTΔ in strains 1272. Gel analysis manifested amplified fragments of ~378 bp with the N-terminus-specific primers in all of the clones examined (Figure 3.40, lanes 7-22), indicating the presence of the intact *CDC13* gene.

As the N-terminus fragment of *cdc13-1* was targeted to be replaced by a marker cassette of the TRP1-PGAL1 through homologous recombination, the integration of TRP1 module was verified by analytic PCR with marker-specific primers, T1 and T2.

3.4.1.3.7.2. Analytic PCR for the TRP1-PGAL1 modular marker

Further analysis of the above tryptophan-positive putative transformants with the marker-specific primers T1 and T2 revealed that the marker cassette of TRP1-PGAL1 did not integrate within the chromosomal DNA of any of the selected transformants tested to replace the N-terminus of *CDC13*. Figure 3.41 (lanes 8-22), confirmed the absence of the tryptophan marker module in all transformants examined for NTΔ. The tested tryptophan^{+} transformants (putative), however, could be the result of spontaneous gene conversion (not by homologous recombination) without integration of the TRP1 marker within the genome.

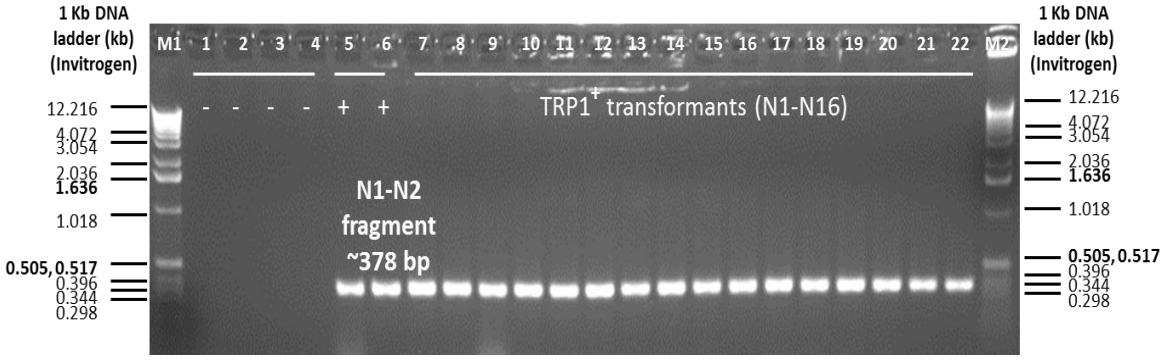

Figure 3.40. PCR screening for *CDC13* N-terminus deletion (NTΔ) mutants (1-16) in the strain 1272: agarose gel electrophoresis of PCR products (N1and N2 primers).

The putative *cdc13-1* NTΔ transformants (#N1-N16) were screened by PCR for *CDC13* N-terminus specific fragment. The PCR was carried out using the N1and N2 diagnostic primers in a 25 µl reaction volume with 2 µl of denatured genomic DNA from cells. The PCR products (10 µl) were examined on a 1.5% agarose gel.

Lanes M1: 1 kb ladder, 500 ng (Invitrogen); **1-2**: NTC, -ve control; **3-4**: PCR products from cells of strains 2607 and 2608 (*cdc13*Δ); **5-6**: PCR products from cells of strains 1272 and 640 (WT, *CDC13*); **7-22**: PCR products from cells of transformants #N1-N16 in strain 1272 (anticipated *CDC13*-NTΔ mutants).
Gel analysis showed fragment of ~378 bp in all 16 transformants examined (lanes, 7-22).

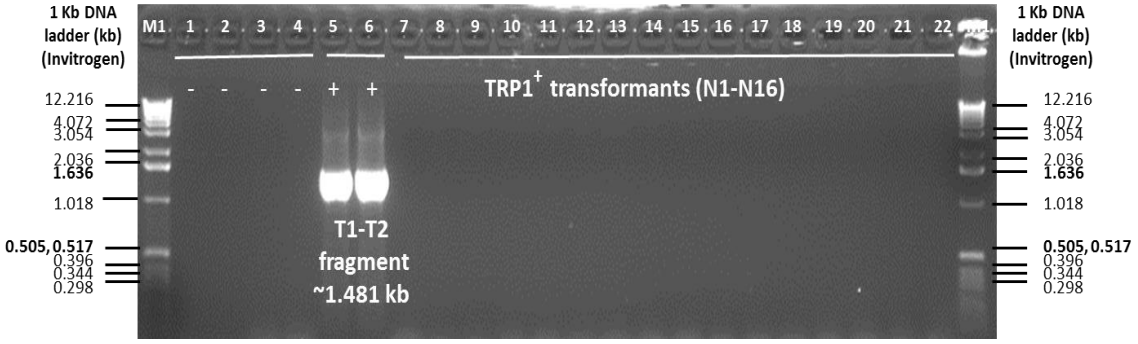

Figure 3.41. PCR for the TRP1-PGAL1 marker module in anticipated *CDC13*-NTΔ mutants (1-16) in the strain 1272: electrophoretic analysis of PCR products (T1-T2 primer pair).

The putative *CDC13*-NTΔ transformants (#N1-16) were screened by diagnostic PCR for the TRP1-PGAL1 marker module. The PCR was carried out using diagnostic primers in a 25 µl reaction volume with 2 µl of denatured genomic DNA from cells. The PCR products (10 µl) were examined on a 0.8% agarose gel.

Lanes M1: 1 kb ladder, 500 ng (Invitrogen); **1-2**: NTC, -ve control; **3**: PCR products from cells of strain 1272 (*CDC13*), control; **4**: PCR products from cells of strains 1296-TR, (*cdc13-1* mutant), control; **5-6**: PCR products with plasmid DNA (pDL515 with TRP1-PGAL1), +ve control; **7-22**: PCR products from cells of transformants #N1-N16 in strain 1272 (anticipated *CDC13*-NTΔ mutants).
The gel analysis showed the absence of fragments ~1.481 kb in all trp1$^+$ transformants examined (N1-N16 with respect to lanes 7-22), indicating no replacement of the N-terminus by the tryptophan marker through homologous recombination.

Overall results for *cdc13-1* N-terminus deletion with the TRP1-PGAL1 marker module and PCR analysis to confirm the correct mutants (NTΔ::TRP1-PGAL1) has been summarised in Table 3.3 that presents the comparative number of mutants generated in all three strains, 1296-TR, 1297-TR and 1272.

Table 3.3. Analysis of tryptophan-positive transformants for *cdc13-1* N-terminus truncation with TRP1-PGAL1 module by homologous recombination

	Strains DLY (selected clones)	**1296-TR** (*cdc13-1*)	**1297-TR** (*cdc13-1*)	**1272** (*CDC13*)
1	T^+L^+ transformants analysed for NTΔ	24	24	16
2	PCR^+ for N-terminus (N1-N2, 378 bp)	18	15	16
3	PCR^+ for TRP1-PGAL1 (T1-T2, 1.845 kb)	6	9	0
4	True mutants NTΔ::TRP1-PGAL1 construct	6/24 (25%)	9/24 (37.5%)	0/16 0%
5	False positive (T^+L^+ revertants)	18/24 (75%)	15/24 (62.5%)	16/16 (100%)
6	Target-specific homologous recombination (HR)	6/24 (25%)	9/24 (37.5%)	0%
7	Non homologous recombination (NHR)	0%	0%	0%
8	Name of the construct generated	N2, N4, N5, N6, N7, N21	N1, N4, N5, N7, N8, N11, N14, N16, N22	-

3.4.1.3.8. PCR screening of H^+L^+ transformants for *cdc13-1* N-terminus deletion (*cdc13-1* NTΔ::HIS3MX6-PGAL1)

To verify disruption of *cdc13-1* or *CDC13* with the marker cassette HIS3MX6-PGAL1 for NTΔ, the H^+L^+ transformants were screened by diagnostic PCR for the *cdc13-1* N-terminus and His marker module with appropriate controls. After a second round of selection, H^+L^+ transformants from strains 1296-TR, 1297-TR and 1272 were analysed by diagnostic PCR for the verification of N-terminus disruption and integration of the marker. In total, 30 transformants each from 1296-TR and 1297-TR (data shown only for 15) and 10 transformants from strain 1272 were analysed systematically for the detection of the N-terminus (PCR with N1-N2 primers), HIS3MX6 marker module (PCR with H1-H2 primers) and finally for the C-terminus (PCR with the C1-C2 primer pair, data not shown).

3.4.1.3.8.1. Screening of *cdc13-1* NTΔ::HIS3MX6-PGAL1 mutants of strain 1296-TR

3.4.1.3.8.1.1. Analytical PCR for the N-terminus

A PCR was performed with the N1 and N2 primer pair to detect the *cdc13-1* N-terminus in 15 histidine-positive transformants in strain 1296. Gel analysis revealed a fragment of ~378 bp in all tested transformants #N1-N15 (Figure 3.42, lanes 8-22 respectively) in agreement with controls *cdc13-1* (lanes 5-6) and *CDC13* (lane 7), indicating the presence of intact *cdc13-1* or *CDC13* without disruption.

The genomic integration of the marker cassette HIS3MX6-PGAL1 was diagnosed by a second analytical PCR with marker-specific primers to test whether these his^+ transformants were revertants or non-homologous recombinants.

3.4.1.3.8.1.2. Analytical PCR for the HIS3MX6-PGAL1 module

In parallel PCR, the same putative his^+ transformants were also examined for the histidine marker module with the H1 and H2 primer pair. No marker-specific band (~1.6 kb) was detected in all transformants examined for NTΔ (Figure 3.43, lanes 8-22). As a result, there was no replacement of the N-terminus with the histidine marker module (HIS3MX6-pGAL1). All $histidine^+$ transformants which were PCR-positive for the N-terminus fragment but did not amplify the marker could be spontaneous revertants, (not non-homologous recombinants) emerging as a result of gene conversion.

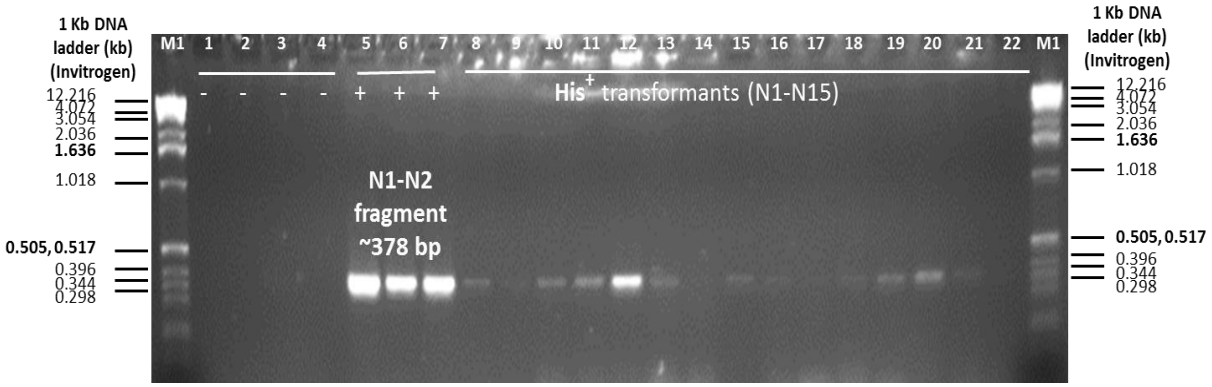

Figure 3.42. PCR screening for *cdc13-1* N-terminus deletion (NTΔ::HIS3MX6-PGAL1) mutants (1-15) of strain 1296-TR: agarose gel electrophoresis of PCR products (N1-N2 primers).

The putative, *cdc13-1* NTΔ transformants (#N1-N15) were screened by PCR for the *cdc13-1* N-terminus. The PCR was carried out with N1 and N2 diagnostic primers in a 25 µl reaction volume with 2 µl of denatured genomic DNA from cells. The PCR products (10 µl) were examined on a 1.5 % agarose gel.

Lanes M1: 1 kb ladder, 500 ng (Invitrogen); **1-2**: NTC, -ve control; **3-4**: PCR products from cells of strains 2607 and 2608 (*cdc13Δ* mutants); **5-6**: PCR products from cells of strains 1296-TR, 1297-TR (*cdc13-1* mutants); **7**: PCR products from cells of strain 640 (WT, *CDC13*); **8-22**: PCR products from cells of transformants # N1-N15 in strain 1296-TR (expected *cdc13-1*-NTΔ mutants).

Gel analysis showed fragments of ~378 bp in all transformants (lanes 8-22). Wild type strains 640 (positive for *CDC13*) and 1296-TR and 1297-TR strains positive for *cdc13-1* showed a single fragment of 378 bp (lanes 5-7 respectively) with almost the same intensity.

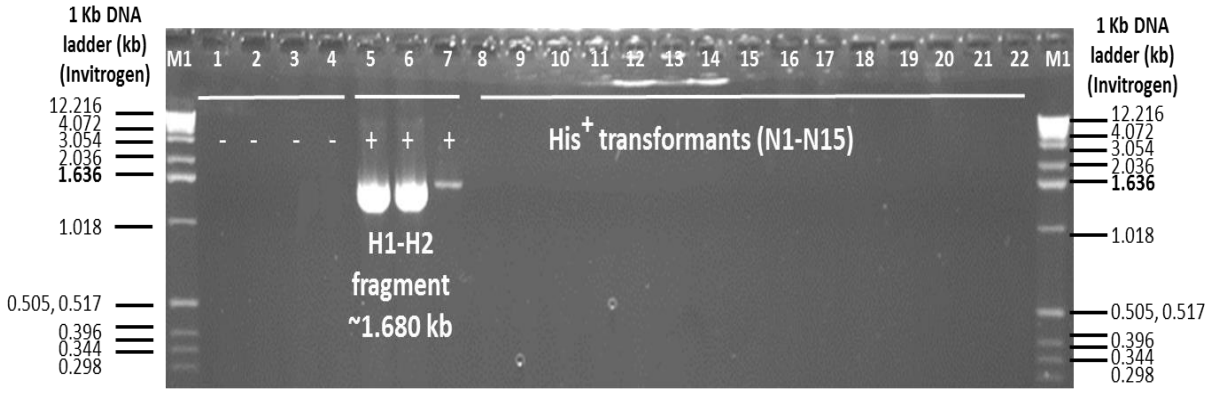

Figure 3.43. PCR to detect HIS3MX6-GAL1 marker module in anticipated *cdc13-1*-NTΔ mutants (1-15) in strain 1296-TR: electrophoretic analysis of PCR products (H1 and H2 primers).

The fifteen (#N1-15) histidine positive putative *cdc13-1* NTΔ transformants were screened by diagnostic PCR for the HIS3MX6-PGAL1 marker module. The PCR was carried out with the H1-H2 diagnostic primers in a 25 µl reaction volume, with 2 µl of denatured genomic DNA. The PCR amplified products (10 µl) were examined on a 0.8 % agarose gel.

Lanes M1: 1 kb ladder, 500 ng (Invitrogen); **1-2**: NTC, -ve control; **3-4**: PCR products from cells of strains 1296-TR, 1297-TR (*cdc13-1* mutant), -ve control; **5-6**: PCR products with DNA of plasmid (pDL504 with HIS3MX6) +ve control; **7**: PCR products from cells of mutant *cdc13-1*-CTΔ::HIS3MX6 in strain 1297-TR, +ve control; **8-22**: PCR products from cells of transformants # N1-N15 in strain 1296-TR.

Gel analysis did not show any fragment of ~1.680 kb for any of the his$^+$ transformants (lanes 8-22), indicating an absence of marker integration in genome.

3.4.1.3.8.2. Screening of *cdc13-1* NTΔ::HIS3MX6-PGAL1 mutants of strain 1297-TR

3.4.1.3.8.2.1. Analytical PCR for the N-terminus

The 15 histidine positive transformants were analysed for strain 1297 survivors. Gels analysis exhibited the faint bands of ~378 bp in all transformants with varying intensity (Figure 3.44, lanes 8-22) with similar size in positive controls, *cdc13-1* (lanes 5-6) and *CDC13* (lane 7) indicating the presence of intact *cdc13-1* or *CDC13* in chromosomal DNA. To test whether his^+ transformants were revertants or non-homologous recombinants with integrated marker (HIS3MX6-PGAL1) second analytical PCR with marker-specific primers was performed.

3.4.1.3.8.2.2. Analytical PCR for the HIS3MX6-PGAL1 modular

The results of diagnostic PCR performed to detect the histidine marker with the H1 and H2 primer pair, did not confirm the presence of a marker-specific band (~1.6 kb) in any of the mutants examined (Figure 3.45, lanes 8-22).

This indicates that, there was no replacement of the N-terminus with the HIS3MX6-PGAL1 module. All $histidine^+$ transformants (which did not amplify the marker but showed the N-terminus fragment) could be spontaneous revertants, (not non-homologous recombinants) emerging as a result of gene conversion.

3.4.1.3.8.3. Screening of *cdc13-1* NTΔ::HIS3MX6-PGAL1 mutants of strain 1272

3.4.1.3.8.3.1. Analytical PCR for the N-terminus

The 10 histidine-positive transformants were analysed for strain 1272. Gel analysis exhibited N-terminus-specific bands of ~378 bp in all examined transformants with varying intensity (Figure 3.46, lanes 10-19) along with positive controls, *cdc13-1* (lane 5) and *CDC13* (lanes 6-7) indicating the presence of non-disrupted *CDC13*.

3.4.1.3.8.3.2. Analytical PCR for HIS3MX6-PGAL1 module marker

To test whether the his^+ transformants were revertants or non-homologous recombinants, a second analytical PCR was performed for the HIS3MX6-PGAL1 marker module using H1 and H2 primers. The results did not confirm the presence of the marker-specific band (~1.6 kb) in any of the transformants examined (Figure 3.47, lanes 8-17).

It could be concluded from the above results that there was no replacement of the N-terminus with the marker module in the analysed transformants. All $histidine^+$ transformants which did not amplify the marker and showed the N-terminus fragment could be spontaneous revertants (not non-homologous recombinants) emerging as a result of gene conversion.

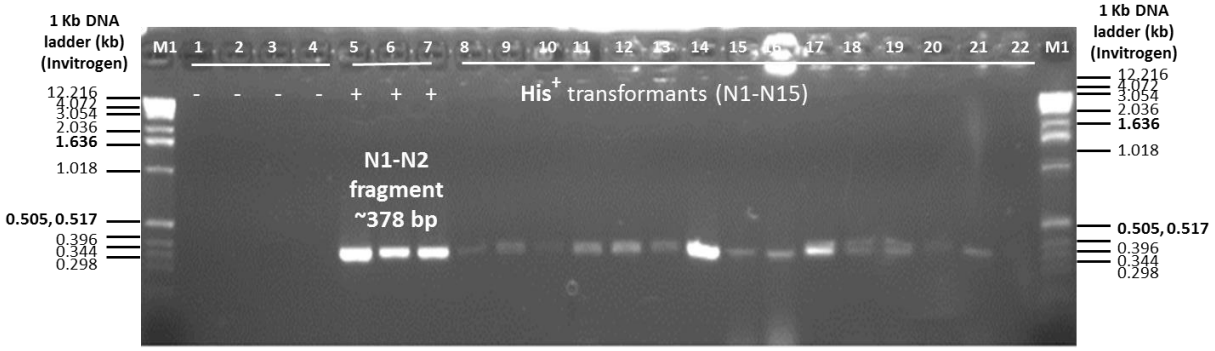

Figure 3.44. PCR screening for *cdc13-1* N-terminus deletion (NTΔ::HIS3MX6-PGAL1) mutants (1-15) of strain 1297-TR: agarose gel electrophoresis of PCR products (N1-N2 primers).

The putative *cdc13-1* NTΔ transformants (#N1-N15) were screened by PCR for the *cdc13-1* N-terminus specific fragment. The PCR was carried out with diagnostic primers in a 25 µl reaction volume, with 2 µl of denatured genomic DNA from cells. The PCR products (10 µl) were examined on a 1.5 % agarose gel.

Lanes M1: 1 kb ladder, 500 ng (Invitrogen); **1-2**: NTC, -ve controls; **3-4**: PCR products from cells of strains 2607 and 2608 respectively (*cdc13Δ*); **5-6**: PCR products from cells of strains 1296-TR, 1297-TR respectively (*cdc13-1*); **7**: PCR products from cells of strain 640, (WT, *CDC13*); **8-22**: PCR products from cells of his$^+$ transformants # N1-N15 in strain 1297-TR (expected *cdc13-1*-NTΔ mutants).

Gel analysis showed fragments of ~378 bp in all examined transformants (lanes 8-22) indicating intact *cdc13-1* without disruption.

Figure 3.45. PCR to detect HIS3MX6-GAL1 modulular DNA in anticipated *cdc13-1*-NTΔ mutants (1-15) in strain 1297-TR: electrophoretic analysis of PCR products (H1-H2 primers).

The potential, *cdc13-1*-NTΔ transformants (#N1-15) were screened by diagnostic PCR for the HIS3MX6-PGAL1 module. The PCR was carried out using H1-H2 diagnostic primers in a 25 µl reaction volume with 2 µl of denatured genomic DNA from cells. The PCR amplified products (10 µl) were examined on a 0.8 % agarose gel.

Lanes M1: 1 kb ladder, 500 ng (Invitrogen); **1-2**: NTC, -ve control; **3-4**: PCR products from cells of strains 1296-TR, 1297-TR (*cdc13-1* mutant)s; **5-6**: PCR products with DNA of plasmid (pDL504 with HIS3MX6), +ve controls; **7**: PCR products from cells of mutant *cdc13-1*-CTΔ::HIS3MX6 in strain 1297-TR, +ve control; **8-22**: PCR products from cells of transformants # N1-N15 in strain 1297-TR (expected *cdc13-1*-NTΔ mutants).

Gel analysis did not show any fragments of ~1.680 kb for any of his$^+$ transformants (lanes 8-22), indicating an intact gene without disruption.

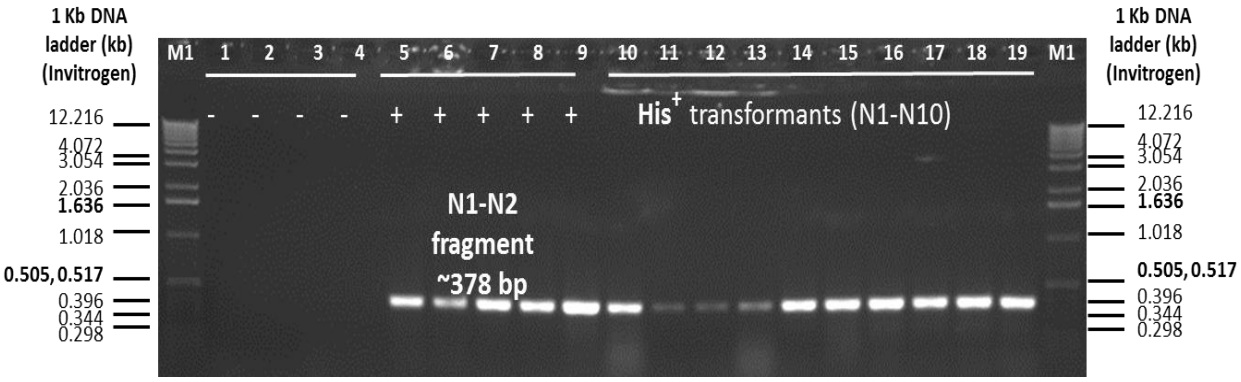

Figure 3.46. PCR screening for *CDC13* N-terminus deletion (NTΔ::HIS3MX6-PGAL1) mutants (1-10) of strain 1272: agarose gel electrophoresis of PCR products (N1-N2 primers).

The putative, *CDC13* NTΔ transformants (#N1-N10) were screened by PCR for the *CDC13* N-terminus specific fragment. The PCR was carried out using N1-N2 diagnostic primers in a 25 µl reaction volume with 2 µl of denatured genomic DNA from cells. The PCR products (10 µl) were examined on a 1.5 % agarose gel.

Lanes M1: 1 kb ladder, 500 ng (Invitrogen); **1-2**: NTC, -ve control; **3-4**: PCR products from cells of strains 2607 and 2608 (*cdc13*Δ); **5**: PCR products from cells of strain 1296-TR (*cdc13-1*); **6-7**: PCR products from cells of strain 1272 (*CDC13*); **8-9**: PCR products from cells of strain 640, (WT, *CDC13*) cells; **10-19**: PCR products from cells of transformants # N1-N10 in strain 1272 (expected *CDC13*-NTΔ mutants).

Gel analysis showed fragments of sizes ~378 bp in all examined transformants (lanes 10-19) indicating intact *CDC13* without disruption.

Figure 3.47. PCR to detect HIS3MX6 marker module in anticipated *CDC13*-NTΔ mutants (1-10) in the strain 1272: electrophoretic analysis of PCR products (H1-H2 primers).

The putative, *CDC13* NTΔ transformants (#N1-10) were screened by diagnostic PCR for the HIS3MX6 marker module. The PCR was carried out with H1-H2 diagnostic primers in a 25 µl reaction volume with 2 µl of denatured genomic DNA from cells. The PCR products (10 µl) were examined on a 0.8 % agarose gel.

Lanes M1: 1 kb ladder, 500 ng (Invitrogen); **1**: NTC, -ve control; **2-3**: PCR products from cells of strains 1296-TR, (*cdc13-1* mutant) and 1272 (*CDC13*) respectively, -ve controls; **4-5**: PCR products with DNA of plasmid (pDL504 with HIS3MX6), +ve control; **6-7**: PCR products from cells of mutants *cdc13-1*-CTΔ::HIS3MX6 in strains 1297-TR, +ve control; **8-17**: PCR products from cells of transformants # N1-N10 in strain 1272 (expected *cdc13-1*-NTΔ mutants).

Gel analysis did not show any fragments of ~1.680 kb for any of his$^+$ transformants (lanes 8-17), indicating the intact *CDC13* gene without disruption.

3.4.1.3.8.4. Summary on transformation experiments and PCR screening for NTΔ

Table 3.4 presents the number of transformants generated as a result of transformation and homologous recombination with the histidine and tryptophan markers cassettes used for the disruption of the N-terminus. The strains 1296, 1297 and 1272 showed different number of revertants on $T^{-}L^{-}$ media (negative control) in transformation experiments. Analysis of $T^{+}L^{+}$ transformants also revealed a varying number of tryptophan revertants with strain 1296 and 1297 survivors, whereas the transformants ($H^{+}L^{+}$ and $T^{+}L^{+}$) analysed for NTΔ in strain 1272, were all proved through PCR to be revertants.

Table 3.4. The comparative analysis of $H^{+}L^{+}$ transformant (HIS3MX6-pGAL1 modular DNA; pDL516) and $T^{+}L^{+}$ transformant (TRP1-pGAL1 DNA; pDL515) for N-terminal truncation.

	Strains	**1296-TR** (*cdc13-1*)	**1297-TR** (*cdc13-1*)	**1272** (*CDC13*)
$H^{+}L^{+}$ transformants	Total $H^{+}L^{+}$ transformants obtained in 100 µl	144	63	10
	$H^{+}L^{+}$ transformants analysed for NTΔ	30	30	10
	$H^{+}L^{+}$revertants on $H^{-}L^{-}$ media	0	0	0
$T^{+}L^{+}$ transformants	$T^{+}L^{+}$ transformants obtained in 100 µl	685	550	TMTC*
	$T^{+}L^{+}$ transformants analysed for NTΔ	24	24	16
	True mutant with NTΔ::TRP1-PGAL1 construct	6	9	0
	$T^{+}L^{+}$ revertants on $T^{-}L^{-}$ media per 100 µl	195	125	220
	Viable count of TR cells in 100 µl	$168x10^{6}$	$52x10^{6}$	$221x10^{6}$
	Frequency of $T^{+}L^{+}$ revertants	$7.5x10^{-6}$	$1.488x10^{-6}$	$0.995x10^{-6}$

TMTC* (too many to count)

Frequency = no of revertants/viable count

3.5.1. *cdc13-1* C-terminal deletion (CTΔ)

The second half of the *cdc13-1/ CDC13* open reading frame sequence between nucleotides 1387 and 2775 (~1389 nt) with respect to the C-terminus half of *CDC13* gene (Figure 3.3D) was targeted for disruption with homologous recombination with the histidine marker module.

3.5.1.1. Modulating DNA template preparation for C-terminal truncation

The plasmid pFA6a-GFP(S65T)-HIS3MX6 (pDL504) with the histidine marker module was used as a template for PCR amplification (synthesis) of the fragment for *cdc13-1* C-terminal deletion (Wach *et al*., 1997, Longtine *et al*., 1998) (Figures 2.9, 2.11 in Methods; Figure 3.17).

3.5.1.1.1. Plasmid DNA extraction and size evaluation

The yeast plasmid pDL504 (pFA6a-GFP(S65T)-His3MX6) for CTΔ was transformed into bacterial cells (*E.coli* NM522 strain K-12) (Figure 3.16). DNA was extracted and evaluated on the basis of molecular size as was explained in the N-terminus deletion section (Figure 3.17 and Figure 3.18, lanes 1, 4 and 7).

3.5.1.1.2. PCR synthesis of HIS3MX6 (*cdc13-1* CTΔ) and HIS3MX6-PGAL1 (*cdc13-1* NTΔ) modulating DNA

3.5.1.1.2.1. Cross check of the homology of deletion primers for the his marker with and without PGAL1 promoter

To verify the specificities of hybrid primers for their respective yeast plasmid, two sets of PCR were performed to amplify the N- and C-terminus deletion cassettes of *cdc13-1* with the histidine marker using opposite primers. Figure 3.48 presents the analysis of the resulting PCR reaction products. The expected disruption cassette for the N-truncation (linear DNA of 1.9 kb) was amplified with the specific primers (FT-N1 and RT-N1) and template DNA of plasmid pFA6a-His3MX6-PGAL1 (lanes 3 and 4). For C-truncation DNA fragment of ~1.6 kb was amplified using primers (FT-C2 and RT-C2) and the plasmid pFA6a-His3MX6 peculiar for that cassette (lanes 10 and 11). However, faint bands of the correct size were amplified with opposite primers (second pairs of primers) from both plasmids. This demonstrated some homology of these histidine plasmids to both set of primers (lanes 5 and 6; 12 and 13).

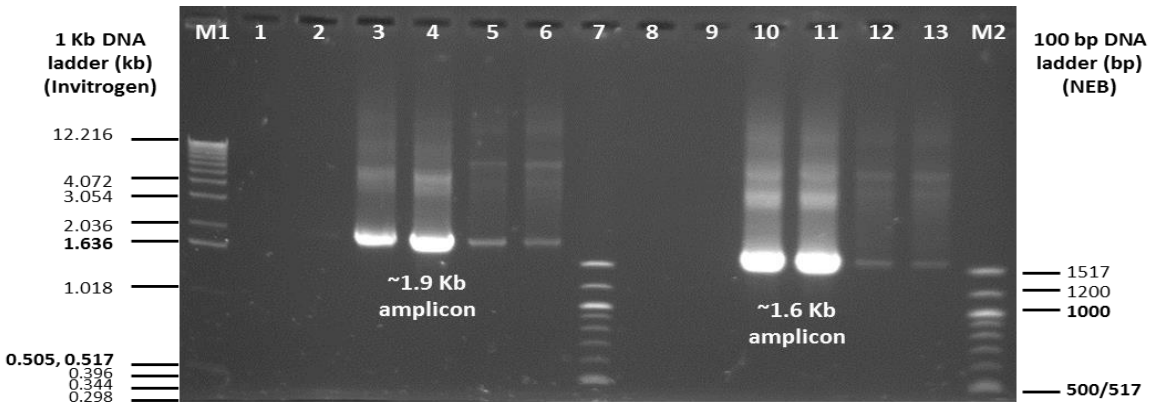

Figure 3.48. PCR amplification using template plasmid pDL504 and pDL516 to cross check hybrid primer specificities: agarose gel electrophoresis of PCR products.

In the first set of PCR hybrid primers, FT-N1 and RT-N1 specific for *cdc13-1* N-terminus deletion modules were used with yeast vectors pDL516 (pFA6a-HIS3MX6-PGAL1) and pDL504 (pFA6a-HIS3MX6) respectively. In the second set of PCR hybrid primers, FT-C2 and RT-C2 specific for *cdc13-1* C-terminus deletion modules were used with yeast vectors pDL504 (pFA6a-HIS3MX6) and pDL516 (pFA6a-HIS3MX6-PGAL1) respectively. For each sample, 10 µl of amplicon was examined on a 0.9% agarose gel.

Lanes M1: 1 kb DNA marker, 500 ng (Invitrogen); **1-2**: negative control (NTC without cells or DNA);

3-4: PCR products using plasmid pDL516 (pFA6a-His3MX6-PGAL1); **5-6**: PCR products using plasmid pDL504 (pFA6a-His3MX6);

7: M2 100 bp quantitative DNA marker, 500 ng (NEB); **8-9**: negative control (NTC without cells or DNA);

10-11: PCR products using plasmid pDL 504 (pFA6a-His3MX6); **12-13**: PCR products using plasmid pDL516 (pFA6a-His3MX6-PGAL1; **M2**: 100 bp DNA marker, 500 ng (NEB).

The N-terminus primers resulted in ~1.943 kb amplicons with the pDL516 template (lanes 3 and 4) and C-terminus primers resulted in ~1.579 kb amplicon with the plasmid template pDL504 (lanes 10 and 11). However, there is a slight amplification with the opposite primers (lanes 5-6, 12 and 13).

3.5.1.1.2.2. PCR amplification of HIS3MX6 modulating DNA for *cdc13-1* C-truncation

Using yeast plasmid DNA pFA6a-HIS3MX6 as a template and hybrid primers (FT-C2 and RT-C2), PCR was performed to amplify the HIS3MX6 marker module with ADH1 terminator to delete the second half of *cdc13-1* (1387-2775 nt). Figure 3.49 represents the result of electrophoresis analysis of amplified products and confirms the amplification of the required size fragments of approximately 1.6 kb for C-terminus truncation (lanes 3-7).

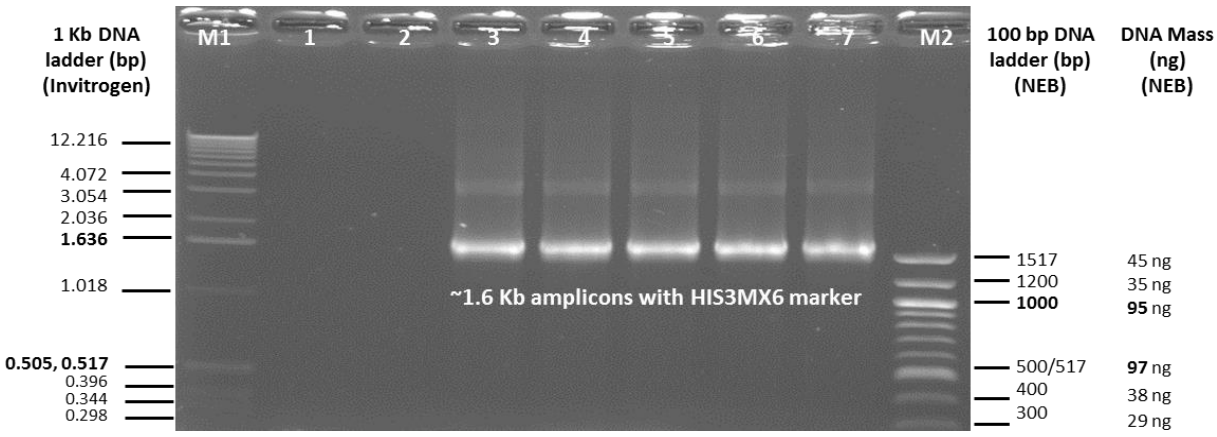

Figure 3.49. PCR amplification for ADH1-HIS3MX6 modulating DNA for *cdc13-1* C-terminus deletion: agarose electrophoretic analysis of PCR reaction products.

cdc13-1 C-terminus deletion modules were amplified using the yeast vector pFA6a-GFP(S65T)-His3MX6 (pDL504) as a template with hybrid primers FT-C2and RT-C2 and 1x green PCR master mix (Promega) in 100 µl of reaction volume. Amplified PCR products (3 µl) from each reaction were analysed on a 0.9% agarose gel.

Lanes M1 and **M2**: 1 kb DNA marker, (Invitrogen) and 100 bp DNA marker quantitative (NEB), 500 ng respectively; **1-2**: negative control (NTC) without cells or DNA; **3-7**: the C-terminal ADH1-HIS3MX6 deletion fragment of ~1.6 kb (1.680 kb without the GFP tag) as expected.

3.5.1.1.2.3. Purification of HIS3MX6 modulating DNA for *cdc13-1* C-terminus truncation

For purification, the PCR products were extracted with phenol-chloroform followed by ethanol precipitation. The agarose gel analysis of purified and non-purified product is shown in Figure 3.50. Lane 1 represents non-purified PCR product whereas lanes 2 exhibits extracted amplicon of C-terminus deletion cassettes (ADH1-HIS3MX6 DNA fragment with flanking target sequences). The intensity of the linear DNA product was compared to that of the DNA masses of the reference standard (M2) to estimate the yield. The approximate concentration of purified fragment was estimated to be ~30-50 ng/µl according to the quantitative marker (NEB 100 bp ladder).

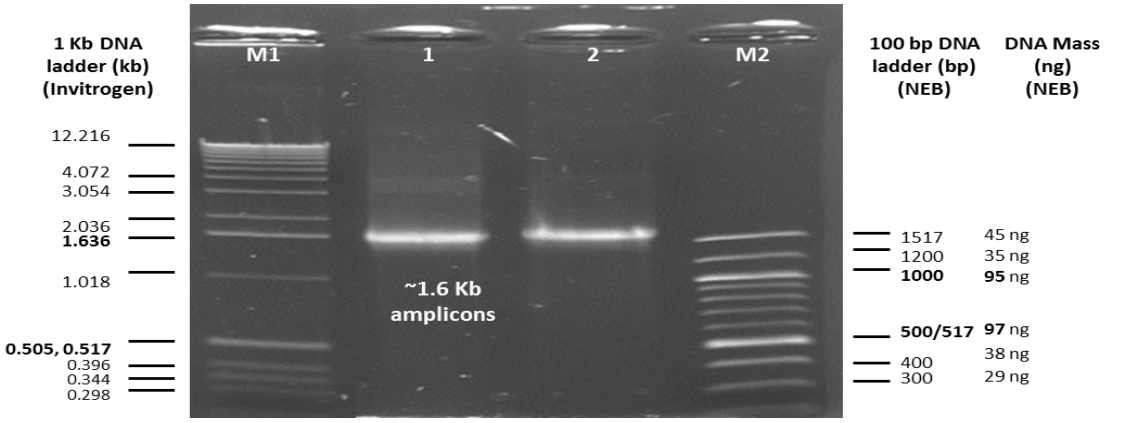

Figure 3.50. Agarose gel analysis of purified PCR amplified products for the *cdc13-1* C-terminus deletion module (ADH1-HIS3MX6 DNA).

PCR amplified product (350 µl) was purified by phenol-chloroform extraction and ethanol precipitation. The purified and non-purified (3 µl) amplicons were examined on a 0.8% agarose gel.

Lanes M1 and **M2**: 1 kb DNA ladder, (Invitrogen) and 100 bp DNA marker quantitative (NEB), 500 ng respectively; **1**: un-purified DNA from PCR reaction; **2**: phenol-chloroform extracted DNA fragment).

The purified fragment, 3 µl (lane 2) was analysed on a gel along with 3 µl un-purified amplicons (lane 1). The approximate concentration of purified fragment was estimated to be ~30-50 ng/µl according to the quantitative marker (NEB 100 bp ladder).

3.5.1.2. Preparation of competent cells for transformation

3.5.1.2.1. Generation and analysis of temperature-resistant (TR) survivors

Temperature-resistant survivors were generated at high temperature (36°C) as explained earlier from *cdc13-1* mutant strains DLY 1296 and DLY 1297 (Figures 3.21-3.26. The strain DLY 1272 with *CDC13* (grown at 36°C) was also used in transformation experiments including above mentioned survivors strains.

The competent cells prepared from these strains were tested for their viability. Figure 3.51 shows an example of viability counts in a 50 µl suspension for each strain. The competent cells were also checked for the frequency of spontaneous revertants at 30°C on dropout media lacking histidine and tryptophan (for H^+ and T^+ revertants). The histidine marker did not show revertants on medium lacking histidine (data not shown).

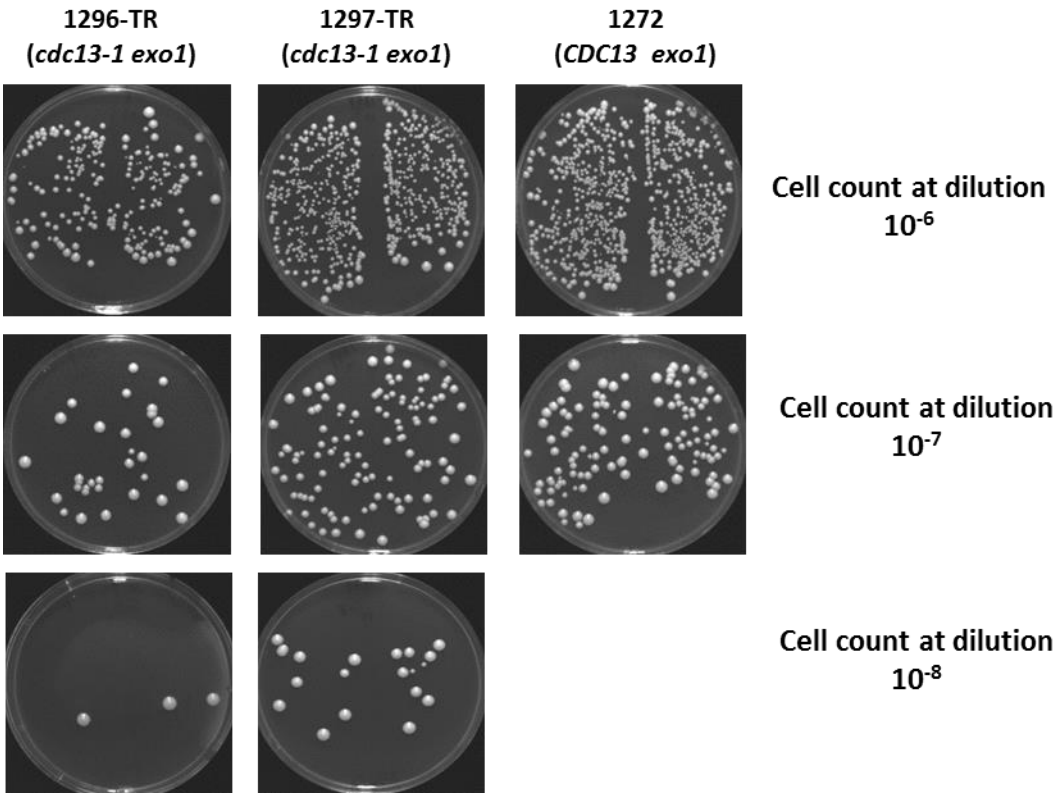

Figure 3.51. Viability count of the yeast competent cells.

The concentrated competent cells from strains (1296-TR, 1297-TR and 1272) were diluted and 50 µl (of the three dilutions 10^{-6}, 10^{-7} and 10^{-8}) were plated on each half of a YEPD plate to estimate the viable count. Cells were cultivated for 5 days at 23°C to get well spaced colonies for counting. The total number of cells in one millilitre was calculated on the basis of colony numbers from 50 µl of suspensions. Strain 1297 showed the highest viable cell number in one millilitre, i.e., 673.66×10^6 cells while the viable cell count in strain 1272 was 497.5×10^6 cells. The strain 1296 exhibited the lowest viable count i.e., 142.33×10^6 cells/ml.

3.5.1.2.2. Transformation of *cdc13-1* C-terminus deletion module into strain 1296-TR, 1297-TR and 1272 competent cells

Transformations of *S. cerevisiae* strains 1296-TR, 1297-TR and 1272 were carried out according to the standard protocol (Materials and Methods). Freshly prepared competent cells previously analysed for viability, marker analysis (Figures 3.21-3.25) and PCR genotyping for *CDC13* (Figure 3.26) were transformed with purified PCR product specific for C-terminus truncation. Transformation was carried out with ~1.5 µg DNA (40 µl) and 10 µl single stranded carrier DNA (sperm DNA) in 100 µl suspension of yeast cells.

For C-terminus deletion, the putative transformants were selected on histidine- and leucine-deficient dropout medium for strain 1296-TR (Figure 3.52, 3a and 4a), 1297-TR (3b and 4b) and 1272 cells (3c and 4c). The non-transformed cells from three strains 1296-TR, 1297-TR and 1272 were also plated on medium lacking histidine and leucine (H^-L^- medium; as negative controls; 1a, 1b and 1c) and on L^- medium (as positive controls; 2a, 2b and 2c). As expected,

there was no growth on H^-L^- dropout plates used as a negative control. However, in case of positive control the plates with L^- medium showed abundant growth for all these three strains. From the first round of selection after transformation, a few colonies grown on H^-L^- medium were picked randomly and diluted suspension of these was plated on H^-L^- dropout medium for a second round of selection to get the purified colonies. The media plates with cell suspension were incubated for 5-7 days at 30°C. Figure 3.53 demonstrates the growth shown by his^+ transformants with colonies which were picked randomly to screen analytically by PCR to verify gene disruption with the integration of the histidine marker module in the genome of the relevant strain.

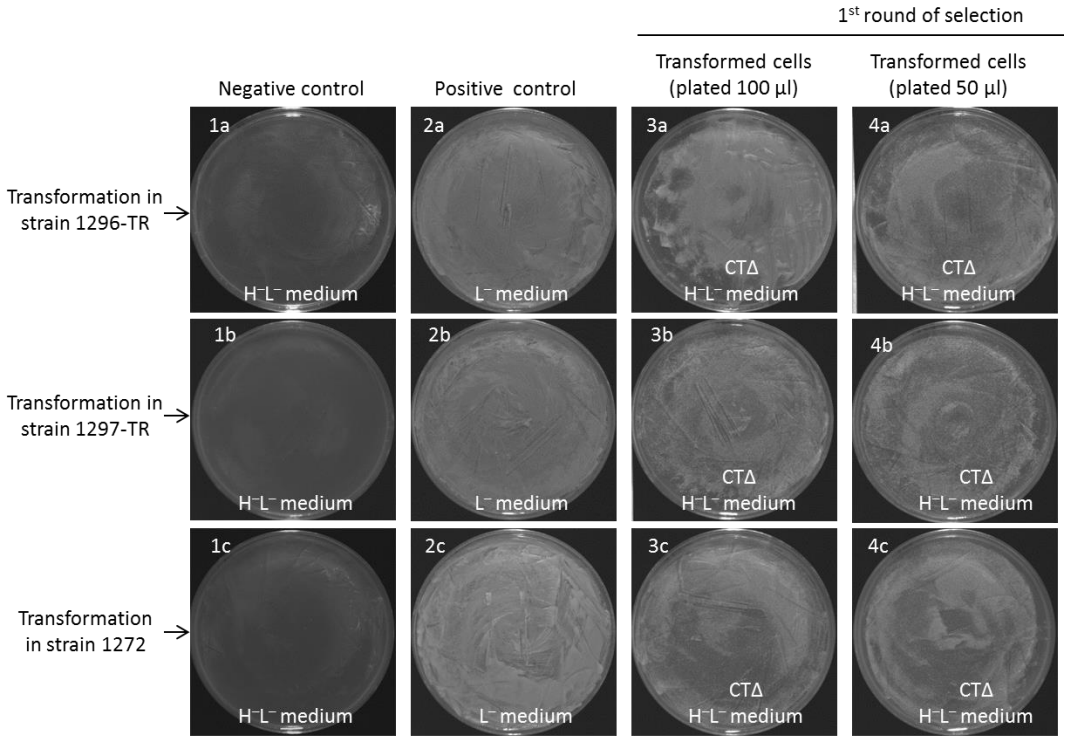

Figure 3.52. Transformation of competent cells from strains 1296-TR, 1297-TR and 1272 with *cdc13-1* C-terminus truncation module.

Freshly prepared competent cells were transformed with purified PCR fragments. Transformation was carried out with ~1.5 µg amplified DNA (40 µl) and 10 µl single stranded carrier DNA (sperm DNA) in 100 µl suspension of yeast cells. Transformants were selected on HL-deficient medium in the first rounds of selection. Abundant colonies grew after five to seven days of incubation at 30°C. A few cells were picked randomly from different places of plate, diluted in 10 µl of sterile water and spread over the HL-deficient medium for a second round selection.

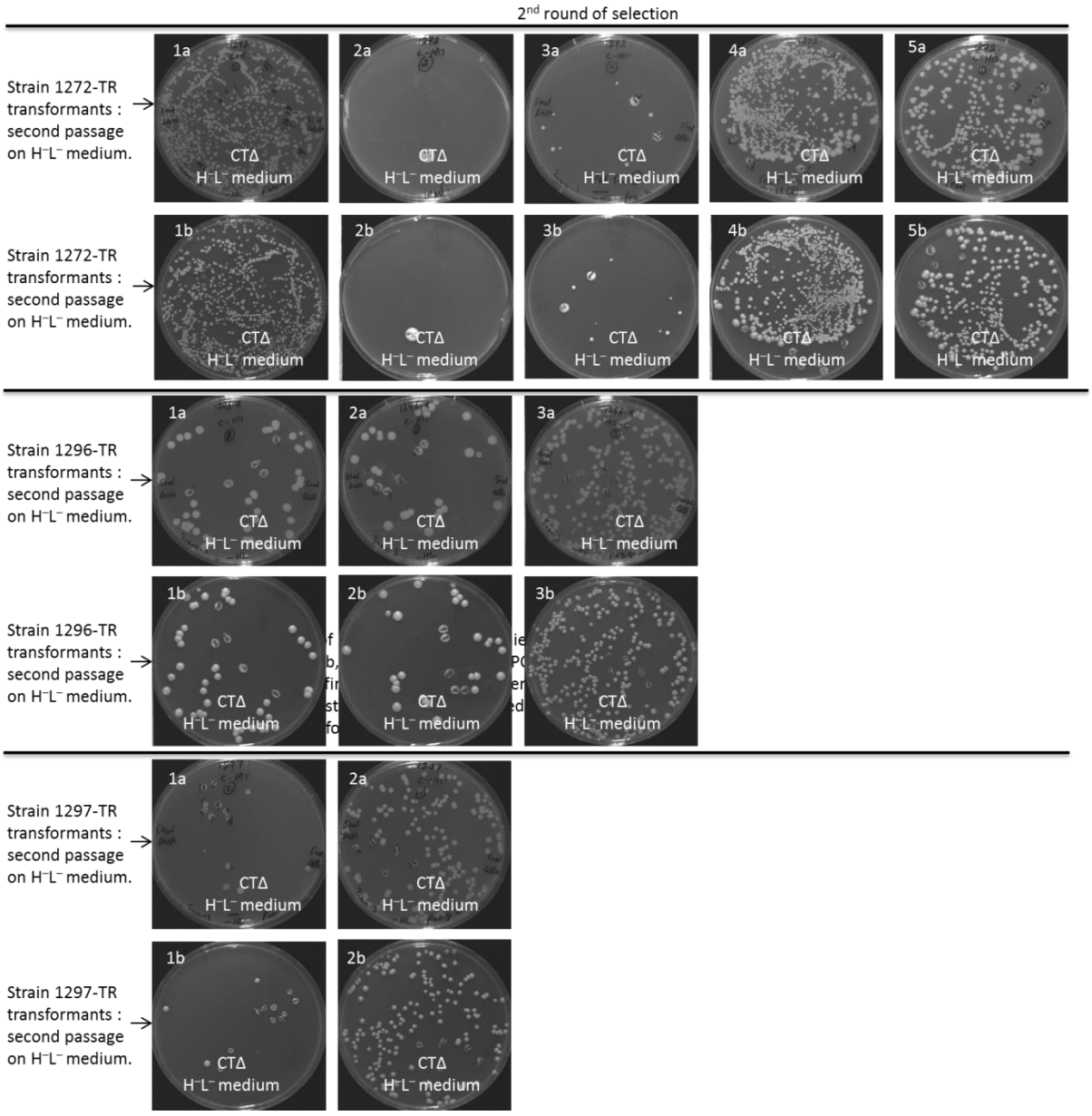

Figure 3.53. Selection of H^+L^+ transformant colonies for PCR analysis for C-terminus truncation.

From the first selection, a few cells were picked randomly from different places of plate, diluted in 10 µl of sterile water and spread over the HL-deficient media for a second round selection.

From the second selection, 25 colonies were picked randomly for strain 1272 transformants, and 15 transformants each for strains 1296-TR and 1297-TR. Selected colonies were analysed for C-terminus deletion and for the genomic integration of the histidine marker with diagnostic PCR directly from denatured cells.

3.5.2. Confirmation of *cdc13-1* disruption and marker module integration through analytical PCR

After a second round of selection, H^+L^+ transformants from strains 1296-TR, 1297-TR and 1272 were analysed by diagnostic PCR for the verification of C-terminus deletion and integration of the marker in chromosomal DNA. In total, 15 transformants each from strains 1296-TR and 1297-TR and 40 transformants from strain 1272 were analysed for the detection of the C-terminus (PCR with C1-C2 primers), HIS3MX6 marker module (PCR with H1-H2 primers) and finally for the N-terminus (PCR with the N1-N2 primer pair).

3.5.2.1. Screening of *cdc13-1* CTΔ::(HIS3MX6) mutants in strain 1296-TR

3.5.2.1.1. Analytical PCR for the C-terminus

The 15 histidine-positive transformants (#C1-C15) were analysed by diagnostic PCR for *cdc13-1* CTΔ in strain 1296 survivors. Gel electrophoresis revealed a fragment of ~276 bp in two transformants #C2 and #C8 (Figure 3.54, lanes 9 and 15 respectively) in consonance with *cdc13-1* (lanes 5-6) or *CDC13* (lane 7) indicating the presence of intact *cdc13-1* or *CDC13*. However, no amplified products were observed in the other transformants analysed (lanes 8, 10-14 and 16-22) confirming successful deletion of the *cdc13-1* gene by target-guided homologous recombination. As the C-terminus fragment of *cdc13-1* should be replaced by a histidine cassette resulting in the *cdc13-1*-CTΔ::ADH1-HIS3MX6 construct, the correct integration of HIS3MX6 was confirmed by analytical PCR with marker-specific primers H1 and H2.

3.5.2.1.2. Analytical PCR for HIS3MX6 modular marker

Figure 3.55 confirmed the presence of the histidine marker module in mutants examined for CTΔ (lanes 8, 10-14 and 16-22). The H^+L^+ transformant #C2 (lane 9), showing discrete gene specific band for the C-terminus did not amplify the marker (spontaneous revertant), whereas transformant #C8 (lane 15) with discrete marker specific fragment confirmed the integration of the marker without deleting the C-terminus, indicating its non-homologous recombination.

3.5.2.1.3. Analytical PCR for the N-terminus

In *cdc13-1*-CTΔ::ADH1-HIS3MX6 mutants, the presence of the intact N-terminus was confirmed by a second PCR with N1 and N2 gene-specific primers for the N-terminal half. Analytical gel shows the presence of ~378 bp fragments in the 15 tested transformants (Figure 3.56A, lanes 7-21). The *Eco*R1 digestion of amplified N-terminus fragments produced two discrete fragments (Figure 3.56B, lanes 7-21) of ~219 bp and ~159 bp corroborating the N-terminus half of the *cdc13-1* mutant in CTΔ::ADH1-HIS3MX6 construct of strain 1296-TR.

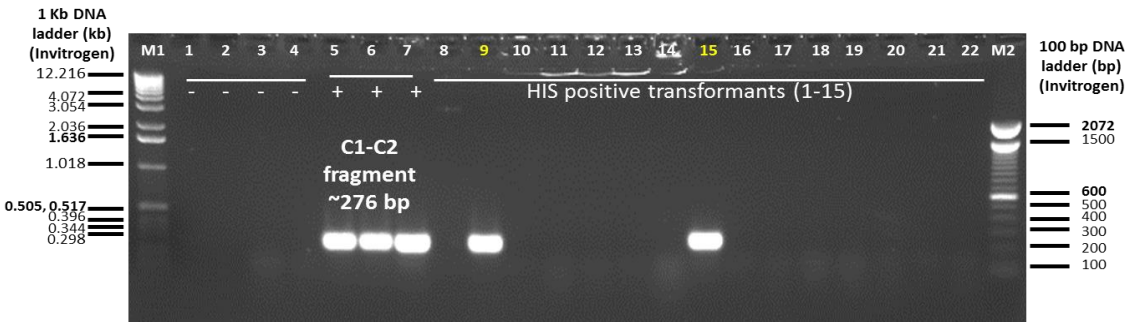

Figure 3.54. PCR screening (1-15) for *cdc13-1* C-terminus deletion (CTΔ) in strain 1296-TR: agarose gel electrophoresis of PCR products (C1 and C2 primer pair).

The putative, *cdc13-1* CTΔ transformants (#C1-15) were screened by PCR for the *cdc13-1* C-terminus. The PCR was carried out with C1 and C2 diagnostic primers in a 25 µl volume with 2-3 µl of denatured genomic DNA from cells. The PCR products (10 µl) were examined on a 1.5 % agarose gel.

Lanes M1: 1 kb ladder, 500 ng (Invitrogen); **1-2**: NTC, -ve control; **3-4**: PCR products from cells of strain 2607 and 2608 (*cdc13*Δ) respectively; **5-7**: PCR products from cells of strains 1296-TR, 1297-TR (*cdc13-1*) and 640 (WT, *CDC13*); **8-22**: PCR products from cells of transformants #C1-C15 in strain 1296-TR (expected *cdc13-1*-CTΔ mutants); **M2**: 100 bp ladder, 500 ng (Invitrogen).

Gel analysis showed fragment of ~276 bp in two clones C2 and C8 (lanes 9 and 15). All other CTΔ mutants examined, lanes 8, 10-14 and 16-22) exhibited no fragments indicating the absence of the C-terminus.

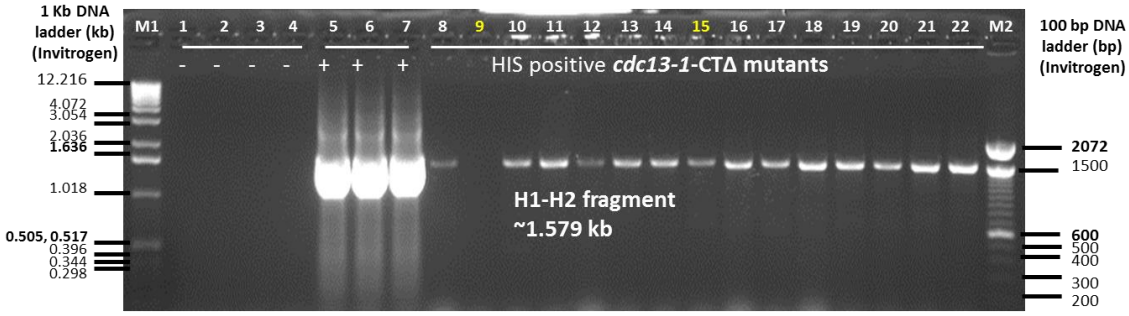

Figure 3.55. PCR confirmation of HIS3MX6 marker module in *cdc13-1*-CTΔ mutants (1-15) in strain 1296-TR: agarose gel electrophoretic analysis of PCR products (H1 and H2 primer pair).

The putative, *cdc13-1* CTΔ transformants (#C1-15) were screened by PCR for the HIS3MX6 marker module. The PCR was carried out with H1 and H2 primers in a 25 µl volume with 2 µl of denatured genomic DNA from cells. The PCR products (10 µl) were examined on a 0.8 % agarose gel.

Lanes M1: 1 kb ladder, 500 ng (Invitrogen); **2**: NTC, -ve control; **3-4**: PCR products from cells of strains 1296-TR, 1297-TR (*cdc13-1* mutant), control; **5-7**: PCR products with plasmid DNA (pDL504 with HIS3MX6) +ve control; **8-22**: PCR products from cells of transformants #C1-C15 in strain 1296-TR (anticipated *cdc13-1*-CTΔ mutants); **M2**: 100 bp ladder, 500 ng (Invitrogen).

Gel analysis showed fragments of ~1.579 kb in all tested clones except one (#C2, lane 9), indicating the replacement of the C-terminus by the histidine marker integrated by homologous recombination. However, clone #C8 (lane 15) exhibited a fragment of 1.5 kb (HIS3MX6) indicating its non-homologous genomic integration without CTΔ.

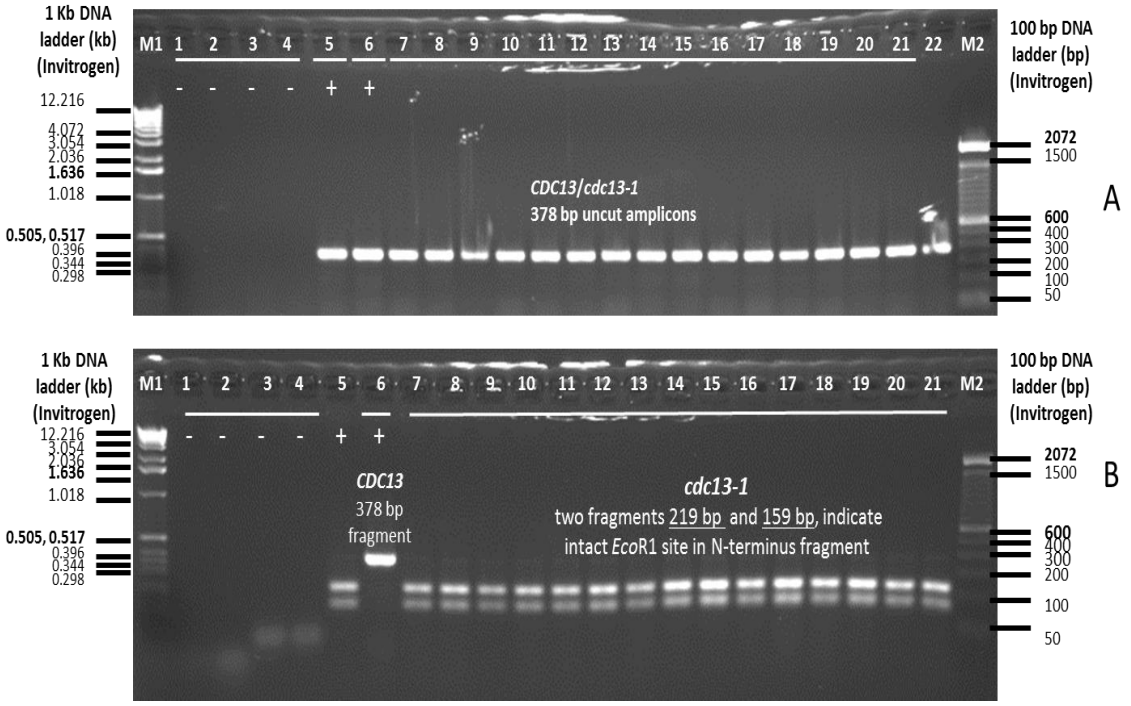

Figure 3.56. PCR confirmation of *cdc13-1* N-terminus in *cdc13-1*-CTΔ mutants (1-15) of strain 1296-TR: electrophoretic analysis of uncut and cut PCR products (amplified using N1 and N2 primer pair).

The *cdc13-1* CTΔ clones (#C1-15) were screened by diagnostic PCR using *CDC13* N-terminus-specific primers (N1 and N2). The PCR products, uncut and digested (7 µl) were examined on a 1.5 % agarose gel.

Lanes M1: 1 kb ladder, 500 ng (Invitrogen); **1-2**: NTC, -ve control; **3-4**: PCR products from cells of strains 2607 and 2608 (*cdc13*Δ), -ve control; **5-6**: PCR products from cells of strains 1296-TR (*cdc13-1*) and 640 (WT, *CDC13*) respectively; **7-21**: PCR products from cells of transformants #C1-C15 with strains 1296-TR (expected *cdc13-1*-CTΔ mutants); **22**: mistake load; **M2**: 100 bp ladder, 500 ng (Invitrogen).

Gel electrophoresis showed the ~378 bp fragment in all clones examined (#C1-C15, lanes 7-21 respectively), confirming the presence of the intact N-terminus in CTΔ mutants.

(**A**) Analytical gel showing uncut PCR fragment from N-terminus (amplified using N1 and N2 primers).

(**B**) Analytical gel showing *Eco*R1 digested N-terminus specific PCR products.

3.5.2.1.4. Screening of *cdc13-1* CTΔ::(HIS3MX6) mutants in strain 1297-TR

3.5.2.1.4.1. Analytical PCR for the C-terminus

The 15 histidine-positive transformants were analysed by diagnostic PCR for *cdc13-1* CTΔ in strain 1297 survivors. Gel analysis did not detect any fragments of ~276 bp in any of the clones examined (Figure 3.57, lanes 8-22 with respect to clones #C1-C15) indicating deletion of the *cdc13-1* gene by target-guided homologous recombination. As the C-terminus fragment of *cdc13-1* is expected to be replaced by a marker cassette of HIS3MX6 in the *cdc13-1*-CTΔ::ADH1-HIS3MX6 construct, the correct integration of HIS3MX6 was verified by analytical PCR with the marker-specific H1 and H2 primers.

3.5.2.1.4.2. Analytical PCR for the HIS3MX6 modular marker

Figure 3.58 confirmed the presence of the histidine marker module in all transformants examined for CTΔ (lanes 8-22). The H^+L^+ transformants #C1-C15 manifested discrete bands of 1.5 kb marker module with varying intensity, proving the integration of the marker in chromosomal DNA replacing the C-terminus, by homologous recombination.

3.5.2.1.4.3. Analytical PCR for the N-terminus

In *cdc13-1*-CTΔ::HIS3MX6 mutants, the presence of the intact N-terminus was confirmed by diagnostic PCR using N1 and N2 gene-specific primers from the N-terminal half. Analytical gel shows the presence of ~378 bp fragments in all clones examined (Figure 3.59A, lanes 7-21). The restriction analysis of the N-terminus amplified fragments with *Eco*R1 enzyme produced two distinct fragments (Figure 3.59B, lanes 7-21) of ~219 bp and ~159 bp corroborating the N-terminus specific fragment of the *cdc13-1* mutant in CTΔ::HIS3MX6 construct of strain 1297-TR.

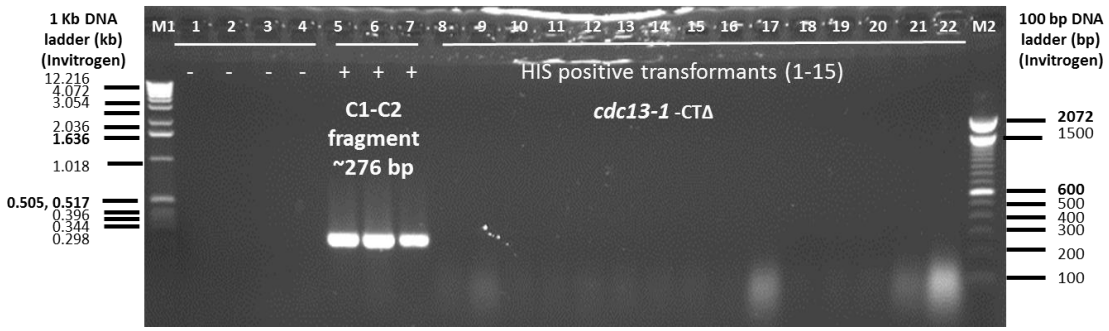

Figure 3.57. PCR screening (1-15) of *cdc13-1* C-terminus deletion (CTΔ) in strain 1297-TR: agarose gel electrophoresis of C1 and C2 amplified PCR products.

The putative, *cdc13-1* CTΔ transformants (#C1-15) were screened by PCR for the *cdc13-1* C-terminus with appropriate positive (lanes 5-7) and negative controls (lanes 1-4). The PCR products (10 µl) were examined on a 1.5 % agarose gel.

Lanes M1: 1 kb ladder, 500 ng (Invitrogen); **1-2**: NTC, -ve control; **3-4**: PCR products from cells of strain 2607 and 2608 (*cdc13*Δ); **5-7**: PCR products from cells of strain 1296-TR, 1297-TR (*cdc13-1*) and 640 (WT, *CDC13*); **8-22**: PCR products from cells of transformants #C1-C15 in strain 1297-TR (expected *cdc13-1*-CTΔ mutants); **M2**: 100 bp ladder, 500 ng (Invitrogen).

The analytical gel did not show any fragments of ~276 bp in any of the clones examined (#C1-C15 with respect to lanes 8-22) indicating the deletion of the C-terminus.

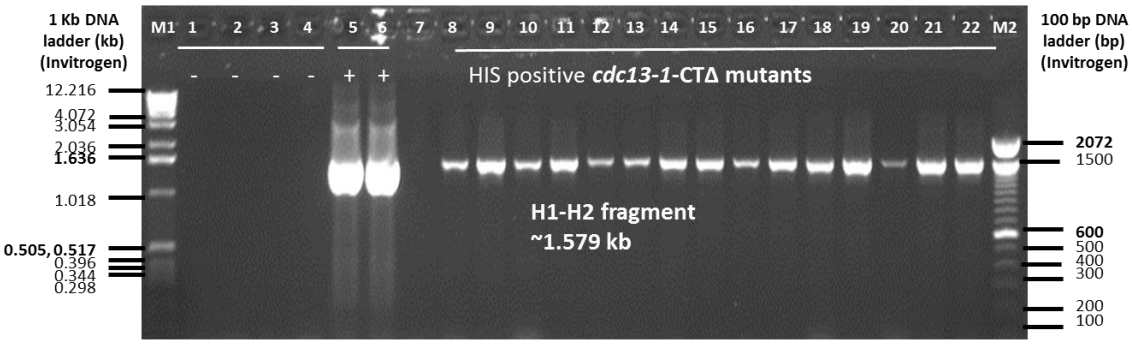

Figure 3.58. PCR confirmation of the HIS3MX6 marker module in *cdc13-1*-CTΔ mutants (1-15) in strain 1297-TR: electrophoretic analysis of PCR products (amplified using H1 and H2 primer pair).

The presumptive, *cdc13-1* CTΔ transformants (#C1-15) were screened by diagnostic PCR for the HIS3MX6 marker module. The PCR products (10 µl) were examined on a 0.8 % agarose gel.

Lanes M1: 1 kb ladder, 500 ng (Invitrogen); **1-2**: NTC, -ve controls; **3-4**: PCR products from cells of strains 1296-TR, 1297-TR (*cdc13-1* mutant), controls; **5-6**: PCR products with plasmid DNA (pDL504 with HIS3MX6), +ve control; **7**: blank; **8-22**: PCR products from cells of transformants #C1-C15 in strain 1296-TR (expected *cdc13-1*-CTΔ mutants); **M2**: 100 bp ladder, 500 ng (Invitrogen).

Gel electrophoresis confirmed the presence of ~1.579 kb fragments (the histidine marker) in all examined clones (C1-C15 with respect to lanes 8-22), indicating the deletion of the C-terminus. The PCR products (10 µl) were examined on a 0.8 % agarose gel.

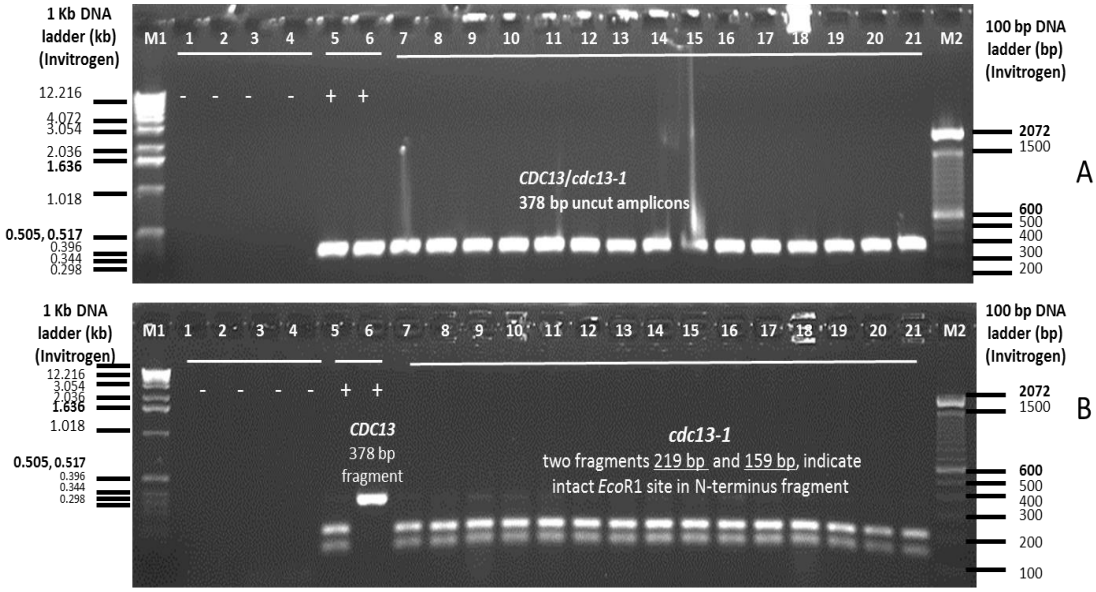

Figure 3.59. PCR confirmation of *cdc13-1* N-terminus in *cdc13-1*-CTΔ mutants (1-15) in strain 1297-TR: electrophoretic analysis of uncut and cut PCR products (amplified using N1 and N2 primer pair).

The *cdc13-1* CTΔ clones (#C1-15) were screened by diagnostic PCR using *CDC13* N-terminus-specific primers. The PCR products, uncut and *Eco*R1 digested (7 µl), were examined on a 1.5 % agarose gel.

Lanes M1: 1 kb ladder, 500 ng (Invitrogen); **1-2**: NTC, -ve control; **3-4**: PCR products from cells of strains 2607 and 2608 (*cdc13*Δ); **5-6**: PCR products from cells of strains 1297-TR, (*cdc13-1*) and 640 (WT, *CDC13*) respectively; **7-21**: PCR products from cells of transformants #C1-C15 in strain 1297-TR (confirmed *cdc13-1*-CTΔ clones); **M2**: 100 bp ladder, 500 ng (Invitrogen).

Gel electrophoresis confirmed fragments of ~378 bp in all clones examined #C1-C15 (lanes 7-21 respectively), indicating the presence of the intact N-terminus with *Eco*R1 site in CTΔ::ADH1-HIS3MX6 constructs.

(**A**) Analytical gel showing uncut PCR fragment from N-terminus (amplified using N1 and N2 primers).

(**B**) Analytical gel showing *Eco*R1 digested N-terminus specific PCR products.

3.5.2.2. Screening of *CDC13* CTΔ::(HIS3MX6) in mutants of strain 1272

3.5.2.2.1. Analytical PCR for the C-terminus

In total, 77 histidine-positive transformants were analysed by diagnostic PCR for *CDC13*-CTΔ in strains 1272 (data are shown for 40 transformants, #C1-C40). The gel analysis confirmed amplified fragments of ~276 bp with the C-terminus-specific primers in all of the examined transformants (Figures 3.60, 3.63 and 3.66, lanes 10-19, 8-22 and 8-22 with respect to transformants #C1-C10, C11-C25 and C26-C40 respectively) indicating the presence of the intact *CDC13* gene.

The genomic integration of the HIS3MX6 marker module was diagnosed by analytical PCR, using marker-specific primers.

3.5.2.2.2. Analytical PCR for the HIS3MX6 modular marker

Further analysis of the histidine-positive transformants with marker-specific primers H1 and H2 revealed that the marker cassette of HIS3MX6, did not replaced the C-terminus of *CDC13* although it integrated within genome of a few of the transformants. Figure 3.61 (lanes 10-13 and 15), Figure 3.64 (faint bands in lanes 8, 11, 13-14, and 17-20), and Figure 3.67 (lane 19) showed the size-specific band of~ 1.5 kb with different intensity and confirmed the presence of the histidine marker module in a few transformants examined for CTΔ. However, further analysis of these transformants for the *CDC13* N-terminus could determine the nature of these H^+L^+ transformants, i.e., whether the result of spontaneous gene conversion or non-homologous recombination of the HIS3MX6 marker within genome.

3.5.2.2.3. Analytical PCR for the N-terminus

In histidine-positive mutants, the presence of the intact N-terminus was confirmed by diagnostic PCR with N1 and N2 gene-specific primers for the N-terminal half of *CDC13*. Analytical gel (Figure 3.62 (lanes 9-18) and Figure 3.65 (lanes 8-22) confirmed the presence of ~378 bp fragments in transformants C1-C25 examined. The restriction analysis of N-terminus amplified fragments with *Eco*R1 enzyme did not cut the ~378 bp fragment (Figure 3.62B, lanes 9-18) corroborating the N-terminus specific fragment of *CDC13* (not *cdc13-1* mutant) in H^+L^+ transformants of strain 1272. The conformation of the full *CDC13* indicates the generation of the tested transformants by non-homologous recombination rather than gene conversion. Overall, the results of PCR analysis of forty histidine$^+$ transformants in strain 1272 did not confirm any CTΔ mutant.

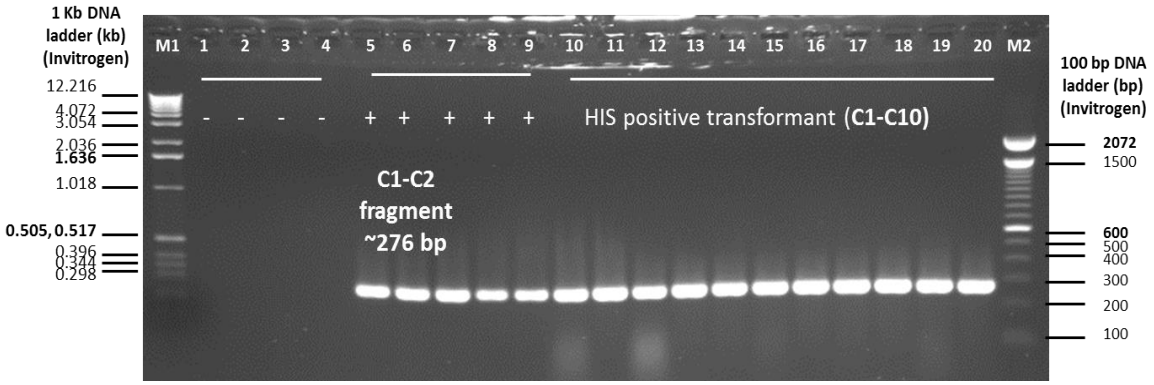

Figure 3.60. PCR screening (1-10) for *CDC13* C-terminus deletion (CTΔ) in strain 1272: agarose gel electrophoresis of C1-C2 amplified PCR products.

The putative, *CDC13*-CTΔ transformants (#C1-10) were screened by PCR for the *CDC13* C-terminus with appropriate positive (lanes 5-9) and negative controls (lanes 1-4). The PCR amplified products (10 µl) were examined on a 1.5 % agarose gel.

Lanes M1: 1 kb ladder, 500 ng (Invitrogen); **1-2**: NTC, -ve control; **3-4**: PCR products from cells of strain 2607 and 2608 respectively (*cdc13*Δ); **5-6**: PCR products from cells of strain 1296-TR and 1297-TR respectively (*cdc13-1*); **7-9**: PCR products from cells of strain 1272 and 640 (WTx2) respectively (*CDC13*); **10-19**: PCR products from H^+L^+ cells of transformants #C1-C10 in strain 1272; **20**: sample #C10 repeated; **M2**: 100 bp ladder, 500 ng (Invitrogen).

The analytical gel shows amplified fragments of ~276 bp in all of the transformants examined (#C1-C10 with respect to lanes 10-19) indicating the presence of C-terminus.

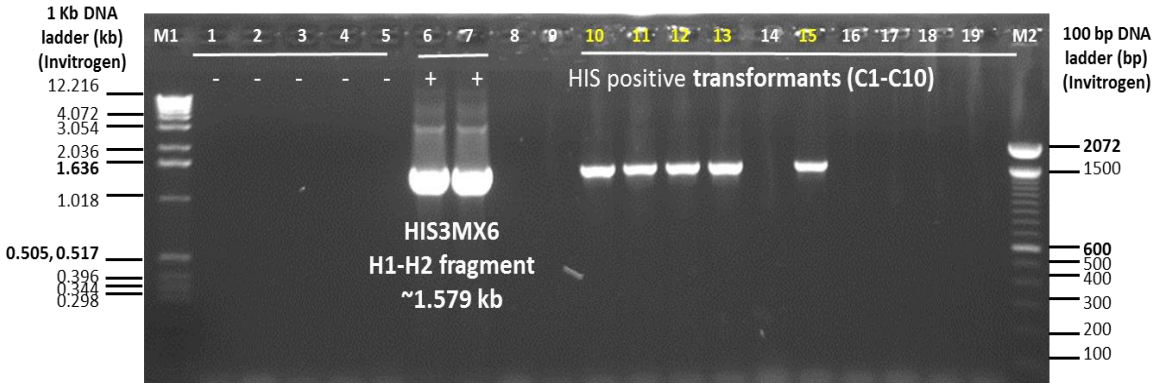

Figure 3.61. PCR confirmation of the HIS3MX6 marker module in *CDC13*-CTΔ mutants (1-10) in strain 1272: electrophoretic analysis of PCR products (amplified using H1and H2 primers).

The H^+L^+ *CDC13*-CTΔ transformants (#C1-10) were screened by diagnostic PCR for the HIS3MX6 marker module. The PCR products (10 µl) were examined on a 0.8 % agarose gel.

Lanes M1: 1 kb ladder, 500 ng (Invitrogen); **1-2**: NTC, -ve control; **3-4**: PCR products from cells of strains 1296-TR, 1297-TR (*cdc13-1* mutant), -ve control; **5**: PCR products from cells of strains 1272 (*CDC13*), -ve control; **6-7**: PCR products with DNA of plasmid (pDL504 with HIS3MX6), +ve control; **8-9**: blank; **10-19**: PCR products from H^+L^+ cells of transformants #C1-C10 in strain 1272 (expected *CDC13*-CTΔ mutants); **M2**: 100 bp ladder, 500 ng (Invitrogen).

Gel analysis confirmed the presence of ~1.579 kb fragment in five out of the 10 clones examined (#C1-C4 and C6 with respect to lanes 10-13, and 15). However, this does not indicate the deletion of the C-terminus by the histidine marker.

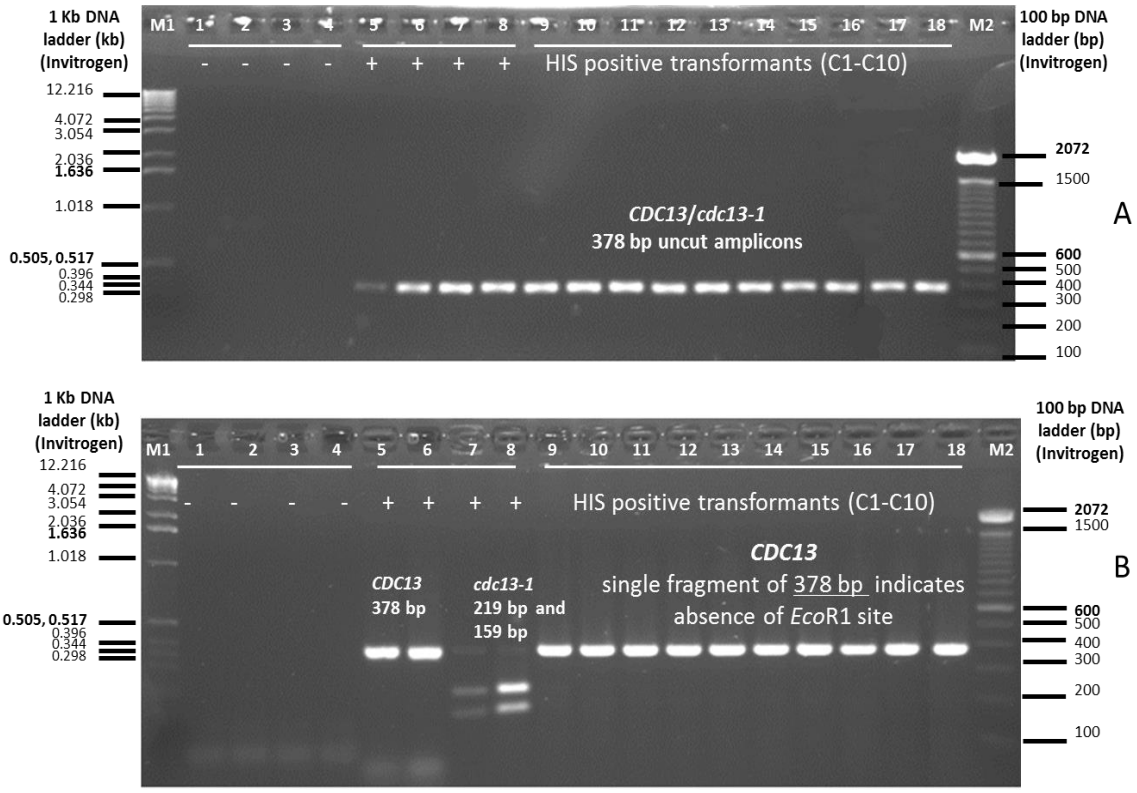

Figure 3.62. PCR confirmation of the *CDC13* N-terminus mutants (1-10) in histidine^{+} transformants in strain 1272: electrophoretic analysis of uncut and cut PCR products (amplified using N1-N2 primers).

The putative *CDC13*-CTΔ, $H^{+}L^{+}$ transformants (#C1-C10) were screened by diagnostic PCR for N-terminus specific fragment. The PCR products of uncut and digested products (7 µl) were examined on 1.5 % agarose gels.

Lanes M1: 1 kb ladder, 500 ng (Invitrogen); **1-2**: NTC, -ve control; **3-4**: PCR products from cells of strains 2607 and 2608 (*cdc13*Δ) respectively; **5-6**: PCR products from cells of strains 1272, (*CDC13*) and 640 (WT, *CDC13*) respectively; **7-8**: PCR products from cells of strains 1296-TR, (*cdc13-1*) and 1297-TR (*cdc13-1*) respectively; **9-18**: PCR products from cells of $H^{+}L^{+}$ transformants #C1-C10 in strain 1272 (*cdc13-1*-C-terminus); **M2**: 100 bp ladder, 500 ng (Invitrogen).

Gel analysis confirmed fragment of ~378 bp in all clones examined (#C1-C10, lanes 9-18 respectively), indicating the presence of the intact N-terminus in the tested $H^{+}L^{+}$ transformants.

(**A**) Analytical gel showing uncut PCR amplified fragmens from N-terminus (amplified using N1 and N2 primers).

(**B**) Analytical gel showing *Eco*R1 digested PCR products of the N-terminus.

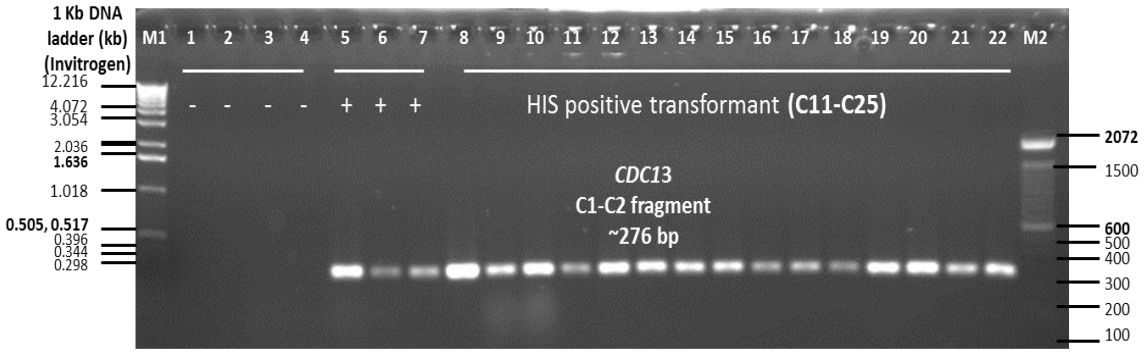

Figure 3.63. PCR screening (11-25) for *CDC13* C-terminus deletion (CTΔ) in strain 1272: agarose gel electrophoresis of PCR products (C1 and C2-specific primers).

The putative, *CDC13*-CTΔ transformants (#C11-C25) were screened by PCR for the *CDC13* C-terminus with appropriate positive (lanes 5-7) and negative controls (lanes 1-4). The PCR products (10 µl) were resolved on a 1.5 % agarose gel.

Lanes M1: 1 kb ladder, 500 ng (Invitrogen); **1-2**: NTC, -ve control; **3-4**: PCR products from cells of strain 2607 and 2608 (*cdc13*Δ) respectively; **5**: PCR products from cells of strain 1296-TR (*cdc13-1*); **6-7**: PCR products from cells of strain 1272 and 640 (WT) *CDC13*, respectively; **8-22**: PCR products from cells of transformants #C11-C25 in strain 1272; **M2**: 100 bp ladder, 500 ng (Invitrogen).

Analytical gel shows fragments of ~276 bp in all of the H^+L^+ transformants examined (C11-C25 with respect to lanes 8-22) indicating the intact C-terminus.

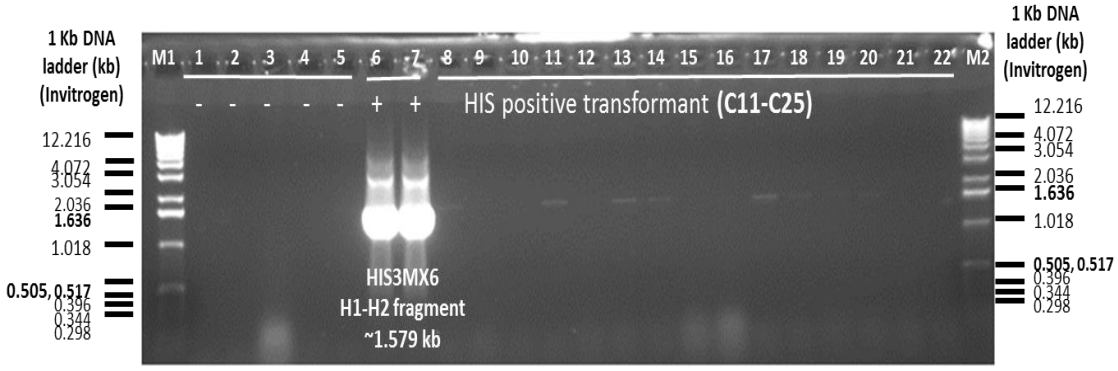

Figure 3.64. PCR confirmation of the HIS3MX6 marker module in *CDC13*-CTΔ mutants (11-25) in the strain 1272: electrophoretic analysis of PCR products (amplified using H1 and H2 primers).

The H^+L^+ putative *CDC13*-CTΔ transformants (#C11-C25) were screened by PCR for the HIS3MX6 marker module. The PCR products (10 µl) were resolved on a 0.8 % agarose gel.

Lanes M1: 1 kb ladder, 500 ng (Invitrogen); **1-2**: NTC, -ve control; **3-4**: PCR products from cells of strains 1296-TR, 1297-TR (*cdc13-1* mutant) respectively; **5**: PCR products from cells of strain 1272, (*CDC13*); **6-7**: PCR products from DNA of plasmid (pDL504 with HIS3MX6) +ve control; **8-22**: PCR products from cells of transformants #C11-C25 in strain 1272 (expected *CDC13*-CTΔ mutants); **M2**: 100 bp ladder, 500 ng (Invitrogen).

Gel analysis showed the presence of a ~1.579 kb fragment (faint bands) in eight out of the 15 clones examined (C11, C14, C16-17 and C20-C23 with respect to lanes 8, 11, 13, 14 and 17-20) indicating its non-homologous genomic integration without CTΔ.

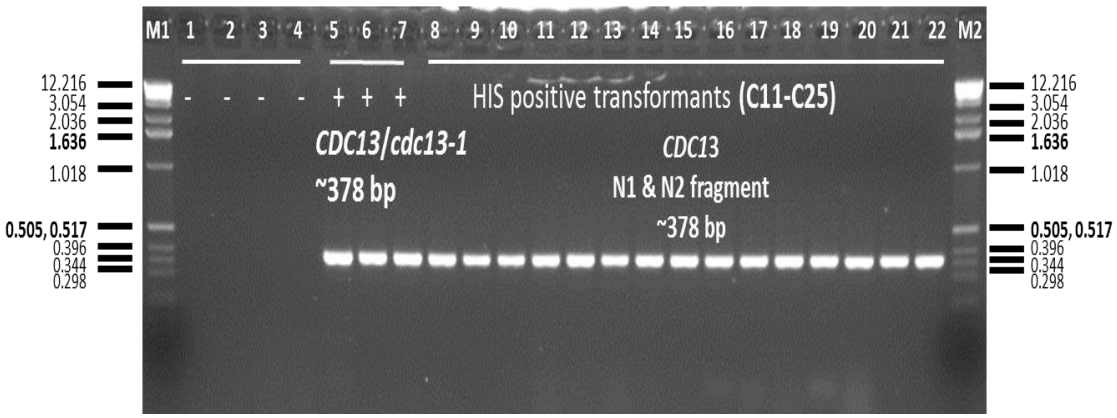

Figure 3.65. PCR confirmation of *CDC13* N-terminus in histidine^{+} transformants (11-25) in strain 1272: electrophoretic analysis of uncut products (amplified with N1 and N2 primers).

The *CDC13*-CTΔ transformants (#C11-C25) were screened by diagnostic PCR for the *CDC13* N-terminus. The PCR products uncut (7 µl) were resolved on 1.5 % agarose gels.

Lanes M1: 1 kb ladder, 500 ng (Invitrogen); **1-2**: NTC, -ve controls; **3-4**: PCR products from cells of strains 2607 and 2608 (*cdc13*Δ), respectively; **5**: PCR products from cells of strains 1296-TR, (*cdc13-1*) ; **6-7**: PCR products from cells of strains 1272, (*CDC13*) and 640 (WT, *CDC13*) respectively; **8-22**: PCR products from cells of transformants #C11-C25 of the strain 1272 (confirmed *cdc13-1*-C-terminus); **M2**: 1 kb ladder, 500 ng (Invitrogen).

Gel analysis confirmed the presence of ~378 bp fragment in all 15 transformants examined (#C11-C25, lanes 8-22 respectively), indicating the presence of the intact N-terminus in his^{+} transformants.

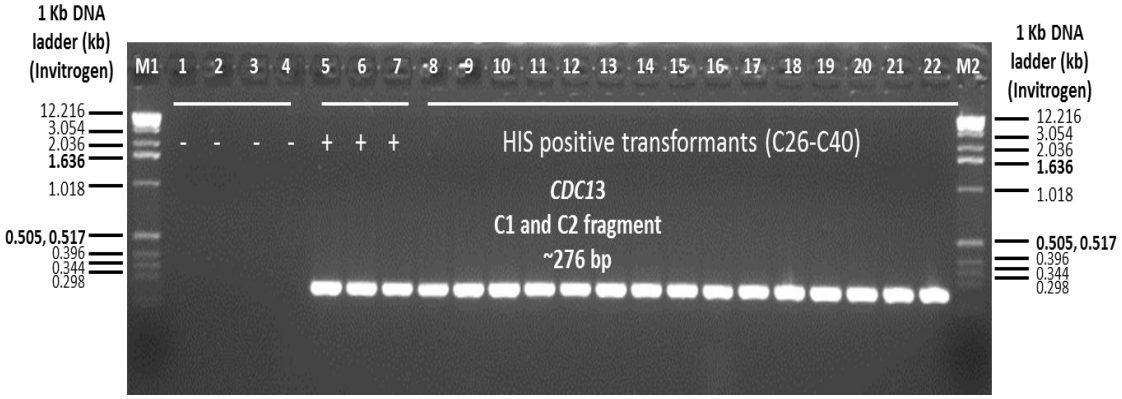

Figure 3.66. PCR screening for *CDC13* C-terminus deletion (CTΔ) transformants (26-40) in strain 1272: agarose gel electrophoresis of PCR products (amplified with C1 and C2 primers).

The presumptive his$^+$ *CDC13*-CTΔ transformants (15) were screened by PCR for the *CDC13* C-terminus deletion using appropriate positive (lanes 5-7) and negative controls (lanes 1-4). The PCR products (10 µl) were examined on a 1.5 % agarose gel.

Lanes M1: 1 kb ladder, 500 ng (Invitrogen); **1-2**: NTC, -ve control; **3-4**: PCR products from cells of strain 2607 and 2608 (*cdc13*Δ), respectively; **5**: PCR products from cells of strain 1296-TR (*cdc13-1*); **6-7**: PCR products from cells of strain 1272 and 640 (WT, *CDC13)*, respectively; **8-22**: PCR products from cells of transformants #C26-C40 of strain 1272; **M2**: 1 kb ladder, 500 ng (Invitrogen).

The analytical gel confirmed amplified fragments of ~276 bp in all of the transformants examined (C26-C40 with respect to lanes 8-22) indicating the presence of the intact C-terminus.

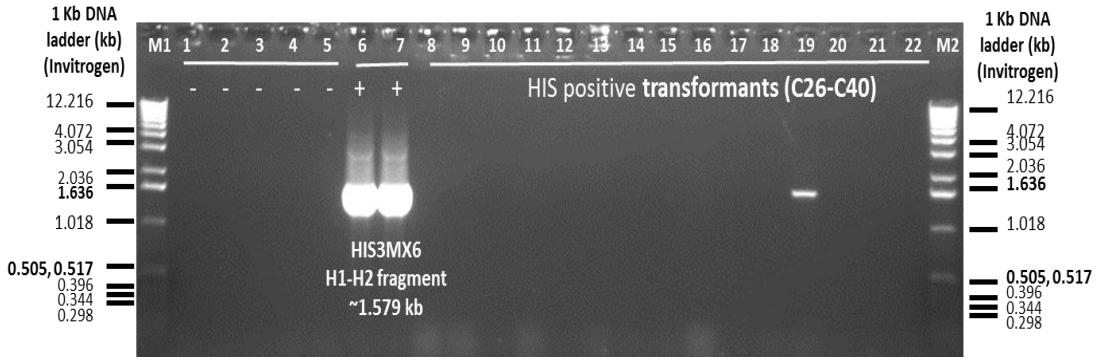

Figure 3.67. PCR confirmation of the HIS3MX6 marker module in *CDC13*-CTΔ mutants (26-40) in strain 1272: electrophoretic analysis of PCR products (amplified with the H1-H2 primer pair).

The presumptive *CDC13*-CTΔ transformants (#C26-#40) were screened by diagnostic PCR for the HIS3MX6 marker module. The PCR products (10 µl) were examined on a 0.8 % agarose gel.

Lanes M1: 1 kb ladder, 500 ng (Invitrogen); **1-2**: NTC, -ve controls; **3-4**: PCR products from cells of strains 1296-TR, 1297-TR (*cdc 13-1* mutant) respectively, -ve controls; **5**: PCR products from cells of strains 1272, cells (*CDC13*), -ve control; **6-7**: PCR products with DNA of plasmid (pDL504 with HIS3MX6), +ve control; **8-22**: PCR products from cells of transformants #C26-C40 in strain 1272 (expected *CDC13*-CTΔ mutants); **M2**: 1 kb ladder, 500 ng (Invitrogen).

Gel analysis confirmed the presence of ~1.579 kb fragments in one (C37 with respect to lane 19) out of 15 tested his$^+$ transformants. However, the presence of histidine fragment does not indicate the deletion of the C-terminus (PCR$^+$ for C-terminus).

3.5.3. Summary of C-terminus truncation results

The results on *cdc13-1* C-terminus deletion with the HIS3MX6 marker module and PCR analysis to confirm the correct mutants (CTΔ::HIS3MX6) are summarised in Table 3.5. The data below present numbers of clones generated in all three strains, 1296-TR, 1297-TR and 1272 as a result of homologous recombination with gene-specific guide oligonucletides.

Table 3.5. Comparative analysis of histidine-positive transformants for C-terminus deletion for *cdc13-1* and *CDC13* strains.

Analysis of C-terminus truncation with ADH1-HIS3MX6 module (pDL504)				
	Selected clones in DLY strains	1296-TR (*cdc13-1*)	1297-TR (*cdc13-1*)	1272 (*CDC13*)
1	H^+L^+ transformants analysed for CTΔ	15	15	77
2	PCR^+ for C-terminus (C1-C2 primer pair)	2	0	77
3	PCR^+ for HIS3MX6 (H1-H2 primer pair)	14	15	14
4	True mutant/ CTΔ::HIS3 construct	13 (86.67%)	15 (100%)	0 %
5	False positive H^+L^+ revertants**)**	2 (13.33%)	0 %	77 (100%)
6	Target specific homologous recombination (HR)	13 (86.67%)	15 (100%)	0%
7	Non homologous recombination (NHR)	1 (6.67%)	0 %	14 (18.18%) (C1-4, C6,C11,C14, C16, C17, C20-C23, C37*)
8	Name of the constructs generated	C1,C3-C7, C9-C15	C1-C15	-

3.6. Genetic crosses

In the past, genetic crosses were performed mainly to map different genes on chromosomes and to estimate the genetic distance between the mapped genes. At present, genetic crosses in yeast are carried out to generate new combinations of known mutations arising as a consequence of meiotic recombination. Analysis of newly derived deletion mutants can provide insights into gene function. In order to monopolise on this technology, two classical techniques were selected for the following studies; genetic crossing and the separation of spores by micromanipulation, to yield new deletion mutants.

3.6.1. Haploid strain crosses and micromanipulation

A number of crosses were performed in this study in an attempt to generate new combinations of mutations of capping proteins from the obtained mutations. A representative example has been shown here to show the generation and analysis of diploids and haploids. Yku70 is another important telomere capping protein beside Cdc13 and Stn1. In order to study the impact of Yku70 in the *STN1* deletion mutants, crosses were performed to obtain deletion combinations, stn1::HIS exo1::LEU2 yku70::URA3 ($H^+L^+U^+$). Other desired deletion combinations was stn1::HIS exo1::LEU2 (H^+L^+).

Two crosses were carried out by mixing a loopful of culture from MATa (strain 3345; MATa *yku70*::URA3) and MATα (strain 2684/2685; MATα *cdc13*::HIS *stn1*::HIS *exo1*::LEU2 rad24::TRP) (Figure 3.68A) on nutrient rich medium YEPD plates and incubated at 28°C for a minimum of 8 hours (Figure 3.68B). The resulting diploid cells were selected on dropout media without complemented for four auxotrophies. Parental strains were used as controls (Figure 3.68A and C). Only diploid cells grew on dropout medium through complementation by compensating nutrients, an indicative of a successful cross. Diploid cells were purified through 2-3 passages (Figure 3.68C), single colonies were selected, grown for sporulation and for micromanipulation analysis.

Diploids cells were analysed by sporulating, saturated cultures for tetrad formation in potassium acetate medium (Figure 3.69A and B). In total, 82 tetrads were analysed by dissecting four-spore tetrads and isolating individual cells by micromanipulation. Germination of 31 spores out of 328 cells isolated, revealed low viability of micromanipulated cells (~9%). Further analysis of the 31 viable spores by replica plating for genotypic markers segregated all spores into 6 groups with the gene combinations presented in Table 3.6
in correlation with Figure 3.70.

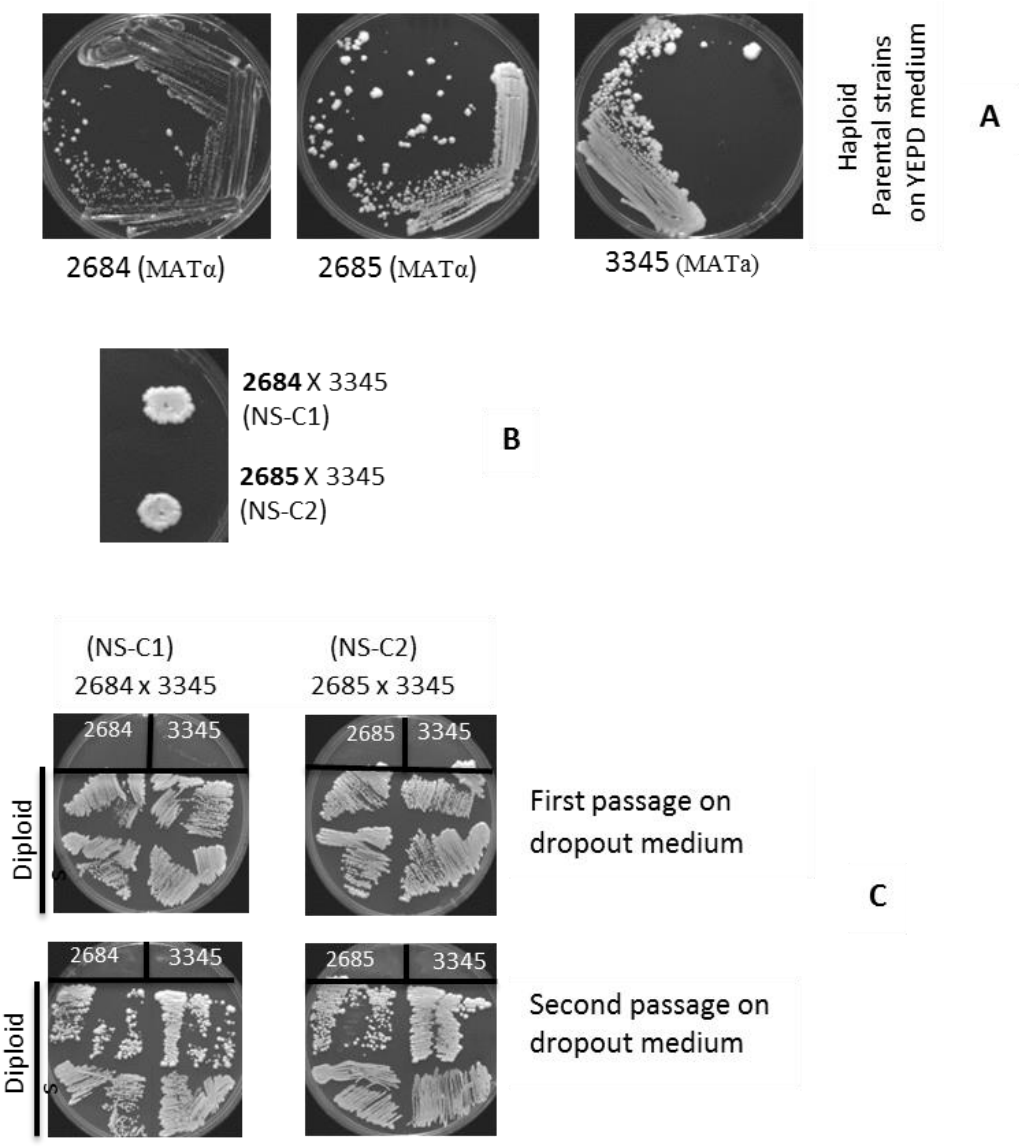

Figure 3.68. Crosses between haploid strains 3345 and 2684/2685 and purification of diploid cells by sub culturing.

(**A**) Growth of parental strains on YEPD medium.

(**B**) Crosses of *S. cerevisiae* strain DLY 3345, Ura$^+$ (MATa *yku*70::URA3) with DLY strains 2684 or 2685, HIS$^+$, LEU$^+$ and TRP$^+$ (MATα *cdc13*::HIS *stn1*::HIS *exo1*::LEU2 *rad24*::TRP), on YEPD plates to generate diploid cells.

(**C**) Selection of diploids cells on dropout medium lacking histidine, leucine, tryptophan and uracil. The parental cells did not grow on this selective medium. The selected diploids cells were further purified by sub culturing on dropout medium without four essential nutrients.

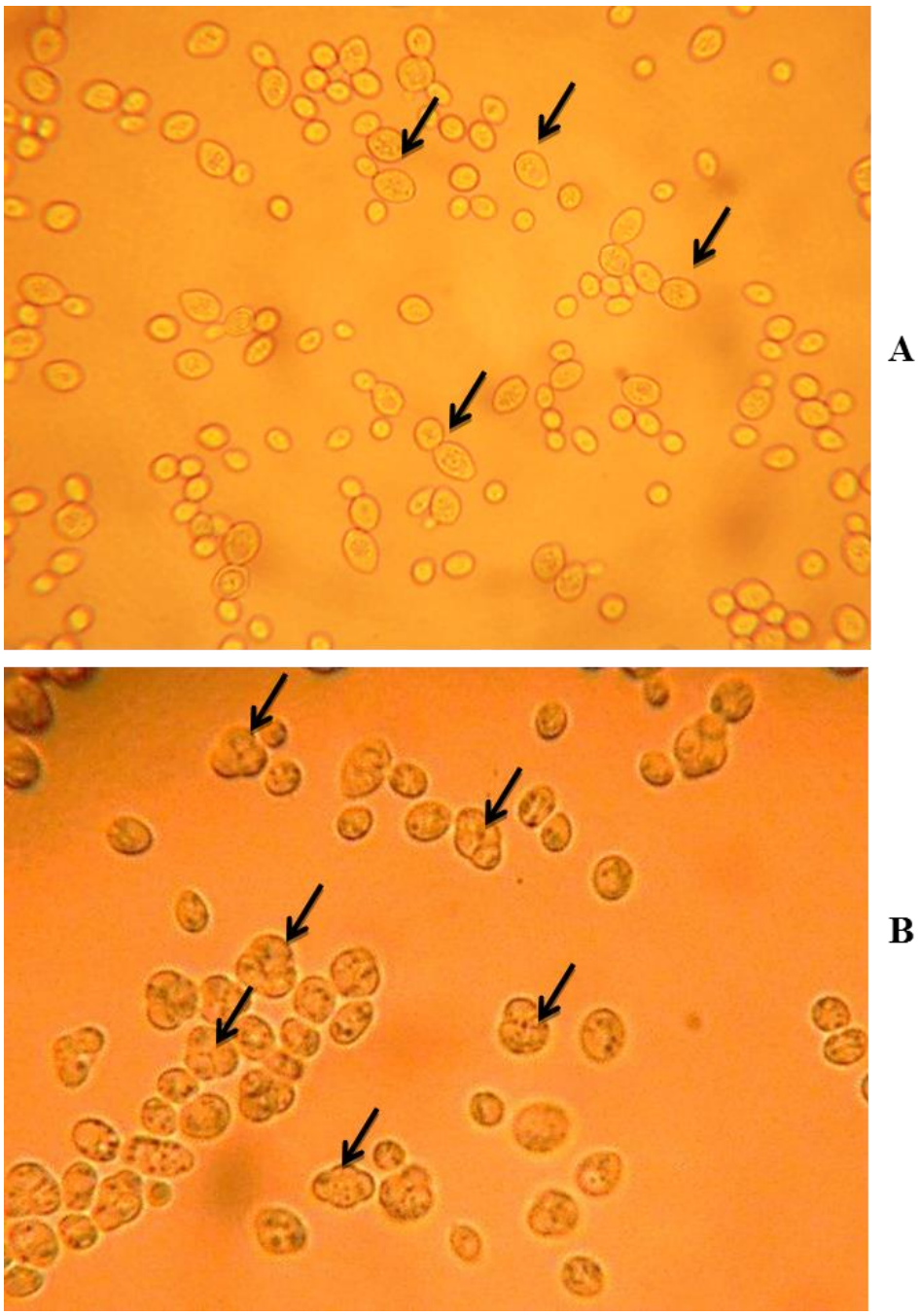

Figure 3.69. Sporulation of diploid culture (NS-C2, 3345 x 2685).

(**A**) Saturated cultures with G1-arrested ovoid cells, sporulation in 1% potassium acetate buffer.

(**B**) Tetrads with four spores as examined with a phase contrast microscope.

Diploid cultures were grown to saturation at 28°C in YEPD broth (approximately two days). Saturated cultures were sporulated in 1% potassium acetate buffer. Tetrads with four cells were examined with a phase contrast microscope. Sporulated cells (asci) were treated with glusulase enzyme to digest sac surrounding tetrads at 30°C for 8 to 10 minutes. Micromanipulation was carried out to separate spores (ascospores) from digested tetrads for genotype analysis by using a dissecting microscope with a micromanipulator attached (Singers). The pictures were taken with Zeis KF microscope at a magnification of 400x fitted with a Nikon Coolpix 4500 camera (4 megapixels 4x optical zoom).

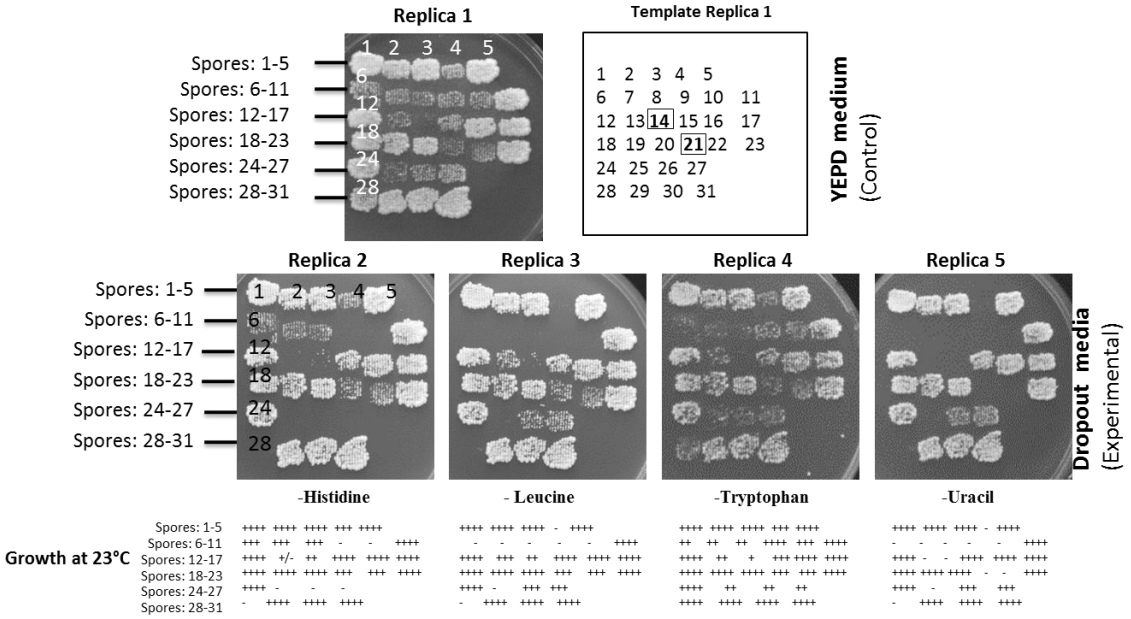

Genotype assessment on the basis of growth on dropout media

Marker combination		Growth patterns on dropout media				Spore number ID
		-Histidine	-Leucine	-Tryptophan	-Uracil	
1.	HLTU	+/++++	+/++++	+/++++	+/++++	1, 2, 3, 5, 11, 12, 15, 16, 17, 18, 19, 20, 23, 24, 29, 30, 31
2.	HT	+/++++	-	+/++++	-	4, 6, 7, 8
3.	T	-	-	+/++++	-	9, 10, 25, 28
4.	LT	-	+/++++	+/++++	-	13
5.	LTU	-	+/++++	+/++++	+/++++	26, 27
6.	**HLT**	+/++++	+/++++	+/++++	-	**14, 21**, 22

Figure 3.70. Replica plating on YEPD and dropout media for random spore genetic analysis revealed six groups of genetic combinations.

In total, 82 tetrads were dissected from sporulated cultures. The cells separated by micromanipulation, showed low viability (31 cells germinated out of 328 showing ~9% viability). Viable spores were replica plated on dropout media for marker analysis. Genotypes were assessed on the basis of marker combination. These combinations (1-6) were further analysed for haploid or diploid cell status on sporulating medium: 0.3-0.5% anhydrous sodium acetate with 1.5 % agar (Fowell, 1952).

Table 3.6. Assessment of genetic combinations on the basis of auxotrophic markers.

	Marker combination	Genotype assessed	Spores	Frequency (%)
1.	HLTU	cdc13::HIS and/or stn1::HIS exo1::LEU2 rad24::TRP yku70::URA3	17	55
2.	HT	cdc13::HIS &/ stn1::HIS rad24::TRP	4	13
3.	T	rad24::TRP	4	13
4.	LT	exo1::LEU2 rad24::TRP	1	3
5.	LTU	exo1::LEU2 rad24::TRP yku70::URA3	2	6
6.	HLT	cdc13::HIS and/ stn1::HIS exo1::LEU2 rad24::TRP	3	~10

The first group incorporated the gene combination (cdc13::HIS and/ stn1::HIS exo1::LEU2 rad24::TRP yku70::URA3) and contained the maximum number of spores (17 out of 31). The other groups include one to four spores, representing less frequent gene combinations. All groups were further investigated for haploid or diploid cell status on sporulating media. Microscopic examination revealed the nature of all cells in first group diploid rather than haploid by the formation of tetrads typical of diploids on sporulating medium.

All spores from group 2 and group 6 were analysed for the presence or absence of *CDC13* and *STN1* genes. The haploids cells were purified by sub-culturing on dropout medium. The freshly grown cells were analysed by two parallel PCR to detect *CDC13* (N-terminus) and *STN1* (full gene). Two haploids ($H^+L^+T^+$) #14 and #21 confirmed the presence of wild type *CDC13* with the deletion of the *STN1* gene. These haploids with resulting genotype *CDC13* stn1::HIS exo1::LEU2 rad24::TRP1 were examined for their chronological life span and growth sensitivity to different genotoxic agents.

However no required combination of *yku70* with $H^+L^+U^+$ (stn1::HIS exo1::LEU2 yku70::URA3) was obtained in these crosses. Further crosses are required to achieve the full complement of required gene combinations by increasing the viability of isolated spores.
A number of crosses were carried out to obtain the required combinations of genes (*CDC13* stn1::HIS exo1::LEU2) in the absence of *rad24*, and quite a few tetrads were dissected to analyse the resulting haploids (~100 tetrads with ~400 spores). The viable hybrids were obtained by selection on minimal medium. However, the putative hybrids could not be achieved (either not propagated or occur with very low frequency).

In addition haploid cells from strain 1296 (mating type a) harbouring *cdc13-1* N-truncated mutation were also crossed to cells from strain 1297 (mating type α) containing *cdc13-1* C-truncated mutation. The resulting diploids were analysed for marker analysis and also for *CDC13* by detecting N- and C-terminals through PCR. Diploids grown for sporulation (three times), however, failed to sporulate or to form tetrads. These diploids were further studied for their sensitivity to genotoxic agents.

3.6.2. Conclusions:

The study reveals:

- potential of the PCR based approach to generate DNA cassette and to detect its integration diagnostically in chromosomal DNA directly from cells;
- the ease of utilisation of PCR-based approach and genetic transformation to generate *CDC13* full gene deletion mutants using *cdc13-1 exo1Δ* mutants of yeast *S. cerevisia*e;
- disruption of *CDC13* N-terminus by PCR generated PGAL1-TRP1 deletion module and its confirmation by diagnostic PCR in *cdc13-1 exo1Δ* mutants;
- *CDC13* C-terminus truncation by ADH1-HIS3MX6 deletion cassette (amplified fragment with target oriented flanking regions) and confirmation of its integration into chromosomal DNA of *cdc13-1 exo1Δ* mutants by performing diagnostic PCR;
- usability of traditional genetic crosses in obtaining new combination of deletions from the existing mutations/deletions through tetrad analysis using micromanipulation e.g., generation of *STN1* deletion mutants ($H^+L^+T^+$, *stn1Δ exo1Δ rad24Δ* with *CDC13*, #14 and #21 haploid in this study)

Chapter 4

Sequencing and Telomere length studies

4.1. Introduction

Essential capping proteins, Cdc13 and Stn1 help to maintain genomic integrity by capping chromosome at ends in budding yeast. It makes them indispensable components of telomeres. In the absence of Cdc13, uncapped telomeres accumulate excessive single-stranded DNA, arrest cell division and die (Garvik *et al*., 1995). However, capping proteins Cdc13 and Stn1 are dispensable in the absence of exonuclease activities on uncapped telomeres in *exo1Δ* mutants (Zubko and Lydall, 2006) indicating existence of alternative mechanism of telomere capping.

In yeast, telomeric DNA consists of multiple repeats of nucleotide sequence $(TG_{1\text{-}3})n$, which varies in length in different chromosomes and strains with an average length of about 300-350 bp (Louis, 1995, Teng and Zakian, 1999). There are two other sub-telomeric structure or repeat elements, Y' and X (Louis and Haber, 1990). Adjacent to the telomere, the Y' elements are present in single or in repeats of two to four copies while X elements vary from 300 bp to 3 kb in length and are present in almost all telomeres. In yeast, the length of the telomere is maintained by the telomerase enzyme, and in its absence, or in telomerase-defective cells, the telomeres are maintained by a Rad52-dependent recombination and Pol32-dependent break-induced replication mechanisms (Lydeard *et al*., 2007, Lundblad and Blackburn, 1993). Two examples of such cells are human senescent cells lacking active telomerase, and telomerase independent survivor cells in budding yeast. Both could maintain telomeres by homologous recombination by amplifying telomeric and sub-telomeric structures (Teng and Zakian, 1999).

The telomeric patterns are characterised on the basis of copy number, location and restriction site differences of Y' elements (Louis and Haber, 1990). In yeast, telomeric repeat lengths are determined by digesting genomic DNA with *Xho*1, which generates ~1.3 kb conserved terminal restriction fragments (TRFs) detectable by Southern blot hybridisation (Parenteau and Wellinger, 1999). In budding yeast, two types of telomeric DNA patterns have been found in cells that survive under condition of telomere dysfunctions (survivors). For example telomerase deficient *tlcΔ* cells (Teng and Zakian, 1999), telomerase deficient human somatic cells or fast rate growing colonies in *sgs1Δ exo1Δ rad9Δ cdc13Δ* yeast cells. These cells shows growth crisis, shortened telomere and post senescence survivors' accumulation, and maintain their telomere using recombination dependent mechanism (Ngo and Lydall, 2010).

In type I survivors (the more common of the two), subtelomeric Y' elements are amplified followed by very short tracts of terminal TG DNA at the end of chromosomes. In type II survivors, terminal $TG_{1\text{-}3}$ telomeric repeats are amplified and are shown as very long and heterogeneous in length with 12 kb or more of TG repeats at the ends of chromosomes (Teng and Zakian, 1999, Signon *et al*., 2001, Chen *et al*., 2001). Type I telomeric patterns can be converted to type II that can return to wild type length upon the reintroduction of telomerase. The yeast type II survivors resemble human ALT cells as both contain long, heterogenous

telomeric repeats (Bryan *et al*., 1997, Teng and Zakian, 1999). Both type II and human ALT cells amplify their telomeric DNA through recombination dependent DNA replication that might involve extrachromosomal circular DNA containing telomeric repeat elements (Henson *et al*., 2009, McEachern and Haber, 2006). In yeast, the type II telomeric DNA mimics immortal or cancerous cells of humans that also maintain telomeric DNA in the absence of telomerase. The Exo1 exonuclease is considered to be an initiator of the recombination process in type I and type II survivors and generates the substrate for the recombination process in the absence of telomerase (Maringele and Lydall, 2004). In yeast, the Southern blot hybridisation pattern with restriction endonuclease-digested genomic DNA is used to determine telomeric DNA patterns, either of type I or Type II, on the basis of fragment sizes. In this study to characterise telomeric DNA in different deletion mutants, genomic DNA was extracted, digested with *Xho*I restriction enzyme (recognition site within the Y' fragment) and was subjected to Southern blot analysis with the Y'+TG probe to examine telomere and Y' lengths.

4.2. Aims and objectives

This part of the study is devoted to determine the sequence of deletion constructs, analysing the telomere length and telomeric DNA patterns in mutants lacking Cdc13 and Stn1 proteins and also in N- and C-terminus truncated variants of Cdc13 mutants using Southern blot hybridisation. This aim involves the following objectives:

- To sequence the integrated N- and C-terminus deletion constructs.
- To study the telomere length patterns in the *CDC13* and *STN1* deletion mutants in the presence of *EXO1* deletion by using Southern blot hybridisation.
- To compare the length of telomeres and their DNA patterns in N- and C-terminus truncated Cdc13 conditional mutants.
- To investigate the effects of temperature on the telomere lengths and telomeric DNA patterns in N- and C-terminus truncated mutants.

4.3. Results

Yeast strains used in this study are listed in Table 4.1. The *STN1* deletion mutants in the presence of *EXO1* and *RAD24* deletions were generated by crosses followed by tetrad analysis using micromanipulation. The *cdc13-1* N- and C-terminus truncated mutants were generated by knock-out PCR techniques using survivor strains 1296-TR and 1297-TR. The truncated mutants of *cdc13-1* were sequenced to determine their DNA.

Table 4.1. Yeast strains and mutants used in telomere length experiments.

	Specification	**DLY strains**	**Essential genotype**
1.	WT	640	MATa ade2-1 trp1-1 can1-100 leu2-3,112 his3-11,15 ura3 GAL+ psi+ ssd1-d2 RAD5
2.	WT	641	MATa ade2-1 trp1-1 can1-100 leu2-3,112 his3-11,15 ura3 GAL+ psi+ ssd1-d2 RAD5
3.	*cdc13-1* survivor at 36°C	1296-TR	MATa *exo1*::LEU2 *cdc13-1*
4.	*cdc13-1* N-terminus deletion mutants in strain 1296-TR: #2, **#4, #5**, #6, #7, #21	1296 NTΔ (TRP1)	*cdc13-1* NTΔ::TRP1 *exo1*::LEU2
5.	*cdc13-1* C-terminus deletion mutants in strain 1296-TR: #3, #4, #6, #7**,#9, #10**	1296 CTΔ (HIS3)	*cdc13-1* CTΔ::HIS3MX6 *exo1*::LEU2
6.	*cdc13-1* survivor at 36°C	1297-TR	MATa *exo1*::LEU2 *cdc13-1*
7.	*cdc13-1* N-terminus deletion mutants in strain 1297-TR: #1, **#7, #8**, #11, #14, #22	1297 NTΔ (TRP1)	*cdc13-1* NTΔ::TRP1 *exo1*::LEU2
8.	*cdc13-1* C-terminus deletion mutants in strain 1297-TR: #3, #4,#7, #8, #**11, #12**	1297 CTΔ (HIS3)	*cdc13-1* CTΔ:: HIS3MX6 *exo1*::LEU2
9.	*EXO1* deletion mutant	1272	MATalpha *exo1*::LEU2 RAD5
10.	*EXO1* deletion mutant	1273	MATalpha *exo1*::LEU2 RAD5
11.	*STN1* deletion mutant	#14 (haploid)	*CDC13 stn1*::HIS *exo1*::LEU2 *rad24*::TRP1
12.	*STN1* deletion mutant	#21 (haploid)	*CDC13 stn1*::HIS *exo1*::LEU2 *rad24*::TRP1
13.	*CDC13* deletion mutant	2607	MAT? (initially alpha) *cdc13*::HIS *exo1*::LEU2
14.	*CDC13* deletion mutant	2608	MAT? (initially alpha) *cdc13*::HIS *exo1*::LEU2 ade2-1 trp1-1 can1-100 leu2-3,112 his3-11,15 ura3 GAL+ psi+ ssd1-d2 RAD5
15.	*CDC13 STN1 RAD24 EXO1* deletion mutant	2684	MATalpha *cdc13*::HIS *stn1*::HIS *exo1*::LEU2 rad24::TRP ade2-1 trp1-1 can1-100 leu2-3,112 his3-11, 15 ura3 GAL+ psi+ ssd1-d2 RAD5?
16.	*CDC13 STN1*, *RAD24 EXO1* deletion mutant	2685	MATalpha *cdc13*::HIS *stn1*::HIS *exo1*::LEU2 *rad24*::TRP

(N- and C-truncated mutants shown in **bold** were used in CLS studies)

4.3.1. DNA sequencing of *CDC13* N- and C-terminus deletion constructs

cdc13-1 N- and C-truncated mutants generated using survivor strains 1296-TR and 1297-TR were selected by their phenotypic auxotrophies and were confirmed by PCR for *cdc13-1* N- and C-termini modification and linked markers (as has been described Chapter 3). In order to determine the correct DNA sequence of the constructs for functional studies, six N- and C-truncated *cdc13-1* constructs each for strains 1296 and 1297 were sequenced (twenty four clones in total with twelve each for N- and C-terminus deletion).

The rapid and elaborate PCR technique was utilised to prepare sequencing templates from genomic DNA of different constructs using the high fidelity Q5 DNA polymerase enzyme (NEB). To overcome the greater error rate of *in vitro* misincorporation of bases, this polymerase enzyme has an associated $3' \rightarrow 5'$ exonuclease that confers a proofreading function by removing errors.

As only the coding region of *cdc13-1* gene was modified, two primers flanking the *CDC13* were designed from upstream and downstream of the gene to amplify an approximately 3 kb fragment that contains *cdc13-1* sequence (in the case of parental strains 1296- and 1297-TR) or the integrated marker linked with the N- and C-truncated part of *cdc13-1* in the case of constructs. The 3 kb amplified fragments were subjected to sequencing to determine any mutations.

The part is related to sequence N- and C-terminal truncated constructs to confirm the nucleotide sequence of truncated Cdc13 (N- or C-terminus) and related markers (TRP1 or HIS3) and to analyse the coding sequence of the construct for any amino acid changes.

4.3.1.1. Primers design for sequencing *cdc13-1* and gene disrupting modular DNA

Three sets of primers were used to sequence ~3 kb region of *cdc13-1*-NTΔ::TRP1, *cdc13-1*-CTΔ::*HIS3MX6* constructs and *cdc13-1* full gene, from mutants strain 1296-TR and 1297-TR. The details of the sequencing primers are shown in Table 4.2.

Table 4.2. Sequencing primers used for *cdc13-1*, N- and C-terminus deletion mutants.

Primer name	Construct sequenced	Primer length (nt)	Primer sequence	Location of primer
F1 (for)*	CTΔ and NTΔ	22	5' ACATGCAGCCTTGATTAACGTG 3'	*CDC13* upstream region
F2 (for)	CTΔ	20	5' CAACTCGCAGCTTATGACGC 3'	*CDC13* N-terminus
F3 (F3-HIS3) (for)	CTΔ	20	5' TGAGGCGCGCCACTTCTAAA 3'	HIS3MX6 modular plasmid (at the start of ADH1 terminator)
R1 (R2-TRP1) (rev)*	NTΔ	20	5 'CATTTTGAGATCCGGGTTTT 3'	TRP1-PGAL1 modular plasmid (at the end of GAL1 promoter)
R2 (rev)	NTΔ	22	5' TTCTGCGAGAGCTGGTGTAGTG 3'	*CDC13* C-terminus
R3 (rev)	CTΔ and NTΔ	22	5' GCATCAAGAAGGAAGGAAGACC 3'	*CDC13* downstream region
N1 (for)	*cdc13-1*	20	5' ATTGGCACGATGATGATTCC 3'	Forward primer from *CDC13* N-terminus half
N2 (rev)	*cdc13-1*	20	5' TTCGATCAGGCTTTTCCAGT 3'	Reverse primer from *CDC13* N-terminus half

*Forward (for) and reverse (rev) primers

4.3.1.1.1. Primers to sequence *cdc13-1* amplicons

The four primers F1, N1, N2 and R3 were selected to sequence *cdc13-1* DNA from strain 1296-TR and 1297-TR. Figure 4.1 shows the relevant position of each primer within the coding sequence and 200 nt upstream and downstream of the *cdc13-1*. F1 and N1 are forward primers whereas N2 and R3 are reverse primers.

***cdc13-1* ORF sequence including the upstream and downstream non-coding region**

F1 →
SQ Sequence 3175 BP;
TGTGGATTAT TTAATATGTA CATGCAGCCT TGATTAACGT GATTATACTT TTTAAACCTT 60
TGATATCCAA ATTTTTCAAC GTCATAAGAG ACGCGAAGGC CTAGTGAGAT GCGAAATGCT 120
AATTCAAAAT GGAAATTTAA GAATATATTC ATATATGTTT CTCTTTGGAT ACGAATGACC 180
GTGGAAACTA TCGCCTAAAA ATGGATACCT TAGAAGAGCC TGAGTGTCCT CCACATAAAA 240
ATCGTATTTT TGTGAGCTCG AGTAAAGATT TTGAAGGCTA TCCCAGCAAA GCAATAGTTC 300
CCGTGCAATT CGTGGCGCTT TTAACCTCAA TACACCTGAC TGAAACAAAA TGTTTGCTAG 360
GCTTTTCTAA TTTTGAGAGG CGAGGAGATC AATCCCAAGA AGATCAATAT TTAATCAAAC 420
TGAAGTTCAA AGATAGGGGC TCGGAGAGGT TAGCCCGGAT CACTATTTCC TTACTTTGCC 480
AATACTTTGA TATTGAACTG CCAGATTTAG ATTCTGACTC AGGCGCATCC CCAACAGTAA 540
TACTGAGAGA TATTCACCTT GAAAGGTTAT GTTTTTCAAG TTGTAAAGCT TTATATGTAT 600
CAAAACACGG GAACTATACT CTATTCTTAG AGGACATAAA ACCGTTGGAT TTGGTAAGTG 660
TGATAAGCAC CATATCTACA AAATCGACAA ATAGCAGCAA GCATTCGTCA TCAGAACTTA 720
TTTCAGAATG TGATTTGAAC AACTCACTTG TGGATATCTT CAACAATTTA ATAGAAATGA 780
ATAGAGACGA GAAAAACAGG TTTAAATTTG TAAAGTTGAT TCACTACGAT ATAGAACTAA 840
AAAAGTTCGT TCAAGACCAA CAAAAGGTAT TATCGCAGAA ATCAAAAGCC GCAGCAATTA 900
ATCCTTTCTT TGTGCCAAAT AGACTAGGGA TACCTTACAT TGAATCCCAA AACGAATTCA 960
ACTCGCAGCT TATGACGCTT AATGTAGATG AACCGACCAC AGATATAAGC AACATGGGAG 1020
AGGAAATGCA TGACAGCGCA GATCCCATTG AGGATTCAGA TTCCTCAACT ACCTCCTCTA 1080
N1 →
CCGGGAAATA TTTCAGCTCA AAATCCTACA TCCAGTCACA GACACCTGAA AGGAAAACAA 1140
GCGTACCAAA TAATTGGCAC GATGATGATT CCGGAAGCAA GAGGAAGAGA AAGCTTTCTT 1200
TCCACAGTCC GAACGCGTCC TCAATCCGCA AAGCCATCAG TTATGAGCAA CTTTCCCTAG 1260
CTAGTGTAGG CTCAGTTGAA AGGTTAGAGG GCAAAATTGT TGGCATGAAT TCACCTCAAT 1320
TCGCCAGTAT AAATGAGTTC AAATATTGCA CATTGAAATT ATATTTTACG CAGCTCTTAC 1380
CAAATGTCCC AGACAAGGTC CTGGTGCCAG GCGTCAATTG CATTGAGATC GTTATCCCGA 1440
N2 ←
CGAGAGAGCG AATCTGTGAG CTCTTCGGTG TTTTAAACTG TCAAAGCGAC AAGATATCGG 1500
ATATTTTACT ACTGGAAAAG CCTGATCGAA TTTCCGTCGA AGTTGAAAGG ATCCTGTGGG 1560
ACAATGACAA GACCGCCAGC CCAGGTATGG CAGTATGGAG TTTGAAGAAC ATTAGCACCG 1620
ACACGCAGGC GCAGGCGCAG GTGCAGGTGC CTGCGCAATC GTCGGCGTCA ATCGATCCGT 1680
CTCGCACAAG GATGAGCAAA ATGGCAAGGA AAGACCCCAC CATCGAATTC TGTCAGTTGG 1740
GACTCGACAC TTTTGAGACC AAATACATAA CAATGTTTGG CATGCTAGTC TCCTGCTCGT 1800
TTGATAAACC TGCCTTTATA TCTTTTGTCT TTAGCGATTT TACCAAGAAC GATATCGTCC 1860
AAAACTATCT TTACGACAGA TATCTAATAG ATTACGAGAA CAAGTTAGAG CTGAACGAGG 1920
GCTTCAAAGC CATCATGTAC AAAAACCAAT TCGAAACGTT TGACTCTAAG CTCAGAAAAA 1980
TATTCAACAA CGGGCTAAGA GATCTACAGA ACGGCCGCGA TGAAAACCTT TCGCAATACG 2040
GCATAGTTTG TAAGATGAAT ATAAAAGTGA AAATGTACAA CGGCAAATTG AATGCCATTG 2100
TGCGCGAATG TGAGCCGGTC CCGCATTCCC AAATAAGCAG CATCGCCTCG CCTTCACAGT 2160
GCGAACATTT AAGATTGTTC TACCAACGAG CGTTCAAGAG AATTGGCGAA TCCGCAATTT 2220
CACGCTATTT CGAAGAGTAC CGGAGGTTTT TCCCCATACA TAGAAACGGT TCTCATCTCG 2280
CGAAACTGAG GTTCGATGAA GTAAAGCATG AACCAAAAAA ATCACCCACT ACACCAGCTC 2340
TCGCAGAACA CATACCCGAC CTGAATGCAG ACGTGTCCTC CTTCGATGTA AAGTTCACAG 2400
ATATATCTTC TCTCTTGGAC TCCTCGGCTC GCCTCCCGCG CCCACAGCAA ACACACAAGA 2460
GCAACACATT ATACAGTTGC GAGGGCCGTA TCATCGCCAT CGAGTACCAC GCATCTGATC 2520
TCTGCTTCCA TATCACGAAT GAGCTCCCAC TTTTACAAAC CCGCGGCTTG GCCCCGGAGC 2580
GAGTGTTGCA ACTACACATC ATTACCTCCA AGAACTTTGC TTATTTTTTC AACCGCTCAA 2640
GCGCCTACTT ACAGCGTCAG CCTCTTGAGG AAAAATATAC GCAATTGGCA CAATTTCTCG 2700
GCCATTCATT TAAATTCAAT ATAACCTCCT CGCTCACGCT GTTCCCTGAC ACTACCGTGG 2760
CACTCCAGAT CTGGTGCCCA ATTGAATGCA CCTTTCGGGA ATTGCAACAA CAGCTGGCCC 2820
ATCCGAAGGT TGCAGCGGCT CCTGATTCAG GGAGTCTTGA TTGCGCAATT AATGCTACCG 2880
TCAATCCTCT GCGACTTCTT GCCGCGCAAA ATGGCGTCAC CGTGAAAAAG GAGGAGGATA 2940
ATGACGATGA CGCCGGAGCC GTTCCCACCT CGTAAGACAT GATCCGCGCA GCCCAACGCG 3000
GCGGTGCCAA ATTGCAGTGA CGTCTCGGAG TAATATAAAA AAAAAAGACC AAATAACCAA 3060
R3 ←
ATTTAAGGGT GCTCTGAATA TAAGGGAGTG GAACGTTTTC ACACGAAGGA AAAGGGAAAG 3120
AGGGGAGTGG TAAGAAGCAA GAGTCAATGA AAGGTCTTCC TTCCTTCTTG ATGCT 3175
//

*Eco*R1 site in *cdc13-1*

Figure 4.1. Selection of primers to sequence 3 kb PCR fragment containing *cdc13-1* ORF (a reference sequence).

CDC13 ORF (1-2775) with upstream and downstream sequences with each being 200 nucleotides in length, accessed from *Saccharomyces* Genome Database (SGD) (http://www.yeastgenome.org/) and primers used to sequence ~3 kb (3175-20=3155) PCR fragment from *cdc13-1* mutants (control sequence from strains 1296-TR and 1297-TR). The ATG and TAA represent the start and stop codons of *cdc13-1* replication. The primers (highlighted sequence) include F1 (22) 5'ACATGCAGCCTTGATTAACGTG 3', N1 (20) 5'ATTGGCACGATGATGATTCC 3', N2 (20) 5'TTCGATCAGGCTTTTCCAGT 3' (reverse complement of ACTGGAAAAGCCTGATCGAA) and R3 (22) 5' GCATCAAGAAGGAAGGAAGACC 3' (reverse complement of GGTCTTCCTTCCTTCTTGATGC).

4.3.1.1.2. Primers to sequence the NTΔ amplicon

Similarly, the primers F1, R1, R2 and R3 were used to sequence the *cdc13-1*-N-truncated construct (NTΔ amplicon, 3 kb). Figure 4.2 shows the relevant position of each primer within 200 nt upstream and downstream of the *cdc13-1*-NTΔ::GAL1-TRP1 region (grey colour sequences). F1 is a forward primer whereas R1, R2 and R3 are reverse primers.


```
TGTGGATTAT TTAATATGTA CATGCAGCCT TGATTAACGT GATTATACTT TTTAAACCTT      60
TGATATCCAA ATTTTTCAAC GTCATAAGAG ACGCGAAGGC CTAGTGAGAT GCGAAATGCT     120
AATTCAAAAT GGAAATTTAA GAATATATTC ATATATGTTT CTCTTTGGAT ACGAATGACC     180
GTGGAAACTA TCGCCTAAAA GAATTCGAGC TCGTTTAAAC CTCCTTACGC ATCTGTGCGG     240
TATTTCACAC CGCAGGCAAG TGCACAAACA ATACTTAAAT AAATACTACT CAGTAATAAC     300
CTATTTCTTA GCATTTTTGA CGAAATTTGC TATTTTGTTA GAGTCTTTTA CACCATTTGT     360
CTCCACACCT CCGCTTACAT CAACACCAAT AACGCCATTT AATCTAAGCG CATCACCAAC     420
ATTTTCTGGC GTCAGTCCAC CAGCTAACAT AAAATGTAAG CTTTCGGGGC TCTCTTGCCT     480
TCCAACCCAG TCAGAAATCG AGTTCCAATC CAAAAGTTCA CCTGTCCCAC CTGCTTCTGA     540
ATCAAACAAG GGAATAAACG AATGAGGTTT CTGTGAAGCT GCACTGAGTA GTATGTTGCA     600
GTCTTTTGGA AATACGAGTC TTTTAATAAC TGGCAAACCG AGGAACTCTT GGTATTCTTG     660
CCACGACTCA TCTCCATGCA GTTGGACGAT ATCAATGCCG TAATCATTGA CCAGAGCCAA     720
AACATCCTCC TTAGGTTGAT TACGAAACAC GCCAACCAAG TATTTCGGAG TGCCTGAACT     780
ATTTTTATAT GCTTTTACAA GACTTGAAAT TTTCCTTGCA ATAACCGGGT CAATTGTTCT     840
CTTTCTATTG GGCACACATA TAATACCCAG CAAGTCAGCA TCGGAATCTA GAGCACATTC     900
TGCGGCCTCT GTGCTCTGCA AGCCGCAAAC TTTCACCAAT GGACCAGAAC TACCTGTGAA     960
ATTAATAACA GACATACTCC AAGCTGCCTT TGTGTGCTTA ATCACGTATA CTCACGTGCT    1020
CAATAGTCAC CAATGCCCTC CCTCTTGGCC CTCTCCTTTT CTTTTTTCGA CCGAATTAAT    1080
TCTTAATCGG CAAAAAAAGA AAAGCTCCGG ATCAAGATTG TACAGATCTG TAAAGAGCCC    1140
CATTATCTTA GCCTAAAAAA ACCTTCTCTT TGGAACTTTC AGTAATACGC TTAACTGCTC    1200
ATTGCTATAT TGAAGTACGG ATTAGAAGCC GCCGAGCGGG TGACAGCCCT CCGAAGGAAG    1260
ACTCTCCTCC GTGCGTCCTC GTCTTCACCG GTCGCGTTCC TGAAACGCAG ATGTGCCTCG    1320
CGCCGCACTG CTCCGAACAA TAAAGATTCT ACAATACTAG CTTTTATGGT TATGAAGAGG    1380
AAAAATTGGC AGTAACCTGG CCCCACAAAC CTTCAAATGA ACGAATCAAA TTAACAACCA    1440
TAGGATGATA ATGCGATTAG TTTTTTAGCC TTATTTCTGG GGTAATTAAT CAGCGAAGCG    1500
ATGATTTTTG ATCTATTAAC AGATATATAA ATGCAAAAAC TGCATAACCA CTTTAACTAA    1560
TACTTTCAAC ATTTTCGGTT TGTATTACTT CTTATTCAAA TGTAATAAAA GTATCAACAA    1620
AAAATTGTTA ATATACCTCT ATACTTTAAC GTCAAGGAGA AAAAACCCGG ATCTCAAAAT    1680
GGCAGTATGG AGTTTGAAGA ACATTAGCAC CGACACGCAG GCGCAGGCGC AGGTGCAGGT    1740
GCCTGCGCAA TCGTCGGCGT CAATCGATCC GTCTCGCACA AGGATGAGCA AAATGGCAAG    1800
GAAAGACCCC ACCATCGAAT TCTGTCAGTT GGGACTCGAC ACTTTTGAGA CCAAATACAT    1860
AACAATGTTT GGCATGCTAG TCTCCTGCTC GTTTGATAAA CCTGCCTTTA TATCTTTTGT    1920
CTTTAGCGAT TTTACCAAGA ACGATATCGT CCAAAACTAT CTTTACGACA GATATCTAAT    1980
AGATTACGAG AACAAGTTAG AGCTGAACGA GGGCTTCAAA GCCATCATGT ACAAAAACCA    2040
ATTCGAAACG TTTGACTCTA AGCTCAGAAA AATATTCAAC AACGGGCTAA GAGATCTACA    2100
GAACGGCCGC GATGAAAACC TTTCGCAATA CGGCATAGTT TGTAAGATGA ATATAAAAGT    2160
GAAAATGTAC AACGGCAAAT TGAATGCCAT TGTGCGCGAA TGTGAGCCGG TCCCGCATTC    2220
CCAAATAAGC AGCATCGCCT CGCCTTCACA GTGCGAACAT TTAAGATTGT TCTACCAACG    2280
AGCGTTCAAG AGAATTGGCG AATCCGCAAT TTCACGCTAT TTCGAAGAGT ACCGGAGGTT    2340
TTTCCCCATA CATAGAAACG GTTCTCATCT CGCGAAACTG AGGTTCGATG AAGTAAAGCA    2400
TGAACCAAAA AAATCACCCA CTACACCAGC TCTCGCAGAA CACATACCCG ACCTGAATGC    2460
AGACGTGTCC TCCTTCGATG TAAAGTTCAC AGATATATCT TCTCTCTTGG ACTCCTCGGC    2520
TCGCCTCCCG CGCCCACAGC AAACACACAA GAGCAACACA TTATACAGTT GCGAGGGCCG    2580
TATCATCGCC ATCGAGTACC ACGCATCTGA TCTCTGCTTC CATATCACGA ATGAGCTCCC    2640
ACTTTTACAA ACCCGCGGCT TGGCCCCGGA GCGAGTGTTG CAACTACACA TCATTACCTC    2700
CAAGAACTTT GCTTATTTTT TCAACCGCTC AAGCGCCTAC TTACAGCGTC AGCCTCTTGA    2760
GGAAAAATAT ACGCAATTGG CACAATTTCT CGGCCATTCA TTTAAATTCA ATATAACCTC    2820
CTCGCTCACG CTGTTCCCTG ACACTACCGT GGCACTCCAG ATCTGGTGCC CAATTGAATG    2880
CACCTTTCGG GAATTGCAAC AACAGCTGGC CCATCCGAAG GTTGCAGCGG CTCCTGATTC    2940
AGGGAGTCTT GATTGCGCAA TTAATGCTAC CGTCAATCCT CTGCGACTTC TTGCCGCGCA    3000
AAATGGCGTC ACCGTGAAAA AGGAGGAGGA TAATGACGAT GACGCCGGAG CCGTTCCCAC    3060
CTCGTAAGAC ATGATCCGCG CAGCCCAACG CGGCGGTGCC AAATTGCAGT GACGTCTCGG    3120
AGTAATATAA AAAAAAAAGA CCAAATAACC AAATTTAAGG GTGCTCTGAA TATAAGGGAG    3180
TGGAACGTTT TCACACGAAG GAAAAGGGAA AGAGGGGAGT GGTAAGAAGC AAGAGTCAAT    3240
GAAAGGTCTT CCTTCCTTCT TGATGCT                                        3267
```

Figure 4.2. Selection of primers used to sequence the *cdc13-1*-N-truncated construct (NTΔ amplicon~3267 bp).

The sequence shows the position of the primers used for sequencing. The highlighted codons 'ATG' and 'TAA' represent start and stop codons for the *cdc13-1* C-terminus half replication after N-truncation. The primers include F1 (22) 5' ACATGCAGCCTTGATTAACGTG 3', R1 (20) 5'CATTTTGAGATCCGGGTTTT 3' (reverse complement of AAAACCCGGATCTCAAAATG), R2 (22) 5'TTCTGCGAGAGCTGGTGTAGTG 3' (reverse complement of CACTACACCAGCTCTCGCAGAA) and R3 (22) 5' GCATCAAGAAGGAAGGAAGACC 3' (reverse complement of GGTCTTCCTTCCTTCTTGATGC).

4.3.1.1.3. Primers to sequence the CTΔ amplicon

Finally, the primers F1, F2, F3 and R3 were used to sequence the *cdc13-1*-C truncated construct (CTΔ amplicon). Figure 4.3 shows the relevant position of each primer within 200 nt upstream and downstream of the *cdc13-1*-CTΔ::ADH1-HIS3MX6 construct region. The F1, F2 and F3 are forward primers whereas R3 is reverse primer.

SQ Sequence 3365 BP;

F1 →
TGTGGATTAT TTAATATGTA CATGCAGCCT TGATTAACGT GATTATACTT TTTAAACCTT 60
TGATATCCAA ATTTTTCAAC GTCATAAGAG ACGCGAAGGC CTAGTGAGAT GCGAAATGCT 120
AATTCAAAAT GGAAATTTAA GAATATATTC ATATATGTTT CTCTTTGGAT ACGAATGACC 180
GTGGAAACTA TCGCCTAAAA **ATG**GATACCT TAGAAGAGCC TGAGTGTCCT CCACATAAAA 240
ATCGTATTTT TGTGAGCTCG AGTAAAGATT TTGAAGGCTA TCCCAGCAAA GCAATAGTTC 300
CCGTGCAATT CGTGGCGCTT TTAACCTCAA TACACCTGAC TGAAACAAAA TGTTTGCTAG 360
GCTTTTCTAA TTTTGAGAGG CGAGGAGATC AATCCCAAGA AGATCAATAT TTAATCAAAC 420
TGAAGTTCAA AGATAGGGGC TCGGAGAGGT TAGCCCGGAT CACTATTTCC TTACTTTGCC 480
AATACTTTGA TATTGAACTG CCAGATTTAG ATTCTGACTC AGGCGCATCC CCAACAGTAA 540
TACTGAGAGA TATTCACCTT GAAAGGTTAT GTTTTTCAAG TTGTAAAGCT TTATATGTAT 600
CAAAACACGG GAACTATACT CTATTCTTAG AGGACATAAA ACCGTTGGAT TTGGTAAGTG 660
TGATAAGCAC CATATCTACA AAATCGACAA ATAGCAGCAA GCATTCGTCA TCAGAACTTA 720
TTTCAGAATG TGATTTGAAC AACTCACTTG TGGATATCTT CAACAATTTA ATAGAAATGA 780
ATAGAGACGA GAAAAACAGG TTTAAATTTG TAAAGTTGAT TCACTACGAT ATAGAACTAA 840
AAAAGTTCGT TCAAGACCAA CAAAAGGTAT TATCGCAGAA ATCAAAAGCC GCAGCAATTA 900
ATCCTTTCTT TGTGCCAAAT AGACTAGGGA TACCTTACAT TGAATCCCAA AACGAATTCA 960
F2 →
ACTCGCAGCT TATGACGCTT AATGTAGATG AACCGACCAC AGATATAAGC AACATGGGAG 1020
AGGAAATGCA TGACAGCGCA GATCCCATTG AGGATTCAGA TTCCTCAACT ACCTCCTCTA 1080
CCGGGAAATA TTTCAGCTCA AAATCCTACA TCCAGTCACA GACACCTGAA AGGAAAACAA 1140
GCGTACCAAA TAATTGGCAC GATGATGATT CCGGAAGCAA GAGGAAGAGA AAGCTTTCTT 1200
TCCACAGTCC GAACGCGTCC TCAATCCGCA AAGCCATCAG TTATGAGCAA CTTTCCCTAG 1260
CTAGTGTAGG CTCAGTTGAA AGGTTAGAGG GCAAAATTGT TGGCAT**GAAT TC**ACCTCAAT 1320
TCGCCAGTAT AAATGAGTTC AAATATTGCA CATTGAAATT ATATTTTACG CAGCTCTTAC 1380
CAAATGTCCC AGACAAGGTC CTGGTGCCAG GCGTCAATTG CATTGAGATC GTTATCCCGA 1440
CGAGAGAGCG AATCTGTGAG CTCTTCGGTG TTTTAAACTG TCAAAGCGAC AAGATATCGG 1500
ATATTTTACT ACTGGAAAAG CCTGATCGAA TTTCCGTCGA AGTTGAAAGG ATCCTGTGGG 1560
F3 →
ACAATGACAA GACCGCCAGC CCAGGTTGAG GCGCGCCACT TCTAAATAAG CGAATTTCTT 1620
ATGATTTATG ATTTTTATTA TTAAATAAGT TATAAAAAAA ATAAGTGTAT ACAAATTTTA 1680
AAGTGACTCT TAGGTTTTAA AACGAAAATT CTTATTCTTG AGTAACTCTT TCCTGTAGGT 1740
CAGGTTGCTT TCTCAGGTAT AGCATGAGGT CGCTCTTATT GACCACACCT CTACCGGCAG 1800
ATCCGCTAGG GATAACAGGG TAATATAGAT CTGTTTAGCT TGCCTCGTCC CCGCCGGGTC 1860
ACCCGGCCAG CGACATGGAG GCCCAGAATA CCCTCCTTGA CAGTCTTGAC GTGCGCAGCT 1920
CAGGGGCATG ATGTGACTGT CGCCCGTACA TTTAGCCCAT ACATCCCCAT GTATAATCAT 1980
TTGCATCCAT ACATTTTGAT GGCCGCACGG CGCGAAGCAA AAATTACGGC TCCTCGCTGC 2040
AGACCTGCGA GCAGGGAAAC GCTCCCCTCA CAGACGCGTT GAATTGTCCC CACGCCGCGC 2100
CCCTGTAGAG AAATATAAAA GGTTAGGATT TGCCACTGAG GTTCTTCTTT CATATACTTC 2160
CTTTTAAAAT CTTGCTAGGA TACAGTTCTC ACATCACATC CGAACATAAA CAACCATGGC 2220
AGAACCAGCC CAAAAAAAGC AAAAACAAAC TGTTCAGGAG CGCAAGGCGT TTATCTCCCG 2280
TATCACTAAT GAAACTAAAA TTCAAATCGC TATTTCGCTG AATGGTGGTT ATATTCAAAT 2340
AAAAGATTCG ATTCTTCCTG CAAAGAAGGA TGACGATGTA GCTTCCCAAG CTACTCAGTC 2400
ACAGGTCATC GATATTCACA CAGGTGTTGG CTTTTTGGAT CATATGATCC ATGCGTTGGC 2460
AAAACACTCT GGTTGGTCTC TTATTGTTGA ATGTATTGGT GACCTGCACA TTGACGATCA 2520
CCATACTACC GAAGATTGCG GTATCGCATT AGGGCAAGCG TTCAAAGAAG CAATGGGTGC 2580
TGTCCGTGGT GTAAAAAGAT TCGGTACTGG GTTCGGCACCA TTGGATGAGG CGCTATCACG 2640
TGCCGTAGTC GATTTATCTA GTAGACCATT TGCTGTAATC GACCTTGGAT TGAAGAGAGA 2700
GATGATTGGT GATTTATCCA CTGAAATGAT TCCACACTTT TTGGAAAGTT TCGCGGAGGC 2760
GGCCAGAATT ACTTTGCATG TTGATTGTCT GAGAGGTTTC AACGATCACC ACAGAAGTGA 2820
GAGTGCGTTC AAGGCTTTGG CTGTTGCCAT AAGAGAAGCT ATTTCTAGCA ATGGCACCAA 2880
TGACGTTCCC TCAACCAAAG GTGTTTTGAT GTGAAGTACT GACAATAAAA AGATTCTTGT 2940
TTTCAAGAAC TTGTCATTTG TATAGTTTTT TTATATTGTA GTTGTTCTAT TTTAATCAAA 3000
TGTTAGCGTG ATTTATATTT TTTTTCGCCT CGACATCATC TGCCCAGATG CGAAGTTAAG 3060
TGCGCAGAAA GTAATATCAT GCGTCAATCG TATGTGAATG CTGGTCGCTA TACTGCTGTC 3120
GATTCGATAC TAACGCCGCC ATCCAGTTTA AACGAGCTCG AATTCGACAT GATCCGCGCA 3180
GCCCAACGCG GCGGTGCCAA ATTGCAGTGA CGTCTCGGAG TAATATAAAA AAAAAAGACC 3240
AAATAACCAA ATTTAAGGGT GCTCTGAATA TAAGGGAGTG GAACGTTTTC ACACGAAGGA 3300
R3 ←
AAAGGGAAAG AGGGGAGTGG TAAGAAGCAA GAGTCAATGA AAGGTCTTCC TTCCTTCTTG 3360
ATGCT 3365

Figure 4.3. Selection of primers used to sequence the *cdc13-1* CTΔ-HIS3MX6 construct (CTΔ amplicon~3365 bp).

The sequence shows the position of primers used for sequencing within the theoretical sequence as accessed from database and online resources. The highlighted codons 'ATG' and 'TAA' represent start and stop codons for the *cdc13-1* N-terminus half replication after C-truncation and for the histidine marker respectively. The primers are F1 (22) 5'ACATGCAGCCTTGATTAACGTG 3', F2 (20) 5'CAACTCGCAGCTTATGACGC 3', F3 (20) 5'TGAGGCGCGCCACTTCTAAA3'and R3 (22) 5' GCATCAAGAAGGAAGGAAGACC 3' (reverse complement of GGTCTTCCTTCCTTCTTGATGC).

Additional details of the sequence of the constructs *cdc13-1* NTΔ-TRP1 (3267 bp) and *cdc13-1* CTΔ-HIS3MX6 are presented in Table 4.3 and 4.4 respectively.

Table 4.3. The sequence details of the *cdc13-1* NTΔ-TRP1 construct (3267 bp).

	Nucleotide sequence	**Name of sequence (*cdc13-1* NTΔ-TRP1 construct)**	**Total length (bp)**
1	1-200	*CDC13* upstream sequence	(200)
2	151-200	NTΔ: forward deletion primer (NF1) 5' part	(50)
3	201-220	NTΔ: forward deletion primer's (NF1) 3' part (F4 primer from TRP1 modulating DNA)	(20)
4	221-300	Blank sequence	(80)
5	301-975	TRP1 marker coding sequence (end to start)	(675)
6	976-1123	TRP1 promoter	(148)
7	1124-1217	Blank sequence	(94)
8	1218-1335	UAC (upstream activating sequence)	(118)
9	1218-1659	GAL1 promoter	(442)
10	1662-1681	NTΔ: reverse deletion primer's (NR1) 3' part (R2 primer from TRP1 modulating DNA)	(20)
11	1682-1729	NTΔ: reverse deletion primer (NR1)'s 5' part	(48)
12	1679-3067	*CDC13*-C-terminus	(1389)
13	3068-3267	*CDC13* downstream sequence	(200)

Table 4.4. The sequence details of the *cdc13-1* CTΔ-ADH1-HIS3MX6 construct (3365 bp).

	Nucleotide sequence	**Name of sequence (*cdc13-1* CTΔ-HIS3MX6 construct)**	**Total length (bp)**
1	1-200	*CDC13* upstream sequence	(200)
2	201-1589	*CDC13*-N-terminus	(1389)
3	1537-1586	C-terminus forward deletion primer (CF2)'s 5' end: gene sequence	(50)
4	1587-1606	C-terminus forward deletion primer (CF2)'s 3' end: F3 modulating primer from HIS3MX6 DNA, used as F3 sequencing primer	(20)
5	1607-1609	Blank sequence	(3)
6	1610-1797	ADH1 terminator	(188)
7	1798-1871	Blank sequence including 30 nucleotide insertion:	(74)
8	1872-2214	TEF promoter	(343)
9	2215	Blank sequence	(1)
10	2216-2914	HIS3MX6 marker coding sequence (start to end)	(699)
11	2915-2917	Blank sequence	(3)
12	2918-3115	TEF terminator	(198)
13	3116-3145	Blank sequence	(30)
14	3146-3165	C-terminus reverse deletion primer (CR2) 's 3' end: (R1 modulating primer from HIS3MX6 marker DNA)	(20)
15	3166-3216	C-terminus reverse deletion primer (CR2)'s 5' end: gene sequence	(51)
16	3166-3365	*CDC13* downstream sequence	(200)

4.3.1.2. Sequencing template preparation

4.3.1.2.1. Total DNA extraction

Total DNA was prepared from 24 constructs and two controls. Figure 4.4 presents the results of gel electrophoresis of genomic DNA extracted from 12 N-truncated (A) and 12 C-truncated (B) constructs of *cdc13-1*. Cells were selected on dropout medium and single colonies cultivated onto YEPD plates for three days at 30°C. DNA was isolated from N- and C-truncated *cdc13-1* clones, re-suspended in 100 µl 1x TE buffer at 4°C overnight (o/n). DNA from 6 independent mutants with N-terminus deletion (Figure 4.4A) and C-terminus deletion (Figure 4.4B) were analysed electrophoretically for strain 1296 (lanes 1-6) and 1297 (lanes 7-12). The genomic DNA from original strains 1296-TR and 1297-TR (*cdc13-1*) are shown in lanes 13 and 14 (B). All DNA bands exhibit an almost identical intensity, with a yield on average of 1-2 µg/µl. The genomic DNAs were diluted (1:100 or 1:200) and used to amplify the 3 kb sequencing templates.

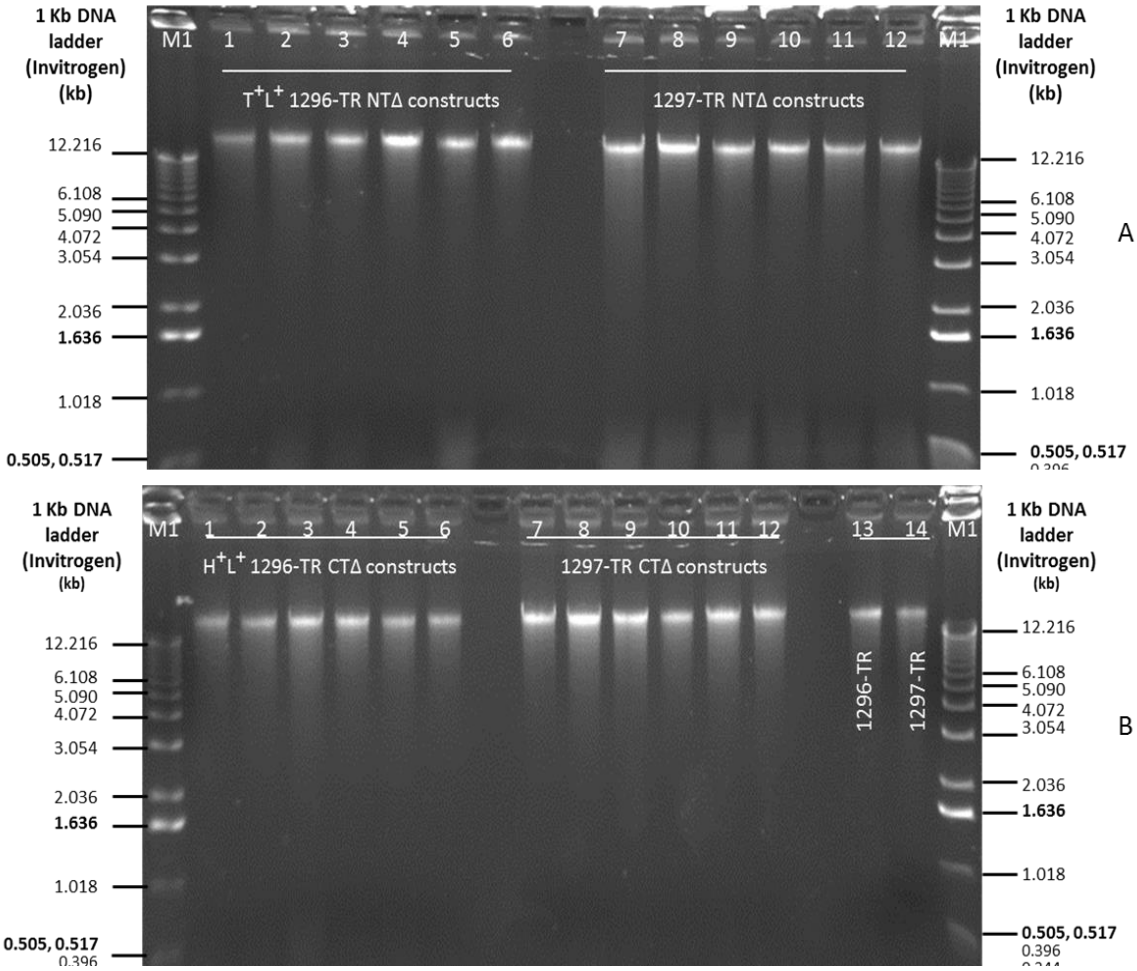

Figure 4.4. Total DNA analysis of *cdc13-1* N-terminus (*cdc13-1*-NTΔ::TRP1-PGAL1) and C-terminus (*cdc13-1*-CTΔ::HIS3MX6) deletion mutants generated in strain 1296-TR and 1297-TR survivors.

For each sample, 2 µl of uncut DNA (mixed with 2 µl of 5x DNA dye and 6 µl of 1x TE buffer) was examined on a 0.7 % agarose gel. M1 represents a 1 kb size marker (Invitrogen) used at a concentration of 1 µg (0.1µg/µl).

(**A**) Agarose gel electrophoresis of genomic DNA from N-terminus truncated clones.
Lanes 1-6: total DNA from NTΔ constructs (*cdc13-1*-NTΔ::TRP1-PGAL1) #2, #4, #5, #6, #7 and #21 in strain 1296-TR; **7-12**: total DNA from NTΔ constructs (*cdc13-1*-NTΔ::TRP1-PGAL1) #1, #7, #8, #11, #14 and #22 in strain 1297-TR.
(**B**) Agarose gel electrophoresis of genomic DNA from C-terminus truncated clones.
Lanes 1-6: total DNA from NTΔ constructs (*cdc13-1*-CTΔ::HIS3MX6) #3, #4, #6, #7, #9, #10 in strain 1296-TR; **7-12**: total DNA from NTΔ constructs (*cdc13-1*-CTΔ::HIS3MX6) #3, #4, #7, #8, #11, #12 in strain 1297-TR; **13 and 14**: total DNA from strain 1296-TR and strain 1297-TR respectively; **M1**: 1 kb marker (Invitrogen) 1 µg (0.1µg/µl).

4.3.1.2.1.1. PCR amplification of 3 kb specific fragments using *CDC13* upstream and downstream primers

PCR product of ~3 kb was amplified from genomic DNA with Q5 polymerase (NEB) using primers F1 and R3 with an initial denaturation during 50 seconds at 98°C followed by 32 cycles of 10 seconds of denaturation at 98°C, 30 seconds of annealing at 60°C and 90 seconds of extension at 72°C. The final extension at 72°C was carried out for 2 minutes. PCR conditions were adapted with the supplementation of enhancer (Figure 4.5A) or $MgCl_2$ (Figure 4.5B). The results of agarose gel electrophoresis of the PCR products show amplification of the desired band of ~3 kb with both concentrated and diluted template DNA (1:100 and 1:200) with more consistent and specific bands with almost similar intensity with $MgCl_2$ (Figure 4.5).

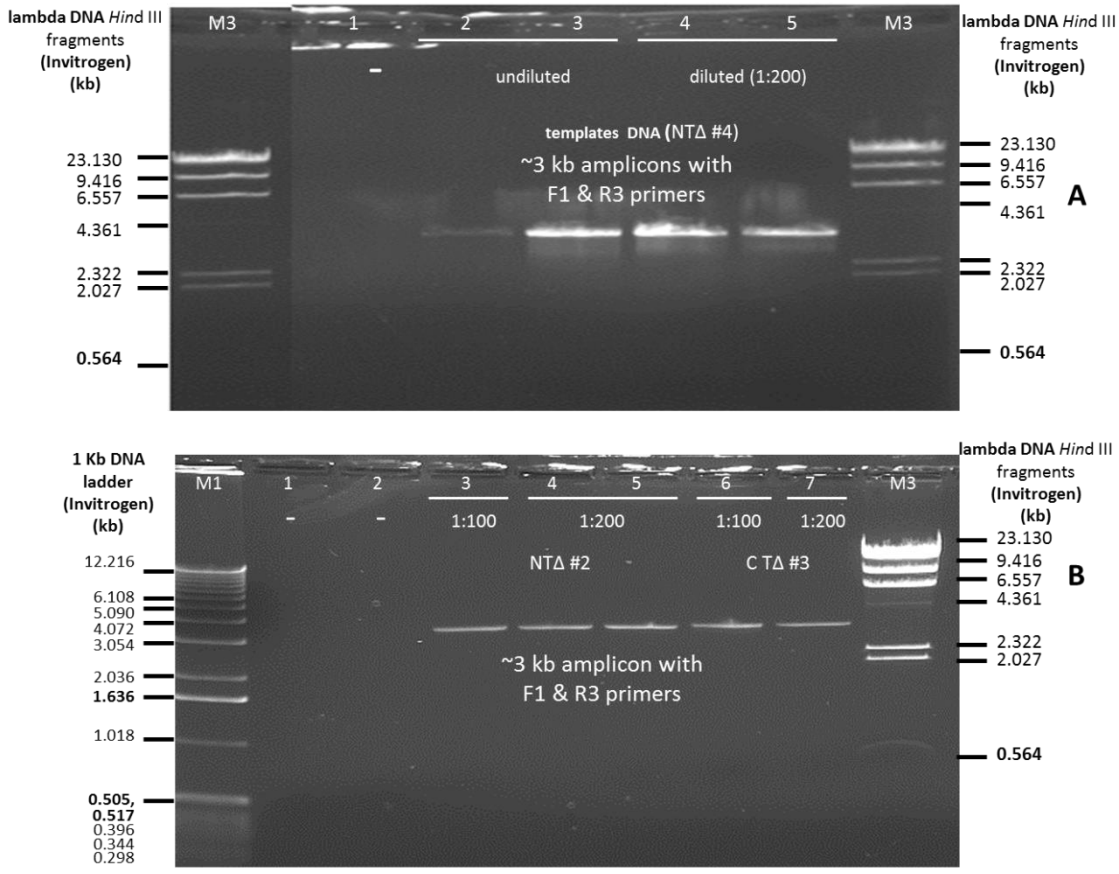

Figure 4.5. PCR amplification of the 3 kb product in the presence of enhancer or $MgCl_2$.

Genomic DNA concentrated and diluted (1:100 and 1:200) from the construct *cdc13-1*-NTΔ/CTΔ in strain 1296-TR were used as a template. PCR was performed in a 50 µl reaction volume with 1 unit of Q5 enzyme in the presence of 1x enhancer/2 mM $MgCl_2$ using forward F1 (5' ACATGCAGCCTTGATTAACGTG 3') and reverse R3 primer (5' GCATCAAGAAGGAAGGAAGACC 3'). Gel electrophoresis shows amplified products with concentrated and diluted DNA templates. 2 µl of PCR products with 2 µl of 5x DNA dye and 6 µl 1x TE buffer were examined on a 0.7% agarose gel for all the samples.

(**A**) Gel electrophoresis of PCR products, amplified in the presence of enhancer.

Lanes **M3**: lambda DNA *Hin*d III fragments (Invitrogen), 1 µg (0.1 µg/µl); **1**: -ve control (Non template control, without DNA); **2** and **3**: PCR amplicons with concentrated template; **4** and **5**: PCR products with diluted (1:200) template (genomic DNA from construct *cdc13-1*-NTΔ #4).

(**B**) Gel electrophoresis of PCR products, amplified in the presence of 2 mM $MgCl_2$.

Lanes M1: 1 kb size marker (Invitrogen) used in a concentration of 1 µg (0.1µg/µl); **1** and **2**: -ve controls (Non template control, without DNA); **3-5**: PCR fragment amplified with 1/100 (lane 3) and 1/200 (lanes 4 and 5) diluted DNA template from construct *cdc13-1*-NTΔ #2 of strain 1296-TR; **6** and **7**: PCR fragment amplified with 1/100 (lane 6) and 1/200 (lane 7) diluted DNA template from construct *cdc13-1*-CTΔ #3 of strain 1296-TR; **M3**: lambda DNA *Hin*d III fragments (Invitrogen), 1 µg (0.1 µg/µl).

4.3.1.2.1.2. PCR amplification for the 3 kb fragment from genomic DNA of *cdc13-1*-N- and C-truncated mutants (1296-TR and 1297-TR).

Sequencing templates were generated through PCR amplification from genomic DNA of N- and C-truncated *cdc13-1* clones. 12 clones were selected for each modification, from strain 1296 and 1297. The genomic DNA used as a template was diluted to 1:200. PCR was performed in a 50 µl reaction volume with 1 unit of Q5 enzyme in the presence of 2 mM $MgCl_2$ with forward, F1 (5-'ACATGCAGCCTTGATTAACGTG-3') and reverse primer, R3 (5'-GCATCAAGAAGGAAGGAAGACC-3'). Figure 4.6 shows PCR fragments amplified from DNA isolated from six independent mutants with N-terminus deletion (A) and C-terminus deletion (B) of strains 1296- (lanes 3-8) and 1297-TR (lanes 10-15). For each sample, 2 µl of PCR product was examined on a 0.7 % agarose gel. The resulting amplified fragments (~3 kb) consisted of truncated *cdc13-1* and a TRP1/HIS3MX6 marker DNA.

For the control sequencing template, the 3 kb target region containing *cdc13-1* coding region plus 200 nt upstream and downstream sequences were amplified using the F1 and R3 primers supplemented with 2 mM $MgCl_2$ and genomic DNA template from original strains 1296-TR and 1297-TR. Agarose gel electrophoresis of the PCR products confirmed the presence of the required DNA fragments (~3 kb) from all tested deletion constructs and controls.

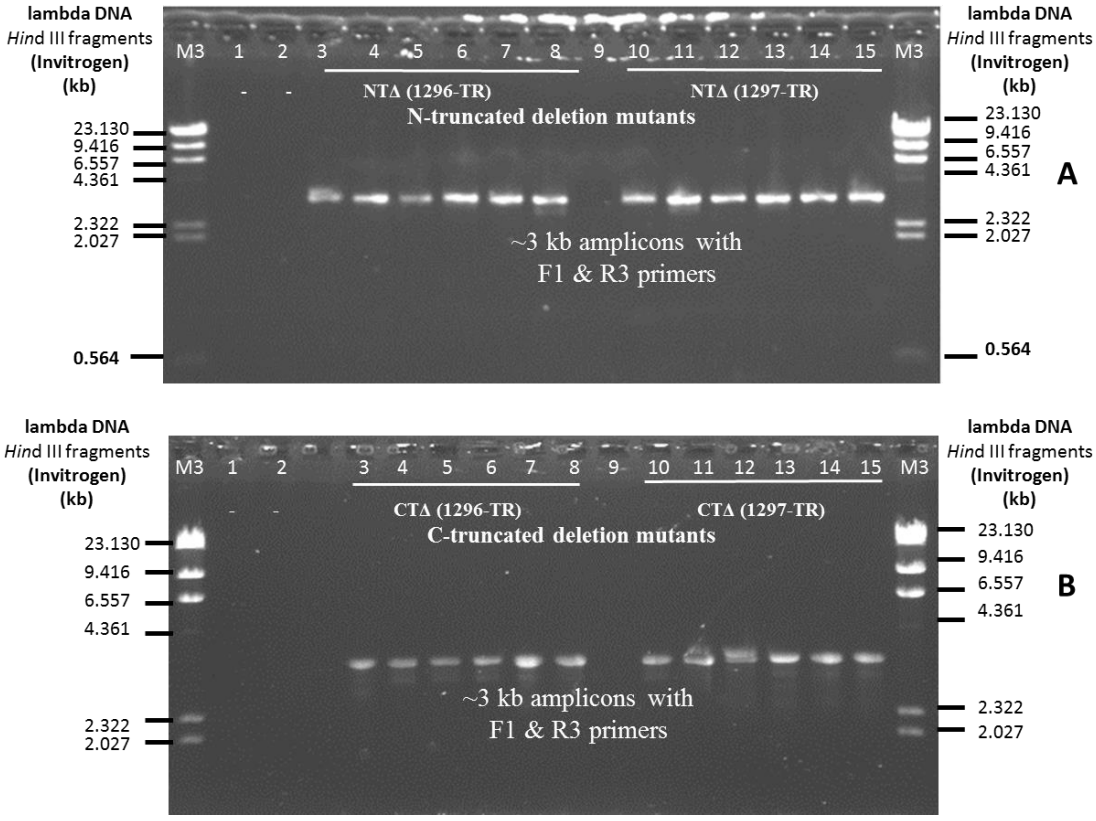

Figure 4.6. Electrophoretic separation of PCR products following amplification with Q5 polymerase from *cdc13-1* N-terminus (*cdc13-1*-NTΔ::TRP1-PGAL1) and C-terminus (*cdc13-1*-CTΔ::HIS3MX6) deletion mutants.

For each sample, 2 µl of PCR product was examined on a 0.7 % agarose gel. **M3** represents lambda DNA *Hin*d III fragments (Invitrogen), 1 µg (0.1 µg/µl). **Lanes 1** and **2** represent -ve controls (Non template control, without DNA).

(A) Gel electrophoresis of PCR products from 12 N-terminus truncated clones (*cdc13-1*-NTΔ::TRP1-PGAL1).
Lanes: **3-8**: PCR products (~3 kb) from N-terminus deletion constructs, #2, #4, #5, #6, #7 and #21 respectively in strain 1296-TR; **10-15**: PCR products (~3 kb) from N terminus deletion constructs, #1, #7, #8, #11, #14 and #22 respectively in strain 1297-TR.
(B) Gel electrophoresis of PCR products from 12 C-terminus truncated clones (*cdc13-1*-CTΔ::ADH1-HIS3MX6).
Lanes 3-8: PCR products (~3 kb) from C-terminus deletion constructs #3, #4, #6, #7, #9, #10 respectively in strain 1296-TR; **10-15**: PCR products (~3 kb) from C-terminus deletion constructs #3, #4, #7, #8, #11, #12 respectively strain 1297-TR.

4.3.1.2.1.3. Purification of 3 kb PCR fragments sequencing template

For automated sequencing, the purification of amplified DNA templates was performed using a commercially available kit (Wizard® PCR preps DNA purification system, Promega). The column purified DNA eluted in sterile water was ready for sequencing. The quality and quantity of purified DNA was first estimated by measuring absorbance using a spectrophotometer (Nanodrop 2000; Table 4.5) and then separating the DNA by agarose gels electrophoresis (Figure 4.7) for N- (A) and C-truncated (B) PCR fragments. The analytical gels showed the quantity of DNA ~30-50 ng/µl on average. The purified DNA fragments from 26 samples (24 clones and 2 controls) were sent for sequencing at a concentration of approximately 30-50 ng/µl along with sequencing primers (at a concentration of 10 pmol/µl). The automated sequencing was performed at GATC-Biotech facilities (Germany) on a ABI 3730xl DNA analyser (Applied Biosystems), which is high throughput, capillary electrophoresis systems and used for analysing fluorescently labelled DNA fragments. . Data was evaluated by the Phred20 system using the Base caller KB 1.4.1.8.

The column purified DNA was successfully sequenced with a read length of 700 to 1000 nt sequences. However, another set of amplified sequencing templates for N- and C-terminus ~3 kb DNA (Figure 4.8A and B respectively), extracted with phenol-chloroform method followed by ethanol precipitation (Figure 4.9 for N- (A) and C-truncated (B) constructs failed in sequencing indicating the non-suitability of phenol extracted template for sequencing although it looked similar on analytical gels. It also indicates that the purity of DNA is a crucial factor for successful sequencing.

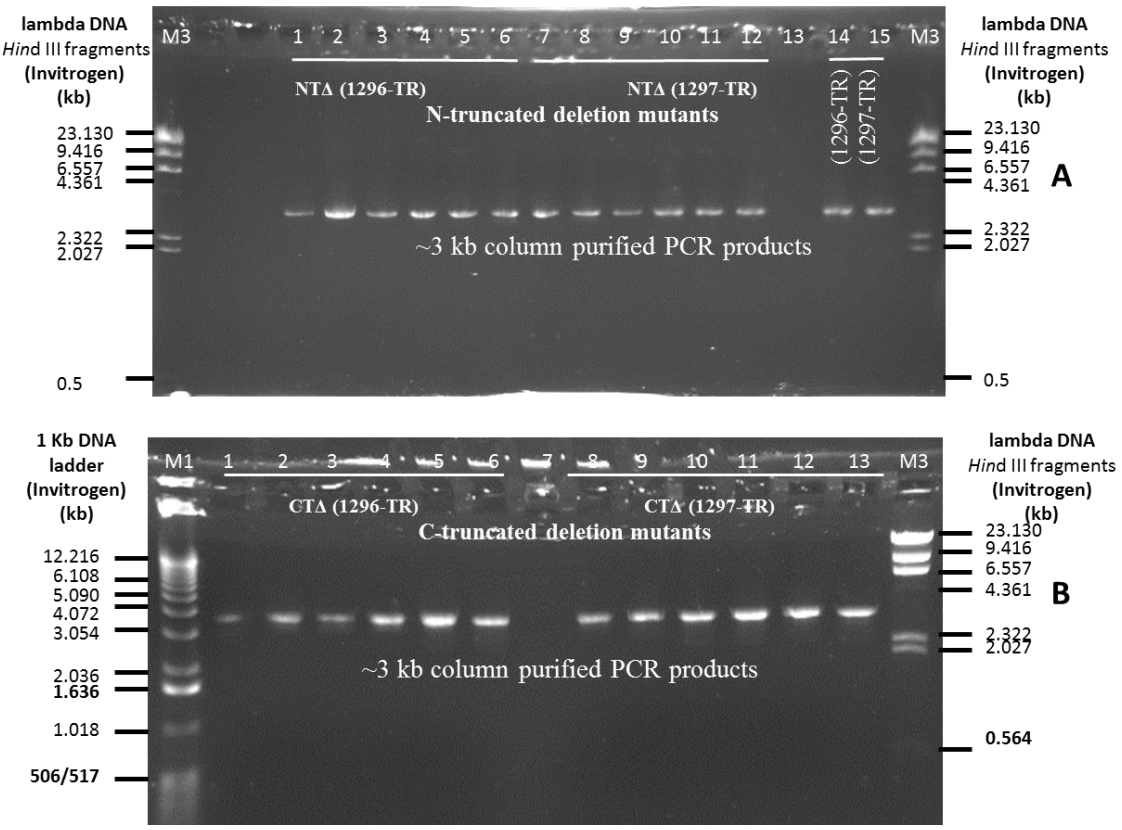

Figure 4.7. Electrophoretic separation of PCR products following purification of amplified products from *cdc13-1* N-terminus (*cdc13-1*-NTΔ::TRP1-PGAL1) and C-terminus (*cdc13-1*-CTΔ::HIS3MX6) deletion mutants.

PCR-amplified 3 kb fragments from 26 samples were cleaned up of unwanted PCR products (PCR primers and remaining dNTPs etc.). Promega's DNA purification columns were used to purify amplified products according to the manufacturer's instruction. Purified DNA was eluted in sterile water and analysed for concentration using a spectrophotometer (Nanodrop 2000). For each sample, 2 µl of the purified DNA was examined on a 0.7 % gel.

(**A**) Gel electrophoresis of purified PCR products from 12 clones with *cdc13-1*-N-truncation.

Lanes 1-6: column purified ~ 3 kb PCR fragments from 6 clones, #2, #4, #5, #6, #7 and #21 respectively in strain 1296-TR; **7-12**: column purified PCR fragments from 6 clones, #1, #7, #8, #11, #14 and #22 respectively in strain 1297-TR; **14-15**: column purified PCR fragments from original strain 1296-TR and 1297-TR (*cdc13-1*).

(**B**) Gel electrophoresis of purified PCR products from 12 clones with *cdc13-1*-C-truncation.

Lanes 1-6: column purified PCR fragments (~3 kb) from 6 clones, #3, #4, #6, #7, #9, #10 respectively in strain 1296-TR; **8-13**: column purified PCR fragments (3 kb) from 6 constructs, #3, #4, #7, #8, #11, #12 respectively in strain 1297-TR.

M1 represents 1 kb size marker (Invitrogen) used at a concentration of 1 µg (0.1µg/µl).

M3 represents lambda DNA *Hin*d III fragments (Invitrogen), 1 µg (0.1 µg/µl).

Table 4.5. The estimation of concentration of column purified DNA by spectrophotometry.

#	Sample ID	Nucleic acid conc. ng/µl	Absorbance 260/230	Absorbance 260/280
1.	1296-N*#2	15.3	0.64	1.91
2.	1296-N #4	42.1	1.54	1.83
3.	1296-N #5	21.7	1.66	1.77
4.	1296-N #6	21.5	1.62	1.78
5.	1296-N #7	19	1.7	1.8
6.	1296-N #21	18.6	1.08	1.84
7.	1297-N #1	17.5	1.56	1.95
8.	1297-N #7	21.7	1.72	1.8
9.	1297-N #8	12.8	0.95	1.88
10.	1297-N #11	18.1	1.43	1.94
11.	1297-N #12	15.5	1.73	1.81
12.	1297-N #22	19.1	0.8	1.87
13.	1296-C*#3	23.5	2.33	1.95
14.	1296-C #4	18.6	2.47	2.01
15.	1296-C #6	16.8	0.86	2.04
16.	1296-C #7	18.6	1.77	1.98
17.	1296-C #9	25.8	0.64	1.84
18.	1296-C #10	21.5	2.1	1.93
19.	1297-C #3	16.5	1.77	1.98
20.	1297-C #4	21.7	2.25	1.89
21.	1297-C #7	24.3	2.06	1.83
22.	1297-C #8	27.6	2.02	1.8
23.	1297-C #11	27.3	2.09	1.91
24.	1297-C #12	21.7	1.87	1.84
25.	1296 #25	22	1.6	1.81
26.	1297 #26	19.8	1.71	1.83

*N denotes N-terminus deletion (NTΔ) mutant.

*C denotes C-terminus deletion (CTΔ) mutant.

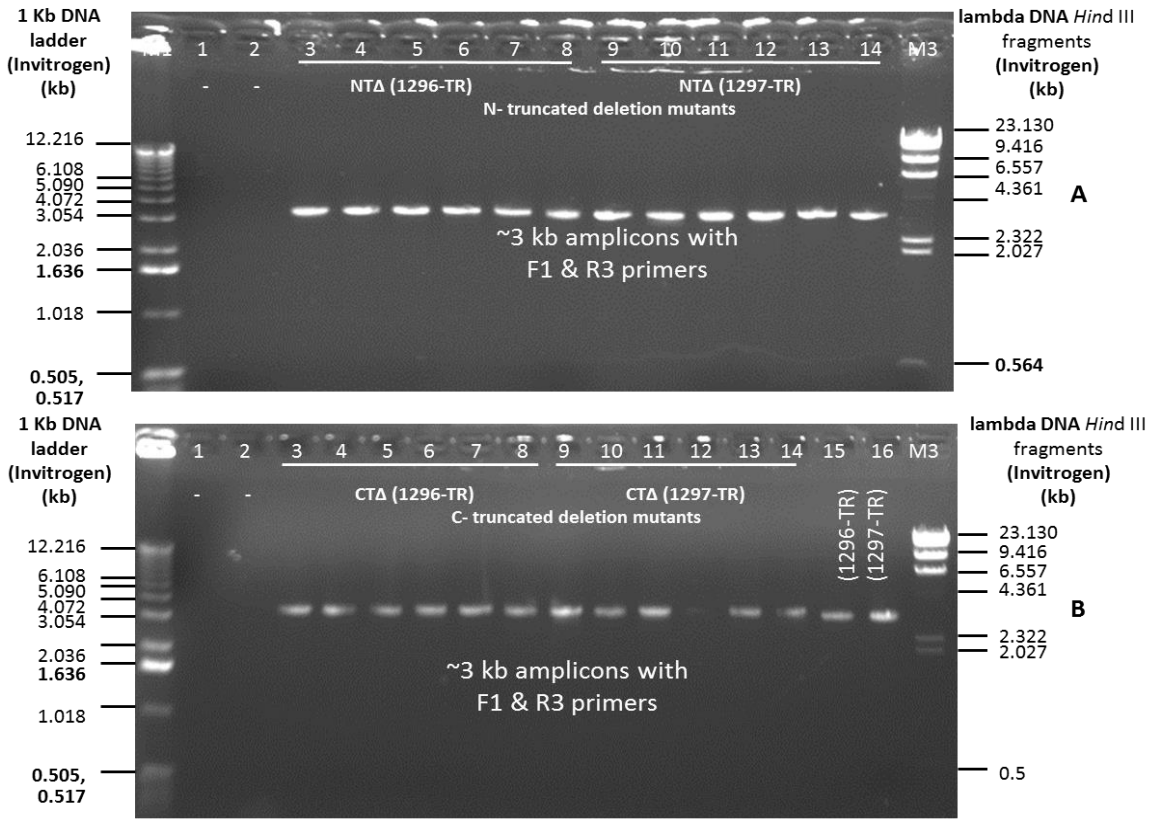

Figure 4.8. Electrophoretic separation of PCR products following amplification with Q5 polymerase from *cdc13-1* N-terminus and C-terminus deletion mutants generated from 1296-TR and 1297-TR survivors.

PCR was performed as explained earlier with Q5 polymerase enzyme in 50 µl volume. For each sample, 2 µl of PCR product was examined on a 0.7 % agarose gel.

(A) Gel electrophoresis of PCR amplified products from 12 N-terminus truncated clones.

Lanes 3-8: PCR fragments (~3 kb) from strain 1296-TR N-terminus deletion constructs (*cdc13-1*-NTΔ::TRP1-PGAL1) #2, #4, #5, #6, #7 and #21 respectively; **9-14**: PCR products (3 kb) from strain 1297-TR N-terminus deletion constructs (*cdc13-1*-NTΔ::TRP1-PGAL1) #1, #7, #8, #11, #14 and #22 respectively.

(B) Gel electrophoresis of PCR amplified products from 12 C-terminus truncated clones.

Lanes 3-8: PCR fragments from strain 1296-TR C-terminus deletion constructs (*cdc13-1*-CTΔ::HIS3MX6) #3, #4, #6, #7, #9, #10 respectively; **9-14**: PCR fragments from strain 1297-TR C-terminus deletion constructs (*cdc13-1*-CTΔ: HIS3MX6) #3, #4, #7, #8, #11, #12 respectively; **15-16**: PCR fragments from control original strains 1296- and 1297-TR with *cdc13-1*.

M1 represents 1 kb size marker (Invitrogen) used at a concentration of 1 µg (0.1µg/µl). **M3** represents lambda DNA *Hin*d III fragments (Invitrogen), 1 µg (0.1 µg/µl). **Lanes 1** and **2** represent -ve controls (Non template control, without DNA).

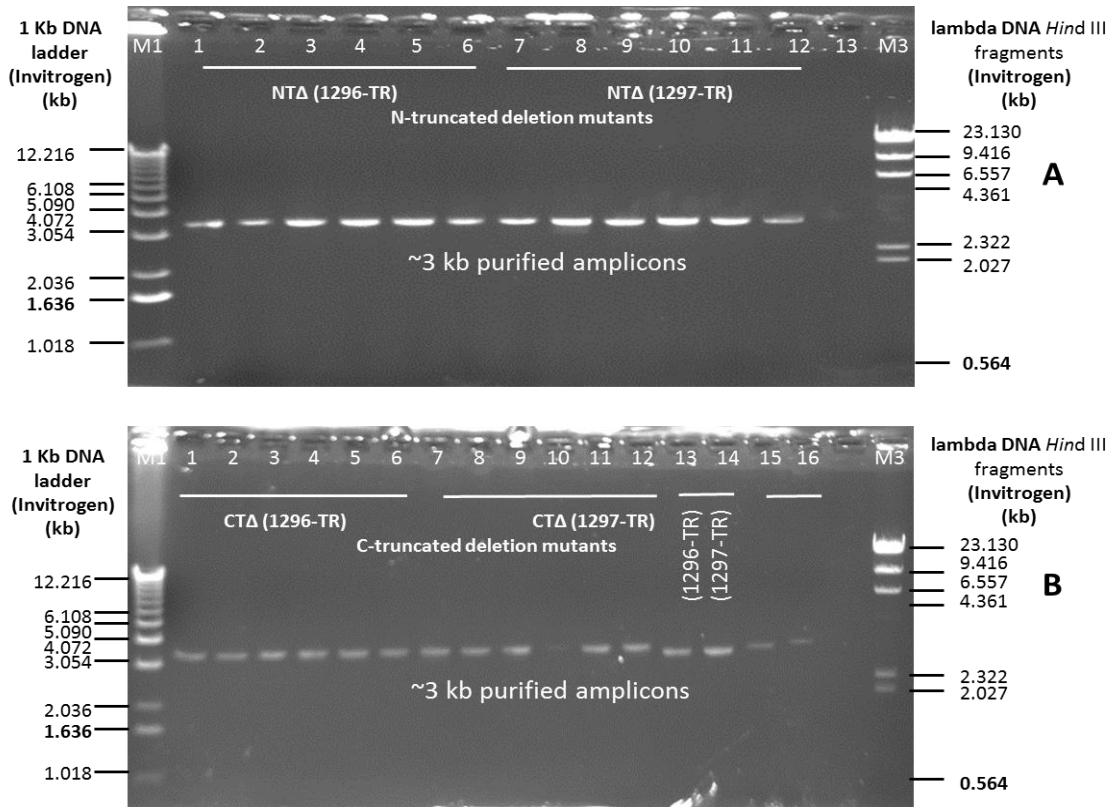

Figure 4.9. Electrophoretic analysis of PCR products following phenol extraction of amplified products from *cdc13-1* N-terminus (*cdc13-1*-NTΔ::TRP1-PGAL1) and C-terminus (*cdc13-1*-CTΔ::HIS3MX6) deletion mutants.

PCR-amplified 3 kb fragments were cleaned up of unwanted PCR products by the phenol/chloroform extraction method. The clean DNA was examined as 2 µl of each sample on a 0.7 % gel.

M1 represents 1 kb size marker (Invitrogen) used at a concentration of 1 µg (0.1µg/µl). **M3** represents lambda DNA *Hin*d III fragments (Invitrogen), 1 µg (0.1 µg/µl).

(**A**) Gel electrophoresis of purified PCR products from 12 clones with *cdc13-1*-N-terminus truncation.

Lanes 1-6: purified PCR products from 6 clones from strain 1296-TR (*cdc13-1*-NTΔ::TRP1-PGAL1) #2, #4, #5, #6, #7 and #21 respectively; **7-12**: purified PCR products from 6 clones from strain 1297-TR (*cdc13-1*-NTΔ::TRP1-PGAL1) #1, #7, #8, #11, #14 and #22 respectively.

(**B**) Gel electrophoresis of purified PCR products from 12 clones with *cdc13-1*-C-terminus truncation.

Lanes 1-6: purified fragments (3 kb) from strain 1296-TR C- terminus deletion constructs (*cdc13-1*-CTΔ::HIS3MX6) #3, #4, #6, #7, #9, #10 respectively; **7-12**: purified fragments from strain 1297-TR C-terminus deletion constructs (*cdc13-1*-CTΔ::HIS3MX6) #3, #4, #7, #8, #11, #12 respectively; **13-14**: purified PCR products from control 1296- and 1297-TR with *cdc13-1*; **15-16**: column-purified PCR fragments from *cdc13-1*-N-terminus-truncated (NTΔ#2) and C-terminus-truncated (CTΔ#3)-1296-TR clones.

4.3.1.3. Analysis of the sequencing data.

Results of automated DNA sequencing were in the form of a four-colour-chromatogram and a text file of primary sequence data as interpreted by computer program (Phred-Phrap). Four nucleotide sequence-reads (forward- and reverse-reads in accordance with 4 primers) were generated for each sample, mutants (24x4) and controls (2x4). The text sequence of DNA was aligned with its relevant theoretical (reference) sequence, mentioned earlier for *cdc13-1* (3175 nt; Figure 4.1), NTΔ- (3267 nt; Figure 4.2) and CTΔ-constructs (3365 nt; Figure 4.3) to find any mismatches. The *cdc13-1* C-terminus, N-terminus in constructs and histidine marker were orientated from 5' to 3' (left to right) on top strand, while the tryptophan marker was in an opposite orientation from right to left.

All miscalled bases and errors at the beginning and end of each sequence reads were manually double-checked by overlapping text data and the chromatogram analysis. On the basis of homology analysis and sequencing results, real sequences were constructed for the individual mutants. The resulting mutations, deletions, insertions and substitution were mapped and were further analysed for the predicted protein sequences (Cdc13-1-N- or C-terminus and linked tryptophan or histidine marker proteins) through translational analysis to see whether it could shift the frame or not. Finally, all the identified (ascertained) modifications were summarised in Tables 4.6, 4.7 and 4.8 for *cdc13-1* controls and N- and C-terminus-truncated constructs respectively.

Table 4.6. Analysis of modifications in *cdc13-1* DNA sequence* in strains 1296-TR and 1297-TR mutants.

DNA ID (#)	Name of Mutant/ construct	Location of nucleotide	Nature of DNA mutations			Position of mutation (within coding region of *cdc13-1*, or non-coding upstream/downstream sequence)	Modification of amino acid	Protein Frame shift: (marker or Cdc13-1 protein)
			Deletion	Insertion	substitution			
25	*cdc13-1 exo1Δ* (strain 1296-TR)	69, 78/79 upstream	A?			*CDC13* upstream (miscounted peaks due to limit of resolution in the beginning of the sequence read, nucleotide 'A' in fact be two A's, not accurate error)		NO
26	*cdc13-1 exo1Δ* (strain 1297-TR)	69, 78/79 upstream	A?			*CDC13* upstream (miscounted peaks due to limit of resolution in the beginning of the sequence read, nucleotide 'A' in fact be two A's, not accurate error)		NO

**cdc13-1* ORF including 200 nt up- and downstream sequence.

Table 4.7. Analysis of modifications in *cdc13-1*-N-terminus-truncated::TRP1-PGAL1 DNA from strains 1296-TR and 1297-TR mutants.

DNA ID (#)	**Name of the construct:** (*cdc13-1*-NTΔ-TRP1-PGAL1)	**Location of nucleotide**	**Nature of DNA mutations**			**Position of mutation (*cdc13-1* coding region, upstream/downstream non-coding sequence, TRP1 marker or promoter of modular DNA)**	**Amino acid modification**	**Protein Frame shift: (marker or truncated Cdc13-1 protein)**
			Deletion	**Insertion**	**substitution**			
1	1296-NTΔ #2	78/79 upstream	A?			*CDC13* upstream (miscounted peaks due to limit of resolution in the beginning of the sequence read, nucleotide 'A' in fact be two A's, not accurate error)		No
		219			A→C	Within F4 primer of TRP1 marker of modular DNA, downstream region of TRP1 marker		No
		254		TAGATC		Within modular DNA, 46 nucleotides outside the end (stop) codon of TRP1 marker		No
		1706	A?			*cdc13* C-half, mutation located within deletion primer		Yes/*cdc13-1*-C-terminus
2	1296-NTΔ #4	69, 78/79 upstream	A?			*CDC13* upstream (miscounted peaks due to limit of resolution in the beginning of the sequence read, nucleotide 'A' in fact be two A's, not accurate error)		No
		254		TAGATC		Within modular DNA, 46 nucleotides outside the end (stop) codon of TRP1 marker		No
3	1296-NTΔ #5	78/79 upstream	A?			*CDC13* upstream (miscounted peaks due to limit of resolution in the beginning of the sequence read, nucleotide 'A' in fact be two A's, not accurate error)		No
		254		TAGATC		Within modular DNA, 46 nucleotides outside the end (stop) codon of TRP1 marker		No
4	1296-NTΔ #6	69, 78/79 upstream	A?			*CDC13* upstream (miscounted peaks due to limit of resolution in the beginning of the sequence read, nucleotide 'A' in fact be two A's, not accurate error)		No
		254		TAGATC		within modular DNA, 46 nucleotides outside the end (stop) codon of TRP1 marker		No
5	1296-NTΔ #7	69, 78/79 upstream	A?			*CDC13* upstream (miscounted peaks due to limit of resolution in the beginning of the sequence read, nucleotide 'A' in fact be two A's, not accurate error)		No
		254		TAGATC		Within modular DNA, 46 nucleotides outside the end (stop) codon of TRP1 marker		No
		457			T→C	In TRP1 marker of modular DNA codon 173 changed from TTA to TTG, both stand for Leucine	No change in AA	No

DNA ID (#)	Name of the construct: (*cdc13-1*-NTΔ-TRP1-PGAL1)	Location of nucleotide	Nature of DNA mutations			Position of mutation (*cdc13-1* coding region, upstream/downstream non-coding sequence, TRP1 marker or promoter of modular DNA)	Amino acid modification	Protein Frame shift: (marker or truncated Cdc13-1 protein)
			Deletion	Insertion	substitution			
6	1296-NTΔ #21	69, 78/79 upstream	A?			*CDC13* upstream (miscounted peaks due to limit of resolution in the beginning of the sequence read, nucleotide 'A' in fact be two A's, not accurate error)		No
		254		TAGATC		Within modular DNA, 46 nucleotides outside the end (stop) codon of TRP1 marker		No
		462			T→C	Within coding sequence of TRP1 marker of modular DNA, codon 172 changed from AGC (Ser) to GGC (Gly)	Change in AA-172 from Ser to Gly	No
		1457			T→C	Within GAL1 promoter of modular DNA (doubly confirmed)		
7	1297-NTΔ #1	78/79 upstream	A?			*CDC13* upstream (miscounted peaks due to limit of resolution in the beginning of the sequence read, nucleotide 'A' in fact be two A's, not accurate error)		
		254		TAGATC		Within modular DNA, 46 nucleotides outside the end (stop) codon of TRP1 marker		No
		879			C→T	Within coding sequence of TRP1 marker of modular DNA, codon 33 changed from GCT (Ala) to ACT (Thr)	Change in AA-33 from Ala to Thr	No
8	1297-NTΔ #7	78/79 upstream	A?			*CDC13* upstream (miscounted peaks due to limit of resolution in the beginning of the sequence read, nucleotide 'A' in fact be two A's, not accurate error)		
		254		TAGATC		Within modular DNA, 46 nucleotides outside the end (stop) codon of TRP1 marker		No
		676			A→G	Within coding sequence of TRP1 marker of modular DNA, codon 100 changed from CAT (His to CAC (His) (double confirmed)	Change in codon-100 of TRP1 marker but not AA	
		2107			C→A	Within C-terminus coding region of N-truncated *cdc13-1,* codon 143 changed from GGC (Gly) to GGA (Gly) in C-terminus half	No change in protein, AA remains the same	
9	1297-NTΔ #8	69, 78/79 upstream	A?			*CDC13* upstream (miscounted peaks due to limit of resolution in the beginning of the sequence read, nucleotide 'A' in fact be two A's, not accurate error)		
		254		TAGATC		Within modular DNA, 46 nucleotides outside the end (stop) codon of TRP1 marker		No

DNA ID (#)	**Name of the construct:** (*cdc13-1*-NTΔ-TRP1-PGAL1)	**Location of nucleotide**	**Nature of DNA mutations**			**Position of mutation (*cdc13-1* coding region, upstream/downstream non-coding sequence, TRP1 marker or promoter of modular DNA)**	**Amino acid modification**	**Protein Frame shift: (marker or truncated Cdc13-1 protein*)***
			Deletion	**Insertion**	**substitution**			
		1092	A?			Within TRP1 promoter region, not reliable		no
		1681	G?			*cdc13* C- half, mutation located within deletion primer (reverse), not reliable		Yes/*cdc13-CT*
10	1297-NTΔ #11	69, 78/79 upstream	A?			*CDC13* upstream (miscounted peaks due to limit of resolution in the beginning of the sequence read, nucleotide 'A' in fact be two A's, not accurate error)		
		254		TAGATC		Within modular DNA, 46 nucleotides outside the end (stop) codon of TRP1 marker		No
		821			A→G	Within coding sequence of TRP1 marker of modular DNA, codon 52 changed from ATT (Iso) to ACT (Thr) (double confirmed)	Change in codon/AA-52 of TRP1 marker from Ile to Thr	No
11	1297-NTΔ #12	69, 78/79 upstream	A?			*CDC13* upstream (miscounted peaks due to limit of resolution in the beginning of the sequence read, nucleotide 'A' in fact be two A's, not accurate error)		
		254		TAGATC		Within modular DNA, 46 nucleotides outside the end (stop) codon of TRP1 marker		No
12	1297-NTΔ #22	69, 78/79 upstream	A?			*CDC13* upstream (miscounted peaks due to limit of resolution in the beginning of the sequence read, nucleotide 'A' in fact be two A's, not accurate error)		
		254		TAGATC		Within modular DNA, 46 nucleotides outside the end (stop) codon of TRP1 marker		No

Table 4.8. Analysis of modifications in *cdc13-1*-C-truncated::ADH1-HIS3MX6 DNA from strains 1296-TR and 1297-TR mutants.

DNA ID (#)	**Name of the construct:** (*cdc13-1*-CTΔ-ADH1-HIS3MX6)	**Location of nucleotide**	**Nature of DNA mutations**			**Position of mutation (*cdc13-1* coding region, upstream/downstream non-coding sequence, HIS3MX6 marker DNA or its promoter or ADH1 terminator)**	**Amino acid modification**	**Protein Frame shift: (marker or truncated Cdc13-1 protein)**
			Deletion	**Insertion**	**substitution**			
13	1296-CTΔ #3	78/79 upstream	A?			*CDC13* upstream (miscounted peaks due to limit of resolution in the beginning of the sequence read, nucleotide 'A' in fact be two A's, not accurate error)		NO
		1763			C→T (Doubly confirmed)	Mutation within ADH1 terminator sequence at the start of HIS3MX6 modular DNA		NO
		2213			A→G (Doubly confirmed)	Mutation within TEF promoter before *S. pombe his5* gene of HIS3MX6 modular DNA		NO
14	1296-CTΔ #4	78 upstream	A?			*CDC13* upstream (miscounted peaks due to limit of resolution in the beginning of the sequence read, nucleotide 'A' in fact be two A's, not accurate error)		NO
		1763			C→T	Mutation within ADH1 terminator sequence at the start of HIS3MX6 modular DNA		NO
		2213			A→G	Mutation within TEF promoter before *S. pombe his5* gene of HIS3MX6 modular DNA		NO
15	1296-CTΔ #6	1763			C→T	Mutation within ADH1 terminator sequence at the start of HIS3MX6 modular DNA		NO
		3115			G→A	Mutation within TEF terminator, the end part of HIS3MX6 modular DNA (This mutation is also present in few other mutants)		
16	1296-CTΔ #7	1763			C→T	Mutation within ADH1 terminator sequence at the start of HIS3MX6 modular DNA		NO
		3115			G→A	Mutation within TEF terminator, the end part of HIS3MX6 modular DNA (This mutation is also present in few other mutants)		No
17	1296-CTΔ #9	1763			C→T	Mutation within ADH1 terminator sequence at the start of HIS3MX6 modular DNA		NO

DNA ID (#)	Name of the construct: (*cdc13-1*-CTΔ-ADH1-HIS3MX6)	Location of nucleotide	Nature of DNA mutations			Position of mutation (*cdc13-1* coding region, upstream/downstream non-coding sequence, HIS3MX6 marker DNA or its promoter or ADH1 terminator)	Amino acid modification	Protein Frame shift: (marker or truncated Cdc13-1 protein)
			Deletion	Insertion	substitution			
		3115			G→A	Mutation within TEF terminator, the end part of HIS3MX6 modular DNA (This mutation is also present in a few other mutants)		NO
		3306? Miscalled nucleotide at the start of sequence run?			G→A?	*CDC13* downstream sequence beyond deletion primer (This mutation is towards the start of sequence run, not very reliable) or modification could be in strain 1296-TR		NO
18	1296-CTΔ #10	1763			C→T	Mutation within ADH1 terminator sequence at the start of HIS3MX6 modular DNA		NO
		3115			G→A	Mutation within TEF terminator, the end part of HIS3MX6 modular DNA (This mutation is also present in a few other mutants)		NO
19	1297-CTΔ #3 (*cdc13-1* CTΔ)	1763			C→T	Mutation within ADH1 terminator sequence at the start of HIS3MX6 modular DNA		NO
		3306? Miscalled nucleotide at the start of R3-sequence runs?			G→A?	*CDC13* downstream sequence beyond deletion primer (This mutation is towards the start of sequence run, not very reliable) or modification could be in strain 1296-TR		NO
20	1297-CTΔ #4	1763			C→T	Mutation within ADH1 terminator sequence at the start of HIS3MX6 modular DNA		NO
		3306? Miscalled nucleotide at the start of R3-sequence runs?			G→A?	*CDC13* downstream sequence beyond deletion primer (This mutation is towards the start of sequence, not very reliable) or modification could be in strain 1296-TR		NO
		1763			C→T	Mutation within ADH1 terminator sequence at the start of HIS3MX6 modular DNA		NO
21	1297-CTΔ #7	1763			C→T	Mutation within ADH1 terminator sequence at the start of HIS3MX6 modular DNA		NO
		3306? Miscalled nucleotide at the start			G→A?	*CDC13* downstream sequence beyond deletion primer (This mutation is towards the start of sequence, not very		NO

DNA ID (#)	Name of the construct: (*cdc13-1*-CTΔ-ADH1-HIS3MX6)	Location of nucleotide	Nature of DNA mutations			Position of mutation (*cdc13-1* coding region, upstream/downstream non-coding sequence, HIS3MX6 marker DNA or its promoter or ADH1 terminator)	Amino acid modification	Protein Frame shift: (marker or truncated Cdc13-1 protein)
			Deletion	Insertion	substitution			
		of R3-sequence runs?				reliable) or modification could be in strain 1296-TR		
22	1297-CTΔ #8	1763			C→T	Mutation within ADH1 terminator sequence at the start of HIS3MX6 modular DNA		NO
		3306? Miscalled nucleotide at the start of R3-sequence runs?			G→A?	*CDC13* downstream sequence beyond deletion primer (This mutation is towards the start of sequence, not very reliable) or modification could be in strain 1296-TR		NO
23	1297-CTΔ #11	1763			C→T	Mutation within ADH1 terminator sequence at the start of HIS3MX6 modular DNA		NO
24	1297-CTΔ #12	1763			C→T	Mutation within ADH1 terminator sequence at the start of HIS3MX6 modular DNA		NO

The *Eco*R1 site was confirmed in the parent strains at position 1311 (Figure 4.10). No sequence modifications were found in the *cdc13-1* coding region in either parent strain 1296 or 1297. However, a few mutations were encountered in N-truncated and C-truncated constructs. These mutations were mainly substitution (occurrence 0-2 per read) with very few (0-1) deletion mutations. Insertion of six nucleotide sequence (TAGATC) was confirmed in every N-terminus-truncated mutant (100% of read) (Figure 4.11). This sequence lies within the modular DNA of marker cassette, 46 nucleotides outside the stop codon of the TRP1 marker at position 254. The *cdc13-1*-NTΔ mutants (in strain 1296-TR) #4, #5 and #6 did not show any mutations (Figure 4.12). Out of 8 substitution mutations identified in rest of the mutants (Figure 4.12 and 4.13), 5 lay within the coding region of the TRP1 marker (Figures 4.14-4.18), one outside the TRP1 marker within the 3' part of the deletion primer (not very reliable) (Figure 4.19) and one lay within the GAL1 promoter region (Figure 4.20). Only one substitution mutation was positioned within the C-terminus half of the *cdc13-1* gene (mutant #7 in strain 1297-TR) (Figure 4.21). However, it does not change the amino acid (codon 143 changes from GGC→GGA, but both encode glycine, a silent mutation) (Figure 4.21B). Only one nucleotide mismatch (deletion mutation?) was identified in NTΔ mutants #2 located within the deletion primer at the start of the C-terminus and might possibly shift the translational frame (however

not very reliable, seems sequencing error rather than a valid mutation from R2 chromatogram analysis) (Figure 4.22).

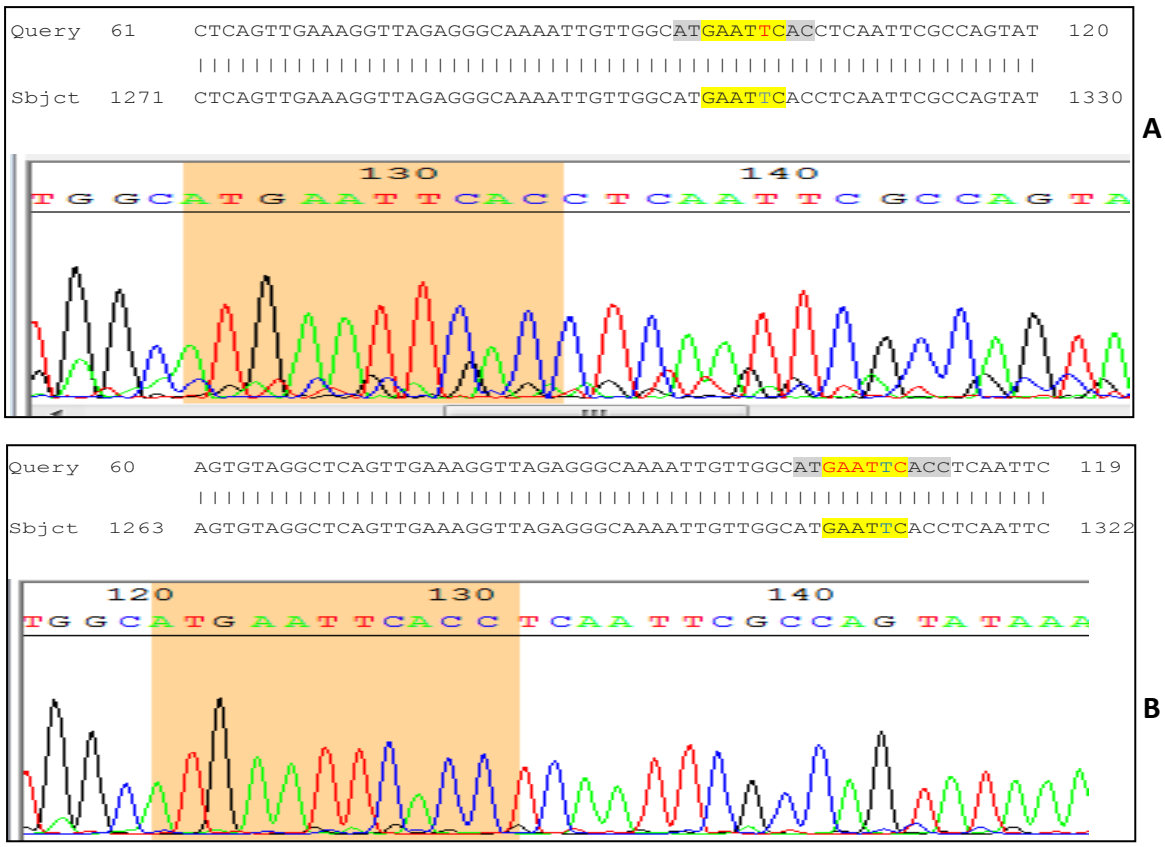

Figure 4.10. Confirmation of *Eco*R1 site in *cdc13-1* ORF sequence through sequencing of PCR fragment. Alignment of N1-sequence read (query) with that of reference sequence (subject) and N1-chromatogram shows *EcoR1* site (GAATTC) at position 1311 in 3 kb amplified DNA from genomic DNA of parent strain 1296-TR (**A**) and 1297-TR (**B**).

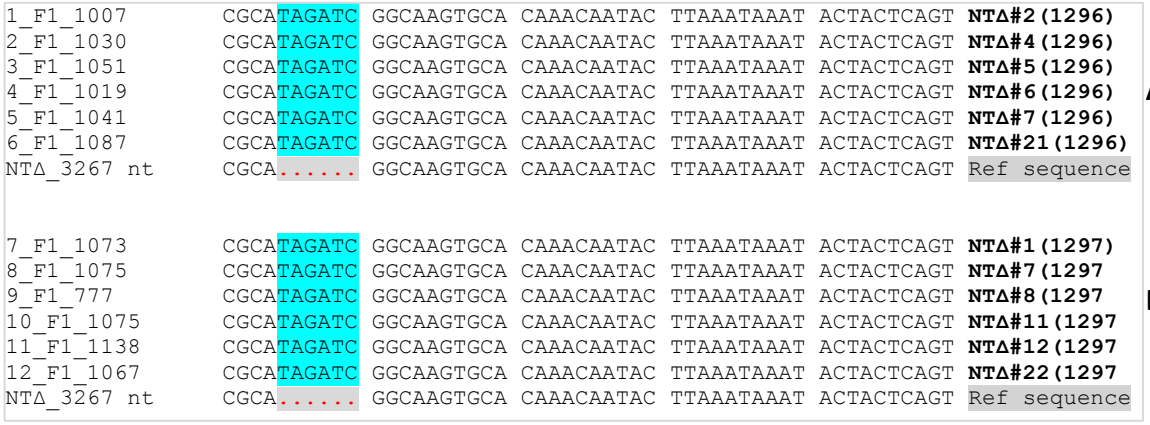

Figure 4.11. Confirmation of TAGATC sequence insertion in N-terminus truncated mutants at position 254 of the reference sequence.

Analysis of F1 sequence-reads by DNA alignment with the reference sequence of NTΔ manifests TAGATC six nucleotide sequence in all tested mutants. F1 sequences (1-12) were generated by automated sequencing of PCR fragments from genomic DNA of *cdc13-1* N-truncated mutants of strain 1296-TR (**A**) and 1297-TR (**B**). Whereas NTΔ reference sequence was constructed from *cdc13-1* C-terminus ORF sequence and modular DNA sequence from yeast plasmid, pFA6a-TRP1-PGAL1 as accessed from online resources.

Figure 4.12. Identification of two substitution mutations within coding region of TRP1 marker in NTΔ-TRP1 constructs (strain 1296) by alignment of F1 sequence reads.

Alignment of F1 sequence reads from six NTΔ-TRP1 (strain 1296) constructs shows substitution of nucleotide T with C in NTΔ clone #7 (**5**) at position 457 and in clone #21 (**6**) at position 462 of reference sequence. Conversely sequencing of PCR products from genomic DNA of NTΔ constructs #4 (2), #5 (3) and #6 (4) (strain 1296-TR) did not show any mutation.

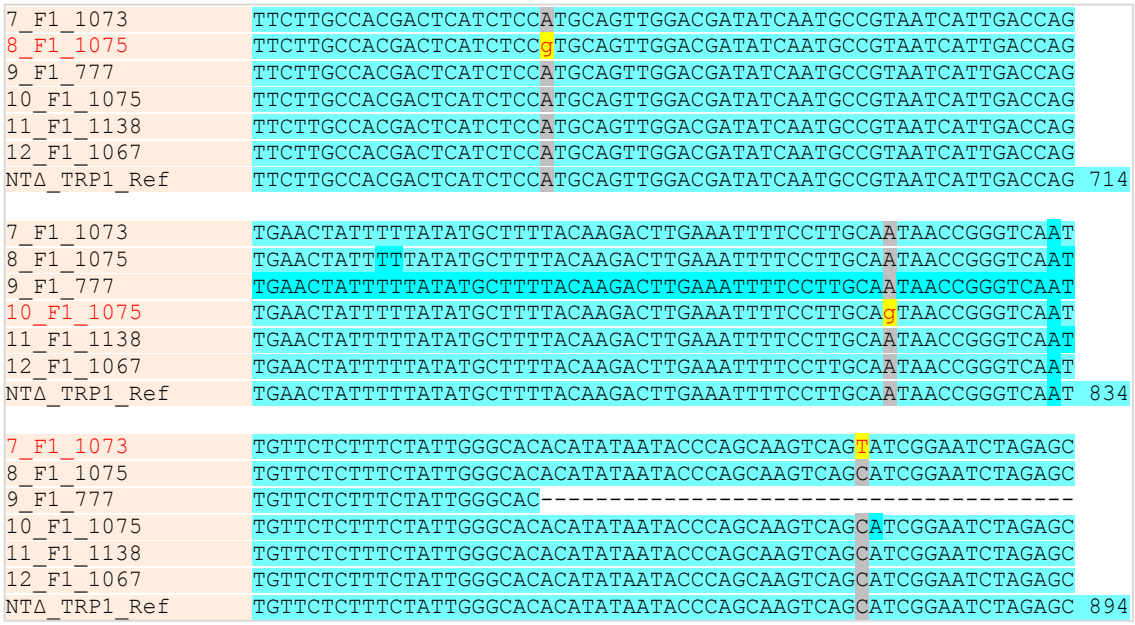

Figure 4.13. Identification of three substitution mutations within coding region of TRP1 marker in NTΔ-TRP1 constructs (strain 1297) by alignment of F1 sequence reads.

Alignment of F1 sequences from six NTΔ-TRP1 (strain 1297) constructs shows substitution of nucleotide A with G in NTΔ clone #7 (**8**) at position 676 and in clone #11 (**10**) at position 821 of reference sequence. F1 sequences alignment in mutant NTΔ clone #1 (**7**) shows substitution of nucleotide C with T at position 879 of construct. The DNA sequencing of PCR fragment from NTΔ constructs #8 (9) could not read sequence after nucleotide 855. F1 sequence alignment in this mutant could not detect any mutation between positions 855 and 894.

F1 text sequence from F1 sequence read of the construct **NTΔ#7(1296)**

```
Query  362   ATCACCAACATTTTCTGGCGTCAGTCCACCAGCTAACATAAAATGCAAGCTTTCGGGGCT  421
             ||||||||||||||||||||||||||||||||||||||||||||| ||||||||||||||
Sbjct  412   ATCACCAACATTTTCTGGCGTCAGTCCACCAGCTAACATAAAATGTAAGCTTTCGGGGCT  471
```

F1 chromatogram

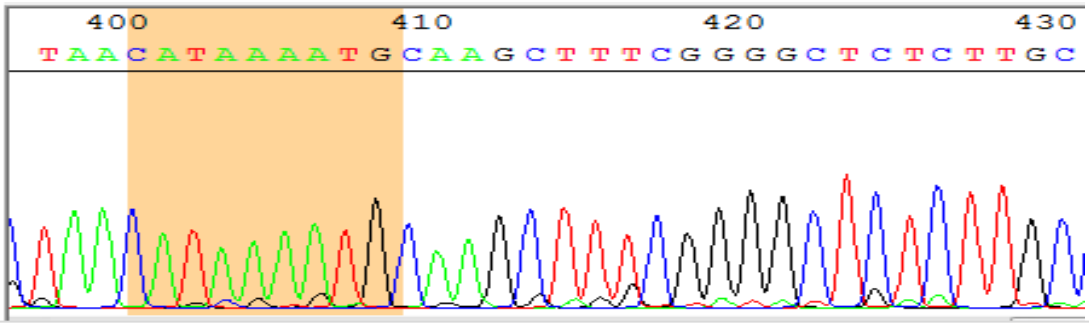


```
Query  481   TCTGACTGGGTTGGAAGGCAAGAGAGCCCCGAAAGCTTGCATTTTATGTTAGCTGGTGGA  540
             ||||||||||||||||||||||||||||||||||||| ||||||||||||||||||||      TRP1 DNA
Sbjct  481   TCTGACTGGGTTGGAAGGCAAGAGAGCCCCGAAAGCTTACATTTTATGTTAGCTGGTGGA  540
Query  121   VFPKDCNILLSAASQKPHSFIPLFDSEAGGTGELLDWNSISDWVGRQESPESLHFMLAGG  180
             ||||||||||||||||||||||||||||||||||||||||||||||||||||||||||||     TRP1 Protein
Sbjct  121   VFPKDCNILLSAASQKPHSFIPLFDSEAGGTGELLDWNSISDWVGRQESPESLHFMLAGG  180

codon 173 changed from TTA to TTG, both encode leucine amino acid
```

Figure 4.14. A silent substitution mutation in NTΔ::TRP1 clone #7 (1296-TR).

(**A**) Mapping of point mutation within construct sequence.

Alignment of F1-sequence (query) with that of reference sequence (subject) and F1-chromatogram show replacement of nucleotide T with C at position 457 of the construct.

(**B**) Mapping of the point mutation within TRP1 protein.

TRP1 coding sequence (query) from NTΔ::TRP1 clone #7 was aligned to that of reference sequence (subject) from yeast plasmid to map point mutation on the protein. This mutation at position 457 of mutant construct, corresponding to coding sequence position 519 of TRP1 marker will change codon 173 of TRP1 marker from TTA to TTG, both encode for leucine amino acid (a silent mutation).

F1 text sequence from F1 sequence read of the construct **NTΔ#21(1296)**

```
Query   364   ATCACCAACATTTTCTGGCGTCAGTCCACCAGCTAACATAAAATGTAAGCCTTCGGGGCT   423
              ||||||||||||||||||||||||||||||||||||||||||||||||||| |||||||||
Sbjct   412   ATCACCAACATTTTCTGGCGTCAGTCCACCAGCTAACATAAAATGTAAGCTTTCGGGGCT   471
```

F1 chromatogram (AAAATGTAAGCC)

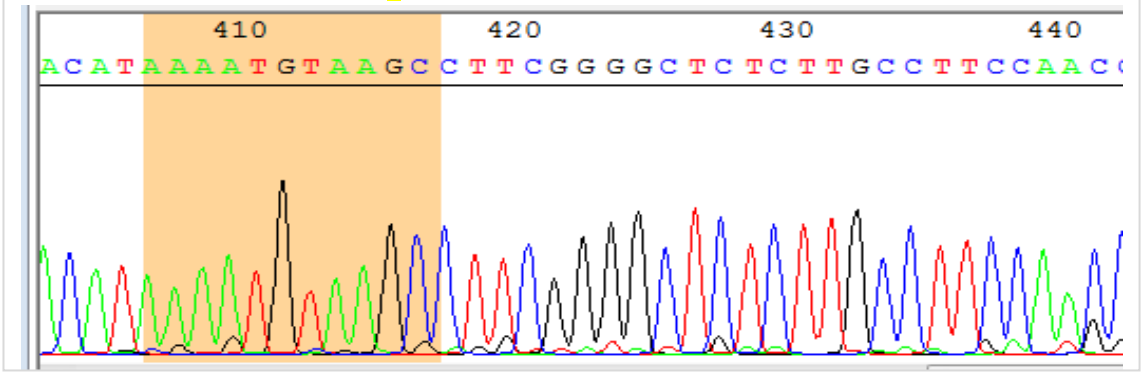


```
Query   481   TCTGACTGGGTTGGAAGGCAAGAGAGCCCCGAAGGCTTACATTTTATGTTAGCTGGTGGA   540
              |||||||||||||||||||||||||||||||| |||||||||||||||||||||||||  TRP1 DNA
Sbjct   481   TCTGACTGGGTTGGAAGGCAAGAGAGCCCCGAAAGCTTACATTTTATGTTAGCTGGTGGA   540

Query   121   VFPKDCNILLSAASQKPHSFIPLFDSEAGGTGELLDWNSISDWVGRQESPEGLHFMLAGG   180
              ||||||||||||||||||||||||||||||||||||||||||||||||.||||||||  TRP1 Protein
Sbjct   121   VFPKDCNILLSAASQKPHSFIPLFDSEAGGTGELLDWNSISDWVGRQESPESLHFMLAGG   180

Codon 172 changed from AGC to GGC, amino acid changed from S (Serine) to G (glycine)
```

Figure 4.15. A missense substitution mutation in the NTΔ::TRP1 clone #21 (1296-TR).

(**A**) Mapping of point mutation within construct sequence.

Alignment of F1-sequence (query) with that of reference sequence (subject) and F1-chromatogram show replacement of nucleotide T with C at position 462 of the construct.

(**B**) Mapping of the point mutation within TRP1 protein.

TRP1 coding sequence (query) from NTΔ::TRP1 clone #21 was aligned to that of reference sequence (subject) from yeast plasmid to map point mutation on the protein. This mutation at position 462 of mutant construct, corresponding to coding sequence position 514 of TRP1 marker will change codon 172 of TRP1 marker from AGC (serine) to GGC (glycine), a missense point mutation.

F1 text sequence from F1 sequence read of the construct **NTΔ#1(1297)**

```
Query  783   CTCTTTCTATTGGGCACACATATAATACCCAGCAAGTCAGTATCGGAATCTAGAGCACAT  842
             ||||||||||||||||||||||||||||||||||||||| ||||||||||||||||||
Sbjct  839   CTCTTTCTATTGGGCACACATATAATACCCAGCAAGTCAGCATCGGAATCTAGAGCACAT  898
```

F1 chromatogram with highlighted sequence GCAAGTCAGT

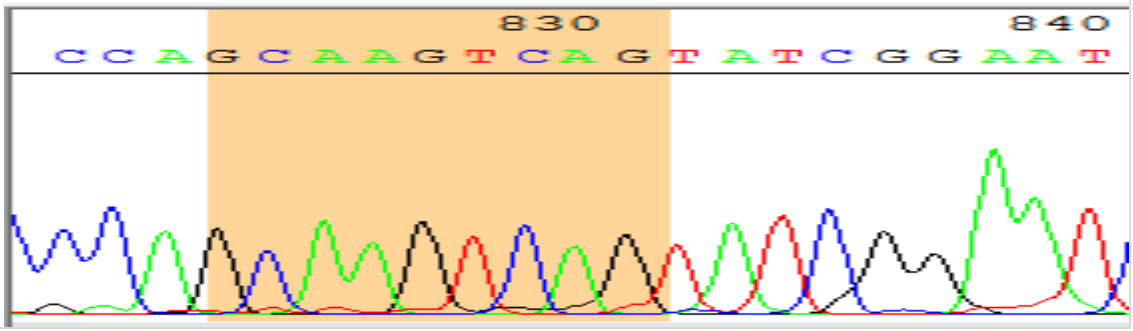


```
Query  61    AGCACAGAGGCCGCAGAATGTGCTCTAGATTCCGATACTGACTTGCTGGGTATTATATGT  120
             |||||||||||||||||||||||||||||||||||| |||||||||||||||||||||| TRP1 DNA
Sbjct  61    AGCACAGAGGCCGCAGAATGTGCTCTAGATTCCGATGCTGACTTGCTGGGTATTATATGT  120

Query  1     MSVINFTGSSGPLVKVCGLQSTEAAECALDSDTDLLGIICVPNRKRTIDPVIARKISSLV  60
             ||||||||||||||||||||||||||||||.||||||||||||||||||||||||||||  TRP1 Protein
Sbjct  1     MSVINFTGSSGPLVKVCGLQSTEAAECALDSDADLLGIICVPNRKRTIDPVIARKISSLV  60
```

Codon 33 changed from GCT to ACT, amino acid changed from A (Alanine) to T (Threonine)

Figure 4.16. A missense substitution mutation in the NTΔ::TRP1 clone #1 (1297-TR).

(**A**) Mapping of point mutation within construct sequence.

Alignment of F1-sequence (query) with that of reference sequence (subject) and F1-chromatogram show replacement of nucleotide C with T at position 879 of the construct.

(**B**) Mapping of the point mutation within TRP1 protein.

TRP1 coding sequence (query) from NTΔ::TRP1 clone #1 was aligned to that of reference sequence (subject) from yeast plasmid to map point mutation on the protein. This mutation at position 879 of mutant construct, corresponding to coding sequence position 97 of TRP1 marker will change codon 33 of TRP1 marker from GCT (alanine) to ACT (threonine), a missense point mutation. This mutation was also confirmed in overlapping R1 sequence read.

F1 text sequence from F1 sequence read of the construct **NTΔ#7(1297)**

```
Query  602   GCCACGACTCATCTCCGTGCAGTTGGACGATATCAATGCCGTAATCATTGACCAGAGCCA  661
              ||||||||||||||||| ||||||||||||||||||||||||||||||||||||||||
Sbjct  660   GCCACGACTCATCTCCATGCAGTTGGACGATATCAATGCCGTAATCATTGACCAGAGCCA  719
```

F1 chromatogram with highlighted sequence CTCATCTCCG

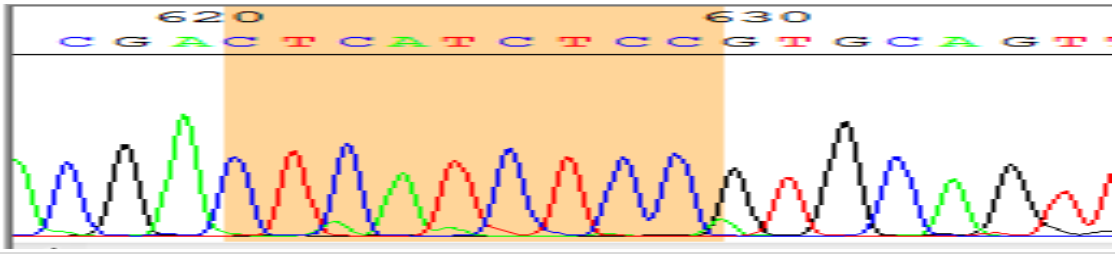


```
Query  241   CCTAAGGAGGATGTTTTGGCTCTGGTCAATGATTACGGCATTGATATCGTCCAACTGCAC  300
              ||||||||||||||||||||||||||||||||||||||||||||||||||||||||||   TRP1 DNA
Sbjct  241   CCTAAGGAGGATGTTTTGGCTCTGGTCAATGATTACGGCATTGATATCGTCCAACTGCAT  300

Query  61    KAYKNSSGTPKYLVGVFRNQPKEDVLALVNDYGIDIVQLHGDESWQEYQEFLGLPVIKRL  120
              ||||||||||||||||||||||||||||||||||.||||||||||||||||||||||||   TRP1 Protein
Sbjct  61    KAYKNSSGTPKYLVGVFRNQPKEDVLALVNDYGIDIVQLHGDESWQEYQEFLGLPVIKRL  120
```

Codon 100 changed from **CAT** to **CAC**, both encode amino acid **H** (Histidine)

Figure 4.17. A silent substitution mutation in the NTΔ::TRP1 clone #7 (1297-TR).

(**A**) Mapping of point mutation within construct sequence.

Alignment of F1-sequence (query) with that of reference sequence (subject) and F1-chromatogram show replacement of nucleotide A with G at position 676 of the construct.

(**B**) Mapping of the point mutation within TRP1 protein.

TRP1 coding sequence (query) from NTΔ::TRP1 clone #7 was aligned to that of reference sequence (subject) from yeast plasmid to map point mutation on the protein. This mutation (positioned at nucleotide 300) will change codon 100 of TRP1 marker from CAT to CAC, both encode for histidine amino acid, a silent point mutation. This mutation was also confirmed in overlapping R1 sequence read.

F1 text sequence from F1 sequence read of the construct **NTΔ#11(1297)** **A**

```
Query  722   TATTTTTATATGCTTTTACAAGACTTGAAATTTTCCTTGCAGTAACCGGGTCAATTGTTC  781
             ||||||||||||||||||||||||||||||||||||||| ||||||||||||||||||
Sbjct  780   TATTTTTATATGCTTTTACAAGACTTGAAATTTTCCTTGCAATAACCGGGTCAATTGTTC  839
```

F1 chromatogram with highlighted sequence TTTCCTTGCAG

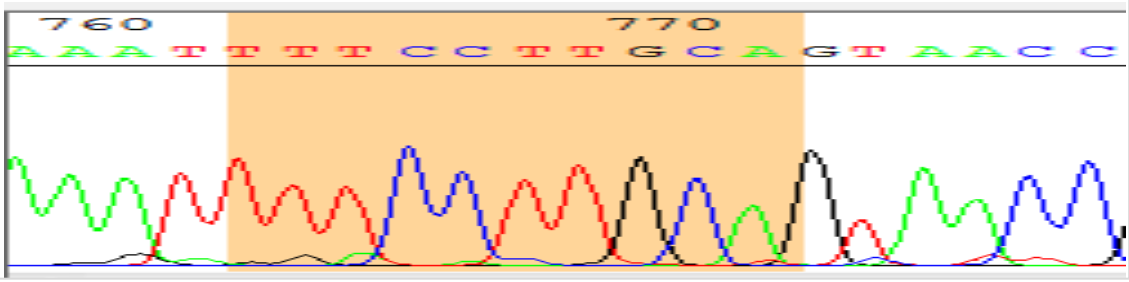

B

```
Query  121   GTGCCCAATAGAAAGAGAACAATTGACCCGGTTACTGCAAGGAAAATTTCAAGTCTTGTA  180
             ||||||||||||||||||||||||||||||||.||||||||||||||||||||||||||  TRP1 DNA
Sbjct  121   GTGCCCAATAGAAAGAGAACAATTGACCCGGTTATTGCAAGGAAAATTTCAAGTCTTGTA  180

Query  1     MSVINFTGSSGPLVKVCGLQSTEAAECALDSDADLLGIICVPNRKRTIDPVTARKISSLV  60
             ||||||||||||||||||||||||||||||||||||||||||||||||||.||||||||  TRP1 Protein
Sbjct  1     MSVINFTGSSGPLVKVCGLQSTEAAECALDSDADLLGIICVPNRKRTIDPVIARKISSLV  60
```

Codon 52 changed from **ATT** to **ACT**, amino acid changed from I (Isoleucine) to T (Threonine)

Figure 4.18. A missenses substitution mutation in *cdc13-1* NTΔ::TRP1 clone #11 (1297-TR).

(**A**) Mapping of point mutation within construct sequence.

Alignment of F1-sequence (query) with that of reference sequence (subject) and F1-chromatogram show replacement of nucleotide A with G at position 821 of the construct.

(**B**) Mapping of the point mutation within TRP1 protein.

TRP1 coding sequence (query) from NTΔ::TRP1 clone #11 was aligned to that of reference sequence (subject) from yeast plasmid to map point mutation on the protein. This mutation positioned at nucleotide 155, will change codon 52 of TRP1 marker from ATT (isoleucine) to ACT (threonine), a missense point mutation. This mutation was also confirmed in overlapping R1 sequence read.

1_F1_1007	GTGGAAACTATCGCCTAAAAGAATTCGAGCTCGTTTAACCTCCTTACGCATCTGTGCGG	
2_F1_1030	GTGGAAACTATCGCCTAAAAGAATTCGAGCTCGTTTAAACCTCCTTACGCATCTGTGCGG	
3_F1_1051	GTGGAAACTATCGCCTAAAAGAATTCGAGCTCGTTTAAACCTCCTTACGCATCTGTGCGG	A
4_F1_1019	GTGGAAACTATCGCCTAAAAGAATTCGAGCTCGTTTAAACCTCCTTACGCATCTGTGCGG	
5_F1_1041	GTGGAAACTATCGCCTAAAAGAATTCGAGCTCGTTTAAACCTCCTTACGCATCTGTGCGG	
6_F1_1087	GTGGAAACTATCGCCTAAAAGAATTCGAGCTCGTTTAAACCTCCTTACGCATCTGTGCGG	
NTΔ_TRP1_Ref	GTGGAAACTATCGCCTAAAAGAATTCGAGCTCGTTTAAACCTCCTTACGCATCTGTGCGG	240

F1 text sequence from F1 sequence read of the construct **NTΔ#2 (1296)**

```
Query  120  TCGCCTAAAAGAATTCGAGCTCGTTTAACCTCCTTACGCATCTGTGCGGTATTTCACAC  179
            ||||||||||||||||||||||||||| ||||||||||||||||||||||||||||||
Sbjct  191  TCGCCTAAAAGAATTCGAGCTCGTTTAAACCTCCTTACGCATCTGTGCGGTATTTCACAC  250
```

B

F1 chromatogram with highlighted sequence CGAGCTCGTTTAAC

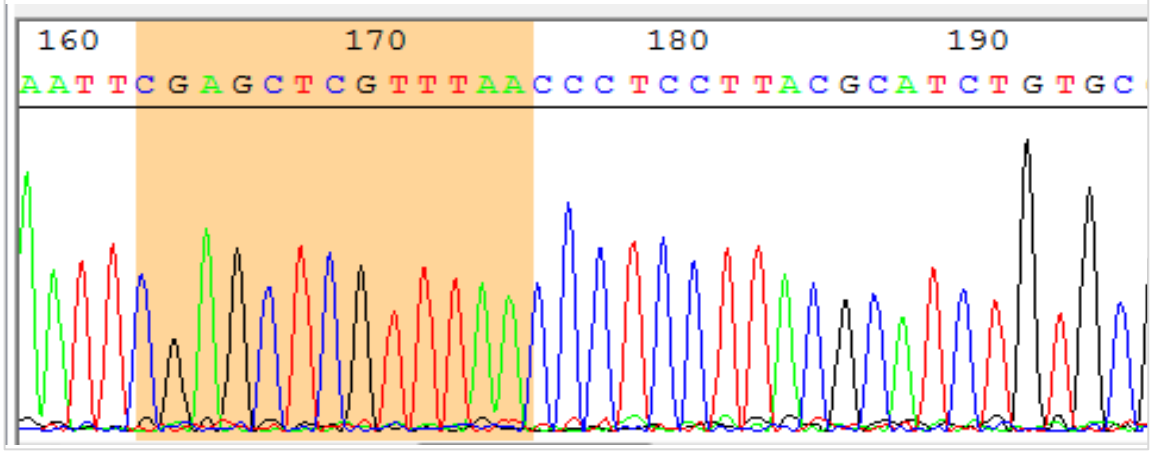

Figure 4.19. Identification of one substitution mutations outside TRP1 coding region in NTΔ::TRP1 clone #2 (strain 1296).

(**A**) Identification of substitution mutations by multiple sequence alignment.
Alignment of F1 sequences from six NTΔ::TRP1 (strain 1296) constructs shows a substitution mutation in NTΔ clone #2 which replaces nucleotide A with C at position 219 of the reference sequence. This mutation is positioned within F4 primer of TRP1 marker of modular DNA and being within 3'part of deletion primer, not very reliable modification.
(**B**) Confirmation of substitution mutation in NTΔ::TRP1 clone #2 (1296-TR) by F1-chromatogram.
Alignment of F1-sequence (query) with that of reference sequence (subject) and F1-chromatogram show replacement of nucleotide A with C at sequence position 219. This is the part of the forward deletion primer (F4 TRP1) with less chances of modification, however two sequencing reactions confirmed this modification.

R1 text sequence from R1 sequence read (reverse complement) from the construct **NTΔ#21 (1296)**

```
Query   132    TAGGATGATAATGCGACTAGTTNTTTAGCCTTATTTCTGGGGTAATTAATCAGCGAAGCG   191
               ||||||||||||||||| ||||| ||||||||||||||||||||||||||||||||||||
Sbjct   1441   TAGGATGATAATGCGATTAGTTTTTTAGCCTTATTTCTGGGGTAATTAATCAGCGAAGCG   1500
```

The reverse complement of sequence ATAATGCGAC is GTCGCATTAT.

R1 chromatogram with highlighted sequence GTCGCATTAT.

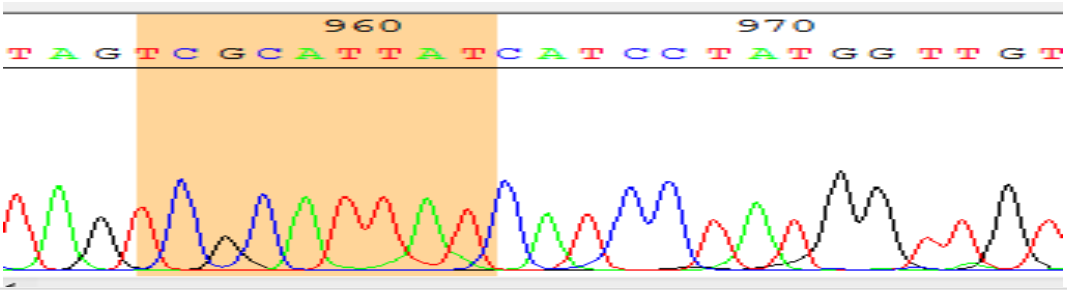

Figure 4.20. A substitution mutation in NTΔ::TRP1 clone #21 (1296-TR).
Alignment of R1-sequence (query) with that of reference sequence (subject) and R1-chromatogram show replacement of nucleotide T with C at sequence position 1457 of the reference DNA. This modification is positioned within *GAL1* promoter sequence and was also confirmed in overlapping R2 sequence.

R2 text sequence from R2 sequence read (reverse complement) from the construct **NTΔ#7 (1297)**

```
Query   721    CTCAGAAAAATATTCAACAACGGGCTAAGAGATCTACAGAACGGACGCGATGAAAACCTT   780
               ||||||||||||||||||||||||||||||||||||||||||||| ||||||||||||||||
Sbjct   2063   CTCAGAAAAATATTCAACAACGGGCTAAGAGATCTACAGAACGGCCGCGATGAAAACCTT   2122
```

The reverse complement of sequence CAGAACGGA is TCCGTTCTG.

R2 chromatogram with highlighted sequence TCCGTTCTG.

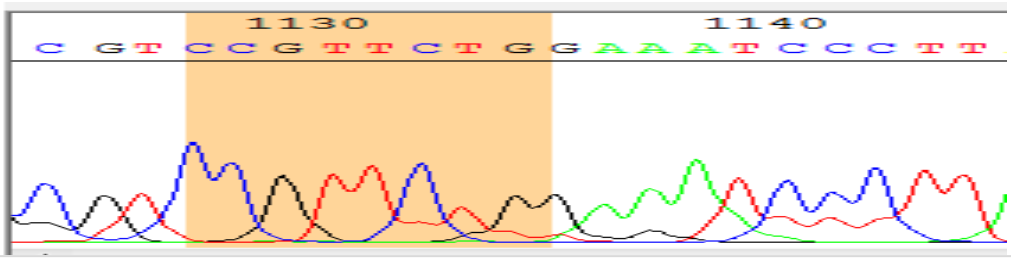


```
Query   421    CAGAACGGACGCGATGAAAACCTTTCGCAATACGGCATAGTTTGTAAGATGAATATAAAA   480
               |||||||| ||||||||||||||||||||||||||||||||||||||||||||||||||||  cdc13-1 C-terminus DNA
Sbjct   421    CAGAACGGCCGCGATGAAAACCTTTCGCAATACGGCATAGTTTGTAAGATGAATATAAAA   480

Query   121    QFETFDSKLRKIFNNGLRDLQNGRDENLSQYGIVCKMNIKVKMYNGKLNAIVRECEPVPH   180
               ||||||||||||||||||||||||||||||||||||||||||||||||||||||||||||  Cdc13-1 C-terminus protein
Sbjct   121    QFETFDSKLRKIFNNGLRDLQNGRDENLSQYGIVCKMNIKVKMYNGKLNAIVRECEPVPH   180
```

Codon 143 changed from GGC to GGA, both encode amino acid G (Glycine)

Figure 4.21. A substitution mutation in NTΔ::TRP1 clone #7 (strain 1297-TR).
Alignment of R2-sequence (query) with that of reference sequence (subject) and R2-chromatogram show replacement of nucleotide C with A at sequence position 2107. This modification is positioned within *cdc13-1* C-terminus coding sequence and will change codon 143 from GGC to GGA, both encode for amino acid glycine (a silent mutation).

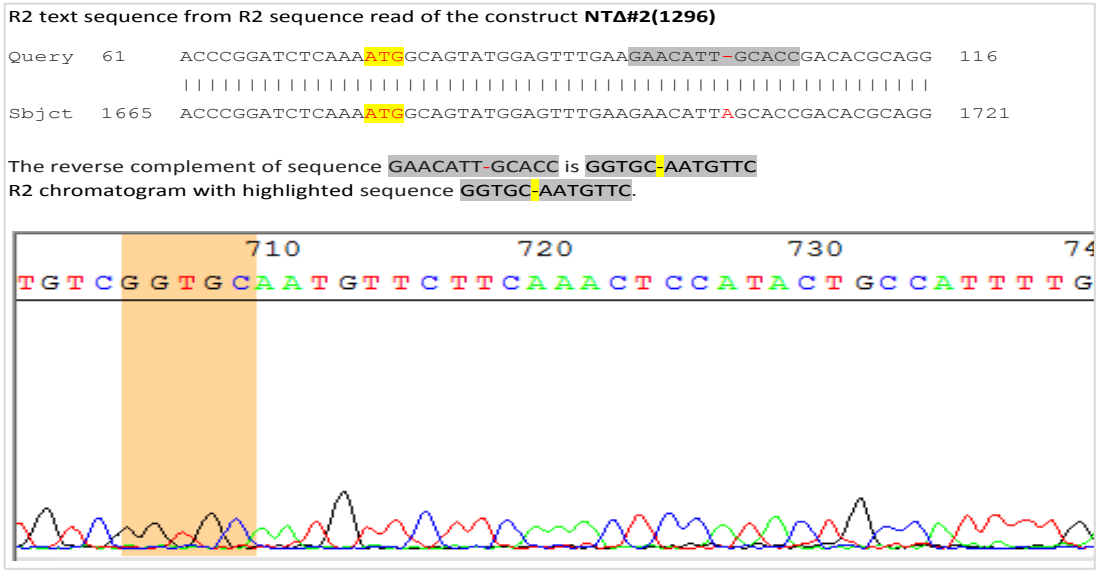

Figure 4.22. A deletion mutation (?) in NTΔ::TRP1 clone #2 (strain 1296) mutant.
Alignment of R2-sequence (query) with that of reference sequence (subject) and R2-chromatogram show nucleotide A missing at sequence position 1706. R2 chromatogram show two broad green peaks (less well resolved) which might indicates three A's not two as mis-counted by computer program This modification lies within deletion primer at the start of the *cdc13-1* C-terminus coding sequence. This mutation being in the beginning of the sequence read not very reliable however can shift frame of the encoded protein.

Homology analysis of C-terminus-truncated mutants with a theoretical (expected) sequence identified 24 substitution mutations (1-3 per sequence read). In 12 of these mutations, a single nucleotide 'C' is replaced with 'T' at position 1763 of all constructs (100%). This modification lies within the ADH1 terminator sequence and common in all tested mutants (Figure 4.23), might possibly be an alteration in the original sequence of the construct not reported in the sequences accessed online. The two substitution mutations were identified at position 2213 (TEF promoter) and occurred in two C-terminus-truncated mutants (#3 and #4) in which nucleotide 'A' was replaced with 'G' (Figure 4.24). In the same way, two other substitution mutations that replaced nucleotide G →A identified at position 3115 and 3306, are common in 4 (Figure 4.25 and 4.26) and 5 mutants (Figure 4.27) respectively. The first one is located within the TEF terminator, but the second one, lying downstream of *CDC13* at the start of the sequence read, is not very reliable (more like a computer program error in nucleotide read not a valid mutation). None of these mutation occurred in the coding region of the protein (Cdc13-1-C-terminus). Moreover, there was no deletion mutation identified in C-terminus-truncated constructs and the *Eco*R1 site was also confirmed in the C-terminus-truncated mutants at position 1311 within the N-terminus (Figure 4.28).

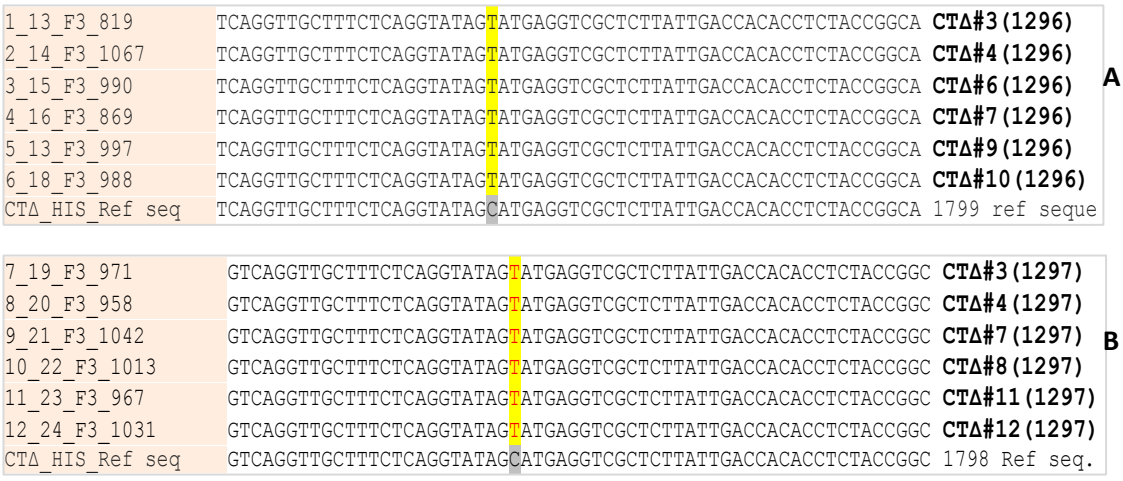

Figure4.23. Alignment of F3 sequences show substitution mutation (C to T) at position 1763 located within ADH1 terminator sequence in *cdc13-1* CTΔ::ADH1-HIS3MX6 constructs.

F3 sequences (1-12) in all tested mutants were generated by automated sequencing of PCR fragments from genomic DNA of *cdc13-1* C-truncated mutants of strain 1296-TR (**A**) and 1297-TR (**B**). Whereas CTΔ reference sequence was constructed from *cdc13-1* N-terminus ORF sequence and modular DNA sequence from yeast plasmid, pFA6a-ADH1-HIS3MX6 as accessed from online resources.

```
1_13_F3_819          CCTTTTAAAATCTTGCTAGGATACAGTTCTCACATCACATCCGAACATAAACAgCCATGG CTΔ#3(1296)
2_14_F3_1067         CCTTTTAAAATCTTGCTAGGATACAGTTCTCACATCACATCCGAACATAAACAgCCATGG CTΔ#4(1296)
3_15_F3_990          CCTTTTAAAATCTTGCTAGGATACAGTTCTCACATCACATCCGAACATAAACAACCATGG CTΔ#6(1296)
4_16_F3_869          CCTTTTAAAATCTTGCTAGGATACAGTTCTCACATCACATCCGAACATAAACAACCATGG CTΔ#7(1296)
5_13_F3_997          CCTTTTAAAATCTTGCTAGGATACAGTTCTCACATCACATCCGAACATAAACAACCATGG CTΔ#9(1296)
6_18_F3_988          CCTTTTAAAATCTTGCTAGGATACAGTTCTCACATCACATCCGAACATAAACAACCATGG CTΔ#10(1296)
CTΔ_HIS_Ref seq      CCTTTTAAAATCTTGCTAGGATACAGTTCTCACATCACATCCGAACATAAACAACCATGG 2219 Ref seq
```

A

```
7_19_F3_971          TCCTTTTAAAATCTTGCTAGGATACAGTTCTCACATCACATCCGAACATAAACAACCATG CTΔ#3(1297)
8_20_F3_958          TCCTTTTAAAATCTTGCTAGGATACAGTTCTCACATCACATCCGAACATAAACAACCATG CTΔ#4(1297)
9_21_F3_1042         TCCTTTTAAAATCTTGCTAGGATACAGTTCTCACATCACATCCGAACATAAACAACCATG CTΔ#7(1297)
10_22_F3_1013        TCCTTTTAAAATCTTGCTAGGATACAGTTCTCACATCACATCCGAACATAAACAACCATG CTΔ#8(1297)
11_23_F3_967         TCCTTTTAAAATCTTGCTAGGATACAGTTCTCACATCACATCCGAACATAAACAACCATG CTΔ#11(1297)
12_24_F3_1031        TCCTTTTAAAATCTTGCTAGGATACAGTTCTCACATCACATCCGAACATAAACAACCATG CTΔ#12(1297
CTΔ_3365             TCCTTTTAAAATCTTGCTAGGATACAGTTCTCACATCACATCCGAACATAAACAACCATG 2218 Ref seq
```

B

Sequence read with F3 primer (query) and its chromatogram from mutant CTΔ#3 (1296-TR)

```
Query  541   TCTTGCTAGGATACAGTTCTCACATCACATCCGAACATAAACAGCCATGGCAGAACCAGC  600
              ||||||||||||||||||||||||||||||||||||||||||| ||||||||||||||||
Sbjct  2170  TCTTGCTAGGATACAGTTCTCACATCACATCCGAACATAAACAACCATGGCAGAACCAGC  2229
```

F3 chromatogram with highlighted sequence GAACATAAACA shows nucleotide G at position 603

C

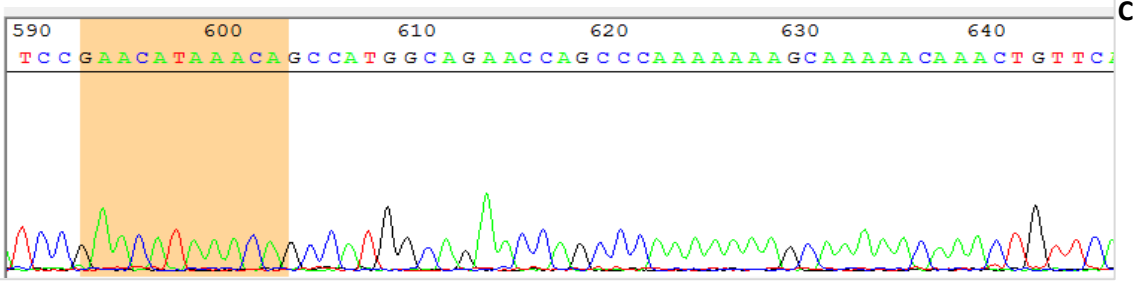

Sequence read with F3 primer (query) and its chromatogram from mutant CTΔ#4 (1296-TR)

```
Query  544   GATACAGTTCTCACATCACATCCGAACATAAACAGCCATGGCAGAACCAGCCCaaaaaaa  603
              ||||||||||||||||||||||||||||||||| ||||||||||||||||||||||||
Sbjct  2179  GATACAGTTCTCACATCACATCCGAACATAAACAACCATGGCAGAACCAGCCCAAAAAAA  2238
```

F3 chromatogram with highlighted sequence ACATAAACA, shows nucleotide G at position 602

D

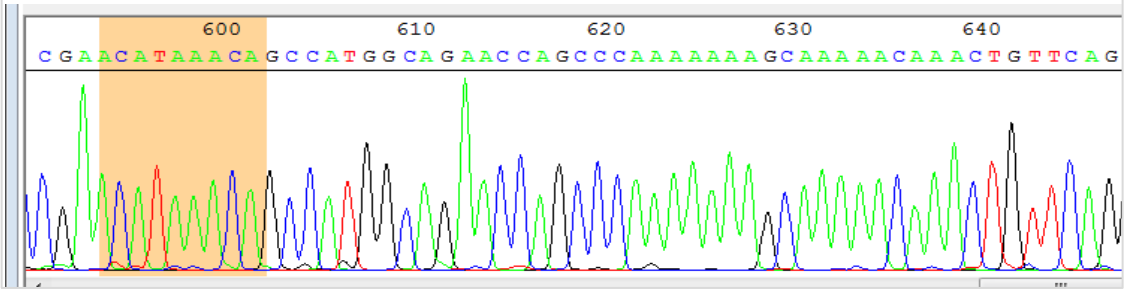

Figure 4.24. Two mutants of *cdc13-1* CTΔ (#3 and #4 in strain 1296) show substitution of A with T at position 2213.

Alignment of F3-sequences with that of CTΔ construct sequence show this substitution mutation (**A** and **B**), positioned within TEF promoter region of His marker (**C** and **D**).

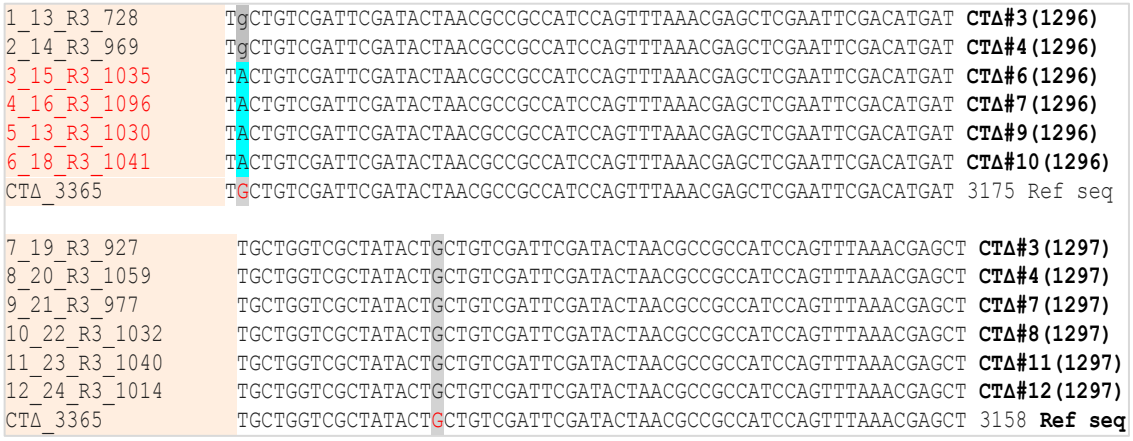

Figure 4.25. Identification of substitution of G with A at position 3115 in four mutants of *cdc13-1* CTΔ (1296-TR) by alignment of R3 sequences.

R3-sequences alignment from all tested mutants with that of CTΔ construct sequence show this substitution mutation in four CTΔ clones #6 (**3**), #7 (**4**), #9 (**5**) and #10 (**6**) in strain 1296-TR. This mutation is positioned within TEF terminator region of His marker. All six tested clones in strain 1297-TR (**7-12**) do not show this mutation.

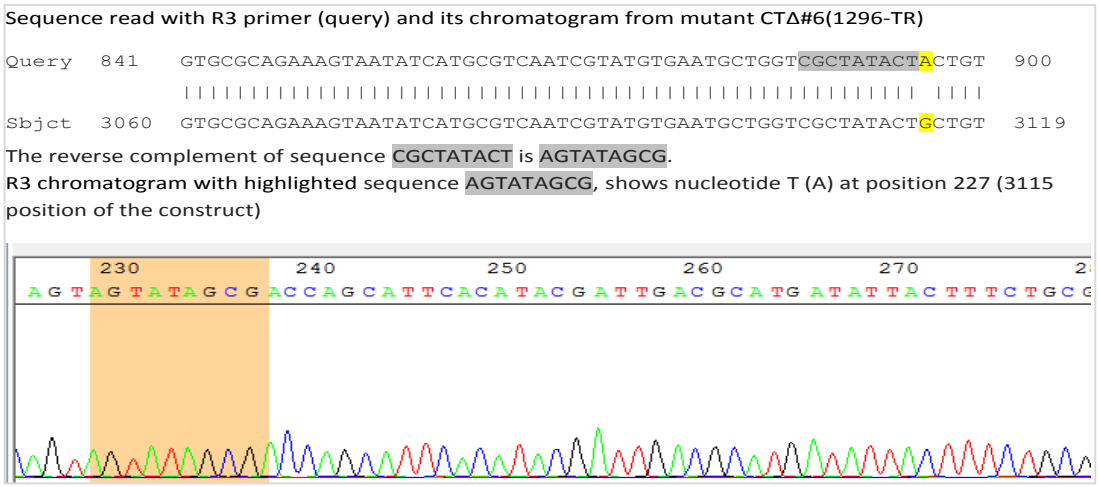

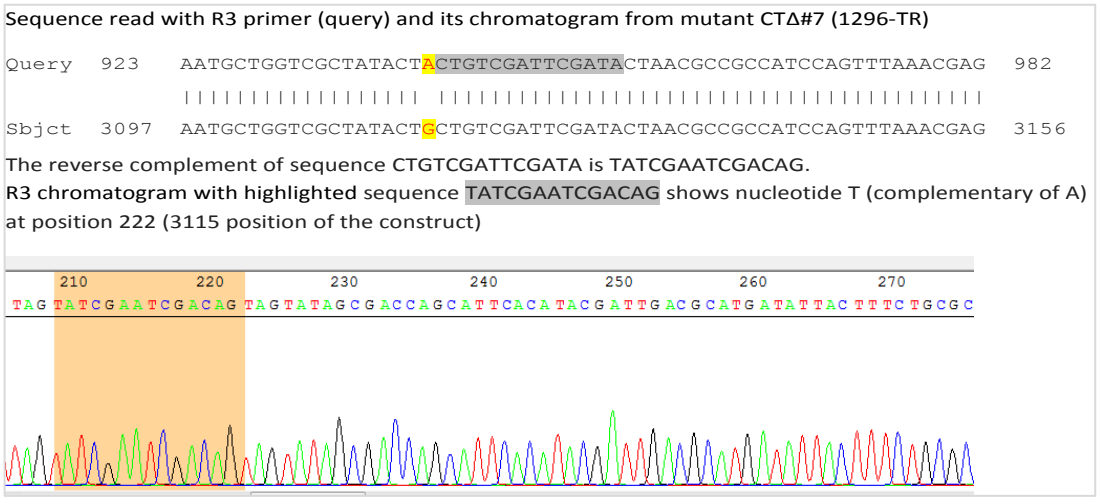

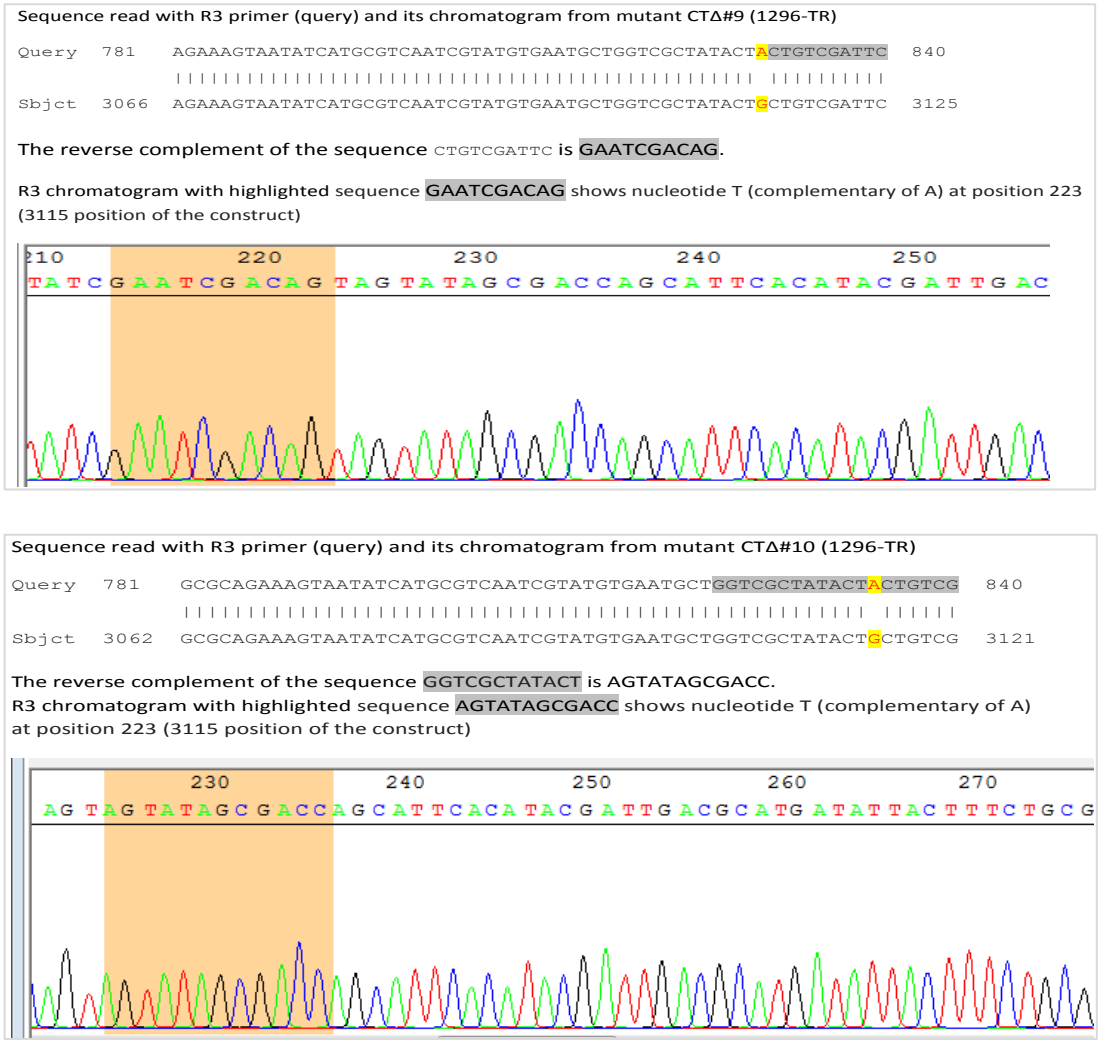

Figure 4.26. Confirmation of substitution mutation at sequence position 3115 in CTΔ::HIS3MX6 clones (1296-TR).

Alignment of R3-sequences (query) with that of reference sequence (subject) and R3-chromatogram from four CTΔ clones, #6 (**A**), #7 (**B**), #9 (**C**) and #10 (**D**) show replacement of nucleotide G with A at sequence position 3115 in TEF terminator region of His3MX6 marker.

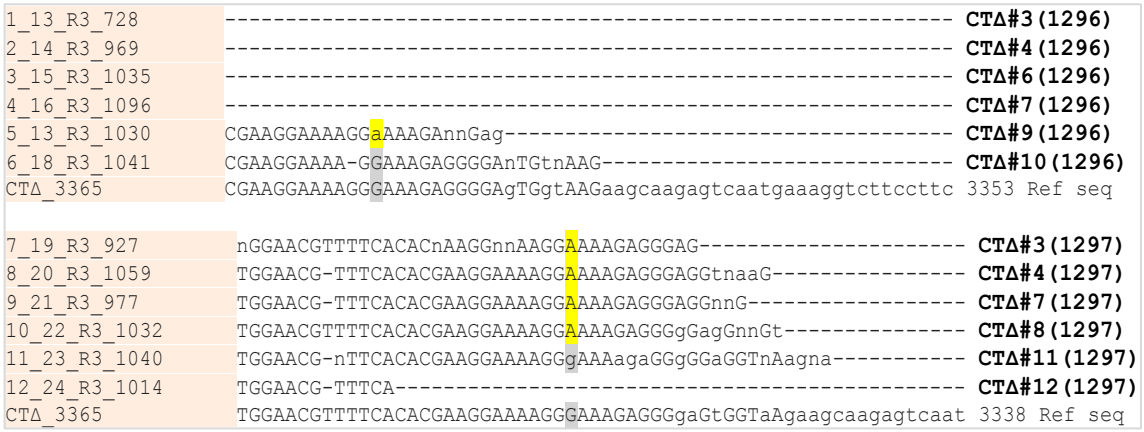

Figure 4.27. Identification of substitution of G with A at position 3306 in fiver clones of *cdc13-1* CTΔ by alignment of R3 sequences.

R3-sequences alignment from tested mutants in strain 1296-TR (**1-6**) and in strain 1297-TR (**7-12**) with that of CTΔ construct sequence show this substitution mutation in five CTΔ clones #9 (**5**, #3 (**7**), #4 (**8**), #7 (**9**) and #8 (**10**). This mismatched nucleotide is located in the start of R3 sequence and not reliable.

Figure 4.28. Confirmation of *Eco*R1 restriction site at position 1311 of the *cdc13-1* CTΔ::ADH1-HIS3MX6 constructs in strain 1296-TR and 1297-TR.
Alignment of F2 sequences from twelve clones show conserved *Eco*R1 site in all tested mutants sequences (aligned by MUSCLE, multiple sequence alignment tool (http://www.ebi.ac.uk/Tools/msa/muscle/).

4.3.2. Studying telomere length patterns in *CDC13* and *STN1* deletion mutants in the presence of *EXO1* deletion.

4.3.2.1. Extraction of total DNA and *Xho*1 digestion of genomic DNA

Southern blot hybridisation of telomeric DNA patterns were studied in *Xho*1-digested genomic DNA from the mutants without essential telomere binding proteins Cdc13 and Stn1 (either alone or in combination), or without either the N- or C-terminus of the essential protein (Cdc13). The genomic DNAs isolated from wild type yeast strains (strains 640 and 641 with *CDC13*) and Cdc13-1 mutants (strains 1296-TR and 1297-TR) were used as controls. Yeast cells primarily selected on dropout media were then grown on YEPD medium for 3 days at different temperatures - 23°C, 30°C or 37°C - as required. DNA was isolated from a loopful of cells, resuspended slowly at 4°C and analysed on agarose gels.

Figure 4.29 shows the results of a representative gel with genomic DNA isolated from *cdc13*Δ and/or *stn1*Δ mutants in the presence of *exo1*Δ. The high molecular weight intact bands on the analytical gel represented the desired genomic DNA. Similarly, the genomic DNA was prepared from *cdc13-1*-N-and C-terminus deletion mutants and from original strains of survivors, 1296-TR and 1297-TR.

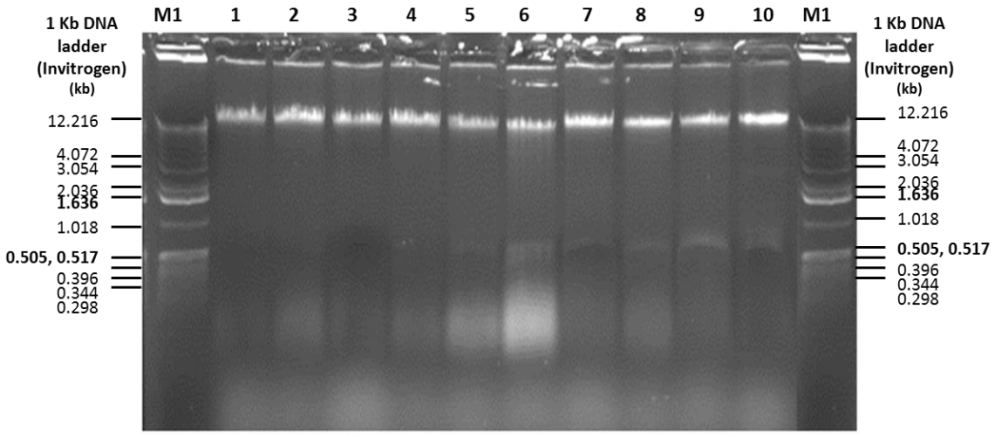

Figure 4.29. A representative analytical gel after electrophoresis of genomic DNA from wild type and mutant strains with *cdc13* and/or *stn1* deletion in the presence of *exo1*Δ.

For each sample, 2 µl of genomic DNA was examined on a 0.7% agarose gel.

lanes M1: 1 kb marker (Invitrogen) 1 µg (0.1 µg/µl); **1-2**: total DNA from strains 640 and 641 (WT); **3-4**: total DNA from strains 1272 and 1273 (*exo1*Δ); **5-6**: total DNA from haploids strains #14 and #21 (*stn1*Δ *exo1*Δ *rad*24Δ); **7-8**: total DNA from strains 2607 and 2608 (*cdc13*Δ *exo1*Δ); **9-10**: total DNA from strains 2684 and 2685 (*cdc13*Δ *stn1*Δ *exo1*Δ *rad*24Δ).

The mutant cultures were selected on dropout media. Single, well separated colonies were cultivated onto YEPD plates for three days at 30°C. For *stn1*Δ (haploids #14 and #21), two types of colonies with slight differences in colour, light and dark shades, were observed. Light coloured colonies were selected and subcultured for the isolation of DNA. The fresh cultures from plate (passage 3) were used to isolate total DNA. The extracted genomic DNA was dissolved in 100 µl 1x TE buffer at 4°C overnight. Two independent DNA samples, from wild type (strains 640 and 641, lanes 1 and 2), *exo1Δ* (strains 1272 and 1273, lanes 3 and 4), *cdc13* deletions (strains 2607 and 2608, lanes 7 and 8), *stn1* deletions (haploids #14 and #21, lanes 5 and 6) and *cdc13 stn1* combined deletions (strains 2684 and 2685, lanes 9 and 10) were analysed on agarose gel. The agarose gel electrophoretic results with uncut DNA clearly showed single intact band of high molecular weight (above 12 kb) containing ~1-2 µg of DNA in each lane in all analysed samples.

After confirmation of DNA integrity on analytical gels, genomic DNA from wild type and other mutants including *cdc13-1* N- and C-truncated clones was digested overnight with *Xho*1 restriction enzyme. Six independent mutants with N-terminus and C-terminus deletions were analysed for both 1296-TR and 1297-TR strains. Digestion was performed with 5 µl genomic DNA in 20 µl reaction volume with *Xho*1 enzyme. Small amounts (10-20%) of DNA from the digested samples were examined electrophoretically. Figure 4.30A showed the results of digested DNAs from wild type (lanes 1, 2), *EXO1* deletion mutants (lanes 3, 4) *CDC13* deletion (lanes 5, 6), *STN1* deletion (lanes 7, 8, 11-14), combined deletions of *CDC13* and *STN1* with *EXO1* and *RAD24* deletions (lanes 9, 10), *cdc13-1 EXO1* deletion mutants (lanes 15, 16) and *cdc13-1* N-terminus deletion (NTΔ) mutants in strain 1296-TR (lanes 17-22). Similarly digested DNA from *cdc13-1* C-terminus deletion mutants in strain 1296-TR (lanes 1-6), *cdc13-1* NTΔ (lanes 7-12), *cdc13-1* CTΔ (lanes 13-18) mutants in strain 1297-TR and uncut DNA samples (lanes 20-22) are shown in Figure 4.30B.

The digested DNA approximately equal amount, were subjected to Southern blot followed by hybridisation with a Y'+TG probe and detection of signals on X-ray film.

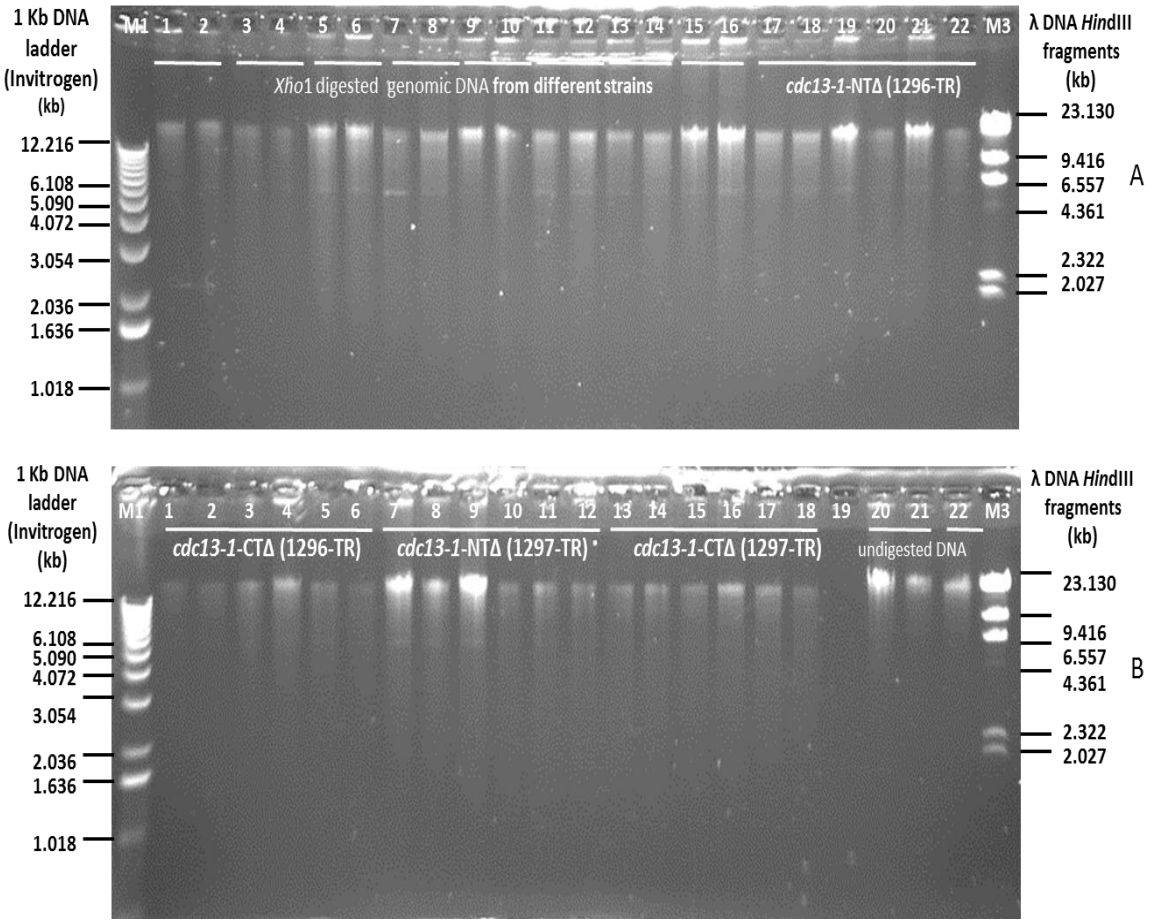

Figure 4.30. A representative gel after electrophoresis of digested genomic DNA, samples for Southern blot analysis.

Cells were cultivated for three days on YEPD plates at 30°C. Total DNA isolated from cells of passage-3., digested overnight with *Xho*1 enzyme and examined on a 0.8% agarose gel. Digested DNA (2 µl) with 1 µl undigested genomic DNA was examined on analytical gels.

M1 represents 1 kb DNA ladder and **M3** represents λ DNA digested with *Hin*dIII used as size references.

(**A**) Agarose gel electrophoresis of *Xho*1digested genomic DNA.

Lanes 1-2: digested genomic DNA samples from strains 640 and 641 (WT); **3-4**: 1272 and 1273 (*exo1Δ*); **5-6**: 2607 and 2608 (*cdc13Δ exo1Δ*); **7-8**: #14 and #21 (haploids, *stn1Δ exo1Δ rad24Δ*; **9-10**: 2684 and 2685 (*cdc13Δ stn1Δ exo1Δ* rad24*Δ*); **11-12**: #14 x2 (haploid, light and dark shades colonies; **13-14**: #21 x2 (haploid, light and dark shades colonies); **15-16**: 1296-TR and 1297-TR respectively (*cdc13-1 exo1Δ*); **17-22**: *cdc13-1* N-terminus deletion in strain 1296-TR (*cdc13-1*-NTΔ #2, **#4, #5,** #6, #7, #21 clones respectively.

(**B**) DNA gel resolution of genomic DNA samples from *cdc13-1*-N or C truncated deletion constructs.

Lanes 1-6: (*cdc13-1* CTΔ clones #3, #4, #6, #7, **#9, #10** in strain 1296-TR); **7-12**: (*cdc13-1*-NTΔ clones #1, #7, #8, #11, #14 and #22 in strain 1297-TR); **13-18**: (*cdc13-1*-CTΔ clones #3, #4, #7, #8, **#11, #12** in strain 1297-TR; **20-21**: uncut DNA from strains 640 and 641 (WT); **22**: 1272 (*exo1Δ*)**.**

4.3.2.2. Preparation of the probe for Southern blot hybridisation analysis

4.3.2.2.1. Transformation of *E. coli* NM522 by plasmid 987

To prepare the probe for Southern blot hybridisation analysis, the plasmid 987 harbouring the Y'+ TG fragment was multiplied in bacterial cells (*E.coli* K-12 strain NM522). The transformed cells were grown overnight on selective medium with 100 mg/L of ampicillin at 37°C (Figure 4.31). Ampicillin-resistant colonies were picked up and used to set overnight cultures in nutrient broth with ampicillin. Overnight grown cells were used for the extraction of plasmid DNA on a midi prep columns.

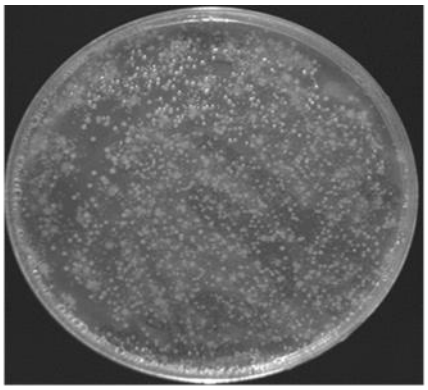

Transformed mixture of *E. coli* NM522 (with plasmid 987), grown overnight at 37°C

Figure 4.31. A representative plate showing growth of transformed *E. coli* (with plasmid DNA, p987) on ampicillin containing selective medium.

The competent cells of host bacteria, *E. coli* K12 (200 µl) were transformed with 2 µl of the diluted plasmid DNA 987 (with cloned Y'+TG fragment). The mixture of cells and DNA (transformed mixture 50 µl) was plated on nutrient agar medium with 100 µg/ml ampicillin and incubated overnight at 37°C to obtain ampicillin-resistant colonies. Random colonies were picked to set cultures for isolation of plasmid DNA.

4.3.2.2.2. Extraction and digestion of plasmid DNA

The plasmid DNA 987 was extracted from host *E. coli* overnight culture with a Qiagen kit. DNA was suspended in sterile 1x TE buffer (10 mM Tris-Cl, pH 8.0, 1 mM EDTA). The purified DNA was digested with *Bam*H1 and *Xho*1 enzymes to release the 1 kb fragment. Uncut DNA and digested DNA were analysed on a 0.8% agarose gel to confirm the completion of digestion.

4.3.2.2.3. Purification of the DNA probe

The *Xho*1 and *Bam*H1 digested plasmid p987 products were resolved on 0.8% agarose gel. The uncut and cut DNA (Figure 4.32A, lanes 1 and 2 respectively) were separated electrophoretically on the agarose gel. The required 1 kb DNA fragment was excised from the gel (Figure 4.32B) and the DNA was extracted from agarose using QIAquick gel extraction kit. Figure 4.33 shows the result of an analytical gel with uncut plasmid (lanes 1 and 2), cut plasmid (lane 3) and purified 1 kb DNA fragment (lane 4). The approximate concentration of purified fragment was estimated to be 10-15 ng/µl. Approximately 10-15 µl of the DNA was labelled with the Amersham gene images AlkPhos direct labelling and detection system. This randomly labelled DNA was used as a probe for Southern blot hybridisation analysis.

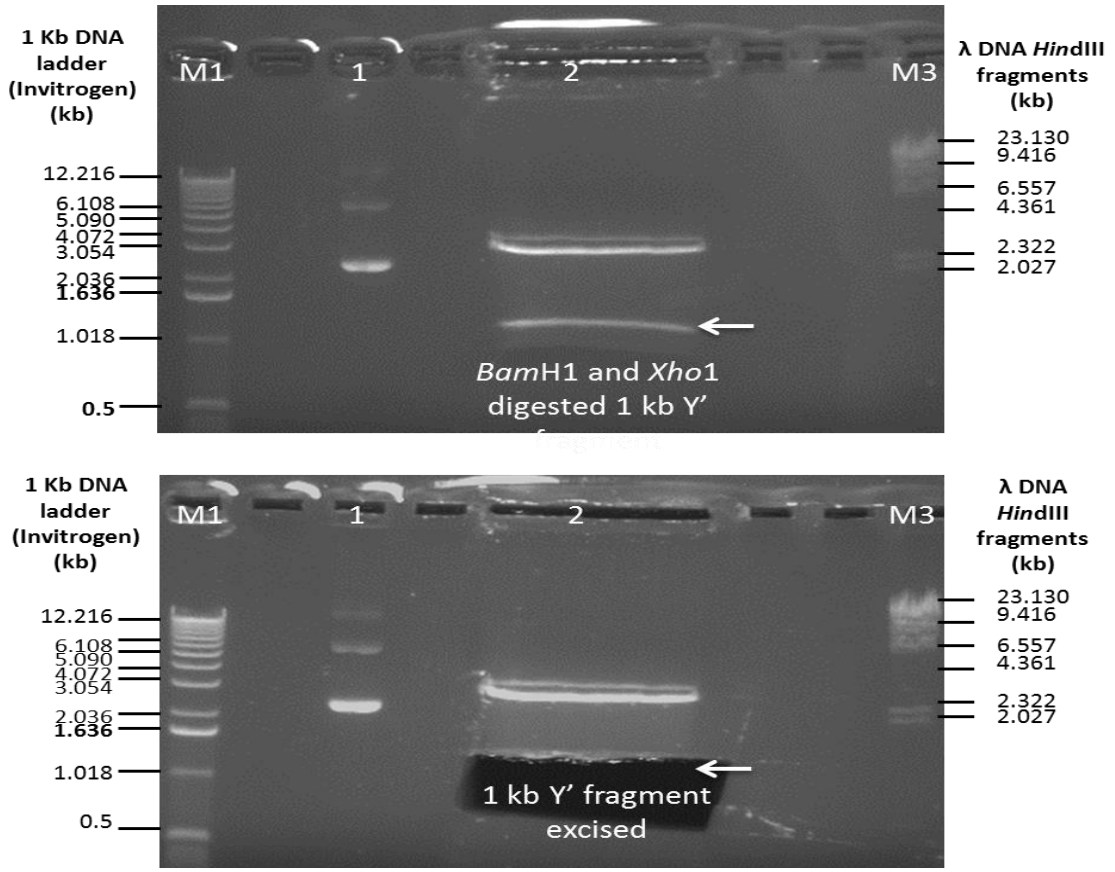

Figure 4.32. The separation and cut out of the 1 kb fragment on an analytical gel following the plasmid DNA digestion to obtain the probe fragment.

The plasmid DNA 987 was digested with *Bam*H1 and *Xho*1 enzymes to cut out the 1 kb Y'+TG fragment. Uncut DNA and digested DNA were separated on a 0.8% agarose gel. The ~1 kb fragment was excised from the gel and purified with a QIAquick gel extraction kit.
Lanes M1: 1 kb DNA ladder; **M3**: λ DNA digested with *Hin*dIII, used as a size references; **1**: uncut plasmid 987 DNA (3 µl); **2**: *Bam*H1 and *Xho*1digested plasmid DNA (150 µl).

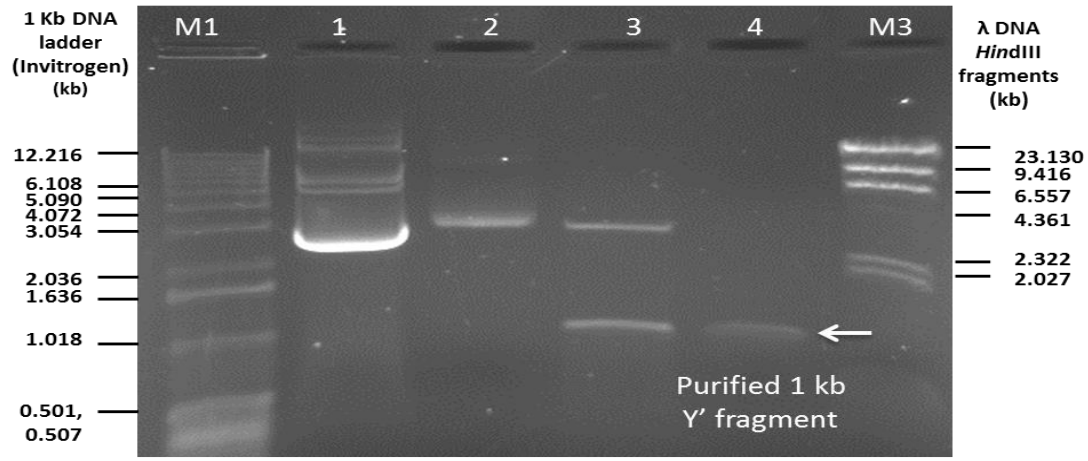

Figure 4.33. The estimation of amount of the 1 kb fragment after electrophoresis in comparison with uncut and cut plasmid.

The 1 kb fragment was gel purified using a QIAquick gel extraction kit (cat. no. 28704) by following the user manual. The purified fragment, 2 µl (**lane 4**) was analysed on the gel along with uncut plasmid DNA (**lanes 1 and 2**) and digested DNA (**lane 3**), 5 µl of each. **M1** represents 1 kb DNA ladder and **M3** represents λ DNA digested with *Hin*dIII, used as size references.

4.3.2.3. A comparative analysis of telomeric DNA from *CDC13* and *STN1* single, combined and partial deletion mutants in the absence of *EXO1*

To understand more about the mechanism of growth of mutants lacking essential telomere capping protein Cdc13 and/or Stn1, or mutants with defective Cdc13 with the N- or C-terminus truncated at 30°C, telomeric DNA patterns were examined. The blot analysis of the Stn1 (Figure 4.34, lanes 5 and 6) and Cdc13 (lanes 9 and 10) deletion mutants alone and in combination (lanes 7 and 8) showed similar diffused and smeary telomere DNA patterns, comparable to type I survivors (Figure 4.35). Two N-truncated *cdc13-1* mutants in strain 1296-TR also exhibited somewhat similar patterns of telomere DNA, with smeary and very short terminal DNA (Figure 4.34 B and C, lanes 13 and 14). In contrast, the other two N-truncated mutants in strain 1297-TR (Figure 4.34 B, lanes 17 and 18) presented different telomeric DNA patterns with distinct bands in the range of 1-5 kb with obvious Y'5.5 kb and 6.5 kb bands, more like type II survivors shown in Figure 4.35. In Figure 4.34 B, the wild type control 640 (lane 1), original strain 1297-TR (lane 12) and Exo1 deletion mutants (lanes 3 and 4) showed distinct 6.5 kb, 5.5 kb and terminal 1.3 kb bands. However, terminal DNA fragments were not obvious in the two N- (lanes 17 and 18) and C-truncated mutants (lanes 15, 16, 19, and 20), which revealed their telomeric pattern similar to type II survivors but with unique patterns in each with very few similarities between them.

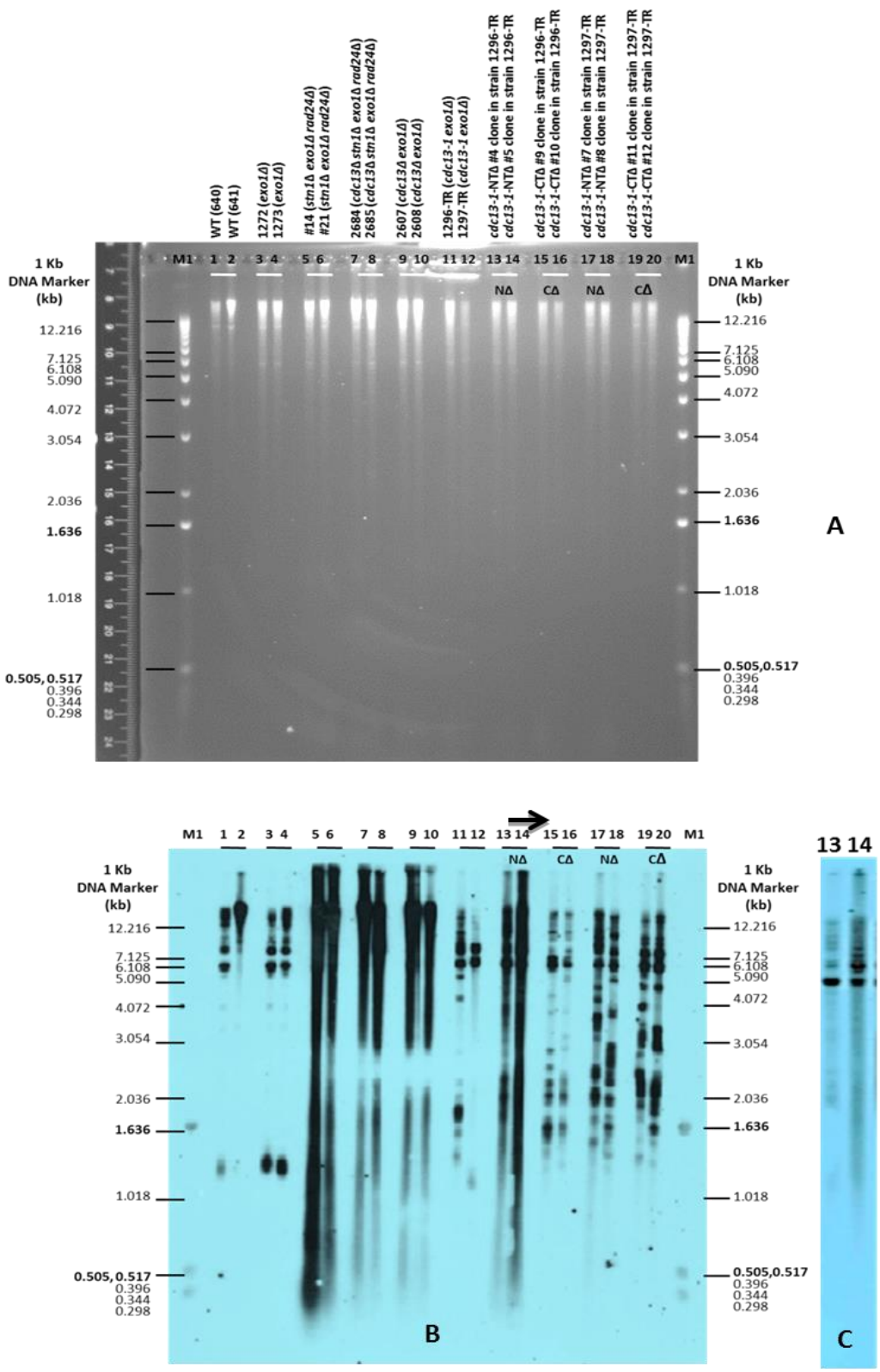

Figure 4.34. An analysis of yeast telomeric DNA from Cdc13 and Stn1 deficient mutants in comparison to mutants of Cdc13-1 with truncated N-terminus (*cdc13-1*-NTΔ) and C-terminus (*cdc13-1*-CTΔ) in the absence of Exo1.

Total DNA was extracted from cells grown on YEPD medium at 30°C from passage 3.

DNA was digested with *Xho*1 enzyme overnight and separated on agarose gel for telomeric DNA analysis by Southern bloting. Two independent mutants were analysed for each deletion including N- (**lanes 13-14 and 17-18**) and C-terminus deletion (**lanes 15-16 and 19-20**).

Wild type strains 640 and 641 (*CDC13*) were used as positive controls (**lanes 1 and 2**) whereas Exo1 deletion mutants were negative control (**lanes 3 and** 4). Stn1 and Cdc13 single deletion (**lanes 5, 6 and 9, 10**) and combined deletion (**lanes 7 and 8**) mutants are presented.

Digestion was performed with 5 µl genomic DNA in a 25 µl reaction volume with *Xho*1 restriction enzyme. Digested DNA (8-12 µl) was resolved on a 0.8 % agarose gel at 40 volts overnight.

(**A**) Agarose gel analysis of digested genomic DNA from Cdc13 and Stn1 deletion mutants, Cdc13-1 N- and C-terminus truncated mutants along with controls.

(**B**) Telomere Southern blot analysis of DNA in the above gel with a Y'+TG probe (randomly labelled telomeric repeat DNA).

(**C**) Short time exposure of above blot, showing two N-truncated mutants (lanes 13 and 14) with distinct fragments of 5.5 kb and 6.5 kb with a Y'+TG probe (telomeric repeat DNA).

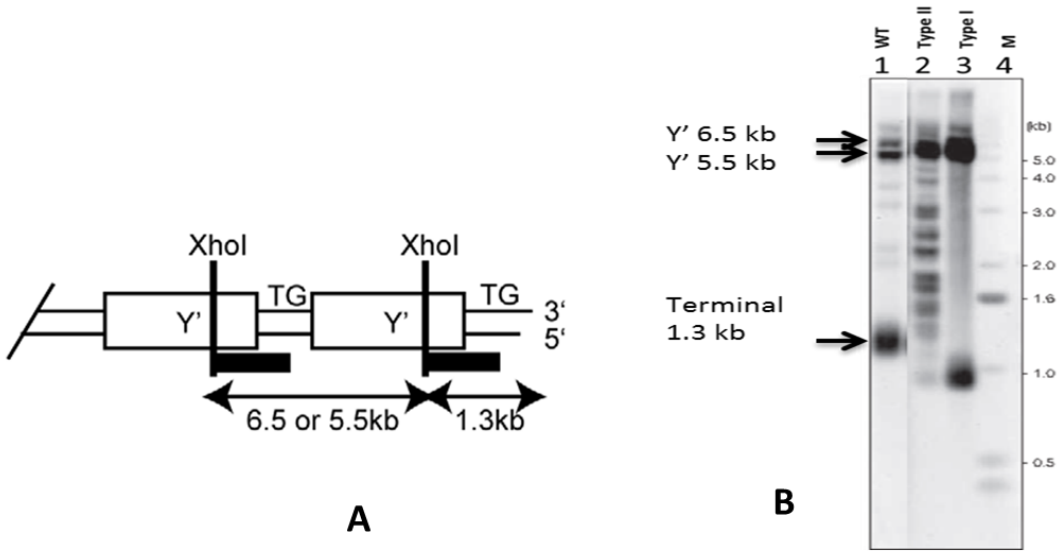

Figure 4.35. Telomere DNA patterns in wild type and temperature-resistant *cdc13-1* cells maintaining telomere length through recombination.

Wild type and type I survivors amplify sub-telomeric Y' repeats (**lanes 1 and 3** respectively) whereas *cdc13-1* and type II survivors amplify the terminal TG_{1-3} repeats (**lane 2**) and show bigger than 1 kb telomeric DNA fragments upon digestion. The probe hybridises to the telomeric end of the Y' repeat (~1 kb) and to ~120 bp sequence of TG repeat (Maringele and Lydall, 2003).

(**A**) Schematic representation of the end of the yeast chromosome with Y' repeat, position of *Xho*I site and hybridisation probe (black bar), (the Figure was taken from Ngo and Lydall, 2010).

(**B**) Southern blot with Y'+TG probe (the Figure taken from Zubko and Lydall, 2006).

4.3.2.4. Comparison of telomeric DNA patterns in *cdc13Δ* and *cdc13-1* N- and C-terminus-truncated mutants

The *cdc13-1 exo1Δ* mutants showed a growth retardation phenotype at 30°C and displayed a permissive temperature of less than 30°C. However, their temperature-resistant survivors were able to grow at 37°C. It has been determined earlier that Cdc13 deletion mutants in the absence of Exo1 could grow normally at both 23°C and 30°C. To examine any differences in telomeric DNA composition the genomic DNA was isolated from N- and C-truncated mutants grown at 30°C, and analysed by Southern blot hybridisation. Figure 4.36 shows the results of electrophoretic separation of digested DNA samples and their hybridisation after using the 1 kb Y'+TG probe. The Y'-terminal restriction fragments (Y'-TRFs) migrate at about 1.3 kb, and some of the other bands correspond to non-Y′-TRFs (Parenteau and Wellinger, 1999). The temperature resistant *cdc13-1* cells from original strain 1296-TR (lane 2) generated telomeric DNA patterns similar to type II survivors which showed discrete bands with amplified terminal TG repeats detectable after digestion with *Xho*1 (Zubko and Lydall, 2006). The cells from wild type and strain 1297-TR (lanes 1 and 29 respectively) produced similar patterns (with amplified Y' terminal repeat fragments, but with a smearing tracks in 1297-TR like in type I survivors). Two individual strains of Cdc13 deficient mutants (lanes 15 and 16) showed a diffused and smeary telomeric DNA similar to that in type I survivors without any distinct bands. All N-truncated mutants exhibited 5.5 kb and 6.5 kb fragments. However, the smaller fragments within the range of 1-5 kb showed variations in size without any specific trend. The four N-truncated mutants in strain 1296 (lanes 4-7) and two N-truncated mutants in strain 1297 (lanes 9 and 14) also showed diffused and smeary telomeric DNA patterns similar to those in *CDC13Δ* mutants (type I survivor pattern). Two N-truncated mutants from strain 1296 manifested slightly similar banding pattern in the size range of 1-2.5 kb, with a common ~4.2 kb fragment (lanes 3 and 8), while other N-terminus deleted mutants in strain 1297 (lanes 10-13) exhibit an overall unique telomeric repeat pattern similar to that in type II survivors. Similarly, telomeric DNA patterns among C-truncated mutants exhibited the 5.5 kb Y' fragment, however, the 6.5 kb fragment was not obvious in the two mutants (lanes17 and 18). Overall, type II specific telomeric DNA patterns were observed in all C-truncated mutants except one (lane 24) that presented a mixed pattern of telomere DNA. The terminal TG repeat fragments in strain 1296-TR C-truncated mutants exhibited the bands spread between ~1.3 kb to 2 kb clumped towards the end as compared to slightly wider spread of bands with a ~1.2 kb to 3 kb range in C-truncated mutants of 1297-TR. Among C-truncated mutants in strain 1296, based on the size homology of terminal TG repeats and bigger than 5 kb fragments, the mutant #3 shared some similarity with #4 (lanes 17 and 18), mutant # 6 with # 9 (lanes 19 and 20), and mutant #7 with #10 (Figure 4.36B and C, lanes 21 and 22). However, 1297-TR C-truncated mutants did not show any common banding patterns among themselves, each showing a unique telomeric pattern. It was concluded from the above results that all Cdc13 C-truncated mutants displayed

homology with telomerase-independent, recombination-dependent type II survivors. In contrast, only half of the N-truncated mutants manifested homology with type II survivors, while rest of the N-truncated mutants exhibited diffuse and smeary telomeric pattern without an obvious terminal 1.3 kb fragment (characteristic of type I survivors). The diffuse DNA could be single-stranded DNA, generated at high temperature.

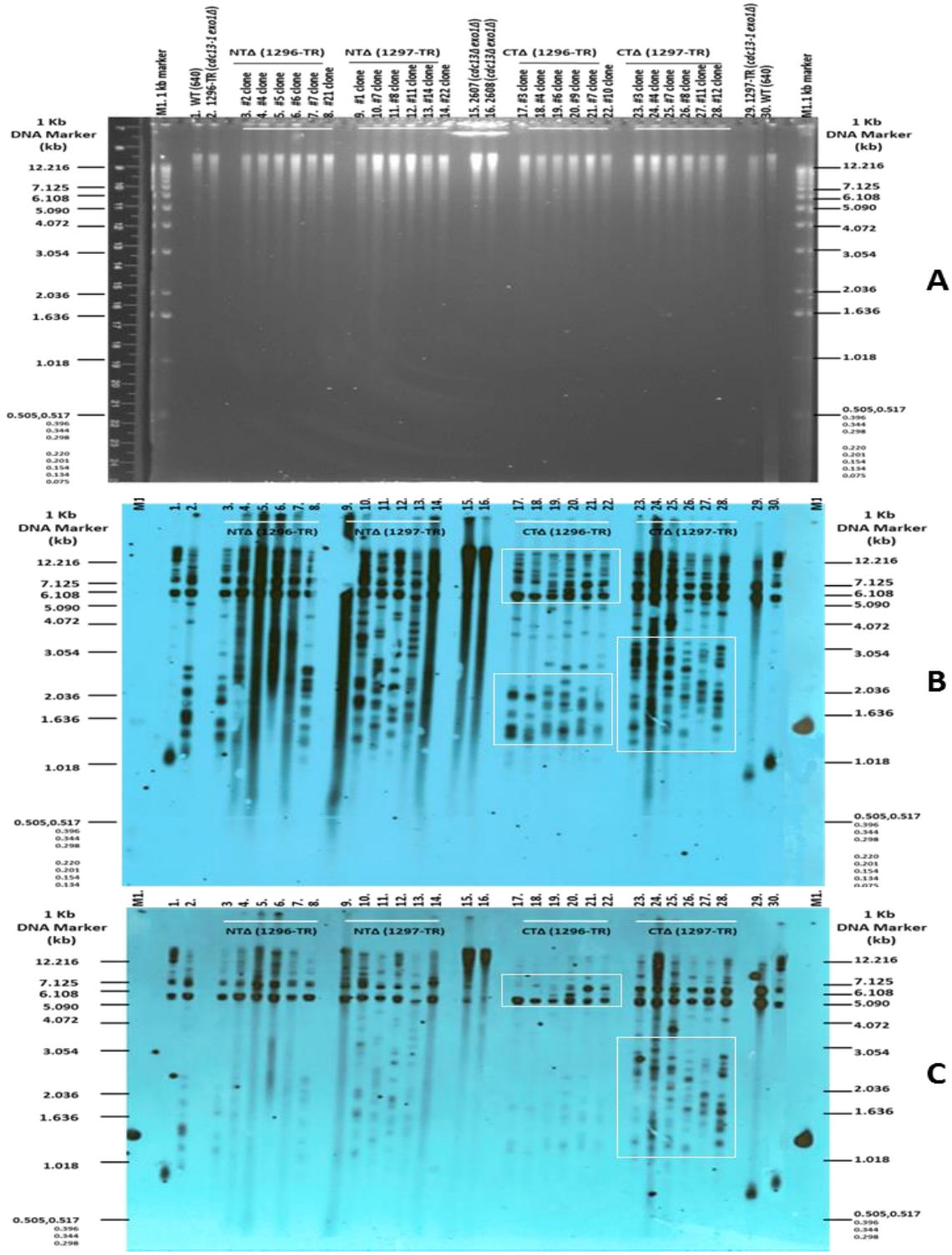

Figure 4.36. Telomeric DNA patterns in *cdc13*Δ and their comparison to those in *cdc13-1* N- and C-truncated mutants in the absence of Exo1.

Total DNA was extracted from cells grown on YEPD media at 30°C. DNA fragments after digestion with *Xho*1 enzyme (overnight) were separated on agarose gel for telomeric analysis by Southern blot hybridisation. Six independent mutants were analysed for N- (lanes 3-8 and 9-14) and C-terminus deletion mutants (lanes 17-22 and 23-28). *CDC13*Δ are in lanes 15 and 16. Wild type strains 640 (lanes 1 and 30) and strains 1296-TR and 1297-TR (lanes 2 and 29 respectively) were used as controls.

Digestion was performed with 5 µl genomic DNA in a 25 µl reaction volume with *Xho*1 restriction enzyme. Digested DNA (8-12 µl) was resolved on a 0.8 % agarose gel at 36 volts overnight.

(**A**) An agarose gel analysis of digested genomic DNA from *cdc13*Δ, *cdc13-1* N- and C-truncated mutants along with controls.

(**B**) Telomere Southern blot hybridisation from the above gel using a Y'+TG probe (randomly labelled telomeric repeat DNA) after a longer exposure to the film, 3 days.

(**C**) Southern blot analysis (short exposure to the film, 1 day).

4.3.2.4.1. Effect of elevated temperature on telomeric DNA patterns of *cdc13-1* N- and C-truncated mutants from 1296-TR

Figure 4.37 represents the results of comparative analysis of telomeric DNA from N- and C-truncated *cdc13-1* mutants in strain 1296-TR grown at 23°C and 37°C. The DNA of truncated mutants grown at 37°C showed more resistance to digestion under similar conditions. These trends were obvious in both N- (lanes 9-14) and C-truncated mutants (lanes 25-30) at 37°C; however, more consistent patterns were exhibited between C-truncated mutants (lanes 25-30). Two N-truncated mutants at 23°C (lanes 5 and 7) also showed partial digestion of DNA. In contrast two telomeric fragments 5.5 kb and 6.5 kb were prominent in all *Xho*1 digested samples while the distinct terminal fragment (1.3 kb) was present only in the wild type (lanes 1, 31 and 32) and strain 1296 (lane 17). Overall, the N-truncated mutants exhibited diffuse telomeric patterns (in the range of 0.5-4 kb or even smaller fragments with weak intensity) similar to the *cdc13* full gene deletion mutant (lane 15). C-truncated mutants grown at 23°C showed telomeric structure similarity to the strain 1296-TR (lane 17) with more distinct terminal bands in the range of 1-2 kb.

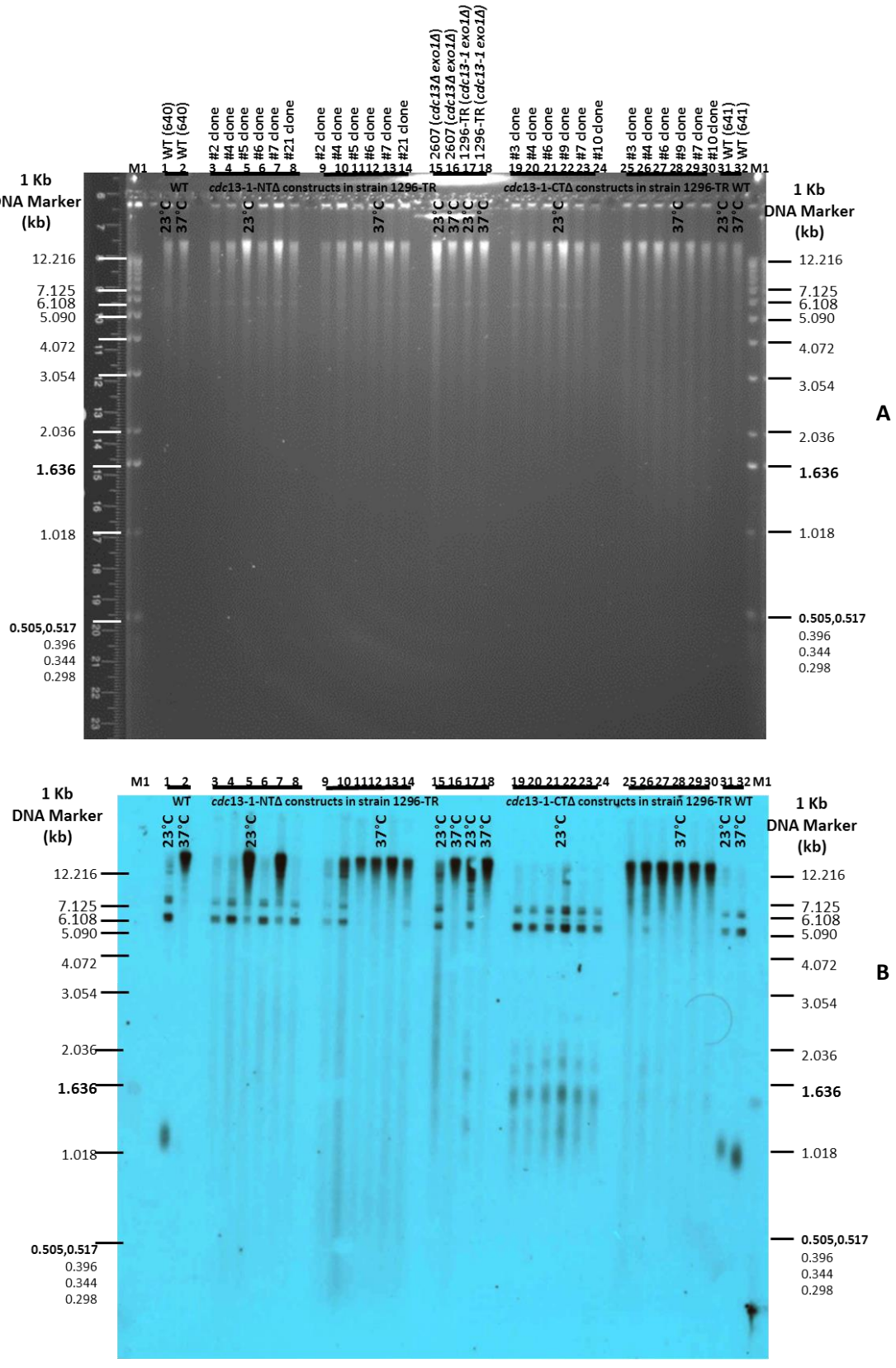

Figure 4.37. Telomeric DNA patterns of *cdc13-1* N- and C-truncated mutants from strain 1296-TR grown at normal and elevated temperatures.

Analysis of yeast telomeric DNA was performed from N-truncated (*cdc13-1*-NTΔ) and C-truncated (*cdc13-1*-CTΔ) mutants in the absence of Exo1 in strain 1296-TR. Total DNA was extracted from passage 3 cells grown on YEPD medium at 23°C and 37°C. Genomic DNA (*Xho*1 digested) was resolved on agarose gel overnight (A), followed by DNA blotting and probing for telomeric Southern blot analysis

using the labelled Y'+TG probe (1kb) (B). Six independent mutants from N- (**lanes 3-8** and **9-14** at 23°C and 37°C respectively) and C-terminus deletion mutants (**lanes 19-24** and **25-30** at 23°C and 37°C respectively) were analysed. **Lanes 15 and 16** represent DNA from the *cdc13*Δ *exo1*Δ mutant (strain 2607) at 23°C and 37°C respectively and **lanes 17 and 18** similarly show DNA from the 1296-TR strain. **M1** represents 1 kb marker (non-labelled). At both ends of the gel/blot **lanes 1, 2** and **31, 32** represent DNA from wild type strains (641 and 640 respectively).

(**A**) Agarose gel analysis of digested genomic DNA from *cdc13-1* N- and C-truncated mutants grown at 23°C and 37°C in strain 1296-TR along with controls.
(**B**) Telomere TRFs analysis using a Y'+TG probe.

4.3.2.4.2. Effect of elevated temperature on telomeric DNA patterns of *cdc13-1* N- and C-truncated mutants from 1297-TR strain

Figure 4.38 represents the results of comparative analysis of telomeric DNA from N- and C-truncated *cdc13-1* mutants in strain 1297-TR grown at 23°C and 37°C. The DNA of truncated mutants from 37°C showed more resistance to digestion (partial digestion) under similar conditions. These trends were obvious in both N- (lanes 9-14) and C-truncated mutants (lanes 25-30) at 37°C. Two N-truncated mutants at 23°C (lanes 3 and 5) also showed partial digestion of DNA. At 23°C, two telomeric fragments of 5.5 kb and 6.5 kb were prominent in all *Xho*1 digested samples from both truncations whereas the 1.3 kb terminal fragment was shown by the wild type (lanes 1, 2, and 31) and strain 1297 (lane 17). Overall, all N-truncated mutants (lanes 3-14) at 23°C and 37°C respectively and C-truncated mutants (lanes 25-30) at 37°C only, reflected diffused telomeric patterns (in the range of 0.5-5 kb) like *Cdc13* full gene deletion (lane 15 and 16) and C-truncated mutants at 23°C manifested telomeric structures similar to the strain 1297-TR (lane 17), with more distinct terminal bands in the range of 1-3 kb.

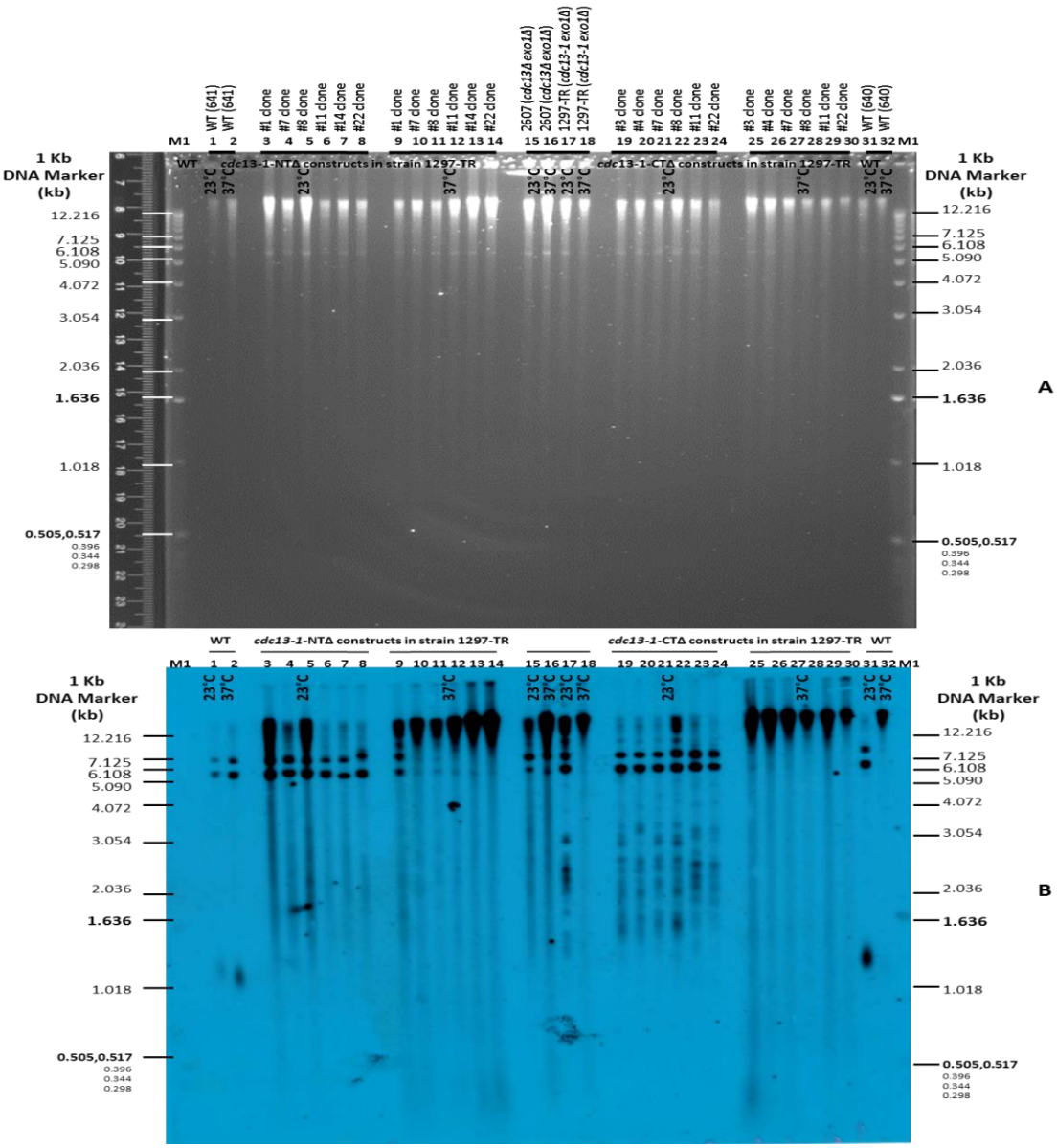

Figure 4.38. Telomeric DNA patterns of *cdc13-1* N- and C-truncated mutants from strain 1297-TR grown at normal and elevated temperatures.

Analysis of yeast telomeric DNA from N-truncated (*cdc13-1*-NTΔ) and C-truncated (*cdc13-1*-CTΔ) mutants was carried out in the absence of Exo1 in the strain 1297-TR. Total DNA was extracted from passage 3 cells grown on YEPD medium at 23°C and 37°C. Genomic DNA (*Xho*1 digested) was resolved on agarose gel overnight (A), followed by DNA blotting and probing for telomeric Southern blot analysis using the labelled Y'+ TG probe (B). Six independent mutants from N- (**lanes 3-8** and **lanes 9-14** at 23°C and 37°C respectively) and C-terminus deletion mutants (**lanes 19-24** and **25-30** at 23°C and 37°C respectively) were analysed. **Lanes 15 and 16** represent DNA from *cdc13*Δ *exo1*Δ mutant (strain 2607) at 23°C and 37°C respectively and **lanes 17 and 18** shows DNA from the 1297-TR parental strain. **M1** represents 1 kb marker (non-labelled). At both ends of the gel/blot, **lanes 1, 2 and 31, 32** represent DNA from the wild type strains (640 and 641 respectively).

(**A**) Agarose gel analysis of *Xho*I digested genomic DNA from *cdc13-1* N- and C-truncated mutants grown at 23°C and 37°C in strain 1297-TR along with controls.
(**B**) Telomere TRFs blot analysis using Y'+TG probe.

4.4. Conclusions

- The analyses of DNA sequences in N- and C-truncated mutants support the expected sequences in most C-truncated and N-truncated generated mutants.
- DNA sequence showed no change in nucleotide sequence in three *cdc13-1*-NTΔ clones (mutants #4, #5 and #6 in strain 1296-TR) potentially useful for extended studies. Out of the five substitution mutations identified in the coding region of the TRP1 marker in NTΔ clones two were founded to be silent (NTΔ clone #7-1296 and clone #7-1297) with three missense mutations. One substitution mutation was located in the GAL1 promoter region and another one was positioned outside the coding region of TRP1 marker. One silent mutation was identified in the C-terminus half of Cdc13-1 (clone #7-1297). Whereas single deletion mutation shown in one mutant (clone #2-1296), positioned within deletion primer of C-terminus of *cdc13-1* ORF (protein frame shift) was interpreted as mis-counted error from the sequencing chromatogram.
- The analysis of C-terminus-truncated mutants revealed only one valid substitution mutations, common in four clones and was positioned within the TEF terminator of HIS3MX6 marker. Sequence analyses of all tested CTΔ mutants, confirmed the intact *Eco*R1 site in the N-terminus-half of the gene.
- Southern blot hybridisation analysis of the Stn1 and Cdc13 deletion mutants, single and in combination showed similar diffused and smeary telomere DNA patterns comparable to type I survivors with distinct 5.5 and 6.5 kb bands indicating the nature of telomere elongation in these strains may be through amplification of sub-telomeric Y' repeats.
- Analysis of N-truncated *cdc13-1* mutants revealed mixed telomeric DNA patterns, smeary with short terminal DNA and telomeric DNA with distinct bigger than 1 kb DNA bands characteristic of type I and type II survivors. These observations demonstrate that telomere length maintenance in these mutants occurs possibly through recombination (amplification of Y' repeats or the terminal TG_{1-3}).
- C-truncated *cdc13-1* mutants displayed similarity with type II survivors (indicating telomere maintenance through amplification of the terminal TG_{1-3}) as manifested by their unique telomeric DNA patterns similar to those in type II survivors.
- Overall, the telomeric DNA patterns in *cdc13-1* N-truncated mutants are similar to the *cdc13* full gene deletion mutants while telomeric DNA patterns in C-truncated mutants showed similarity to the *cdc13-1* mutants (strains 1296, 1297).

Chapter 5

Cellular responses of *CDC13* and *STN1* mutants to different stress factors

5.1. Introduction

Yeast are eukaryotes that are highly adaptable to different environments and can survive under adverse conditions. This ability of *S. cerevisiae* makes it an ideal organism for dissecting the genomic and molecular bases of adaptive responses (Gladieux *et al*., 2014). Adaptive phenotypes under different endogenous or exogenous genotoxic agents reflect the underlying complex genetic and genomic processes (Alfoldi and Lindblad-Toh, 2013).

To respond to abrupt changes, the yeast expression programme maintains its internal milieu by inducing or supressing groups of genes (genomic expression pattern) under specific environmental stresses (Gasch *et al*., 2000). The physiological effects of the stresses reflect the cellular mechanisms that cells use to cope with these stresses and the nature of distinct traits the cell acquired to adapt (Olson-Manning *et al*., 2012).

It has been identified in previous studies that genes involved in similar cellular processes are similarly expressed and show common sequence motifs of the transcription factors and promoters involved in their regulation (Gasch *et al*., 2000). The similar responses of the group of genes under the same environmental stress, however, might depend upon different signalling pathways that regulate these genes in a condition-specific or gene-specific way. Beside the cell type, the nature and duration of the stress collectively determines the activation of protective (survival pathways) or destructive (programmed cell death) cellular responses (Fulda *et al*., 2010).

The cell cycle of the yeast is under tight regulation of cell cycle checkpoint genes that eliminate errors in DNA replication and maintain cell viability. Previous studies have shown that exposure to genotoxic agents (toxic chemicals and radiation) affects the progression of cells through the cell division cycle (Alic *et al*., 2001).

Previous studies have also revealed that genotoxic agents [methyl methanesulfonate (MMS) and hydroxyurea (HU)] disrupt multiple cell cycle checkpoint responses resulting in replication stress while replication stress signals activate the S-phase checkpoint accompanied by cell sensitivity to the replication inhibitor (Gasparyan *et al*., 2009). In contrast hydrogen peroxide (H_2O_2) induces G2 arrest through *RAD9* mediated pathway (Flattery-O'Brien and Dawes, 1998).

These genotoxic agents act at different pathways of cell cycle checkpoints, e.g., G1-S phase, S phase or G2-M phase, to trigger the underlying regulatory mechanism. The cell cycle checkpoint responses are reflected by sensitivity patterns of the phenotypical growth of the mutant.

In yeast *S. cerevisiae,* the essential roles of telomere capping proteins Cdc13 and Stn1 in DNA replication are still under investigation. Cdc13 interacts physically with the Stn1 protein to regulate the telomere length. The temperature-sensitive mutant's alleles, *cdc13-1* and *stn1-13* at

the restrictive temperature generate single-stranded DNA that activates the damage response pathway and arrests cell cycle (Garvik *et al*., 1995). The loss of Cdc13 function induces recombination and leads to Mec1-dependent cell cycle arrest. The Stn1 deletion stimulates Rad9, a checkpoint mediator protein, and activates Mec3 modulated G2-M checkpoints.

To explore further the possible roles of Cdc13 and Stn1 in the stress-response pathways through the cell cycle checkpoints, *S. cerevisiae* mutant cells deficient in Stn1and Cdc13 proteins or mutant cells with N- and C-terminus truncated alleles of *cdc13-1* were allowed to grow in chronic conditions in the presence of exogenous DNA damaging agents (i.e., UV and MMS, HU), or under the oxidative stress ($H_2O_{2)}$ and were analysed for their phenotypical growth patterns. The sensitivities of different mutants were determined under DNA replication stress induced by MMS or HU, oxidative stress caused by H_2O_2 and DNA damaging effects by exposing cells to UV irradiation.

5.2. Aims and objectives

This part of the study was focused on determining the sensitivity of different yeast mutants, (*cdc13*Δ and *stn1*Δ single mutants or in combination, and also *cdc13-1*- N- and C-terminus deletion mutants) to different genotoxic agents like UV irradiations, MMS, H_2O_2 and HU.

This aim involves the following objectives:

- To study the response of *cdc13* and *stn1* deletion mutant cells (in the presence of *exo1* deletion) to genotoxic agents.
- To compare the genotoxic effects in N- and C-terminus truncated *cdc13-1* conditional mutants.
- To investigate the effects of the genotoxic agents on *cdc13-1* N- and C-terminus truncated haploid and diploids mutants (heterozygous).

The following exogenous genotoxic agents with varying concentrations were implemented in toxicity assays.

- UV irradiations: environmental DNA-damaging agent.
- MMS: DNA alkylating agent/ DNA-damaging agent.
- H_2O_2: oxidizing agent (oxidative stress causing agent).
- HU: DNA replication inhibitor.

5.3. Results

The yeast strains used in this study are listed in Table 4.1 (Chapter 4). The additional diploids #31 and #32 used for toxicity assays were generated in crosses between N- and C-truncated haploid mutants of 1296-TR and 1297-TR strains respectively, and PCR verified for both N- and C-terminus of *cdc13-1* in diploid cells.

5.3.1. The effects of genotoxic agents on the growth of *cdc13* and *stn1* deletion mutants.

5.3.1.1. Effects of UV on the growth of conditional mutants lacking Cdc13 and Stn1 proteins.

To determine the effects of UV irradiation, a potent DNA damaging environmental factors, on the growth of yeast cells, the *cdc13* and/or *stn1* deletion mutants of *S. cerevisiae* were analysed under different UV exposures. The preliminary experiments were performed to determine the effective dose of UV irradiation by comparing phenotypic growth inhibition patterns of *cdc13*Δ and *stn1*Δ mutants' cells with those in *exo1*Δ (1272) and WT (640) controls.

The YEPD plates spotted with serial dilutions of 8 cultures (two sets - one set for each temperature regime) were exposed to UV irradiation (x100 μJ/cm^2) (in UV time exposure mode) from a UV dose of 10 J/m^2 to one of 100 J/m^2 (UV10-UV 100). The plates were incubated at 23°C and 30°C for 3 and 5 days. The growth inhibition in *stn1Δ (*haploid #14, #21*)* and *stn1Δ cdc13Δ* (2684 and 2685) mutants in the absence of *rad24* (a component of checkpoint proteins) and *exo1* initiated at the minimum UV exposure of 10 J/m^2, with severe inhibition exhibited between UV 20 J/m^2 and UV 30 J/m^2 exposure and with no growth at UV 40 J/m^2 or above at 23°C for 3 days (Figure 5.1). Similar growth patterns in response to UV sensitivity were observed for these mutants at 23°C for 5 days with minimal growth recovery at UV 30 J/m^2 and 40 J/m^2. Conversely, the wild type control (WT, 640) and *exo1Δ* mutant (1272), showed no obvious growth inhibition at lower exposures, with least inhibition at UV 40 J/m^2 and 50 J/m^2, with significant growth arrest at UV 60 J/m^2 and at higher exposures at 23°C for 3 days. However, the partial recovery of these control cells was well pronounced at 23°C and 30°C for 5 days.

In *cdc13Δ* mutant strains 2607 and 2608, the sensitivity to UV initiated at high UV exposures (UV 50 J/m^2 and 60 J/m^2), and was more obvious at UV 70 J/m^2 at 23°C after 3 days incubation when compared to 23°C for 5 days, indicating some recovery of growth after longer incubation. In all strains, control and mutants cells displayed no growth or minimal growth at UV 100 J/m^2. The *cdc13Δ* mutants in the absence of *exo1* (2607 and 2608) displayed weak resistance to UV 100 J/m^2 similar to controls (640) and *exo1* deletion mutants (1272). The *exo1* deletion mutant

(1272) showed slightly more resistance to UV (UV 70) as compared to WT, obvious at 23°C after 5 days incubation only.

Overall, the strain 2685 (combined deletion of *stn1* and *cdc13* in the absence of *exo1* and *rad24*) revealed maximum sensitivity to UV when compared to *stn1Δ* (#14 and #21) and *cdc13Δ* (2607 and 2608) mutants. In the previous study, the *rad24Δ* mutant cells were shown to be sensitive to UV (Lydall and Weinert, 1995). So it was difficult to conclude whether this high sensitivity displayed by the *stn1Δ cdc13Δ* (2685) mutants was actually a combined deletions response or it was the effect of the *rad24Δ* background.

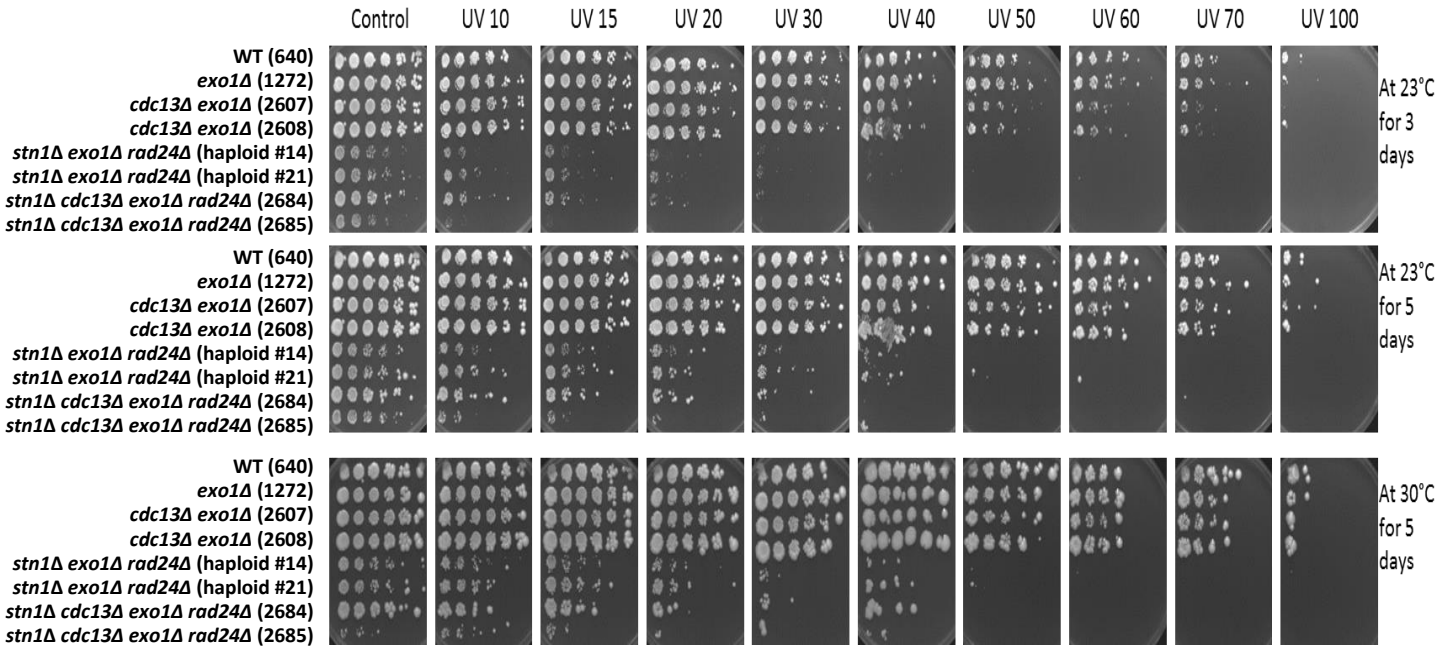

Figure 5.1. Effect of UV irradiation (10-100 J/m^2) on the growth of *cdc13* and *stn1* deletion mutants.

Eight strains including mutants and controls (640, 1272, 2607, 2608, #14, #21, 2684 and 2685) were analysed for UV sensitivity of *cdc13* and *stn1* deletion mutants. Five-fold serial dilutions of the strains in sterile water were spotted onto YEPD medium plates and exposed to different doses of UV irradiations (in UV time exposure mode, 10 J/m^2 to 100 J/m^2). The UV irradiated plates were incubated for 3-5 days at 23°C and 30°C before being photographed.

Further experiments were carried out to draw conclusive results of the UV sensitivity of these mutants. The results presented in Figure 5.2, clearly showed the resistance of the *cdc13*Δ mutant cells (consistent in both strains 2607 and 2608) to UV 25 J/m^2 and 50 J/m^2 when compared with *stn1*Δ mutants (#14 and #21) and *stn1*Δ *cdc13*Δ (2684 and 2685) mutants, however, *cdc13*Δ mutants manifested similar to WT and *exo1*Δ mutants resistance at high temperature (30°C) and after longer incubation (5 days at 23°C and 30°C; Figure 5.2B). The comparison of *stn1* deletion mutants between haploid #14 and #21, however, manifested

slightly variable UV (UV 25 J/m^2 and 50 J/m^2) susceptibility. The haploid #14's cells appeared to be more UV sensitive as compared to cells from haploid #21. This difference in sensitivity pattern was obvious at 23°C and 30°C for 3 (Figure 5.2A) and 5 days (Figure 5.2B). To test whether this response was because of a smaller initial cell number, further assays were conducted at the same UV exposure (UV 25 J/m^2 and 50 J/m^2) and also at higher UV exposures (UV 25, 50, 55, 50, 65 and 70 J/m^2; Figure 5.3AB). However, these intra-mutant UV sensitivity differences were repeatedly observed. Altogether, it was obvious that double deletion mutants *cdc13*Δ *stn1*Δ were more sensitive to UV than either *cdc13*Δ or *stn1*Δ mutants with some reservation regarding the presence of *rad24*Δ.

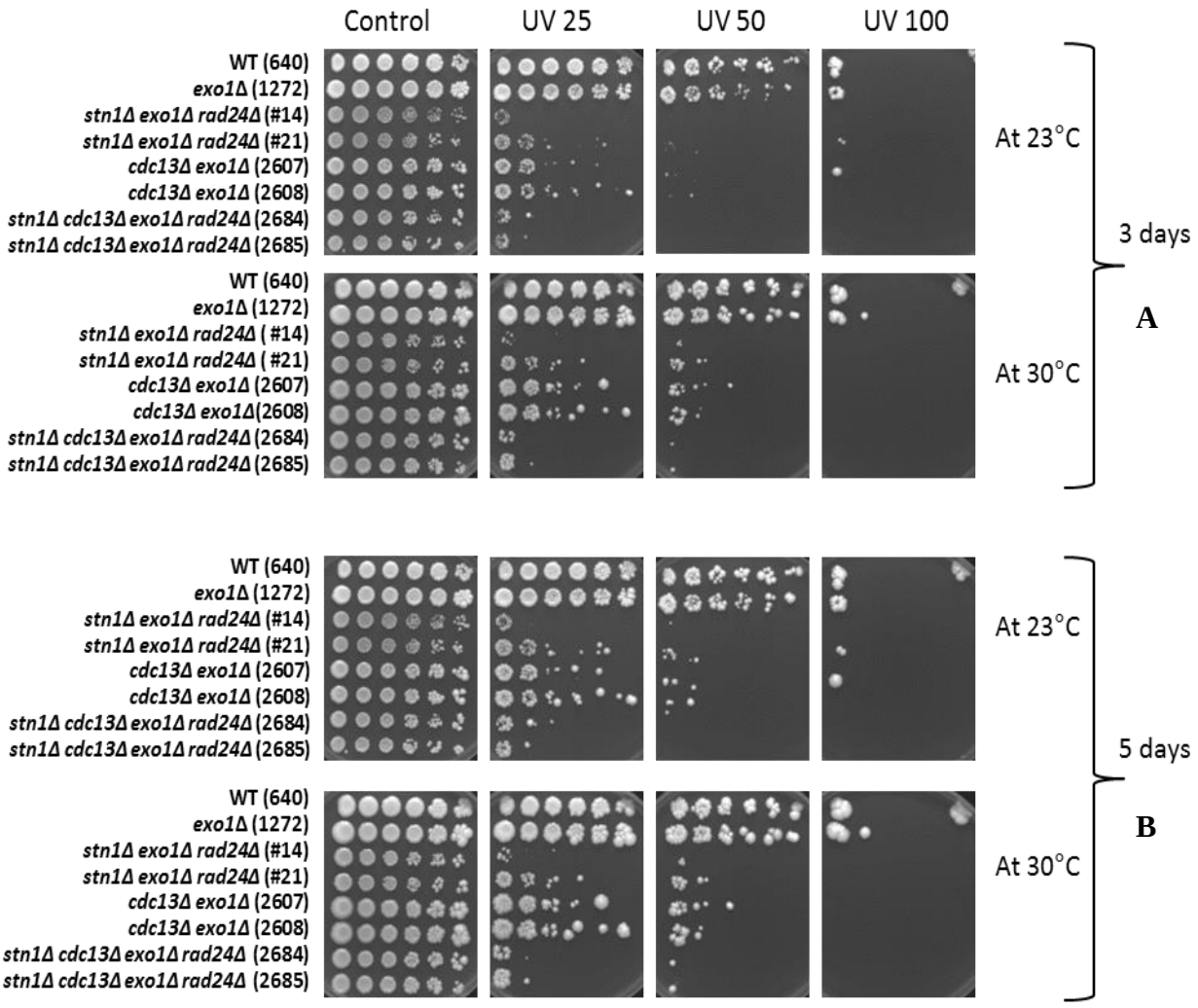

Figure 5.2. Effect of selective UV irradiation (25, 50 and 100 J/m^2) on the growth of *cdc13* and *stn1* deletion mutants.

Eight strains including mutants and controls (640, 1272, #14, #21, 2607, 2608, 2684 and 2685) were analysed for UV sensitivity of *cdc13* and *stn1* deletion mutants. Five-fold serial dilutions of the strains in sterile water were spotted onto YEPD medium plates and exposed to three different doses of UV irradiation (in UV time exposure mode, 25 J/m^2, 50 J/m^2 and 100 J/m^2). The UV irradiated plates were incubated for 3-5 days at 23°C and 30°C before being photographed. Strain numbers are indicated in brackets.

(**A**) Incubation of plates for 3 days at 23°C and 30°C.

(**B**) Incubation of plates for 5 days at 23°C and 30°C.

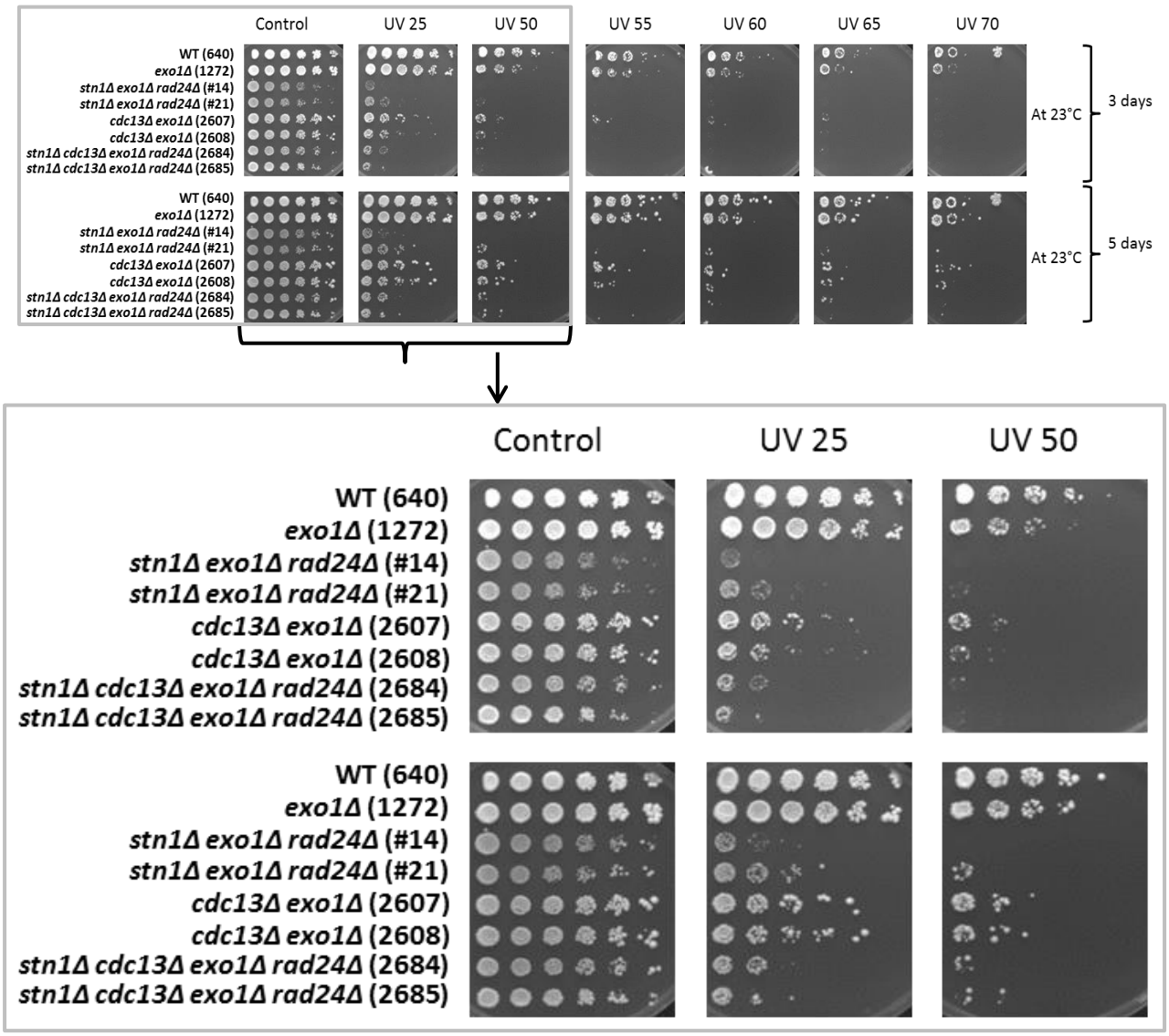

Figure 5.3. Effect of UV irradiation (25-70 J/m^2) on the growth of *cdc13* and *stn1* deletion mutants.

Eight strains including mutants and controls (640, 1272, #14, #21, 2607, 2608, 2684 and 2685) were analysed for UV sensitivity of *cdc13* and *stn1* deletion mutants. Five-fold serial dilutions of the strains in sterile water were spotted onto YEPD medium plates and exposed to six different doses of UV irradiation (in UV time exposure mode, 25, 50, 55, 60, 65 and 70 J/m^2). The UV irradiated plates were incubated for 3-5 days at 23°C and 30°C before being photographed. Strain numbers are indicated in brackets.

5.3.1.2. Effect of MMS on the growth of *cdc13* and *stn1* deletion mutants

MMS is another potent DNA-damaging agent. Previous studies have shown that MMS can cause random DNA fragmentation. In *S. cerevisiae* MMS induces heat-labile damage in recombination-deficient cells (Lundin *et al*., 2005).

The study described in this section was conducted to determine the responses of *cdc13* and *stn1* deletion mutants' cells to chronic exposure of the DNA alkylating agent, MMS. Freshly prepared YEPD plates containing three different concentrations of MMS (0.010%, 0.015% and 0.020%; w/v) were spotted with serial dilutions of 8 cultures (two sets, one for each temperature regime). The plates were incubated at 23°C and 30°C for 3 and 5 days. The growth of *stn1Δ (*haploid #14, #21*)* and *stn1Δ cdc13Δ* (2684 and 2685) mutants in the background of *rad24Δ* and *exo1Δ* was moderately inhibited at 0.010% concentration of MMS, with severe inhibition observed at 0.015% and 0.020% MMS after 3 days of incubation at 23°C (Figure 5.4A). All mutants displayed severe sensitivity to MMS at 0.015 and 0.020% of MMS at 23°C after 3 days of incubation. In contrast, *cdc13Δ* mutants (strains 2607 and 2608) in the background of *exo1Δ* deletion displayed relative resistance to MMS, prominent at 23°C after 5 days of incubation as compared to 3 days of incubation at 23°C (Figure 5.4A). However, this pattern of resistance gradually decreased with increased susceptibility of *cdc13Δ* mutant cells at increasing doses of MMS (0.020%) after longer incubation (5 days) at lower temperature (23°C). The *cdc13Δ exo1Δ* mutant cells also exhibited similar trends of MMS resistance, obvious at 0.010%, 0.015 and 0.020% of MMS at 30°C after 3-5 days of incubation (Figure 5.4B). However, no distinct susceptibility was observed with increasing dose (0.020%) at 30°C after a longer incubation of 5 days. Similarly, the *stn1Δ* (haploid #14, #21*)* and *stn1Δ cdc13Δ* (2684 and 2685) mutants cells displayed sensitivity to all three doses of MMS (0.010%, 0.015% and 0.020%) but to variable extents at 30°C after incubation of 3-5 days (Figure 5.4B). The wild type and the *exo1Δ* deletion mutants were mildly arrested in their growth at low temperature (23°) after 3 days of incubation, obvious at 0.020% MMS, however, most of these cells restored their growth after 5 days of incubation at 23° (Figure 5.4A). Taken together, the growth of the wild type (640) and *exo1* deletion mutant (1272) were negligibly affected at 0.010%, 0.015% and 0.020% concentrations of MMS after 3-5 days of incubation at 30°C (Figure 5.4B).

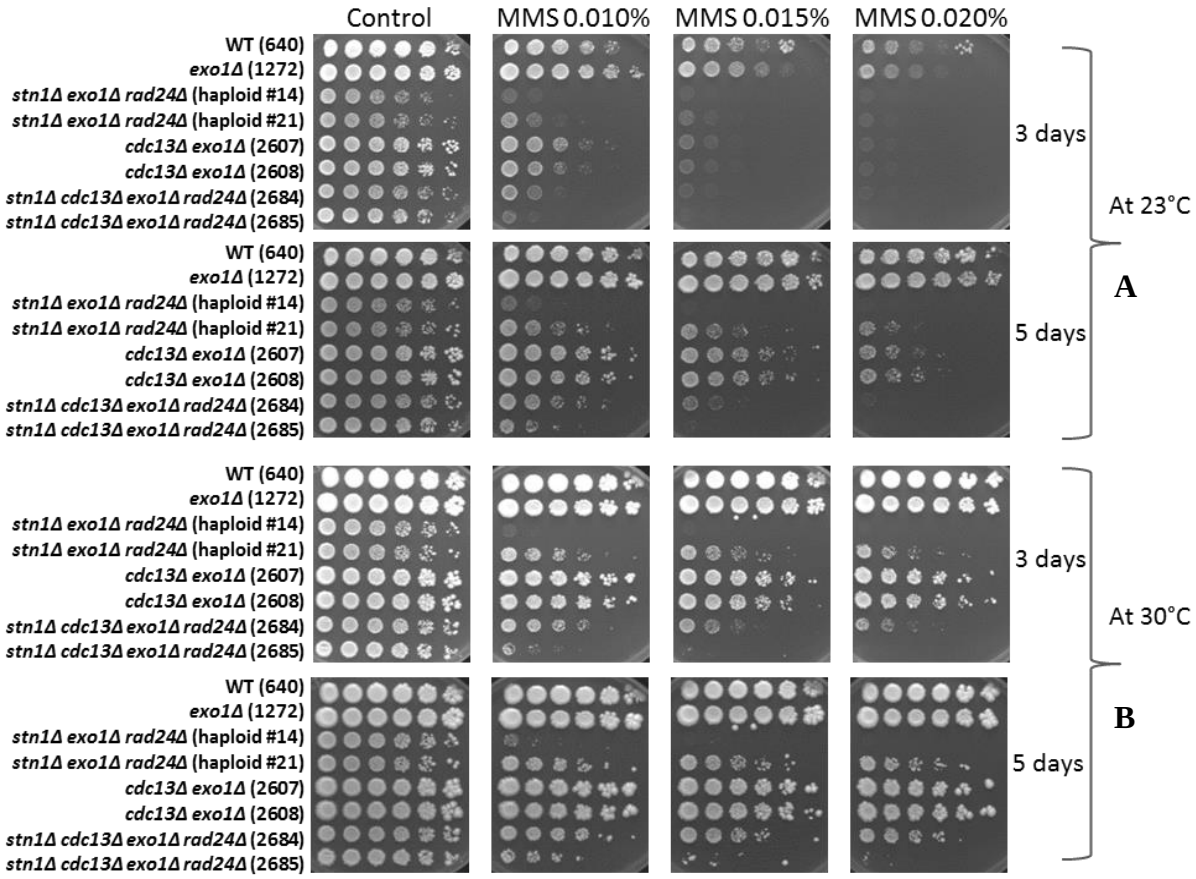

Figure 5.4. Effect of MMS (0.01-0.02%) on the growth of *cdc13* and *stn1* deletion mutants.

Eight strains including mutants and controls (640, 1272, #14, #21, 2607, 2608, 2684 and 2685) were analysed for MMS-mediated sensitivity of *cdc13* and *stn1* deletion mutants. Five-fold serial dilutions of the indicated yeast strains in sterile water were spotted onto YEPD agar plates containing 0.010%, 0.015% and 0.020% of MMS. The plates were incubated for 3-5 days at 23°C and 30°C before being photographed. Strain numbers are indicated in brackets.

(**A**) Incubation of plates for 3-5 days at 23°C.

(**B**) Incubation of plates for 3-5 days at 30°C.

The susceptibility of all *cdc13Δ*, *stn1Δ* and *stn1Δ cdc13Δ* mutants was further tested at one higher dose of MMS (0.015%, 0.020% and 0.030%; w/v) (Figure 5.5). One plate was also exposed to a UV dose of 15 J/m^2 (UV 15). The plates were incubated at 23°C and 30°C for 3 and 5 days.

The growth of *stn1Δ (*haploid #14, #21*)* and *stn1Δ cdc13Δ* (2684 and 2685) mutants in the background of *rad24Δ* and *exo1Δ* was moderately inhibited at 0.015% (w/v) of MMS with severe inhibition observed at 0.020 and 0.030% at 23°C after 3 days of incubation (Figure 5.5). The similar growth patterns in response to MMS sensitivity were observed for *stn1Δ* and *stn1Δ cdc13Δ* mutants and controls at 23°C for 5 days with partial growth recovery at 0.020% and

0.030% MMS. However, the *stn1Δ (*haploid #14, #21*)* and the *stn1Δ cdc13Δ* (2684 and 2685) mutants' cells displayed less sensitivity at 0.020% of MMS as compared to 0.030% of MMS at 30°C after 3-5 days of incubation.

In contrast, *cdc13* deletion mutants (strains 2607 and 2608) in the background of *exo1Δ* displayed obvious resistance to MMS, which was pronounced at 0.020% of MMS after 3 days of incubation at 23°C and 30°C. However, the sensitivity of *cdc13Δ* mutant cells to 0.030% MMS was less obvious at the higher temperature (30°C).
There was some growth restoration of *cdc13Δ exo1Δ* mutant cells after longer incubation of 5 days at 23°C and 30°C. The sensitivity patterns of all mutants and controls at UV 15 J/m^2 (23°C and 30°C) were comparable to MMS 0.015% after 3 and 5 days of incubation at 23°C and to MMS 0.020% after 3 and 5 days of incubation at 30°C.

The variable susceptibilities presented by *stn1Δ* (haploid #14 versus #21) and *stn1Δ cdc13Δ* (combined deletions, 2684 versus 2685) mutants in earlier experiments, were still obvious however, to a lesser extent, revealing mutant #14 (*stn1Δ rad24Δ exo1Δ*) to be slightly more sensitive as compared to mutant #21 and mutant strain 2685 (*stn1Δ cdc13Δ rad24Δ exo1Δ*) as compared to mutant 2684 to MMS at 23°C and 30°C after 3 and 5 days incubation (Figure 5.5AB). This differential sensitivity pattern was well pronounced with the low dose of MMS (0.010%) at 23°C and 30°C after 3 and 5 days incubation Figure 5.5AB).

It was clear that *cdc13Δ* mutants showed more resistant to MMS than other two mutants (more obvious at longer incubation, e.g., 23°C after 5 days (Figure 5.5A) and also at higher temperature, e.g., 30°C after 3-5 days) (Figure 5.5B) indicating different underlying mechanisms. Moreover, at an increased concentration of MMS i.e., 0.030%, the *cdc13Δ* mutant cells also became susceptible to MMS after 3 days of incubation at 23°C and 30°C. However, the extent of the sensitivities was difficult to determine because of the variable phenotypes in *stn1*Δ mutants #14 and #21 and *cdc13*Δ *stn1*Δ (combined deletions) in strains 2684 and 2685 in the background of *exo1*Δ *rad24*Δ.

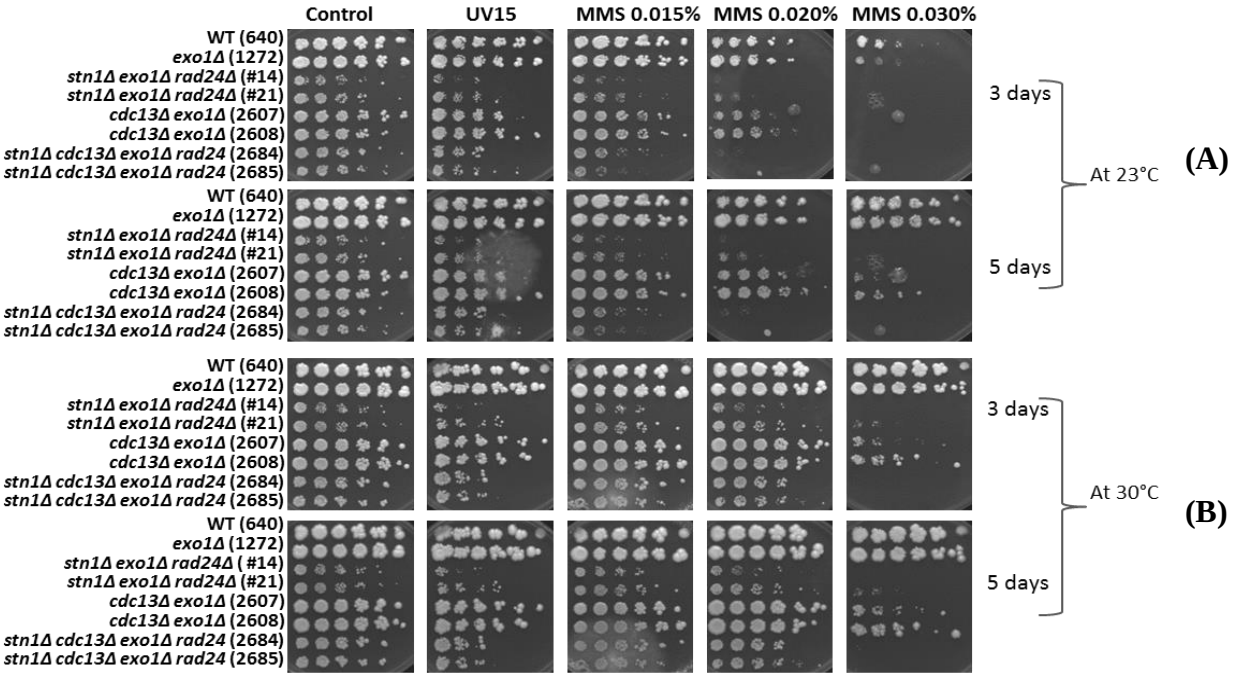

Figure 5.5. Effect of selective MMS (0.015, 0.02 and 0.03%) and UV on the growth of *cdc13* and *stn1* deletion mutants.

Eight strains including mutants and controls (640, 1272, #14, #21, 2607, 2608, 2684 and 2685) were analysed for MMS-mediated sensitivity of *cdc13Δ* and *stn1Δ* mutants. Five-fold serial dilutions of the strains in sterile water were spotted onto YEPD agar plates containing 0.015%, 0.020% and 0.030% of MMS. One plate was also exposed to UV irradiation (UV 15 J/m^2). Plates were incubated for 3-5 days at 23°C and 30°C before being photographed. Strain numbers are indicated in brackets.

(**A**) Incubation of plates for 3-5 days at 23°C.
(**B**) Incubation of plates for 3-5 days at 30°C.

5.3.1.3. Effect of H_2O_2 on the growth of *cdc13* and *stn1* deletion mutants

H_2O_2 is an oxidising DNA-damaging agent that is also used as a biocide. It can generate hydroxyl radicals that react with various cellular components including biomolecules like DNA, RNA, proteins and especially lipids (Alic *et al*., 2001) and create oxidative stress to the cell. Based on its damaging characteristics, it is used to model chronic oxidative damage to cells through oxidative stress and to investigate the effect of its toxicity on the viability of cells with different mutations. It has been reported in recent studies that, based on its concentration, H_2O_2 genotoxicity works through two distinct mechanisms that generate free radicals which react with proximal DNA and cause damage. At low concentrations, it damages DNA and at higher concentrations it oxidises proteins and lipids and cell membranes. Yeast cells exposed to oxidative stress or DNA damaging agents respond through impaired progression of cell cycle or cell cycle arrest under cell cycle checkpoint mechanisms (Weinert, 1998). H_2O_2 induced cell

cycle arrest at the G2 phase is dependent on radiation-sensitive *RAD9* gene (Weinert and Hartwell, 1988).

This study was carried out to investigate the effect of H_2O_2 on the growth of *cdc13Δ* and *stn1Δ* mutants' cells. The freshly prepared YEPD plates containing three different concentrations of H_2O_2 (2 mM, 3 mM and 4 mM; w/v) were spotted with serial dilutions of 8 cultures (two sets, one for each temperature regime). The plates were incubated at 23°C and 30°C for 3 and 5 days. The growth of *stn1Δ* mutants (haploid #14 and #21) in the presence of *rad24Δ exo1Δ* was the most abundant on 3 mM H_2O_2, and still observed on 4 mM H_2O_2 after 3 and 5 days of incubation at 23°C and 30°C where other strains did not grow at all (Figure 5.6AB).

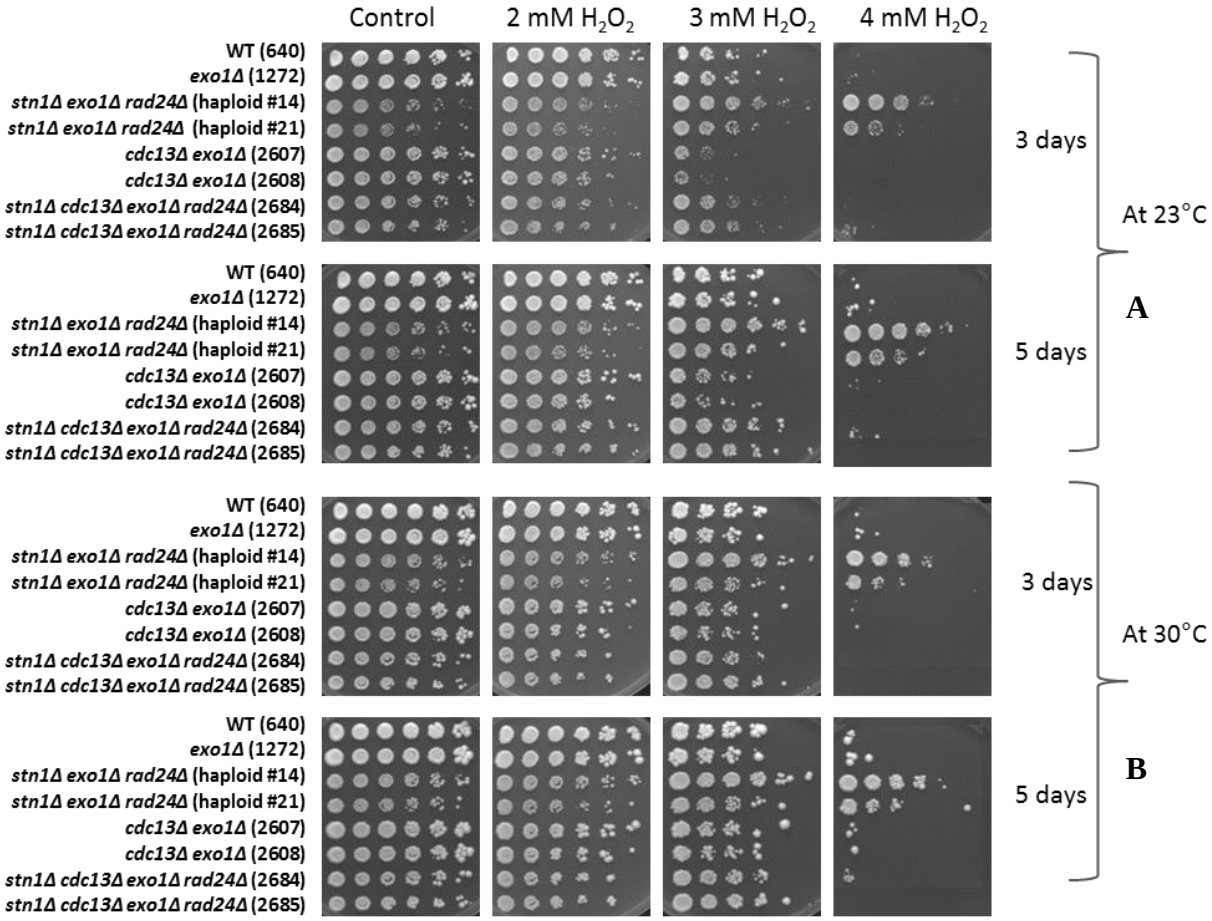

Figure 5.6. Effect of H_2O_2 (2 mM, 3 mM and 4 mM) on the growth of *cdc13Δ* and *stn1Δ* mutants**.**
Eight strains including mutants and controls (640, 1272, #14, #21, 2607, 2608, 2684 and 2685) were analysed for H_2O_2-mediated sensitivity of *cdc13Δ* and *stn1Δ* mutants. Five-fold serial dilutions of the strains in sterile water were spotted onto YEPD agar plates containing 2 mM, 3 mM and 4 mM of H_2O_2. Plates were incubated for 3-5 days at 23°C and 30°C before being photographed. Strain numbers are indicated in brackets.
(**A**) Incubation of plates for 3-5 days at 23°C.
(**B**) Incubation of plates for 3-5 days at 30°C.

The *stn1Δ* mutant #14 manifested slightly more resistance to H_2O_2 at 3 and 4 mM H_2O_2 when compared to mutant #21, in contrast to the MMS sensitivity pattern, where #14 showed an increased level of sensitivity as compared to #21. The *cdc13Δ* mutants and *cdc13Δ stn1Δ* mutant cells were moderately inhibited at 3 mM H_2O_2; the *cdc13Δ* mutants (2607 and 2608) manifested slightly more sensitivity as compared to the *cdc13Δ stn1Δ* mutants (2684 and 2685). In *cdc13Δ exo1Δ* mutants (2607 and 2608) H_2O_2-mediated growth inhibition at 3 mM concentration was more pronounced after 3 days of incubation as compared to 5 days of incubation at 23°C. The growth of wild type (640) and *exo1Δ* deletion mutant (1272) were also mildly affected at 3 mM H_2O_2 after 3-5 days of incubation at 23°C and 30°C. Overall the same toxicity patterns were exhibited at 23°C and 30°C with minimal or no growth at longer incubation (5 days) or at higher temperature (30°C). The growth of all mutants and controls was severely inhibited at increased doses of H_2O_2, 5 mM and 8 mM (Figure 5.7), with minimal growth of *stn1Δ* mutant at 5 mM showing its resistance to H_2O_2 even at higher concentration as compared to other mutants and controls. Based on these results it could be suggested that *STN1* gene might play some unknown role distinct from the *CDC13* gene through a different mechanism associated with tolerating oxidative stress.

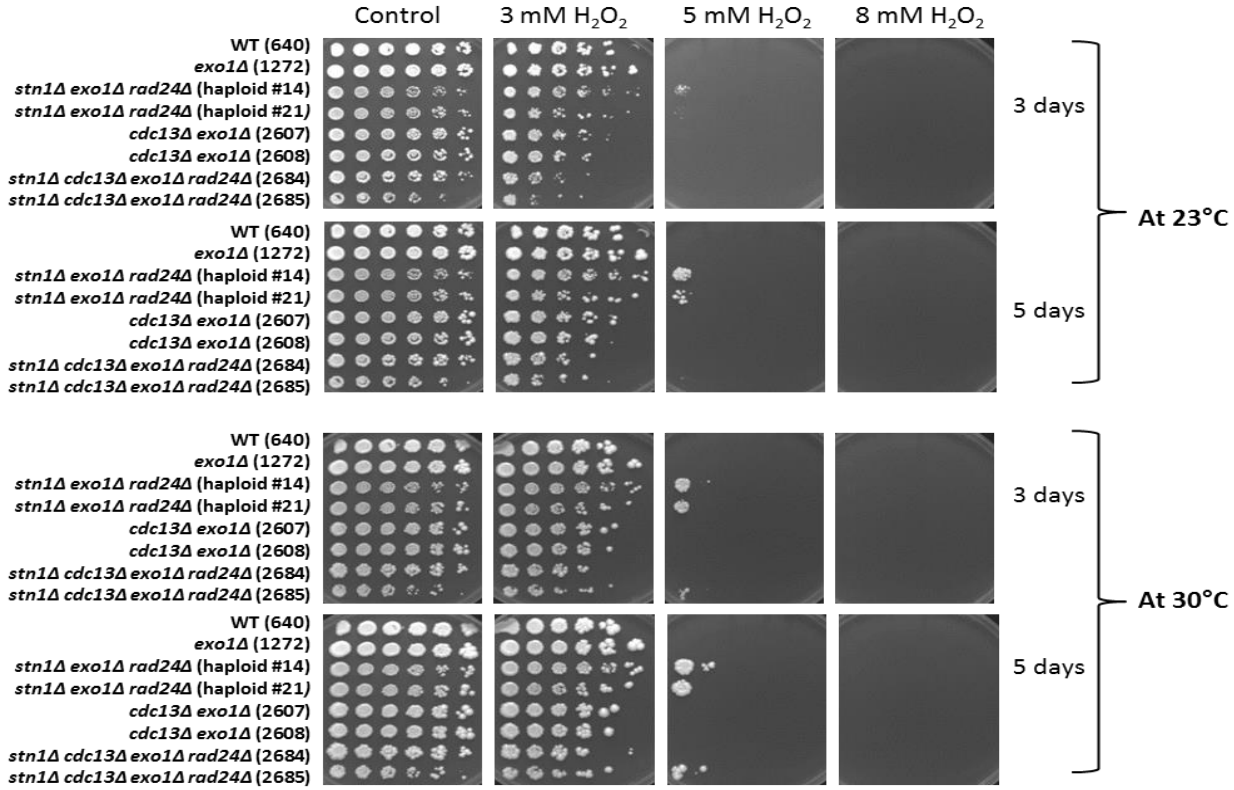

Figure 5.7. Effect of H_2O_2 (3 mM, 5 mM and 8 mM) on the growth of *cdc13Δ* and *stn1Δ* mutants.
Eight strains including mutants and controls (640, 1272, #14, #21, 2607, 2608, 2684 and 2685) were analysed for H_2O_2-mediated sensitivity of *cdc13* and *stn1* deletion mutants. Five-fold serial dilutions of the strains in sterile water were spotted onto YEPD agar plates containing 3 mM, 5 mM and 8 mM of H_2O_2. Plates were incubated for 3-5 days at 23°C and 30°C before being photographed. Strain numbers are indicated in brackets.

5.3.1.4. Effect of HU on the growth of *cdc13Δ* and *stn1Δ* deletion mutants

HU is a potent replication inhibitor. In yeast *S. cerevisia*e HU inhibits DNA replication by inhibiting ribonucleotide reductase and blocks DNA synthesis by preventing dNTP pool expansion at G1-S phase of cell cycle (Koc *et al*., 2004).

This study was aimed to examine the response of *cdc13* and *stn1* deletion mutants' cells to HU. The freshly prepared YEPD plates containing different concentrations of HU were spotted with serial dilutions of 8 cultures (two sets, one for each temperature regime). The plates were incubated at 23°C and 30°C for 3 and 5 days.

The preliminary results with 10 mM, 25 mM and 30 mM of HU (w/v) showed mild inhibition of growth to varying extents in all mutants as compared to wild type and *exo1Δ* mutants. The *cdc13Δ stn1Δ* mutants (2684 and 2685) in the presence of *exo1Δ* and *rad24Δ* showed a moderate susceptibility to HU with a slight increase in inhibition of growth as compared to either *stn1Δ* (#14 and #21) or *cdc13Δ* mutants (2607, 2608) marked at 30 mM HU after 3 and 5 days of incubation at 23°C. There was a general trend of growth restoration after 5 days of incubation in mutants and wild type strains. However, the *stn1Δ* mutant #14 exhibited less growth restoration as compared to mutant *stn1Δ cdc13Δ* (2684) after 5 days of incubation at 23°C and 30°C. The *cdc13Δ* mutants (2607 and 2608), however, displayed slightly increased resistance to HU at 30 mM as compared to other mutants.

Toxicity assays with increased doses of HU (10 mM, 25 mM and 50 mM; w/v) (Figure 5.8) revealed the same trends of growth inhibition with *stn1Δ cdc13Δ* (2684 and 2685) showing more pronounced HU-induced growth inhibition at 23°C (Figure 5.8) and 30°C (Figure 5.8) after 3 days of incubation. The *stn1Δ* mutants, haploid #14, showed slightly more sensitivity to 50 mM HU when compared to mutant #21, with the sensitivity pattern comparable to MMS-induced sensitivity of *stn1Δ* mutants (#14 with an increased level of sensitivity as compared to #21, earlier in this section). Similarly, the inhibition of growth in the *stn1Δ* mutant #14 was comparable to the *cdc13Δ stn1Δ* mutant strain 2684 at 23°C and 30°C after 3 days of incubation but this pattern changed after 5 days of growth where combined deletion mutants exhibited increased growth restoration as compared to *stn1Δ* mutant #14. The *cdc13Δ* mutants (2607 and 2608) persistently displayed slightly increased resistance to HU at 50 mM as compared to other mutants. Further assays at even higher concentrations of HU (50 mM, 75 mM and 100 mM HU; w/v) (Figure 5.9AB) clearly showed that strains containing *stn1Δ cdc13Δ* (2684 and 2685) mutations with *exo1Δ rad24Δ* were completely inhibited in the presence of 100 mM HU at 23°C and 30°C after 3 and 5 days of incubation with a mild restoration of cell growth after 5 days of incubation at 23°C and 30°C. The strains *stn1Δ* (#14 and #21) mutants showed much better growth sensitivity, than strains with combined deletions (2684 and 2685) and slightly less growth as compared to *cdc13Δ* mutants (2607 and 2608) at 23°C. Results also showed that at

23°C (Figure 5.9A) and 30°C (Figure 5.9B) the growth of *cdc13Δ* mutants (2607 and 2608) were partially inhibited in the presence of increased concentrations of 50, 75 and 100 mM HU (pronounced at 23°C) after 3 and 5 days of incubation, though it still manifested resistance as compared to WT, *exo1Δ* and 2684 and 2685 strains (*cdc13Δ stn1Δ*). The growth of wild type (640) and *exo1Δ* mutants (1272) were not, or negligibly, affected at 30, 50 or 100 mM concentration of HU after 3-5 days of incubation at 23°C and 30°C.

The stronger inhibition of growth in combined deletion mutants *stn1Δ cdc13Δ* (2684 and 2685) suggests that *cdc13Δ* and *stn1Δ* might contribute to the sensitivity via different pathways.

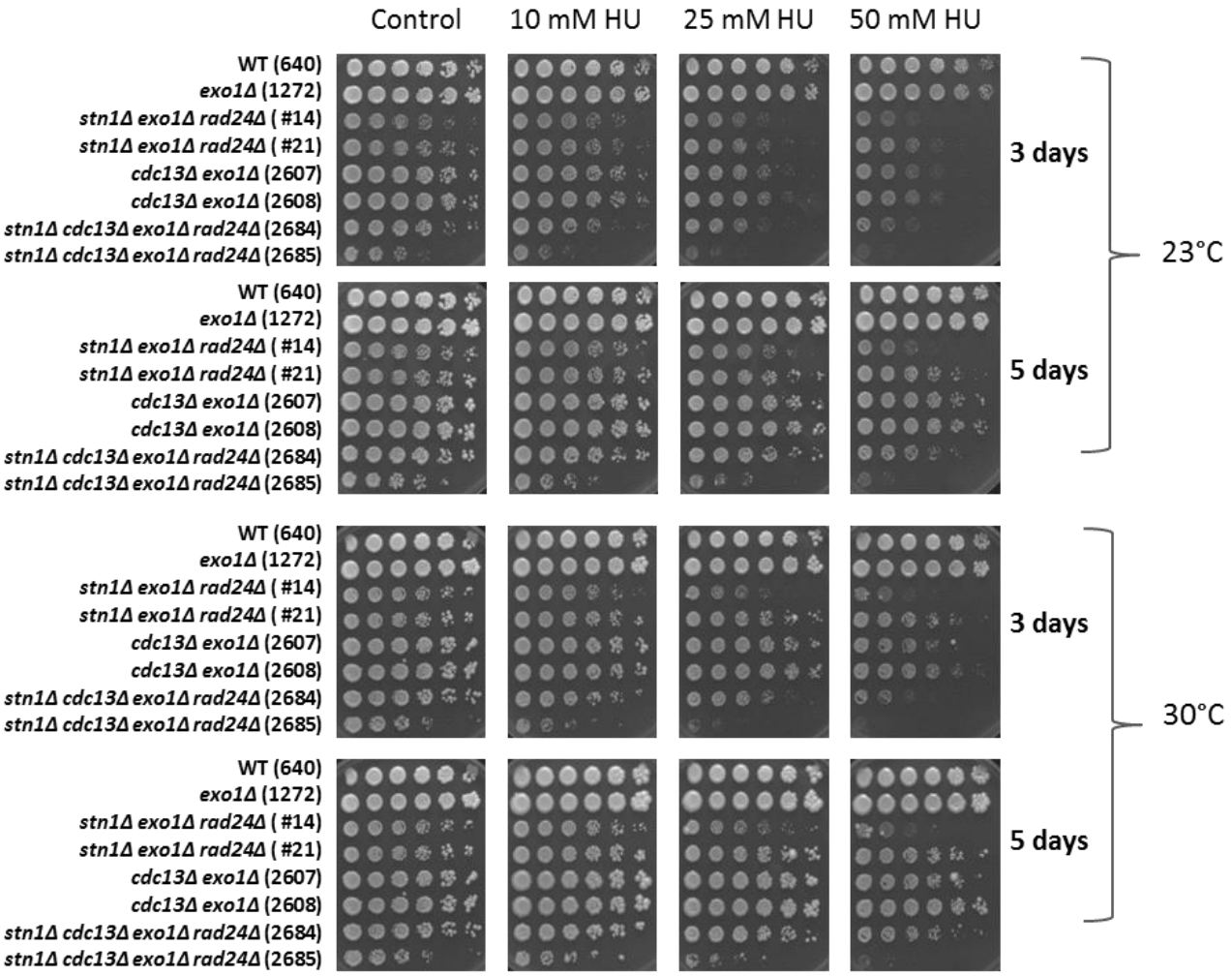

Figure 5.8. Effect of low concentration of HU (10 mM, 25 mM and 50 mM) on the growth of *cdc13Δ* and *stn1Δ* mutants.

Eight strains including mutants and controls (640, 1272, #14, #21, 2607, 2608, 2684 and 2685) were analysed for HU-mediated sensitivity of *cdc13Δ* and *stn1Δ* mutants. Five-fold serial dilutions of the strains in sterile water were spotted onto YEPD agar plates containing 10 mM, 25 mM and 50 mM of HU. Plates were incubated for 3-5 days at 23°C and 30°C before being photographed. Strain numbers are indicated in brackets.

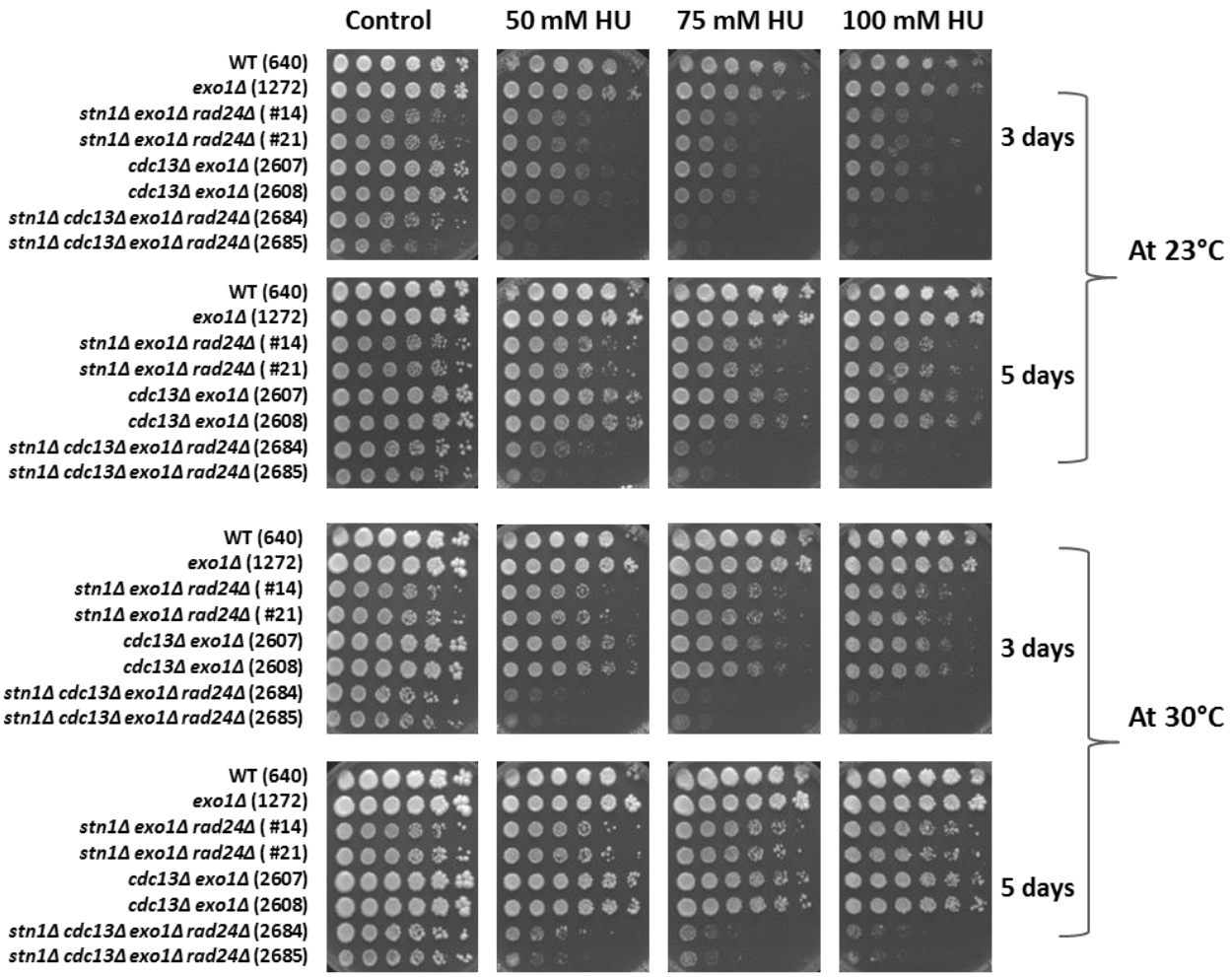

Figure 5.9. Effect of higher doses of HU (50 mM, 75 mM and 100 mM) on the growth of *cdc13Δ* and *stn1Δ* mutants.

Eight strains including mutants and controls (640, 1272, #14, #21, 2607, 2608, 2684 and 2685) were analysed for HU-mediated sensitivity of *cdc13Δ* and *stn1Δ* mutants. Five-fold serial dilutions of the strains in sterile water were spotted onto YEPD agar plates containing 50 mM, 75 mM and 100 mM of HU. Plates were incubated for 3-5 days at 23°C and 30°C before being photographed. Strain numbers are indicated in brackets.

5.3.2. Synergistic effect of genotoxic agents on the growth of different deletion mutants

5.3.2.1. Synergistic effect of UV and MMS on the growth of *cdc13Δ* and *stn1Δ* mutants

It was shown earlier in this chapter that *cdc13Δ* mutants (2607 and 2608) were more resistant to MMS as compared to *stn1Δ* (#14 and #21) and *stn1Δ cdc13Δ* (2684 and 2685) mutants. However, to see the combined effect of UV and MMS, freshly prepared YEPD plates containing different concentrations of MMS (0.010 %, 0.015 %, and 0.020 %; w/v) were spotted with serial dilutions of 8 cultures (two sets, one for each temperature regime). The plates were exposed to different doses of UV (25, 50, 60 and 75 J/m^2). The results clearly showed that low

concentration of MMS (0.010%) enhanced the genotoxic effect of UV on the growth of all deletion mutants (Figure 5.10A-D). The combined effects of MMS with UV enhanced the inhibitory effects cooperatively, e.g., UV exposure of 25 J/m^2 at MMS 0.010% concentration increased the sensitivity to the level exhibited at MMS 0.015%-0.020% or UV 75 J/m^2 at 23°C after 3 and 5 days of incubation (Figure 5.10AB) or comparable to MMS 0.015% or UV 50 J/m^2 at 30°C after 3 and 5 days of incubation (Figure 5.10CD). However, differences between sensitivity of *cdc13*Δ and *stn1*Δ single mutants were not distinguishable at 23°C after 3 days because of the strong inhibition of growth.

Under conditions of the combined treatment, the *cdc13Δ* mutants (2607 and 2608) also exhibited resistance to MMS (0.010%) at UV 25 J/m^2, as compared to *stn1Δ* (#14 and #21), *stn1Δ cdc13Δ exo1Δ rad24Δ* (2684 and 2685), which were more obvious at 30°C after 3 and 5 days of incubation. The *stn1* deletion mutant #14 appeared to be more sensitive than #21. The *cdc13Δ* and *stn1Δ* mutant, 2685 strain exhibited increased sensitivity to MMS as compared to the 2684 strain.

It could be concluded that both genotoxic agents enhanced lethality of the cells cooperatively.

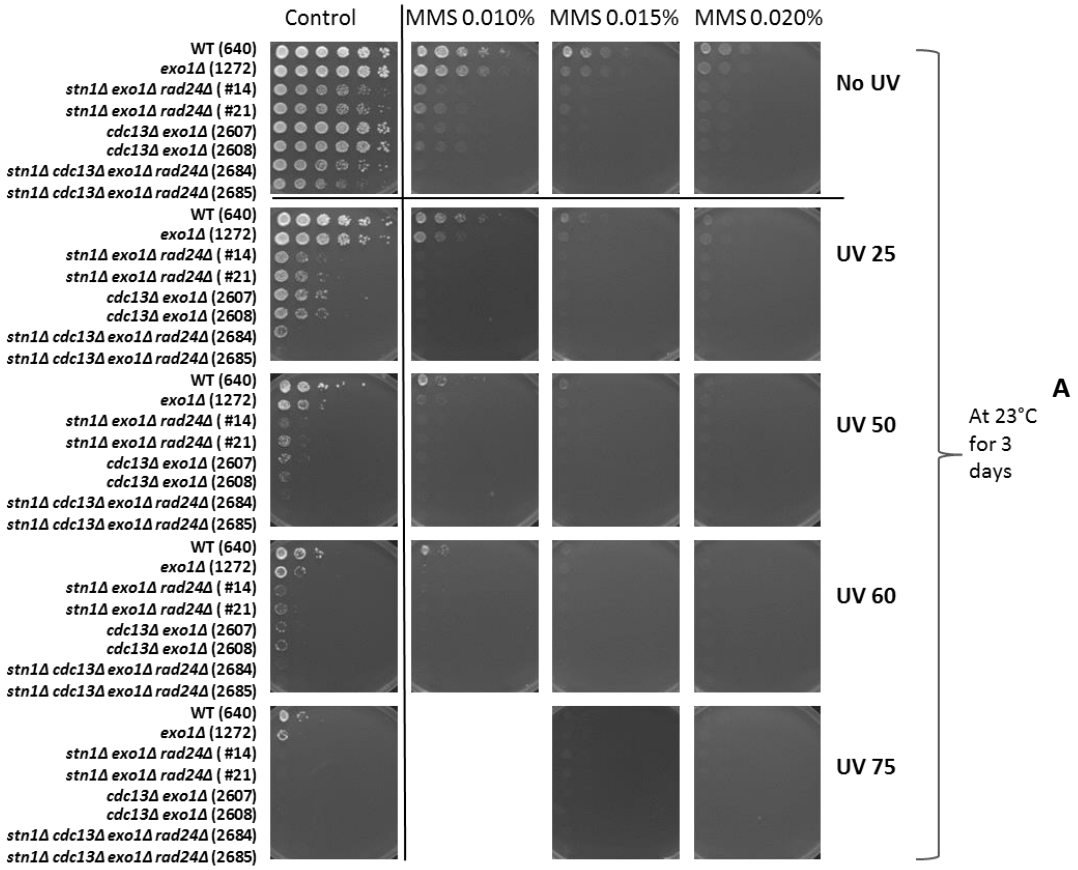
Control
MMS 0.010%
MMS 0.015%
MMS 0.020%
WT (640)
exo1Δ (1272)
stn1Δ exo1Δ rad24Δ (#14)
stn1Δ exo1Δ rad24Δ (#21)
cdc13Δ exo1Δ (2607)
cdc13Δ exo1Δ (2608)
stn1Δ cdc13Δ exo1Δ rad24Δ (2684)
stn1Δ cdc13Δ exo1Δ rad24Δ (2685)
No UV
UV 25
UV 50
UV 60
UV 75
At 23°C for 3 days
A

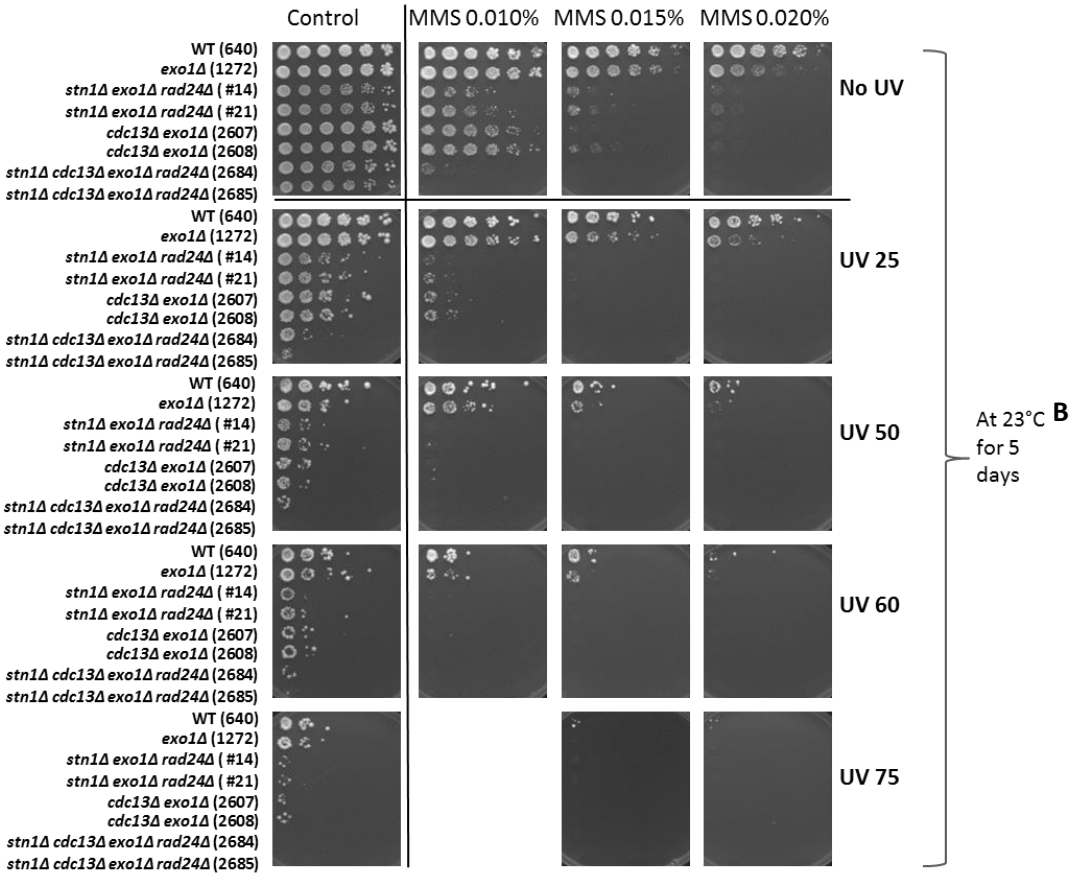
Control
MMS 0.010%
MMS 0.015%
MMS 0.020%
WT (640)
exo1Δ (1272)
stn1Δ exo1Δ rad24Δ (#14)
stn1Δ exo1Δ rad24Δ (#21)
cdc13Δ exo1Δ (2607)
cdc13Δ exo1Δ (2608)
stn1Δ cdc13Δ exo1Δ rad24Δ (2684)
stn1Δ cdc13Δ exo1Δ rad24Δ (2685)
No UV
UV 25
UV 50
UV 60
UV 75
At 23°C for 5 days
B

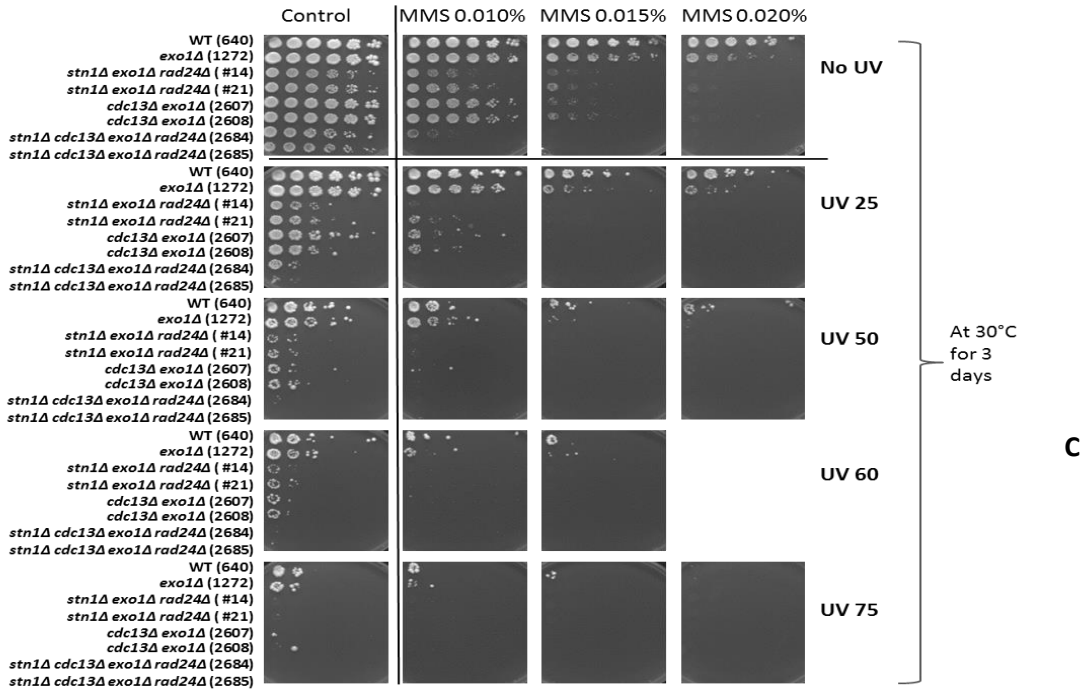

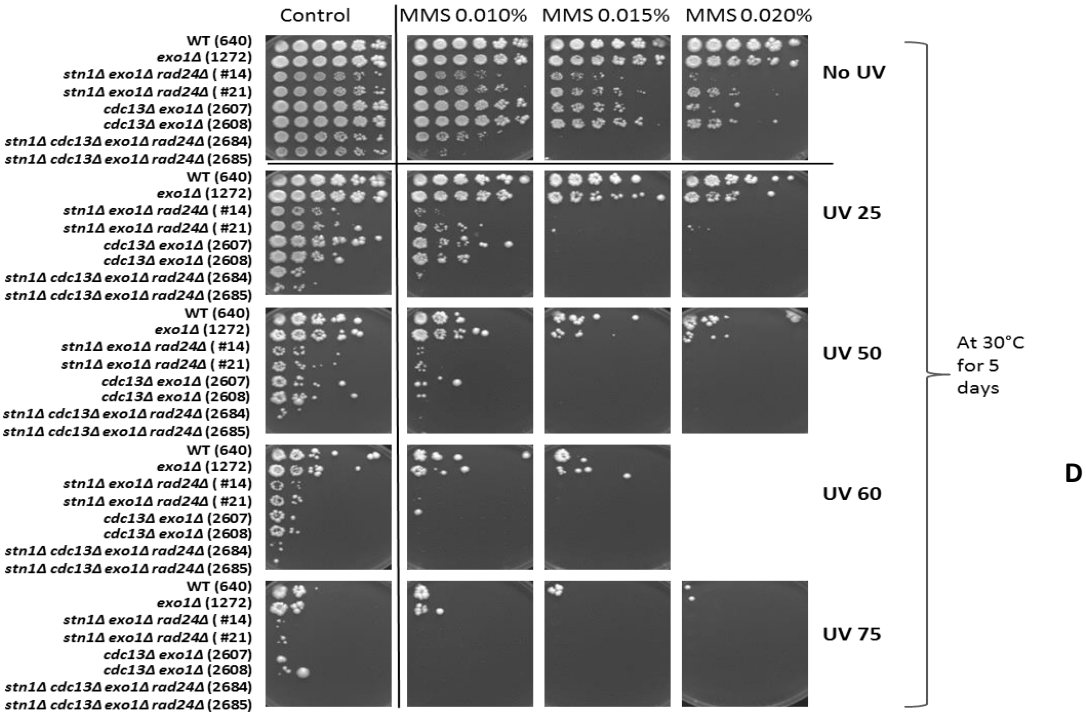

Figure 5.10. Combined effects of MMS and UV on the growth of *cdc13Δ* and *stn1Δ* mutants.

Eight strains including mutants and controls (640, 1272, #14, #21, 2607, 2608, 2684 and 2685) were analysed for MMS+UV-mediated sensitivity of *cdc13Δ* and *stn1Δ* mutants. Five-fold serial dilutions of the strains in sterile water were spotted onto YEPD agar plates containing 0.010%, 0.015%, 0.020% of MMS. Plates were exposed to different doses of UV irradiation (25, 50, 60 and 75 J/m^2) and incubated for 3-5 days at 23°C and 30°C before being photographed. Strain numbers are indicated in brackets.

(**A**) At 23°C after 3 days of incubation.

(**B**) At 23°C after 5 days of incubation.

(**C**) At 30°C after 3 days of incubation.

(**D**) At 30°C after 5 days of incubation.

5.3.2.2. Synergistic effect of UV and H_2O_2 on the growth of *cdc13Δ* and *stn1Δ* mutants

The *stn1Δ* (#14 and #21) mutants exhibited resistance to H_2O_2 as compared to *stn1Δ cdc13Δ* (2684 and 2685) mutants and *cdc13Δ* mutants (2607 and 2608) as shown earlier in this chapter. To determine the combined effect of UV and H_2O_2, the freshly prepared YEPD plates containing different concentrations of H_2O_2 (2 mM, 3 mM and 4 mM; w/v) were spotted with serial dilutions of 8 cultures. The plates were exposed to UV (in UV time exposure mode) with different doses of UV (25 50, 60 and 75 J/m^2). The results showed that H_2O_2 at higher doses of 4 mM enhanced the resistance of *stn1Δ* (#14 and #21) to UV 25 J/m^2 (Figure 5.11A-D). However, the growth of other mutants, *stn1Δ cdc13Δ* (2684 and 2685) and *cdc13Δ* (2607 and 2608), was severely inhibited at this concentration of H_2O_2 under the effect of UV. The growth of *stn1Δ* (#14 and #21) mutants was comparable to growth of wild type and *exo1Δ* mutants at 4 mM H_2O_2 and UV 25 J/m^2 at 23°C (Figure 5.11AB) and 30°C (Figure 5.11CD) after 3 and 5 days of incubation. However, at lower concentration of H_2O_2 (2 mM), the growth pattern of all mutants and controls were comparable to growth exhibited under the respective UV exposure. It could be concluded from these results that H_2O_2 enhanced the resistance of *stn1Δ* (#14 and #21) mutants under the effect of UV in a concentration-dependent manner.

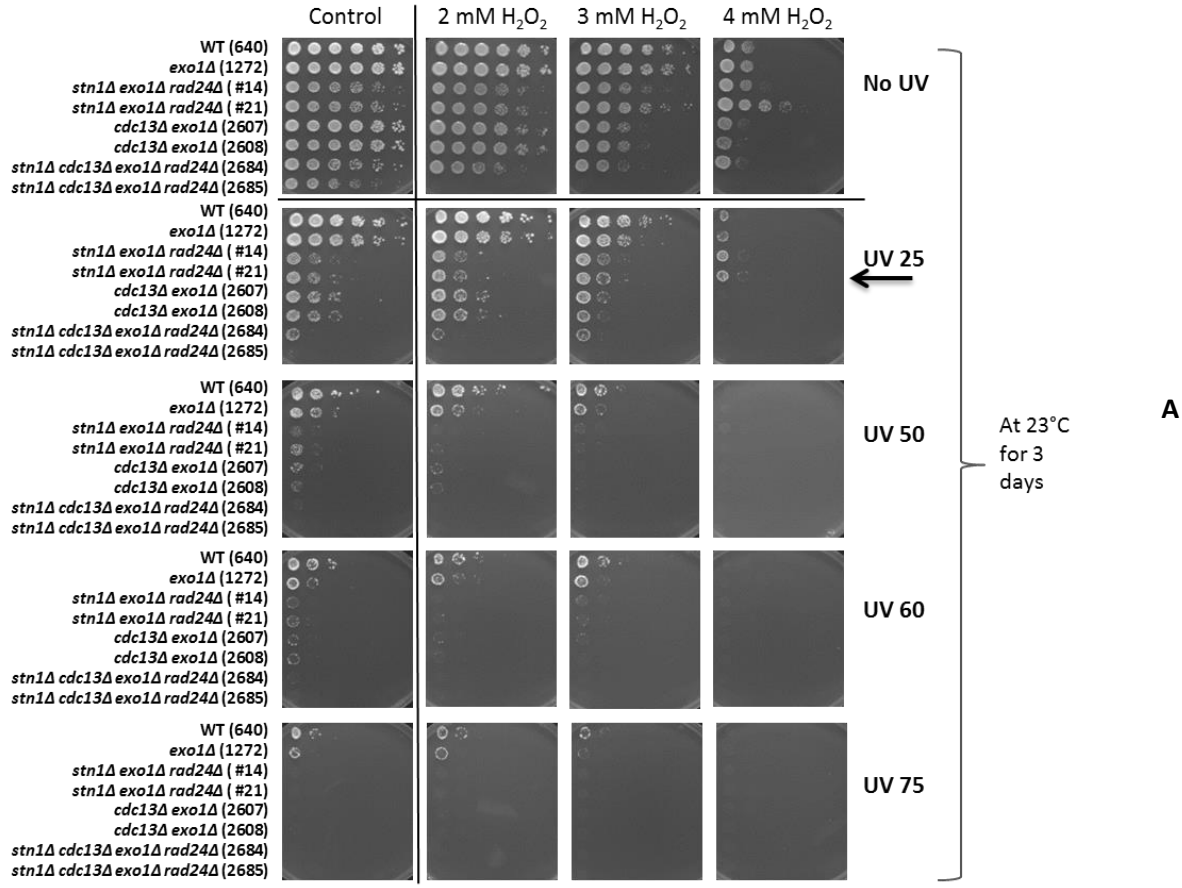
Control
2 mM H_2O_2
3 mM H_2O_2
4 mM H_2O_2
WT (640)
exo1Δ (1272)
stn1Δ exo1Δ rad24Δ (#14)
stn1Δ exo1Δ rad24Δ (#21)
cdc13Δ exo1Δ (2607)
cdc13Δ exo1Δ (2608)
stn1Δ cdc13Δ exo1Δ rad24Δ (2684)
stn1Δ cdc13Δ exo1Δ rad24Δ (2685)
No UV
UV 25
UV 50
UV 60
UV 75
At 23°C for 3 days
A

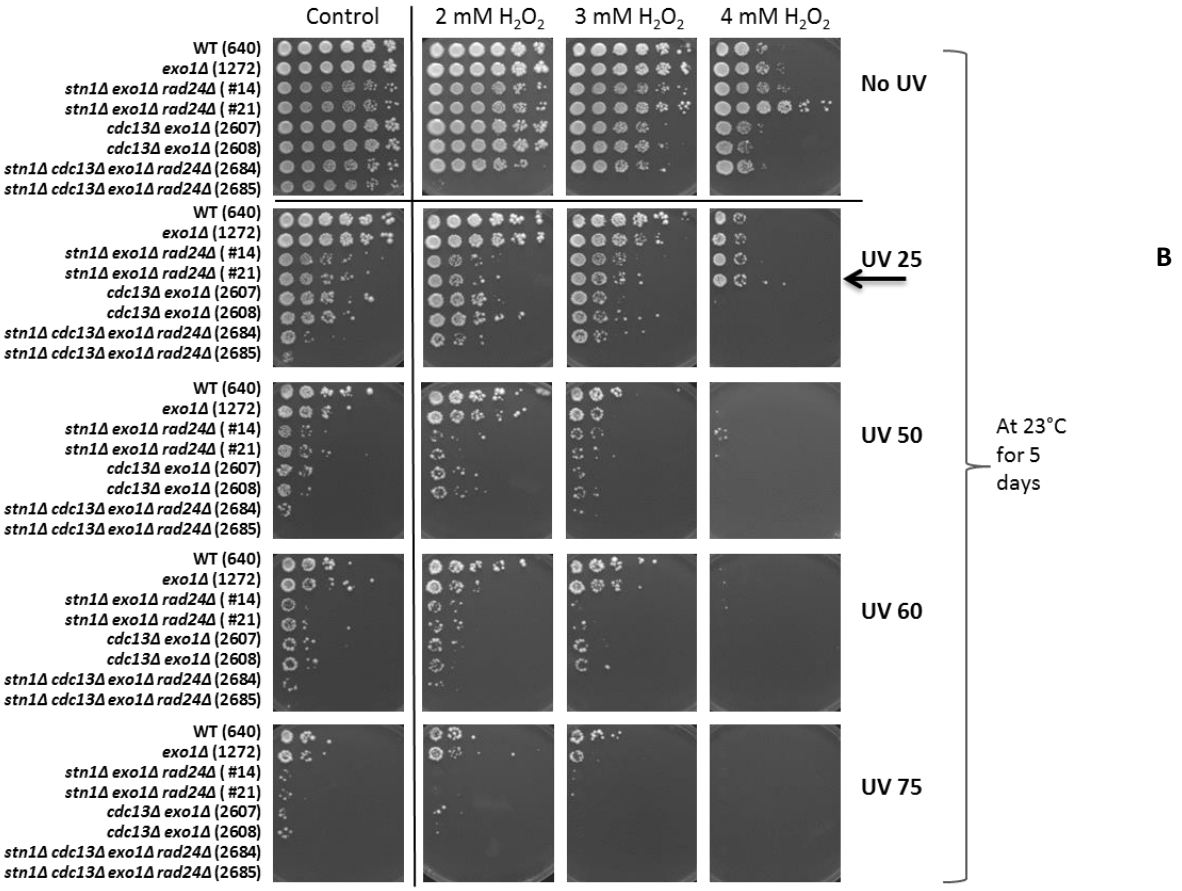
Control
2 mM H_2O_2
3 mM H_2O_2
4 mM H_2O_2
WT (640)
exo1Δ (1272)
stn1Δ exo1Δ rad24Δ (#14)
stn1Δ exo1Δ rad24Δ (#21)
cdc13Δ exo1Δ (2607)
cdc13Δ exo1Δ (2608)
stn1Δ cdc13Δ exo1Δ rad24Δ (2684)
stn1Δ cdc13Δ exo1Δ rad24Δ (2685)
No UV
UV 25
UV 50
UV 60
UV 75
At 23°C for 5 days
B

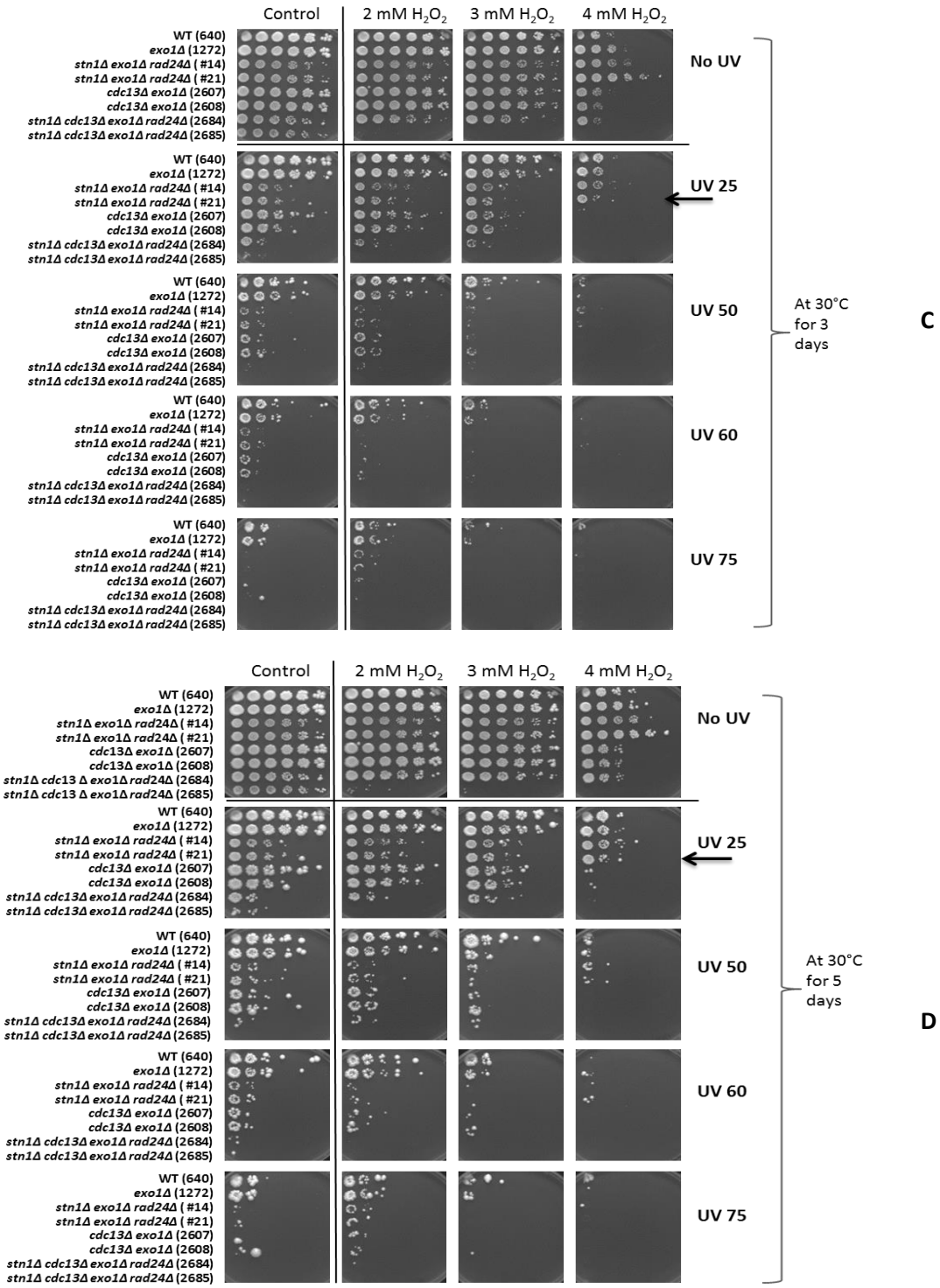

Figure 5.11. Combined effect of H_2O_2 and UV on the growth of *cdc13Δ* and *stn1Δ* mutants.
Eight strains including mutants and controls (640, 1272, #14, #21, 2607, 2608, 2684 and 2685) were analysed for H_2O_2+UV-mediated sensitivity of *cdc13Δ* and *stn1Δ* mutants. Five-fold serial dilutions of the strains in sterile water were spotted onto YEPD agar plates containing 2 mM, 3 mM, 4 mM of H_2O_2. Plates were exposed to different doses of UV irradiation (25, 50, 60 and 75 J/m^2) and incubated for 3-5 days at 23°C and 30°C before being photographed. Strain numbers are indicated in brackets.

(**A**) At 23°C after 3 days of incubation.
(**B**) At 23°C after 5 days of incubation.
(**C**) At 30°C after 3 days of incubation.
(**D**) At 30°C after 5 days of incubation.

5.3.2.3. Synergistic effect of UV and HU on the growth of *cdc13Δ* and *stn1Δ* mutants

In this section, the cooperative effect of HU was determined in the presence of UV. It was shown earlier in this chapter that combined deletion *stn1Δ cdc13Δ* (2684 and 2685) mutants exhibited severe growth arrest in the presence of HU (50 mM or above) as compared to *stn1Δ* (#14 and #21) or *dc13Δ* mutants (2607 and 2608) at 23°C or 30°C for 3 and 5 days. At increased concentration of HU (50 mM, 75 mM and 100 mM HU) the *cdc13Δ* mutants (2607 and 2608) appeared to be slightly susceptible to HU, however, comparatively less than *stn1Δ* (#14 and #21). The synergetic effects of UV and HU were tested at different concentrations of HU (50 mM, 75 mM and 100 mM HU; w/v) combined with UV exposures of different doses (25, 50, 60 and 75 J/m^2).

The results showed that 50 mM HU enhanced the genotoxic effect of UV on the growth of all deletion mutants and controls at 23°C and 30°C after 3 and 5 days of incubation (Figure 5.12A-D). The combined effects of HU with UV exposure of 25 J/m^2 enhanced the inhibitory effects cooperatively, e.g., UV exposure of 25 j/m^2 with 50 mM of HU increased the sensitivity to the level exhibited between UV 60 and UV 75 at 23°C (Figure 5.12AB) and 30°C (Figure 5.12CD) after 3 and 5 days of incubation. However, 50 mM HU increased the resistance of the *stn1*Δ mutant (#14 and #21) to UV 25 exhibited at 23°C and 30°C after 3 and 5 days of incubation to a lesser extent. This could be the concentration-dependent effect of HU similar to the effect of H_2O_2 at 4 mM concentration shown in the previous section. This phenomenon of HU resistance, however, was not distinguishable at 50 mM, 75 mM or 100 mM HU in the absence of UV.

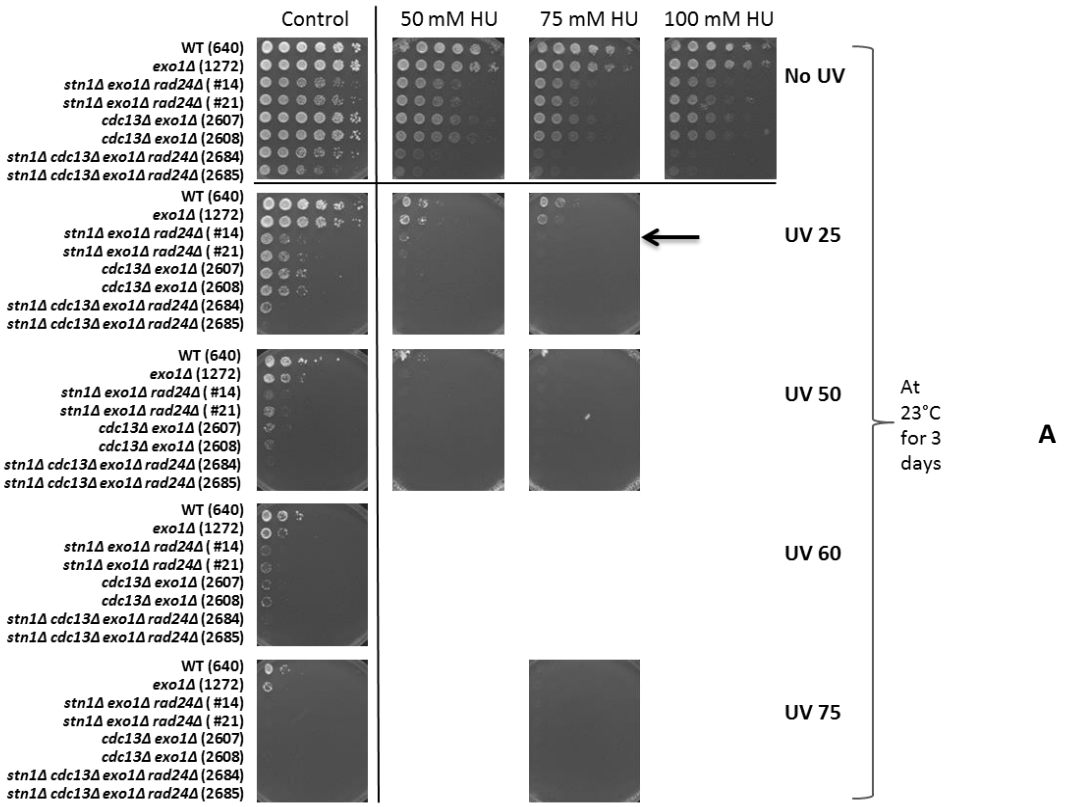
Control
50 mM HU
75 mM HU
100 mM HU
WT (640)
exo1Δ (1272)
stn1Δ exo1Δ rad24Δ (#14)
stn1Δ exo1Δ rad24Δ (#21)
cdc13Δ exo1Δ (2607)
cdc13Δ exo1Δ (2608)
stn1Δ cdc13Δ exo1Δ rad24Δ (2684)
stn1Δ cdc13Δ exo1Δ rad24Δ (2685)
No UV
UV 25
UV 50
UV 60
UV 75
At 23°C for 3 days
A

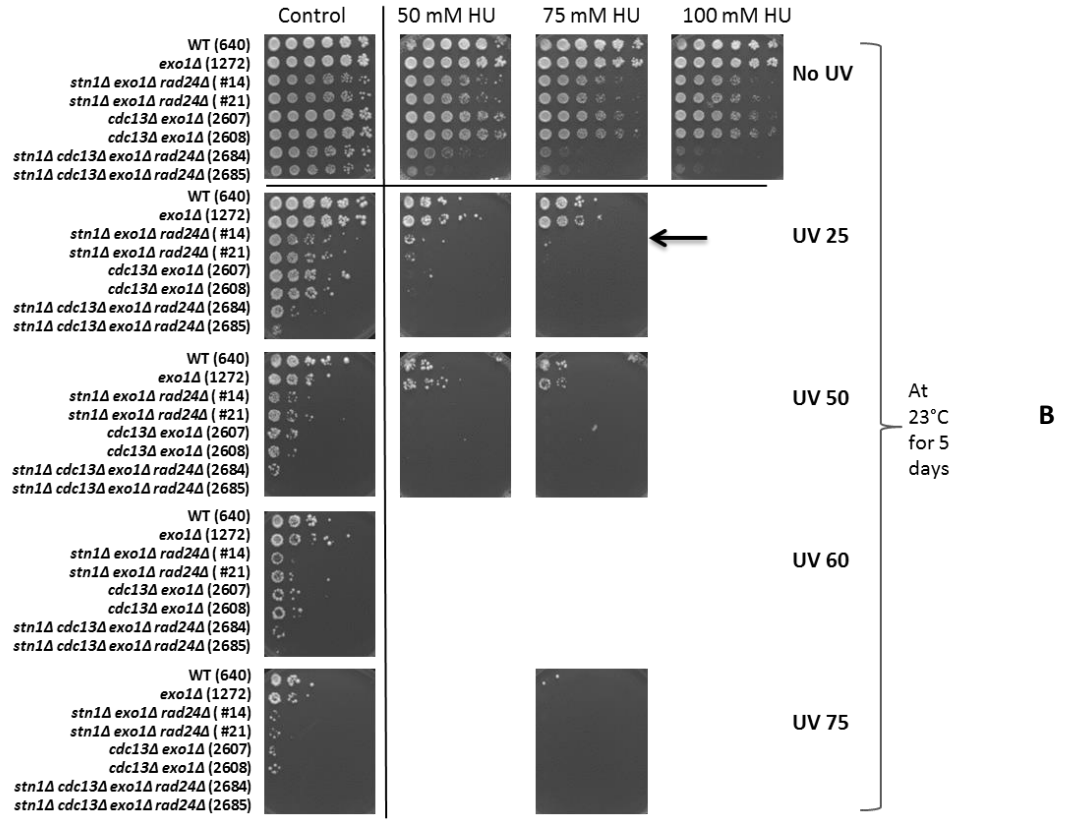
Control
50 mM HU
75 mM HU
100 mM HU
WT (640)
exo1Δ (1272)
stn1Δ exo1Δ rad24Δ (#14)
stn1Δ exo1Δ rad24Δ (#21)
cdc13Δ exo1Δ (2607)
cdc13Δ exo1Δ (2608)
stn1Δ cdc13Δ exo1Δ rad24Δ (2684)
stn1Δ cdc13Δ exo1Δ rad24Δ (2685)
No UV
UV 25
UV 50
UV 60
UV 75
At 23°C for 5 days
B

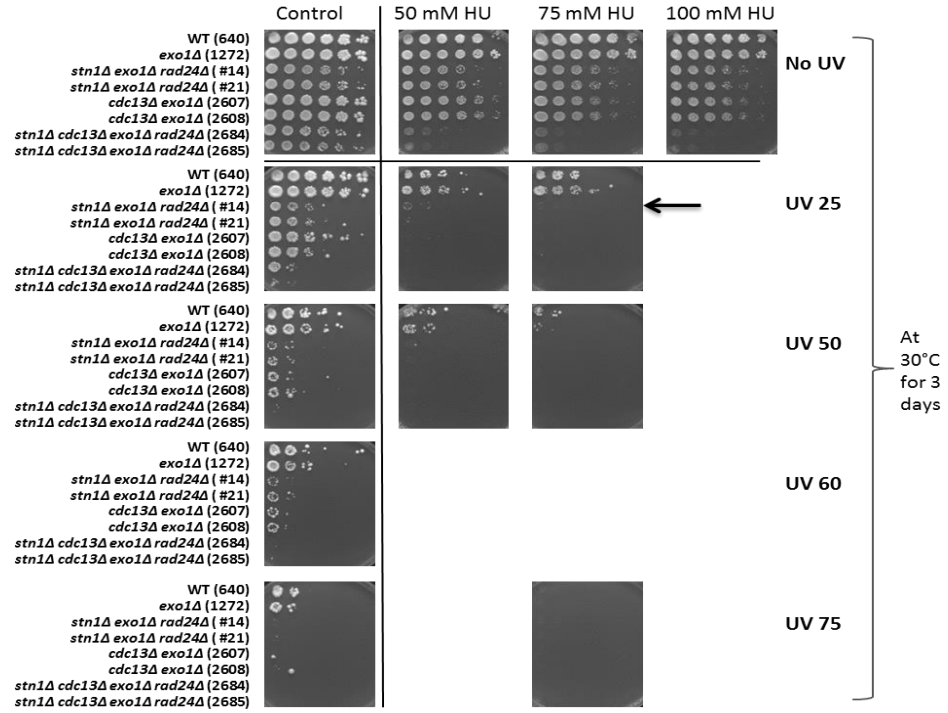

C

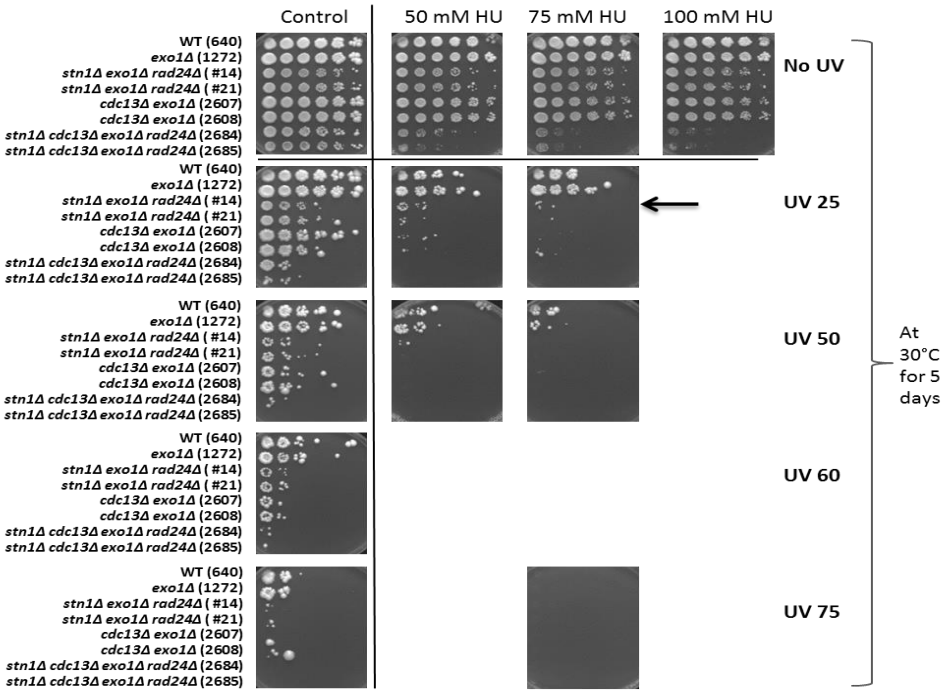

D

Figure 5.12. Combined effect of HU and UV on the growth of *cdc13Δ* and *stn1Δ* mutants.

Eight strains including mutants and controls (640, 1272, #14, #21, 2607, 2608, 2684 and 2685) were analysed for HU +UV-mediated sensitivity of *cdc13Δ* and *stn1Δ* mutants. Five-fold serial dilutions of the strains in sterile water were spotted onto YEPD agar plates containing 50 mM, 75 mM and 100 mM (w/v) of HU. Plates were exposed to different doses of UV irradiation with 25, 50, 60 and 75 J/m^{2}of UV and incubated for 3-5 days at 23°C and 30°C before being photographed. Strain numbers are indicated in brackets.

(**A**) At 23°C after 3 days of incubation.

(**B**) At 23°C after 5 days of incubation

(**C**) At 30°C after 3 days of incubation.

(**D**) At 30°C after 5 days of incubation.

Looking at the response of *cdc13Δ* and *stn1Δ* mutants on MMS, H_2O_2 and HU, it could be hypothesised that a) sensitivity to both MMS and HU might be under the control of the same pathways, b) sensitivity to H_2O_2 could possibly be under a different controlling mechanism, c) increased sensitivity of combined deletion could be due to the effect of either *rad24Δ* or due to interaction of *cdc13Δ* and *stn1Δ* cooperatively.

5.3.3. The effects of genotoxic agents on the growth of *cdc13-1* mutants lacking N- or C-terminus

5.3.3.1. Effects of UV on N- and C-terminal truncated variants of *cdc13-1*

These studies were carried out to compare the growth pattern of *cdc13-1* mutants lacking the N- or C-terminus under the effect of UV. Initial experiments were performed to determine the effective dose of UV irradiation by exposing N- and C-terminus deleted (NTΔ and CTΔ) variants of *cdc13-1* to a range of UV exposures. Two YEPD plates (P1 and P2) each spotted with serial dilutions of 8 cultures containing parent strains (1296-TR and 1297-TR), wild type (640 and 641), *cdc13Δ* (2607 and 2608), *cdc13-1*-NTΔ and *cdc13-1*-CTΔ mutants (two construct from each parent strain) were exposed to different doses of UV irradiation (2, 4, 6, 8, 10, 20, 30, 50 and 100 J/m^2). The plates were incubated at 23°C and 30°C for 3 and 5 days.

The mutants *cdc13Δ*, *cdc13-1*-NTΔ and -CTΔ exhibited distinct patterns of growth inhibition initiated at UV 10 J/m^2, obvious at UV 30 J/m^2 and severe growth arrest at UV 50 J/m^2 at 23°C and 30°C after 3 days of incubation. The *cdc13Δ* (2607 and 2608) mutants showed the maximum sensitivity to UV with the least growth as compared to NTΔ and CTΔ mutant at UV 30 J/m^2 and 50 J/m^2, well pronounced at 23°C with minimal growth recovery at UV 30 J/m^2 and 50 J/m^2) as compared to 30°C after 3 days of incubation. Similarly, *cdc13-1*-NTΔ mutants also displayed severe inhibition of growth, with slightly better growth as compared to *cdc13Δ* (2607 and 2608) at UV 30 J/m^2 and 50 J/m^2. In contrast, *cdc13-1*-CTΔ mutants displayed significant resistance to UV with growth patterns comparable to the original strains 1296-TR, 1297-TR and wild type strains (640 and 641) at UV 30, 50 and 100 J/m^2 at 23°C and 30°C after 3 days of incubation. However, *cdc13-1* mutants strains (1296-TR and 1297-TR) manifested pronounced resistance to UV with growth comparable to wild type (640 and 641), obvious at 30°C after 3 days of incubation. Similar trends of growth arrest were observed at 23°C and 30°C after 5 days of incubation. However, some restoration of growth was observed in all mutants and in the wild type after a longer incubation of 5 days at 23°C or at the higher temperature of 30°C after 3-5 days of incubation.

Considering the effective range of UV exposures (30 J/m^2 or above), further experiments were performed with the above mentioned mutants and controls to elucidate the inhibition of growth observed in preliminary experiments. Figure 5.13 presents the gradual increase in inhibition of growth with increasing exposures to UV (from UV 30 to UV 100 J/m^2) in a dose-dependent

manner. The maximum growth arrest was observed in case of *cdc13Δ* mutants (2607 and 2608) in the range of UV 50-UV 70 J/m^2. *cdc13-1*-NTΔ also exhibited moderate growth arrest in the same UV range, while CTΔ mutants displayed comparatively weak sensitivity in this UV range. The growth decline patterns in four *cdc13-1*-NTΔ mutants from two parent strains (with *cdc13-1 exo1*Δ) consistently manifested the similar trends. The wild type (640 and 641) and strains 1296-TR and 1297-TR also showed moderate sensitivity to UV 60 J/m^2 and above with least growth at UV 100 J/m^2. However, these distinct trends in UV sensitivity and resistance were more pronounced at 23°C as compared to 30°C. The parent strains also displayed increased resistance to UV to varying extents as compared to wild type (640 and 641) at higher UV exposure (100 J/m^2).

Further analysis of these mutants at narrow selective UV exposures (25, 50, 55, 60, 65 and 70 J/m^2) also revealed the same distinct trends among *cdc13Δ, cdc13-1*-NTΔ and *cdc13-1*-CTΔ mutants, with maximum, moderate and least sensitivities to UV. However at this range of UV exposure, the sensitivity difference was less distinct between wild type and parent strains (Figure 5.14). This difference however could only be limited at higher UV exposures (UV 100 J/m^2). The growth in parent and wild type strains were slightly less, however the overall sensitivity of *cdc13-1*-CTΔ were still comparable to wild type and parent strains, well pronounced at UV 65 J/m^2 and UV 70 J/m^2 at 23°C after 3 and 5 days of incubation.

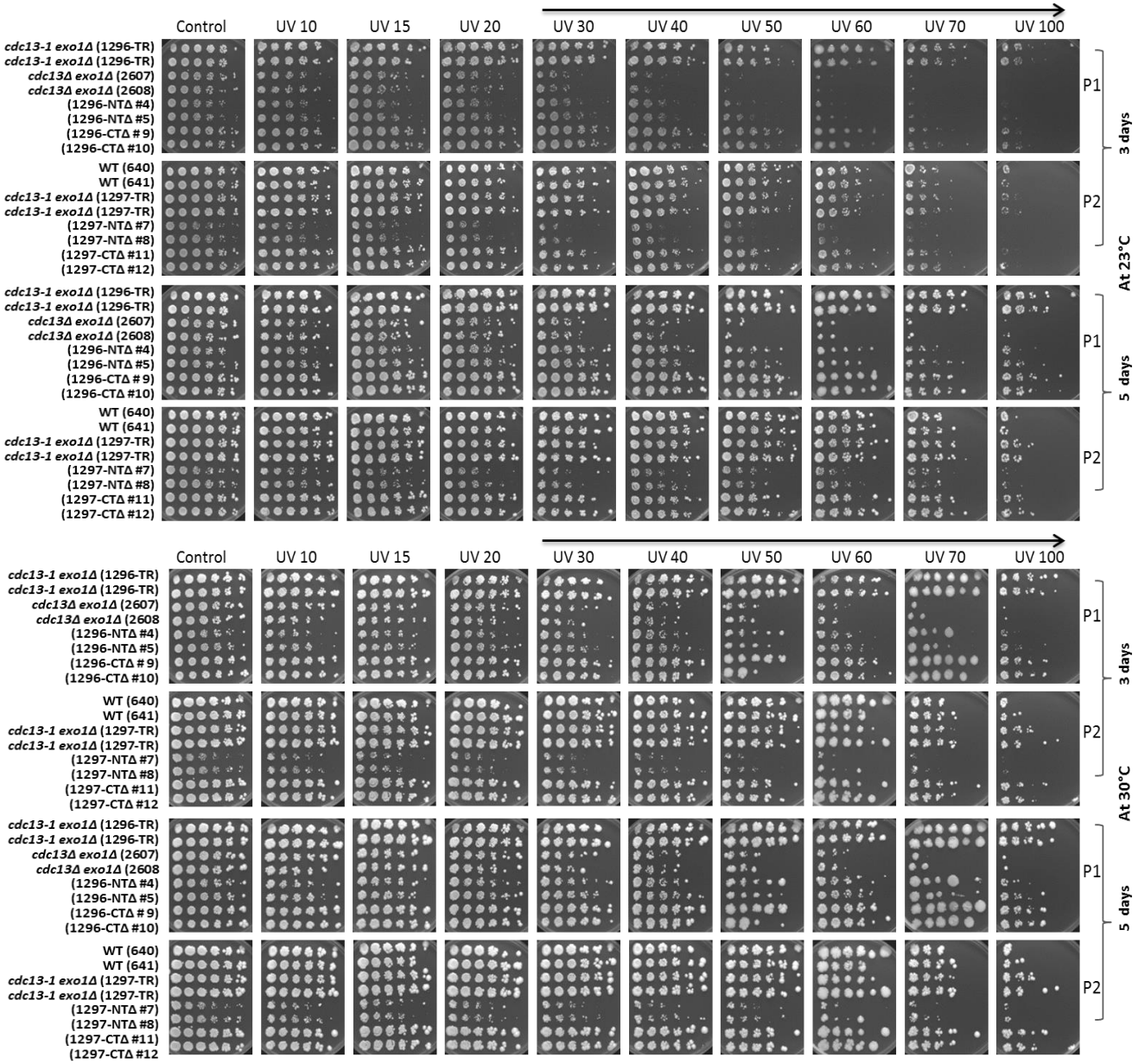

Figure 5.13. Effect of wide-range of UV irradiation (10, 15, 20, 30, 40, 50, 60, 70 and 100 J/m^2) on the growth of *cdc13-1* N- and C-terminus truncated mutants of 1296-TR and 1297-TR strains.

Sixteen strains on two plates (P1 and P2) including mutants and controls (1296-TR x2, 2607, 2608, *cdc13-1*-NTΔ x2 (1296) and *cdc13-1*-CTΔ x2 (1296), 640, 641, 1297-TR x2, *cdc13-1*-NTΔ x2 (1297) and *cdc13-1*-CTΔ x2 (1297) were analysed for UV sensitivity. Five-fold serial dilutions of the strains in sterile water were spotted onto YEPD medium plates and exposed to nine different doses of UV irradiation (in UV time exposure mode, 10, 15, 20, 30, 40, 50, 60, 70 and 100 J/m^2). The UV irradiated plates were incubated for 3-5 days at 23°C and 30°C before being photographed. Strain numbers are indicated in brackets.

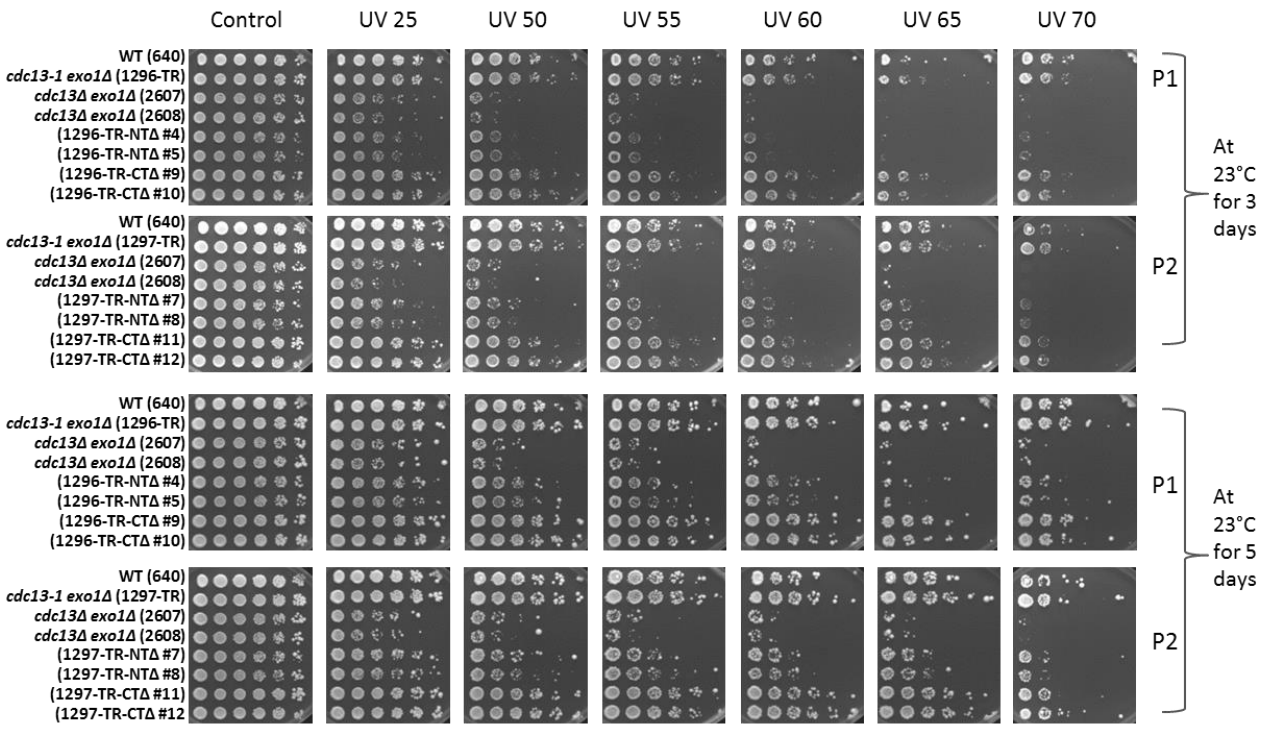

Figure 5.14. Effect of selective UV irradiation 25, 50, 55, 60, 65, and 70 J/m^2) on the growth of *cdc13-1* N- and C-terminus truncated mutants in 1296-TR and 1297-TR strains.

Sixteen strains on two plates (P1 and P2) including mutants and controls (640, 1296-TR, 2607, 2608, 1296-*cdc13-1*-NTΔ x2 and 1296-*cdc13-1*-CTΔ x2, 640, 1297-TR, 1297-*cdc13-1*-NTΔ x2 and 1297-*cdc13-1*-CTΔ x2) were analysed for UV sensitivity of *cdc13-1* N- and C-terminus truncated mutants. Five-fold serial dilutions of the indicated yeast strains in sterile water were spotted onto YEPD medium plates and exposed to six different doses of UV irradiation (in UV time exposure mode, 25, 50, 55, 60, 65 and 70 J/m^2). The UV irradiated plates were incubated for 3-5 days at 23°C and 30°C before being photographed. Strain numbers are indicated in brackets.

A final experiment was carried out to determine the effect of UV irradiation on a few more *cdc13-1* N- and C-terminus truncated mutants from *cdc13-1* strains (1296-TR and 1297-TR). Figure 5.15 represented the results of UV-mediated growth responses of six *cdc13-1*-NTΔ and CTΔ mutants at three UV exposures (UV 25, UV 50 and UV 100 J/m^2). The distinct trends of growth inhibition of two N- and C-terminus truncated mutants were more pronounced at exposure of UV 50 J/m^2, at 23°C and 30°C after 3 and 5 days of incubation (Figure 5.15AB). The UV resistance of C-truncated mutants was also comparable to the wild type and parent strains at exposure UV 50 J/m^2. Interestingly, both CTΔ mutants displayed slightly more growth at UV 100 J/m^2, which was significant at 30°C after 3 and 5 days of incubation. The four other NTΔ and CTΔ deletion mutants (P4 and P5) exhibited the same distinct pattern of UV sensitivity with increased growth inhibition in NTΔ mutants as compared to CTΔ mutants with few exceptions (Figure 5.15CD), that could be due to an unequal number of initial cells. These distinct sensitivity patterns were more pronounced at the lower temperature (23°C as compared to 30°C), and with the shorter incubation period (3 days as compared to 5 days) (Figure 5.15C). Significant growth restoration was observed in four NTΔ and CTΔ mutants at 23°C after 5 days of incubation and at 30°C after 3 and 5 days of incubation. The distinct sensitivity pattern became less obvious after the longer incubation of 5 days due to the partial recovery of arrested cells.

Based on these observations, it was concluded that there were at least three domains in the Cdc13 protein that contributed to the resistance to UV. However, on the basis of comparable sensitivities among wild type (slightly less resistant) and CTΔ mutants it could be hypothesised that C-domain could contain a suppressor of WT resistance to UV that might make CTΔ mutants more resistant to UV at high doses.

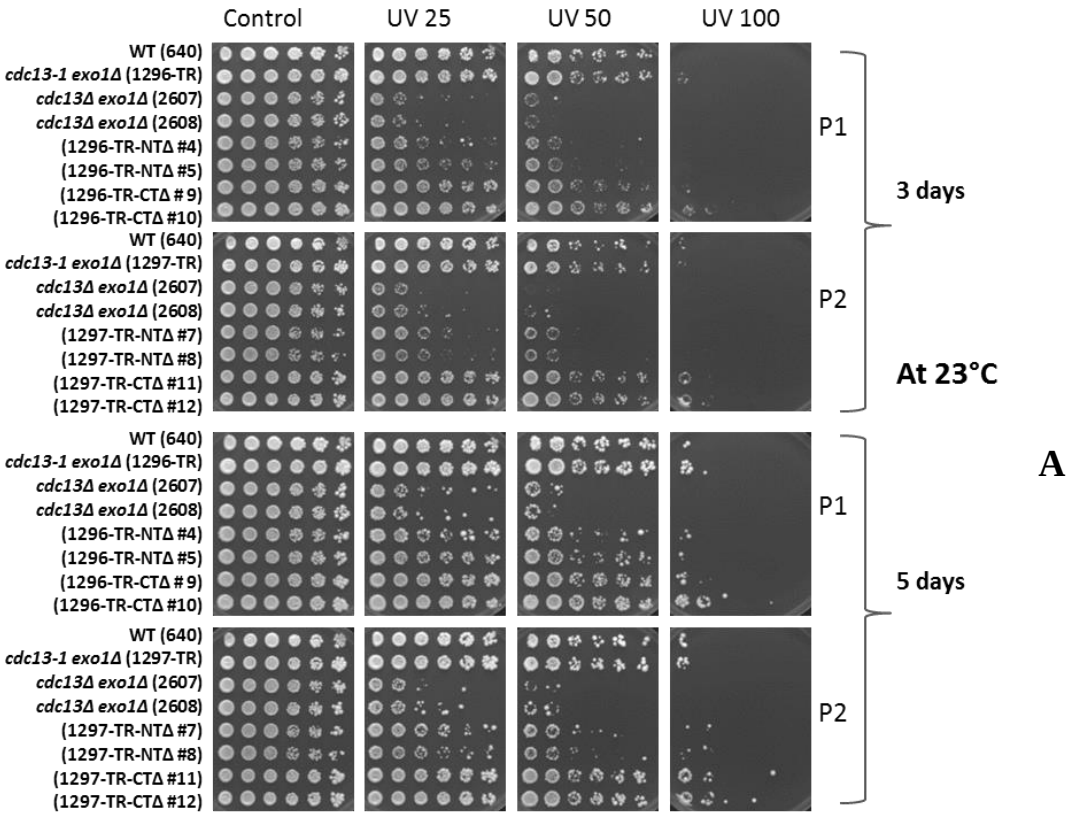
Control
UV 25
UV 50
UV 100
WT (640)
cdc13-1 exo1Δ (1296-TR)
cdc13Δ exo1Δ (2607)
cdc13Δ exo1Δ (2608)
(1296-TR-NTΔ #4)
(1296-TR-NTΔ #5)
(1296-TR-CTΔ # 9)
(1296-TR-CTΔ #10)
WT (640)
cdc13-1 exo1Δ (1297-TR)
cdc13Δ exo1Δ (2607)
cdc13Δ exo1Δ (2608)
(1297-TR-NTΔ #7)
(1297-TR-NTΔ #8)
(1297-TR-CTΔ #11)
(1297-TR-CTΔ #12)
P1
P2
3 days
At 23°C
5 days

A

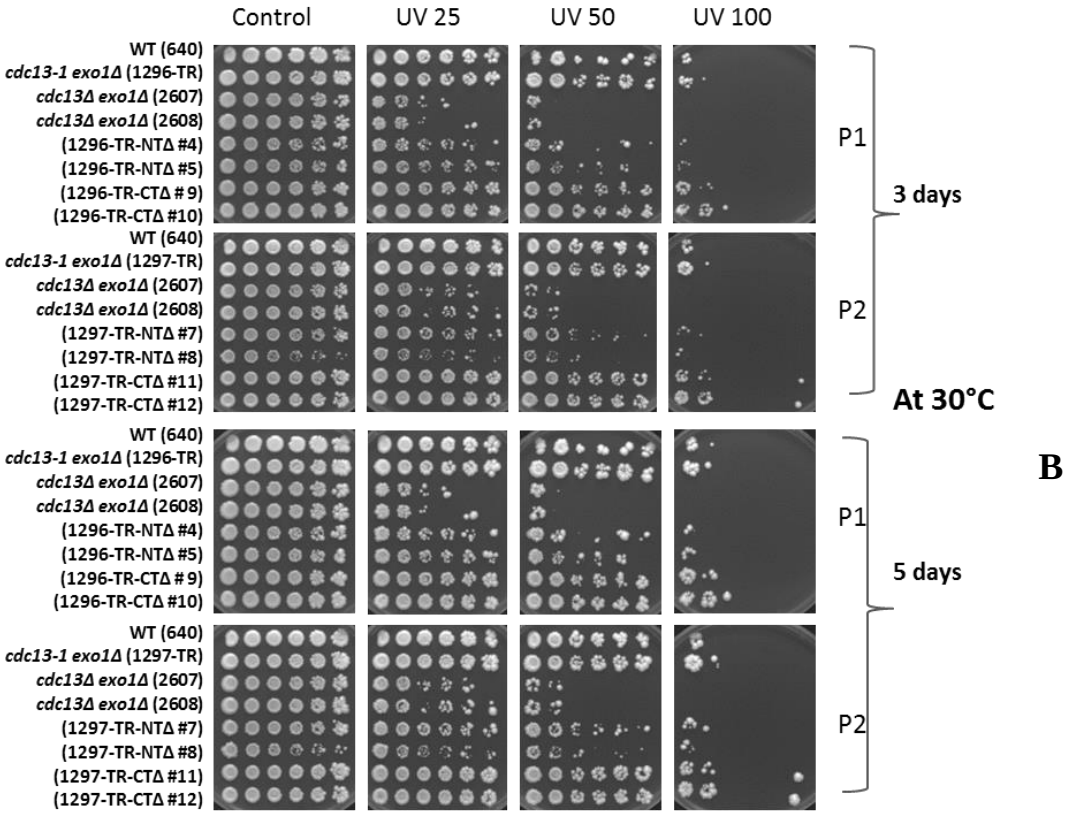
Control
UV 25
UV 50
UV 100
WT (640)
cdc13-1 exo1Δ (1296-TR)
cdc13Δ exo1Δ (2607)
cdc13Δ exo1Δ (2608)
(1296-TR-NTΔ #4)
(1296-TR-NTΔ #5)
(1296-TR-CTΔ # 9)
(1296-TR-CTΔ #10)
WT (640)
cdc13-1 exo1Δ (1297-TR)
cdc13Δ exo1Δ (2607)
cdc13Δ exo1Δ (2608)
(1297-TR-NTΔ #7)
(1297-TR-NTΔ #8)
(1297-TR-CTΔ #11)
(1297-TR-CTΔ #12)
P1
P2
3 days
At 30°C
5 days

B

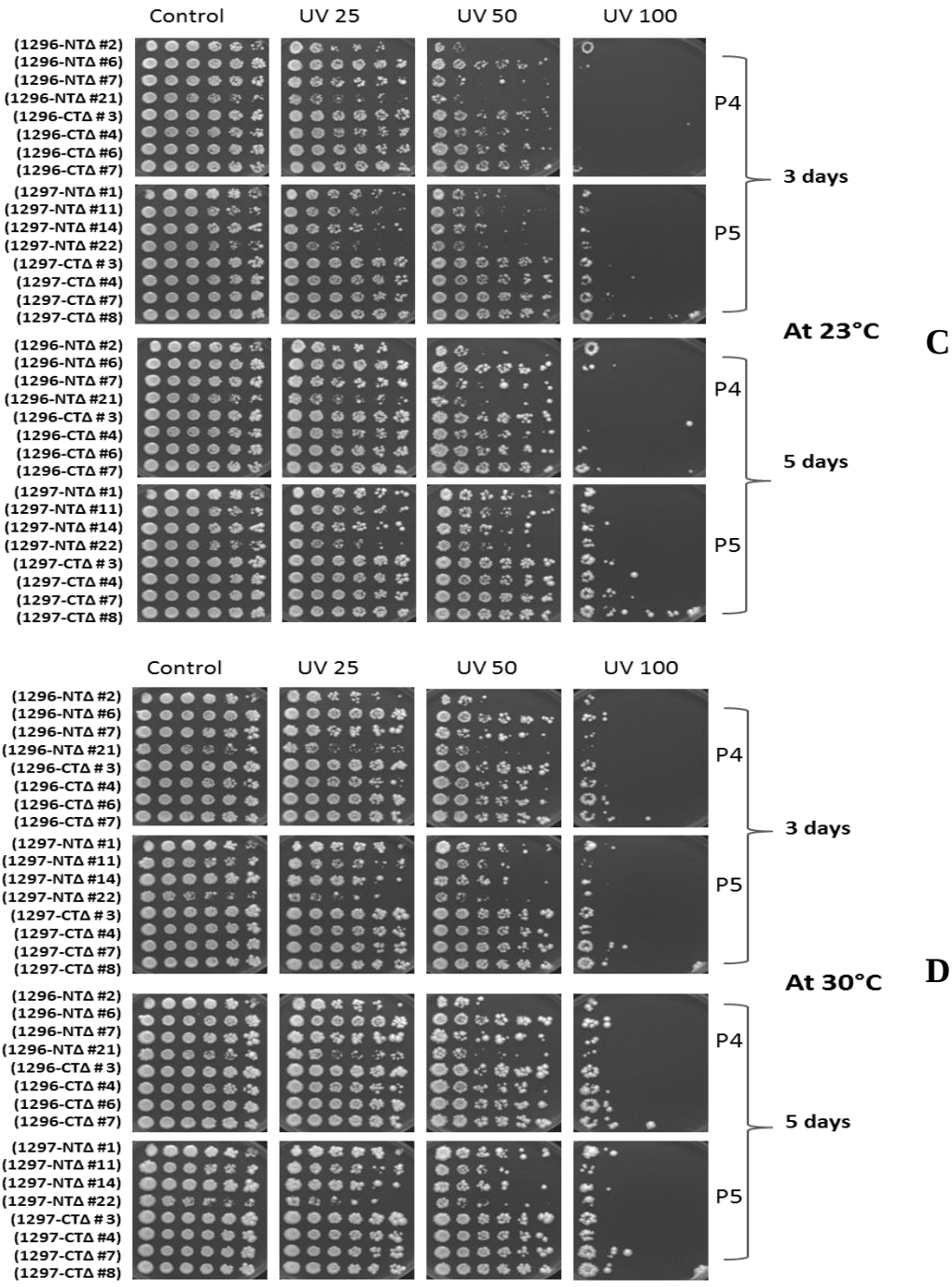

Figure 5.15. Effect of UV irradiation (25, 50, and 100 J/m^2) on the growth of *cdc13-1* N- and C-terminus truncated mutants in 1296-TR and 1297-TR strains.

Different strains on four plates (P1, P2, P4 and P5) including mutants and controls [640, 1296-TR, 2607, 2608, *cdc13-1*-NTΔ x2 (1296), *cdc13-1*-CTΔ x2 (1296) (P1); 640, 1297-TR, *cdc13-1*-NTΔ x2 (1297) and *cdc13-1*-CTΔ x2 (1296) (P2), *cdc13-1*-NTΔ x4 (1296), *cdc13-1*-NTΔ x4 (1296) (P4) and *cdc13-1*-NTΔ x4 (1297), *cdc13-1*-CTΔ x4 (1297) (P5)] were analysed for UV sensitivity. Five-fold serial dilutions of the strains in sterile water were spotted onto YEPD medium plates and exposed to three different doses of UV irradiation (in UV time exposure mode, 25, 50, and 100 J/m^2). The UV irradiated plates were incubated for 3-5 days at 23°C and 30°C before being photographed. Strain numbers are indicated in brackets.

(**A**) Plates 1 and 2 (P1 and P2) 3-5 days of incubation at 23°C.
(**B**) Plates 1 and 2 (P1 and P2) 3-5 days of incubation at 30°C.
(**C**) Plates 4 and 5 (P4 and P5) 3-5 days of incubation at 23°C.
(**D**) Plates 4 and 5 (P4 and P5) 3-5 days of incubation at 30°C.

5.3.3.2. Effects of MMS on the growth of *cdc13-1* mutants lacking N- or C-terminus

This study was conducted to determine the MMS-mediated growth responses of *cdc13-1*-NTΔ and *cdc13-1*-CTΔ mutants' cells.

Serial dilutions of 32 different cultures including 12 *cdc13-1*-NTΔ and CTΔ mutants of 1296-TR and 1297-TR strains, wild type strain (640), *cdc13-1* strain (1296-TR and 1297-TR) and *cdc13Δ exo1Δ* mutants strains (2607 and 2608) were spotted on YEPD plates containing three different concentrations of MMS (0.010%, 0.015% and 0.020%; w/v). The plates were incubated at 23°C and 30°C for 3 and 5 days.

The results showed that *cdc13Δ exo1Δ* (2607 and 2608) mutants were more sensitive to MMS when compared with *cdc13-1*-NTΔ mutants which in turn were slightly more susceptible to MMS as compared to *cdc13-1* CTΔ (Figure 5.16). Additionally, MMS-mediated growth arrest was influenced by three factors; concentration of MMS, incubation temperature and incubation time. For example, maximum inhibition of growth was observed at the highest concentration of MMS (0.020%), at the lowest temperature (23°C) and after the shortest incubation time (3 days).

The *cdc13Δ exo1Δ* (2607 and 2608) mutants displayed a moderate growth arrest at 0.010% MMS, with a significant growth inhibition in response to 0.015% MMS. However, severe inhibition of growth was observed at 0.020% of MMS at 23°C and 30°C after 3 and 5 days of incubation with a highest inhibition level detected at 23°C after 3 days of incubation. The pronounced inhibition of *cdc13Δ* at 0.020% MMS as compared to 0.015% MMS, however, was not recovered (or partially recovered) after 5 days of incubation at 23°C. The *cdc13-1*-NTΔ mutants demonstrated sensitivity to all tested doses of MMS (0.010%, 0.015% and 0.020%; w/v) but appeared to be more susceptible to 0.015% and 0.020% MMS, obvious at 23°C and 30°C after 3 days of incubation (Figure 5.16A). In contrast, *cdc13-1*-CTΔ mutants displayed a partial resistance to 0.020% MMS with growth patterns comparable to *cdc13-1* strain (1296-TR and 1297-TR) and wild type strain (640) that was less pronounced at the lower temperature (23°C) as compared to 30°C. All mutants and the wild type showed inhibition of growth to some extent at 23°C after 3 and 5 days of incubation. The wild type strain 640 appeared to be more sensitive to MMS with inhibited growth, obvious at 0.015% and 0.020% (w/v) at 23°C after 3 and 5 days of incubation. However, the wild type and parent strains presented no or minimal growth inhibition at 30°C after 3 and 5 days of incubation.

The MMS sensitivity patterns observed among *cdc13Δ exo1Δ*, *cdc13-1*-NTΔ and *cdc13-1*-CTΔ mutants were slightly less pronounced at 30°C as compared to 23°C after 5 days of incubation, and obvious only at 0.015% and 0.020% of MMS (Figure 5.16B). However, more restoration of cell growth was noticed at 30°C after 5 days of incubation.

The four other NTΔ and CTΔ deletion mutants (P4 and P5) also exhibited the distinct pattern of MMS-mediated sensitivity; slightly increased inhibition in NTΔ as compared to CTΔ, more obvious at 23°C and 30°C after 3 days of incubation (Figure 5.16C). The significant growth restoration was observed in four NTΔ and CTΔ mutants after 5 days of incubation at 23°C and 30°C, and the distinct sensitivity pattern became less obvious due to recovery of arrested cells. After 5 days incubation the distinct sensitivity patterns were much less pronounced at 23°C and 30°C (Figure 5.16D).

Overall, the results manifested a similar trend as was observed earlier with UV-mediated sensitivity in NTΔ and CTΔ mutants. The CTΔ mutant also manifested resistance to 0.020% MMS at 23°C, with the growth comparable to that in the wild type (640) indicating that the presence of the C-domain might contribute to the mechanisms of the sensitivity of wild type cells.

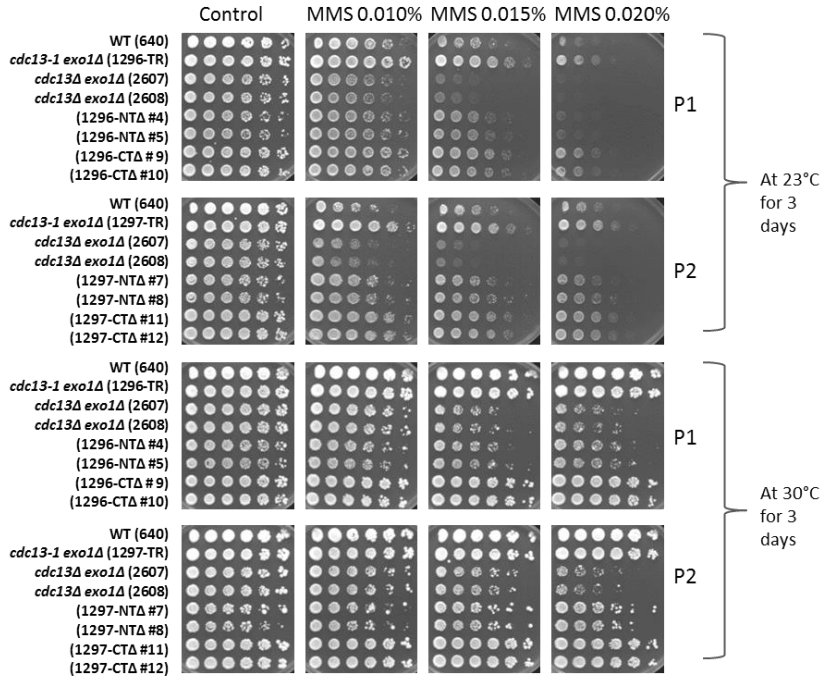
Control
MMS 0.010%
MMS 0.015%
MMS 0.020%
WT (640)
cdc13-1 exo1Δ (1296-TR)
cdc13Δ exo1Δ (2607)
cdc13Δ exo1Δ (2608)
(1296-NTΔ #4)
(1296-NTΔ #5)
(1296-CTΔ # 9)
(1296-CTΔ #10)
WT (640)
cdc13-1 exo1Δ (1297-TR)
cdc13Δ exo1Δ (2607)
cdc13Δ exo1Δ (2608)
(1297-NTΔ #7)
(1297-NTΔ #8)
(1297-CTΔ #11)
(1297-CTΔ #12)
P1
P2
At 23°C for 3 days
At 30°C for 3 days

A

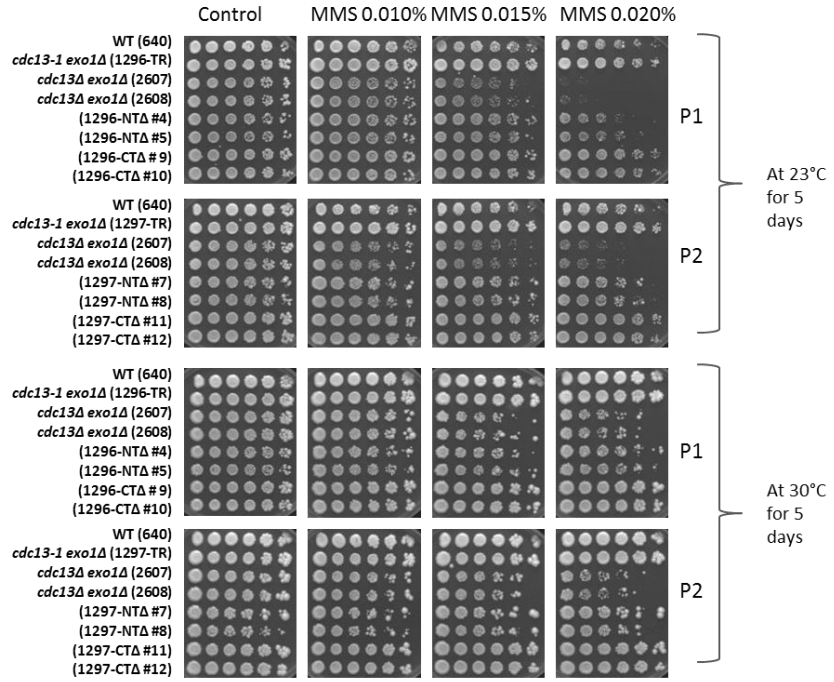
Control
MMS 0.010%
MMS 0.015%
MMS 0.020%
WT (640)
cdc13-1 exo1Δ (1296-TR)
cdc13Δ exo1Δ (2607)
cdc13Δ exo1Δ (2608)
(1296-NTΔ #4)
(1296-NTΔ #5)
(1296-CTΔ # 9)
(1296-CTΔ #10)
WT (640)
cdc13-1 exo1Δ (1297-TR)
cdc13Δ exo1Δ (2607)
cdc13Δ exo1Δ (2608)
(1297-NTΔ #7)
(1297-NTΔ #8)
(1297-CTΔ #11)
(1297-CTΔ #12)
P1
P2
At 23°C for 5 days
At 30°C for 5 days

B

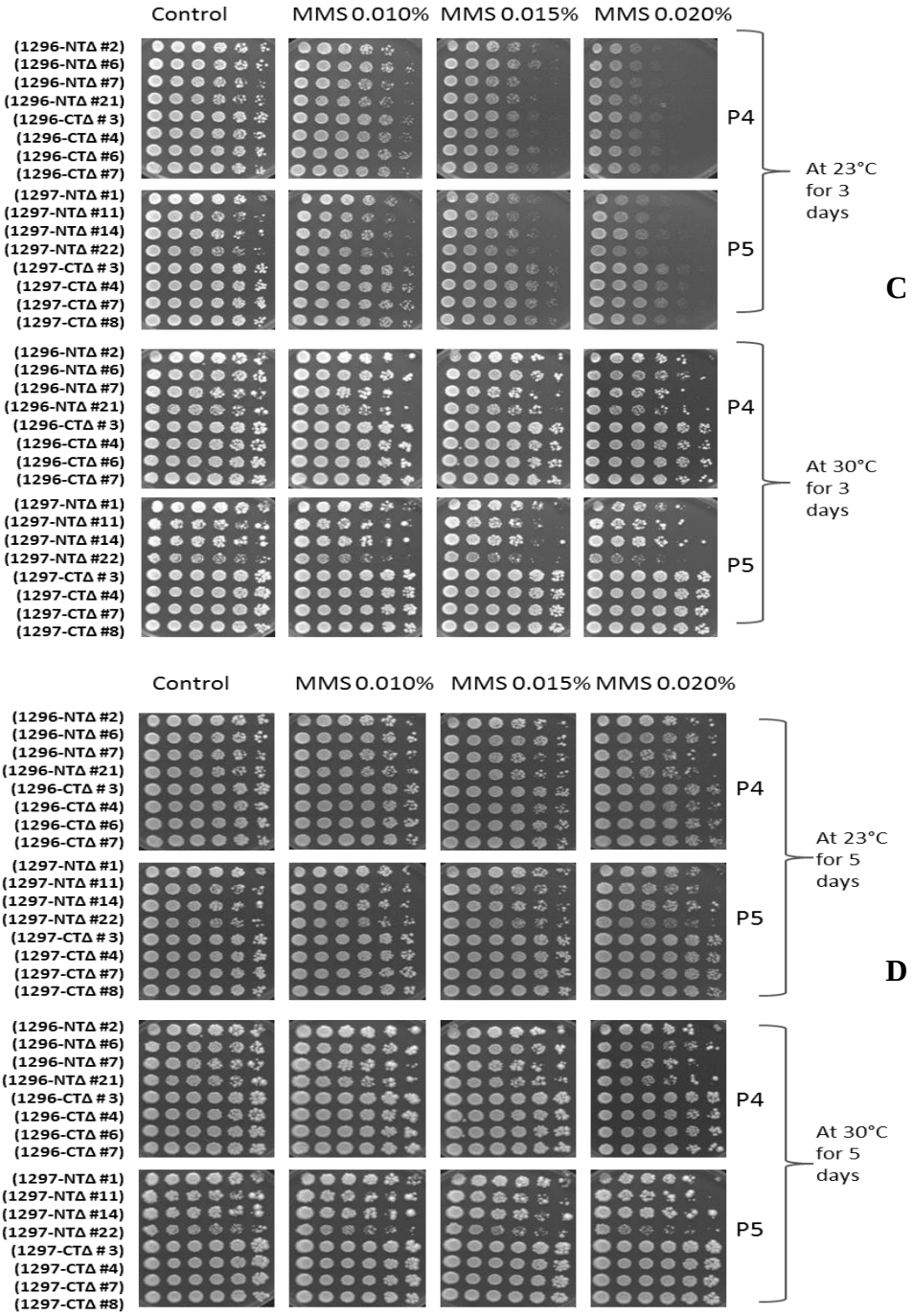

Figure 5.16. Effect of MMS (0.010%, 0.015% and 0.020%; w/v) on the growth of *cdc13-1*-NTΔ and CTΔ mutants of 1296-TR and 1297-TR strains.

Different strains on four plates (P1, P2, P4 and P5) including mutants and controls [640, 1296-TR, 2607, 2608, *cdc13-1*-NTΔ x2 (1296) and *cdc13-1*-CTΔ x2 (1296) (P1); 640, 1297-TR, 2607, 2608, *cdc13-1*-NTΔ x2 clones (1297) and *cdc13-1*-CTΔ x2 clones (1297) (P2); *cdc13-1*-NTΔ x4 clones (1296) and *cdc13-1*-CTΔ x4 clones (1296) (P4); and *cdc13-1*-NTΔ x4 clones (1297) and *cdc13-1*-CTΔ x4 clones (1296) (P5)] were analysed for MMS-mediated sensitivity. Five-fold serial dilutions of the indicated yeast strains in sterile water were spotted onto YEPD medium plates containing three different concentrations of MMS 0.010%, 0.015% and 0.020%; w/v). The plates were incubated for 3-5 days at 23°C and 30°C before being photographed. Strain numbers are indicated in brackets.

(**A**) Plates 1 and 2 (P1 and P2) 3 days of incubation at 23°Cand 30°C

(**B**) Plates 1 and 2 (P1 and P2) 5 days of incubation at 23°Cand 30°C

(**C**) Plates 4 and 5 (P4 and P5) 3 days of incubation at 23°Cand 30°C

(**D**) Plates 4 and 5 (P4 and P5) 5 days of incubation at 23°Cand 30°C

5.3.3.3. Effect of H_2O_2 on the growth of *cdc13-1* mutants lacking N- or C-terminus

To determine the H_2O_2-mediated oxidative stress responses on the growth of *cdc13-1*-NTΔ and *cdc13-1*-CTΔ mutant cells, serial dilutions of 16 different cultures were spotted on YEPD plates containing three different concentrations of H_2O_2 (2 mM , 3 mM and 4 mM; w/v). The plates were incubated at 23°C and 30°C for 3 and 5 days.

The results showed that all mutants and wild type strains were severely inhibited in their growth at 4 mM H_2O_2 at 23°C and 30°C after 3 and 5 days of incubation (Figure 5.17). The result also indicated that *cdc13Δ exo1Δ* (2607 and 2608) mutants were moderately arrested at 3 mM H_2O_2 at 23°C and 30°C after 3 and 5 days of incubation, to a higher extent at 23°C. *cdc13-1*-NTΔ mutants were slightly more sensitive to 3 mM of H_2O_2 as compared to *cdc13-1*-CTΔ mutants. Strains 1296-TR and 1297-TR exhibited slightly better growth at 23°C and 30°C after 3 and 5 days of incubation, indicating their increased resistance to 3 mM H_2O_2 as compared to the wild type (640). The growth rate of *cdc13-1*-CTΔ at 3 mM H_2O_2 was comparable to the wild type at 23°C and 30°C after 3 and 5 days of incubation. A slight effect of H_2O_2 on the growth of all mutants was also observed at 2 mM, when cells were incubated at 23°C and 30°C for 3 days. However, due to growth restoration, this effect was not obvious after 5 days of incubation. The inhibitory effect of H_2O_2 was concentration dependent and become pronounced at the concentration of 3 mM. At a higher concentration of H_2O_2 (5 mM) the growth of all mutants and controls was severely inhibited, however there was weak growth of *cdc13-1*-CTΔ mutants indicating their resistance as compared to the wild type. This might be further evidence for the existence of C-terminus domain that might contribute to wild type sensitivity to H_2O_2, consistent with the MMS and UV effects on *cdc13-1*-CTΔ mutants.

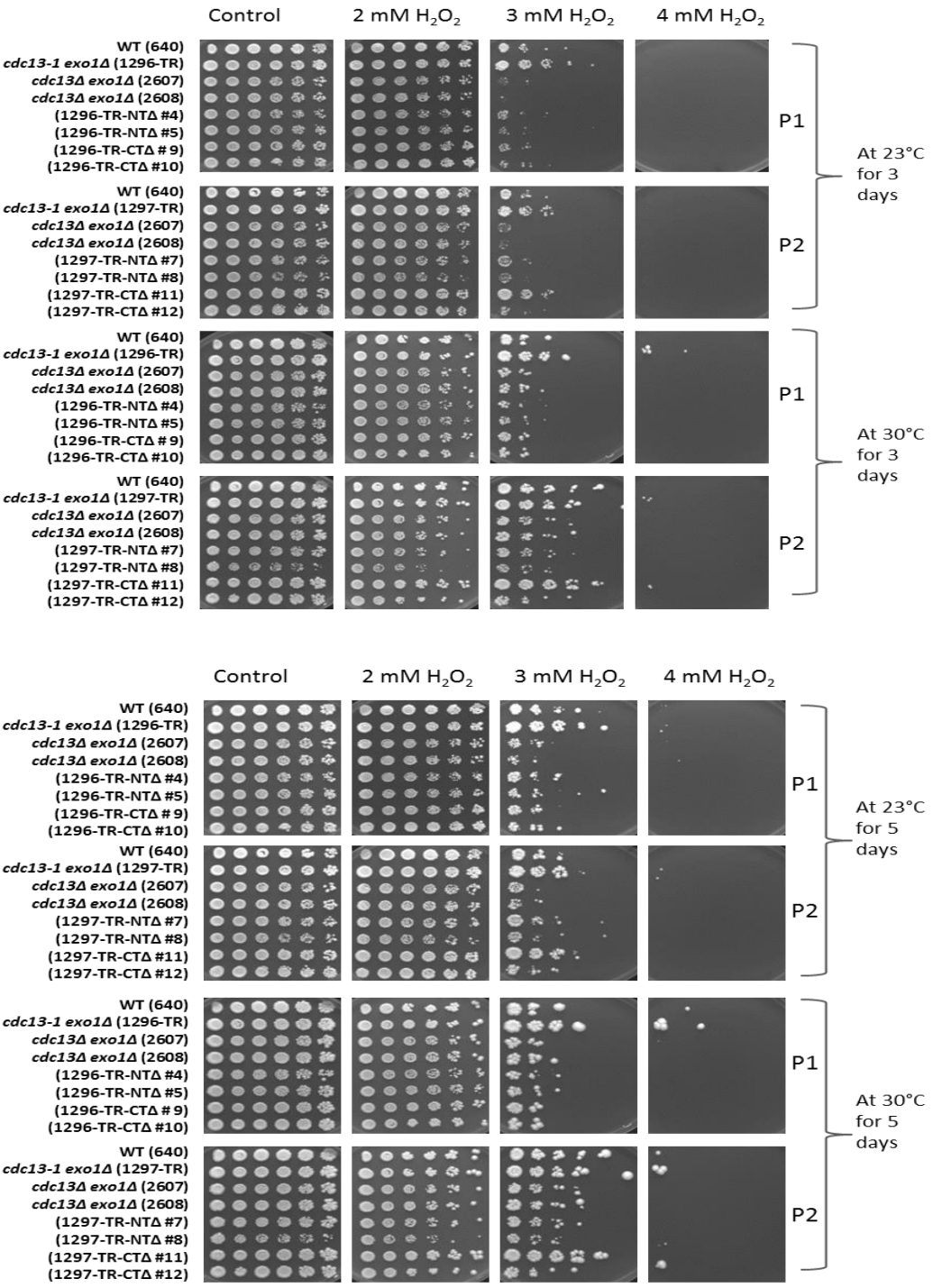

Figure 5.17. Effect of H_2O_2 (2 mM, 3 mM and 4 mM; w/v) on the growth of *cdc13-1*-N- and C-terminus truncated mutants in strains 1296-TR and 1297-TR.

Different strains on two plates (P1, P2) including mutants and controls [640, 1296-TR, 2607, 2608, *cdc13-1*-NTΔ (1296) x2 clones, *cdc13-1*-CTΔ (1296) x2 clones (P1) and 640, 1297-TR, 2607, 2608, *cdc13-1*-NTΔ (1299) x2 clones, *cdc13-1*-CTΔ (1297) x2 clones (P2] were analysed for H_2O_2-mediated sensitivity. Five-fold serial dilutions of the strains in sterile water were spotted onto YEPD medium plates containing three different concentrations of H_2O_2 (2 mM, 3 mM and 4 mM; w/v). The plates were incubated for 3-5 days at 23°C and 30°C before being photographed. Strain numbers are indicated in brackets.

5.3.3.4. Effect of HU on the growth of *cdc13-1* mutants lacking N- or C-terminus

In this study, *cdc13-1*-NTΔ and *cdc13-1*-CTΔ mutants (12 of each) were tested for their response to the presence of HU, a DNA replication inhibitor. YEPD agar plates containing different concentrations of HU (10 mM, 25 mM and 30 mM; w/v) were spotted with serially diluted cultures. The plates were incubated at 23°C and 30°C for 3 and 5 days.

At 10, 25 and 30 mM, (w/v) HU concentration, all mutants and controls exhibited inhibition of growth to some extent that varied with concentration and temperature (Figure S5.7). The higher growth inhibition was observed at 30 mM of HU at 23°C after 3 days of incubation (Figure S5.7A). The *cdc13Δ exo1Δ* mutants (2607 and 2608) and *cdc13-1*-NTΔ mutants displayed a moderate inhibition of growth in the presence of HU as compared to the wild type (640 and 641) and parent strains (1296-TR and 1297-TR) and to the *cdc13-1*-CTΔ mutants which was more obvious at 30 mM HU at 23°C after 3 days of incubation. In contrast, *cdc13-1*-CTΔ mutants revealed minimal growth susceptibility to HU with a better growth pattern comparable to the wild type (640 and 641) and strains (1296-TR and 1297-TR). The wild type and parent strains, however, exhibited no or negligible growth arrest at 23°C and 30°C after 3 and 5 days of incubation at all tested concentration of HU (Figure S5.7AB). The distinct pattern of HU-mediated growth, with weak, moderate and increased susceptibility of cells in *cdc13-1* CTΔ, *cdc13-1* NTΔ, and *cdc13Δ exo1Δ* mutants (2607 and 2608) respectively, were less obvious after 5 days (Figure S5.7BD). The resistance of *cdc13-1*-CTΔ mutants to HU-mediated toxicity was consistently reflected by all 12 analysed mutants, a phenomenon in agreement with previous results with UV, MMS and H_2O_2. Similar trends were discovered with remaining *cdc13-1*-NTΔ and *cdc13-1*-CTΔ mutants [four of each type with either parent strain (1296-TR or 1297-TR)] (Figure S5.7CD).

At increased doses of HU (10 mM, 25 mM and 50 mM; w/v) (Figure S5.8) , a similar pattern of growth inhibition was revealed with *cdc13Δ exo1Δ* mutants (2607 and 2608) showing a pronounced growth inhibition at 23°C and 30°C after 3 days of incubation as compared to NTΔ and CTΔ mutants (Figure S5.8AC). However, the inhibition patterns at 50 mM HU were more profound at 23°C and 30°C after 3 days of incubation as compared to 30 mM HU-mediated inhibition that was observable only at 23°C after 3 days of incubation. However, after 5 days of growth, most of the inhibition shown at day 3 was restored, resulting in a less distinguishable inhibition pattern of growth (Figure S5.8BD).

Finally, these results were justified with even higher concentrations of HU (50 mM, 75 mM and 100 mM; w/v). The inhibition of growth was distinct at 23°C and 30°C after 3 and 5 days of incubation (Figure 5.18). The *cdc13Δ* mutants (2607 and 2608) were severely inhibited in their growth while partial growth arrest, to varying extents, was shown by *cdc13-1*-NTΔ and *cdc13-*

1-CTΔ mutants. The wild type (640) and parent strains (1296-TR and 1297-TR) presented no or mild inhibition in their growth at 23°C and 30°C after 3 (Figure 5.18AC) and 5 days of incubation (Figure 5.18BD). The growth patterns of *cdc13-1*-CTΔ mutants were consistent in all 12 analysed CTΔ mutants and were comparable in their HU-mediated growth susceptibility to wild type strain (640). The three *cdc13-1*-NTΔ (1296-NTΔ #2 and #6, 1297-NTΔ #8) however, showed slight resistance to inhibition, which could be due to the variable number of starter cells used for serial dilution (Figure 5.18CD). All other mutants were consistent in their growth inhibition pattern.

Taken together, *cdc13Δ* mutants, *cdc13-1*-NTΔ and *cdc13-1*-CTΔ mutants exhibited severe, moderate and mild phenotypic growth inhibition respectively under the toxic effect of HU. The distinct growth patterns observed were consistent with earlier results obtained with the exogenous genotoxic agent UV, DNA damaging, MMS and H_2O_2.

Based on these results, it could be concluded that there are at least 3 domains in the Cdc13 protein that might contribute to WT-sensitivity to UV, MMS, H_2O_2 and HU. Moreover, the resistance pattern of CTΔ, comparable with wild type strain, indicates that the C-domain might also contain a suppressor of WT-resistance to UV, MMS and HU.

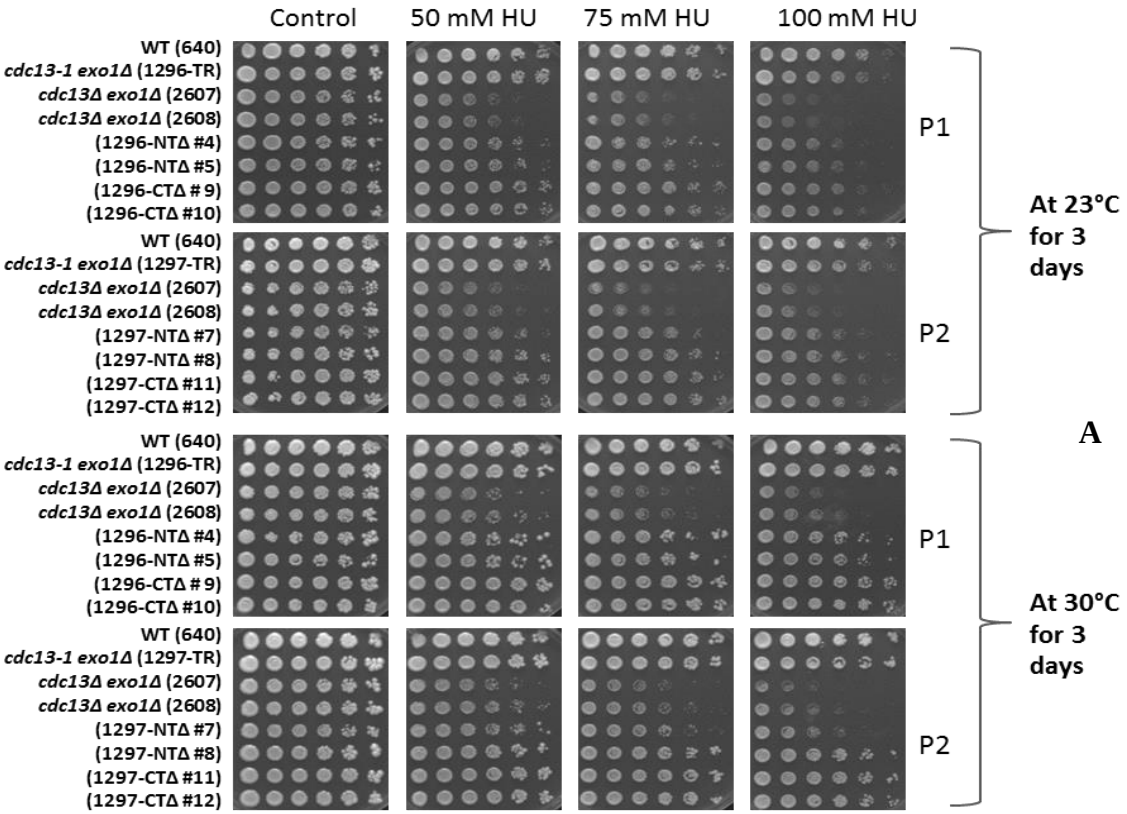
Control
50 mM HU
75 mM HU
100 mM HU
WT (640)
cdc13-1 exo1Δ (1296-TR)
cdc13Δ exo1Δ (2607)
cdc13Δ exo1Δ (2608)
(1296-NTΔ #4)
(1296-NTΔ #5)
(1296-CTΔ # 9)
(1296-CTΔ #10)
WT (640)
cdc13-1 exo1Δ (1297-TR)
cdc13Δ exo1Δ (2607)
cdc13Δ exo1Δ (2608)
(1297-NTΔ #7)
(1297-NTΔ #8)
(1297-CTΔ #11)
(1297-CTΔ #12)
P1
P2
At 23°C for 3 days
A
At 30°C for 3 days

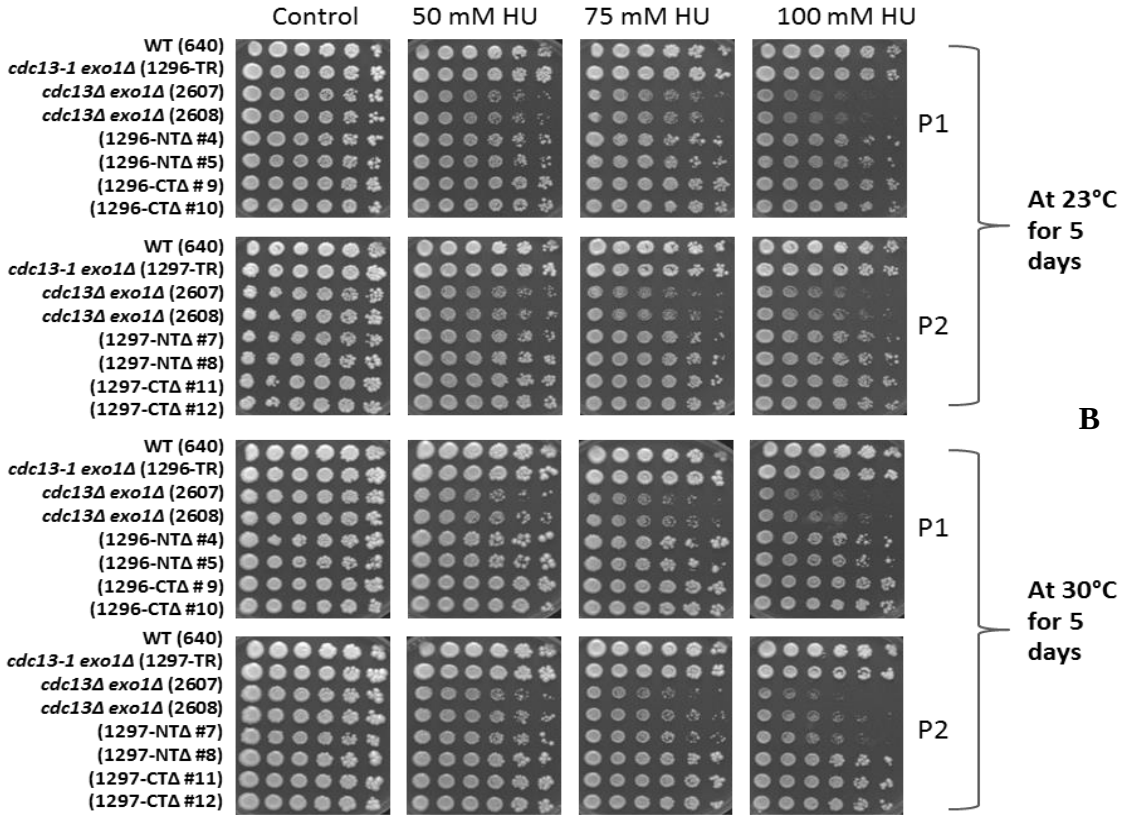
Control
50 mM HU
75 mM HU
100 mM HU
WT (640)
cdc13-1 exo1Δ (1296-TR)
cdc13Δ exo1Δ (2607)
cdc13Δ exo1Δ (2608)
(1296-NTΔ #4)
(1296-NTΔ #5)
(1296-CTΔ # 9)
(1296-CTΔ #10)
WT (640)
cdc13-1 exo1Δ (1297-TR)
cdc13Δ exo1Δ (2607)
cdc13Δ exo1Δ (2608)
(1297-NTΔ #7)
(1297-NTΔ #8)
(1297-CTΔ #11)
(1297-CTΔ #12)
P1
P2
At 23°C for 5 days
B
At 30°C for 5 days

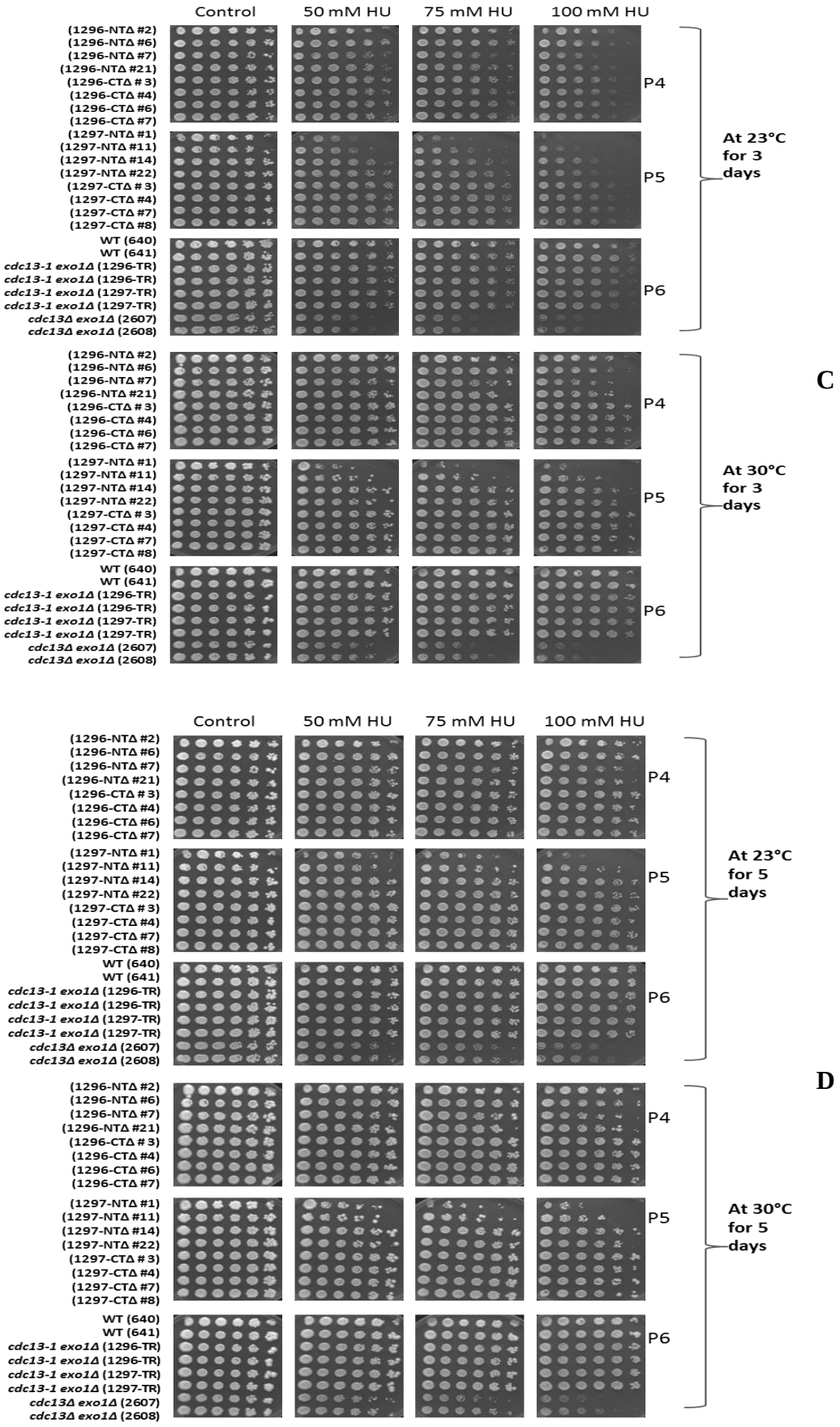

Figure 5.18. Effect of HU (50 mM, 75 mM and 100 mM) on the growth of *cdc13-1* N- and C-terminus truncated mutants of 1296-TR and 1297-TR strains.

Different strains on five plates (P1, P2, P4, P5 and P6) including mutants and controls [640, 1296-TR , 2607, 2608, *cdc13-1*-NTΔ x2 clones, (1296), *cdc13-1*-CTΔ x2 clones (1296), (P1); 640, 1297-TR, *cdc13-1*-NTΔ x2 clones (1297), *cdc13-1*-CTΔ x2 clones (1297), (P2); *cdc13-1*-NTΔ x4 clones (1296), *cdc13-1*-CTΔ x4 clones (1296), (P4); *cdc13-1*-NTΔ x4 clones (1297), *cdc13-1*-CTΔ x4 clones (1297), (P5) and 640, 641, 1296-TR x2, 1297-TR x2, 2607 and 2608 (P6)] were analysed for HU-mediated sensitivity. Five-fold serial dilutions of the indicated yeast strains in sterile water were spotted onto YEPD medium plates containing three different concentrations of HU 50 mM, 75 mM and 100 mM). The plates were incubated for 3-5 days at 23°C and 30°C before being photographed. Strain numbers are indicated in brackets.

(**A**) Plates 1 and 2 (P1 and P2) after 3 days of incubation at 23°C and 30°C.

(**B**) Plates 1 and 2 (P1 and P2) after 5 days of incubation at 23°C and 30°C.

(**C**) Plates 4, 5 and 6 (P4, P5 and P6) after 3 days of incubation at 23°C and 30°C.

(**D**) Plates 4, 5 and 6 (P4, P5 and P6) after 5 days of incubation at 23°C and 30°C.

5.3.4. The effects of genotoxic agents on the growth of *cdc13-1* N- or C-terminus truncated (haploids) in comparison with diploid (NTΔ x CTΔ) mutants

5.3.4.1. Effects of UV on *cdc13-1* mutants lacking NTΔ or CTΔ (haploids) and diploid mutants

Two diploid (#31 and #32) mutants harbouring the NTΔ/CTΔ alleles were analysed and compared to haploids, *cdc13Δ exo1Δ* (2607 and 2608), *cdc13-1*-NTΔ and *cdc13-1*-CTΔ mutants in their growth responses after exposures to UV 25, UV 50 and UV 100 J/m^2, at two different temperature regimes (23°C and 30°C), after 3 and 5 days of growth. As illustrated in Figure 5.19AB, the haploids *cdc13Δ exo1Δ* mutants (2607 and 2608) were severely inhibited in their growth at a UV exposure of 100 J/m^2 (UV 100); they showed no growth at UV 100 J/m^2 and weak growth at UV 50 J/m^2 at 23°C and 30°C after 3 and 5 days of incubation. In comparison, the haploid *cdc13-1*-NTΔ mutants also had severe growth arrest, and *cdc13-1*-CTΔ mutants with moderate growth arrest manifested their distinct sensitivity pattern at UV 25, 50 and 100 J/m^2 at 23°C and 30°C after 3 and 5 days. The haploid *cdc13-1*-CTΔ also exhibited mild to moderate growth at UV 100 J/m^2 significantly obvious as compared to growth of wild type (640 and 641) strains that exhibited limited growth at UV 100 J/m^2 at 23°C and 30°C within 3 and 5 days. Strains 1296-TR and 1297-TR as well as wild type (640 and 641) strains exhibited weak growth after UV 100 J/m^2, representing severe growth arrest, and much better growth after UV 25 and 50 J/m^2 representing no or limited growth arrest. Strains 1296-TR and 1297-TR (P6) exhibited slightly less susceptibility to UV as compared to wild type (640 and 641) but slightly more sensitivity as compared to *cdc13-1*-CTΔ [1296-CTΔ #9, #10 (P7), 1297-CTΔ #11, #12 (P8)] at UV 100 at 23°C after 3 days of incubation (Figure 5.19A). In contrast, the two diploids [#31 and #32 (P7 and P8)] exhibited intermediate inhibition of growth at UV 50 and 100 J/m^2 at

23°C and 30°C after 3 and 5 days. The diploid #31 manifested slightly less growth (when compared with diploid #32), more obvious at UV 50 and 100 at 23°C after 3 days of growth (Figure 5.19A). The growth pattern in diploid #31 indicated that the growth inhibition was either equal or slightly more when compared with *cdc13-1*-NTΔ mutants but slightly less when compared to *cdc13-1*-CTΔ mutants, also comparable with wild type at UV 100 after 3 days of incubation at 23°C. Similarly, in diploid number #32, the inhibition in growth was slightly more when compared with the wild type but less than in the *cdc13-1*-CTΔ mutant.

Overall, diploid #31 displayed comparatively more inhibition of growth when compared with diploid #32. In general, diploids displayed intermediate growth, when compared with *cdc13-1*-CTΔ and *cdc13-1* NTΔ.

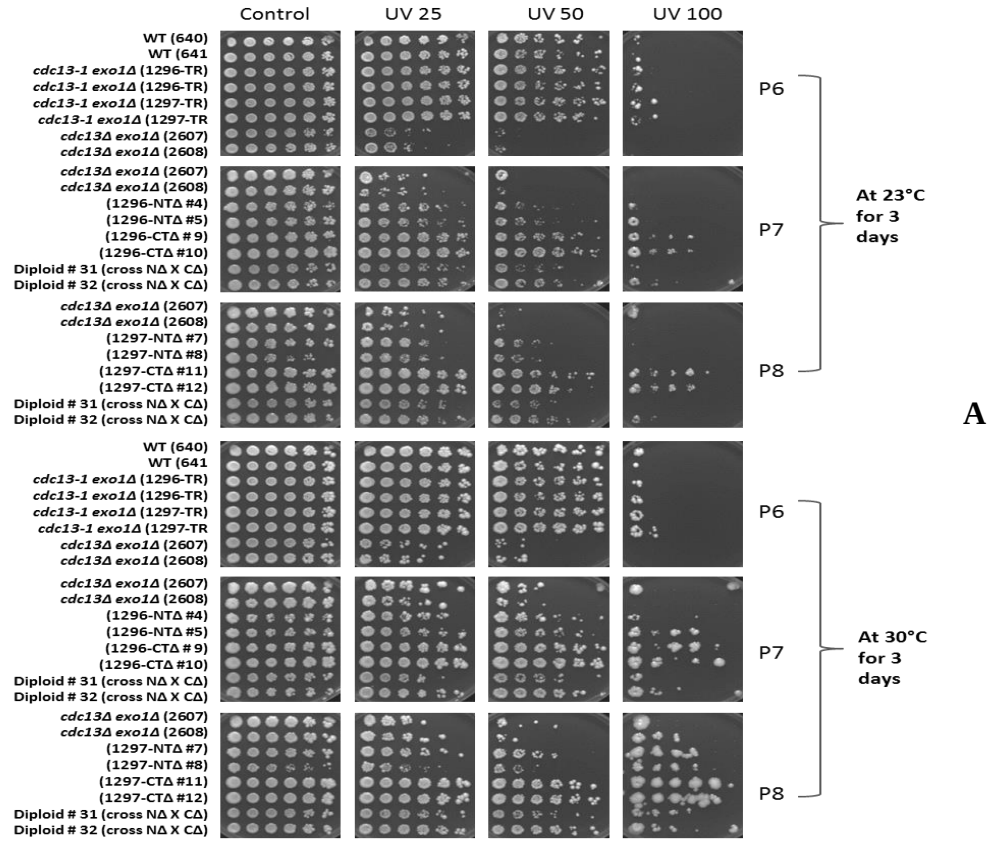

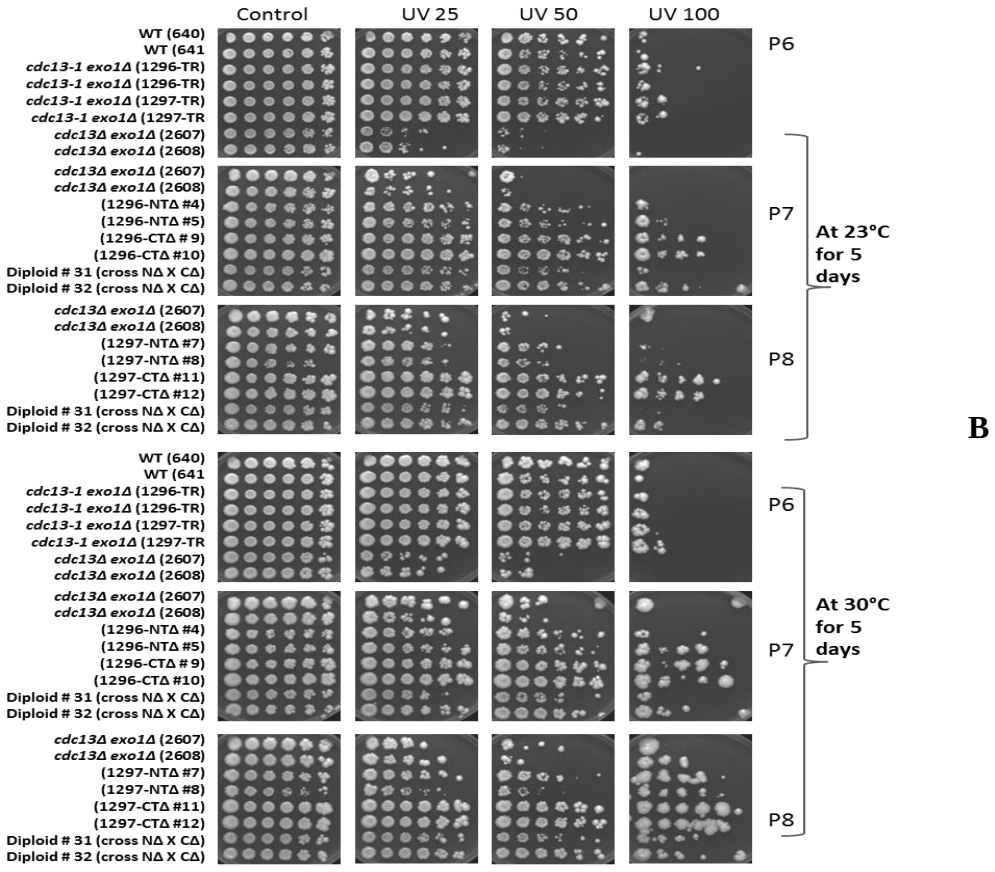

Figure 5.19. Effect of UV irradiation (25, 50, and 100 J/m^2) on the growth of *cdc13-1* N- and C-terminus truncated (haploids) in comparison to diploid mutants.

Different strains on three plates (P6, P7 and P8) including mutants and controls [640, 641, 1296-TR x2, 1297-TR x2, 2607, 2608 (P6); 2607, 2608, *cdc13-1*-NTΔ (1296) x2 clones, *cdc13-1*-CTΔ (1296) x2 clones, diploid #31, diploid #32 (P7); 2607, 2608, *cdc13-1*-NTΔ (1297) x2 clones, *cdc13-1*-CTΔ (1297) x2 clones, diploid #31, diploid #32 (P8)] were analysed for UV-mediated sensitivity. Five-fold serial dilutions of the strains in sterile water were spotted onto YEPD medium plates and exposed to three different doses of UV irradiation (25, 50, and 100 J/m^2). The UV irradiated plates were incubated for 3-5 days at 23°C and 30°C before being photographed. Strain numbers are indicated in brackets.

(**A**) Plates 6, 7 and 8 (P6, P7 and P8) after 3 days of incubation at 23°C and 30°C.

(**B**) Plates 6, 7 and 8 (P6, P7 and P8) after 5 days of incubation at 23°C and 30°C.

5.3.4.2. Effect of MMS on *cdc13-1* mutants lacking NTΔ or CTΔ (haploids) and diploid mutants

The MMS stress-mediated growth responses were determined for two diploids (#31 and #32, containing the *cdc13-1* N- and C-terminus deleted allele of the *cdc13-1* gene) growing at three concentrations of MMS (0.010%, 0.015% and 0.020%; w/v). The haploid mutants *cdc13Δ exo1Δ* (2607 and 2608), *cdc13-1*-NTΔ and *cdc13-1*-CTΔ were used for comparison with wild type strains (640 and 641) and mutant strains 1296-TR and 1297-TR. All serially diluted cultures were spotted on YEPD agar plates (P6, P7 and P8) containing above mentioned concentration of MMS and incubated at two different temperature regimes (23°C and 30°C) during 3 and 5 days. As shown in Figure 5.20, the haploid *cdc13Δ exo1Δ* mutants (2607 and 2608) showed sensitivity to all three concentrations of MMS and were severely inhibited in their growth at 0.015% MMS (mild growth) and 0.020% MMS (no growth) at 23°C as compared to 30°C after 3 days of incubation (Figure 5.20A). In comparison, the haploid *cdc13-1*-NTΔ and *cdc13-1*-CTΔ mutants, manifested their distinct sensitivity pattern (more growth in CTΔ as compared to NTΔ) at 0.010%, 0.015% and 0.020% MMS at 23°C and 30°C after 3 days of incubation (Figure 5.20A). Strains 1296-TR and 1297-TR (P6) exhibited obviously less susceptibility to 0.015% and 0.020% MMS at 23°C. The haploid *cdc13-1*-CTΔ [1296-CTΔ #9, #10 (P7), 1297-CTΔ #11, #12 (P8) also exhibited stronger resistance to 0.020% MMS (obvious at 23°C and 30°C after 3 days of incubation), as compared to strains 1296-TR and 1297-TR (P6) and wild type strains. Wild type strains (640 and 641), however, were less resistant at an increased concentration of MMS 0.020%. The diploids [#31 and #32 (P7 and P8)] appeared to be mildly inhibited in their growth under the effect of MMS and exhibited an intermediate level of growth inhibition at 0.010%, 0.015% and 0.020% MMS at 23°C and 30°C after 3 days and 5 days of incubation. The diploid #31 showed slightly less growth (possibly due to fewer cells in the starter culture as the growth difference was also shown in controls) when compared with diploid #32. There was partial growth restoration after 5 days of incubation at 23°C and 30°C but the inhibitory pattern of all mutants and controls were still comparable (Figure 5.20B). The growth pattern in diploids indicated that the MMS stress- mediated growth inhibition was either

equal to or slightly more when compared to *cdc13-1*-NTΔ mutants but slightly less when compared with *cdc13-1*-CTΔ mutants and wild type at 0.020% MMS at 23°C after 3 and 5 days of incubation. Overall, diploids manifested intermediate inhibition of growth phenotype, contributed from both alleles of *cdc13-1*, CTΔ and NTΔ, and possibly reflected the effect of allele dosage.

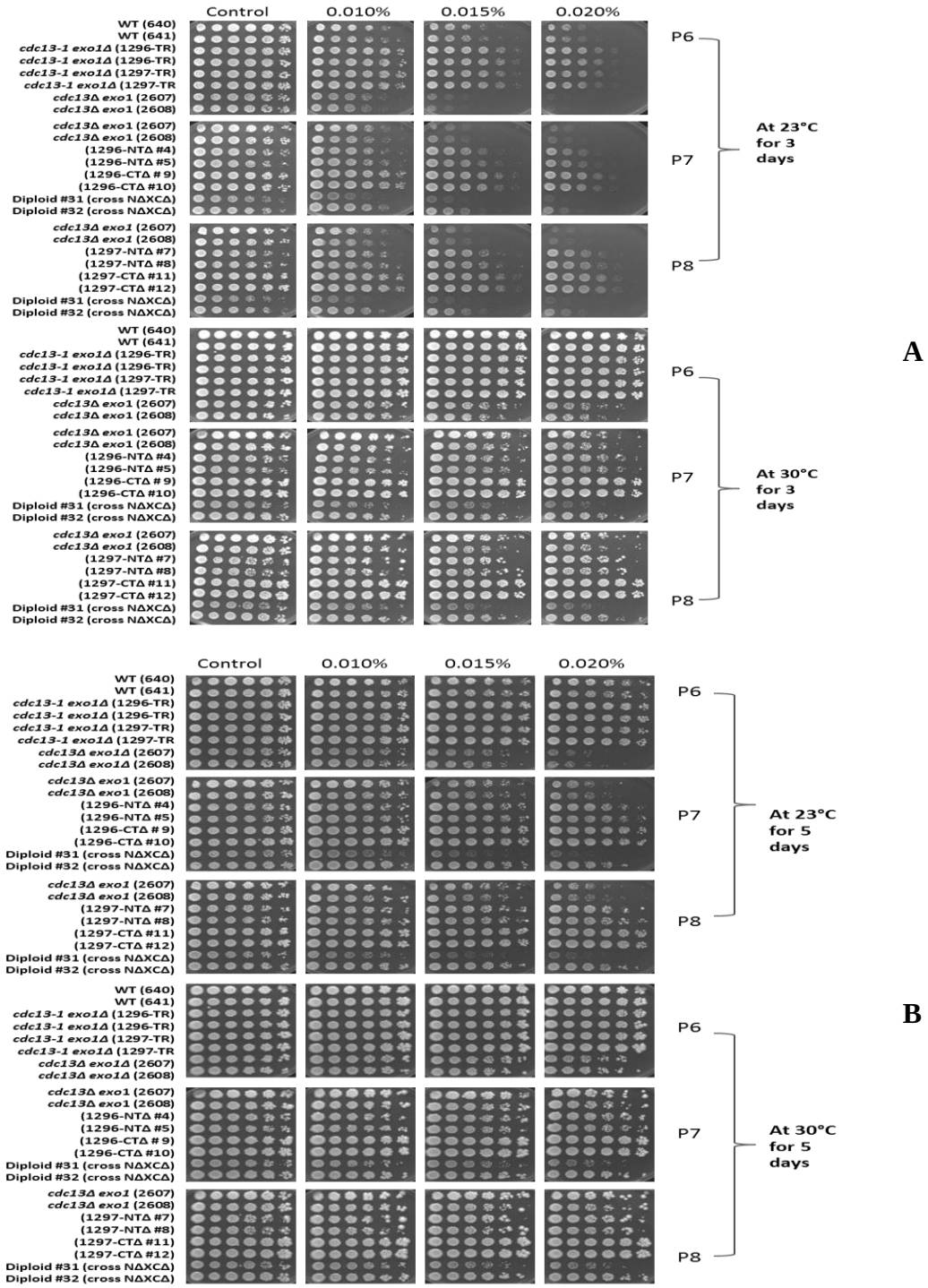

Figure 5.20. Effect of MMS (0.010%, 0.015% and 0.020%; w/v) on the growth of *cdc13-1* N- and C-terminus truncated mutants (haploids) in comparison to diploid mutants of 1296-TR and 1297-TR strains.

Different strains on three plates (P6, P7 and P8) including mutants and controls [640, 641, 1296-TR x2, 1297-TR x2, 2607, 2608 (P6); 2607, 2608, *cdc13-1*-NTΔ (1296) x2 clones, *cdc13-1*-CTΔ (1296) x2 clones, diploid #31, diploid #32 (P7); 2607, 2608, *cdc13-1*-NTΔ (1297) x2 clones, *cdc13-1*-CTΔ (1297) x2 clones, diploid #31, diploid #32 (P8)] were analysed for MMS-mediated sensitivity. Five-fold serial dilutions of the indicated yeast strains in sterile water were spotted onto YEPD medium plates containing three concentrations of MMS, (0.010%, 0.015% and 0.020%; w/v). The plates were incubated for 3-5 days at 23°C and 30°C before being photographed. Strain numbers are indicated in brackets.

(**A**) Plates 6, 7 and 8 (P6, P7 and P8) after 3 days of incubation at 23°C and 30°C.

(**B**) Plates 6, 7 and 8 (P6, P7 and P8) after 5 days of incubation at 23°C and 30°C.

5.3.4.3. Effects of H_2O_2 on *cdc13-1* mutants lacking NTΔ or CTΔ (haploids) and on diploid (NTΔ/CTΔ) mutants

This part of the study aimed to determine the effects of H_2O_2 on the growth of diploids containing both alleles (*cdc13-1*-NTΔ and *cdc13-1* CTΔ) in comparison with haploid, *cdc13-1*-NTΔ and CTΔ mutants. Serially diluted cultures were spotted on the YEPD agar plates (P6, P7 and P8) contained three different concentrations of H_2O_2, (2 mM, 3 mM and 4 mM), and incubated at two different temperature (23°C and 30°C) for 3 and 5 days.

All cultures were severely inhibited in their growth at 4 mM H_2O_2, while mild inhibition of growth was observed at 2 mM H_2O_2 at 23°C and 30°C after 3 and 5 days of incubation (Figure 5.21). However, differential growth patterns were observed at 3 mM H_2O_2 reflecting distinct individual responses of *cdc13Δ exo1Δ* (2607 and 2608), *cdc13-1*-NTΔ [1296-NTΔ #4 and #5 (P7); 1297- NTΔ #7 and #8 (P8)] and *cdc13-1*-CTΔ [1296-CTΔ #9 and #10 (P7); 1297-CTΔ #11 and #12 (P8)] mutants (haploid) and diploids (#31 and #32; P7 and P8) strains, wild type (640 and 641; P6) and strains 1296-TR and 1297-TR; P6.

The haploid *cdc13Δ exo1Δ* mutants (2607 and 2608) were the most sensitive to 3 mM H_2O_2 (Figure 5.21). The haploid *cdc13-1*-NTΔ and *cdc13-1*-CTΔ mutants also manifested a partial growth inhibition, with slightly less growth in the NTΔ mutant (P7, P8) as compared to CTΔ mutant (P7, P8), more obvious at 3 mM H_2O_2 at 23°C and 30°C after 3 days of incubation (Figure 5.21A). The wild type strains (640 and 641; P6) exhibited slightly more sensitivity to 3 mM H_2O_2 as compared to strains 1296-TR and 1297-TR; (P6), more obvious at 23°C. However, the sensitivity difference between *cdc13-1*-CTΔ (P7 and P8) and *cdc13-1*-NTΔ (P7 and P8) deletion mutants were not very distinguishable at 23°C after 3 and 5 days of incubation.

The haploid *cdc13-1*-CTΔ mutants on 3 mM and 4 mM H_2O_2 were comparable in growth inhibition to strains 1296-TR and 1297-TR (P6) and wild type strains as well as to the diploid strains (#31 and #32) that displayed some resistance to 3 mM H_2O_2 and also to 4 mM H_2O_2 (to some degree) as mild growth was observed at 4 mM H_2O_2 comparable to the growth of *cdc13-1*-CTΔ mutants (haploid), obvious after the longer incubation (at 23°C after 5 days of incubation)

and at higher temperature (30°C after 3 and 5 days of incubation). The partial recovery of growth was observed after 5 days of incubation at 23°C and 30°C but it did not mask the distinct inhibitory growth pattern displayed after 3 days of incubation (Figure 5.21B). The inhibition of growth in diploids was comparable to the growth exhibited by *cdc13-1*-CTΔ or better than NTΔ mutants at 30°C after 3 and 5 days of incubation.

Overall, the growth of the diploids on H_2O_2 exceeded the growth of the two haploids with C- and N- truncated *cdc13-1* and all other strains in the experiment.

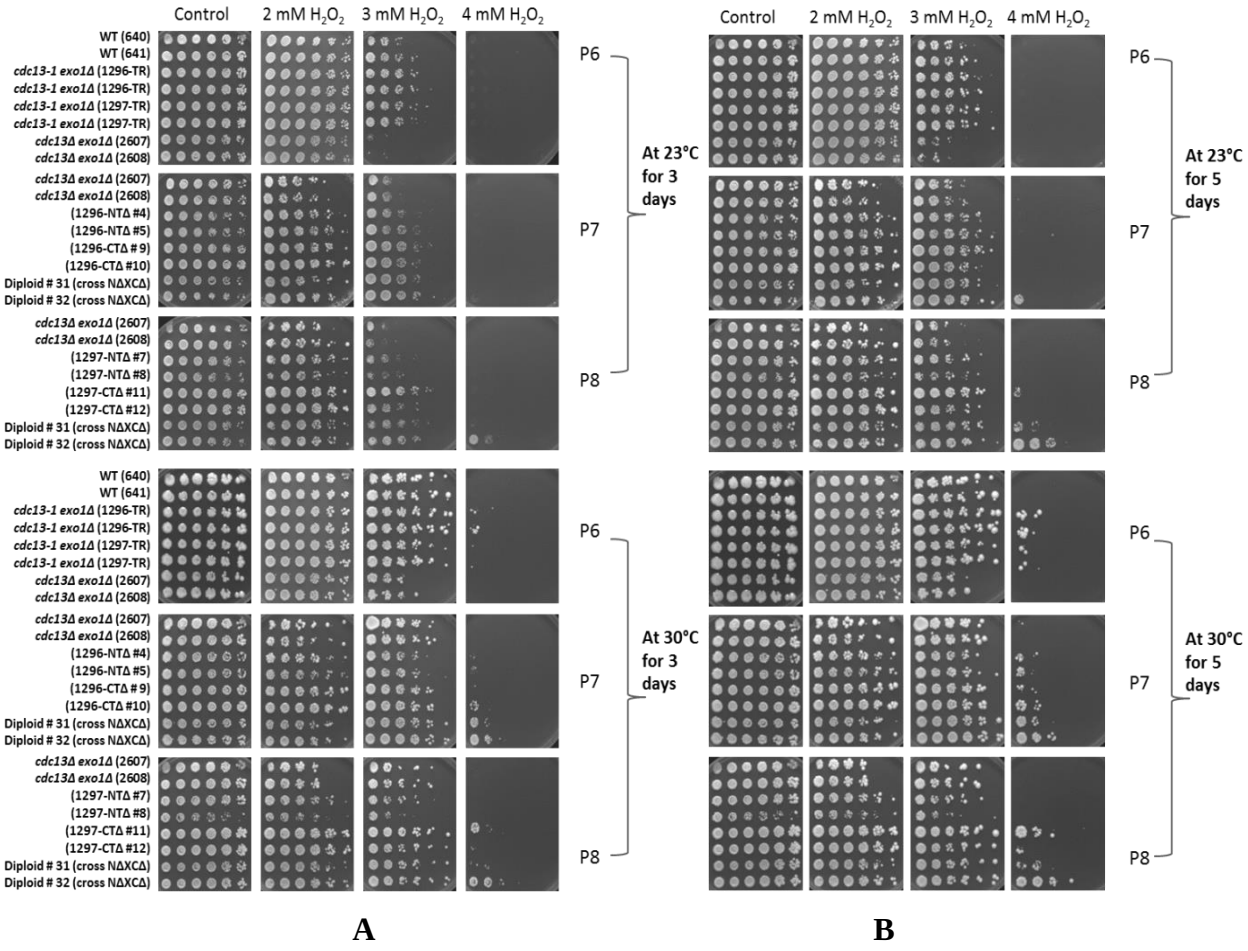

Figure 5.21. Effect of H_2O_2 (2 mM, 3 mM and 4 mM) on the growth of *cdc13-1* N- and C-terminus truncated haploids in comparison to diploid mutants of 1296-TR and 1297-TR strains.
Different strains on three plates (P6, P7 and P8) including mutants and controls [640, 641, 1296-TR x2, 1297-TR x2, 2607, 2608 (P6); 2607, 2608, *cdc13-1*-NTΔ (1296) x2 clones, *cdc13-1*-CTΔ (1296) x2 clones, diploid #31, diploid #32 (P7); 2607, 2608, *cdc13-1*-NTΔ (1297) x2 clones, *cdc13-1*-CTΔ (1297) x2 clones, diploid #31, diploid #32 (P8)] were analysed for sensitivity to H_2O_2 in order to compare it in *cdc13-1* N- and C-terminus truncated haploids and diploid mutants. Five-fold serial dilutions of the strains in sterile water were spotted onto YEPD medium plates containing three concentration of H_2O_2 (2 mM, 3 mM and 4 mM). The plates were incubated for 3-5 days at 23°C and 30°C before being photographed. Strain numbers are indicated in brackets.
(**A**) Plates 6, 7 and 8 (P6, P7 and P8) after 3 days of incubation at 23°C and 30°C.
(**B**) Plates 6, 7 and 8 (P6, P7 and P8) after 5 days of incubation at 23°C and 30°C.

Effect of HU on *cdc13-1* mutants lacking NTΔ or CTΔ (haploids) and on diploid (NTΔ/CTΔ) mutants

To determine growth responses to HU in diploids (#31 and #32) and haploids, the *cdc13-1* NTΔ, *cdc13-1*-CTΔ and *cdc13Δ* (2607 and 2608) mutant cultures were tested at two concentrations of HU (25 mM and 50 mM; w/v). Serially diluted cultures were spotted on HU containing YEPD agar plates (P7 and P8) incubated at 23°C and 30°C for 3 and 5 days

As shown in Figure 5.22, there was a slight to moderate effect of inhibition of growth at 50 mM HU after 3 days of incubation at 23°C and 30°C, (obvious in last two to three dilutions of all cultures when compared to controls). The haploids *cdc13Δ exo1Δ* mutants (2607 and 2608) showed partial sensitivity to both concentrations of HU, more obvious at 50 mM, HU (partial growth in last three dilutions) at 23°C as compared to 30°C after 3 days of incubation (Figure 5.22A). In comparison, the haploid *cdc13-1*-NTΔ and *cdc13-1*-CTΔ mutants with mild growth arrest, manifested their distinct sensitivity pattern (more growth in CTΔ as compared to NTΔ) at 50 mM HU at 23°C and 30°C after 3 days of incubation (Figure 5.22A).

Due to growth restoration after 5 days of incubation at 23°C and 30°C, the inhibition trends were less comparable (Figure 5.22B). The growth of diploids was either equal or slightly enhanced when compared to *cdc13-1*-NTΔ mutants (P7, at 23°C after 3 days) but obviously less when compared to *cdc13-1*-CTΔ mutants at 50 mM HU at 23°C after 3 and 5 days of incubation.

Overall, the observed growth inhibition trends in haploids and diploids were consistent with previous experiments with UV and MMS. The *cdc13Δ* mutants showed the maximum inhibition in growth, while medium inhibition was observed in *cdc13-1* NTΔ. The *cdc13-1*-CTΔ mutants, however, displayed the best growth and maximum resistance to HU, obvious at 23°C after 3 days of incubation. The diploid [#31 and #32 (P7 and P8)] appeared to be mildly inhibited in their growth under the effect of HU. In diploids, the growth inhibition was not very significant. They presented the intermediate growth inhibition as compared to haploids obvious at 30°C after 3 and 5 days of incubation that could be the result of an allele dosage effect as seen in the previous experiments.

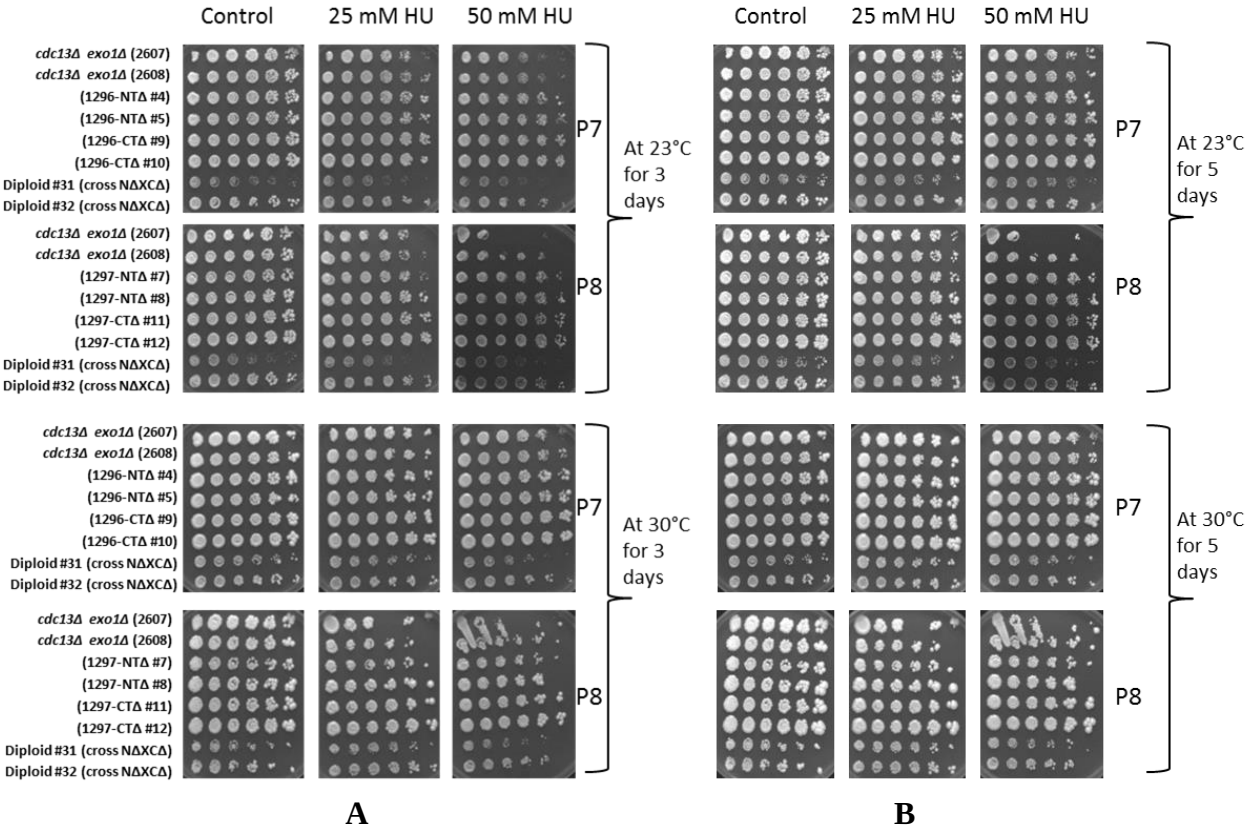

Figure 5.22. Effect of HU (25 mM, and 50 mM) on the growth of *cdc13-1* N- and C-terminus truncated haploids in comparison to diploid mutants of 1296-TR and 1297-TR strains.

Different strains on three plates (P6, P7 and P8) including mutants and controls [640, 641, 1296-TR x2, 1297-TR x2, 2607, 2608 (P6); 2607, 2608, *cdc13-1*-NTΔ (1296) x2 clones, *cdc13-1*-CTΔ (1296) x2 clones, diploid #31, diploid #32 (P7); 2607, 2608, *cdc13-1*-NTΔ (1297) x2 clones, *cdc13-1*-CTΔ (1297) x2 clones, diploid #31, diploid #32 (P8)] were analysed for sensitivity to HU in order to compare it in *cdc13-1* N- and C-terminus truncated haploids and diploid mutants. Five-fold serial dilutions of the strains in sterile water were spotted onto YEPD medium plates containing two concentrations of HU (25 mM, and 50 mM). The plates were incubated for 3-5 days at 23°C and 30°C before being photographed. Strain numbers are indicated in brackets.

(**A**) Plates 6, 7 and 8 (P6, P7 and P8) after 3 days of incubation at 23°C and 30°C.

(**B**) Plates 6, 7 and 8 (P6, P7 and P8) after 5 days of incubation at 23°C and 30°C.

5.4. Conclusions:

- The similar responses of *cdc13Δ* (more resistant) and *stn1Δ* (less resistant) mutants to UV, MMS and HU indicate the existence of sensitivity control under the same pathways.
- The resistance to oxidative stress (H_2O_2) in *STN1* deletion mutants as compared to *CDC13* deletion mutants indicates the involvement of different mechanism to cope the oxidative stress.
- Increased sensitivity of combined deletion to UV, MMS and HU could be due to the effects of either *rad24Δ* or due to interaction of *cdc13Δ* and *stn1Δ* cooperatively.
- The peculiar sensitivity trends in N- and C-terminus mutants of Cdc13-1, implies that different domains exist in the Cdc13 protein that contribute to UV resistance.
- The slightly less resistance of wild type as compared to C-terminus truncated mutants of Cdc13-1 protein indicate the presence of suppressor of WT-resistance to UV, MMS and replication inhibitor HU.
- The growth inhibition trends in heterozygous diploid containing N- and C-terminus of Cdc13-1 suggest the allele dosage effect to DNA damaging and replication inhibitor stress factors.

  In summary, mutants without essential telomere capping proteins Cdc13 and Stn1, and N- and C-terminus truncated variants of Cdc13-1 show distinct patterns of sensitivity to DNA replication inhibitors (MMS and HU), DNA damaging agents (UV) and oxidative stress factor (H_2O_2). These cellular responses to genotoxic agents highlight potentially new roles of telomere capping proteins, Cdc13 and Stn1.

Chapter 6

Chronological lifespan studies

6.1. Introduction

In yeast chronological lifespan (CLS) assays measure the time cells can remain viable in the post-replicative stationary phase (Piper, 2006, Fabrizio and Longo, 2003). These assays provide direct screening of genes involved in longevity pathways and identify chronologically long-lived gene deletions.

In the past, yeast has been used to study basic cellular processes such as DNA repair, the cell cycle, the mechanism of cellular interaction, cell signalling and differentiation (Piper, 2006, Vachova *et al*., 2012). At present, budding yeast, *Saccharomyces cerevisiae* is used as an ideal eukaryotic model to study ageing at the organismal, cellular and molecular level (Jazwinski, 2002, Guarente and Kenyon, 2000, Kaeberlein *et al*., 2007). The phenomenon of ageing is a result of the complex interplay of molecular and cellular processes (Uzunova *et al*., 2013). The CLS of yeast is measured as the survival time of cells in a non-dividing stationary phase and has been implicated into identification of genes and pathways involved in the regulation of ageing. In yeast, nutrient-sensing the Tor/Sch9 and the Ras/adenylate cyclase/PKA (protein kinase A) pathways are involved in the mechanisms of lifespan regulation (Guarente and Kenyon, 2000). Yeast can survive in adverse conditions in different environments. The Ras/cAMP pathway controls the adaptation in response to nutrient limitation (Pedruzzi *et al*., 2000). Analogous to these pathways, in higher eukaryotes are the 'insulin/IGF-I (insulin-like growth factor) like' pathway that regulates longevity (Dorman *et al*., 1995).

Yeasts are highly adaptable eukaryotes and can survive for more than three months without showing a decrease in cellular viability under normal conditions (Lillie and Pringle, 1980). Traditionally, two media have been used to study the CLS of yeast: synthetic complete medium (SC/SDC) (Fabrizio *et al*., 2004, Fabrizio and Longo, 2003) and nutrient-rich, YEPD medium (Longo and Fabrizio, 2012). The SDC medium promotes short survival with high metabolism. In contrast, YEPD leads to reduced metabolism with longer survival. Both media were utilised in this study to find measureable differences in cellular viability of Cdc13- and Stn1-deficient strains.

Maintenance of telomere integrity ensures the genomic stability of cells. Loss of protective proteins or the presence of defective protein unmasks the telomere that activates DNA damage checkpoint signalling pathways. The activation of exonucleolytic degradation on the uncapped telomere can lead to genomic instability and early senescence, the hallmarks of ageing (Mason and Skordalakes, 2010, Aubert and Lansdorp, 2008).

Cdc13 binds to telomere G-rich tails through a sequence specific central OB-(oligosaccharide/oligonucleotide binding) fold essential for its capping function (Eldridge and

Wuttke, 2008). The interaction between Cdc13 and Stn1 is mediated through C-terminal located conserved OB4-fold (Sun *et al*., 2011). The structural analysis of Cdc13 has revealed another conserved region/OB1 fold in its N-terminal end (Sun *et al*., 2011), that might bind with Po1I; catalytic subunit of pol α primase complex (Qi and Zakian, 2000). Cdc13 protein also interacts with Est1 through its recruitment domain, second fold in N-terminus that facilitate telomerase recruitment to telomere.

Cdc13 N- and C-terminal ends interact with different components of telomere capping machinery, implying their different structural motifs or domains. In this study, the chronologic lifespan of different yeast strains lacking Cdc13 and Stn1 were compared to WT to find possible roles of telomere capping proteins in cellular senescence and ageing. CLS of N- and C-terminus deletions were also investigated to dissect the role of both halves of the Cdc13 protein in cellular senescence under different paradigms, including calorie restriction.

In yeast, chronological ageing is strictly temperature-dependent. To facilitate ageing studies, strains were tested for appropriate growth temperature and also for sensitivity of mutants to higher temperature.

6.2. Aims and objectives

The main focus of this part of work was to determine differences in chronological lifespans of mutants, lacking essential telomere capping proteins, Stn1and Cdc13, under present laboratory conditions.

This aim involves the following objectives:

- To test the mutant strains at a range of temperatures to determine appropriate conditions allowing facilitation of CLS studies at higher temperature (above 23˚C).
- To test the sensitivity of the mutants to higher temperature (30˚C) and to compare it with that at low temperature (23˚C).
- To test the viability of the mutants after short-term of preserving in glycerol.
- To measure the CLS of mutant strains without essential telomere capping proteins, Stn1 and Cdc13.
- To measure the CLS of mutants with N- and C-terminal deletion variants of protein Cdc13-1.

6.3. Results

CLS of *S. cerevisiae* wild type, *EXO1* deletion, *STN1* deletion, *CDC13* deletion and *cdc13-1* without N- and C-terminus were studied. Yeast strains used in this study are listed in Table 4.1 (Chapter 4).

6.3.1. The cultivation of yeast cells in solid and liquid media

cdc13 and *stn1* single and combined mutants were cultivated on YEPD agar and in broth media to determine cell growth rate, efficiency and cellular viability. Overnight cultures (set with approximately equal numbers of cells) grown in YEPD broth at 30°C showed variable growth rates. Total cell numbers were confirmed spectrophotometrically by measuring the optical densities (OD_{660}) in 1 ml of cultures. Combined deletion mutants with genotype *cdc13*Δ *stn1*Δ *exo1*Δ *rad24*Δ showed three to four times less OD_{660} as compared to the wild type implying only 25% (DLY 2684 with $p<0.00008$) and 30% (DLY 2685 with $p<0.00014$) of the growth rate compared to the controls (DLY 640) (Figure 6.1). Reduced cell number was also observed in single mutants with *STN1* deletion (DLY 2625: 34%; DLY 2626: 23% survival, with $p<0.0004$ and $p<0.00009$ respectively, highly significant) as compared to the wild type. However, strains DLY 2607 and 2608 with *CDC13* and *EXO1* deletions, and strains 1272 and 1273 with *EXO1* deletion did not show a significant difference ($p< 0.8, 0.2, 0.2$ and 0.2 respectively) in growth (101%, 98%, 102% and 103% respectively) on YEPD agar (Figure 6.3) and broth media.

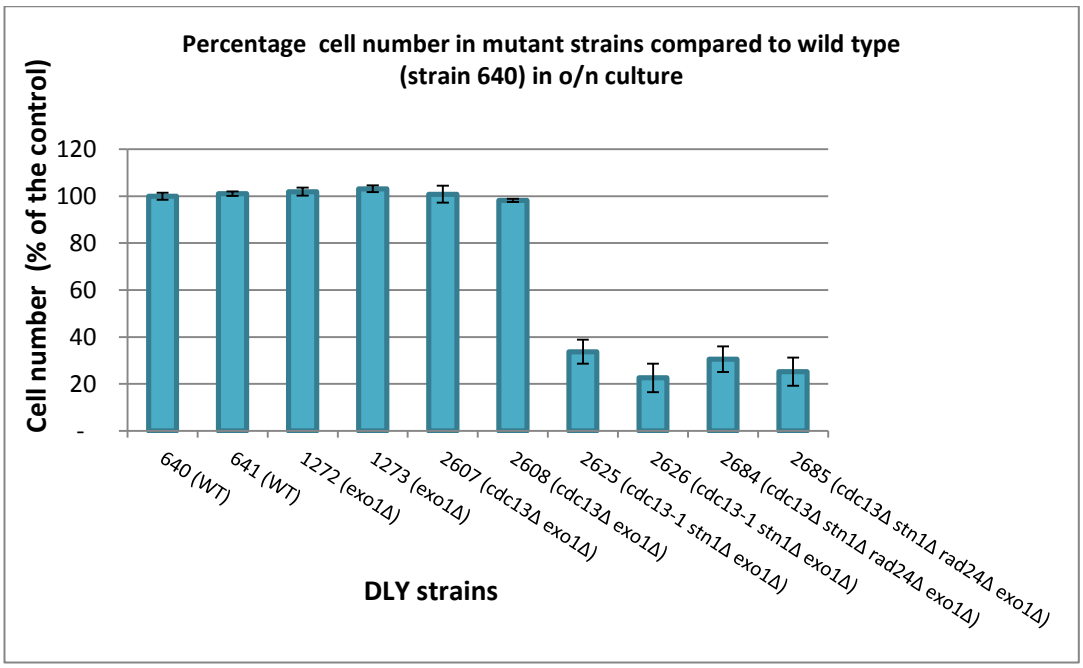

Figure 6.1. Spectrophotometric analysis of cell densities in overnight cultures. Variable OD_{660} values correlate with different cell numbers in the wild type (WT) and mutant strains. The cell number is expressed as percentage of the control (WT) cells considered as 100%, and the differences in cell numbers in mutants were calculated from controls. Results are expressed as mean ± SEM (n=5). The cell number variations in strains 641, 1272, 1273, 2607 and 2608 are statistically non-significant ($p > 0.05$), whereas low cell number in strains 2625, 2626, 2684 and 2685 with p values 0.00042, 0.00009, 0.00008, 0.00014, respectively, shows statistically highly significant variations as compared to the wild type ($p < 0.0001$).

The differences in growth capacity and, therefore, final cell numbers of different mutants were correlated with variable number of colony-forming units on YEPD agar medium (Figure 6.2). Colony formation was reduced in *stn1* deletion mutants (*stn1*Δ, strains 2625 and 2626) and *cdc13* and *stn1* combined deletion mutant (strain 2685) as compared with wild type. Colony morphology also appeared altered in mutant strains as compared to the wild type; in particular, colony shape was irregular and "flowery" in strains 2625 and 2685 as compared to the wild type (640), which was smooth and circular (Figure 6.3).

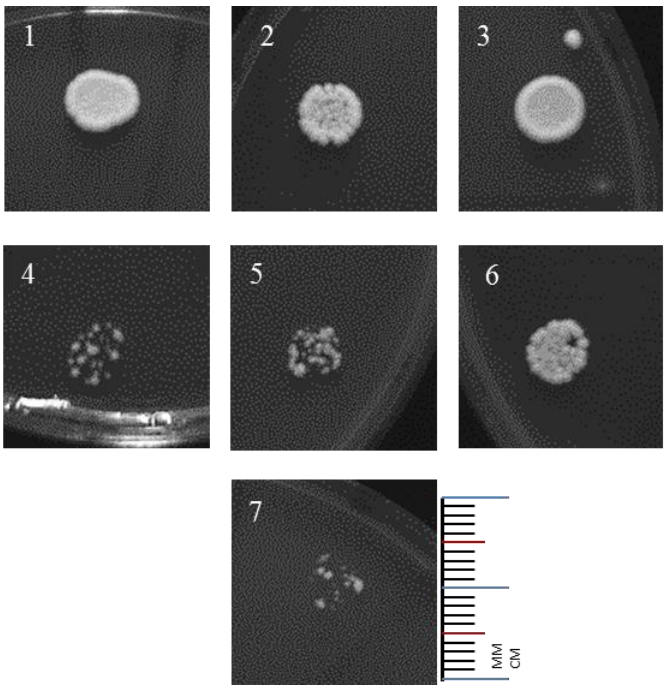

1: WT (DLY 640)

2: WT (DLY 641)

3: *exo1*Δ (DLY 1273)

4: *stn1*Δ *exo1*Δ *cdc13-1* (DLY 2625)

5: *stn1*Δ *exo1*Δ *cdc13-1* (DLY 2626)

6: *cdc13*Δ *exo1*Δ (DLY 2607)

7: *cdc13*Δ *stn1*Δ *exo1*Δ *rad24*Δ (DLY 2685)

Figure 6.2. The abundance of the colony formation by different strains propagated on YEPD medium after overnight (o/n) incubation at 30°C.

Mutant *stn1Δ exo1Δ cdc13-1* (strains DLY 2625 and DLY 2626) and *cdc13Δ stn1Δ exo1Δ rad24Δ* (strain DLY 2685) showed less effective colony formation, heterogeneous (various) cell sizes (4, 5 and 7) as compared to the wild type strains DLY 640 and 641 (1 and 2). Overnight-grown cultures from a single colony were diluted in 1:2 in YEPD broth and 5 µl of each diluted culture was spotted on a YEPD agar plate and incubated at 30°C. Scale bar equal to 20 mm.

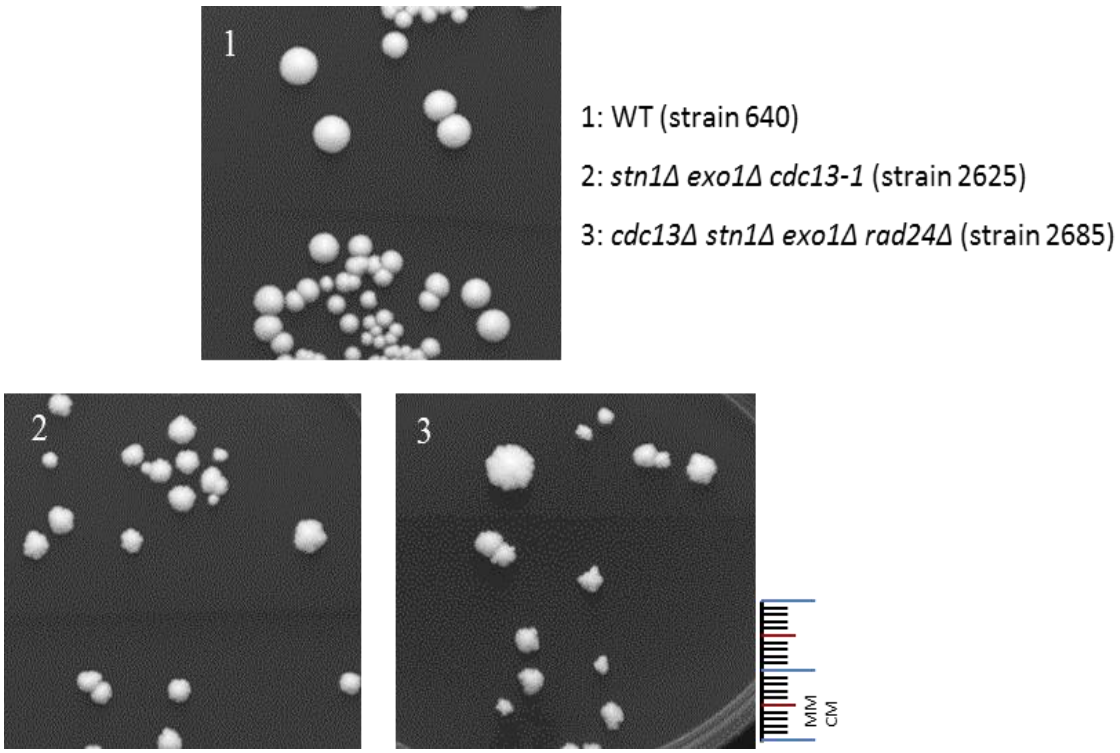

Figure 6.3. Colony morphologies in WT and mutant strains grown on YEPD agar medium.

Mutant strains *stn1*Δ (2625) and *stn1Δ cdc13Δ* (2685) (2 and 3 respectively) showed "flowery" colony shapes with wavy margins as compared to uniform circular colonies in wild type strain 640 (1). Scale bar equal to 20 mm. Cultures were grown for 3 days before being photographed.

6.3.2. Spot tests

Yeast strains selected for the ageing studies (mutants with *CDC13* and *STN1* deletions and wild type) showed variable growth patterns on YEPD agar plates and broth at 23°C in preliminary cultivation assays. Spot tests were carried out to assess the viability of these strains at a range of temperatures to determine the optimal temperature regimes to grow mutant strains in order to facilitate chronological lifespan (CLS) studies (Figure 6.4). Yeast ageing slows at low temperature, and therefore it takes longer (up to 3-6 months) to study CLS at low temperature as compared to high temperature (Fabrizio and Longo, 2003, Piper, 2006).

Serial dilutions (5-fold serial dilution) of cells from fresh cultures (five cultures of each mutant set with single independent colony) were spotted on YEPD plates using replica plating and incubated for 3-5 days at defined temperatures (23°C-40°C) to determine the viability of cultures in different dilutions. Mutant strain 2625 (*exo1*Δ *stn1*Δ *cdc13-1*) showed mild sensitivity to high temperature growing slightly better at 23°C as compared to 36°C and 38°C (colonies 1-4 on plates 1-4). However, colony 5 (plate 3) did not exhibited marked sensitivity

to high temperature. The mutant strain 2685 (*cdc13*Δ *exo1*Δ *stn1*Δ *rad24*Δ*)* grew better at 36°C and 38°C as compared to 23°C; other mutant strains [1272 and 1273 (*exo1*Δ), 2607 (*exo1*Δ *cdc13*Δ] and wild type strain (640) did not show any sensitivity to high temperatures (36°C-38°C).

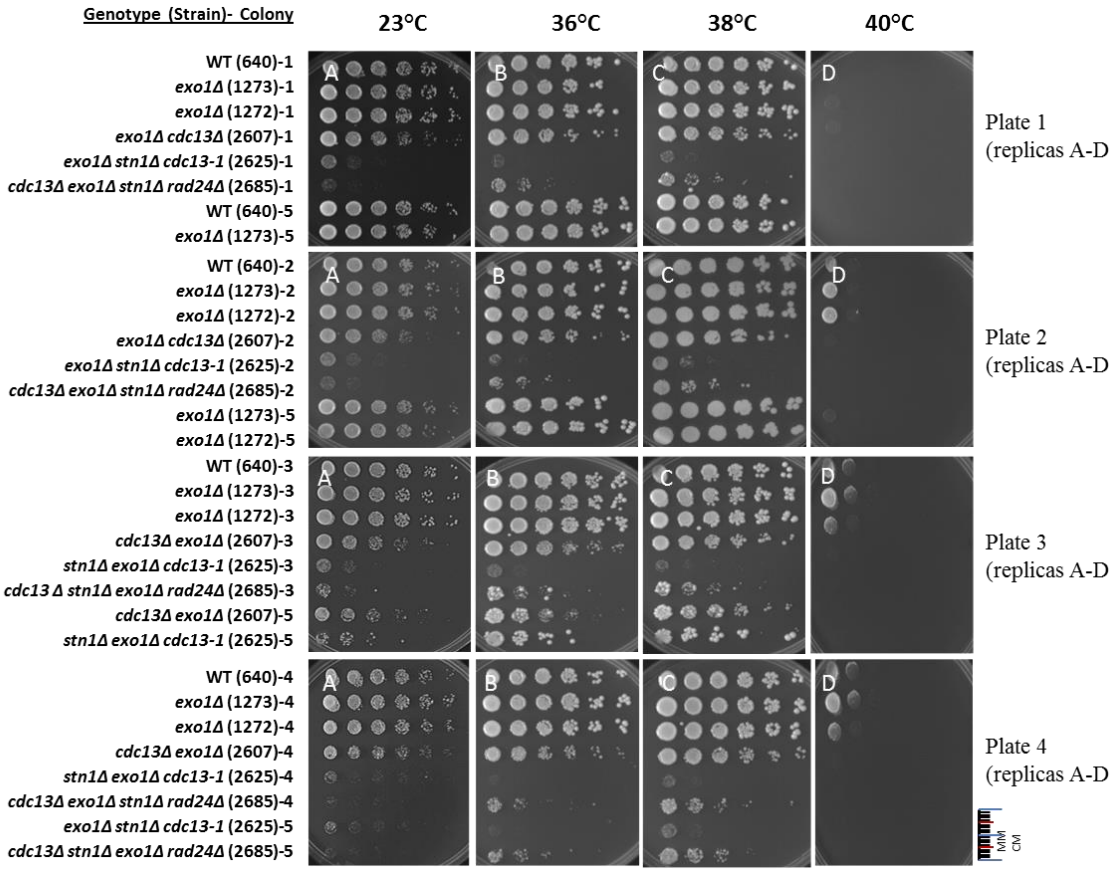

Figure 6.4. Growth of mutant and wild type strains at different temperatures.

Five independent colonies (1-5) were analysed for their growth at 23°C to 40°C. Yeast cultures were serially (five-fold) diluted, cell number equalised by measuring OD_{660}, spotted onto YEPD agar plates and incubated at the indicated temperatures for 3-5 days before being photographed. Scale bar equal to 20 mm.

For further verification of temperature sensitivity, another spot test was conducted with temperature-sensitive (ts) controls i.e., strains 1108 (ts) and 1296 (ts), to establish whether less growth in *stn1*Δ containing mutants (strains 2625, 2685) was a valid finding. Two mutant strains were selected for *stn1*Δ *exo1*Δ *cdc13-1* (2625 and 2626) and *stn1*Δ *cdc13*Δ *exo1*Δ *rad24*Δ (2684 and 2685) deletion each. The results showed that strain 2625 did not grow well at low temperature (23°C) and showed better growth at 30°C (Figure 6.5, plate 1, A and B). Reduced growth in mutant strain 2625 (*exo1*Δ *stn1*Δ *cdc13-1*) could result from reduced cell numbers or reduced rate of growth, or high mortality in this strain. However, another *stn1* deletion mutant, strain 2626 (*stn1*Δ *exo1*Δ *cdc13-1*), did not grow well at both temperatures at

the same cell density (plate 2, A and B). Similarly strains 2684 and 2685 (*cdc13*Δ *exo1*Δ *stn1*Δ) grew better at 30°C as compared to 23°C: other mutant strains 1272 and 1273 (*exo1*Δ), 2607 (*exo1*Δ *cdc13*Δ), and wild type (640) did not show any sensitivity to high temperature (30°C). Strains 1108-ts (*cdc13-1*) and 1296-ts (*exo1*Δ *cdc13-1*) were temperature sensitive (ts), used as experimental controls, did not grow at 30°C due to sensitivity to high temperature. Strain 2605 was a temperature-resistant (TR) survivor, used as a control that could grow at high temperature.

It was determined from spot analysis results that mutant strains were not sensitive to high temperature i.e., 30°C and all yeast strains could grow well; hence CLS studies can be facilitated at 30°C rather than 23°C. On the basis of spot test experiment, the strain 2625 was selected to use in ageing experiments as the *STN1* deletion mutant instead of strain 2626.

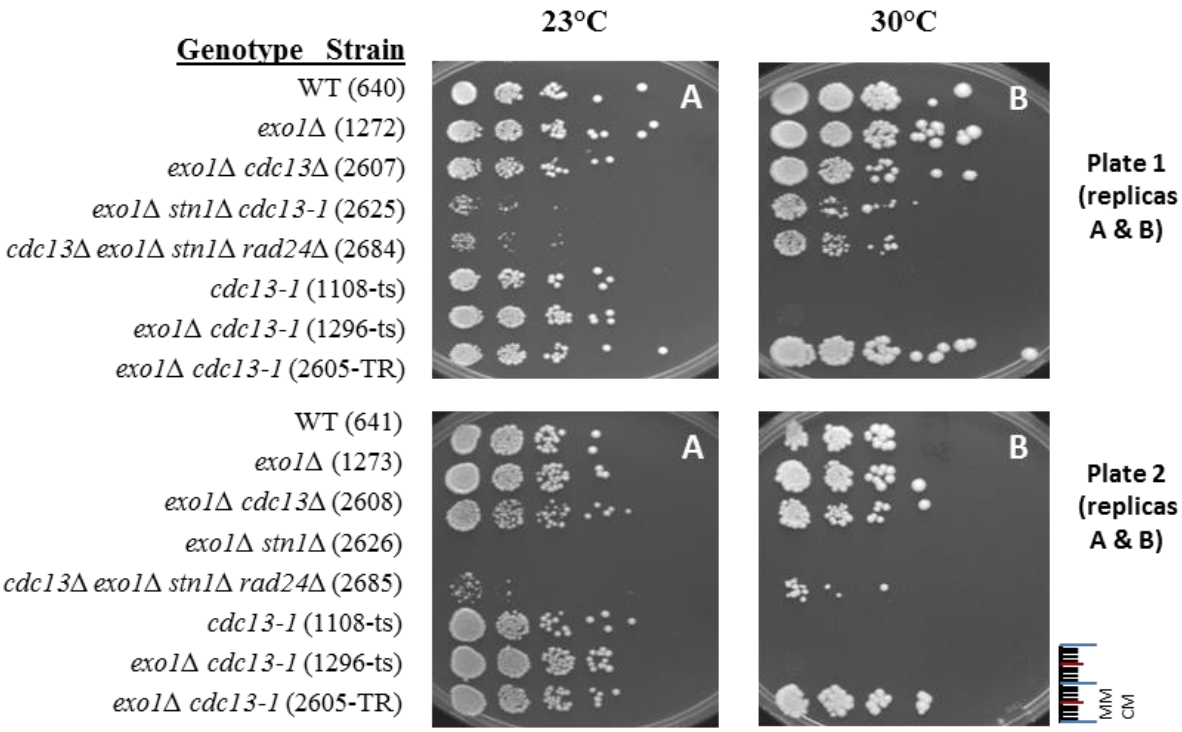

Figure 6.5. Spot test analysis to check sensitivity of different mutants at 23°C and 30°C.

Two independent isolates of the same mutation, experimental and control were tested for their sensitivity to 30°C in comparison with 23°C. Serially diluted cultures with equal number of cells, estimated by measuring OD_{660}, were spotted onto YEPD agar plates in replicates and incubated at 23°C and 30°C for three days before being photographed. Strain numbers are indicated in brackets. Scale bar equal to 20 mm.

6.3.3. Testing viability of yeast cultures after preservation in glycerol

Viability tests were carried out to examine if different growth rates take place in different deletion mutants. The viability of cultures preserved in glycerol could be affected over a period of time. Therefore, it was important to investigate the viability of *stn1* and *cdc13* deletion mutants kept in 25% glycerol at -80°C (in comparison with the wild type strain) before investigating any potentially reproducible differences in chronological survival. This test was performed also to establish how long a strain can be preserved without affecting its viability.

Yeast strains selected for this experiment included control strain 640 and mutants 1273 (*exo1*Δ), 2607 (*exo1*Δ *cdc13*Δ) and 2685 (*cdc13*Δ *exo1*Δ *stn1*Δ *rad24*Δ). These mutant strains were selected due to their reduced growth and high mortality rates. The combined deletion mutants (*STN1* and *CDC13*) grow slowly as compared to the wild type and *EXO1* deletion mutant. It is possible to grow fast growing strains overnight at a particular temperature (30°C) and preserve them at -80°C until slow growing strains achieve the same cell density prior to set CLS experiments in broth medium with equal cell numbers.

The cultures of haploid strains were grown overnight at 30°C from single colonies (see Methods section 2.3.1.8 for details). The approximate cell number in the o/n culture was calculated by measuring cell densities and confirmed with the haemocytometer cell count. Table 6.1 shows the relevant absorbance of experimental strains at OD_{660} (with approximate absorbance 0.6 at $OD_{660)}$.

Table 6.1. Total number of cells per 1 ml as measured by using spectrophotometer and haemocytometer.

Strain	Genotype	OD_{660}	No of cells /ml (spectrophotometer)	No of cells /ml (haemocytometer)
640	Wild type	0.641	9,330,000	8,361,111
1273	*exo1Δ*	0.663	9,660,000	10,555,556
2607	*exo1Δ cdc13Δ*	0.640	9,330,000	10,250,000
2685	*cdc13Δ exo1Δ stn1Δ rad24*	0.647	9,500,000	11,250,000

For comparison, cell suspensions from freshly grown cultures (washed cells) were prepared in water and 25% glycerol with approximately equal numbers of cells (calculated per 1 ml by spectrophotometer absorbance) in all strains.

Two set of samples (water and 25% glycerol with 5 aliquots of each) with concentration of approximate 1000 cells/ml, preserved at -80°C were tested for viable cell count on YEPD agar plates over a period of one week. Viable cell count was calculated by counting CFUs from 50 µl of suspension on each half of a YEPD plate of two replicates for zero time periods (0H), one hour (1H), one day (1D), three days (3D) and one week (1W) samples. The average viable cell count (from duplicate) at 0H was considered 100% and taken to calculate % viability for different time periods.

The percent survival in water and glycerol are presented in Figure 6.6 and showed the survival comparison between wild type and different mutants in water and glycerol over a period of one week. The single deletion mutant strain 2607 without Cdc13 showed a gradual loss of viability in water samples; 65% loss within a period of one week whereas glycerol samples showed a lower decrease in viable colony count over the same time, with 19% loss in viability. The wild type strain 640 also exhibited a significant reduction in viable count in water samples with 60% loss in viability as compared to 29% loss in glycerol samples over a period of 1 week. The strain 1273 with *EXO1* deletion however, did not show a remarkable loss in viability (only 8%) in glycerol samples. In comparison, water samples in this mutant manifested 32% viability loss. The strain 2685, without two core proteins, Cdc13 and Stn1 did not show proper growth at this cell density in water and in glycerol ~50% reduction in viability was observed over a time of 3 days. The strain 2685 without two core proteins, Cdc13 and Stn1 at the same initial cell density showed a very high mortality rate with very low viable count in water and in glycerol; with a 50% reduction in viability over a period of 3 days in glycerol samples whereas there was no any growth in water samples. Gradual loss of viable cells in mutant stains in glycerol and water suggested that this approach might not be suitable to store mutant cells for CLS studies.

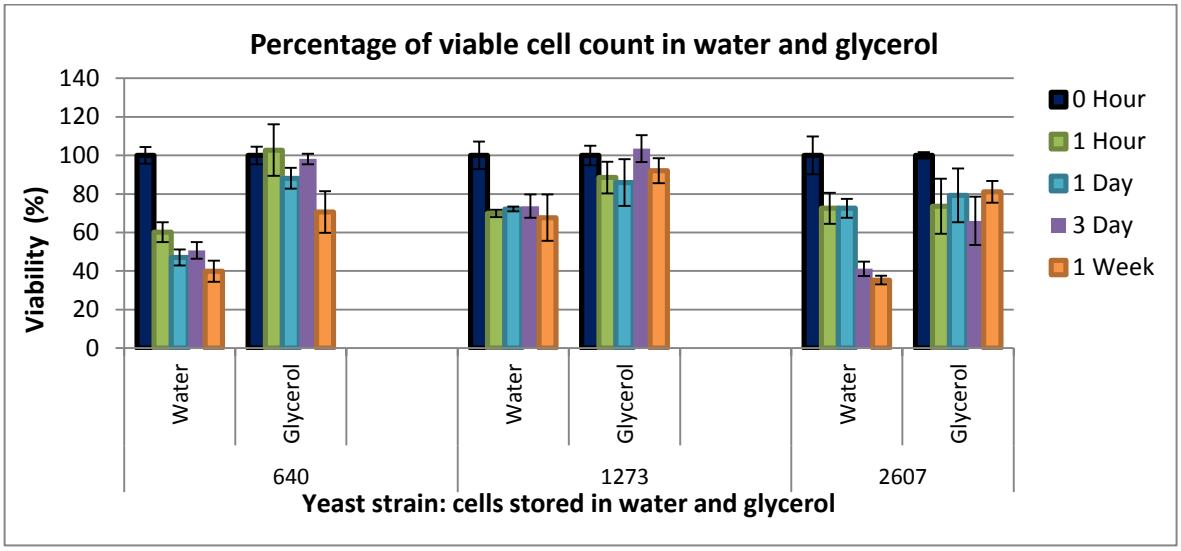

Figure 6.6. The loss of viability in yeast strains stored at -80°C in glycerol and water.

Diluted suspensions (of washed cells) in glycerol and water with approximately equal number of cells (estimated by measuring OD_{660}) from frozen samples for different time periods were plated 50 µl on both halves of YEPD plates and incubated for 2-3 days before being counted. Average viable colony count was estimated per 50 µl volume of water and glycerol. The percentage of viable count was calculated considering 0 hour viable count as 100%. Results are expressed as mean ± SEM (n=4).

640 (wild type strain), 1273 (*EXO1* deletion mutant), 2607 (*EXO1 CDC13* deletion mutant), 2685 (*EXO1 CDC13 STN1* deletion mutant).

6.3.4. CLS studies in synthetic complete (SC) medium (postdiauxic phase)

CLS studies were carried out adopting the method reported by Fabrizio and Longo (2003), with a few modifications as reported by Murakami *et al*. (2008). Six strains of yeast (*S. cerevisiae*) were used for chronological ageing experiment (Table 6.2). Wild type strain (640) was used as an experimental control for single (*cdc13*Δ or *stn1*Δ) or combined deletion mutants (*cdc13*Δ *stn1*Δ) without essential telomere capping proteins Cdc13 and Stn1, to reveal the impact of these genes and their mutations on telomere uncapping, rate of growth, cell mortality, ageing and cellular senescence that leads eventually to cell death.

Table 6.2. Relevant genotypes of strains used in CLS studies.

	Strains DLY	**Strain's relevant genotype**	**Strain's essential genotype**
1	**640**	WT	MAT a ade2-1 trp1-1 can1-100 leu2-3,112 his3-11,15 ura3 GAL+ psi+ ssd1-d2 RAD5
2	**1272**	*exo1*Δ	MAT alpha *exo1*::LEU2
3	**1273**	*exo1*Δ	MAT alpha *exo1*::LEU2
4	**2607**	*exo1*Δ *cdc13*Δ	MAT not known (initially alpha) *cdc13*::HIS *exo1*::LEU2
5	**2625**	*exo1*Δ *stn1*Δ *cdc13-1*	MAT not known (initially alpha) *cdc13-1 stn1*::HIS *exo1*::LEU2
6	**2685**	*exo1*Δ *cdc13*Δ *stn1*Δ *rad24*Δ	MAT alpha *cdc13*::HIS *stn1*::HIS *exo1*::LEU2 *rad24*::TRP

All strains were grown in YEPD medium with 2% glucose at 30°C, with shaking. Total number of cells in overnight-grown cultures was estimated by measuring the spectrophotometric absorbance at OD_{660} (Table 6.3). For fast-growing cultures (cultures #1 to #20) absorbance were measured at dilution 1:2 (500 culture and 500 µl medium), while for slow-growing cultures (cultures #21 to #30) the absorbance at OD_{660} was measured directly from 1 millilitre overnight culture (without any dilution). For CLS measurement, all cultures were adjusted to an approximately equal number of washed cells ~$1x10^6$/ml, (based on OD_{660}) in 20 ml of SC broth (Protocol S2.1). Whereas 50 µl o/n culture to inoculate 5 ml volume of SC medium (Murakami, 2008) or cell number density of ~$1.85x10^5$/ml at inoculum has been reported in other studies.
The ageing cultures were maintained at 30°C with constant agitation for 4 weeks with pooling samples for colony counts at particular intervals (at 3 days, 6 days, 9 days, 12 days and so for four weeks).

Table 6.3. Parameters of inoculums in SC medium (with approximately equal cell numbers).

Key No	Strains DLY	OD_{660} (o/n culture)	Vol. of o/n culture used for inoculums (µl)	OD_{660} at day 3	Auxotrophies requirement
1	640	1.695	196	1.799	HLTU
2	640	1.680	198	1.784	HLTU
3	640	1.661	200	1.770	HLTU
4	640	1.640	202	1.783	HLTU
5	640	1.663	200	1.776	HLTU
6	1272	1.695	196	1.091	H-TU
7	1272	1.672	199	1.782	H-TU
8	1272	1.693	196	1.000	H-TU
9	1272	1.643	202	1.770	H-TU
10	1272	1.708	194	1.792	H-TU
11	1273	1.684	196	1.777	H-TU
12	1273	1.685	197	1.793	H-TU
13	1273	1.670	199	1.719	H-TU
14	1273	1.698	196	1.789	H-TU
15	1273	1.707	195	1.786	H-TU
16	2607	1.569	212	1.638	--TU
17	2607	1.687	197	1.657	--TU
18	2607	1.698	196	1.681	--TU
19	2607	1.692	196	1.630	--TU
20	2607	1.706	195	1.639	--TU
21	2625	1.253	530	1.563	--TU
22	2625	1.393	477	1.530	--TU
23	2625	1.412	470	1.469	--TU
24	2625	1.752	379	1.458	--TU
25	2625	1.220	544	1.507	--TU
26	2685	1.460	454	1.492	---U
27	2685	1.518	437	1.494	---U
28	2685	0.806	824	1.502	---U
29	2685	1.272	522	1.550	---U
30	2685	0.850	781	1.516	---U

Cultures (o/n) #1-#20 were diluted (1:2) to measure OD_{660} while cultures #21-#30 were measured for OD without dilution. To estimate cell number in 3 day-grown culture, all cultures (#1-#30) were diluted (1:2) to measure OD_{660}.

It has been reported earlier that cell division stops after 2-3 days, cells enter in stationary phase or arrest in the G0 phase and ethanol starts accumulating in the medium (Fabrizio and Longo, 2003). Cultures were examined microscopically at day 3, day 6 and day 30 (Figures 6.7-6.11) for stationary phase cell arrest. Un-budded cells were prominent in day 3 and day 6 cultures, while big, flattened, aged cells were observed in day 30 cultures in all strains.

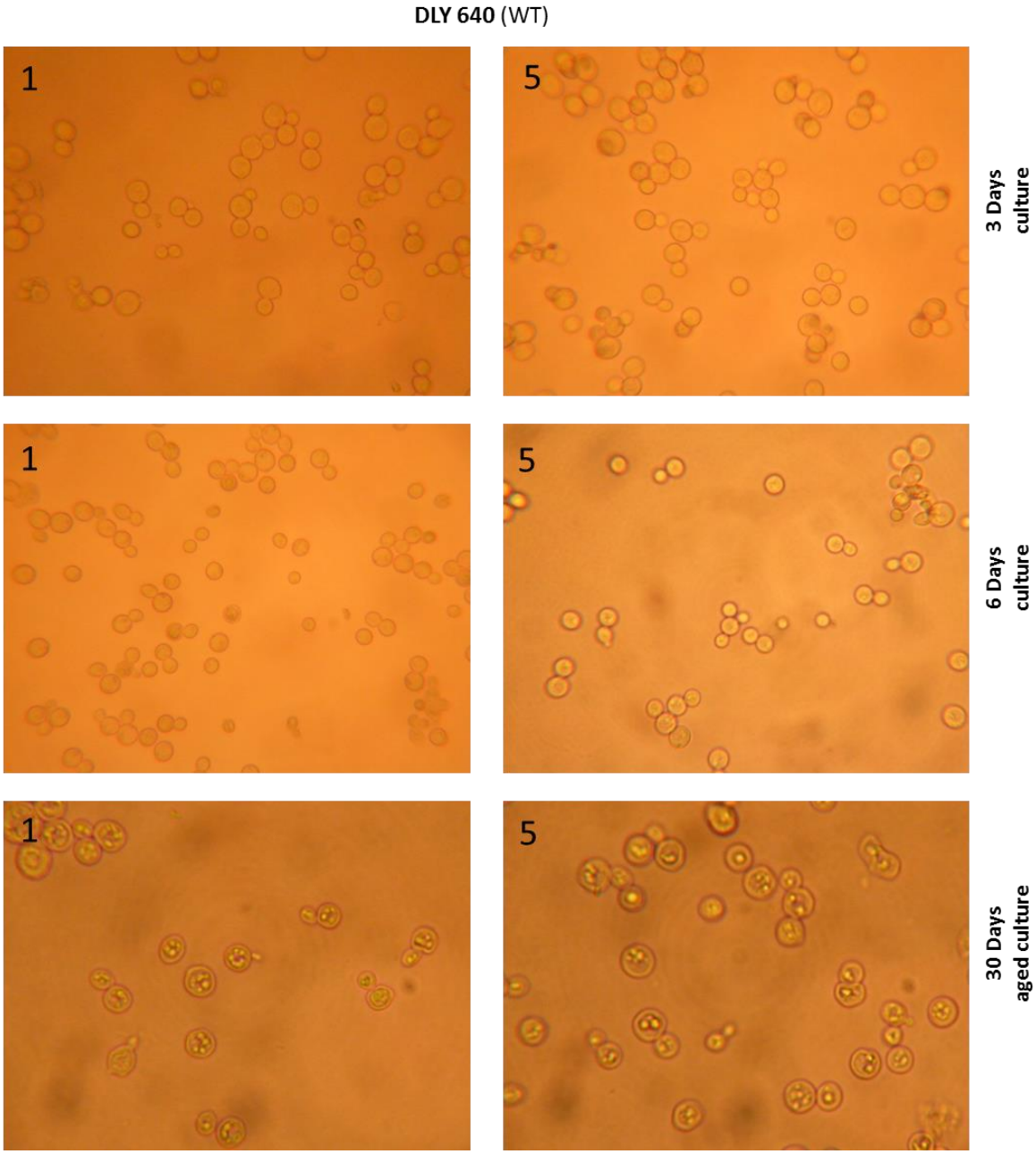

Figure 6.7. Microscopy of ageing culture of the strain DLY 640.

Digital images of 3, 6 and 30 days cultures of strains 640 (WT, control) as manifested by the representative replicas (#1 and #5). Many budded cells were observed in three days culture as compared to a few cells with small buds in 6 day culture. In 30 days-aged culture most of the cells were un-budded, with scarce buds and large vacuoles. Cultures were grown in SC medium supplemented for their auxotrophies at 30°C in a shaking incubator for 30 days. The pictures were taken with a Zeis KF microscope at a magnification of 400x fitted with a Nikon Coolpix 4500 camera (4 Megapixels 4x optical zoom).

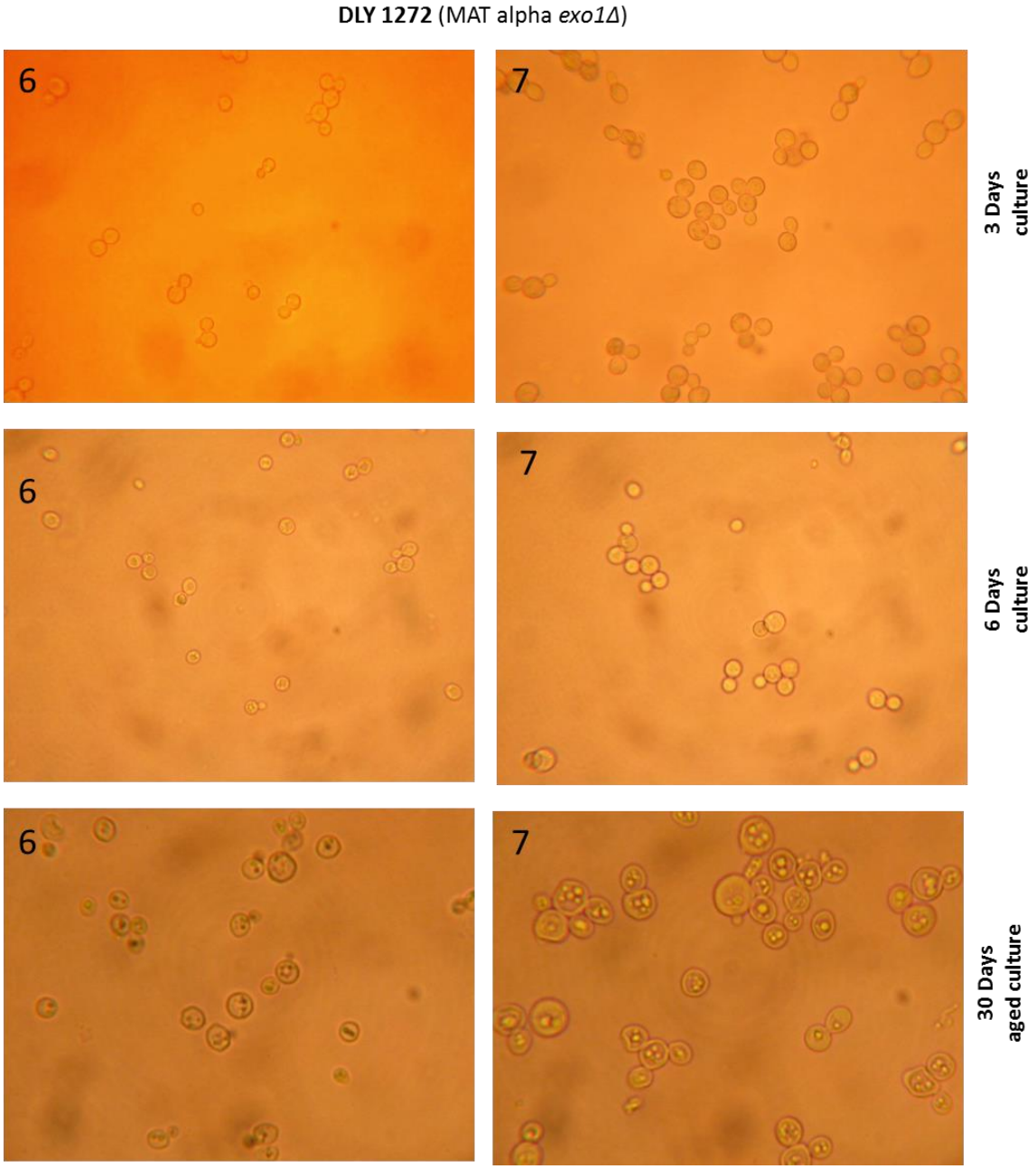

Figure 6.8. Microscopy of ageing culture of the strain DLY 1272.

Digital images of 3, 6 and 30 days cultures of strain 1272 (*exo1* deletion mutant) as manifested by the representative replicas (#6 and #7). Many budded cells were observed in three days' culture as compared to few cells with small buds in 6 day culture. In 30 days' aged culture most of the cells were un-budded, with scarce buds and large vacuoles. Cultures were grown in SC medium supplemented for their auxotrophies at 30°C in a shaking incubator for 30 days. The pictures were taken with a Zeis KF microscope at a magnification of 400x fitted with a Nikon Coolpix 4500 camera (4 Megapixels 4x optical zoom).

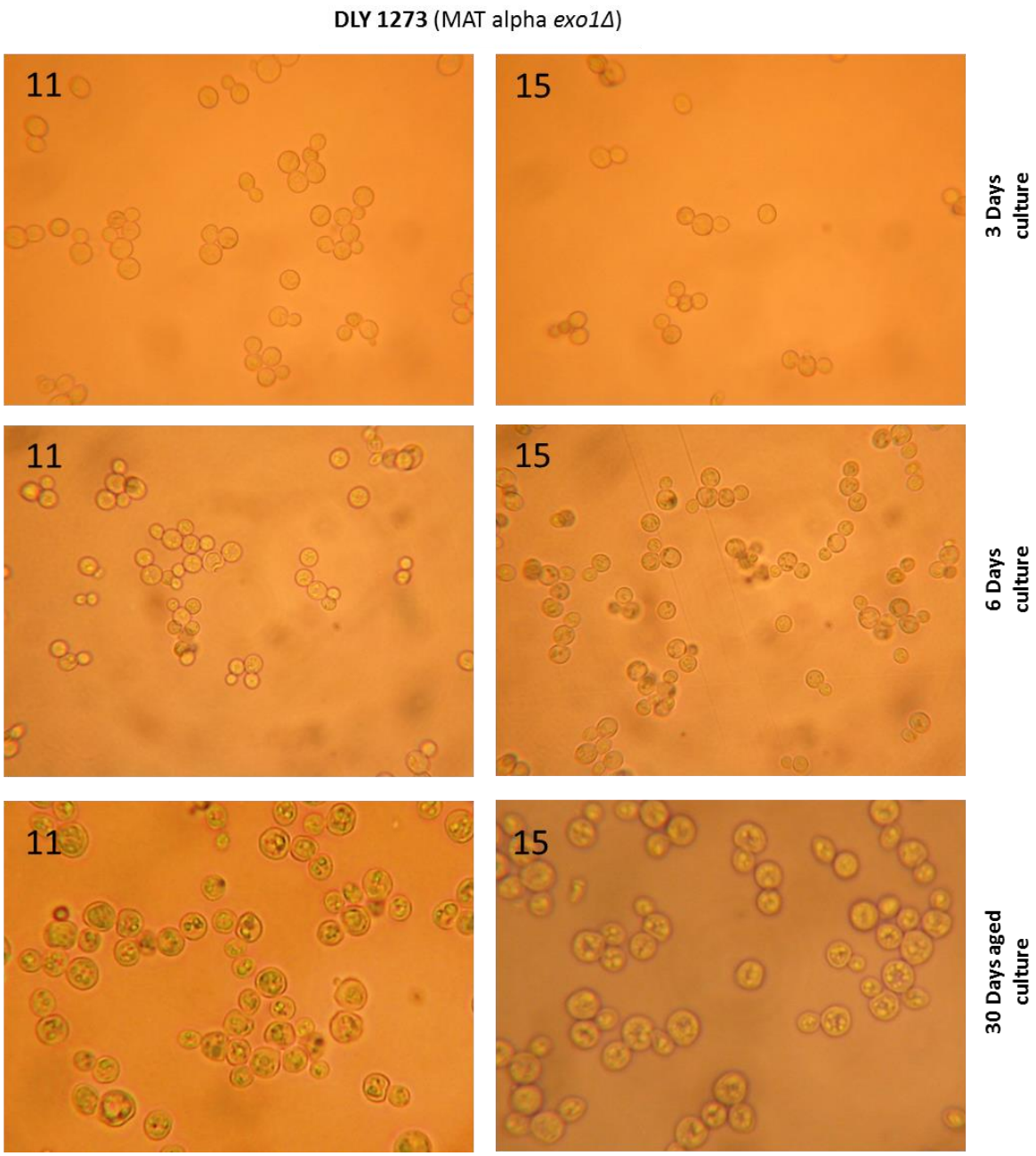

Figure 6.9. Microscopy of ageing culture of the strain DLY 1273.

Digital images of 3, 6 and 30 days cultures of strains 1273 (*exo1* deletion mutant) as manifested by the representative replicas (#11 and #15). Many budded cells were observed in three days' culture as compared to few cells with small buds in 6 day culture. In 30 days aged culture, most of the cells were un-budded, with scarce buds and large vacuoles. Cultures were grown in SC medium supplemented for their auxotrophies at 30°C in a shaking incubator for 30 days. The pictures were taken with a Zeiss KF microscope at a magnification of 400x fitted with a Nikon Coolpix 4500 camera (4 Megapixels 4x optical zoom).

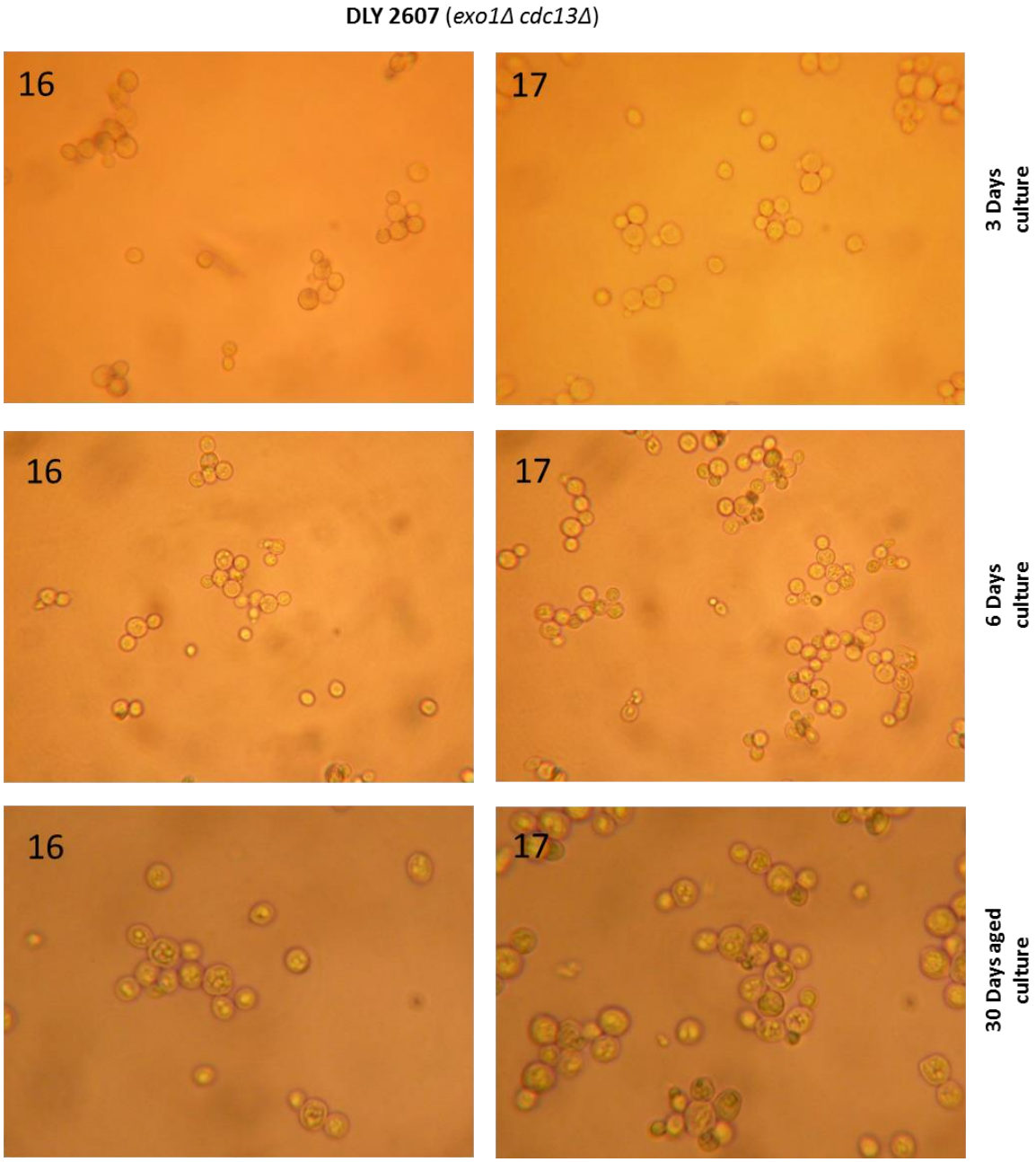

Figure 6.10. Microscopy of ageing culture of the DLY strain 2607.

Digital images of 3, 6 and 30 days cultures of strain 2607 (*exo1Δ cdc13*Δ mutant) as manifested by the representative replicas (#16 and #17). Many budded cells were observed in three days' culture as compared to a few cells with small buds in 6 day culture. In 30 days aged culture most of the cells were un-budded, with scarce buds and large vacuoles. Cultures were grown in SC medium supplemented for their auxotrophies at 30°C in a shaking incubator for 30 days. The pictures were taken with a Zeiss KF microscope at a magnification of 400x fitted with a Nikon Coolpix 4500 camera (4 Megapixels 4x optical zoom).

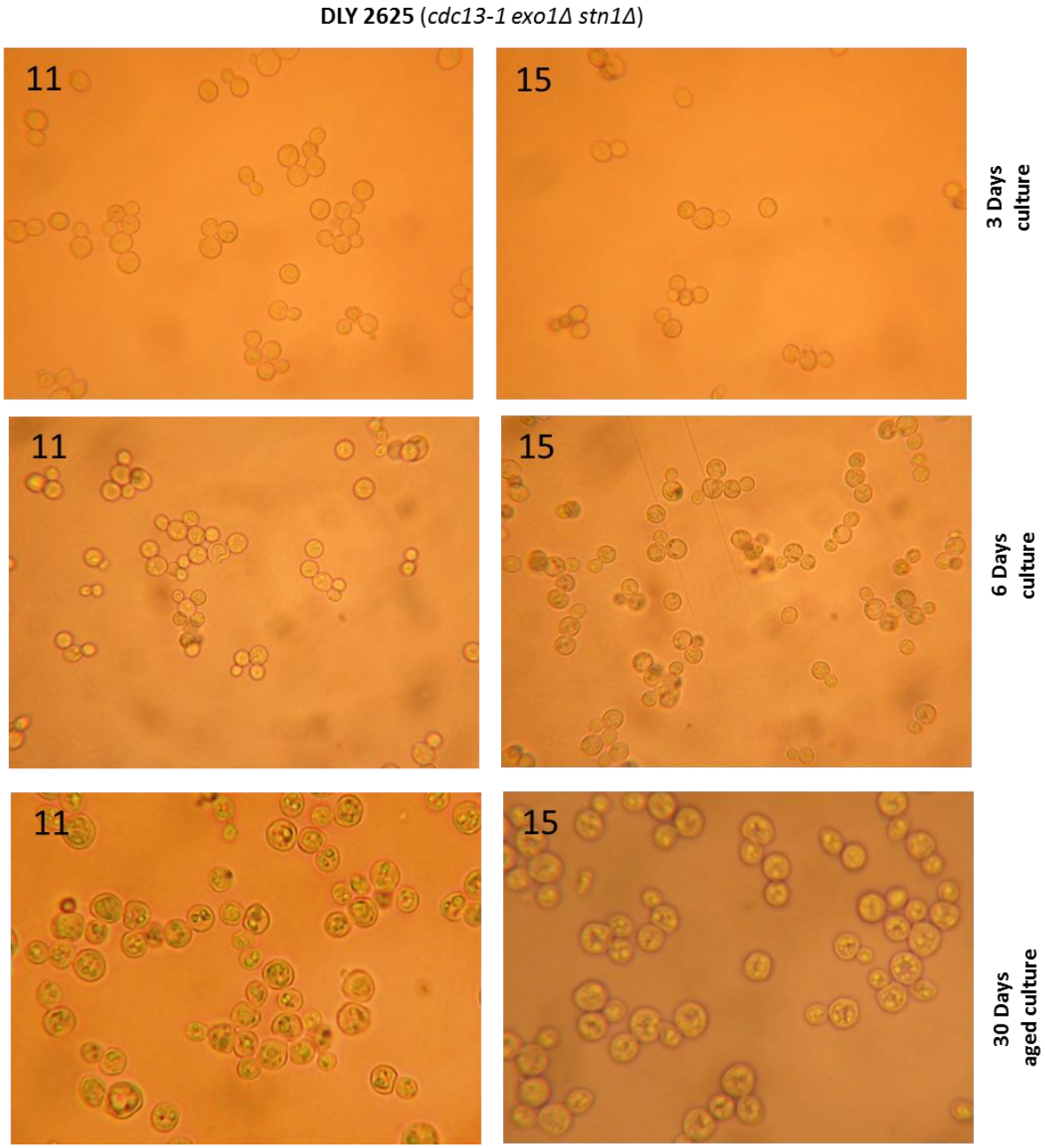

Figure 6.11. Microscopy of ageing culture of the strain DLY 2625.

Digital images of 3, 6 and 30 days cultures of strains 2625 (*exo1Δ stn1Δ cdc13-1* mutant) as manifested by the representative replicas (#11 and #15). Many budded cells were observed in three days' culture as compared to few cells with small buds in 6 day culture. In 30 days aged culture, most of the cells were un-budded, with scarce buds and large vacuoles. Cultures were grown in SC medium supplemented for their auxotrophies at 30°C in a shaking incubator for 30 days. The pictures were taken with a Zeiss KF microscope at a magnification of 400x fitted with a Nikon Coolpix 4500 camera (4 Megapixels 4x optical zoom).

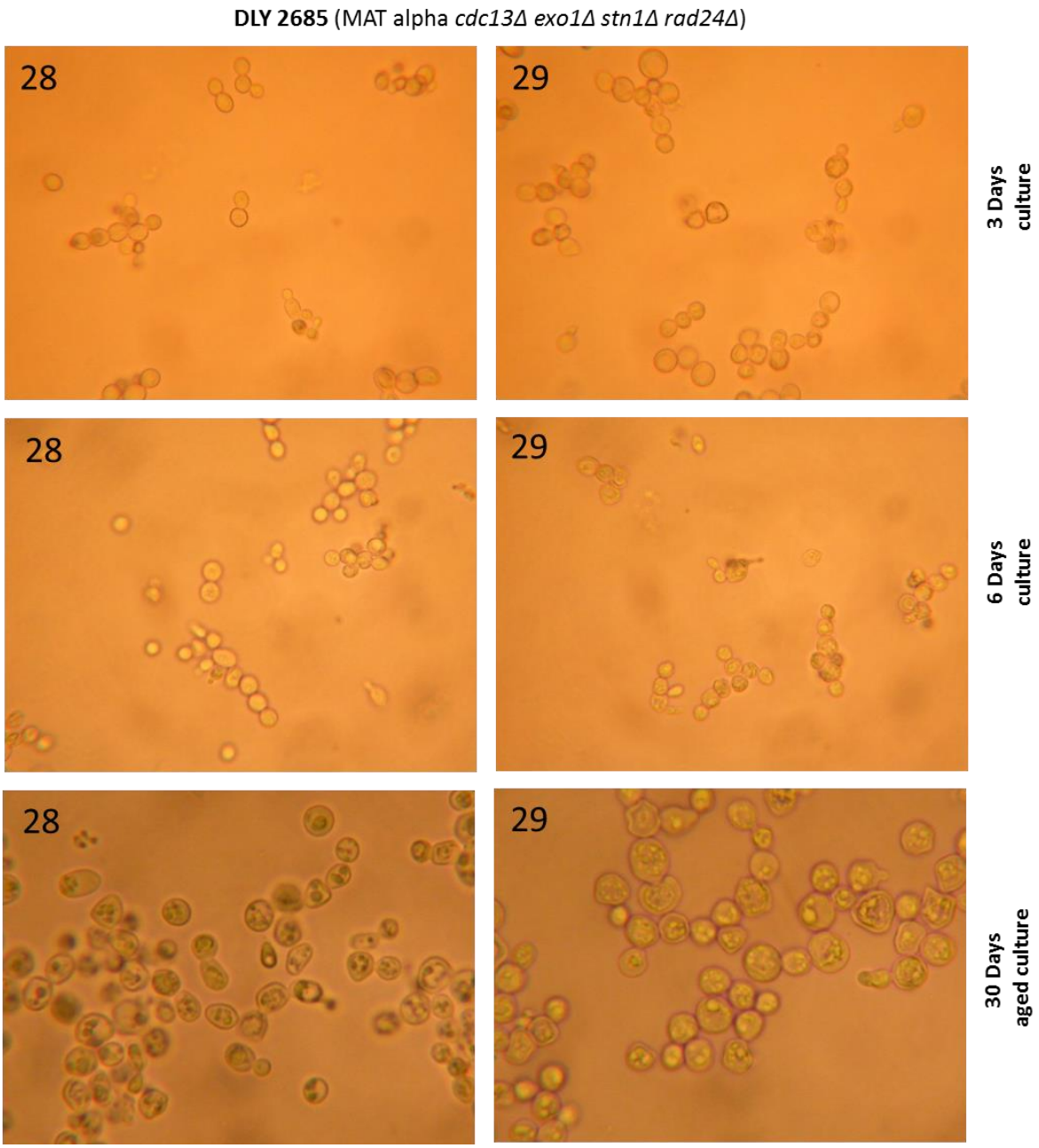

Figure 6.12. Microscopy of ageing culture of the strain DLY 2685.

Digital images of 3, 6 and 30 days cultures of strain 2685 (*exo1Δ stn1Δ cdc13Δ rad24Δ* mutant) as manifested by the representative replicas (#28 and #29). Many budded cells were observed in three days' culture as compared to few cells with small buds in 6 day culture. In 30 day aged culture most of the cells were un-budded, with scarce buds and large vacuoles. Cultures were grown in SC medium supplemented for their auxotrophies at 30°C in a shaking incubator for 30 days. The pictures were taken with a Zeiss KF microscope at a magnification of 400x fitted with a Nikon Coolpix 4500 camera (4 Megapixels 4x optical zoom).

Figure 6.13 shows genotypic markers testing by replica plating at the start (A) and at the end (B) of ageing study, to ensure the maintenance of the genotype throughout the experiment.

Strains 1272 and 1273 (*exo1*Δ) showed growth on YEPD and dropout media in the absence of leucine [replicas 1 and 3 (A) and 1 and 4 (B)] indicating the presence of the *LEU2* marker gene for *de novo* synthesis of l-leucine amino acid while strains 2607 (*exo1*Δ *cdc13*Δ) and 2625 (*cdc13-1 exo1*Δ *stn1*Δ) were auxotrophic to nutrition markers tryptophan and uracil (replica 4 and 5 (A) 5 and 6 (B) and can grow in media that do not contain histidine and leucine. Strain 2685 (*cdc13*Δ *exo1*Δ *stn1*Δ *rad24*Δ TR) did not manifest growth in the absence of uracil, replica 5 (A) and 6 (B) but grew on the media deficient in histidine or leucine or tryptophan showing the presence of marker genes *HIS3*, *LEU2* and *TRP1*. None of the strains showed any growth in the absence of uracil while strain 640 (wild type) could grow only in the presence of all marker-related components in YEPD medium YEPD only. Master plate and its replicas 1 and 2 on YEPD medium (B) also represents the comparative growth of all individual cultures from a particular strain (1-6) at the end of the CLS experiment; e.g., strain 1272, colony 1 did not show any growth, while all replicas of strain 2625 showed less growth on YEPD.

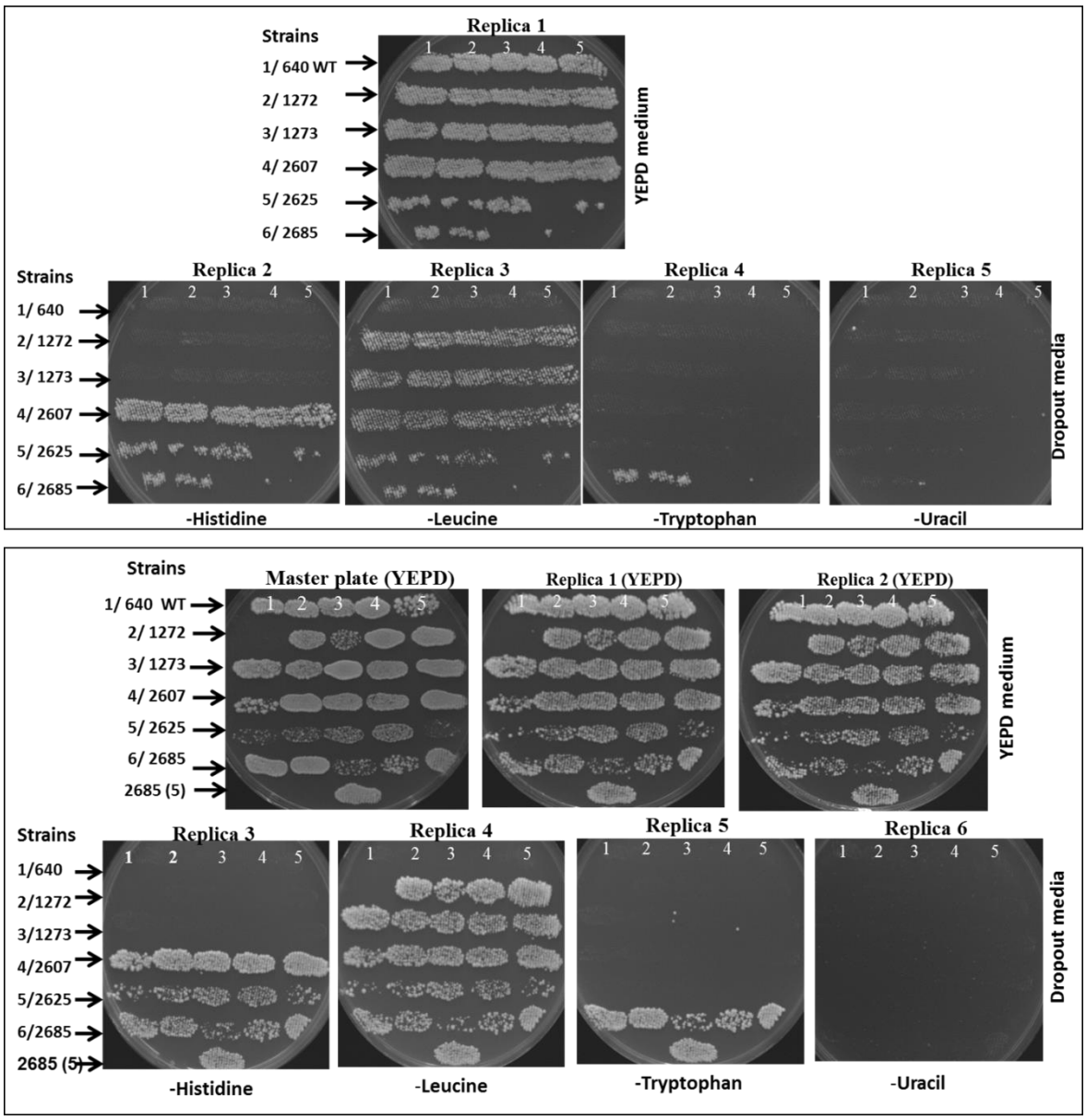

Figure 6.13. Replica plating on YEPD and dropout media for confirmation of appropriate metabolic markers of experimental strains with their auxotrophies.

Master plates (YEPD medium) were streaked with cultures/suspension from individual colonies (1-5) at the start and end of the CLS experiment from all strains and were incubated to get light growth which was replica plated on YEPD and dropout media. Replica plates were incubated at 23°C for 5 days before being photographed. Numbers 1-5 represent the culture number from five independent colonies for each strain.

(**A**) Replica plating at the start of CLS studies.
(**B**) Replica plating at the end of CLS studies.

Towards the end of experiment, mutant strains took longer for colonies to appear (4-5 days incubation at 30°C). The sizes of the colonies were observed as comparatively larger at the start of experiment (Figure 6.14A) as compared to small colony size with number of minute colonies observed in aged cultures at the end of CLS (Figure 6.14B), as a result of a progressive decrease

in the rate of cell division during senescence (Enomoto *et al.*, 2002). The mutant strains 2625 and 2685 manifested colonies with wavy margins as compared to smooth margins on colonies of strains 640 (wild type) or 1272 or 1273 (*EXO1* deletion) mutants. The sizes of colonies in mutant strains DLY 2607, 2625 and 2685 were relatively small as compared to DLY 640 (wild type), 1272 and 1273 (*EXO1* deletion mutant) strains.

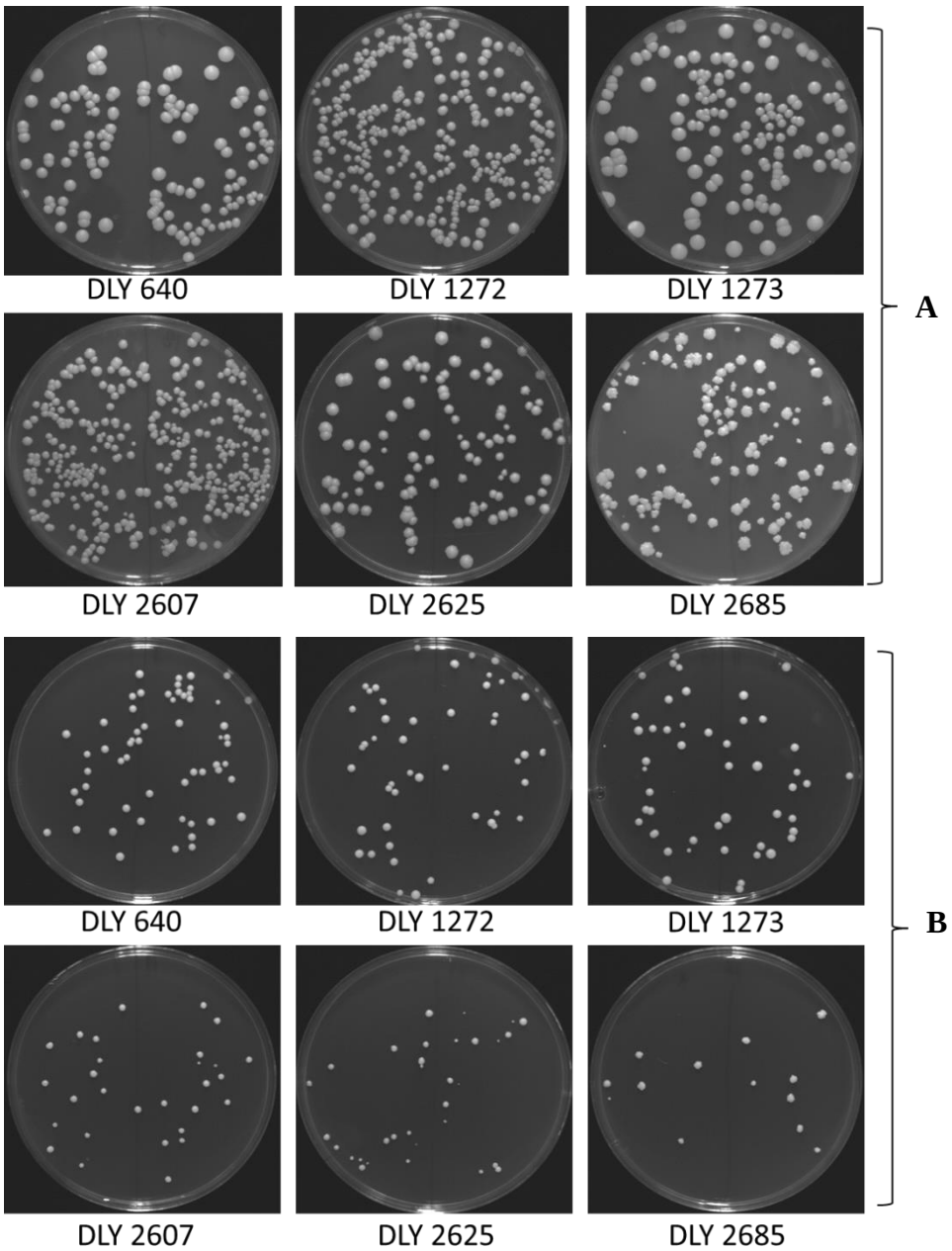

Figure 6.14. Digital images of colonies on YEPD plates from the representative cultures as exhibited at the start and end of CLS studies.

The samples were pooled from the ageing cultures (30 in total), serially diluted to get ~1000 cells/ml density and 50 µl from each sample was plated on YEPD medium in duplicates. The plates were incubated at 30° C for 3 days with 2 additional days for strains 2607, 2625 and 2685 (due to their slow growth rate) towards the end of experiment, before being photographed. Colonies were counted manually. Averages of each count were used to calculate the total viable count in 50 µl or 1 ml of culture. Scale bar equal to 20 mm.

(**A**) Plates showing colonies at day 6 of CLS experiment.

(**B**) Plates showing colonies (aged cells) at day 30 of CLS experiment.

The viable cell counts were estimated from plating 50 µl at specific dilutions at different time points for 30 days and colony count data was tabulated for further analysis. Average viable counts/50 µl from five replicas were taken into account to calculate the total viable cell number in 1 ml by multiplying it by the dilution factor.

In wild type (strain 640), *EXO1* deletion mutants (strains 1272 and 1273) and *CDC13* and/or *STN1* deletion mutants individual replicas showed similar trends, of viability (at day 3), rate of growth and ageing patterns (Figure 6.15A-F). In strain 640, viable counts reached their maximum values on day 9 after culture dilution (Figure 6.15A). Similarly, in *EXO1* deletion mutants (strains 1272 and 1273), 60% of cultures (6 out of 10 replicas) showed their maximum value on day 9 (Figure 6.15B and C). However, replica number 6 (strain 1272) showed a maximum viable count on day 3 and aged earlier than all replicas, with 0 survival value on day 12 (outlier; Figure 6.15B). The strains 2607 and 2685 also manifested the similar trends of viability and ageing among individual replicas (Figure 6.15D and F). The strain 2625 however showed some fluctuations at different time points (Figure 6.15E).

The total numbers of viable cells in 1 ml and the average values of these for each strain from five individual replicas were calculated for each time period. Despite keeping the same initial cell number ($1x10^6$, by measuring at OD_{660}) in all cultures, the total number of viable cells in 1 millilitre volume showed variable cell numbers in different mutant strains at day 3 of CLS studies. For example the strain 2625 (*STN1* deletion) on day 3 showed the least viable cells per ml, 2.5 times less as compared to combined mutant 2685 and 4 times less as compared to 2607 (*CDC13* deletion) that could be due to either the highest mortality or slow rate of growth. Cell number variations among strains 1272 and 1273 (p= 0.67 and 0.91 respectively, p>0.05) were statistically non-significant when compared with controls (640, WT), whereas strains 2625, 2607, and 2685 (p= 0.0013, 0.048 and 0.008 respectively, p< 0.05) represented decreased cell numbers, statistically significant as compared to the wild type. However, the low initial viable cell number at day 3 in strains 2625 and 2685 did not grow further over longer incubation after day 9, indicating early senescence in these strains.

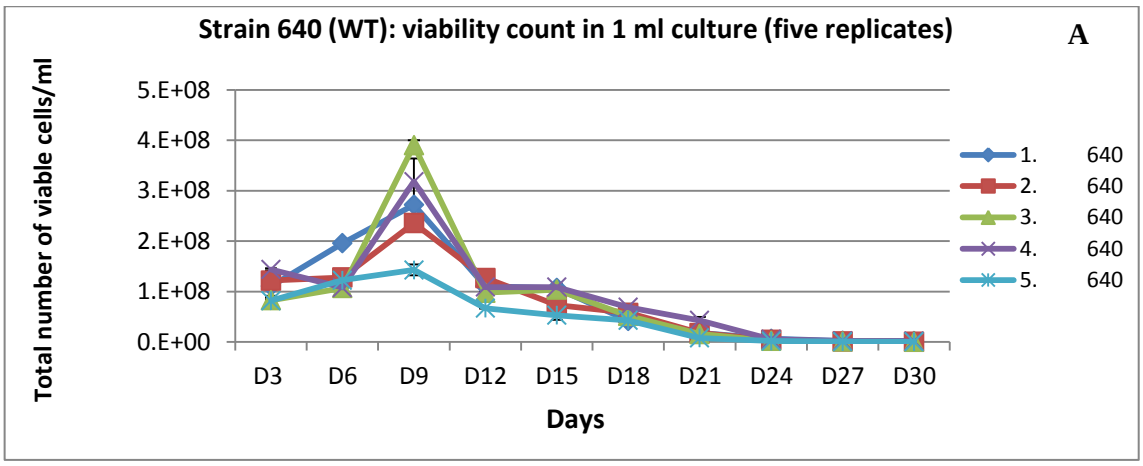
Strain 640 (WT): viability count in 1 ml culture (five replicates)
A
Total number of viable cells/ml
5.E+08
4.E+08
3.E+08
2.E+08
1.E+08
0.E+00
D3
D6
D9
D12
D15
D18
D21
D24
D27
D30
Days
1. 640
2. 640
3. 640
4. 640
5. 640

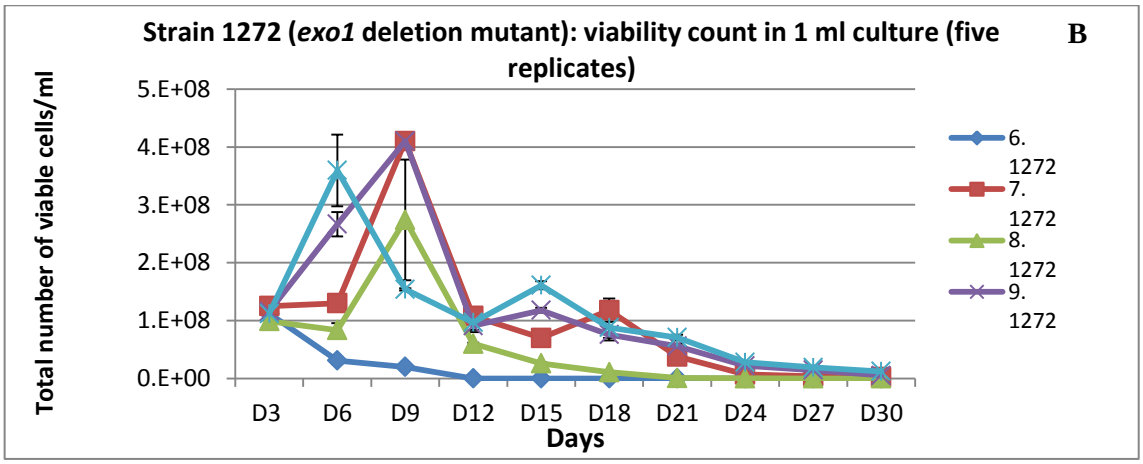
Strain 1272 (exo1 deletion mutant): viability count in 1 ml culture (five replicates)
B
Total number of viable cells/ml
5.E+08
4.E+08
3.E+08
2.E+08
1.E+08
0.E+00
D3
D6
D9
D12
D15
D18
D21
D24
D27
D30
Days
6. 1272
7. 1272
8. 1272
9. 1272

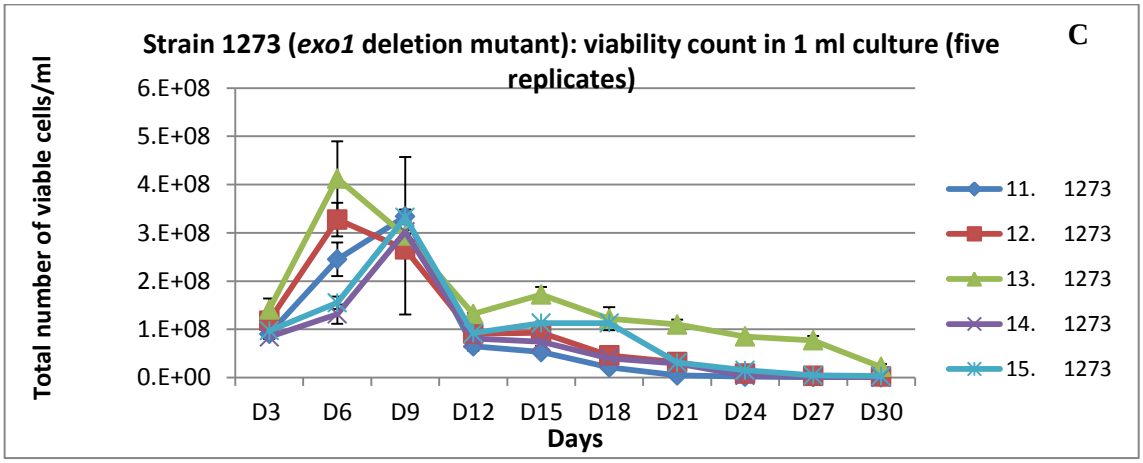
Strain 1273 (exo1 deletion mutant): viability count in 1 ml culture (five replicates)
C
Total number of viable cells/ml
6.E+08
5.E+08
4.E+08
3.E+08
2.E+08
1.E+08
0.E+00
D3
D6
D9
D12
D15
D18
D21
D24
D27
D30
Days
11. 1273
12. 1273
13. 1273
14. 1273
15. 1273

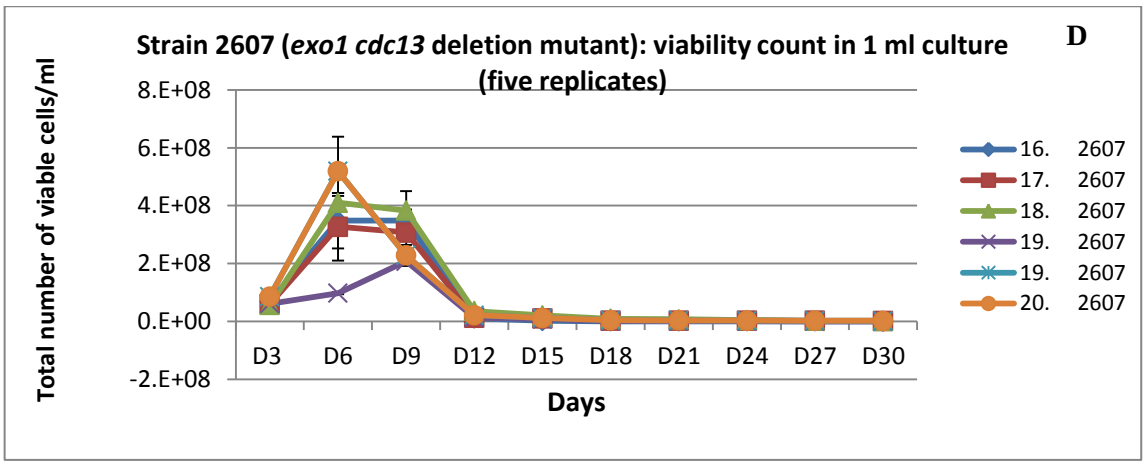

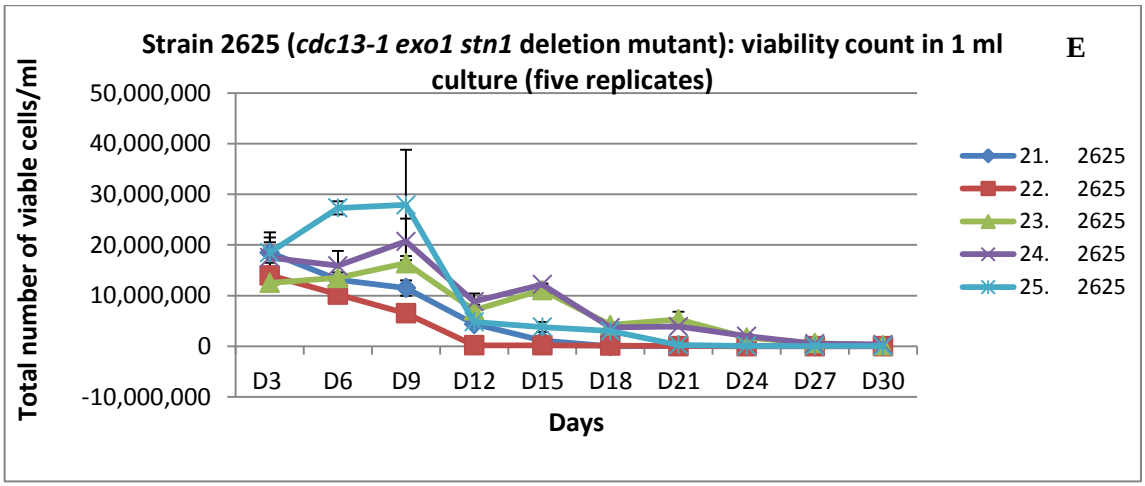

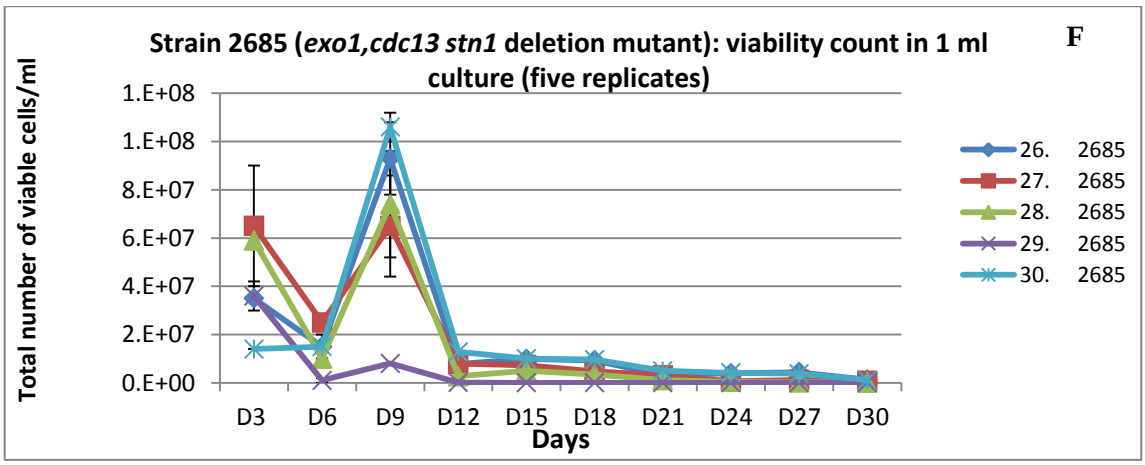

Figure 6.15. The trends of viable cells' decline estimated in 1 ml (five individual replicates) of wild type and mutant strains over a period of 30 days.

Each graph shows total number of viable cells in 1 ml from 5 replicas of the strain, WT or a mutant. The absolute values for cell numbers are presented.

(**A**) DLY 640, (**B**) DLY 1272, (**C**) DLY 1273, (**D**) DLY 2607, (**E**) DLY 2625, (**F**) DLY 2685.

The average viable cell number in 1 ml versus sample pooling days manifested day 9 with maximum value (saturation state) for most of the cultures. After day 9, there was very sharp decline in viable (total) cell number in all cultures. On day 12 of the ageing experiment, mutant strains lacking Cdc13 or Stn1 showed increased loss in viable counts at a much faster rate as compared to viable cells in the wild type and Exo1 mutants. These patterns of growth continued with further loss of viability in a total number of cells until the last day counts of the experiment, day 30 (Figure 6.16).

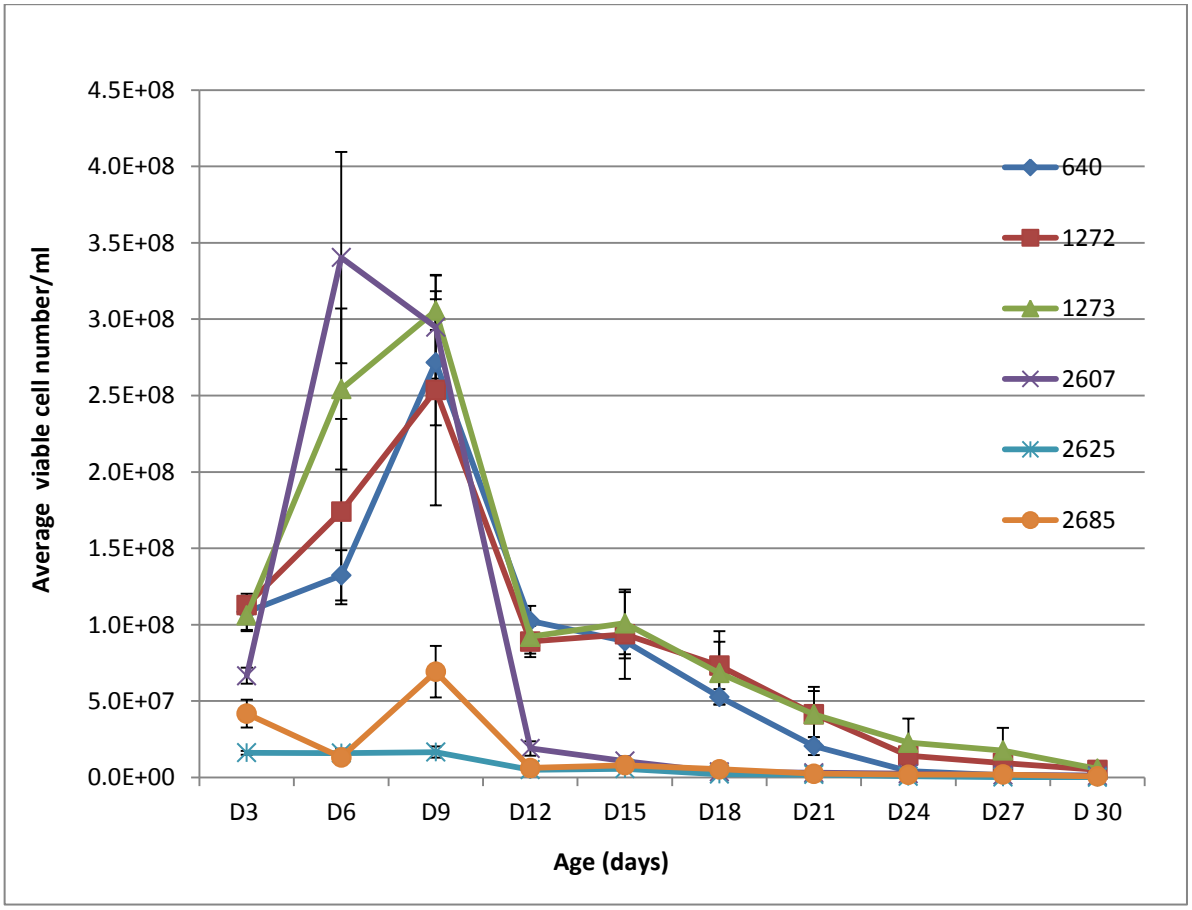

Figure 6.16. The gradual loss of viable cells in different strains over a period of 30 days.

Cells were kept in SC media during a period of CLS studies. The viable cell counts (CFUs) were estimated in 50 µl of the ageing culture for 30 days. Total viable cell number in 1 ml was calculated from average viable counts/50 µl by multiplying it by the dilution factor. The wild type strain (640), and *EXO1* deletion mutants 1272 and 1273 (p= 0.821 and 0.91616 respectively, p values >0.05) and strain 2607 (*CDC13* deletion; p= 0.5689) showed no significant difference in viable count at day 9, whereas strains 2625 (*STN1* and *EXO1* deletion) and 2685 (*CDC13*, *STN1* and *EXO1* deletions; p= 0.0038, 0.0172 respectively; p<0.05) exhibited statistically significant decrease in cell numbers as compared to the wild type. Results are expressed as mean ± SEM (n=5).

Most of the cultures exhibited a maximum value (of colony count) on day 9 after dilution (20 cultures out of 30; 67%), a few (6 out of 30 samples; 20%) showed 100% values on day 6 of CLS experiments and 13% replicas (4 samples out of 30) reached to maximum value on day 3 after dilution. For simplicity, the percentage of viable cell numbers was calculated from average viable counts in 50 µl and considering day 9 viable counts as 100%.

The percent survival of individual replicas of each strain versus chronological age considering 100% survival as day 0 (0 age point) revealed that different mutants without essential capping proteins aged more progressively than wild type. Wild type strain (640) aged slowly showing a typical survival curve "descending staircase" shape of chronological survival. The overall pattern for 5 replicates of strain 640 was more consistent as compared to other mutants. Strains 1272 and 1273 with the *EXO1* deletion also aged at a slow rate showing more cell fluctuations among individual replicates and slightly longer survival. In a single deletion mutant (*cdc13Δ*) most of the cells died at age point 3, three days after their maximum value, showing a sharp loss in cell survival. Similarly, strain 2685 without *CDC13* and *STN1* genes also exhibited a sharp decline in viability at age point 3, with few fluctuations that could be due to survivors that can grow at higher temperature as cells appeared on plates after 5 days incubation, rather than 2-3 days.

Figure 6.17 shows the comparison of survival between different mutants during their chronological lifespan. Age points in CLS experiments were assigned with reference to day 9 cell viability. For example, age point 0 represents the day when strains have the highest cell numbers (100%). The presence of *EXO1* deletion in strains 1272 and 1273 did not have any pronounced effect on ageing as compared to the wild type. Wild type strain 640 exhibited ~38% viable cell number on age point 3, with approximately 60% viability loss whereas *EXO1* deletion in strains 1272 and 1273 showed 35% and 30% viability respectively within 3 days after saturation. Comparatively, there was a sharp reduction in viability in strain 2607 at age point 3 (with viable value 6.45, the lowest survival in all strains). Again, at age point 6, strain 2607 was the fastest ageing strain with survival value ~ 4% and strain 2685 with 12% viable cells became the second most rapidly ageing strain. In strain 2625, without Stn1 protein, 34% of cells were still viable at this stage. The pattern of survival difference exhibited between these three strains at age point 3 was maintained throughout the rest of the chronological life-span experiment until age point 21 where most of the cells were dead (Figure 6.17).

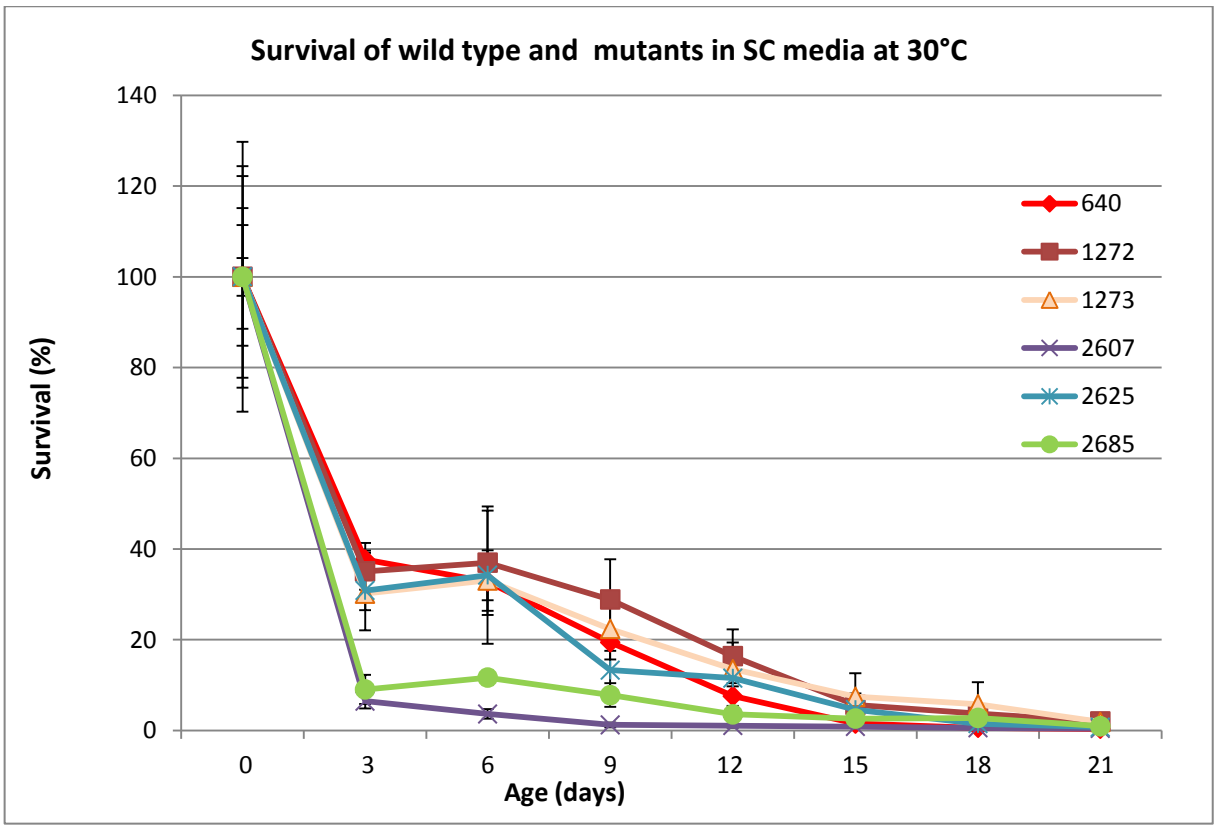

Figure 6.17. Survival (%) of all strains displaying gradual loss of cell survival during chronological ageing.

Wild type strains did not sustain longer survival in this experiment and showed less survival as compared to *EXO1* deletion mutants (strains 1272 and 1273). However, in a repeated experiments (Figure 6.18), the wild type strain displayed longer survival with slightly different ageing patterns among *STN1* (strain 2625) and *CDC13* (strain 2607) deletion mutants. At age point 6, the fastest ageing strain was 2685 with combined deletions of *STN1* and *CDC13*; strain 2607 (*CDC13* deletion) showed better survival as compared to strain 2625 (with *STN1* deletion in the presence of Cdc13-1 mutation).

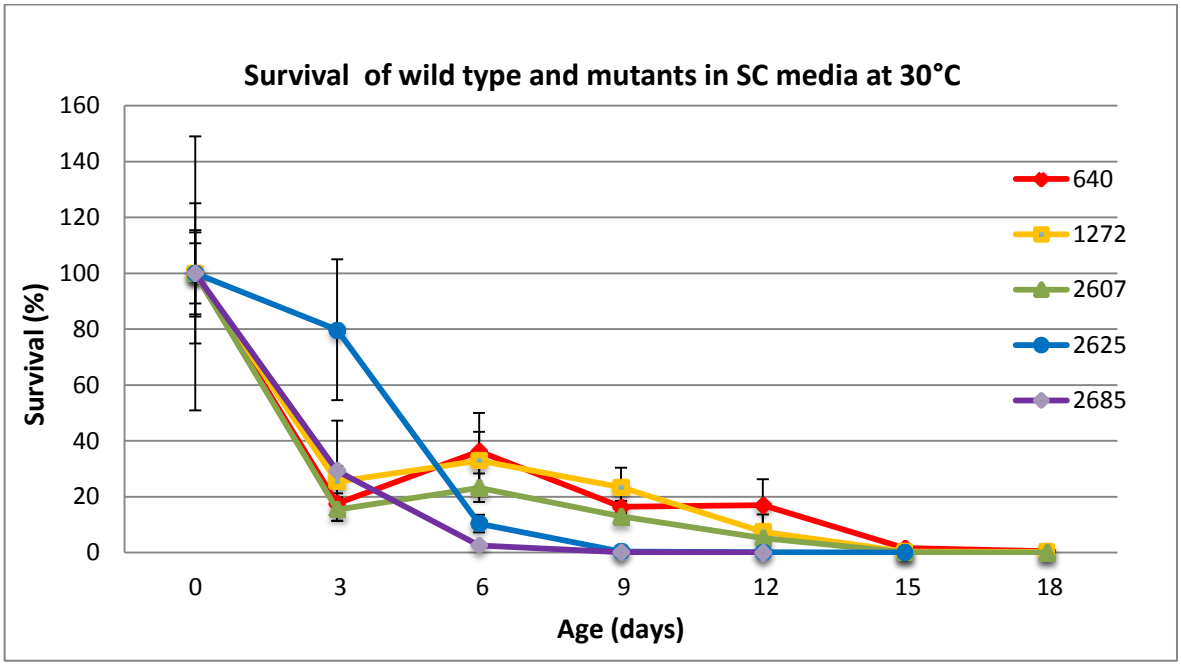

Figure 6.18. Average survival of *cdc13* and *stn1* mutants compared with the wild type strain.

It can be concluded that despite some fluctuations, mutant strains showed a reduction of viability in comparison to the wild type. Each mutation has its own effect and different mutations together (strain 2685 with *CDC13*, *STN1*, *EXO1* and *RAD24* deletion mutations) enhanced the effect of other mutations additively. Strain 2685, without of Cdc13 and Stn1 proteins, exhibited ~ 3% survival at age point 6 as compared to 10% and 23% survival manifested by strains 2625 and 2607 respectively with the removal of Stn1 and Cdc13 respectively (Figure 6.18). Further at age point 9, *STN1* deletion exhibited 2.5 times more viability as compared to the combined deletion, whereas *CDC13* removal exhibited 81 times higher viability as compared to the combined deletion mutant 2685 (0.16% , 0.41% and 13% survival for strains 2685, 2625 and 2607 respectively), while 16% of the wild type cells were still viable. These results showed that deletion mutants without essential capping proteins display reduced survival ability, however, there were few fluctuation of survival curve possibly due to generation of survivors at higher temperatures.

6.3.5. Carrying out CLS experiments in water

To reduce fluctuations in the survival curve observed at certain time points during CLS study in SC medium, further assays were performed to carrying out CLS experiments in water under calorie restriction. The first experiment was performed with wild type strain 640 (Protocol S2.2). The culture was cultivated for o/n (~18 hours) in YEPD broth at 30°C from a freshly grown (mixture of 4-5) colonies. After washing the cells, 3 aliquots of 15% glycerol stock were prepared and kept at -80°C for further dilution in SD medium. Three independent cultures of strain 640 were inoculated with 15% glycerol stock of cells at 1:20 in 10 ml of SD medium in a way that all cultures were ready to start CLS measurements on the same day. They were set up so that they had been grown for 9 days (9-D), 6 days (6-D) and 3 days (3-D) in duplicates, referred as 1 and 2 by the start of these experiments. The saturated cultures of 3-D, 6-D and 9-D grown cells were washed and transferred to sterile water to keep the cells in the stationary phase under calorie restrictions. The cells were equalised in all 6 samples by measuring the OD at 660 nm as shown in Table 6.4.

Table 6.4. Estimation of the number of cells in 3, 6 and 9 day cultures from strain 640 (WT) by measuring the OD_{660}.

Serial No	Strain 640 (grown for 3, 6 and 9 days)	OD_{660}	Cell number (estimated/ml)
1	3-D (1)*[1]	1.018	$1.926x10^7$
2	3-D (2)*[2]	1.037	$2x10^7$
3	6-D (1)	1.021	$1.926x10^7$
4	6-D (2)	1.030	$1.963x10^7$
5	9-D (1)	1.007	$1.890x10^7$
6	9-D (2)	0.968	$1.736x10^7$

*[1] indicates replicate 1

*[2] indicates replicate 2

For ageing study the cells were incubated at 30°C with slow shaking (50 rpm), and CLS was monitored for a period of 52 days (0 to 52) with pooling aliquots at an interval of three days. The viability of the cells was assessed quantitatively at two different dilutions (dilution factor 15625 and 3125), with a low and high number of cells in a 20 µl volume. Two dilutions of cell suspension were plated on YEPD medium to count the viable cells from CFUs. Figure 6.19 shows the colony count after 3 days of incubation at 30°C from high and low dilution at day 19 of CLS measurement.

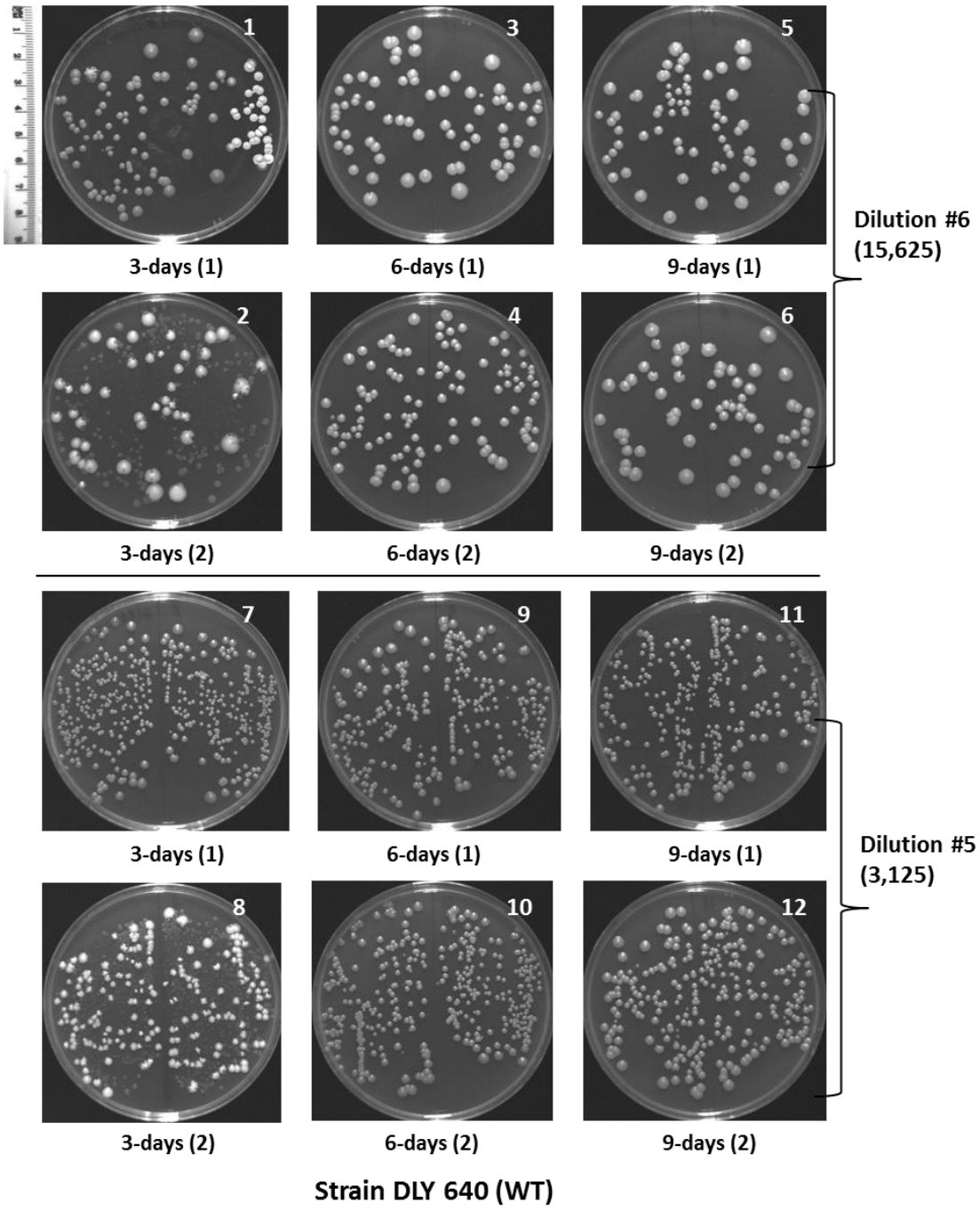

Figure 6.19. An example of plates for colony count at day 19 of CLS studies involving wild type strain 640.

Digital images were taken from colonies on YEPD medium from day 19 of CLS assays. They represent cells from 3-days (plates 1, 2, 7 and 8), 6-days, (plates 3, 4, 9 and 10) and 9-days (5, 6, 11 and 12) cultures with high and low cell number. Colonies were counted from 5-fold diluted cultures from the last two dilutions #5 low (3125), #6 high (15625). Average values of each count were used to calculate the total viable count in 20 µl by multiplying it by the respective dilution factor. Images 2 and 8 showed contamination (small colonies in background) on D 19 of CLS while other cultures have smooth margin circular colonies typical of 640 (wild type). The plates were incubated at 30° C for 2-3 days before being photographed.

For each sample, the average cell count was calculated from two independent preparations. Colony count data was collected for 17 ageing points over a period of 52 days. Considering day 0 values as maximum, the percentages of survival were calculated. The average of survival (%) from low and high numbers of cells and combined average of percent for 3-D, 6-D and 9-D are presented in Figure 6.20.

Results showed a sharp decrease in viability of cells at day 7 of CLS in low (L) and high (H) cell number samples. Both dilutions, showed a gradual decline of viable cell number over the entire period of the CLS, and there were no significant differences in viability on last day (day 52) of the CLS (11%, 12% and 24% with low cell number as compared with 12%, 20% and 16% with high cell number in 3-D, 6-D and 9-D samples respectively). However, the survival curves were more consistent with high cell number (Figure 6.20B) with markedly less fluctuation as compared with low cell number (Figure 6.20A). The 3-D cultures manifested the lowest survival as compared with 9-D samples in both dilutions consistently and also in overall average survival curve (Figure 6.21). The relative pattern of survival remained similar from day 22 to day 52, with a further decrease in viable cell count and increased decline in 3-D as compared to 9-D culture. In contrast, 6-D culture exhibited marked fluctuations at different time points.

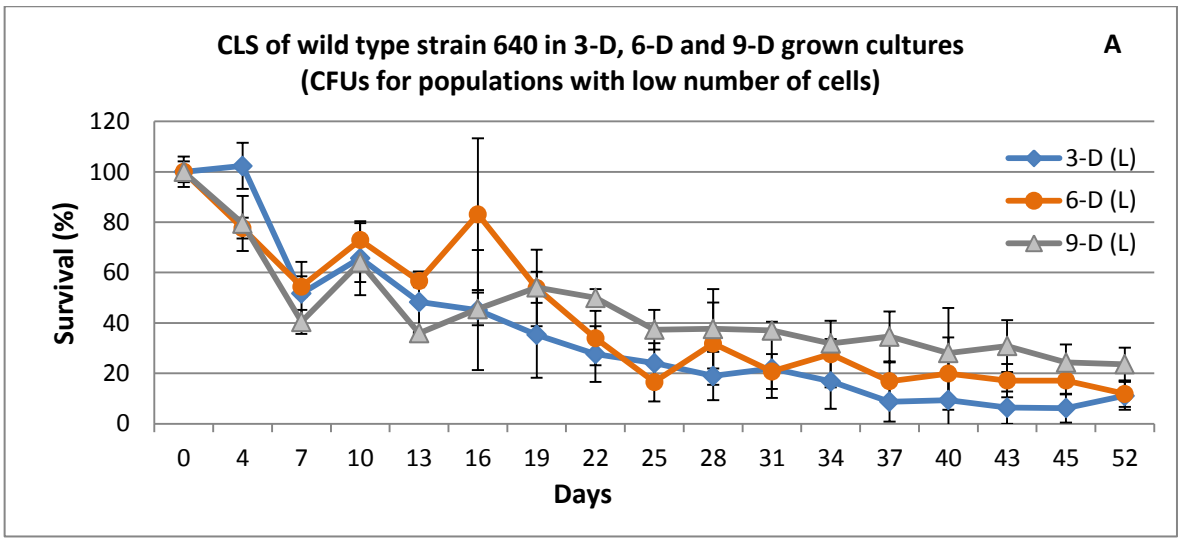

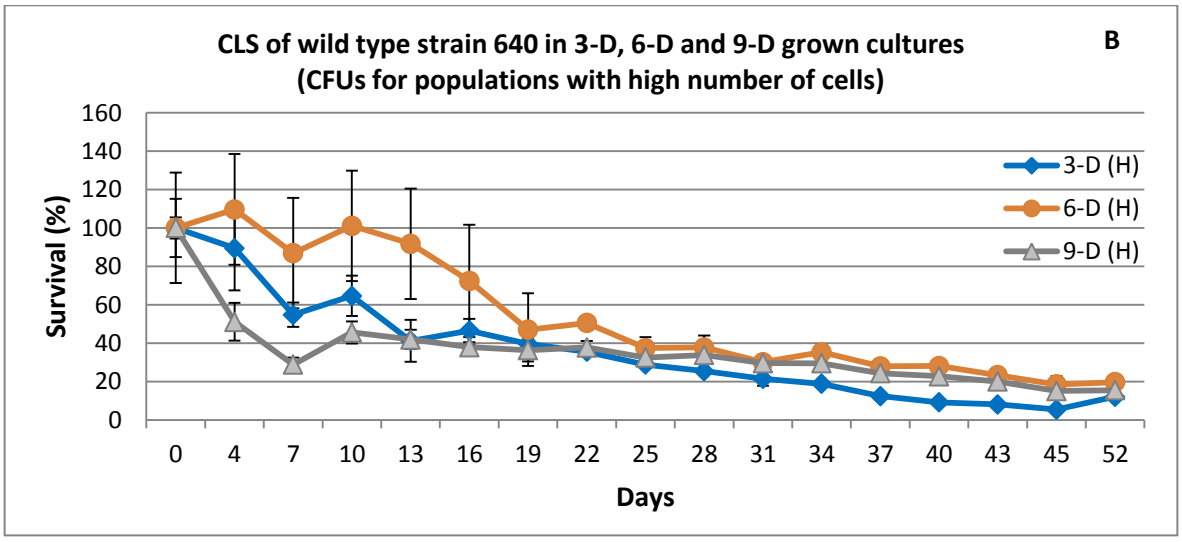

Figure 6.20. Percentage survival of strain 640 (WT) displaying loss of cell survival during chronological ageing in two different dilution at 30°C

The cells were kept in water at 30°C with slow agitation for a period of 52 days. The relative viability is expressed as a percentage of CFUs (maximum of viable cells at day 0 was considered as 100% survival). Results are expressed as mean ± SEM (n=2).

(**A**) Decline of viable cell count at low number of cells (dilution factor 15625) over a period of 52 days.

(**B**) Decline of viable cell count at high number of cells (dilution factor 3125) over a period of 52 days.

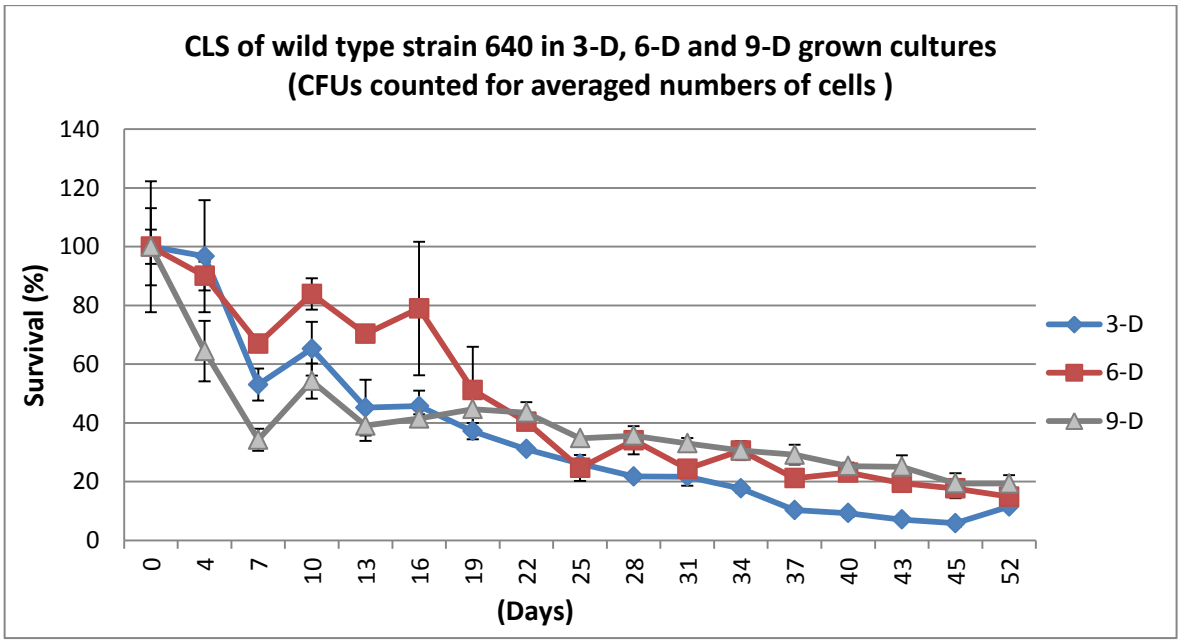

Figure 6.21. Average survival of strain 640 (WT) from low and high CFUs during chronological ageing in water at 30°C.

The cells were kept in water at 30°C with slow agitation for a period of 52 days. The relative viability is expressed as a percentage of CFUs (viable cells (maximum) at day 0 were considered as 100% survival). Percent survival was determined from two populations with low and high cell number. Results are expressed as mean ± SEM (n=4).

6.3.6. Viabilities of yeast mutants after exposure at 40°C and 45°C in water

Further two experiments were conducted with strains 640 (WT), 2607and 2608 (*cdc13Δ*) and 2685 (*cdc13Δ stn1Δ*) exposed at 40°C and 45°C in an attempt to reduce the time required to detect differences in the CLS in water under calorie restriction (low metabolism in stationary phase) following Protocol S2.3. For quantitative measurements of viability, an equal number of cells (based on OD at 660 nm) from G1 phase were exposed to 40°C and 45°C in a shaking water bath over a period of 9 and 7 hours. Samples were pooled after every one hour for analysis and were transferred to ice for half an hour and then to 4°C for 48 hours (G1 phase). After two days, 50 µl of 10-fold serially diluted cells were plated on each half of a YEPD plate. The plates were incubated for 3-5 days at 30°C. The viability was estimated by calculating the CFUs. The average colony count from 0 to 7 hr/9 hr was calculated from the last two dilutions #4 and #5 (10^{-4} and 10^{-5}) for strains 640, 2607 and 2608 and dilution #3 and #4 (10^{-3} and 10^{-4}) for strain 2685.

The relative viability was calculated from the average values from low dilution (with higher number) of cells. The viability of wild type cells (640) dropped to 90% as compared to 49% in strain 2685 (Figure 6.22) for the cells exposed to 40°C during 9 hrs. However, the relative viability in other two mutant strains, 2607 and 2608 showed an increase in viable cell number (163% and 149% respectively) at time point 9 hr with a marked fluctuation at all points of the CLS measurement. On the other hand, the cell exposed to 45°C, strain 2685 exhibited 0% survival as compared to 74% survival in strain 640 (WT) at time point 7 hr (Figure 6.23). The *CDC13* deficient mutants, 2607 and 2608, however, showed 104% and 103% survival at this time point indicating an increase in cell number as compared to the wild type. Based on these results, further experiments were carried out with a traditional standard protocol as recommended by Fabrizio and Longo (2003) under calorie restriction at 4°C to detect viability differences between different mutants lacking essential capping proteins.

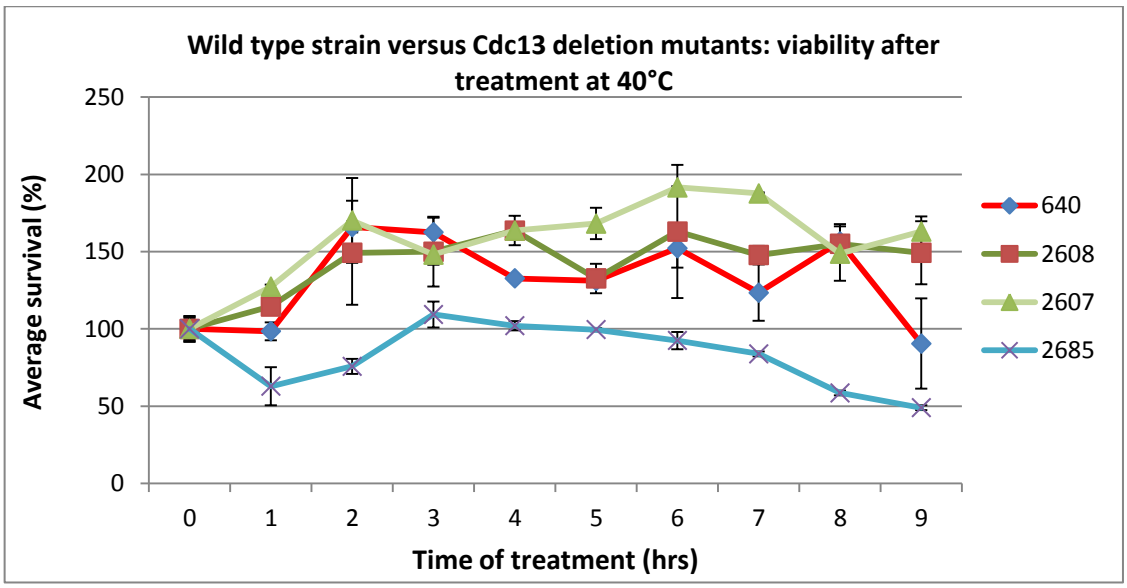

Figure 6.22. Viability dynamics after treatment of cells at 40°C.

The cells were incubated in water bath at 40°C with slow agitation for a period of 9 hours. The relative viability is expressed as a percentage (maximum of viable cells at 0 hr was considered as 100%). Results are expressed as mean ± SEM (n=2).

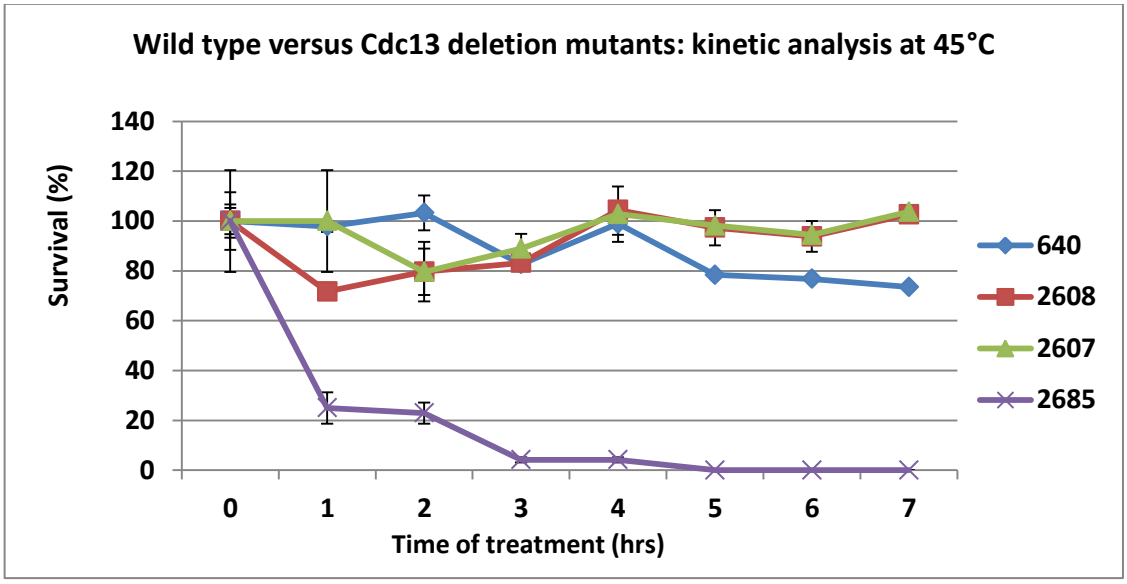

Figure 6.23. Relative viabilities of cells after treatments at 45°C.

The cells were incubated in water bath at 45°C with slow agitation for a period of 7 hours. The relative viability is expressed as a percentage (maximum of viable cells at 0 hr was considered as 100%). Results are expressed as mean ± SEM (n=2).

6.3.7. CLS assay with yeast culture at 4°C in water (stationary phase)

Chronological lifespan of wild type, *cdc13Δ*, *stn1Δ*, and truncated variants of *cdc13-1* mutant strains were studied in the stationary phase under a calorie restriction paradigm (water), as has been reported in previous studies (Fabrizio and Longo, 2003, Smith *et al*., 2007, Santos *et al*., 2012) following Protocol S2.4. Two independent strains were used for each mutation (Table 6.5). The 22 overnight cultures each set with a mixture of few colonies (4-5), were grown at 30°C in YEPD broth which was further diluted in 30 ml of YEPD broth in flasks by keeping an equal cell number as assessed by measuring optical densities at 660 nm. All cultures (1-22) were grown in YEPD medium at 30°C for 6 days until saturation. The cells were washed, equalised by measuring OD at 660 nm and transferred to water at 4°C to measure CLS under calorie restriction in the stationary phase.

Table 6.5. The setup of CLS experiment with mutants lacking *CDC13* and/or *STN1* and truncated variant of *cdc13-1*.

	DLY Strains	**OD_{660}** (at inoculation)	**o/n culture** (volume diluted in 30 ml of YEPD broth)	**YEPD broth**
1	640 (WT)	0.090	500 µl	30 ml
2	641 (WT)	0.107	500 µl	30 ml
3	1272 (*exo1*Δ)	0.092	400 µl	30 ml
4	1273 (*exo1*Δ)	0.086	400 µl	30 ml
5	2607 (*cdc13Δ exo1*Δ)	0.105	500 µl	30 ml
	2608 (*cdc13Δ exo1*Δ)	0.120	500 µl	30 ml
6	1296-TR1 (*cdc13-1 exo1*Δ)	0.092	400 µl	30 ml
7	1296-TR2 (*cdc13-1 exo1*Δ)	0.100	400 µl	30 ml
8	*cdc13-1*-NTΔ-1296 (#4)	0.104	500 µl	30 ml
10	*cdc13-1*-NTΔ-1296 (#5)	0.114	500 µl	30 ml
11	*cdc13-1*-CTΔ-1296 (#9)	0.089	400 µl	30 ml
12	*cdc13-1*-CTΔ-1296 (#10)	0.087	400 µl	30 ml
3	1297-TR1 (*cdc13-1 exo1*Δ)	0.098	400 µl	30 ml
14	1297-TR2 (*cdc13-1 exo1*Δ)	0.100	400 µl	30 ml

15	*cdc13-1*-NTΔ-1297 (#7)	0.110	500 µl	30 ml
16	*cdc13-1*-NTΔ-1297 (#8)	0.113	500 µl	30 ml
17	*cdc13-1*-CTΔ-1297 (#11)	0.094	400 µl	30 ml
18	*cdc13-1*-CTΔ-1297 (#12)	0.093	400 µl	30 ml
19	#14 (haploid with *stn1Δ*)	0.100	1200 µl	30 ml
20	#21 (haploid with *stn1Δ*)	0.167	1200 µl	30 ml
21	2684 (*cdc13Δ stn1Δ exo1*Δ *rad24Δ*)	0.154	600 µl	30 ml
22	2685 (*cdc13Δ stn1Δ exo1*Δ *rad24Δ*)	0.152	2400 µl	30 ml

Strains used in CLS studies and overnight culture used to dilute broth.

6.3.7.1. Morphological characteristics of colonies from different mutants of *CDC13* and *STN1* and N- and C-truncated variants of *cdc13-1*

The *cdc13Δ* and *stn1Δ* cells exhibited irregularly-shaped colonies with wavy margins as compared to circular colonies with smooth margins in the wild type (640, 641) and *EXO1* deletion (1272 or 1273) strains (Figure 6.24). The wavy margined colonies were evident in *stn1Δ*, haploids #14 and #21 and combined deletion mutants strains, 2684 and 2685 - , more so in strain 2685, presumably reflecting genetic instability (Enomoto *et al*., 2002).

The margins of the colonies of *cdc13-1*-NTΔ were also obviously irregular as compared to those in colonies from *cdc13-1*-CTΔ mutants (Figure 6.25). The morphological characteristics of colonies of the mutants used in the CLS studies are shown in Table 6.6.

6.3.7.2. Occurrence of small colonies in *cdc13Δ*, *stn1Δ*, *cdc13-1*-NTΔ and *cdc13-1*-CTΔ mutants

Variable in size colonies were observed in *cdc13Δ* and *stn1Δ* mutants as compared to the wild type (Figure 6.24). The marked differences in colony size were clearly evident in mutants lacking *STN1 ((*#14 and #21) or *STN1* and *CDC13* (strains 2684 and 2685) as compared to wild type (strain 640 and 641) and *EXO1* deficient mutants (strains 1272 and 1273). The occurrence of very small (tiny) colonies as compared to large colonies was apparent in *stn1Δ* (#14 and #21) and *cdc13Δ stn1Δ exo1Δ rad24*Δ (2684 and 2685). However, the size differences were less obvious in *cdc13Δ exo1*Δ (strains 2607 and 2608) mutants.

Similar phenotypical differences were also observed among *cdc13-1* N- and C terminal deletion variants of 1296-TR and 1297-TR. The *cdc13-1*-N-terminal truncated mutants manifested various sizes of colonies (obvious in all 4 NTΔ mutants analysed) as compared to *cdc13-1*-C-

terminal mutants and *cdc13-1* original strains (Figure 6.25). The relative abundance of minute colonies was evident as compared to large size and a few colonies, with enormous size at low cell numbers (10^{-4} dilutions) in *cdc13-1* NTΔ clones of both 1296-TR) and 1297-TR) strains. However, the variations in colony size were not very obvious in C-terminal truncated clones, in which there were slight differences in colony size.

The small colonies upon further sub-culturing also revealed a mixture of tiny and large colonies on solid medium (data not shown) with respect to large and small size cells within minute colonies. The differences in size between individual, small and large colonies were approximately ~3 to 7 fold among *stn1Δ* (#14 and #21) and *cdc13-1* NTΔ mutants, whereas they were ~2-3 fold among *cdc13Δ*, and *cdc13Δ stn1Δ* and *cdc13-1* CTΔ mutants.

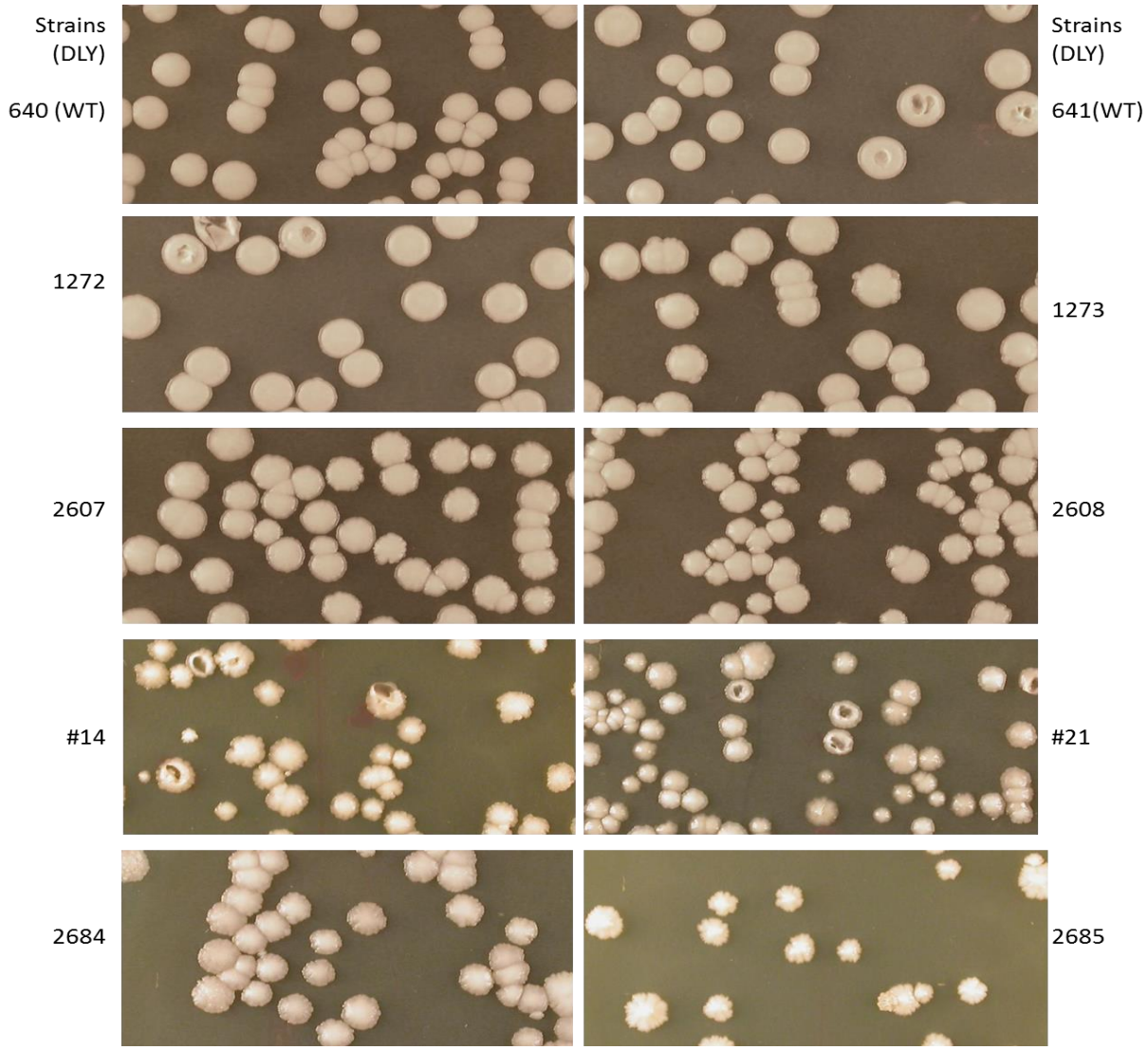

Figure 6.24. Morphological variations of shape and colony size in mutants lacking Cdc13- and Stn1 as compared to wild type and *EXO1* deletion strains.

WT (strains 640 and 641), *exo1Δ* (strains 1272 and 1273), *exo1Δ cdc13Δ* (strains 2607 and 2608), *exo1Δ rad24Δ stn1Δ* (strains #14 and #21) and *exo1Δ rad24Δ cdc13Δ stn1Δ* (strains 2684 and 2685).

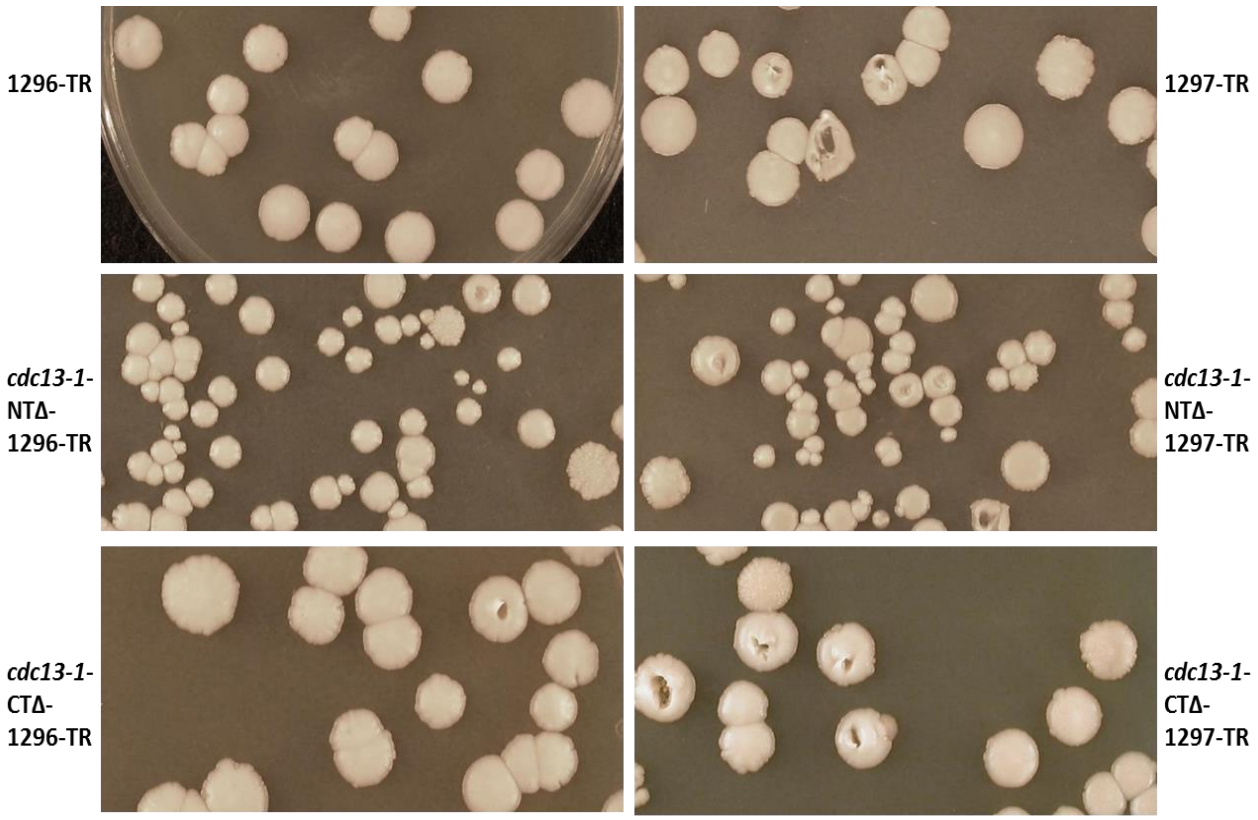

Figure 6.25. Morphological variations of shape and colony size in *cdc13-1* N- and C-terminal deletion variants of 1296-TR and 1297-TR.

cdc13-1 exo1Δ (strains 1296-TR and 1297-TR).

Table 6.6. Morphological characteristics of colonies from *CDC13* and *STN1* deletion mutants, in comparison with wild type.

Strain	**Colour**	**Margin**	**Shape**	**Culture**	**Size** (in 3 day grown colonies at 30°C)
1296-TR 12967-TR	Pale creamy	Smooth edged	Round shape	Almost homogenous, rare small colonies	Bigger size colonies (~3-4 mm)
cdc13-1-NTΔ-1296-TR and *cdc13-1*-NTΔ-1297-TR	Pinkish colour indicating adenine synthesis deficiency	Broken edges or wavy margins	Irregular shape	non-homogenous with big and small colonies	Small (0.5-2 mm), medium (2-2.5 mm) and large (4 mm) size colonies
cdc13-1-CTΔ-1296-TR *cdc13-1*-CTΔ-1297-TR	Mixture of pink and creamy colonies	Round but slightly wavy margin	Round shape, More like *CDC13* deletion mutants	Almost homogenous, with the same size of colonies	bigger (3-4 mm), size slightly smaller than WT colonies, more similar to 1296-TR
Wild type strains (640 and 641)	Pale creamy	Smooth edges	Round	Homogenous, similar size colonies	Bigger in size (4-6 mm)
*exo1*Δ mutants (1272 and 1273)	Same as WT	Smooth edges	Round	Homogenous, similar size colonies	Bigger in size, (4-6 mm)
*cdc13Δ exo1*Δ (2607 and 2608)	Pinkish in colour	Wavy margins	Irregular	Non homogenous, a mixture of big and small colonies	Big size (4-6 mm) and small size (0.5-2 mm)
*stn1Δ exo1*Δ (#14 and #21 haploids)	Pale, mixture of dark and light colour colonies	Wavy margins, slightly less wavy as compared to *stn1Δ cdc13Δ exo1*Δ *rad24*Δ mutants	Irregular	Non homogenous, a mixture of big and small colonies	Mixture of small (0.5-2.5 mm) and large (3-3.5 mm)
*stn1Δ cdc13Δ exo1*Δ *rad24*Δ mutants (2684 and 2685)	Dark pale colonies in strain 2684, turns pinkish with ageing	Wavy margin	Star shape	Non homogenous, a mixture of big and small colonies	Mixture of small and large
	Whitish in strain 2685	Wavy margin/broken edges	Star shape	Non homogenous, a mixture of big and small colonies	Mixture of small, minute and a few large sized; smaller in size as compared to colonies in strain 2684

6.3.7.3. Analysis of genetic markers by replica plating on YEPD and dropout media

All strains (1-22) used in the final part of CLS studies (Table 6.5) were analysed for their genetic markers on YEPD and dropout media to confirm the presence of the appropriate markers and their auxotrphies (Figure 6.26). Four colonies of similar size represented by four streaks (1-4) were selected from ageing cultures and tested for their metabolic markers.
Figure 6.26A shows the result of replica plating of the first 10 samples (1-10) after 5 days of growth at 23°C. The wild type strains 640 and 641 (streaks 1 and 2) did not show any growth on any of the dropout media owing to their auxotrophies for these markers (replicas 2, 3, 4 and 5). Strains 1272 and 1273 (*exo1::LEU2*) confirmed the presence of the *LEU2* gene by growing on dropout media lacking leucine (streaks 3 and 4 in replicas 3). Strains 2607 and 2608 (*exo1::LEU2 cdc13::HIS3*) were auxotrophic for tryptophan and uracil (replicas 4 and 5) and grew on media without histidine and leucine (streaks 5 and 6 in replicas 2 and 3). The strains 1296-TR (*cdc13-1 exo1::LEU2*) exhibited auxotrophies for histidine, tryptophan and uracil (streaks 7 and 8, replicas 2, 4 and 5) but grew on media without leucine indicating the presence of the marker gene *LEU2*. The *cdc13-1*-NTΔ-1296-TR clones #4 and #5 (*cdc13-1* NTΔ::*TRP1 exo1::LEU2*) were auxotrophic for histidine and uracil and grew on media lacking tryptophan (due to integration of tryptophan marker by substituting N-terminus of *cdc13-1*) and leucine (streaks 9 and 10, replicas 3 and 4). None of the strains showed any growth in the absence of uracil (replica 5) while strains 640 and 641 (wild type) grew only in the presence of the four essential marker related components on YEPD medium.

The results for the next 10 samples (streaks 11-20) are shown in Figure 6.26B. Streaks 11, 12, 17 and 18 corresponding to *cdc13-1*-CTΔ clones #9, #10 and #11, #12 of 1296-TR and 1297-TR (*cdc13-1*-CTΔ::*HIS3 exo1::LEU2*) showed growth on dropout media without histidine (replica 2) and leucine (replica 3) confirming the proficiency for leucine synthesis and the integration of the histidine gene. In contrast, *cdc13-1*-NTΔ-1297-TR clones #7 and #8 (*cdc13-1* NTΔ::*TRP1 exo1::LEU2*) were unable to grow in the absence of histidine and uracil but showed growth on media without leucine and tryptophan, confirming the presence of tryptophan and leucine marker genes (streaks 15 and 16, replica 3 and 4). In contrast, strain 1297-TR (*cdc13-1 exo1::LEU2*) did not grow in the absence of histidine, tryptophan and uracil nutrition markers (streaks 13 and 14, replica 2, 4 and 5) but did grow in the medium without leucine (replica 3) confirming the presence of *LEU2* gene. Similarly, *STN1* deletion mutants (*exo1::LEU stn1::HIS rad24::TRP1*) mutants confirmed the presence of all three marker genes in strains #14 and #21 (streaks 19 and 20, replica 2, 3 and 4). All strains were auxotrophic for uracil (replica 5).

Haploid mutants #14 and #21, *stn1*Δ exhibited two types of colonies, dark and light in colour, on YEPD medium. Four dark and light coloured colonies from haploids #14 (streaks 19ab) and #21 (streaks 20ab) were analysed for markers (Figure 6.26C). All colonies showed growth on dropout media lacking histidine, leucine and tryptophan (streaks 19a to 20b in replicas 2, 3 and 4) confirming their genetic markers. However, one patch - represented by streak number 20a (1) - did not show any growth on dropout medium lacking leucine indicating the conversion of the *LEU* marker (from leu^+ to leu^-). The strain 1273 (*exo1::LEU2*) showed a few, fast-growing colonies (in comparison to the normal sized colonies; Figure 6.27). The marker analysis of these big size colonies (streak 4/1273) revealed the presence of marker genes *URA3* in addition to *LEU2* (indicating the conversion of ura^- to ura^+, replicas 3 and 5) owing to their heavy growth on media without these two ingredients. Strains 2684 and 2685 (*exo1::LEU stn1::HIS cdc13::HIS rad24::TRP1*) grew in the media without histidine, leucine or tryptophan confirming the presence of these marker genes *HIS3, LEU2* and *TRP1*.

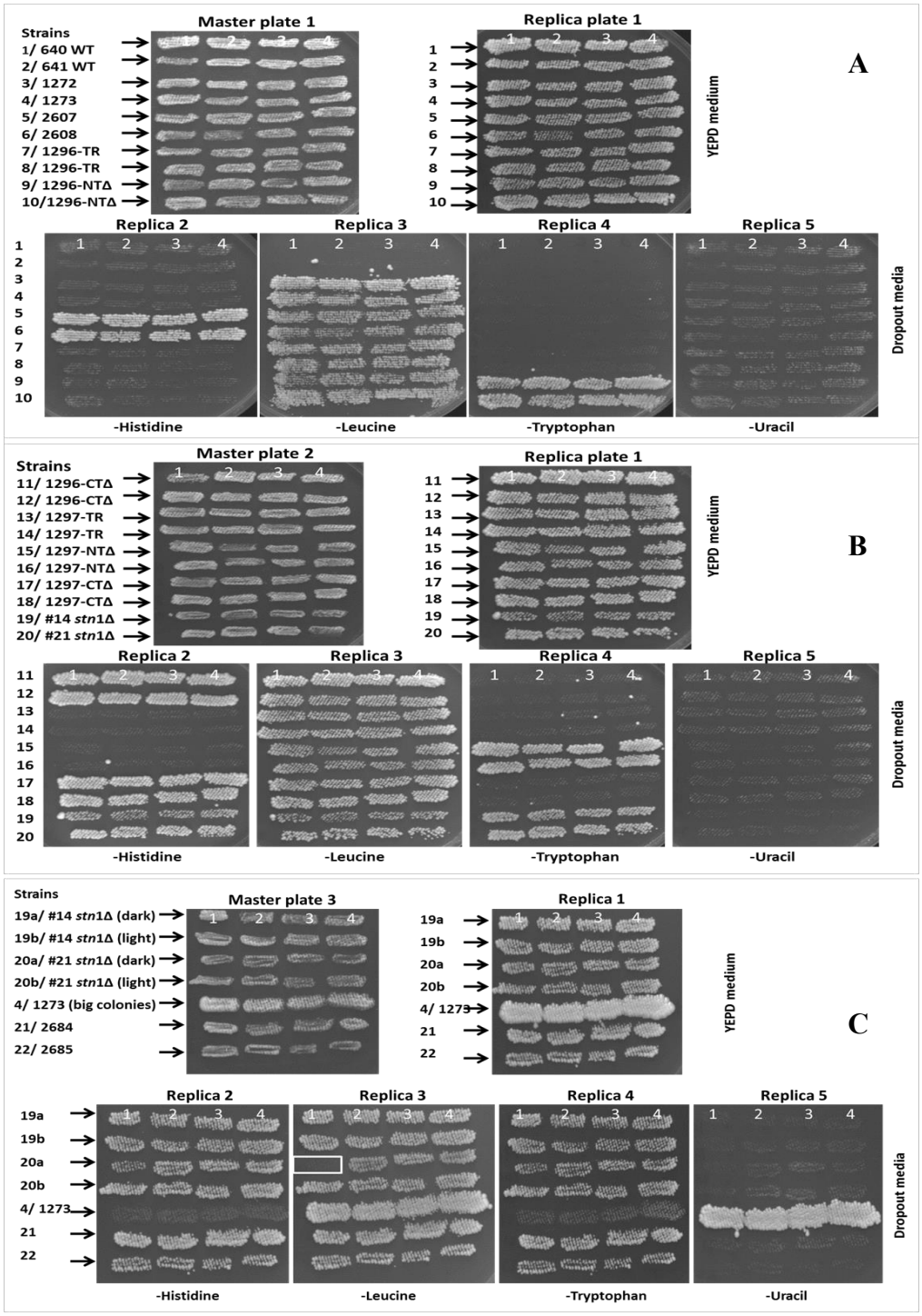

Figure 6.26. Analysis of genetic markers by replica plating on YEPD and dropout media in randomly picked colonies from ageing samples.

(**A**) Replica plating of samples #1-10 (strains 640, 641, 1272, 1273, 2607, 2608, 1296-TR and two clones of *cdc13-1*-NTΔ-1296-TR), each with four colonies (1-4).
(**B**) Replica plating of samples #11-20 (two clones of *cdc13-1*-CTΔ-1296-TR mutants, strains 1297-TR, two clones of *cdc13-1*-NTΔ , two clones of *cdc13-1*-CTΔ, #14 and #21 *stn1* deletion mutants), each with four colonies (1-4).
(**C**) Replica plating of samples #19-22 (*stn1* deletion mutants #14, dark- and light-coloured colonies, #21, dark- and light-coloured colonies; strain 1273, enormous sized colonies; strains 2684 and 2685), each with four colonies (1-4).
Plates were incubated at 23°C for 5 days before being photographed.

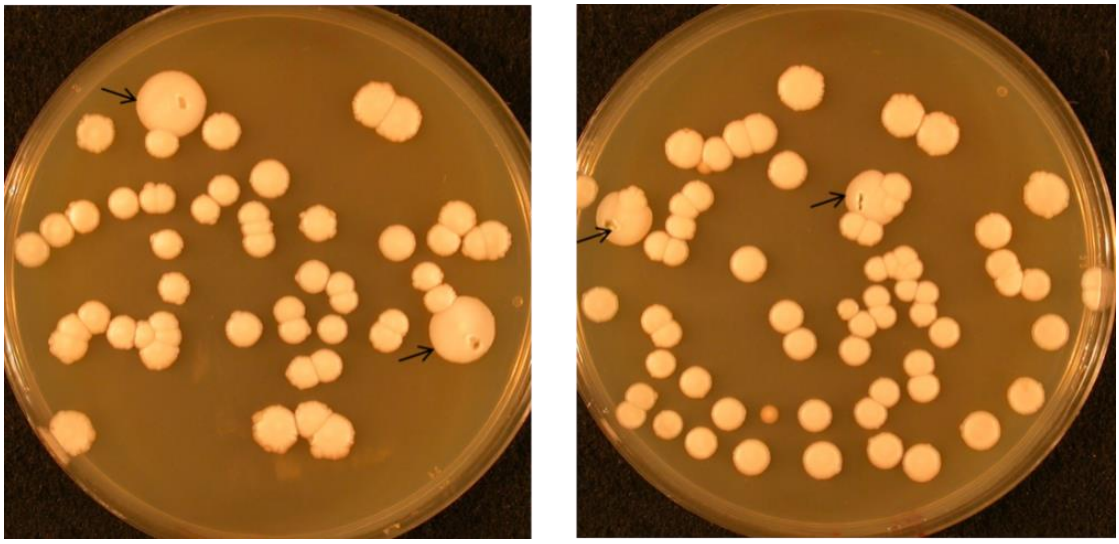

Figure 6.27. Strain DLY 1273 (*exo1*::LEU2) *EXO1* deletion mutant with fast growing Ura$^+$ revertants. The culture of *EXO1* deletion mutant shows a few enormous size colonies. Marker analysis revealed the phenotypes of these colonies as leu+ ura+ not leu+ ura$^-$ as anticipated, indicating the instability of the uracil marker.

6.3.7.4. PCR confirmation of *CDC13* through detection of *cdc13-1* N-terminus and C-terminus fragments

Gel electrophoresis of PCR products (Figure 6.28A) shows the *CDC13* N-terminal-specific fragment of ~378 bp in wild type strains 640 and 641 (lanes 3 and 4), *EXO1* deletion mutant strains 1272 and 1273 (lanes 5 and 6), *cdc13-1* mutant strain 1296-TR (lanes 9 and 10), *cdc13-1*-CTΔ-1296 clones #9 and #10 (lanes 13 and 14), *cdc13-1* mutant strain 1297-TR (lanes 15 and 16), *cdc13-1*-CTΔ-1297 clones #11 and #12 (lanes 19 and 20), *STN1* deletion mutant (lanes 21 and 22) and two diploids (lanes 25 and 26) from crosses between N- and C-terminus mutants (NTΔ-1296 clone #4 x CTΔ-1297 clone #11 and CTΔ-1296 clone #9 x NTΔ-1297 clone #7) respectively. There was no amplification for strains 2607 and 2608 (*cdc13Δ*, lanes 7 and 8), *cdc13-1*-NTΔ-1296 clones #4 and #5 (lanes 11 and 12), *cdc13-1*-NTΔ-1297 #7 and #8 (lanes 17 and 18) and *CDC13* and *STN1* combined deletions mutants strains 2684, 2685 (lanes 23 and 24).

Similarly, PCR products (Figure 6.28B) showed the *CDC13* C-terminal-specific fragment of ~276 bp in wild type strains 640 and 641 (lanes 3 and 4), *EXO1* deletion mutant strains 1272, 1273 (lanes 5, 6), *cdc13-1* mutant strain 1296-TR (2 lanes, 9 and 10), *cdc13-1*-NTΔ-1296 mutants clone #4 and #5 (11, 12), strain 1297-TR, 2 lanes (15, 16), *cdc13-1*-NTΔ-1297 clone #7 and #8 (17, 18), *STN1* deletion haploids #14 and #21 (21, 22) and two diploids from *cdc13-1* N- and C-truncated mutants (25 and 26). However, no C-terminus specific fragment was observed

in lanes 7 and 8 (strains 2607 and 2608), lanes 13 and 14 (*cdc13-1*-CTΔ-1296 clones #9 and #10), lanes 19 and 20 (*cdc13-1*-CTΔ-1297 clones #11 and #12) and lanes 24 and 25 (strains 2684 and 2685), as expected.

The cells from subculture of a single colony were suspended in sterile water (20 µl), and denatured in boiling water for 10 minutes. The supernatant was separated after centrifugation and used as a template for PCR. The PCR was carried out using N1-N2 and C1 and C2 primers (from the N- and C-terminus of *CDC13* respectively), in independent reactions in 25 µl of reaction volume using 3 µl of denatured suspension. The PCR amplified products, (10 µl from each sample), were analysed on a 1.5% agarose gel.

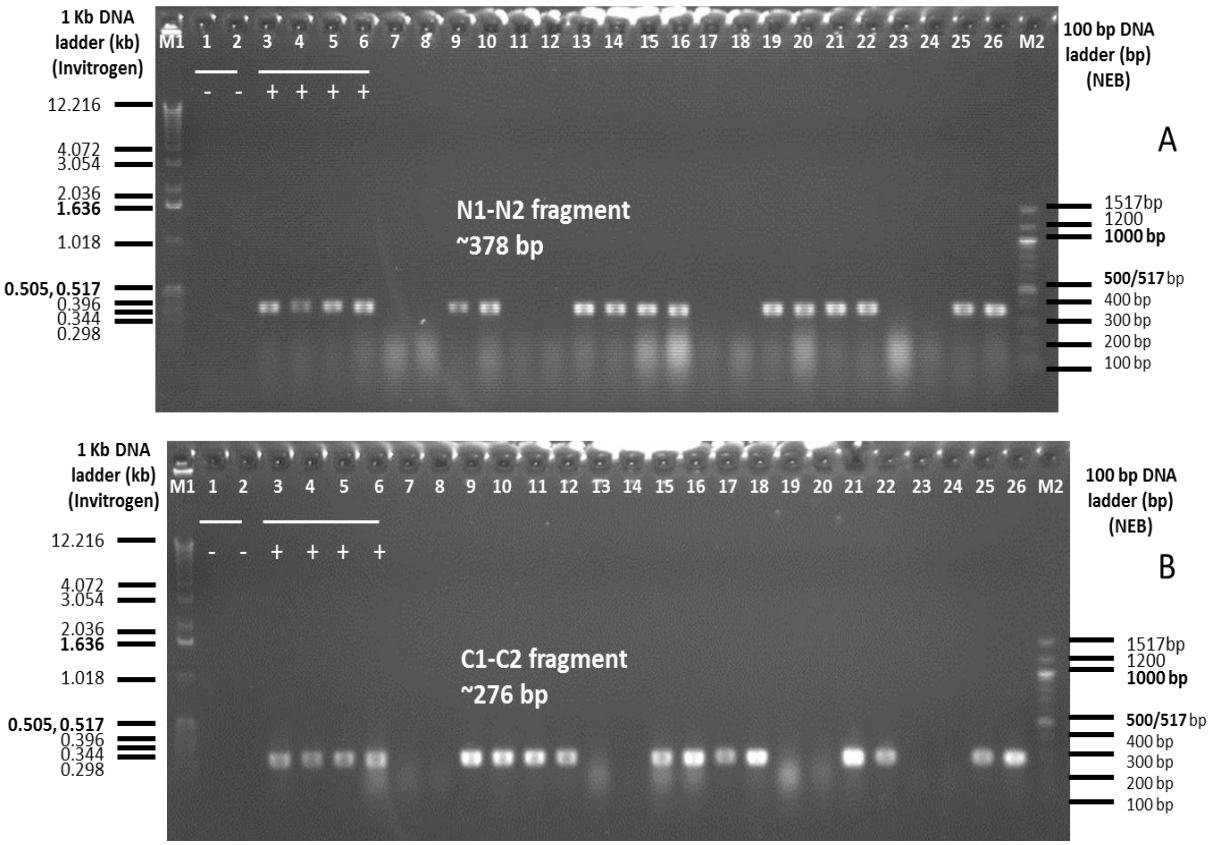

Figure 6.28. PCR detection of *cdc13-1* N- and C-terminals in samples used in the CLS assay: electrophoretic analysis of PCR products from two sets of PCR performed using N- and C-terminal-specific primers (N1-N2 and C1-C2 primers pairs) on agarose gel.

PCR reaction was carried out in a 25 µl volume with 2-3 µl of denatured genomic DNA from cells of sample strains including *CDC13* and *STN1* deletion mutants. From each reaction, 10 µl of PCR product was analysed on a 1.5% agarose gel along with reference markers.

Lanes M1: 1 kb ladder (Invitrogen); **1-2**: NTC, -ve controls; **3-6**: PCR products from cells of strains 640, 641 (WT), 1272 and 1273 (*EXO1* deletion), positive controls; **7-8**: PCR products with strains 2607 and

2608 (*CDC13* deletion mutants), negative controls; **9-14**: PCR products with strain 1296-TR (2 lanes), *cdc13-1*-NTΔ-1296 (clones #4 and #5), *cdc13-1*-CTΔ-1296 (clones #9 and #10), two lanes for each; **15-20**: PCR fragments with strains 1297-TR (2 lanes), *cdc13-1*-NTΔ-1297 (clones #7 and #8), *cdc13-1*-CTΔ-1297 (clones #11 and #12), two lanes for each; **21-22**: PCR fragments with haploid #14 and #21 (*stn1* deletion); **23-24**: PCR products with cells of strain 2684 and 2685 (*cdc13 and stn1* double deletion mutants); **25-26**: PCR products with cells of diploids (from a cross of N- and C-truncated Cdc13-1 mutants); **M2**: 100 bp ladder (NEB).

(**A**) Agarose gel analysis of the PCR fragments (~378 bp) from the PCR carried out using *CDC13* N-terminal-specific primer pair (N1 and N2).

(**B**) Agarose gel analysis of the PCR fragments (~276 bp) from the PCR carried out using *CDC13* C-terminal-specific primer pair (C1 and C2).

6.3.7.5. CLS measurement

For measuring viable count, each sample (1-22) was split into 3 replicates. Each replica was diluted to a density of ~1000 cells/ ml. Two measurements were taken for each replica after every 5 days until day 40, and then after every 10 days until day 90. To measure cellular viability, two aliquots of 50 µl were taken from each sample (4°C) and plated on each half of a YEPD plate, then cultivated at 30°C for 3 days with additional 2 days of incubation towards the end of the CLS measurements. CFUs were counted for individual replicates, and the average values of three replicas were used to calculate the mean value for each strain, which was used to assess the percentage of survival and also to calculate the total cell viability per ml at each age point.

The colony count data from the CLS assay were collected during 90 days and recorded for further analysis. The total number of cells at each age point was calculated by multiplying the average number of cells by correspondent dilution factor. The percentage of survival was calculated to show the decline in the number of viable cells of different mutants over the entire period of the CLS. Results were plotted as line charts representing the percentage of survival and the age over the period of the CLS (Figures 6.29-6.31).

To compare the impact of different deletions on chronological lifespan, two strains were selected for each mutation e.g., 2607 and 2608 for *cdc13Δ* , #14 and #21 for *stn1Δ*, 2684 and 2685 for *cdc13Δ stn1Δ*, along with two wild type controls (640 and 641) and two *exo1*Δ mutants (1272 and 1273). Figure 6.29 presents CLS results for mutants lacking Cdc13 and Stn1essential telomere capping proteins, under calorie restriction. Strain 2685 in the absence of Cdc13, Stn1, Rad24 and Exo1 proteins, manifested the highest mortality on day 5 of the survival curve with ~17% survival only as compared to 98%, 83% in Cdc13-1-deficient strains (2607 and 2608), and 92% and 88% in Stn1-lacking strains, (#14 and #21). This rapid decline of viability clearly

showed the additive effects of the two capping proteins (five-fold) as compared to the viabilities loss in the absence of either protein Cdc13 or Stn1.

At day 15, there was a clear segregation of mutant strains without essential telomere capping proteins and other controls, WT (640 and 641) and mutants lacking Exo1 protein (1272 and 1273). All four controls showed much better survival (77%-87%, of viability of cells) whereas mutants with uncapped telomeres exhibited a remarkable decrease in viability showing 10% to 45% survival with two exceptions (strain 2684 with 64% and strain 2607 with 76% survival). These patterns of ageing and mortality continued until day 40 with a slow rate of ageing in controls as compared to a faster decline of viability in mutants with telomere capping dysfunctions. Strain 2685 at day 40 showed only 0.15% survival and almost 100% mortality, whereas strain 2684, exhibited a sharp decline of viability between day 35 and day 50, still manifesting 27% survival with 73% viable cell loss (statistically significant with *p* value of 0.0015 as compared to WT). However, strain 2684 aged at a much faster rate between day 50 and day 90, exhibiting 17%, 15%, 11%, 11% and 10% of survival at day 50, day 60, day 70, day 80 and day 90 of CLS.

Both Stn1 deficient mutants (#14 and #21) and one Cdc13 deficient mutant (2608) presented consistently fast rates of ageing over the entire period of 90 days. Haploid #14 showed the highest decline, with 18% survival, 2608 with 24% survival, and haploid #21 with 31% survival at day 40. Keeping the same trends of mortality rate and ageing, these three mutants (in the absence of either single essential protein), haploid #14, strain 2608 and haploid #21, exhibited 10%, 16% and 16% survival respectively at day 90 of CLS (statistically highly significant with *p* values of 0.0074, 0.0084 and 0.0071 respectively). In contrast, the second Cdc13-lacking mutant (2607) showed 48% survival at day 90 (with 32% survival difference from strain 2608) as compared to WT (68% survival). The difference was statistically significant (p=0.0112). This might suggest that not only Cdc13 but also some other factors are also involved into regulation of senescence.

All controls (WT 640 and 641) and mutant lacking Exo1 protein (1272 and 1273) displayed a gradual viability decline, keeping a consistent pattern of survival between day 10 and 25. Strain 1273 showed slightly better survival at day 25 (78%), as compared to WT 640 and 641 and 1272 manifesting 76%, 73% and 69% survival respectively, without significant differences [with *p* value of 0.334 (641), 0.070 (1272) and 0.260 (1273)]. The WT 640 later showed a slow rate of mortality with better survival as compared to 1273, 641 and 1272 between day 30 and 90 (68%, 64%, 52% and 52% survival respectively).

Unexpectedly, the same mutations did not show the same effect in two strains at different ageing points. All strains and mutants showed individual variations. The two WT strains (640 and 641) displayed 1% to 16% difference from each other at different days of the CLS.

Similarly, Exo1 deficient strains 1272 and 1273 showed a 12% difference in survival, and Cdc13 lacking mutants displayed a 31% difference between strains 2607 and 2608 at age point 90. Overall, at day 90 of the CLS, 6% to 31% survival differences were seen between different groups of two strains with same mutation. These inter-strain variations in the presence of same mutation could result from epistatic interactions between the mutations understudy and genetic determinants in the genome (Lehner, 2011).

Overall, the absence of two essential capping proteins Cdc13 and Stn1 (2685), resulted in the highest mortality rate, and led to a shorter CLS (35-40 days with 0.15% survival) as compared to the deletion of Stn1 alone (longer CLS of 90 days with 10-16% survival) or Cdc13 alone (CLS of 90 days with 16-48% survival). The dramatic loss of viability and the faster rate of ageing in single and combined mutants highlighted the significance of these capping proteins in the protection of the telomeres and cumulative effects of these mutations in determining the chronological survival.

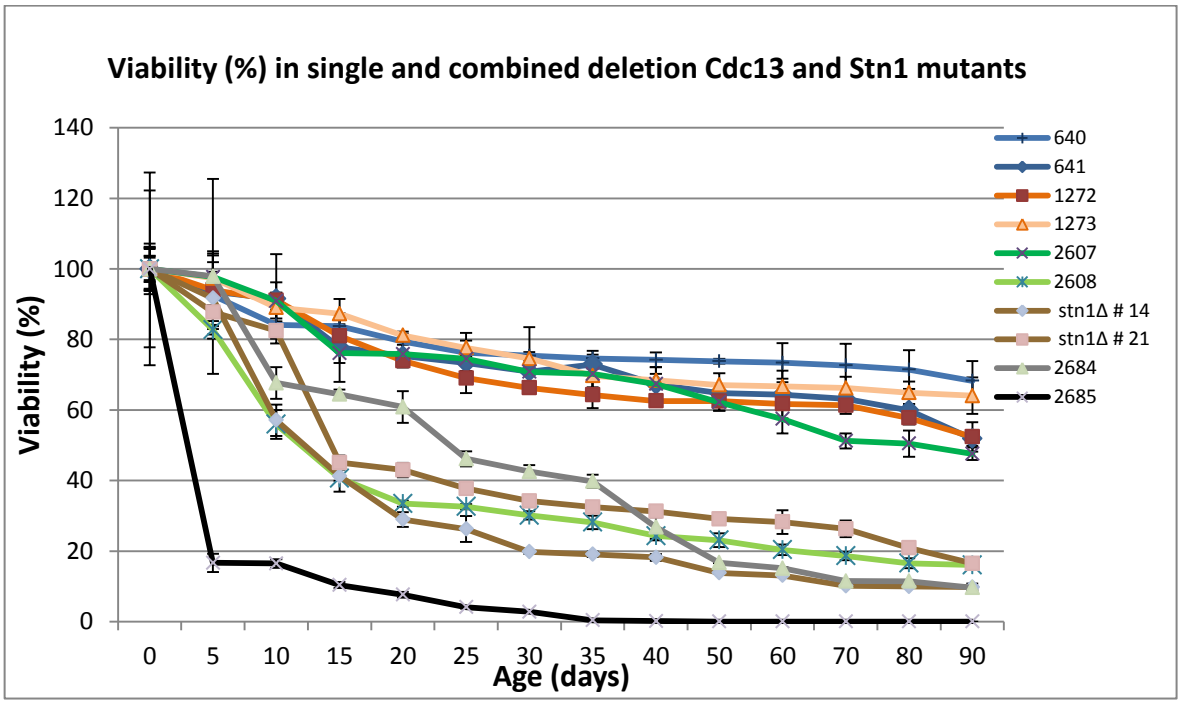

Figure 6.29. Survival (%) in single and combined deletion mutants (Cdc13 and Stn1) over a period of 90 days.

Cells were grown at 30°C in a shaking incubator for six days until saturation, washed with sterile water, and then kept in sterile water at 4°C for the whole period of the CLS studies. Samples were pooled and diluted in water and plated on YEPD plates to estimate the viable counts. Colonies were counted, and relative viability was calculated over a period of 90 days, taking the 0 day count as 100%.

Figure 6.30A shows the CLS for *cdc13-1* full gene deletion strain (2608) and its NTΔ and CTΔ variants from the strain 1296-TR. The average viability of *cdc13-1*-NTΔ-1296 was dramatically reduced as compared to CTΔ-1296 at age points 5-20 with 56% viability as

compared to 65% at day 20 of the CLS. However, the cell survival difference gradually became reduced and remarkably low with further ageing from day 25 to day 60 (with the difference of 2%, 4%, 1%, 1%, 6% and 3%). The strain 1296-TR displayed less viability as compared to CTΔ, but better survival as compared to NTΔ until age point 25. Then, it gradually appeared to be closer to NTΔ from age points 60 and 90. At day 90, *cdc13-1* mutant (strain 1296-TR) showed a survival of 29% as compared to 30% survival in NTΔ and 20% in CTΔ. The viabilities of, both mutants were significantly lower as compared to wild type (641) and *EXO1* deletion mutant (1273) but were higher when compared to strains 2685, #14 and 2608.

However, when survival values for individual NTΔ and CTΔ clones were plotted, the result was somewhat different (Figure 6.30B). Both CTΔ clones showed a similar pattern of survival with higher viability than that in NTΔ, from age point 5 to age point 20 (with survival difference of 2%-8% at different age points). However, further down the survival curves individual NTΔ clones exhibited wide fluctuations, with a 9-21% difference in viability. At age point 90, CTΔ clone #10 manifested 26% survival as compared to 14% shown by CTΔ clone #9.

Similarly, NTΔ clones #4 and #5 showed variable survival loss with a viability difference of 9-21% at various age points. Both NTΔ and CTΔ clones showed significantly lower survival as compared to WT (640 and 641) and higher survival as compared to *CDC13* deletion (2608) (lower than that for strain 2607). However, no particular trend was evident for N- and C-truncated mutants of strain 1296.

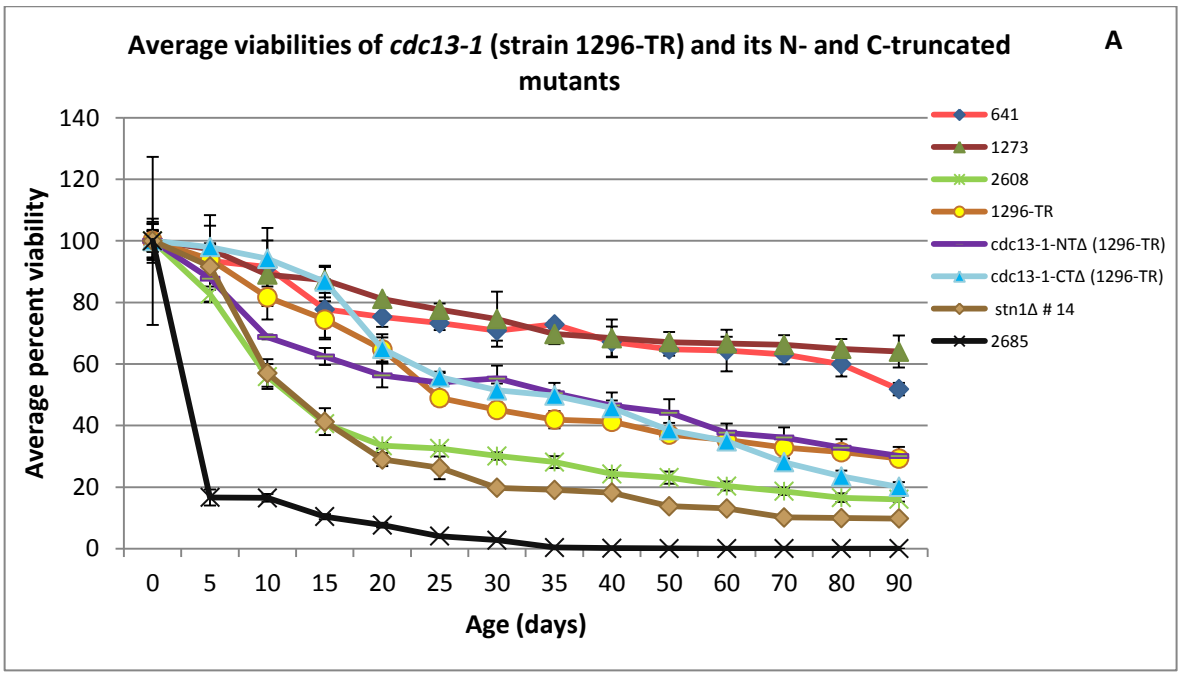

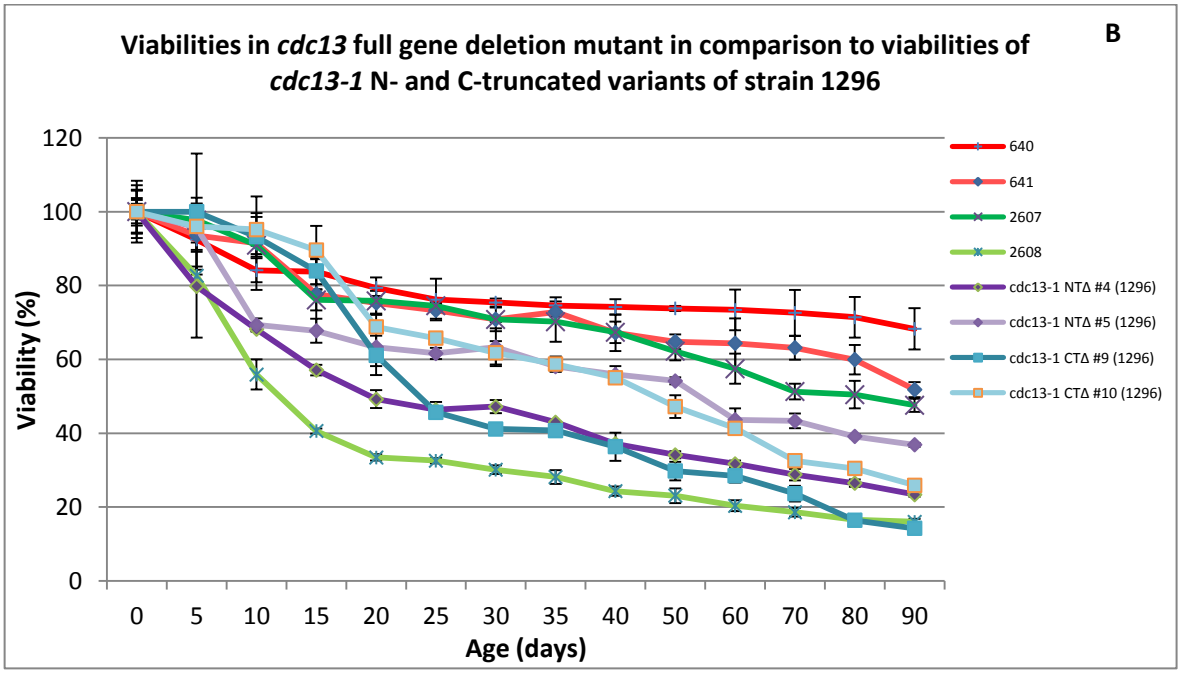

Figure 6.30. Viability loss in the *CDC13* deletion mutant and its comparison with N- and C-truncated variants of 1296-TR over a period of 90 days in CLS studies.

Cells were grown at 30°C shaking incubator for one week, washed with sterile water and kept at 4°C for the whole period of the CLS studies. Samples were pooled and diluted in water and plated on YEPD plates to estimate the viable counts. Colonies were counted, and relative viability was calculated for a period of 90 days by taking the 0 day count as 100%.

(**A**) Average viabilities of NTΔ and CTΔ mutants of strain 1296

(**B**) Viability% of individual NTΔ and CTΔ clones of strain 1296 during chronological ageing

The average percentage of viabilities for NTΔ and CTΔ variants in strain 1297-TR are shown in Figure 6.31A. The average survival of NTΔ was clearly higher as compared to CTΔ, with a difference of 29-37% in viability at different age points- from age point 15 to age point 50. However, a sharp decline in viable cell number was shown between age point 50 and age point 90, with a difference of 8-21% (remarkably less when compared to 29-37% in the first half of the survival curve). Finally, cell survival in NTΔ dropped to 18% as compared to 10% in CTΔ. For comparison, the CTΔ manifested a sharp decline of the survival at age point 10, with a 57% drop of survival (from 97% viable cells to 40%). However, a gradual decrease of viability was apparent from age point 15 to age point 90, (10% survival at age point 90 of the CLS.

The parental strain 1297-TR manifested a less than average viability as compared to NTΔ but better survival (as compared to CTΔ) until age point 90. It appeared to be closer to NTΔ (similar to 1296-TR) from age points 15 to 70. At day 90, it showed a survival of 12% as compared to 18% in NTΔ and 10% in CTΔ. The survival rates were significantly lower as compared to the wild type (641) and *Exo1* deletion mutant (1273) but were higher when compared to strains 2685, #14 and 2608.

The survival pattern of individual NTΔ and CTΔ clones also showed the same trends as seen with combined average survival of two clones Figure 6.31B. The both CTΔ clones showed a consistently similar pattern of survival with remarkably lower viability compared to that of NTΔ, from age point 15 to age point 70 (with a survival difference of 0.32%-6% at different age points). However, individual NTΔ clones exhibited a few fluctuations at the start of survival curve between age point 5 and 20 showing viabilities differences of 11-21% between the two clones. The viability pattern changed at age point 25, and clone #7 showed a slightly higher survival further down the curve as compared to clone #8 with a difference of 1-12% at different age points. At age point 90, NTΔ clone #7 manifested 23% survival as compared to 13% shown by NTΔ clone #8. In contrast to N- and C-truncated variants of 1296, the NTΔ and CTΔ of 1297 strain exhibited a clear survival trend: NTΔ with higher survival values as compared to CTΔ. The percentage of survival in NTΔ and CTΔ clones were lower as compared to both WT (640 and 641) strains. However, CTΔ clones manifested a lower survival as compared to the *CDC13* deletion (2608).

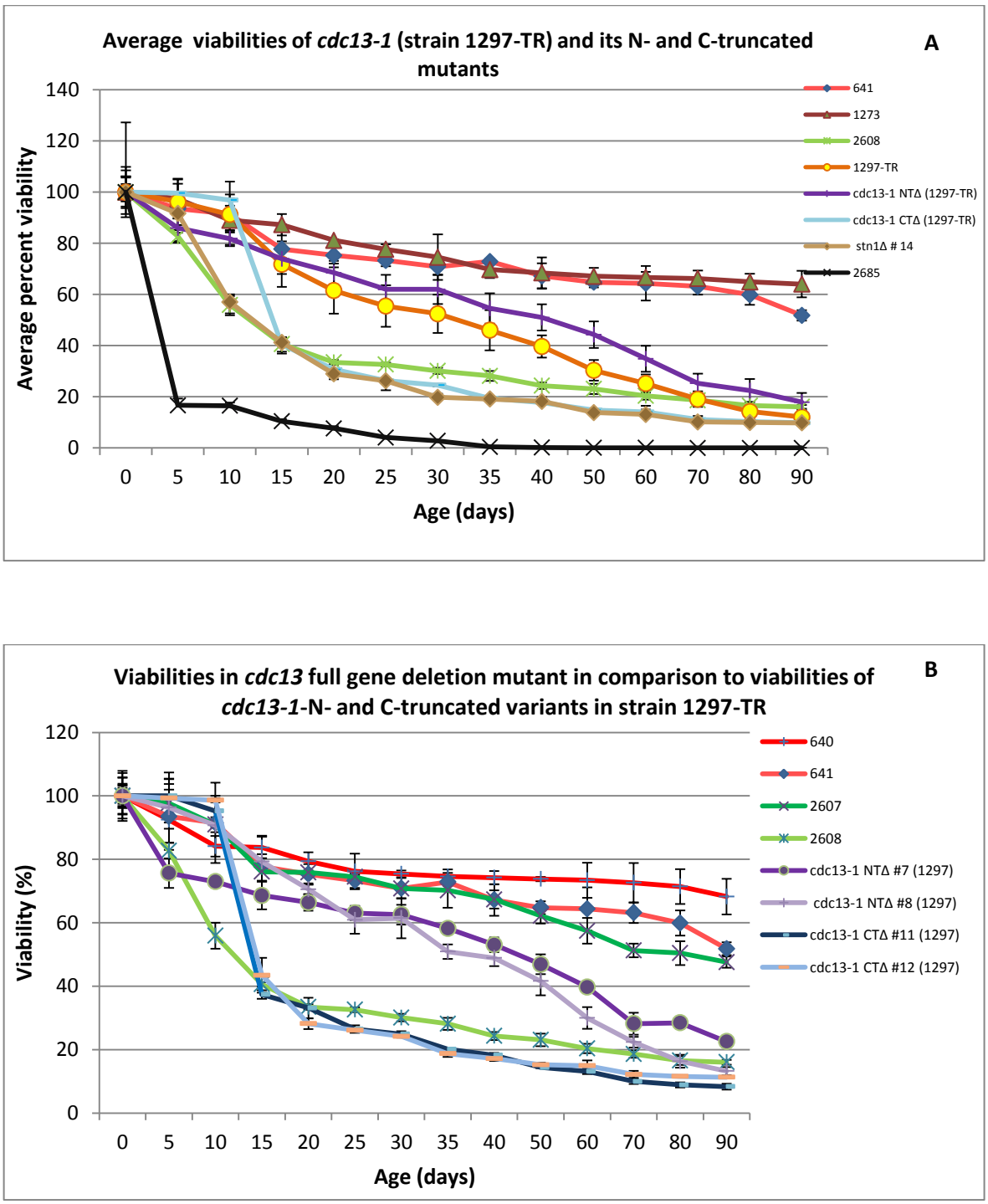

Figure 6.31. Viability loss in *CDC13* deletion mutant and its comparison with two N- and C-truncated variants of 1297-TR over a period of 90 days in CLS studies.

(**A**) Average viabilities of *cdc13*-1 NTΔ and CTΔ mutants of strain 1297.

(**B**) Viabilities of individual NTΔ and CTΔ clones of strain 1297 during chronological ageing.

6.4. Conclusions:

This study has documented the following novel findings.

- The dramatic loss of viability and the faster rate of ageing in, *STN1* and *CDC13* deletion mutants (single and combined) under different conditions, including calorie restriction, highlighted the significance of these capping proteins in the protection of the telomeres and cumulative effects of these mutations in determining the chronological survival.

- Significant differences in viability observed in N- and C-terminal deletion variants of *cdc13-1* mutant reveal different roles of structural motifs or domains in cellular senescence and ageing.

- The marked differences in colony size and irregularly-shaped colonies with wavy margins in single (*stn1Δ* or *cdc13Δ*, – more so in mutants lacking *STN1*) and combined deletion (*cdc13Δ stn1Δ exo1Δ* and *rad24Δ*) mutants as compared to uniformly sized circular colonies with smooth margins in the wild type might reflect genetic instability.

Chapter 7

Overall discussion and future plan of work

7.1 Generation of *CDC13* deletion/modification mutants

Deletion of a gene or ORF sequence is one of the approaches used in systematic functional analysis of genes to study the effect of deletion of a particular gene on cellular functions. In modern genetic analysis generating a null allele or inactivation of a chromosomal gene require '*ex vivo'* synthesis of a gene-targeting construct using multiple cloning steps. In yeast, efficient homologous recombination systems enable genomic integration and manipulations of a foreign gene of interest (Rothstein, 1991, Huber *et al*., 2014). One-step PCR-targeted modification/deletion of a specific gene by means of DNA transformation in yeast is a commonly used technique to understand gene function. Previously, it has been reported that the *cdc13-1* temperature-sensitive (ts) allele of *CDC13* with single amino acid missense mutation within DNA binding domain (DBD; 557-694 aa), shows a decrease in the maximum permissive temperature, and *cdc13-1* mutants can grow only at a lower temperature (Hughes *et al*., 2000). Cells die at higher temperature due to the accumulation of ssDNA, recombination and cell cycle arrest. However, *cdc13-1* temperature-resistant (TR) survivors in the absence of exonuclease activity at telomere can grow at higher temperatures (Zubko and Lydall, 2006).

Depending on experimental needs numerous selectable markers are employed in the yeast manipulation such as prototrophic, autoselection, counterselectable and markers conferring drug resistance (Siewers, 2014). Plasmids with different markers (kanamycin resistance, histidine, tryptophan and leucine prototrophy) are available commercially to be used as templates for the amplification of the deleting module (Wach *et al*., 1997, Longtine *et al*., 1998).

In the 1st set of experiments, the *cdc13-1* full gene of the *S. cerevisiae* mutants (strains 1296 and 2605) containing prototrophic marker *LEU* (*cdc13-1 exo1::LEU2 RAD5 trp1-1 leu2-3,112 his3-11,15 ura3*) was deleted. The heterologous marker module HIS3MX6 used for this purpose is able to complement *S. cerevisiae his3* mutation and has been reported to work better as a selectable marker with less chances of undergoing homologous recombination (less than 5% incorrectly targeted transformants) with the host yeast genome (Wach *et al*., 1997).

Chimeric primers were used for the amplification of the deletion module. Each primer consisted of two parts; a 5' target gene-specific sequence and 3' marker-specific sequence. The gene-specific guided deleting sequences at the 5' ends allows homologous recombination at the desired locus within the genome and requires range of 35-51/30-50/38-50 nucleotides in length, while 3' sequences used for amplification of the marker could be 17-22 nucleotides in length (Wach *et al*., 1997, Baudin *et al*., 1993, Lorenz *et al*., 1995). In previous studies, even smaller

primers with 5'end consisting of 30-35 nucleotides have been used to synthesize PCR product with *HIS3* marker (Baudin *et al*., 1993). However, M. S. Longtine *et al.*, (1998) have suggested that the longer target-/gene-specific flanking sequences may improve the efficiency of homologous recombination. Primers used in this study to generate ~ 1409 bp linear DNA to delete full *cdc13-1* had 46 (forward) and 40 (reverse) nucleotides from upstream and downstream regions of the *CDC13* gene (5' ends) with 20 nucleotides (3' ends) homologous to the histidine marker from the reported sequences (Longtine *et al*., 1998). In this study, the potassium acetate precipitated, ethanol washed PCR DNA was used to transform *cdc13-1* mutants, however, crude PCR mixture can also be used to transform yeast cells as was reported previously (Baudin *et al*., 1993, Gietz *et al*., 1992). Host yeast strains used for DNA transformation should contain non-reversible mutant allele against selectable marker gene otherwise, it could be difficult to maintain the yeast with, or screen for, the integration of foreign selectable markers in homologous recombination experiments (Lorenz *et al*., 1995). The strains 1296 and 2605 used in the transformation experiments contain *his3-11,15* mutation for selectable marker HIS3MX6 gene In preliminary experiments, transformation efficiency of yeast cells as a result of homologous recombination was very low and produced only one histidine^{+} transformant out of $2.53x10^{6}$ cells. These results are consistent with a previous study that showed one to two His^{+} clones by using 3 µg of PCR product with *HIS3* marker module of *S. kluyveri* origin (Wach *et al*., 1997). However, variable levels of genuine transformants (5-10%) are reported by other studies (Lorenz *et al*., 1995), 16-80% (Baudin *et al*., 1993), and 20-95% (Longtine *et al*., 1998). Increased incubation time for transformation (from 15 to 30 min) and a higher quantity of DNA (from 1 to ~3 µg) appeared to increase the number of transformants by almost 11 fold in strain 1296-TR in the current study.

In gene manipulation studies different techniques are employed for the confirmation of target sequence deletion or alteration with the integration of marker module in the recipient genome. Putative clones could be screened on the basis of selectable markers (phenotypic analysis) and examined on DNA level either through traditional Southern blotting technique for the detection of the marker integration and gene modification (Baudin *et al*., 1993) or examined by rapid analytical PCR for the integration of the PCR module in the yeast genome (genetic analysis) (Wach *et al*., 1997). Diagnostic primers from the ORF of *CDC13/cdc13-1* were used for the genotypic detection of disrupted gene. Systematic PCR analysis of 10 His^{+} transformed cells from strain 1296-ts and its TR survivors (*cdc13-1 exo1*::LEU2) showed that all tested clones from ts-cells were PCR positive for *cdc13-1* mutation while all tested TR-transformats were PCR negative for *cdc13-1*gene confirming the deletion of gene in only TR cells of strain 1296. However, it was not determined whether these *cdc13-1*-His^{+} ts-cells were generated as a result of non-homologous recombination of HIS3MX6 marker with host genome or were autonomous revertants due to conversion of auxotrophic mutation or other recombination.

The appearance of His^+ pseudotransformants due to unavoidable background of gene conversion has been reported previously with less than 5% frequency (Wach *et al*., 1997). The deletion of genotypic *cdc13-1* gene in all tested His^+ 1296-TR clones indicated that the yield of correctly targeted transformants with heterologous *HIS3* marker of non *S. cerevisiae* origin could be above 95% (100% in case of TR cells). However, *cdc13-1* disruption with *HIS3* heterologous maker was not quite successful in this study. These results suggest that absence of *cdc13-1* knockout in temperature sensitive cells of strain 1296, may be due to its essential functions in telomere capping and DNA stability at low temperature.

Overall, *cdc13* full gene deletion mutants were developed successfully at high temperature (36C°) in strains of survivors 1296-TR and 2605-TR: (genotype *cdc13-1*::HIS3 *exo1*::LEU2). This indicates that yeast cells can grow and divide without essential telomere capping protein Cdc13 conditionally in the absence of exonuclease activities (*exo1Δ*) on uncapped telomere in survivors (TR cell), in agreement with the previous finding that Cdc13 might be dispensable in *exo1Δ* mutants in temperature resistant survivors (Zubko and Lydall, 2006). Similarly, another study reported that inactivation of checkpoint machinery (by deletion of *RAD9*) and attenuation of telomeric DNA resection pathways (by deletion of both *SGS1* and *EXO1*) are sufficient to allow cells to grow in the absence of Cdc13 telomere capping protein (Ngo and Lydall, 2010).
The telomere cap is adaptable. Loss of nucleases activities at uncapped telomere (*exo1Δ*) and inactivation of DNA damage checkpoint pathways (*rad24Δ*) either promote telomere capping and maintenance through Cdc13-independent mechanism by involving other capping proteins in absence of Cdc13 or Cdc13-mediated capping that is not needed in this case (Zubko and Lydall, 2006). A recent report has also shown that diverse groups of proteins including CST complex, NMD and DDR proteins are involved in telomere capping and replication. The essential roles of Cdc13 protein in telomere capping may be bypassed in the presence of inactive DDR and NMD (Holstein *et al*., 2014).

These finding criticises the essential roles of Cdc13 in cell survival and point towards the involvement of alternative mechanisms in telomere maintenance. It can be hypothesised that at a conditional Cdc13 uncapping other proteins might compensate Cdc13-mediated capping via an alternative mechanism to maintain telomeres and ensure genomic stability. In future studies, it would be interesting, to investigate the mechanism that exists in temperature-resistant *cdc13-1* cells to maintain telomeres in the absence of Cdc13 and makes cell survival possible.

Cdc13 protein binds to telomeric specific ssDNA TG-rich DNA tail with high specificity and affinity. Its interaction with Stn1 through its C-terminal specific domain ensures genomic integrity by protecting telomere ends from nucleases attacks. The sequence analysis of Cdc13 has shown five different conserved OB domains including OB1, RD, OB2, OB3 (DBD) and

OB4 from N- to C-terminus (Anderson *et al*., 2002, Mitchell *et al*., 2010, Mason *et al*., 2013). . N-terminal region is considered crucial part of Cdc13 (Hsu *et al*., 2004). Previous studies have established that N-terminal OB1 fold of Cdc13 is involved in its interaction with Pol1 (a catalytic subunit of polymerase α) for C-rich strand re-synthesis and telomerase RNA associated protein Est1 for G-strand lengthening and regulate telomere length (Qi and Zakian, 2000). While it's C-terminal OB4 domain is utilised to interact with Stn1 protein for the essential roles in telomere end capping and telomerase recruitment. Cdc13 bind to single stranded DNA through its OB3 (DBD) domain for its capping function. Cdc13 exists as a dimer in the solution. A newly discovered OB2 domain between recruitment fold and DNA binding domain is appeared to involve in Cdc13 dimerization. The disruption of OB2 fold affects the binding of Stn1 and Cdc13 and telomere maintenance (Sun *et al*., 2011). Although Cdc13 have been studied extensively in relation to telomere capping functions, the precise role of its N- and C-terminal in telomere length regulation and ageing and senescence are still not clear.

To further understand the roles of Cdc13 and molecular dissection of its functions, N- and C-termini truncated variants of Cdc13-1 were generated in this study. The *CDC13* N-terminal half (1386 nt corresponding to 462 aa) truncated mutants were attempted to generate using modulating plasmid pFA6a-TRP1-PGAL1 in recipient yeast strains: 1296-TR, 1297-TR (*cdc13-1 exo1::LEU2*) and 1272 (*CDC13 exo1::LEU2*). Cells from these three strains were tested for growth at 23°C and 36°C. The fast growing survivors were observed in strain 1296 and 1297 with heterogeneous growth pattern (large and small colonies, with rough edges) but not in the tested strain 1272 (homogenous growth with equal sized smooth edged colonies), which apparently showed no difference in growth at 23°C and 36°C. This type of growth could indicate genetic instability and senescence. When examined for their auxotrophic markers, all three strains showed spontaneous revertants for trp1 marker with varying frequencies, rare for histidine marker (only one cell out of $26x10^6$ cells in strain 1296-TR). High frequency of trp1 revertants ($2.88x10^{-6}$ in strain 1296-TR as compared to $0.46x10^{-6}$ in 1297-TR) could be correlated with increased incidence of false positive transformants (75% in 1296-TR as compared to 63% in strain 1297-TR respectively).

cdc13-1 N- and C-terminus deleting DNA fragments of ~1.576 kb (TRP1-PGAL1) and ~1.6 kb (ADH1-HIS3MX6) respectively DNA were PCR synthesized using 68-71 nt hybrid primers and trp1- and his-plasmids DNA templates. In contrast to potassium acetate/ethanol precipitated PCR product that was used to delete *cdc13-1* full gene, phenol-chloroform extracted and ethanol precipitated (~1-3 µg) linear DNA fragments were used to transform yeast cells for N- and C-terminal specific truncation. Analytical PCRs negative for *cdc13-1* N-terminus (PCR^- for 378 bp fragments) and positive for TRP1 marker module (PCR^+ for ~1.5 kb fragments) indicates truncation of *cdc13-1* N-terminal region with integration of marker module. The results

demonstrated that out of randomly tested Trp1$^+$ (T^+L^+) clones, 25% (6/24) T^+L^+ transformants were true mutants for N-terminus truncation with target specific homologous recombination in survivors strain 1296-TR as compared to 37.5% (9/24) in strain 1297-TR. All other tested T^+L^+ transformants (PCR negative for *TRP1* gene) were considered false positive (spontaneous revertants) generated possibly as a result of endogenous marker gene conversion, (rather than recombinants). There was no false positive mutant as a result of non-homologous recombination of *TRP1* marker gene. Although there are reports that the *TRP1* marker of *S. cerevisiae* origin can recombine efficiently with the endogenous *trp1* locus (Longtine *et al*., 1998, Sikorski and Hieter, 1989) and should be used in strains that contain *TRP1* deletion i.e., *trp1Δ-63* or *trpl-Δ1*. Another yeast vector, pFA6a-HIS3MX6-PGAL1 was also tried for *CDC13* N-terminal truncation with histidine module but without success in obtaining true clones i.e. 0/30 screened His$^+$ transformants in strain 1296-TRand 1297-TR and 0/10 in strain 1272.

Similarly, the second half of *CDC13* ORF (from 1387-2775 nt corresponding to 462 aa) was disrupted by using heterologous histidine (ADH1-HIS3MX6) marker to generate C-terminus deletions of *cdc13-1* mutant under ADH1 terminator. The results of integrative DNA transformation for C-terminus deletion demonstrated high frequencies of true mutants, 86.67% (13/15) and 100% (15/15), in strains 1296-TR and 1297-TR respectively as a result of target specific homologous recombination. Low background of spontaneous revertants for histidine marker mutation resulted higher frequency of *HIS*$^+$ C-truncated mutants. However, two false positive, H^+L^+ (13.33%) mutants were also observed in strain 1296-TR. Further analysis using analytical PCR for the ADH1-HIS3MX6 marker showed that one of the pseudo positive mutant was generated as a result of NHR (PCR$^+$ for marker) while other, PCR negative for marker was determined to be revertant. No true construct (0/77) with C-truncated *CDC13* was achieved in the tested H^+L^+ transformants in strain 1272 (non-survivor strain). However detection of 14 (18.18%) H^+L^+ false positive mutants (also PCR$^+$ for marker) indicate non homologous integration of marker in chromosome; other could be revertants (> 80%) due to marker gene conversion.

The *CDC13* disruption results indicated that endogenous *trp1-1* deletion locus is not very stable and generated unavoidable background because of gene conversion of auxotrophic mutations which decrease the yield of correctly targeted tansformants: 25-37% yield with TRP1 marker as compared to 87-100% with HIS marker. Taken together, PCR based homologous recombination approach and rapid screening assay involving PCR detection of mutants directly from the colonies can be efficient for generating mutants of yeast for functional analysis.

The N-terminus truncated variants of *cdc13-1* generated in this study are expected to exclude OB1 motif (1-190) and RD (227-340/340) domains and most of the OB2 fold (344-494). While C-terminus deleted construct of *cdc13-1* are presumed to exclude small part of OB2 fold (463 onwards) and whole of the OB3/DBD (494-694) and the OB4 fold (694-924) (Anderson *et al*., 2002, Mitchell *et al*., 2010, Mason *et al*., 2013, Sun *et al*., 2011). OB2 motif is disrupted in both N- and C-terminus truncated alleles of *cdc13-1*generated in this study. Previous study has shown that introducing point mutations in full length Cdc13 protein at OB2 fold prevent Cdc13 N-dimerization that leads to telomere shortening. Mutations within DBD affect its DNA binding ability and cause telomere elongation (Mitchell *et al*., 2010). The N- and C-disrupted alleles of Cdc13-1 generated in this study may provide an invaluable tool for exploring the important roles of different motifs of Cdc13 with respect to its N or C-terminus on uncapped telomeres.

7.2 Generation of Stn1 mutants and diploids cells using genetic crosses

Genetic crosses are routinely carried out using haploid strains of opposite mating type to generate new meiotic recombination of existing mutations for phenotypic analysis. They are studied for the interaction of different mutations and combined effects of two or more gene deletions. The diploid cells are sporulated in the presence of 1-2% potassium acetate and non-fermentable carbon source under starvation of nitrogen to generate four cell asci containing haploid meiotic products (Rothstein *et al*., 1977).

To further explore the role of Stn1 protein haploids progeny of *stn1Δ*, triple mutants in new combination (*CDC13 stn1*::HIS *exo1*::LEU2 *rad24*::TRP1) were generated by crossing two haploids mutants. The process of generation of mutants involved inducing sporulation of diploid cells, dissection of tetrads, and separation of individual spores by using micromanipulation tools. It is necessary for genetic analysis to get all four spores from the same ascus. However, in the present study it was not possible to carry out segregation analysis, because of high mortality of spores (31 spores germinated out of 328 spores separated resulting in 9% viability). Random analysis of spores was carried out to find the required genetic combination (*cdc13*Δ *stn1*Δ *rad24*Δ *yku70*Δ *or stn1*Δ *exo1*Δ). Genetic analysis of viable spores by replica plating segregated all spores in five groups of different mutations but none with the desired combination with *yku70*Δ. Presence of only two spore progenies with gene combination *stn1*Δ *exo1*Δ *rad24*Δ *CDC13* (#14 and #21) indicates low frequency of viable recombinants. The presence of wild type *CDC13* in this combination was confirmed by using PCR and

analytical gel electrophoresis for the confirmation of gene specific fragments. Stn1 deletion haploids showed heterogeneous colony growth with small and large colonies and were further studied for their chronological lifespan and cellular responses to oxidative and genotoxic stresses. Diploid cells were also generated by crossing N- and C-truncated haploids of Cdc13-1 mutants. However, the sporulation of these heterozygous diploid cells failed to generate haploid progeny, could be because of deleterious effect of protein misfolding resulting in impaired meiosis.

7.3 Maintenance of telomere in the absence of Cdc13 and Stn1

Maintenance of telomere capping is essential for genomic stability and the survival of eukaryotic cells. Fission yeast can survive telomere dysfunction-mediated chromosome fusion by generating independent replicating circular chromosome (Wang and Baumann, 2008). Unprotected telomere in yeast can be repaired by recombination-dependent break-induced DNA replication (McEachern and Haber, 2006). Budding yeast can maintain their linear chromosome in the absence of telomere capping proteins through recombination-dependent or -independent mechanisms (Zubko and Lydall, 2006) or in the absence of telomerase through recombination based ALT mechanisms (Teng and Zakian, 1999).

Telomere capping protection counteracts the proliferative barrier imposed by DDR machinery. Dysfunctional telomere triggers DDR, cell cycle arrest and contributes to cellular senescence and ageing. It was shown previously that survivors can grow at low rate in telomerase deficient mutants (*tlc1Δ*) or *cdc13-1 rad9Δ exo1Δ* cells in the absence of functional Cdc13 (Teng *et al*., 2000). Further simultaneous inactivation of nucleases activities of Sgs1 (the RecQ helicase in budding yeast) and Exo1 together with cell cycle checkpoint activity of Rad9 allow cell to grow in the absence of capping function of Cdc13 (Ngo and Lydall, 2010).

The overexpression of an OBFC1 (homolog of yeast Stn1 protein) mutant results in elongated telomeres in human cells, implicating OBFC1 in telomere length regulation (Wan *et al*., 2009). In this study deletion of Stn1 and/or Cdc13 in the absence of nucleases activities manifested common diffuse and smeary telomere DNA patterns at 30°C, more diffuse in the *stn1Δ exo1Δ rad24Δ* deletion mutants with a major smear observed between 0.3 kb and 2 kb. These telomeric DNA patterns were different from type I survivors of WT, *EXO1* deletion mutants (strains 1272 and 1273) and *cdc13-1 exo1Δ* (strain 1297-TR) in not having distinct terminal fragment. Type I survivors mainly maintain their telomere through recombination mediated mechanism and by amplifying sub-telomeric Y' repeats (Maringele and Lydall, 2004).

The presence of broad smear in *STN1* deletion mutants observed in this study could correspond to a subset of TRFs of similar sizes, in accordance with possible conservation of sub-telomeric sequences between a subset of chromosomes. Alternatively, the smeary DNA could be ssDNA (extra-chromosomal DNA) in agreement with a previous report where marked increase in ssDNA was observed in cells lacking *STN1* function (Grossi *et al*., 2004). However, it needs to be verified by hybridization of non-denatured DNA by using ssDNA probe. It was shown previously that *cdc13-1 stn1Δ exo1Δ rad24Δ* and *cdc13Δ stn1Δ exo1Δ rad24Δ* mutants at high temperature (36°C) and at late passages also generate ssDNA similar to but in higher amount as observed in type I and type II survivors. The generation of ssDNA could also be Rad52 dependent that is involved in homologous recombination (Zubko and Lydall, 2006). The presence of increased level of ssDNA (an indication of increased accumulation of damages) in *stn1Δ exo1Δ rad24Δ* mutant as compared to *stn1Δ cdc13Δ exo1Δ rad24Δ* mutants or *cdc13Δ exo1Δ* grown at 30°C indicates that Stn1 might has different role in telomere capping and cell survival. This observation is supported from a recent study that showed that Stn1 can bind to telomere in Cdc13 independent manner in the presence of inactive DDR and NMD, and bypass the need of Cdc13 for its capping functions (Holstein *et al*., 2014).

The distinct banding patterns with unique fragments of 1 kb-5 kb with obvious Y' 5.5 kb and 6.5 kb fragments without prominent terminal DNA fragments in N- and C-truncated Cdc13-1 mutants in both strains 1296 and 1297 exhibited telomeric DNA patterns resembling to type II survivors. Presence of predominantly type II survivors suggests that dysfunctional telomere in the presence of defective capping protein Cdc13-1 restore telomere function through amplification of telomeric repeats ($TG_{1\text{-}3}$), using recombination-based mechanisms or ALT (Teng and Zakian, 1999). The patterns of telomere DNA were similar to those in checkpoint-deficient *cdc13-1* cells (*cdc1-1 mec1* strain) at 29°C, which survive through homologous recombination triggered by the accumulation of DNA damage, and telomerase-deficient, recombination dependent (*cdc13-1* cells with Rad52) type II survivors as shown previously (Grandin *et al*., 2001). However the *cdc13-1 exo1Δ* mutant (original strain 1296-TR) displayed telomeric structure resembling to type II survivors whereas strain 1297-TR with similar genotype revealed telomeric DNA structure similar to type I survivors (more like WT) at 30°C indicating the effect of other determinants in the genome. N-truncated mutants of Cdc13 from both strains of *cdc13-1 exo1Δ* exhibited more smeary and diffused background (could be ssDNA, need further verification) as compared to C-truncated mutants at 30°C and showed similarity to *cdc13Δ exo1Δ* mutants.

Further growth of N-terminus truncated variant of *cdc13-1 exo1Δ* (strains 1296-TR and 1297-TR) cultured at 23°C and 37°C for passage 3 (~60-75 divisions) showed telomeric DNA structure that resembled those of *cdc13Δ exo1Δ* mutant at respective temperatures. Telomeric DNA from mutants (N- and C-terminus truncated) grown at 37°C offered more resistance to

digestion as compared to those grown at 23°C. Increased level of diffuse and smeary telomeric DNA (more like type I survivors) without obvious terminal fragment, might indicate the accumulation of ssDNA with successive culturing at 37°C. Telomeric DNA of C-terminus truncated mutants grown at 23°C and 37°C showed resemblance to DNA patterns of original *cdc13-1 exo1Δ* mutant (similar to recombination-proficient type II survivors). Appearance of weak smeared DNA at 37°C was also obvious in C-terminus variants of *cdc13-1 exo1Δ*. At passage 3 the overall trends in telomeric DNA structure of N- and C-terminus mutants of Cdc13-1 appeared to be in transition from type II like telomere to type I like telomere as the individual fragments (> 1 kb) turned more diffuse and smeary with distinct 5.5 kb and 6.5 kb fragments. The disappearance of bigger than 1 kb fragments but the presence of distinct 5.5 kb and 6.5 kb fragments further suggested the maintenance of telomere at passage 3 with the amplification of sub-telomeric-Y' repeats, and degradation of X-repeats.

The N-terminus truncated Cdc13-1 mutants (1-462 aa) used in this study are without OB1 fold, RD motif and most of the OB2 domains. Loss of Cdc13-Pol1 interaction is correlated with telomere elongation (Qi and Zakian, 2000). The RD motif plays an important role in telomerase recruitment through its interaction with Est1 protein. Intact OB2 fold of Cdc13 is required for Cdc13-Stn1 interaction for telomere maintenance (Sun *et al*., 2011). The loss of N-terminus could prevent access of telomerase to telomere overhangs and blocking of extension of G strand, which are required for continuous cell division.

The C-terminus truncated Cdc13-1 mutants (463-924 aa) are without complete DBD (OB3) and OB4 domains and a part of OB2 domain. The absence of DBD could affect binding of Cdc13 with ssDNA, loss of its capping function and exonucleolytic degradation. The essential function of Stn1 is considered to promote telomere end protection through its binding with Cdc13p and is supported by the finding that truncation of C-terminal (123 aa) failed to support viability, however, endogenous expression of *stn1* allele with extensive truncation of C-terminus (removal of 208 aa) allowed cell to grow (Petreaca *et al*., 2007). Stn1 interacts with Pol12 to maintain telomere end protection and length regulation (Grossi *et al*., 2004). The deletion of OB4 fold could result in the loss of interaction of Cdc13-Stn1, loss of telomere end protection and maintenance. These events could lead to genomic instability and early senescence.

The N- and C-truncated Cdc13-1 mutants generated in this study may provide useful tools to investigate genomic instability in response to telomere uncapping in the presence or absence of different domains of Cdc13. These results also support that the attenuation of nucleases Exo1 and Rad24 is sufficient to allow yeast cells to grow and to divide in the absence of telomere capping by Cdc13 or Stn1, or both (Zubko and Lydall, 2006) indicating the plasticity of telomere capping and the maintenance of telomere by other alternative mechanism of capping.

7.4 Cellular responses of cells lacking Cdc13 and Stn1 to genotoxic agents

Genetic interaction analysis is commonly used to study gene function, the role of genes in different cellular pathways and to identify functionally related or functionally redundant genes (Memarian *et al*., 2007). Lethality of a double deletion mutant verifies genetic and functional relationships between two genes. Genotoxic stresses affect growth patterns reflecting distinct traits that cells acquired to adapt to adverse environment (Olson-Manning *et al*., 2012). Cell cycle checkpoints of yeast: G1 phase, S phase and G2-M regulate cell cycle progression (Alic *et al*., 2001). Cells undergo cell cycle arrest in response to defects in DNA replication, chromosome segregation, DNA damages, nuclear migration, and spindle errors under the control of cell checkpoints (Weinert, 1998b, Weinert, 1998a).

Mutant cells display sensitivity and resistance to a wide range of exogenous genotoxic agents. Analysing the growth of a mutant yeast strain in the presence or absence of the sub-lethal concentration of a genotoxic agent is a fast and efficient way to determine the targets of inhibitory compounds. Yeast cells exposed to oxidative stress or DNA damaging agents respond by arrest of cell cycle progression via cell cycle checkpoint mechanisms. Different toxic chemicals activate G1 phase, S phase or G2-M phase cell cycle checkpoints (Harrison and Haber, 2006).

The UV-induced DNA damages occur through photo-dimerization of proximal pyrimidines bases (Kladwang *et al*., 2012). These DNA lesions have adverse effects on genomic and non-coding RNA (Wurtmann and Wolin, 2009). In *S. cerevisiae,* hydroxy urea (HU) inhibits ribonucleotide reductase function and blocks DNA replication. As a result, DNA synthesis is blocked by preventing dNTP pool expansion at G1/S phase of cell cycle (Koc *et al*., 2004). Methyl methanesulfonate (MMS) and HU disrupt multiple cell cycle checkpoint responses resulting in replication stress. Replication stress signal activates S phase checkpoint accompanied by cell sensitivity to the replication inhibitor (Gasparyan *et al*., 2009). The sensitivity of cells to MMS also increases significantly when other DNA repair pathways are compromised (Lundin *et al*., 2005). Hydrogen peroxide is used to model chronic oxidative damage to cell through oxidative stress and induces G2-M arrest through different mechanisms that involve *RAD9* mediated pathway. DNA is considered to be a primary cellular target for many cytotoxic agents. DNA strand breaks, a major class of DNA damage, can be induced by endogenous and exogenous genotoxic agents (Rasouli-Nia *et al*., 2004).

The phenotypical growth patterns of mutant strains lacking Cdc13 and Stn1 (single or in combination) and N- and C-terminus truncated variants of *cdc13-1* were monitored at 23°C and 30°C in the presence of different DNA damaging agents i.e., UV and MMS, HU (DNA

replication inhibitor) H_2O_2 (oxidative stress factor). Responses of mutants lacking Cdc13 and/or Stn1 (in the absence of exonuclease activity) to genotoxic agents UV, MMS and HU were, distinct from WT, whereas combined deletion mutants of *cdc13Δ stn1Δ* (in the absence of *EXO1* and *RAD24* genes) showed the highest sensitivity as compared to *stn1Δ* mutants (in the absence of *RAD24* and *EXO1* genes) and *cdc13Δ* mutants (in the absence of *EXO1* gene). The strong growth inhibition observed in combined deletions mutants as compared to moderate sensitivity of Stn1 lacking mutants might suggest the interaction between Cdc13 and Stn1 cooperatively, with some reservation regarding the presence of *rad24Δ* or involvement of both proteins via different pathways to the overall sensitivity.

In previous studies, it has been shown that overproduction of Stn1 protein makes cells highly sensitive to the replication inhibitors HU and MMS (Gasparyan *et al*., 2009). However, in the present study the absence of Stn1 made cells sensitive to UV, MMS and HU (S phase checkpoint) but highly resistant to H_2O_2 (G2-M checkpoint pathways) as compared to combined deletion mutants (*cdc13Δ stn1Δ*), *cdc13Δ* mutants (in the absence of *EXO1* gene), *exo1Δ* mutants and wild type strains suggesting that the resistance to H_2O_2 could possibly be under a novel controlling mechanisms. The sensitivity to HU and MMS in *stn1Δ* deletion mutants observed in this study is contradictory to the previous results where over expression of Stn1 lead to the same effects (Gasparyan *et al*., 2009). Alternatively, there are different mechanisms of sensitivity in cases of overexpression and the lack of Stn1. Overall, it could be suggested that there is interplay between amounts of Stn1 and some other proteins including Cdc13 in the cell. However this hypothesis needs further exploration.

The essential capping function of Cdc13 can be bypassed by overexpression of N-terminal OB fold of Stn1, and its interaction with Ten1 that allowed cell to grow and divide in the absence of Cdc13 (Petreaca *et al*., 2006). It is obvious that Cdc13 and Stn1 proteins have independent contribution into sensitivity to HU (because the removal of both proteins leads to more dramatic effect of sensitivity to HU (but not to MMS or UV where *stn1Δ* mutants are as sick as *cdc13Δ stn1Δ* combined mutants). Overall, the results on sensitivity to MMS and HU (both impacting DNA stability) indicate that these two proteins might contribute to the maintenance of DNA integrity – may be playing roles in DNA repair, or some other mechanisms. Understanding these mechanisms in future research is important in terms of showing other roles of these essential proteins (behind telomere protection). This observation is further supported by a recent study suggesting that *STN1* and *TEN1* play more critical roles in CST complex as compared to *CDC13* and the requirement of Stn1 cannot be bypassed with the inactivation of DDR and NMD pathways (Holstein *et al*., 2014).

The behaviour of the *STN1* and *CDC13* deletion mutants on H_2O_2 is opposite to that on MMS and UV in a way that single mutant of *cdc13Δ* showed moderate sensitivity implying that Cdc13

plays a role in normal homeostasis towards tolerance to oxidative stress in WT cells. Paradoxically, these results on more tolerance to H_2O_2 in Stn1 mutants indicate that presence of Stn1 protein reduces tolerance to oxidative stress in WT cells. Based on these results, it could be suggested that *STN1* gene might play some unknown role distinct from the *CDC13* gene through a different mechanism associated with tolerating oxidative stress.

The comparison of stress effects in *cdc13Δ* mutants, and *cdc13-1* N- and C-terminus truncated variants also disclosed different extent of growth inhibition to UV, MMS, HU and H_2O_2. The highest sensitivity was observed in *cdc13Δ* mutants with mild effect in its *cdc13-1 CTΔ* allele manifesting slightly more resistance as compared to wild type and *EXO1* deletion mutants. These trends are consistent with those for all tested oxidative **(**H_2O_2) and genotoxic stresses **(**UV, MMS, HU). The resistance pattern of C-terminus truncated *cdc13-1* allele indicates that the C-domain might also contain a suppressor of WT-resistance to UV, MMS and HU. Genotoxicity-induced sensitivity patterns of the diploids cells (heterozygous on both *cdc13-1* N- and C-terminus truncations alleles) show intermediate growth inhibition when compared with *cdc13-1* N- and C-terminus truncated haploids under UV, MMS and HU. This suggests that the allele dosage effect in diploids could play a role in some regulatory pathways. In response to oxidative stress of H_2O_2, increased growth of diploids from the C- and N-truncated *cdc13-1* haploids reflect either allele dosage effect or a hybrid vigour.

Similar to telomeric DNA patterns, the genotoxicity trends in *cdc13-1* C-terminus deletion mutants and *cdc13-1 exo1Δ* mutants (strains 1296-TR and 1297-TR) were very much alike, a phenomenon could be attributed to the presence of point mutation of *cdc13-1* that disrupts the dimerization of protein and is common in both proteins. Comparably, the sensitivity responses manifested by *cdc13-1* N-terminus truncated mutants to damage causing agents are similar to those in full gene deletion mutant, *cdc13Δ exo1Δ* (strains 2607 and 2608) though less severe. This could be due to the involvement of N-terminus residing domains OB1 which recruits Pol1 and/or RD that binds to Est1 in telomere length regulation. Alternatively, it might indicates that an amino-terminal region of Cdc13 (C-truncated *cdc13-1*) is sufficient for its essential functions in cell survival as compared to its carboxyl C-terminal region (N-truncated *cdc13-1*). This is in agreement with a previous study which showed that lack of N-terminal 1-252 amino acids cause defects in successive cell growth and arrest cell cycle in G2-M phase (Hsu *et al*., 2004). Another more likely explanation could be that in *stn1* allele, lack of 123 residues from C-terminal region of Stn1 does not support viability of cells as compared to its allele with more extensive deletions with the removal of additional 185 C-terminal residues which allows growth at endogenous level (Petreaca *et al*., 2007). Therefore, Cdc13-1 C-terminal region might negatively regulate the essential function or destabilizes Cdc13 mutant protein in the absence of N-terminal.

7.5 Chronological lifespan in the absence of Cdc13 and Stn1

The direct effect of the disruption and removal of essential genes *CDC13*/*STN1* individually and in combination (*cdc13Δ stn1Δ)* in the absence of *EXO1* and *RAD24* genes was investigated to find out any impact on chronological lifespan (CLS). Yeasts can switch rapidly between non-reproductive, G0 arrested phase under starvation to a high metabolic rapid proliferative phase in the presence of nutrients (Piper, 2006). Yeasts survive and age in postdiauxic or stationary phase characterised by high resistance to cellular stresses (Werner-Washburne *et al*., 1996). The CLS assays measure the survival of yeast cells arrested in stationary (G0) phase over time, and provide a model to study ageing of non-dividing cells in higher eukaryotes (Werner-Washburne *et al*., 1996, Maclean *et al*., 2003). Previous studies have reported that in natural isolates of *S. cerevisiae*, genotypic variations accounts for about 22% of the total variation of RLS. CLS and RLS appear to be regulated by overlapping but distinct mechanism (Fabrizio and Longo, 2003). CLS of natural isolates (average ~ 7.4 days) are significantly shorter as compared to laboratory strains (Qin and Lu, 2006).

In yeast *S. cerevisiae* CLS assays are conducted at a population level. Yeast cultures are grown either in SDC/SC or YEPD media (high metabolism) in the presence of glucose. For CLS measurements, the saturated cultures are either kept in the same media or are transferred in water (under calorie restriction in stationary phase). The initial logarithmic growth phase has been reported to affect the ability of cells to enter the stationary phase and influence CLS measurements (Maclean *et al*., 2003). Cells from different strains are grown in glucose containing media (YEPD or SC) to post logarithmic phase of growth where cell start entering the stationary phase, characterised by un-budded cells (>80%) under microscope. For the majority of strains it may take 24-48 hours to enter to stationary phase but it may vary in different strains (Qin and Lu, 2006). The three day and six day cultures in this study were examined, and many budded cells were observed indicating that many cells still did not reach the low metabolism stationary phase.

Despite variations in survival, (possibly due to unavoidable manual errors) the fast decline was observed in average viability count within the first 3 days after saturation of cultures of both single and double deletion mutants. Quick drop in cell survival (%) within the first 3 days in all ageing cultures including wild type and *EXO1* deletion mutants (controls) could be due to diauxic switch (shifting from fermentable carbon source to non-fermentable glycerol under respiratory metabolism) that is consistent with a previous study (Pedruzzi *et al*., 2000).

Overall, the results of CLS studies highlighted the importance of different capping proteins (Cdc13 and Stn1) in cell survival and ageing beside telomere maintenance. The loss of

telomere functions in the absence of capping proteins Cdc13 and Stn1 resulted in the gradual loss of cell survival. Each gene showed its own specific role either independently or in combination with other genes. The presence of capping proteins is important for the normal growth of cells with minimum rate of senescence as has been demonstrated with wild type strain (640). The removal of Cdc13 and Stn1 in deletion mutants has obviously increased the rate of senescence over the period of the CLS studies as compared to the wild type strain. The removal of the two proteins (Cdc13 and Stn1) has different deleterious effects on cell survival. The simultaneous removal of both *STN1* and *CDC13* in the absence of *EXO1* and *RAD24* (strain 2685) exhibited high mortality rate with fast ageing as compared to single mutants. The slow rate of ageing in *EXO1* deletion mutants (strain 1272 and 1273) comparable to the wild type (significantly low as compared to fast ageing mutants) indicated the negligible effect of *exo1*Δ on ageing. The strain 2685 has the *rad24* mutation. Rad24 cell cycle checkpoint protein has been associated with processing of ssDNA at telomere (Lydall and Weinert, 1995). The *rad24*Δ cells show delay in the process and repair of broken ends due to delay in resection of DSB ends in *rad24* mutants compared to resection in wild type (Aylon and Kupiec, 2003). The absence of Rad24 could also contribute to a higher rate of senescence in combined deletion mutants. These results emphasise the importance of checkpoint genes in the cell cycle and their roles in enhancing the rate of ageing. Similarly, removal of Stn1 alone in *cdc13-1* (strain 2625) mutant resulted in early ageing of cells at a lesser rate whereas the strain 2607 with *CDC13*, and, *EXO1* deletions showed 2 times faster ageing compared to *stn1*Δ but 4 times faster than in the combined deletions mutants. These patterns of ageing with the lowest survival value in strain 2685 and the highest survival in strain 2607 observed at age point 6 were maintained until the end of CLS assay over a period of one month. The differences in values of survival, however, were only significant from age points 9-12. Due to fast rate of ageing in all cultures, the differences in survival were not significant after this point. However, it is evident that each gene contributes to the overall process of ageing to some extent by causing slow rates of growth and cellular senescence. At age point 12, slightly higher survival % was observed in *cdc13*Δ (strain 2607) as compared to the other two mutants. It suggests that the mutant lacking Stn1 protein (in *cdc13*Δ *stn1*Δ or in *stn1*Δ mutants) aged faster compared to the *cdc13*Δ mutant, which may be due to the cumulative effect of both deletions.

In traditional CLS methods, ageing cultures are maintained at low temperature (4°-8°C) in water in the stationary phase after early growth in YEPD medium until saturation i.e., entering in stationary phase after 3-6 days of growth (Piper, 2006). However, it takes longer (several months) to determine cell lifespan at low temperature (Fabrizio *et al*., 2004, Fabrizio and Longo, 2003). Higher temperatures (35C°-37°C) have been recommended for the initial measurements of survival to see any potential difference (Piper, 2006, Murakami *et al*., 2008). It was the reason for using temperature 30°C in preliminary experiments in this study.

However, it prompted unavoidable high fluctuations in viability at different time points (reflected in CFUs counts and resulting in survival curves). Due to fluctuations of CFUs the shapes of chronological survival curves do not always resemble 'descending stair case', a feature of a regular survival curve (Qin and Lu, 2006). The experimentation with yeast cells aged in SDC/SC media is simple, with low chances of contamination due to low pH of the media while incubation in water at low temperature is risky for longer period of time with high chances of contamination (Fabrizio and Longo, 2007). It was also observed in this study while carrying out CLS experiment using wild type strain 640 in water at 30C° when one of the samples (3 days grown culture) appeared contaminated at day 18 resulting in the elimination of sample.

The stationary phase survival of *S. cerevisiae* is temperature dependent. Longer survival is observed at low temperature under starvation. Loosing viability could be very slow at low temperature (for cells pre-grown on glycerol medium), and it takes very long time to measure CLS (Piper, 2006). High temperature (between 35°C -37°C) is used for the early measurement of stationary survival that could be reproducible at 30°C for measureable differences in survival. In this study, heat inactivation of single and double deletion mutants and wild type at high temperature (40°C and 45°C) were attempted to detect measureable differences in CLS in water within a short time. Samples were pooled after every hour for CFUs count (within 7-9 hours). Due to marked fluctuations in viability (especially in *cdc13Δ*) this protocol could not be adapted to monitor CLS at high temperature.

For the second stage of this study, stationary survival measurements were carried out at 4°C in water to avoid growth fluctuations and to find out possible differences between these mutants. The viability fluctuations observed at different time points may be due to the fraction of arrested cells that may re-enter the cell cycle after using nutrients released from dead cells, as it occurs in nature under adverse conditions (Fabrizio *et al*., 2004). This phenomenon could be detected because of the sudden increase in survival by (10- to 100 fold) in SD media. SD media, however, promotes a shorter lifespan characterised by high metabolism followed and rapid cell death (Fabrizio and Longo, 2003) that was observed in this study by the sharp decline in the survival at age point 3. Initial growth in rich media like YEPD, induce large fluctuations in viability, a common problem that could be overcome by incubating the culture in water and washing the culture to minimise the chances of survivor re-growth in long term survival experiments (Fabrizio *et al*., 2004).

Ageing is characterised by morphological and physiological changes: change in cell size (as big size in old cells) slowdown of cell cycle and protein synthesis, loose and wrinkled appearance of cells. Appearance of aged colonies after longer incubation (required additional 1-2 days in the mutants lacking Stn1 or Stn1 Cdc13) towards the end of the CLS experiment indicates the

change in rates of growth in these mutants with capping dysfunctions in agreement with previous studies where older cells take longer and entered the cell cycle slowly (Fabrizio *et al*., 2004). Different genetic mutations in yeast can cause observable differences in morphological characteristics during growth of cells e.g., difference in colony size and shape (Memarian *et al*., 2007). In CLS experiments mutants without essential telomere capping proteins showed rough edges of their colonies with a mixture of small and large colonies, more obvious in *stn1Δ* or *stn1Δ cdc13Δ* as compared to *cdc13Δ.* In wild type and *EXO1* deletion mutants, all colonies were round shaped with a smooth surface. The rough edges of colonies may be due to senescence of cells (McEachern and Blackburn, 1996) in ageing cultures owing to genomic instability due to telomere uncapping. The occurrence of small colonies in combined deletion mutants, and *stn1Δ* mutants was also enhanced towards the end of the experiment obvious in combined deletion mutants and could be due to cooperative effect of removal of two essential genes. Similar affects were also observed in N- and C-truncated mutants of *cdc13-1* with obvious difference in colony size (heterogeneous) and shape observed in N-truncated mutants. Further studies are required to determine the fate of these small colonies and their correlation with ageing.

CLS experiments using mutants with telomere capping dysfunction disclosed significant differences in survival as assessed in viability assays under two conditions, in SC medium and in water over a period of 30 days and 90 days respectively. In SC medium at 30°C quick decline in survival (%) with highest mortality observed in combined deletion, *cdc13Δ* and *stn1Δ* mutant (strain 2685, with ~3% survival), as compared to *stn1Δ cdc13-1* mutant (strain 2625, with 10% survival) and *cdc13Δ* mutant (strain 2607, with 23% survival) at day 6 of CLS assay, indicates the impact of telomere uncapping (removal of essential proteins) on ageing of the mutant cells. Most of the cells in control strains 1272 (*exo1Δ*), 640 (WT) and 1273 (*exo1Δ*) were still viable with higher values of survival i.e. ~33%, 36% and ~44% respectively at this age point.

The slow reduction in viability in water at 4°C with survival of ~3% attained in combined mutant (strain 2685) in comparison with 20% and 34% viability in *stn1Δ rad24Δ exo1Δ* mutants (haploid #14 and 21) and 71% and 30 % survival in *cdc13Δ exo1Δ* (strain 2607 and 2608) at day 30, indicated the similar trend as was observed in SC medium. These patterns of survival with highest mortality in combined deletion mutants as compared to either single deletion mutants (in the absence of Stn1 or Cdc13) continued until day 90 with further significant reduction in survival rates, as compared to WT. The variations in survival rate in two Cdc13 deletion mutants (strain 2607 and 2607) might indicate the epistatic interactions from cryptic mutations and the role of other genetic determinants within genome (Gibson and Dworkin, 2004). The dramatic loss of viability and faster ageing in combined deletion mutants also highlighted the additive effects of the two capping proteins in chronological survival. *EXO1* deletion (63% and

75% survival at day 35) did not show any pronounced effect on the CLS as compared to wild type strains (75% and 71%).

The observed difference in survival in SC medium (at 30°C) and in water (at 4°C) lead to conclusion that maintenance of ageing cultures for CLS measurement in SC medium prompts fast decline of viability with marked difference in survival within two weeks. However, CLS measured in water promote longer slow rate survival with obvious differences that could be observed between 30 to 60 days. The first approach (SC medium at 30°C) is, therefore, could be utilised for a quick screen of mutants in short time, to investigate any potential difference in survival whereas the CLS measurement in water at 4°C could be used for the reproducible results with less fluctuations in survival curve.

Furthermore, the marked difference in viability in N- and C-truncated variants of Cdc13-1 as compared to WT and control mutants without Exo1 protein also suggested their role in ageing and cellular senescence. The N-terminus end of Cdc13 is considered essential for the viability of cell (Hsu *et al.*, 2004). However, its deletion showed slightly better average survival as compared to C-truncated Cdc13-1 allele, indicating different roles of Cdc13 termini in cell survival and specifically the involvement of C-terminus in cell longevity.

In yeast RLS studies on cell level (with ~60-100 virgin cells) were conducted to investigate the proliferative potential of cells in different mutants and also to investigate the correlation between CLS and RLS in the absence of essential genes. Preliminary experiments with the wild type and double deletion mutant (*cdc13*Δ *stn1*Δ *exo1*Δ *rad24*Δ) were attempted to carry out RLS by micromanipulation (data not shown). The mortality rate of newly separated daughter cells used as virgin cells was very high: almost 80-95 % cells after isolating daughter cells could not survive. The experimental conditions are required be adapted in order to overcome the viability problems of micromanipulated cells in future studies.

7.6 Conclusions

In this study, detrimental impacts of deficiencies in telomere capping proteins, Cdc13 and Stn1, on chronological lifespan and on the tolerance to oxidative and genotoxic stress factors (UV, MMS, HU and H_2O_2) were shown using budding yeast as a model organism. In the light of well-established essentiality of Cdc13 and Stn1 for the survival, this study was focussed on questioning roles of these proteins as well as N- and C-termini of Cdc13-1 in aging and telomeric DNA metabolism.

The analyses of sequences in N- and C-truncated mutants support the expected sequences in most of the generated mutants that can be used in further extended studies. The presence of intact *Eco*R1 site was also confirmed in the N-terminus of *cdc13-1* gene in all tested mutants.

The incidence of diffused and smeary telomere DNA patterns in *cdc13*Δ and/or *stn1*Δ mutants (type I survivors like) and type II survivors like in N- and C-truncated variants of Cdc13-1 (in strains 1296-TR and 1297-TR) indicates the instability of telomere at 23°C and 30°C. The mutants without capping proteins or with defective Cdc13 proteins showed short survival spans with cumulative effects in the presence of combined deletion (*stn1*Δ and *cdc13*Δ) with the absence of Exo1 and Rad24 linking the role of cell cycle checkpoints in the activation of signalling pathways regulating ageing. The distinct patterns of sensitivity in these mutants in response to UV, HU and MMS might indicate the involvement of S phase checkpoint in the signalling pathways triggered by genotoxic agents. Stn1 deletion mutants, however indicate different underlying mechanisms associated with resistance to oxidative stress (H_2O_2). The H_2O_2-resistance pattern of C-terminus truncated *cdc13-1* mutants indicates that the C-domain might also contain a suppressor of WT-resistance to UV, MMS and HU.

The results of this study highlight potentially new roles of Cdc13 and Stn1 that are related to senescence and ageing, and to cellular responses to genotoxic agents and will contribute to existing knowledge on Cdc13 and Stn1 in relation to telomere capping and to better understand the function of their homologs in higher eukaryotes.

7.7 Future work plan

Future developments from the current work would include further clarification and more extended elaboration of the obtained results. In the present study, the nucleotide sequences of N and C-truncated mutants of the disrupted *cdc13-1* were determined through DNA sequencing. Analysis of expression of the mutated proteins in N- and C-truncated variants of Cdc13-1 by using SDS-PAGE and Western blot in future studies will provide further insights into results of the present work.

Cellular analyses of mutants generated in this study are required to measure the RLS of these mutants and also to find any correlation between CLS and RLS. It would be interesting to analyse gene expression of disrupted *cdc13-1* quantitatively by measuring the mRNA levels in N- and C-truncated mutants using real time PCR approach. Furthermore, the interaction between Stn1 and Ten1 proteins in the presence of disrupted Cdc13-1 can be elucidated by analysing the expression of *STN1* and *TEN1* on RNA level and more specifically on protein level.

Construction of Cdc13 N- and C-deletion cassettes with tag (HA tag or c-myc tag) will facilitate accurate detection of expressed proteins in Western blot analysis and also to conduct comparative analysis of the recombinant proteins in mutants with/without tag to determine effects of protein tagging if any on the expression of fusion proteins.

Cdc13 interact with Stn1, Ten1 and Pol1 proteins through its different domains. New partial deletion constructs of Cdc13, Stn1and Ten1 can also be generated by PCR mediated technique to further elucidate the functions of individual domains of Cdc13 [OB1, RD, OB2, OB3 (DBD) and OB4], Stn1 (OB5) and Ten1 (OB6) proteins and to analyse their biological functions in context of ageing and cellular senescence. Further combination of these deletion mutants can be generated by performing genetic crosses to study interaction between Cdc13, Stn1 and Ten1 proteins and the effect of these mutations on other biological aspect of cells such as CLS, RLS, and responses to different genotoxic agents to link molecular interaction, genetic instability, cellular senescence and checkpoint controls with new insights into molecular functions of these essential proteins.

Systematic analysis of truncated mutants for their telomeric DNA lengths could be conducted after growing these mutants at different temperatures such as 23°C, 26°C, 30°C and 37°C for different passages (p3, p6, p9 and p12) in comparison with original strain (*cdc13-1*) and *cdc13* deletion mutants to observe the effect of multiple passages on telomere DNA length/pattern and also to explore cellular responses to short and long term absence of the protein.

Chapter 8

References

References

Abbotts, R., Thompson, N. and Madhusudan, S. (2014) 'DNA repair in cancer: emerging targets for personalized therapy', Cancer Manag Res, 6, pp. 77-92.

Adams, A., Kaiser, C. and Cold Spring Harbor, L. (1998) Methods in yeast genetics : a Cold Spring Harbor Laboratory course manual. Plainview, N.Y.: Cold Spring Harbor Laboratory Press.

Alfoldi, J. and Lindblad-Toh, K. (2013) 'Comparative genomics as a tool to understand evolution and disease', Genome Res, 23(7), pp. 1063-8.

Alic, N., Higgins, V. J. and Dawes, I. W. (2001) 'Identification of a Saccharomyces cerevisiae gene that is required for G1 arrest in response to the lipid oxidation product linoleic acid hydroperoxide', Mol Biol Cell, 12(6), pp. 1801-10.

Allsopp, R. C., Chang, E., Kashefi-Aazam, M., Rogaev, E. I., Piatyszek, M. A., Shay, J. W. and Harley, C. B. (1995) 'Telomere shortening is associated with cell division in vitro and in vivo', Exp Cell Res, 220(1), pp. 194-200.

Amberg, D. C., Burke, D. J. and Strathern, J. N. (2005) Methods in Yeast Genetics: A. Cold Spring Harbor Laboratory Course Manual. 1. Cold Spring Harbor, New York, USA.: Cold Spring Harbor Laboratory Press.

Anderson, E. M., Halsey, W. A. and Wuttke, D. S. (2002) 'Delineation of the high-affinity single-stranded telomeric DNA-binding domain of Saccharomyces cerevisiae Cdc13', Nucleic Acids Res, 30(19), pp. 4305-13.

Aragona, M., Maisano, R., Panetta, S., Giudice, A., Morelli, M., La Torre, I. and La Torre, F. (2000) 'Telomere length maintenance in aging and carcinogenesis', Int J Oncol, 17(5), pp. 981-9.

Arantes-Oliveira, N., Apfeld, J., Dillin, A. and Kenyon, C. (2002) 'Regulation of life-span by germ-line stem cells in Caenorhabditis elegans', Science, 295(5554), pp. 502-5.

Arneric, M. and Lingner, J. (2007) 'Tel1 kinase and subtelomere-bound Tbf1 mediate preferential elongation of short telomeres by telomerase in yeast', EMBO Rep, 8(11), pp. 1080-5.

Aubert, G. and Lansdorp, P. M. (2008) 'Telomeres and aging', Physiol Rev, 88(2), pp. 557-79.

Autexier, C. and Lue, N. F. (2006) 'The structure and function of telomerase reverse transcriptase', Annu Rev Biochem, 75, pp. 493-517.

Aylon, Y. and Kupiec, M. (2003) 'The checkpoint protein Rad24 of Saccharomyces cerevisiae is involved in processing double-strand break ends and in recombination partner choice', Mol Cell Biol, 23(18), pp. 6585-96.

Bassett, D. E., Jr., Boguski, M. S., Spencer, F., Reeves, R., Kim, S., Weaver, T. and Hieter, P. (1997) 'Genome cross-referencing and XREFdb: implications for the identification and analysis of genes mutated in human disease', Nat Genet, 15(4), pp. 339-44.

Baudin, A., Ozier-Kalogeropoulos, O., Denouel, A., Lacroute, F. and Cullin, C. (1993) 'A simple and efficient method for direct gene deletion in Saccharomyces cerevisiae', Nucleic Acids Res, 21(14), pp. 3329-30.

Baumann, P. (2006) 'Are mouse telomeres going to pot?', Cell, 126(1), pp. 33-6.

Baumann, P. and Cech, T. R. (2001) 'Pot1, the putative telomere end-binding protein in fission yeast and humans', Science, 292(5519), pp. 1171-5.

Baynes, J. W. and Thorpe, S. R. (1999) 'Role of oxidative stress in diabetic complications: a new perspective on an old paradigm', Diabetes, 48(1), pp. 1-9.

Bitterman, K. J., Medvedik, O. and Sinclair, D. A. (2003) 'Longevity regulation in Saccharomyces cerevisiae: linking metabolism, genome stability, and heterochromatin', Microbiol Mol Biol Rev, 67(3), pp. 376-99, table of contents.

Blackburn, E. H. (1991) 'Structure and function of telomeres', Nature, 350(6319), pp. 569-73.

Blackburn, E. H. (2000) 'Telomere states and cell fates', Nature, 408(6808), pp. 53-6.

Blackburn, E. H. (2001) 'Switching and signaling at the telomere', Cell, 106(6), pp. 661-73.

Blankley, R. T. and Lydall, D. (2004) 'A domain of Rad9 specifically required for activation of Chk1 in budding yeast', J Cell Sci, 117(Pt 4), pp. 601-8.

Blasco, M. A. (2003) 'Telomeres and cancer: a tale with many endings', Curr Opin Genet Dev, 13(1), pp. 70-6.

Blow, J. J. (1993) 'Preventing re-replication of DNA in a single cell cycle: evidence for a replication licensing factor', J Cell Biol, 122(5), pp. 993-1002.

Boddy, M. N. and Russell, P. (2001) 'DNA replication checkpoint', Curr Biol, 11(23), pp. R953-6.

Bodnar, A. G., Ouellette, M., Frolkis, M., Holt, S. E., Chiu, C. P., Morin, G. B., Harley, C. B., Shay, J. W., Lichtsteiner, S. and Wright, W. E. (1998) 'Extension of life-span by introduction of telomerase into normal human cells', Science, 279(5349), pp. 349-52.

Bonetti, D., Clerici, M., Manfrini, N., Lucchini, G. and Longhese, M. P. (2010) 'The MRX complex plays multiple functions in resection of Yku- and Rif2-protected DNA ends', PLoS One, 5(11), pp. e14142.

Borghouts, C., Benguria, A., Wawryn, J. and Jazwinski, S. M. (2004) 'Rtg2 protein links metabolism and genome stability in yeast longevity', Genetics, 166(2), pp. 765-77.

Bork, S., Pfister, S., Witt, H., Horn, P., Korn, B., Ho, A. D. and Wagner, W. (2010) 'DNA methylation pattern changes upon long-term culture and aging of human mesenchymal stromal cells', Aging Cell, 9(1), pp. 54-63.

Branzei, D. and Foiani, M. (2006) 'The Rad53 signal transduction pathway: Replication fork stabilization, DNA repair, and adaptation', Exp Cell Res, 312(14), pp. 2654-9.

Brush, G. S. and Kelly, T. J. (2000) 'Phosphorylation of the replication protein A large subunit in the Saccharomyces cerevisiae checkpoint response', Nucleic Acids Res, 28(19), pp. 3725-32.

Bryan, T. M., Englezou, A., Dalla-Pozza, L., Dunham, M. A. and Reddel, R. R. (1997) 'Evidence for an alternative mechanism for maintaining telomere length in human tumors and tumor-derived cell lines', Nat Med, 3(11), pp. 1271-4.

Bryan, T. M., Englezou, A., Gupta, J., Bacchetti, S. and Reddel, R. R. (1995) 'Telomere elongation in immortal human cells without detectable telomerase activity', Embo j, 14(17), pp. 4240-8.

Callegari, A. J. and Kelly, T. J. (2007) 'Shedding light on the DNA damage checkpoint', Cell Cycle, 6(6), pp. 660-6.

Campisi, J. (2003a) 'Analysis of tumor suppressor gene-induced senescence', Methods Mol Biol, 223, pp. 155-72.

Campisi, J. (2003b) 'Cellular senescence and apoptosis: how cellular responses might influence aging phenotypes', Exp Gerontol, 38(1-2), pp. 5-11.

Cech, T. R. (2004) 'Beginning to understand the end of the chromosome', Cell, 116(2), pp. 273-9.

Cenci, G., Ciapponi, L. and Gatti, M. (2005) 'The mechanism of telomere protection: a comparison between Drosophila and humans', Chromosoma, 114(3), pp. 135-45.

Chakhparonian, M. and Wellinger, R. J. (2003) 'Telomere maintenance and DNA replication: how closely are these two connected?', Trends Genet, 19(8), pp. 439-46.

Chalfie, M., Tu, Y., Euskirchen, G., Ward, W. W. and Prasher, D. C. (1994) 'Green fluorescent protein as a marker for gene expression', Science, 263(5148), pp. 802-5.

Chen, Q., Ijpma, A. and Greider, C. W. (2001) 'Two survivor pathways that allow growth in the absence of telomerase are generated by distinct telomere recombination events', Mol Cell Biol, 21(5), pp. 1819-27.

Clerici, M., Paciotti, V., Baldo, V., Romano, M., Lucchini, G. and Longhese, M. P. (2001) 'Hyperactivation of the yeast DNA damage checkpoint by TEL1 and DDC2 overexpression', Embo j, 20(22), pp. 6485-98.

Collins, K. (2000) 'Mammalian telomeres and telomerase', Curr Opin Cell Biol, 12(3), pp. 378-83.

Collins, K. and Mitchell, J. R. (2002) 'Telomerase in the human organism', Oncogene, 21(4), pp. 564-79.

Cooke, H. J. and Smith, B. A. (1986) 'Variability at the telomeres of the human X/Y pseudoautosomal region', Cold Spring Harb Symp Quant Biol, 51 Pt 1, pp. 213-9.

Coppe, J. P., Patil, C. K., Rodier, F., Krtolica, A., Beausejour, C. M., Parrinello, S., Hodgson, J. G., Chin, K., Desprez, P. Y. and Campisi, J. (2010) 'A human-like senescence-associated secretory phenotype is conserved in mouse cells dependent on physiological oxygen', PLoS One, 5(2), pp. e9188.

Cross, F. R. (1997) "Marker swap' plasmids: convenient tools for budding yeast molecular genetics', Yeast, 13(7), pp. 647-53.

Da Silva, N. A. and Srikrishnan, S. (2012) 'Introduction and expression of genes for metabolic engineering applications in Saccharomyces cerevisiae', FEMS Yeast Res, 12(2), pp. 197-214.

d'Adda di Fagagna, F. (2008) 'Living on a break: cellular senescence as a DNA-damage response', Nat Rev Cancer, 8(7), pp. 512-22.

Davidovic, M., Sevo, G., Svorcan, P., Milosevic, D. P., Despotovic, N. and Erceg, P. (2010) 'Old age as a privilege of the "selfish ones"', Aging Dis, 1(2), pp. 139-46.

de Lange, T. (2002) 'Protection of mammalian telomeres', Oncogene, 21(4), pp. 532-40.

de Lange, T. (2004) 'T-loops and the origin of telomeres', Nat Rev Mol Cell Biol, 5(4), pp. 323-9.

de Lange, T. (2005) 'Shelterin: the protein complex that shapes and safeguards human telomeres', Genes Dev, 19(18), pp. 2100-10.

de Lange, T. (2009) 'How telomeres solve the end-protection problem', Science, 326(5955), pp. 948-52.

Dehe, P. M. and Cooper, J. P. (2010) 'Fission yeast telomeres forecast the end of the crisis', FEBS Lett, 584(17), pp. 3725-33.

Di Domenico, E. G., Romano, E., Del Porto, P. and Ascenzioni, F. (2014) 'Multifunctional role of ATM/Tel1 kinase in genome stability: from the DNA damage response to telomere maintenance', Biomed Res Int, 2014, pp. 787404.

Dimri, G. P., Lee, X., Basile, G., Acosta, M., Scott, G., Roskelley, C., Medrano, E. E., Linskens, M., Rubelj, I., Pereira-Smith, O. and et al. (1995) 'A biomarker that identifies senescent human cells in culture and in aging skin in vivo', Proc Natl Acad Sci U S A, 92(20), pp. 9363-7.

D'Mello N, P., Childress, A. M., Franklin, D. S., Kale, S. P., Pinswasdi, C. and Jazwinski, S. M. (1994) 'Cloning and characterization of LAG1, a longevity-assurance gene in yeast', J Biol Chem, 269(22), pp. 15451-9.

Donehower, L. A. (2002) 'Does p53 affect organismal aging?', J Cell Physiol, 192(1), pp. 23-33.

Dorman, J. B., Albinder, B., Shroyer, T. and Kenyon, C. (1995) 'The age-1 and daf-2 genes function in a common pathway to control the lifespan of Caenorhabditis elegans', Genetics, 141(4), pp. 1399-406.

Dubrana, K., Perrod, S. and Gasser, S. M. (2001) 'Turning telomeres off and on', Curr Opin Cell Biol, 13(3), pp. 281-9.

Dynan, W. S. and Yoo, S. (1998) 'Interaction of Ku protein and DNA-dependent protein kinase catalytic subunit with nucleic acids', Nucleic Acids Res, 26(7), pp. 1551-9.

Edwards, P. A. (1999) 'The impact of developmental biology on cancer research: an overview', Cancer Metastasis Rev, 18(2), pp. 175-80.

Eldridge, A. M. and Wuttke, D. S. (2008) 'Probing the mechanism of recognition of ssDNA by the Cdc13-DBD', Nucleic Acids Res, 36(5), pp. 1624-33.

Elledge, S. J. (1996) 'Cell cycle checkpoints: preventing an identity crisis', Science, 274(5293), pp. 1664-72.

Enomoto, S., Glowczewski, L. and Berman, J. (2002) 'MEC3, MEC1, and DDC2 are essential components of a telomere checkpoint pathway required for cell cycle arrest during senescence in Saccharomyces cerevisiae', Mol Biol Cell, 13(8), pp. 2626-38.

Espejel, S., Franco, S., Sgura, A., Gae, D., Bailey, S. M., Taccioli, G. E. and Blasco, M. A. (2002) 'Functional interaction between DNA-PKcs and telomerase in telomere length maintenance', Embo j, 21(22), pp. 6275-87.

Fabrizio, P. and Longo, V. D. (2003) 'The chronological life span of Saccharomyces cerevisiae', Aging Cell, 2(2), pp. 73-81.

Fabrizio, P. and Longo, V. D. (2007) 'The chronological life span of Saccharomyces cerevisiae', Methods Mol Biol, 371, pp. 89-95.

Fabrizio, P., Liou, L. L., Moy, V. N., Diaspro, A., Valentine, J. S., Gralla, E. B. and Longo, V. D. (2003) 'SOD2 functions downstream of Sch9 to extend longevity in yeast', Genetics, 163(1), pp. 35-46.

Fabrizio, P., Pletcher, S. D., Minois, N., Vaupel, J. W. and Longo, V. D. (2004) 'Chronological aging-independent replicative life span regulation by Msn2/Msn4 and Sod2 in Saccharomyces cerevisiae', FEBS Lett, 557(1-3), pp. 136-42.

Festing, S. and Wilkinson, R. (2007) 'The ethics of animal research. Talking Point on the use of animals in scientific research', EMBO Rep, 8(6), pp. 526-30.

Finkel, T. and Holbrook, N. J. (2000) 'Oxidants, oxidative stress and the biology of ageing', Nature, 408(6809), pp. 239-47.

Flattery-O'Brien, J. A. and Dawes, I. W. (1998) 'Hydrogen peroxide causes RAD9-dependent cell cycle arrest in G2 in Saccharomyces cerevisiae whereas menadione causes G1 arrest independent of RAD9 function', J Biol Chem, 273(15), pp. 8564-71.

Foiani, M., Pellicioli, A., Lopes, M., Lucca, C., Ferrari, M., Liberi, G., Muzi Falconi, M. and Plevani, P. (2000) 'DNA damage checkpoints and DNA replication controls in Saccharomyces cerevisiae', Mutat Res, 451(1-2), pp. 187-96.

Fowell, R. R. (1952) 'Sodium acetate agar as a sporulation medium for yeast', Nature, 170(4327), pp. 578.

Fulda, S., Gorman, A. M., Hori, O. and Samali, A. (2010) 'Cellular stress responses: cell survival and cell death', Int J Cell Biol, 2010, pp. 214074.

Gartner, A., Milstein, S., Ahmed, S., Hodgkin, J. and Hengartner, M. O. (2000) 'A conserved checkpoint pathway mediates DNA damage--induced apoptosis and cell cycle arrest in C. elegans', Mol Cell, 5(3), pp. 435-43.

Garvik, B., Carson, M. and Hartwell, L. (1995) 'Single-stranded DNA arising at telomeres in cdc13 mutants may constitute a specific signal for the RAD9 checkpoint', Mol Cell Biol, 15(11), pp. 6128-38.

Gasch, A. P., Spellman, P. T., Kao, C. M., Carmel-Harel, O., Eisen, M. B., Storz, G., Botstein, D. and Brown, P. O. (2000) 'Genomic expression programs in the response of yeast cells to environmental changes', Mol Biol Cell, 11(12), pp. 4241-57.

Gasparyan, H. J., Xu, L., Petreaca, R. C., Rex, A. E., Small, V. Y., Bhogal, N. S., Julius, J. A., Warsi, T. H., Bachant, J., Aparicio, O. M. and Nugent, C. I. (2009) 'Yeast telomere capping protein Stn1 overrides DNA replication control through the S phase checkpoint', Proc Natl Acad Sci U S A, 106(7), pp. 2206-11.

Gavrilov, L. A. and Gavrilova, N. S. (2002) 'Evolutionary theories of aging and longevity', ScientificWorldJournal, 2, pp. 339-56.

Gerschman, R., Gilbert, D. L., Nye, S. W., Dwyer, P. and Fenn, W. O. (1954) 'Oxygen poisoning and x-irradiation: a mechanism in common', Science, 119(3097), pp. 623-6.

Ghosal, G. and Chen, J. (2013) 'DNA damage tolerance: a double-edged sword guarding the genome', Transl Cancer Res, 2(3), pp. 107-129.

Gibson, G. and Dworkin, I. (2004) 'Uncovering cryptic genetic variation', Nat Rev Genet, 5(9), pp. 681-90.

Gietz, D., St Jean, A., Woods, R. A. and Schiestl, R. H. (1992) 'Improved method for high efficiency transformation of intact yeast cells', Nucleic Acids Res, 20(6), pp. 1425.

Gietz, R. D., Schiestl, R. H., Willems, A. R. and Woods, R. A. (1995) 'Studies on the transformation of intact yeast cells by the LiAc/SS-DNA/PEG procedure', Yeast, 11(4), pp. 355-60.

Gladieux, P., Ropars, J., Badouin, H., Branca, A., Aguileta, G., de Vienne, D. M., Rodriguez de la Vega, R. C., Branco, S. and Giraud, T. (2014) 'Fungal evolutionary genomics provides insight into the mechanisms of adaptive divergence in eukaryotes', Mol Ecol, 23(4), pp. 753-73.

Gomez, M., Wu, J., Schreiber, V., Dunlap, J., Dantzer, F., Wang, Y. and Liu, Y. (2006) 'PARP1 Is a TRF2-associated poly(ADP-ribose)polymerase and protects eroded telomeres', Mol Biol Cell, 17(4), pp. 1686-96.

Gospodinov, A. and Herceg, Z. (2013) 'Chromatin structure in double strand break repair', DNA Repair (Amst), 12(10), pp. 800-10.

Goytisolo, F. A. and Blasco, M. A. (2002) 'Many ways to telomere dysfunction: in vivo studies using mouse models', Oncogene, 21(4), pp. 584-91.

Grandin, N. and Charbonneau, M. (2009) 'Telomerase- and Rad52-independent immortalization of budding yeast by an inherited-long-telomere pathway of telomeric repeat amplification', Mol Cell Biol, 29(4), pp. 965-85.

Grandin, N., Damon, C. and Charbonneau, M. (2000) 'Cdc13 cooperates with the yeast Ku proteins and Stn1 to regulate telomerase recruitment', Mol Cell Biol, 20(22), pp. 8397-408.

Grandin, N., Damon, C. and Charbonneau, M. (2001) 'Cdc13 prevents telomere uncapping and Rad50-dependent homologous recombination', Embo j, 20(21), pp. 6127-39.

Grandin, N., Damon, C. and Charbonneau, M. (2001) 'Ten1 functions in telomere end protection and length regulation in association with Stn1 and Cdc13', Embo j, 20(5), pp. 1173-83.

Grandin, N., Reed, S. I. and Charbonneau, M. (1997) 'Stn1, a new Saccharomyces cerevisiae protein, is implicated in telomere size regulation in association with Cdc13', Genes Dev, 11(4), pp. 512-27.

Gray, J. V., Petsko, G. A., Johnston, G. C., Ringe, D., Singer, R. A. and Werner-Washburne, M. (2004) '"Sleeping beauty": quiescence in Saccharomyces cerevisiae', Microbiol Mol Biol Rev, 68(2), pp. 187-206.

Griffith, J. D., Comeau, L., Rosenfield, S., Stansel, R. M., Bianchi, A., Moss, H. and de Lange, T. (1999) 'Mammalian telomeres end in a large duplex loop', Cell, 97(4), pp. 503-14.

Grossi, S., Puglisi, A., Dmitriev, P. V., Lopes, M. and Shore, D. (2004) 'Pol12, the B subunit of DNA polymerase alpha, functions in both telomere capping and length regulation', Genes Dev, 18(9), pp. 992-1006.

Guarente, L. and Kenyon, C. (2000) 'Genetic pathways that regulate ageing in model organisms', Nature, 408(6809), pp. 255-62.

Gutteridge, J. M. (1981) 'Thiobarbituric acid-reactivity following iron-dependent free-radical damage to amino acids and carbohydrates', FEBS Lett, 128(2), pp. 343-6.

Gutteridge, J. M. (1995) 'Lipid peroxidation and antioxidants as biomarkers of tissue damage', Clin Chem, 41(12 Pt 2), pp. 1819-28.

Hadfield, C., Jordan, B. E., Mount, R. C., Pretorius, G. H. and Burak, E. (1990) 'G418-resistance as a dominant marker and reporter for gene expression in Saccharomyces cerevisiae', Curr Genet, 18(4), pp. 303-13.

Hall, D. M., Oberley, T. D., Moseley, P. M., Buettner, G. R., Oberley, L. W., Weindruch, R. and Kregel, K. C. (2000) 'Caloric restriction improves thermotolerance and reduces hyperthermia-induced cellular damage in old rats', Faseb j, 14(1), pp. 78-86.

Hamilton, M. L., Van Remmen, H., Drake, J. A., Yang, H., Guo, Z. M., Kewitt, K., Walter, C. A. and Richardson, A. (2001) 'Does oxidative damage to DNA increase with age?', Proc Natl Acad Sci U S A, 98(18), pp. 10469-74.

Harman, D. (1956) 'Aging: a theory based on free radical and radiation chemistry', J Gerontol, 11(3), pp. 298-300.

Harman, D. (1981) 'The aging process', Proc Natl Acad Sci U S A, 78(11), pp. 7124-8.

Harman, D. (1992a) 'Free radical theory of aging', Mutat Res, 275(3-6), pp. 257-66.

Harman, D. (1992b) 'Free radical theory of aging: history', Exs, 62, pp. 1-10.

Harman, D. (2006) 'Free radical theory of aging: an update: increasing the functional life span', Ann N Y Acad Sci, 1067, pp. 10-21.

Harrison, J. C. and Haber, J. E. (2006) 'Surviving the breakup: the DNA damage checkpoint', Annu Rev Genet, 40, pp. 209-35.

Hartwell, L. H. (1970) 'Periodic density fluctuation during the yeast cell cycle and the selection of synchronous cultures', J Bacteriol, 104(3), pp. 1280-5.

Hartwell, L. H. and Weinert, T. A. (1989) 'Checkpoints: controls that ensure the order of cell cycle events', Science, 246(4930), pp. 629-34.

Hayflick, L. (2000) 'The illusion of cell immortality', Br J Cancer, 83(7), pp. 841-6.

Hayflick, L. and Moorhead, P. S. (1961) 'The serial cultivation of human diploid cell strains', Exp Cell Res, 25, pp. 585-621.

Hedbacker, K. and Carlson, M. (2008) 'SNF1/AMPK pathways in yeast', Front Biosci, 13, pp. 2408-20.

Hekimi, S., Burgess, J., Bussiere, F., Meng, Y. and Benard, C. (2001) 'Genetics of lifespan in C. elegans: molecular diversity, physiological complexity, mechanistic simplicity', Trends Genet, 17(12), pp. 712-8.

Hekimi, S., Lapointe, J. and Wen, Y. (2011) 'Taking a "good" look at free radicals in the aging process', Trends Cell Biol, 21(10), pp. 569-76.

Hemann, M. T. and Greider, C. W. (2000) 'Wild-derived inbred mouse strains have short telomeres', Nucleic Acids Res, 28(22), pp. 4474-8.

Hemann, M. T., Strong, M. A., Hao, L. Y. and Greider, C. W. (2001) 'The shortest telomere, not average telomere length, is critical for cell viability and chromosome stability', Cell, 107(1), pp. 67-77.

Henson, J. D., Cao, Y., Huschtscha, L. I., Chang, A. C., Au, A. Y., Pickett, H. A. and Reddel, R. R. (2009) 'DNA C-circles are specific and quantifiable markers of alternative-lengthening-of-telomeres activity', Nat Biotechnol, 27(12), pp. 1181-5.

Herman, P. K. (2002) 'Stationary phase in yeast', Curr Opin Microbiol, 5(6), pp. 602-7.

Herrera, E., Samper, E., Martin-Caballero, J., Flores, J. M., Lee, H. W. and Blasco, M. A. (1999) 'Disease states associated with telomerase deficiency appear earlier in mice with short telomeres', Embo j, 18(11), pp. 2950-60.

Herskowitz, I. (1988) 'Life cycle of the budding yeast Saccharomyces cerevisiae', Microbiol Rev, 52(4), pp. 536-53.

Hockemeyer, D., Daniels, J. P., Takai, H. and de Lange, T. (2006) 'Recent expansion of the telomeric complex in rodents: Two distinct POT1 proteins protect mouse telomeres', Cell, 126(1), pp. 63-77.

Holstein, E. M., Clark, K. R. and Lydall, D. (2014) 'Interplay between nonsense-mediated mRNA decay and DNA damage response pathways reveals that Stn1 and Ten1 are the key CST telomere-cap components', Cell Rep, 7(4), pp. 1259-69.

Horvath, M. P., Schweiker, V. L., Bevilacqua, J. M., Ruggles, J. A. and Schultz, S. C. (1998) 'Crystal structure of the Oxytricha nova telomere end binding protein complexed with single strand DNA', Cell, 95(7), pp. 963-74.

Hsu, C. L., Chen, Y. S., Tsai, S. Y., Tu, P. J., Wang, M. J. and Lin, J. J. (2004) 'Interaction of Saccharomyces Cdc13p with Pol1p, Imp4p, Sir4p and Zds2p is involved in telomere replication, telomere maintenance and cell growth control', Nucleic Acids Res, 32(2), pp. 511-21.

Huber, F., Meurer, M., Bunina, D., Kats, I., Maeder, C. I., Stefl, M., Mongis, C. and Knop, M. (2014) 'PCR Duplication: A One-Step Cloning-Free Method to Generate Duplicated Chromosomal Loci and Interference-Free Expression Reporters in Yeast', PLoS One, 9(12), pp. e114590.

Hughes, T. R., Weilbaecher, R. G., Walterscheid, M. and Lundblad, V. (2000) 'Identification of the single-strand telomeric DNA binding domain of the Saccharomyces cerevisiae Cdc13 protein', Proc Natl Acad Sci U S A, 97(12), pp. 6457-62.

Inoue, M., Sato, E. F., Nishikawa, M., Park, A. M., Kira, Y., Imada, I. and Utsumi, K. (2003) 'Mitochondrial generation of reactive oxygen species and its role in aerobic life', Curr Med Chem, 10(23), pp. 2495-505.

Itahana, K., Campisi, J. and Dimri, G. P. (2007) 'Methods to detect biomarkers of cellular senescence: the senescence-associated beta-galactosidase assay', Methods Mol Biol, 371, pp. 21-31.

Ja, W. W., West, A. P., Jr., Delker, S. L., Bjorkman, P. J., Benzer, S. and Roberts, R. W. (2007) 'Extension of Drosophila melanogaster life span with a GPCR peptide inhibitor', Nat Chem Biol, 3(7), pp. 415-9.

Jazwinski, S. M. (2002) 'Growing old: metabolic control and yeast aging', Annu Rev Microbiol, 56, pp. 769-92.

Jia, X., Weinert, T. and Lydall, D. (2004) 'Mec1 and Rad53 inhibit formation of single-stranded DNA at telomeres of Saccharomyces cerevisiae cdc13-1 mutants', Genetics, 166(2), pp. 753-64.

Jung, M. and Pfeifer, G. P. (2015) 'Aging and DNA methylation', BMC Biol, 13, pp. 7.

Kachouri-Lafond, R., Dujon, B., Gilson, E., Westhof, E., Fairhead, C. and Teixeira, M. T. (2009) 'Large telomerase RNA, telomere length heterogeneity and escape from senescence in Candida glabrata', FEBS Lett, 583(22), pp. 3605-10.

Kaeberlein, M., Burtner, C. R. and Kennedy, B. K. (2007) 'Recent developments in yeast aging', PLoS Genet, 3(5), pp. e84.

Kaeberlein, M., Powers, R. W., 3rd, Steffen, K. K., Westman, E. A., Hu, D., Dang, N., Kerr, E. O., Kirkland, K. T., Fields, S. and Kennedy, B. K. (2005) 'Regulation of yeast replicative life span by TOR and Sch9 in response to nutrients', Science, 310(5751), pp. 1193-6.

Kalmbach, K. H., Fontes Antunes, D. M., Dracxler, R. C., Knier, T. W., Seth-Smith, M. L., Wang, F., Liu, L. and Keefe, D. L. (2013) 'Telomeres and human reproduction', Fertil Steril, 99(1), pp. 23-9.

Kastenmayer, J. P., Ni, L., Chu, A., Kitchen, L. E., Au, W. C., Yang, H., Carter, C. D., Wheeler, D., Davis, R. W., Boeke, J. D., Snyder, M. A. and Basrai, M. A. (2006) 'Functional genomics of genes with small open reading frames (sORFs) in S. cerevisiae', Genome Res, 16(3), pp. 365-73.

Kennedy, B. K., Austriaco, N. R., Jr. and Guarente, L. (1994) 'Daughter cells of Saccharomyces cerevisiae from old mothers display a reduced life span', J Cell Biol, 127(6 Pt 2), pp. 1985-93.

Kennedy, B. K., Austriaco, N. R., Jr., Zhang, J. and Guarente, L. (1995) 'Mutation in the silencing gene SIR4 can delay aging in S. cerevisiae', Cell, 80(3), pp. 485-96.

Kennedy, B. K., Gotta, M., Sinclair, D. A., Mills, K., McNabb, D. S., Murthy, M., Pak, S. M., Laroche, T., Gasser, S. M. and Guarente, L. (1997) 'Redistribution of silencing proteins from telomeres to the nucleolus is associated with extension of life span in S. cerevisiae', Cell, 89(3), pp. 381-91.

Kim, N. W., Piatyszek, M. A., Prowse, K. R., Harley, C. B., West, M. D., Ho, P. L., Coviello, G. M., Wright, W. E., Weinrich, S. L. and Shay, J. W. (1994) 'Specific association of human telomerase activity with immortal cells and cancer', Science, 266(5193), pp. 2011-5.

Kirkwood, T. B. (1977) 'Evolution of ageing', Nature, 270(5635), pp. 301-4.

Kirkwood, T. B. (2002) 'Evolution of ageing', Mech Ageing Dev, 123(7), pp. 737-45.

Kirkwood, T. B. and Holliday, R. (1979) 'The evolution of ageing and longevity', Proc R Soc Lond B Biol Sci, 205(1161), pp. 531-46.

Kirkwood, T. B. and Melov, S. (2011) 'On the programmed/non-programmed nature of ageing within the life history', Curr Biol, 21(18), pp. R701-7.

Kirkwood, T. B. and Rose, M. R. (1991) 'Evolution of senescence: late survival sacrificed for reproduction', Philos Trans R Soc Lond B Biol Sci, 332(1262), pp. 15-24.

Kladwang, W., Hum, J. and Das, R. (2012) 'Ultraviolet shadowing of RNA can cause significant chemical damage in seconds', Sci Rep, 2, pp. 517.

Koc, A., Wheeler, L. J., Mathews, C. K. and Merrill, G. F. (2004) 'Hydroxyurea arrests DNA replication by a mechanism that preserves basal dNTP pools', J Biol Chem, 279(1), pp. 223-30.

Krtolica, A. and Campisi, J. (2002) 'Cancer and aging: a model for the cancer promoting effects of the aging stroma', Int J Biochem Cell Biol, 34(11), pp. 1401-14.

Latre, L., Tusell, L., Martin, M., Miro, R., Egozcue, J., Blasco, M. A. and Genesca, A. (2003) 'Shortened telomeres join to DNA breaks interfering with their correct repair', Exp Cell Res, 287(2), pp. 282-8.

Lederberg, J. and Lederberg, E. M. (1952) 'Replica plating and indirect selection of bacterial mutants', J Bacteriol, 63(3), pp. 399-406.

Lee, H. W., Blasco, M. A., Gottlieb, G. J., Horner, J. W., 2nd, Greider, C. W. and DePinho, R. A. (1998) 'Essential role of mouse telomerase in highly proliferative organs', Nature, 392(6676), pp. 569-74.

Lehner, B. (2011) 'Molecular mechanisms of epistasis within and between genes', Trends Genet, 27(8), pp. 323-31.

Li, G. M. (2008) 'Mechanisms and functions of DNA mismatch repair', Cell Res, 18(1), pp. 85-98.

Lillie, S. H. and Pringle, J. R. (1980) 'Reserve carbohydrate metabolism in Saccharomyces cerevisiae: responses to nutrient limitation', J Bacteriol, 143(3), pp. 1384-94.

Lin, J. J. and Zakian, V. A. (1996) 'The Saccharomyces CDC13 protein is a single-strand TG1-3 telomeric DNA-binding protein in vitro that affects telomere behavior in vivo', Proc Natl Acad Sci U S A, 93(24), pp. 13760-5.

Lin, S. J., Kaeberlein, M., Andalis, A. A., Sturtz, L. A., Defossez, P. A., Culotta, V. C., Fink, G. R. and Guarente, L. (2002) 'Calorie restriction extends Saccharomyces cerevisiae lifespan by increasing respiration', Nature, 418(6895), pp. 344-8.

Lingner, J., Cooper, J. P. and Cech, T. R. (1995) 'Telomerase and DNA end replication: no longer a lagging strand problem?', Science, 269(5230), pp. 1533-4.

Liu, D., O'Connor, M. S., Qin, J. and Songyang, Z. (2004) 'Telosome, a mammalian telomere-associated complex formed by multiple telomeric proteins', J Biol Chem, 279(49), pp. 51338-42.

Lobo, V., Patil, A., Phatak, A. and Chandra, N. (2010) 'Free radicals, antioxidants and functional foods: Impact on human health', Pharmacogn Rev, 4(8), pp. 118-26.

Longhese, M. P. (2008) 'DNA damage response at functional and dysfunctional telomeres', Genes Dev, 22(2), pp. 125-40.

Longhese, M. P., Foiani, M., Muzi-Falconi, M., Lucchini, G. and Plevani, P. (1998) 'DNA damage checkpoint in budding yeast', Embo j, 17(19), pp. 5525-8.

Longo, V. D. and Fabrizio, P. (2012) 'Chronological Aging in Saccharomyces cerevisiae', Subcell Biochem, 57, pp. 101-21.

Longtine, M. S., McKenzie, A., 3rd, Demarini, D. J., Shah, N. G., Wach, A., Brachat, A., Philippsen, P. and Pringle, J. R. (1998) 'Additional modules for versatile and economical PCR-based gene deletion and modification in Saccharomyces cerevisiae', Yeast, 14(10), pp. 953-61.

Lorenz, M. C., Muir, R. S., Lim, E., McElver, J., Weber, S. C. and Heitman, J. (1995) 'Gene disruption with PCR products in Saccharomyces cerevisiae', Gene, 158(1), pp. 113-7.

Louis, E. J. (1995) 'The chromosome ends of Saccharomyces cerevisiae', Yeast, 11(16), pp. 1553-73.

Louis, E. J. and Haber, J. E. (1990) 'The subtelomeric Y' repeat family in Saccharomyces cerevisiae: an experimental system for repeated sequence evolution', Genetics, 124(3), pp. 533-45.

Lundblad, V. and Blackburn, E. H. (1993) 'An alternative pathway for yeast telomere maintenance rescues est1- senescence', Cell, 73(2), pp. 347-60.

Lundin, C., North, M., Erixon, K., Walters, K., Jenssen, D., Goldman, A. S. and Helleday, T. (2005) 'Methyl methanesulfonate (MMS) produces heat-labile DNA damage but no detectable in vivo DNA double-strand breaks', Nucleic Acids Res, 33(12), pp. 3799-811.

Lustig, A. J. (2001) 'Cdc13 subcomplexes regulate multiple telomere functions', Nat Struct Biol: Vol. 4. United States, pp. 297-9.

Lydall, D. (2003) 'Hiding at the ends of yeast chromosomes: telomeres, nucleases and checkpoint pathways', J Cell Sci, 116(Pt 20), pp. 4057-65.

Lydall, D. and Weinert, T. (1995) 'Yeast checkpoint genes in DNA damage processing: implications for repair and arrest', Science, 270(5241), pp. 1488-91.

Lydeard, J. R., Jain, S., Yamaguchi, M. and Haber, J. E. (2007) 'Break-induced replication and telomerase-independent telomere maintenance require Pol32', Nature, 448(7155), pp. 820-3.

Maclean, M. J., Aamodt, R., Harris, N., Alseth, I., Seeberg, E., Bjoras, M. and Piper, P. W. (2003) 'Base excision repair activities required for yeast to attain a full chronological life span', Aging Cell, 2(2), pp. 93-104.

Mager, W. H. and Winderickx, J. (2005) 'Yeast as a model for medical and medicinal research', Trends Pharmacol Sci, 26(5), pp. 265-73.

Maringele, L. and Lydall, D. (2002) 'EXO1-dependent single-stranded DNA at telomeres activates subsets of DNA damage and spindle checkpoint pathways in budding yeast yku70Delta mutants', Genes Dev, 16(15), pp. 1919-33.

Maringele, L. and Lydall, D. (2004) 'EXO1 plays a role in generating type I and type II survivors in budding yeast', Genetics, 166(4), pp. 1641-9.

Martinez, P., Thanasoula, M., Carlos, A. R., Gomez-Lopez, G., Tejera, A. M., Schoeftner, S., Dominguez, O., Pisano, D. G., Tarsounas, M. and Blasco, M. A. (2010) 'Mammalian Rap1 controls telomere function and gene expression through binding to telomeric and extratelomeric sites', Nat Cell Biol, 12(8), pp. 768-80.

Mason, M. and Skordalakes, E. (2010) 'Insights into Cdc13 dependent telomere length regulation', Aging (Albany NY), 2(10), pp. 731-4.

Mason, M., Wanat, J. J., Harper, S., Schultz, D. C., Speicher, D. W., Johnson, F. B. and Skordalakes, E. (2013) 'Cdc13 OB2 dimerization required for productive Stn1 binding and efficient telomere maintenance', Structure, 21(1), pp. 109-20.

Masoro, E. J. (2005) 'Overview of caloric restriction and ageing', Mech Ageing Dev, 126(9), pp. 913-22.

Mates, J. M., Perez-Gomez, C. and Nunez de Castro, I. (1999) 'Antioxidant enzymes and human diseases', Clin Biochem, 32(8), pp. 595-603.

Mather, K. A., Jorm, A. F., Parslow, R. A. and Christensen, H. (2011) 'Is telomere length a biomarker of aging? A review', J Gerontol A Biol Sci Med Sci, 66(2), pp. 202-13.

Mathieu, N., Pirzio, L., Freulet-Marriere, M. A., Desmaze, C. and Sabatier, L. (2004) 'Telomeres and chromosomal instability', Cell Mol Life Sci, 61(6), pp. 641-56.

McCall, M. R. and Frei, B. (1999) 'Can antioxidant vitamins materially reduce oxidative damage in humans?', Free Radic Biol Med, 26(7-8), pp. 1034-53.

McEachern, M. J. and Blackburn, E. H. (1996) 'Cap-prevented recombination between terminal telomeric repeat arrays (telomere CPR) maintains telomeres in Kluyveromyces lactis lacking telomerase', Genes Dev, 10(14), pp. 1822-34.

McEachern, M. J. and Haber, J. E. (2006) 'Break-induced replication and recombinational telomere elongation in yeast', Annu Rev Biochem, 75, pp. 111-35.

McPherson, J. P., Hande, M. P., Poonepalli, A., Lemmers, B., Zablocki, E., Migon, E., Shehabeldin, A., Porras, A., Karaskova, J., Vukovic, B., Squire, J. and Hakem, R. (2006) 'A role for Brca1 in chromosome end maintenance', Hum Mol Genet, 15(6), pp. 831-8.

Memarian, N., Jessulat, M., Alirezaie, J., Mir-Rashed, N., Xu, J., Zareie, M., Smith, M. and Golshani, A. (2007) 'Colony size measurement of the yeast gene deletion strains for functional genomics', BMC Bioinformatics, 8, pp. 117.

Metcalfe, J. A., Parkhill, J., Campbell, L., Stacey, M., Biggs, P., Byrd, P. J. and Taylor, A. M. (1996) 'Accelerated telomere shortening in ataxia telangiectasia', Nat Genet, 13(3), pp. 350-3.

Mitchell, M. T., Smith, J. S., Mason, M., Harper, S., Speicher, D. W., Johnson, F. B. and Skordalakes, E. (2010) 'Cdc13 N-terminal dimerization, DNA binding, and telomere length regulation', Mol Cell Biol, 30(22), pp. 5325-34.

Mittler, R. (2002) 'Oxidative stress, antioxidants and stress tolerance', Trends Plant Sci, 7(9), pp. 405-10.

Miyake, Y., Nakamura, M., Nabetani, A., Shimamura, S., Tamura, M., Yonehara, S., Saito, M. and Ishikawa, F. (2009) 'RPA-like mammalian Ctc1-Stn1-Ten1 complex binds to single-stranded DNA and protects telomeres independently of the Pot1 pathway', Mol Cell, 36(2), pp. 193-206.

Mogila, V., Xia, F. and Li, W. X. (2006) 'An intrinsic cell cycle checkpoint pathway mediated by MEK and ERK in Drosophila', Dev Cell, 11(4), pp. 575-82.

Mordes, D. A., Nam, E. A. and Cortez, D. (2008) 'Dpb11 activates the Mec1-Ddc2 complex', Proc Natl Acad Sci U S A, 105(48), pp. 18730-4.

Mortimer, R. K. and Johnston, J. R. (1959) 'Life span of individual yeast cells', Nature, 183(4677), pp. 1751-2.

Mu, J. and Wei, L. X. (2002) 'Telomere and telomerase in oncology', Cell Res, 12(1), pp. 1-7.

Mulleder, M., Capuano, F., Pir, P., Christen, S., Sauer, U., Oliver, S. G. and Ralser, M. (2012) 'A prototrophic deletion mutant collection for yeast metabolomics and systems biology', Nat Biotechnol, 30(12), pp. 1176-8.

Murakami, C. J., Burtner, C. R., Kennedy, B. K. and Kaeberlein, M. (2008) 'A method for high-throughput quantitative analysis of yeast chronological life span', J Gerontol A Biol Sci Med Sci, 63(2), pp. 113-21.

Navadgi-Patil, V. M. and Burgers, P. M. (2008) 'Yeast DNA replication protein Dpb11 activates the Mec1/ATR checkpoint kinase', J Biol Chem, 283(51), pp. 35853-9.

Ngo, H. P. and Lydall, D. (2010) 'Survival and growth of yeast without telomere capping by Cdc13 in the absence of Sgs1, Exo1, and Rad9', PLoS Genet, 6(8), pp. e1001072.

Nugent, C. I., Hughes, T. R., Lue, N. F. and Lundblad, V. (1996) 'Cdc13p: a single-strand telomeric DNA-binding protein with a dual role in yeast telomere maintenance', Science, 274(5285), pp. 249-52.

Ohouo, P. Y. and Smolka, M. B. (2012) 'The many roads to checkpoint activation', Cell Cycle, 11(24), pp. 4495.

Olson-Manning, C. F., Wagner, M. R. and Mitchell-Olds, T. (2012) 'Adaptive evolution: evaluating empirical support for theoretical predictions', Nat Rev Genet, 13(12), pp. 867-77.

O'Sullivan, R. J. and Karlseder, J. (2010) 'Telomeres: protecting chromosomes against genome instability', Nat Rev Mol Cell Biol, 11(3), pp. 171-81.

Palm, W. and de Lange, T. (2008) 'How shelterin protects mammalian telomeres', Annu Rev Genet, 42, pp. 301-34.

Pamplona, R. and Barja, G. (2006) 'Mitochondrial oxidative stress, aging and caloric restriction: the protein and methionine connection', Biochim Biophys Acta, 1757(5-6), pp. 496-508.

Pandita, R. K., Sharma, G. G., Laszlo, A., Hopkins, K. M., Davey, S., Chakhparonian, M., Gupta, A., Wellinger, R. J., Zhang, J., Powell, S. N., Roti Roti, J. L., Lieberman, H. B. and Pandita, T. K. (2006) 'Mammalian Rad9 plays a role in telomere stability, S- and G2-phase-specific cell survival, and homologous recombinational repair', Mol Cell Biol, 26(5), pp. 1850-64.

Parenteau, J. and Wellinger, R. J. (1999) 'Accumulation of single-stranded DNA and destabilization of telomeric repeats in yeast mutant strains carrying a deletion of RAD27', Mol Cell Biol, 19(6), pp. 4143-52.

Park, S. K., Kim, K., Page, G. P., Allison, D. B., Weindruch, R. and Prolla, T. A. (2009) 'Gene expression profiling of aging in multiple mouse strains: identification of aging biomarkers and impact of dietary antioxidants', Aging Cell, 8(4), pp. 484-95.

Pedruzzi, I., Burckert, N., Egger, P. and De Virgilio, C. (2000) 'Saccharomyces cerevisiae Ras/cAMP pathway controls post-diauxic shift element-dependent transcription through the zinc finger protein Gis1', Embo j, 19(11), pp. 2569-79.

Pedruzzi, I., Dubouloz, F., Cameroni, E., Wanke, V., Roosen, J., Winderickx, J. and De Virgilio, C. (2003) 'TOR and PKA signaling pathways converge on the protein kinase Rim15 to control entry into G0', Mol Cell, 12(6), pp. 1607-13.

Petreaca, R. C., Chiu, H. C. and Nugent, C. I. (2007) 'The role of Stn1p in Saccharomyces cerevisiae telomere capping can be separated from its interaction with Cdc13p', Genetics, 177(3), pp. 1459-74.

Petreaca, R. C., Chiu, H. C., Eckelhoefer, H. A., Chuang, C., Xu, L. and Nugent, C. I. (2006) 'Chromosome end protection plasticity revealed by Stn1p and Ten1p bypass of Cdc13p', Nat Cell Biol, 8(7), pp. 748-55.

Pfander, B. and Diffley, J. F. (2011) 'Dpb11 coordinates Mec1 kinase activation with cell cycle-regulated Rad9 recruitment', Embo j, 30(24), pp. 4897-907.

Piper, P. W. (2006) 'Long-lived yeast as a model for ageing research', Yeast, 23(3), pp. 215-26.

Poloumienko, A., Dershowitz, A., De, J. and Newlon, C. S. (2001) 'Completion of replication map of Saccharomyces cerevisiae chromosome III', Mol Biol Cell, 12(11), pp. 3317-27.

Price, C. M., Boltz, K. A., Chaiken, M. F., Stewart, J. A., Beilstein, M. A. and Shippen, D. E. (2010) 'Evolution of CST function in telomere maintenance', Cell Cycle, 9(16), pp. 3157-65.

Proctor, C. J., Lydall, D. A., Boys, R. J., Gillespie, C. S., Shanley, D. P., Wilkinson, D. J. and Kirkwood, T. B. (2007) 'Modelling the checkpoint response to telomere uncapping in budding yeast', J R Soc Interface, 4(12), pp. 73-90.

Puddu, F., Granata, M., Di Nola, L., Balestrini, A., Piergiovanni, G., Lazzaro, F., Giannattasio, M., Plevani, P. and Muzi-Falconi, M. (2008) 'Phosphorylation of the budding yeast 9-1-1 complex is required for Dpb11 function in the full activation of the UV-induced DNA damage checkpoint', Mol Cell Biol, 28(15), pp. 4782-93.

Puglisi, A., Bianchi, A., Lemmens, L., Damay, P. and Shore, D. (2008) 'Distinct roles for yeast Stn1 in telomere capping and telomerase inhibition', Embo j, 27(17), pp. 2328-39.

Qi, H. and Zakian, V. A. (2000) 'The Saccharomyces telomere-binding protein Cdc13p interacts with both the catalytic subunit of DNA polymerase alpha and the telomerase-associated est1 protein', Genes Dev, 14(14), pp. 1777-88.

Qin, H. and Lu, M. (2006) 'Natural variation in replicative and chronological life spans of Saccharomyces cerevisiae', Exp Gerontol, 41(4), pp. 448-56.

Rahman, K. (2007) 'Studies on free radicals, antioxidants, and co-factors', Clin Interv Aging, 2(2), pp. 219-36.

Rasouli-Nia, A., Karimi-Busheri, F. and Weinfeld, M. (2004) 'Stable down-regulation of human polynucleotide kinase enhances spontaneous mutation frequency and sensitizes cells to genotoxic agents', Proc Natl Acad Sci U S A, 101(18), pp. 6905-10.

Rattan, S. I. (2008) 'Increased molecular damage and heterogeneity as the basis of aging', Biol Chem, 389(3), pp. 267-72.

Raynard, S., Niu, H. and Sung, P. (2008) 'DNA double-strand break processing: the beginning of the end', Genes Dev, 22(21), pp. 2903-7.

Reddel, R. R. (2000) 'The role of senescence and immortalization in carcinogenesis', Carcinogenesis, 21(3), pp. 477-84.

Rothstein, R. (1991) 'Targeting, disruption, replacement, and allele rescue: integrative DNA transformation in yeast', Methods Enzymol, 194, pp. 281-301.

Rothstein, R. J., Esposito, R. E. and Esposito, M. S. (1977) 'The effect of ochre suppression on meiosis and ascospore formation in Saccharomyces', Genetics, 85(1), pp. 35-54.

Rubin, G. M., Yandell, M. D., Wortman, J. R., Gabor Miklos, G. L., Nelson, C. R., Hariharan, I. K., Fortini, M. E., Li, P. W., Apweiler, R., Fleischmann, W., Cherry, J. M., Henikoff, S., Skupski, M. P., Misra, S., Ashburner, M., Birney, E., Boguski, M. S., Brody, T., Brokstein, P., Celniker, S. E., Chervitz, S. A., Coates, D., Cravchik, A., Gabrielian, A., Galle, R. F., Gelbart, W. M., George, R. A., Goldstein, L. S., Gong, F., Guan, P., Harris, N. L., Hay, B. A., Hoskins, R. A., Li, J., Li, Z., Hynes, R. O., Jones, S. J., Kuehl, P. M., Lemaitre, B., Littleton, J. T., Morrison, D. K., Mungall, C., O'Farrell, P. H., Pickeral, O. K., Shue, C., Vosshall, L. B., Zhang, J., Zhao, Q., Zheng, X. H. and Lewis, S. (2000) 'Comparative genomics of the eukaryotes', Science, 287(5461), pp. 2204-15.

Sambrook, J. and Russell, D. W. (2001) Molecular Cloning: A Laboratory Manual. Cold Spring Harbor, NY: Cold Spring Harbor Laboratory Press.

Samper, E., Flores, J. M. and Blasco, M. A. (2001) 'Restoration of telomerase activity rescues chromosomal instability and premature aging in Terc-/- mice with short telomeres', EMBO Rep, 2(9), pp. 800-7.

Sancar, A., Lindsey-Boltz, L. A., Unsal-Kacmaz, K. and Linn, S. (2004) 'Molecular mechanisms of mammalian DNA repair and the DNA damage checkpoints', Annu Rev Biochem, 73, pp. 39-85.

Santos, J., Leao, C. and Sousa, M. J. (2012) 'Growth culture conditions and nutrient signaling modulating yeast chronological longevity', Oxid Med Cell Longev, 2012, pp. 680304.

Scherer, S. and Davis, R. W. (1979) 'Replacement of chromosome segments with altered DNA sequences constructed in vitro', Proc Natl Acad Sci U S A, 76(10), pp. 4951-5.

Sedivy, J. M. (2007) 'Telomeres limit cancer growth by inducing senescence: long-sought in vivo evidence obtained', Cancer Cell, 11(5), pp. 389-91.

Sgro, C. M. and Partridge, L. (1999) 'A delayed wave of death from reproduction in Drosophila', Science, 286(5449), pp. 2521-4.

Shakirov, E. V., Surovtseva, Y. V., Osbun, N. and Shippen, D. E. (2005) 'The Arabidopsis Pot1 and Pot2 proteins function in telomere length homeostasis and chromosome end protection', Mol Cell Biol, 25(17), pp. 7725-33.

Shanley, D. P. and Kirkwood, T. B. (2006) 'Caloric restriction does not enhance longevity in all species and is unlikely to do so in humans', Biogerontology, 7(3), pp. 165-8.

Shay, J. W. and Wright, W. E. (2001) 'Telomeres and telomerase: implications for cancer and aging', Radiat Res, 155(1 Pt 2), pp. 188-193.

Shay, J. W. and Wright, W. E. (2005) 'Senescence and immortalization: role of telomeres and telomerase', Carcinogenesis, 26(5), pp. 867-74.

Siewers, V. (2014) 'An overview on selection marker genes for transformation of Saccharomyces cerevisiae', Methods Mol Biol, 1152, pp. 3-15.

Signon, L., Malkova, A., Naylor, M. L., Klein, H. and Haber, J. E. (2001) 'Genetic requirements for RAD51- and RAD54-independent break-induced replication repair of a chromosomal double-strand break', Mol Cell Biol, 21(6), pp. 2048-56.

Sikorski, R. S. and Hieter, P. (1989) 'A system of shuttle vectors and yeast host strains designed for efficient manipulation of DNA in Saccharomyces cerevisiae', Genetics, 122(1), pp. 19-27.

Sinclair, D. A. and Guarente, L. (1997) 'Extrachromosomal rDNA circles--a cause of aging in yeast', Cell, 91(7), pp. 1033-42.

Sinha, R. P. and Hader, D. P. (2002) 'UV-induced DNA damage and repair: a review', Photochem Photobiol Sci, 1(4), pp. 225-36.

Slijepcevic, P. (2006) 'The role of DNA damage response proteins at telomeres--an "integrative" model', DNA Repair (Amst), 5(11), pp. 1299-306.

Smith, D. L., Jr., McClure, J. M., Matecic, M. and Smith, J. S. (2007) 'Calorie restriction extends the chronological lifespan of Saccharomyces cerevisiae independently of the Sirtuins', Aging Cell, 6(5), pp. 649-62.

Smith, J. S. and Boeke, J. D. (1997) 'An unusual form of transcriptional silencing in yeast ribosomal DNA', Genes Dev, 11(2), pp. 241-54.

Smith, J. S., Brachmann, C. B., Pillus, L. and Boeke, J. D. (1998) 'Distribution of a limited Sir2 protein pool regulates the strength of yeast rDNA silencing and is modulated by Sir4p', Genetics, 149(3), pp. 1205-19.

Smogorzewska, A. and de Lange, T. (2004) 'Regulation of telomerase by telomeric proteins', Annu Rev Biochem, 73, pp. 177-208.

Sohal, R. S., Mockett, R. J. and Orr, W. C. (2002) 'Mechanisms of aging: an appraisal of the oxidative stress hypothesis', Free Radic Biol Med, 33(5), pp. 575-86.

Soni, R., Carmichael, J. P. and Murray, J. A. (1993) 'Parameters affecting lithium acetate-mediated transformation of Saccharomyces cerevisiae and development of a rapid and simplified procedure', Curr Genet, 24(5), pp. 455-9.

Steinkraus, K. A., Kaeberlein, M. and Kennedy, B. K. (2008) 'Replicative aging in yeast: the means to the end', Annu Rev Cell Dev Biol, 24, pp. 29-54.

Stewart, S. A. and Weinberg, R. A. (2006) 'Telomeres: cancer to human aging', Annu Rev Cell Dev Biol, 22, pp. 531-57.

Strehler, B. L. (1986) 'Genetic instability as the primary cause of human aging', Exp Gerontol, 21(4-5), pp. 283-319.

Sun, J., Kale, S. P., Childress, A. M., Pinswasdi, C. and Jazwinski, S. M. (1994) 'Divergent roles of RAS1 and RAS2 in yeast longevity', J Biol Chem, 269(28), pp. 18638-45.

Sun, J., Yang, Y., Wan, K., Mao, N., Yu, T. Y., Lin, Y. C., DeZwaan, D. C., Freeman, B. C., Lin, J. J., Lue, N. F. and Lei, M. (2011) 'Structural bases of dimerization of yeast telomere protein

Cdc13 and its interaction with the catalytic subunit of DNA polymerase alpha', Cell Res, 21(2), pp. 258-74.

Surovtseva, Y. V., Shakirov, E. V., Vespa, L., Osbun, N., Song, X. and Shippen, D. E. (2007) 'Arabidopsis POT1 associates with the telomerase RNP and is required for telomere maintenance', Embo j, 26(15), pp. 3653-61.

Swindell, W. R. (2007) 'Gene expression profiling of long-lived dwarf mice: longevity-associated genes and relationships with diet, gender and aging', BMC Genomics, 8, pp. 353.

Teng, S. C. and Zakian, V. A. (1999) 'Telomere-telomere recombination is an efficient bypass pathway for telomere maintenance in Saccharomyces cerevisiae', Mol Cell Biol, 19(12), pp. 8083-93.

Teng, S. C., Chang, J., McCowan, B. and Zakian, V. A. (2000) 'Telomerase-independent lengthening of yeast telomeres occurs by an abrupt Rad50p-dependent, Rif-inhibited recombinational process', Mol Cell, 6(4), pp. 947-52.

Tsubouchi, H. and Ogawa, H. (2000) 'Exo1 roles for repair of DNA double-strand breaks and meiotic crossing over in Saccharomyces cerevisiae', Mol Biol Cell, 11(7), pp. 2221-33.

Uzunova, K., Georgieva, M. and Miloshev, G. (2013) 'Saccharomyces cerevisiae linker histone-Hho1p maintains chromatin loop organization during ageing', Oxid Med Cell Longev, 2013, pp. 437146.

Vachova, L., Cap, M. and Palkova, Z. (2012) 'Yeast colonies: a model for studies of aging, environmental adaptation, and longevity', Oxid Med Cell Longev, 2012, pp. 601836.

Valko, M., Izakovic, M., Mazur, M., Rhodes, C. J. and Telser, J. (2004) 'Role of oxygen radicals in DNA damage and cancer incidence', Mol Cell Biochem, 266(1-2), pp. 37-56.

Valko, M., Rhodes, C. J., Moncol, J., Izakovic, M. and Mazur, M. (2006) 'Free radicals, metals and antioxidants in oxidative stress-induced cancer', Chem Biol Interact, 160(1), pp. 1-40.

van den Berg, M. A. and Steensma, H. Y. (1997) 'Expression cassettes for formaldehyde and fluoroacetate resistance, two dominant markers in Saccharomyces cerevisiae', Yeast, 13(6), pp. 551-9.

Vaziri, H., Dragowska, W., Allsopp, R. C., Thomas, T. E., Harley, C. B. and Lansdorp, P. M. (1994) 'Evidence for a mitotic clock in human hematopoietic stem cells: loss of telomeric DNA with age', Proc Natl Acad Sci U S A, 91(21), pp. 9857-60.

Vialard, J. E., Gilbert, C. S., Green, C. M. and Lowndes, N. F. (1998) 'The budding yeast Rad9 checkpoint protein is subjected to Mec1/Tel1-dependent hyperphosphorylation and interacts with Rad53 after DNA damage', Embo j, 17(19), pp. 5679-88.

Vina, J., Borras, C. and Miquel, J. (2007) 'Theories of ageing', IUBMB Life, 59(4-5), pp. 249-54.

von Zglinicki, T., Saretzki, G., Ladhoff, J., d'Adda di Fagagna, F. and Jackson, S. P. (2005) 'Human cell senescence as a DNA damage response', Mech Ageing Dev, 126(1), pp. 111-7.

Wach, A., Brachat, A., Alberti-Segui, C., Rebischung, C. and Philippsen, P. (1997) 'Heterologous HIS3 marker and GFP reporter modules for PCR-targeting in Saccharomyces cerevisiae', Yeast, 13(11), pp. 1065-75.

Wan, M., Qin, J., Songyang, Z. and Liu, D. (2009) 'OB fold-containing protein 1 (OBFC1), a human homolog of yeast Stn1, associates with TPP1 and is implicated in telomere length regulation', J Biol Chem, 284(39), pp. 26725-31.

Wang, F. and Lei, M. (2011) 'Human telomere POT1-TPP1 complex and its role in telomerase activity regulation', Methods Mol Biol, 735, pp. 173-87.

Wang, W., Skopp, R., Scofield, M. and Price, C. (1992) 'Euplotes crassus has genes encoding telomere-binding proteins and telomere-binding protein homologs', Nucleic Acids Res, 20(24), pp. 6621-9.

Wang, X. and Baumann, P. (2008) 'Chromosome fusions following telomere loss are mediated by single-strand annealing', Mol Cell, 31(4), pp. 463-73.

Weinert, B. T. and Timiras, P. S. (2003) 'Invited review: Theories of aging', J Appl Physiol (1985), 95(4), pp. 1706-16.

Weinert, T. (1998a) 'DNA damage and checkpoint pathways: molecular anatomy and interactions with repair', Cell, 94(5), pp. 555-8.

Weinert, T. (1998b) 'DNA damage checkpoints update: getting molecular', Curr Opin Genet Dev, 8(2), pp. 185-93.

Weinert, T. A. and Hartwell, L. H. (1988) 'The RAD9 gene controls the cell cycle response to DNA damage in Saccharomyces cerevisiae', Science, 241(4863), pp. 317-22.

Weinert, T. A. and Hartwell, L. H. (1993) 'Cell cycle arrest of cdc mutants and specificity of the RAD9 checkpoint', Genetics, 134(1), pp. 63-80.

Wellinger, R. J. (2009) 'The CST complex and telomere maintenance: the exception becomes the rule', Mol Cell, 36(2), pp. 168-9.

Werner-Washburne, M., Braun, E. L., Crawford, M. E. and Peck, V. M. (1996) 'Stationary phase in Saccharomyces cerevisiae', Mol Microbiol, 19(6), pp. 1159-66.

Werner-Washburne, M., Braun, E., Johnston, G. C. and Singer, R. A. (1993) 'Stationary phase in the yeast Saccharomyces cerevisiae', Microbiol Rev, 57(2), pp. 383-401.

Winzeler, E. A., Shoemaker, D. D., Astromoff, A., Liang, H., Anderson, K., Andre, B., Bangham, R., Benito, R., Boeke, J. D., Bussey, H., Chu, A. M., Connelly, C., Davis, K., Dietrich, F., Dow, S. W., El Bakkoury, M., Foury, F., Friend, S. H., Gentalen, E., Giaever, G., Hegemann, J. H., Jones, T., Laub, M., Liao, H., Liebundguth, N., Lockhart, D. J., Lucau-Danila, A., Lussier, M., M'Rabet, N., Menard, P., Mittmann, M., Pai, C., Rebischung, C., Revuelta, J. L., Riles, L., Roberts, C. J., Ross-MacDonald, P., Scherens, B., Snyder, M., Sookhai-Mahadeo, S., Storms, R. K., Veronneau, S., Voet, M., Volckaert, G., Ward, T. R., Wysocki, R., Yen, G. S., Yu, K., Zimmermann, K., Philippsen, P., Johnston, M. and Davis,

R. W. (1999) 'Functional characterization of the S. cerevisiae genome by gene deletion and parallel analysis', Science, 285(5429), pp. 901-6.

Wright, W. E., Piatyszek, M. A., Rainey, W. E., Byrd, W. and Shay, J. W. (1996) 'Telomerase activity in human germline and embryonic tissues and cells', Dev Genet, 18(2), pp. 173-9.

Wu, L., Multani, A. S., He, H., Cosme-Blanco, W., Deng, Y., Deng, J. M., Bachilo, O., Pathak, S., Tahara, H., Bailey, S. M., Behringer, R. R. and Chang, S. (2006) 'Pot1 deficiency initiates DNA damage checkpoint activation and aberrant homologous recombination at telomeres', Cell, 126(1), pp. 49-62.

Wu, Y. and Zakian, V. A. (2011) 'The telomeric Cdc13 protein interacts directly with the telomerase subunit Est1 to bring it to telomeric DNA ends in vitro', Proc Natl Acad Sci U S A, 108(51), pp. 20362-9.

Wurtmann, E. J. and Wolin, S. L. (2009) 'RNA under attack: cellular handling of RNA damage', Crit Rev Biochem Mol Biol, 44(1), pp. 34-49.

Xin, H., Liu, D., Wan, M., Safari, A., Kim, H., Sun, W., O'Connor, M. S. and Songyang, Z. (2007) 'TPP1 is a homologue of ciliate TEBP-beta and interacts with POT1 to recruit telomerase', Nature, 445(7127), pp. 559-62.

Zainal, T. A., Oberley, T. D., Allison, D. B., Szweda, L. I. and Weindruch, R. (2000) 'Caloric restriction of rhesus monkeys lowers oxidative damage in skeletal muscle', Faseb j, 14(12), pp. 1825-36.

Zambrano, M. M. and Kolter, R. (1996) 'GASPing for life in stationary phase', Cell, 86(2), pp. 181-4.

Zhang, J. R., Andrus, P. K. and Hall, E. D. (1993) 'Age-related regional changes in hydroxyl radical stress and antioxidants in gerbil brain', J Neurochem, 61(5), pp. 1640-7.

Zhou, Z. and Elledge, S. J. (1993) 'DUN1 encodes a protein kinase that controls the DNA damage response in yeast', Cell, 75(6), pp. 1119-27.

Zubko, M. K. and Lydall, D. (2006) 'Linear chromosome maintenance in the absence of essential telomere-capping proteins', Nat Cell Biol, 8(7), pp. 734-40.

Zubko, M. K., Guillard, S. and Lydall, D. (2004) 'Exo1 and Rad24 differentially regulate generation of ssDNA at telomeres of Saccharomyces cerevisiae cdc13-1 mutants', Genetics, 168(1), pp. 103-15.

Supplementary Information

Methods and Protocols

List of Supplementary Method and Protocols:

Supplementary Methods and Protocols

Method S2.1. Preparation of Yeast Extract Peptone Dextrose (YEPD) agar and broth medium with adenine (0.5 L).

YEPD agar medium (500 ml) required:

Yeast Extract (#LP0021)	5 g
Bacteriological peptone (LP0037)	10 g
Agar Bacteriological N1 (LP0037)	10 g

All above ingredients were mixed in distilled water with final volume up to 0.5L, followed by autoclaving with regime B at 121°C for 15 minutes. Media was cooled and at about 60°C following sterile solutions were added in aseptic environment:

- 40% Dextrose* (Glucose) 25 ml
- 0.5% Adenine*(Sulphate) 7.5 ml

To make homogenous composition, mixture was mixed immediately without bubbles. Media was cooled down to 55°C and plates were poured. The media plates were allowed to dry, wrapped in to avoid evaporation and stored at 4°C till use.

To prepare YEPD broth method was followed as above without adding bacteriological agar.

*40% Dextrose:

200 g Glucose was dissolved in 500 ml final volume and solution was autoclaved at 121°C for 15 minutes.

* 0.5% Adenine (sulphate):

0.5 g Adenine sulphate was dissolved in 100 ml final volume distilled water and autoclaved at 121°C for 15 minutes.

Method S2.2. Preparation of Synthetic Defined or Synthetic Dextrose Minimal Medium **(**SD), agar and broth(1 L).

Synthetic Defined medium (SD) used for chronological aging studies contained following components.

- D-glucose 20 g
- Yeast nitrogen base*(-AA/-AS) 1.7 g
- Ammonium sulphate 5.0 g
- Adenine(hemisulphate) 0.04 g

Amino acids	**Concentration (g/L)**
• L-Arginine (HCl)	0.02 g
• L-Aspartic acid	0.1 g
• L-Glutamic acid(monosodium salt)	0.1 g
• L-**Histidine**	0.1 g
• **L-Leucine**	0.3 g
• L-Lysine (mono-HCl)	0.03 g
• L-Methionine	0.02 g
• L-Phenylalanine	0.05 g
• L-Serine	0.375 g
• L-Threonine	0.2 g
• **L-Tryptophan**	0.04 g
• L-Tyrosine	0.03 g
• L-Valine	0.15 g
• **Uracil**	0.1 g

All above components except glucose were mixed in distilled water with final volume of 1 L. The medium was autoclaved at 121°C for 15 minutes. Following autoclaving medium was cooled down to about 60°C and 25ml of sterile 40% Dextrose (Glucose) was added.

To make homogenous composition, medium was mixed immediately without bubbles, cooled down to 55°and plates were poured. Plates were allowed to dry, wrapped in to avoid evaporation and stored at 4°C.

To prepare Synthetic Defined (SD) broth method was followed as above without adding bacteriological agar.

Amino acid auxotrophies were compensated for by adding 5X final concentration to dropout or **synthetic complete medium (SC).**

*****Yeast nitrogen base did not contain amino acids (AA) or ammonium sulfate (AS).

Method S2.3. Preparation of Dropout agar and broth medium (0.5 L).

Dropout agar medium was prepared by mixing following ingredients:

- Dropout amino acid powders* 0.65 g
- Yeast nitrogen base (without Amino acids and ammonium sulphate) 0.85 g
- Ammonium sulphate 2.5 g
- Agar Bacteriological N1 10g
- 1M NaOH 3 ml

All above ingredients were mixed in distilled water with final volume up to 0.5 L, followed by autoclaving at 121°C for 15 minutes. Media was cooled down and at about 60°C sterile solutions of dextrose was added in aseptic environment:

- 40% Dextrose (Glucose) 25 ml

To make homogenous composition, media was mixed immediately avoiding any bubbles, cooled down to 55° and plates were poured. The plates were allowed to dry at room temperature, wrapped in to avoid evaporation and stored at 4°C till use.

To prepare **Dropout broth** method was followed as above without adding bacteriological agar.

***Dropout amino acid powders:** Combination of different amino acids in specific concentration as given below was used to make media with minimal requirements.

Amino acids	**Quantity used for dropout powders**
Adenine (hemisulphate)	2.5 g
L-Arginine (HCl)	1.2 g
L-Aspartic acid	6.0 g
L-Glutamic acid(monosodium salt)	6.0 g
L-Histidine	1.2 g
L-Leucine	3.6 g
L-Lysine(mono-HCl)	1.8 g
L-Methionine	1.2 g
L-Phenylalanine	3.0 g
L-Serine	22.5 g
L-Threonine	12.0 g
L-Tryptophan	2.4 g
L-Tyrosine	1.8 g
L-Valine	9.0 g
Uracil	1.2g

Any amino acid from above list can be dropped or missed to make medium deficient in that specific amino acid. For example medium deficient in histidine was prepared by leaving histidine from the list and using all other amino acids to prepare minus (-) histidine dropout medium.

Protocol S2.1. CLS in SC medium (postdiauxic phase).

- Streaking out cultures of control and experimental strains from frozen stock onto YEPD agar plates and cultivating at 30°C for 48 hrs or more to get well-separated single colonies.
- Picking up single colonies and inoculating 5 ml liquid YEPD medium in a test tube (starter culture). Growing o/n at 30°C in a shaker at 200 rpm.
- Inoculating 5 ml of synthetic complete (SC) medium with 50 µl of starter culture (200 µl in 20 ml SC in flask).
- Setting out five replicates for each strain at this stage for the validity of the experiment.
- Maintaining culture at 30°C with constant agitation for 4 weeks.

Measuring cell survival/viability count through serial dilution and plating

- Taking an aliquot of ageing culture at day 3, 6, 9, 12, 15, 18, 21 etc., for 4 weeks or more and estimating the viability count through colony-forming unit (CFU) after diluting the culture.
- Pooling out culture aliquots and serially diluting them in sterile water to achieve a cell density ~$1x10^3$-$5x10^3$ cells/ml.
- Spreading out 50 µl of diluted suspension on each half of a YEPD agar plate (Kaeberlein, 2006 and incubating at 30°C for 3 days and counting cells for each strain. Calculating viability based on the number of colonies arising (CFUs) on the YEPD.

Data Analysis

All cultures were presumed to be 100% viable at the day showing the maximum number of cells/ml. Averages and standard deviations for five biological replicates were calculated using Microsoft Excel 2010.

Protocol S2.2. CLS experiments in water: CLS-Optimisation using strain 640 by keeping cells at 30°C CLS experiments in water.

- Streaking out culture (640) on YEPD media and cultivating for three days at 23°C for well-separated colonies.
- Picking up a few (4-5) colonies and setting up o/n culture in YEPD broth (10 ml). Cultivating at 30°C in a shaking incubator overnight.
- Washing the culture three times with sterile water.
- Making glycerol stock (15%) and freezing at -80°C until further dilution.
- Inoculating three sets of cultures by diluting 500 µl of glycerol stock in 10 ml of SD broth supplemented with histidine, leucine, tryptophan and uracil (5 times) in a sterile universal. The cell number was kept between 1-2x10^6 cells /ml (Fabrizio and Longo, 2004) and 2-6x10^8 (Qiu and Lu, 2006) according to OD_{660} = 0.1-0.2 (0.2 = 0.255x10^7 cells /ml). First two cultures for 9 days (9-D) were set and cultivating at 30°C in a shaking incubator at 50 rpm. After three days, two cultures were set for 6 days (6-D) and finally, after another three days, last two cultures were set for 3 days (3-D). All cultures were grown to pass the logarithmic phase (24-48 hrs). All cultures were ready at the same time to start CLS measurement. At the end of 9, 6 and 3 days, all cultures were harvested by centrifugation.
- Spinning out 10 ml culture for each sample at low speed (3800 rpm for 5 minutes) to harvest cell pellet.
- Washing out cell pellet three times with sterile water by spinning at the same speed and re-suspending in 10 ml sterile water.
- Measuring absorbance at 660 nm to estimate cell number (starting cell concentration for CLS assay should be ~ 2-6x10^8 cells/ml).
- Keeping cell suspensions at 4°C (G1 phase) over night.
- Transferring and keeping cells at 30°C for CLS assay and pooling out samples for viability count at three day intervals (0, 3 D, 6 D, 9 D and so on).

Making serial dilution for plating:

- Measuring OD_{660} of 1/5 diluted suspension (200 µl with 800 µl of sterile water).
- Making 6 five-fold serial dilutions (40 µl suspensions (A-F) with 160 µl sterile water in a total volume of 200 µl in 96-well plates). Expected cell number in sixth dilution was 6000 cells/ml according to OD_{660}.

- Plating 20 µl of last two dilutions (6^{th}) and dilution 5^{th} on each half of a YEPD plate (two plates) and cultivating at 30°C for three days before counting colonies.
- Counting colonies and tabulating data for each count. Calculating average and % viability and plotting on graph to see viable cell number decline over the period of the assay.

Protocol S2.3. Protocol S2.3. CLS-Optimisation: viability dynamics after exposure of cells to 40°C/ 45°C in shaking water bath.

- Streaking cultures of wild type (DLY 640) and *cdc13* mutants (DLY 2607, 2608 and 2685 strains) on YEPD medium and incubating plates for three days at 30°C for well-separated colonies.
- Picking up a few (4-5) colonies and inoculating with them YEPD broth (10 ml) in a glass universals. Growing at 30°C in a shaking incubator (at 150 rpm) overnight.
- Diluting 400 µl, 500 µl, 500 µl and 800 µl of o/n cultures of strains DLY 640, DLY 2607, DLY 2608 and DLY 2685 respectively in 25 ml YEPD broth in flasks (1/4 volume ratio). Growing cultures for three days in shaking incubator (24-48 hrs, to pass the logarithmic phase).
- Washing out the cultures three times with sterile water (first wash with 40 ml, second wash with 40 ml and third wash with 25 ml sterile water respectively) and centrifuging at 3000 rpm for 5 minutes.
- Re-suspending cell pellet in sterile water (strains 640 in 35 ml, 2607 in 30 ml, 2608 in 25 ml and 2685 in 15 ml respectively) to keep cell number approximately equal.
- Measuring optical density at 660 nm to estimate the number of cells (starting cell concentration 2-6x10^8 cells/ml).
- Keeping cell suspension at 4°C (G1 phase) for 48 hours.
- Setting cultures for analysis in a water bath at 40°C or 45°C. Pooling out samples, 1ml each after every hour (for 7-9 hours) and transferring it first to ice for half an hour and then to 4°C overnight.

Making serial dilutions for plating:

- Measuring OD_{660} of 1/10 diluted suspension (500 µl culture with 4500 µl sterile water) to estimate number of cells /ml.
- Making 5- and10-fold serial dilutions of 500 µl suspension in 5 ml sterile water (1:5, 500 µl culture+ 4500 µl sterile water, dilutions #1-#5 in a total volume of 5000 µl) in small bijou tubes.

- Expected cell number in wild type DLY 640 in dilution #3 was ~4000 cells/ml according to the absorbance 0.011 at OD_{660}.
- Plating 50 µl of last two dilutions (#4 and #5) for strains 640, 2607, 2608 and dilutions #3 and #4 for strain 2685 on each half of a YEPD plate (two plates) and incubating at 30°C for three days before counting colonies.

Protocol S2.4. CLS experiments in water (4°C) under calorie restriction (stationary phase).

(utilised for *cdc13-1* NTΔ and CTΔ mutants and other *cdc13Δ stn1Δ* mutants)

- Streaking out cultures from frozen stocks on YEPD plates and incubating at 30°C for 2-3 days.
- Inoculating 4-5 colonies in 5 ml of YEPD broth and growing in a shaking incubator at 30°C overnight (16-18 hrs).
- Diluting overnight culture to a density of 1-2x10^6 cells /ml (OD_{660} 0.1-0.2) in 25 ml of YEPD broth in a 125 ml flask (keeping culture to flask volume 1:5; for 30 ml culture, a 150 ml flask should be used).
- Growing cultures for 6 days at 30°C in a shaking incubator.
- Washing out cells at 3000 rpm for 5 min (three times with 25 ml sterile distilled water).
- Resuspending cell pellet in 25 ml of sterile distilled water and measuring OD_{660} using the appropriate dilution (1/20 dilution was used to measure OD at 660 nm: mixing 50 µl of culture with 950 µl of water in a final volume of 1 ml, or 150 µl of culture with 2850 µl of water in a final volume of 3 ml).
- Equalising cell number in all cultures, based on the OD_{660} measurement.
- Keeping cells at 4°C for the entire period of CLS and taking measurements after equal time intervals, 5 to 10 days.